INTERNATIONAL REVIEW OF CELL AND MOLECULAR BIOLOGY

Edited by
Kwang W. Jeon

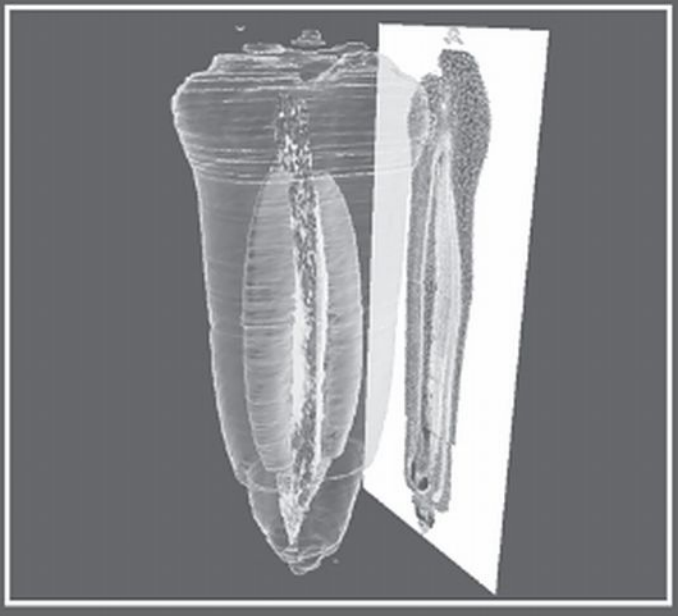

Volume 281

VOLUME TWO EIGHTY ONE

International Review of CELL AND MOLECULAR BIOLOGY

INTERNATIONAL REVIEW OF CELL AND MOLECULAR BIOLOGY

VOLUME TWO EIGHTY ONE

International Review of CELL AND MOLECULAR BIOLOGY

EDITED BY

KWANG W. JEON
Department of Biochemistry
University of Tennessee
Knoxville, Tennessee

ELSEVIER

AMSTERDAM • BOSTON • HEIDELBERG • LONDON
NEW YORK • OXFORD • PARIS • SAN DIEGO
SAN FRANCISCO • SINGAPORE • SYDNEY • TOKYO
Academic Press is an imprint of Elsevier

Front Cover Photography: Cover figure by Felix Bollenbeck, Fraunhofer Institute for Factory Operation and Automation IFF, Magdeburg, Germany

Academic Press is an imprint of Elsevier
525 B Street, Suite 1900, San Diego, CA 92101-4495, USA
30 Corporate Drive, Suite 400, Burlington, MA 01803, USA
32 Jamestown Road, London NW1 7BY, UK
Radarweg 29, PO Box 211, 1000 AE Amsterdam, The Netherlands

First edition 2010

British Library Cataloguing in Publication Data
A catalogue record for this book is available from the British Library

Library of Congress Cataloging-in-Publication Data
A catalog record for this book is available from the Library of Congress

For information on all Academic Press publications
visit our website at elsevierdirect.com

ISBN: 978-0-12-381258-2

PRINTED AND BOUND IN USA
10 11 12 10 9 8 7 6 5 4 3 2 1

Contents

Contributors *vii*

1. Interactions Between Plants and Arbuscular Mycorrhizal Fungi **1**

Shingo Hata, Yoshihiro Kobae, and Mari Banba

1. Introduction 2
2. Studies on Model Legumes 3
3. Studies on Other Plants 14
4. Concluding Remarks 32

Acknowledgments 33
References 33

2. Barley Grain Development: Toward an Integrative View **49**

Nese Sreenivasulu, Ljudmilla Borisjuk, Björn H. Junker, Hans-Peter Mock, Hardy Rolletschek, Udo Seiffert, Winfriede Weschke, and Ulrich Wobus

1. Introduction 50
2. Barley Grain Development 51
3. 3-D/4-D Models of Developing Barley Grains 55
4. Omics Technologies and Molecular-Physiological Events During Grain Development 59
5. Systems Biology View of Barley Grain Development 77
6. Concluding Remarks 79

Acknowledgments 81
References 81

3. New Insights into the Regulation of the Actin Cytoskeleton by Tropomyosin **91**

C.-L. Albert Wang and Lynne M. Coluccio

1. Introduction 92
2. Biochemical and Biophysical Properties of Tropomyosin 92
3. Roles of Tropomyosin in Muscle and Nonmuscle Cells 99
4. Intracellular Distribution of Tropomyosin Isoforms 105
5. Caldesmon and Tropomyosins 108
6. Potential Roles of Tropomyosin in Cancer Metastasis 114

7. Concluding Remarks 116
Acknowledgments 116
References 117

4. Regulation of Sulfate Transport and Assimilation in Plants 129
Hideki Takahashi

1. Introduction 130
2. Sulfate Transport Systems 132
3. Regulation of Sulfate Transport and Metabolism 145
4. Concluding Remarks 152
Acknowledgments 153
References 153

5. Metabolic Pathways in the Apicoplast of Apicomplexa 161
Frank Seeber and Dominique Soldati-Favre

1. Introduction 162
2. Morphology, Acquisition, and Evolutionary Origin of the Apicoplast 164
3. Genome, Proteome, and Protein Trafficking 165
4. Potential and Limitations of *In Silico* Predictions of Metabolic Pathways 168
5. Biosynthesis of Various Metabolites and Factors 170
6. Apicoplast Metabolic Pathways as Drug Targets and the Phenomenon of Delayed Death 208
7. Conclusions 210
Acknowledgments 211
References 211

6. Molecular Mechanisms of Pathogenesis of Parkinson's Disease 229
M.I. Shadrina, P.A. Slominsky, and S.A. Limborska

1. Introduction 230
2. Clinical Features of Parkinson's Disease 231
3. Neuropathology of Parkinson's Disease 233
4. Genetic Causes of Parkinson's Disease 234
5. Conclusion 256
References 257

Index 267

Contributors

Mari Banba
Laboratory of Crop Science, Graduate School of Bioagricultural Sciences, Nagoya University, Nagoya, Japan

Ljudmilla Borisjuk
Leibniz Institute of Plant Genetics and Crop Plant Research, Gatersleben, Germany

Lynne M. Coluccio
Boston Biomedical Research Institute, Watertown, Massachusetts, USA

Shingo Hata
Laboratory of Crop Science, Graduate School of Bioagricultural Sciences, Nagoya University, Nagoya, Japan

Björn H. Junker
Leibniz Institute of Plant Genetics and Crop Plant Research, Gatersleben, Germany

Yoshihiro Kobae
Laboratory of Crop Science, Graduate School of Bioagricultural Sciences, Nagoya University, Nagoya, Japan

S.A. Limborska
Institute of Molecular Genetics, Russian Academy of Sciences, Moscow, Russia

Hans-Peter Mock
Leibniz Institute of Plant Genetics and Crop Plant Research, Gatersleben, Germany

Hardy Rolletschek
Leibniz Institute of Plant Genetics and Crop Plant Research, Gatersleben, Germany

Frank Seeber
Robert-Koch-Institut, Berlin; and FB Biologie/Parasitologie, Philipps-Universität Marburg, Marburg, Germany

Udo Seiffert
Fraunhofer Institute for Factory Operation and Automation IFF, Magdeburg, Germany

M.I. Shadrina
Institute of Molecular Genetics, Russian Academy of Sciences, Moscow, Russia

P.A. Slominsky
Institute of Molecular Genetics, Russian Academy of Sciences, Moscow, Russia

Dominique Soldati-Favre
Department of Microbiology and Molecular Medicine, CMU, University of Geneva, Geneva, Switzerland

Nese Sreenivasulu
Leibniz Institute of Plant Genetics and Crop Plant Research, Gatersleben, Germany

Hideki Takahashi
RIKEN Plant Science Center Joint Laboratory, Kihara Institute for Biological Research, Yokohama City University, Maioka-cho, Totsuka-ku, Yokohama, Japan

C.-L. Albert Wang
Boston Biomedical Research Institute, Watertown, Massachusetts, USA

Winfriede Weschke
Leibniz Institute of Plant Genetics and Crop Plant Research, Gatersleben, Germany

Ulrich Wobus
Leibniz Institute of Plant Genetics and Crop Plant Research, Gatersleben, Germany

CHAPTER ONE

Interactions Between Plants and Arbuscular Mycorrhizal Fungi

Shingo Hata, Yoshihiro Kobae, *and* Mari Banba

Contents

1. Introduction 2
2. Studies on Model Legumes 3
   2.1. The presymbiotic phase 3
   2.2. The endosymbiotic phase 9
3. Studies on Other Plants 14
   3.1. Bryophytes 14
   3.2. Lessons from *Arabidopsis* 16
   3.3. Crops 18
   3.4. Variability of plant responses as to AM colonization 24
   3.5. Toward sustainable agriculture 26
4. Concluding Remarks 32
Acknowledgments 33
References 33

Abstract

Arbuscular mycorrhizal (AM) fungi inhabit the root cortical cells of most plants and obtain photosynthates from the host plants while they transfer mineral nutrients from the soil to the hosts. In this review, we first summarize recent progress regarding signal molecules involved in the recognition of each symbiont, the signaling pathways in the host plants, and the characteristics of AM-inducible nutrient transporters, which were elucidated mainly using model legumes. Then, we summarize studies on the colonization by AM fungi of lower plants and of the roots of major crops. There are not only ''AM-responsive'' crops like maize, sorghum, and soybean but also ''AM-nonresponsive'' ones like wheat, barley, and rice. Finally, we mention the worldwide problems of limited and biased agricultural resources and discuss future directions as to how we can make use of AM symbiosis for improving crop production and establishing sustainable agriculture.

Laboratory of Crop Science, Graduate School of Bioagricultural Sciences, Nagoya University, Nagoya, Japan

International Review of Cell and Molecular Biology, Volume 281
ISSN 1937-6448, DOI: 10.1016/S1937-6448(10)81001-9

Key Words: Symbiosis, Signal transduction, Nutrient exchange, Phosphate transporter, Ammonium transporter, MicroRNA, Sustainable agriculture.

1. Introduction

Arbuscular mycorrhizae are symbiotic associations between plants and fungi, the term arbuscular mycorrhiza (AM) being derived from the Latin word ''arbusculum'' and the Greek words ''mycos'' and ''rhiza,'' which mean little tree, fungus, and root, respectively. In fact, the fungi often form little tree-like structures, arbuscules, in plant root cells. Arbuscular mycorrhizal symbiosis has a long history of more than 400 million years (Redecker et al., 2000; Remy et al., 1994) and is thought to have contributed greatly to the colonization of the land by plants (Pirozynski and Malloch, 1975; Simon et al., 1993). Such symbiosis occurs between 70% and 90% of extant land plant species and soil fungi that belong to a single phylum, the Glomeromycota (Schüßler et al., 2001; Smith and Read, 2008). The AM fungal hyphae extend into the rhizosphere and thereby improve the absorption of water and nutrients such as phosphate and nitrogen, which are two of the three major nutrients, from the soil through arbuscules (Chalot et al., 2006; Govindarajulu et al., 2005; Karandashov and Bucher, 2005). Therefore, it is true that ''mycorrhizae, not roots, are the chief organs of nutrient uptake by land plants'' (Smith and Read, 2008). The AM fungi also endow host plants with tolerance to pathogens and abiotic stress (Liu et al., 2007; Marschner, 1995). During the long period of coevolution, asexual AM fungi became obligate biotrophs that depended on the host plants for their sole carbon supply (Bago et al., 2000; Smith and Read, 2008; Zhu and Miller, 2003). Thanks to the application of cell and molecular biological techniques, studies on AM symbiosis are greatly expanding (Bonfante and Genre, 2008; Bucher et al., 2009; Harrison, 2005; Parniske, 2008).

The molecular mechanisms of interactions between plants and AM fungi have mainly been investigated using model legumes, that is, *Medicago truncatula* and *Lotus japonicus* (Harrison, 2005; Parniske, 2008). Here, we will start by highlighting recent progress regarding signal molecules as to the symbionts and signaling pathways in plants. Then, we will describe aspects of the nutrient trading between two symbionts, and turn our attention to other plants including important crops. We will discuss the potential of AM symbiosis from the viewpoint of agriculture.

2. Studies on Model Legumes

M. truncatula (barrel medic) and *L. japonicus* (birdsfoot trefoil) were postulated to be model legumes in the 1990s (Barker et al., 1990; Cook, 1999; Handberg and Stougaard, 1992). They have small plant bodies, small diploid genomes (less than 500 Mbp), and a self-fertile nature; exhibit a rapid generation time and prolific seed production; and are also amenable to genetic transformation with the aid of *Agrobacterium*. In addition, genome sequencing projects on *M. truncatula* (http://www.jcvi.org/cgi-bin/medicago/index.cgi) and *L. japonicus* (http://www.kazusa.or.jp/lotus/) started rather early and thus related resources are ample. Both model legumes are very suitable for the investigation of plant–microbe interactions such as AM symbiosis and nitrogen-fixing root nodule formation, because *Arabidopsis thaliana*, the leading model plant, does not exhibit either symbiosis.

2.1. The presymbiotic phase

2.1.1. Signal molecules

Historically, model legumes contributed earlier to research on nitrogen-fixing nodule production, another important mode of plant–microbe symbiosis, than to that on AM symbiosis. Regarding the presymbiotic stage of nodulation, the mechanism of recognition between leguminous plants and rhizobial soil bacteria has been well characterized (Spaink, 2000). Each legume secretes particular inducers, usually flavonoid compounds, from its roots. A bacterium recognizes the plant inducers through its NodD proteins (Horvath et al., 1987; Spaink et al., 1987), and then synthesizes and secretes specific Nod factors, lipochitin oligosaccharides. The plant genes for Nod factor receptors have also been identified (Madsen et al., 2003; Radutoiu et al., 2003).

Through analogy to the above mechanism, plant inducers responsible for activation of AM hyphae were sought. Under suitable conditions, the spores of AM fungi germinate, and the elongation of the hyphae stops repeatedly if they do not receive any plant signals (Logi et al., 1998; Mosse, 1959). In contrast, the respiration of hyphae is activated in the presence of compound(s) secreted from plant roots (Tamasloukht et al., 2003). Such diffusible compounds are referred to as "branching factors," because they cause continuous hyphal growth and hyphal branching of some AM fungi as well as respiratory activation (Buee et al., 2000). As a landmark of research on AM symbiosis, Akiyama et al. (2005) identified the chemical structures of branching factors as those of strigolactones, a group of sesquiterpene lactones. Fortuitously, for Akiyama et al., *L. japonicus* is a model legume that secretes unusually high amounts of branching factors for

an unknown reason. Strigolactones were already known at that time as seed-germination stimulants for witchweeds like *Striga* and *Orobanche* (Yoder, 1999). Finally, it turned out that strigolactones are novel plant hormones that inhibit shoot branching in both monocotyledonous and dicotyledonous plants (Gomez-Roldan et al., 2008; Umehara et al., 2008). Therefore, both AM fungi and witchweeds make use of the unstableness of a kind of plant hormone for the recognition of nearby roots of host plants (Parniske, 2005).

Now that plant-derived inducers have been identified, the main aim for natural product chemists would be the identification of diffusible signal compound(s) from AM fungi, collectively called Myc factor(s), which correspond to Nod factors in the case of root nodule formation. For example, a diffusible AM fungal factor activated an early AM-inducible plant genes encoding MtEnod11 (Chabaud et al., 2002; Kosuta et al., 2003) and steroid-binding protein 1 (Kuhn et al., 2010), also stimulating lateral root formation of *M. truncatula* (Olah et al., 2005). In addition, with regard to that the calcium levels in plant cells respond to AM fungi (Kosuta et al., 2008), a fungal signal molecule was reported to cause transient calcium elevation in plant cells (Navazio et al., 2007). Recently, another presymbiotic factor was shown to induce starch accumulation in host roots (Gutjahr et al., 2009b). Unfortunately, the chemical identification of those factors seems to be far from completion. Whether or not these diffusible fungal factors are identical is not yet known. It is also unknown whether or not strigolactones are necessary for the production of these factors.

2.1.2. The prepenetration apparatus

After reaching the epidermis of the host roots, AM fungal extraradical hyphae form hyphopodia (or appressoria), a special fungal organ from which hyphae penetrate into the roots. Since the fungi do not form hyphopodia on nonhost roots, they seem to perform contact recognition of the cell wall of the hosts (Nagahashi and Douds, 1997). However, the details of the recognition mechanism are not understood well. Once hyphopodia are formed, plant cells accept the intraradical hyphae in a very active manner, as follows. First, the nucleus of an epidermal cell attached to a hyphopodium migrates close to the hyphopodium and then moves to the opposite end of the cell. Tracing the nuclear movement exactly, the membranes of the endoplasmic reticulum, cytoplasmic microtubules, and microfilaments are deposited and arranged as a tunnel-like structure, the prepenetration apparatus (PPA). A gene for an expansin-like protein is induced during PPA formation (Siciliano et al., 2007). A fungal hypha is only invited into the epidermal cell after formation of the PPA (Genre et al., 2005). A similar event often occurs in the second plant cell layer before the tip of a fungal hypha reaches it, guiding the hypha through a region of

weakened cell walls that lies between the two plant cells. After reaching the root cortex, a hypha sometimes stays in an apoplast and elongates longitudinally in the root, depending on the host plant species. Then, the fungus forms arbuscules within the cortical cells. During the arbuscule formation, an intracellular structure similar to the PPA is observed again (Genre et al., 2008). The signal for PPA formation is a total mystery at present, but the similarity between AM symbiosis and nitrogen-fixing root nodule formation, specifically the PPA and preinfection threads formed in leguminous roots, was pointed out again (Parniske, 2008). It is noteworthy that arbuscules are surrounded by plant plasma membrane-derived periarbuscular membranes. The thin space between the periarbuscular and fungal plasma membranes, the periarbuscular space, is thought to contain both plant and fungal cell wall components. The thick intracellular hyphae are surrounded by plant membranes, too. In the case of root nodules, nitrogen-fixing bacteria are also surrounded by plant membranes called peribacteroid membranes. Such apparatuses are called symbiosomes. In other words, plant cells accept AM fungi and rhizobial bacteria into them but exclude the microbes from their cytoplasm. Overall, it is obvious that the host plants lead in the infection by symbiotic microbes.

2.1.3. The common symbiosis pathway

In 1996, an epoch-making discovery was reported, that is, that rapid oscillations in peri- and intranuclear calcium, termed calcium spiking, were induced on host roots challenged with a specific Nod factor of a rhizobium (Ehrhardt et al., 1996). Since then, extensive forward genetic studies involving model legumes have been carried out to dissect the signaling pathway involving the calcium spiking in nodule and AM symbioses. It was found that some mutants originally isolated as defective as to the formation of root nodules were also unable to establish AM symbiosis (Bonfante et al., 2000; Parniske, 2000; Wegel et al., 1998). The infection by AM fungi of roots of these mutants results in running extraradical hyphae exhibiting aberrant appressoria, an absence of internal fungal colonization, ceasing of elongation of intraradical hyphae or incomplete formation of arbuscules in the inner cortex. These phenotypes show that AM fungal infection is mainly aborted at the root epidermis (Banba et al., 2008; Bonfante et al., 2000; Kistner et al., 2005; Wegel et al., 1998). Now, at least seven genes in *L. japonicus* are known to be involved in the establishment of both types of symbiosis (Kistner et al., 2005), and most of their counterparts in *M. truncatula* have also been investigated. The signaling pathway comprising these genes is called the common symbiosis pathway (CSP; Fig. 1.1). Based on the presence of the CSP and the above-described similarity between the two types of symbiosis, it is generally accepted that leguminous plants co-opted the preexisting mechanism of AM symbiosis

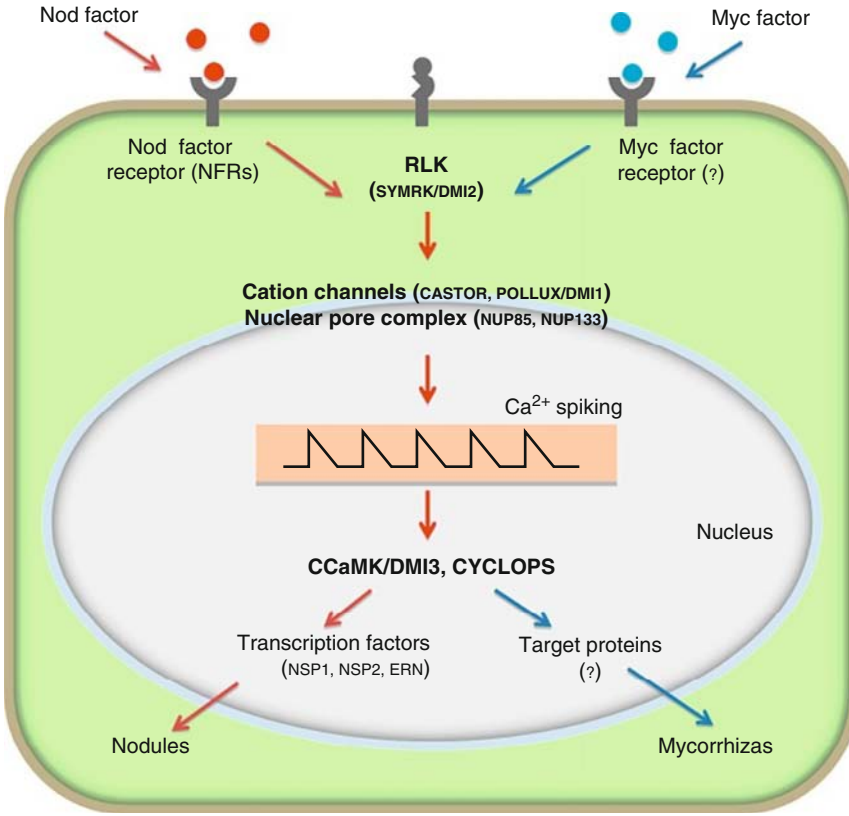

Figure 1.1 Simplified signaling pathways that lead to root nodule formation and AM synbiosis. The common symbiosis pathway is indicated in boldface.

with rhizobial bacteria when they obtained the ability to form nitrogen-fixing root nodules (Kistner and Parniske, 2002). Among the CSP genes of *L. japonicus*, *SYMRK*, *CASTOR*, *POLLUX*, *NUP85*, and *NUP133* lie upstream of calcium spiking, whereas *CCaMK* and *CYCLOPS* are downstream of it (Miwa et al., 2006; Fig. 1.1). Differences in the frequency and amplitude of Ca oscillations between AM symbiosis and root nodule formation have been pointed out (Kosuta et al., 2008). Interestingly, *Arabidopsis* lacks orthologs of *SYMRK*, *CASTOR*, *CCaMK*, and *CYCLOPS*, which explains the inability of *Brassica* plants to perform AM symbiosis (Chen et al., 2009). We will summarize recent progress regarding these genes briefly in the following paragraphs.

SYMRK of *L. japonicus* (*DMI2* in *M. truncatula*) encodes a receptor-like kinase on plasma membranes with an N-terminal leucine-rich repeat

domain on the apoplastic side, a middle transmembrane domain, and a C-terminal kinase domain on the cytoplasmic side (Endre et al., 2002; Stracke et al., 2002). The SYMRK proteins are thought to act at the most upstream of the CSP, but their ligand has not been identified. The target of phosphorylation has not been elucidated, either. The SYMRK proteins in a wide variety of plant species fall into roughly three types that differ in length, domain structure, and biological function. All of the shortest type in monocots, the intermediate type in nonleguminous dicots and the longest type in legumes are enough to establish AM symbiosis, whereas only the longest type acts in the formation of nitrogen-fixing nodules (Gherbi et al., 2008; Markmann et al., 2008). Therefore, the molecular evolution of *SYMRK* seems to be one of the necessary events for legumes to obtain the ability to form root nodules.

The twin genes *CASTOR* and *POLLUX* (the *M. truncatula* ortholog of the latter being *DMI1*) encode potassium-permeable channels in the nuclear envelope, the functions of which are essential for calcium spiking (Ané et al., 2004; Charpentier et al., 2008; Imaizumi-Anraku et al., 2005; Matzke et al., 2009). A gene of *M. truncatula* orthologous to *CASTOR* had long been missing, but was identified in 2009 at last (Chen et al., 2009). Two *L. japonicus* genes for nucleoporins, *NUP85* (Saito et al., 2007) and *NUP133* (Kanamori et al., 2006), were reported to be essential for induction of calcium spiking. An ortholog of *NUP133* in *M. truncatula* was recently found (Grimsrud et al., 2010), but that of *NUP85* has not yet been identified. *NUP85* and *NUP133* are thought to be constituents of a specific subcomplex in the nuclear pore, but whether they function directly or indirectly in the signaling pathway remains to be elucidated (Parniske, 2008).

CCaMK of *L. japonicus* and its *M. truncatula* ortholog *DMI3* encode a plant-specific calcium-calmodulin-dependent protein kinase (CCaMK), which appears to decode calcium spiking (Lévy et al., 2004; Mitra et al., 2004). Strikingly, overexpression of a mutant CCaMK protein that lost the ability of autoinhibition of the enzyme activity induced empty white nodules, suggesting that activation of CCaMK is the only key that triggers the entire processes of nodule formation (Gleason et al., 2006; Tirichine et al., 2006). Genre et al. (2009) recently reported that CCaMK/DMI3 exhibits another function, that is, it protects cells from death upon physical contact, extending its biological importance to outside the CSP.

CYCLOPS of *L. japonicus* (*IPD3* of *M. truncatula*) encodes a unique protein with a nuclear localization signal and a coiled-coil domain (Messinese et al., 2007; Yano et al., 2008). The protein product interacts physically with CCaMK in plant nuclei, and is also phosphorylated by CCaMK *in vitro* (Yano et al., 2008) and *in vivo* (Grimsrud et al., 2010). Therefore, at least three proteins, CCaMK, CYCLOPS, and calmodulin, appear to form a complex within plant nuclei and decipher the signals hidden behind the calcium spiking.

Basically, nothing is known about the upstream part of the CSP in AM symbiosis. Also, much less is known about the downstream events in the CSP in AM symbiosis, except that lysophosphatidylcholine was postulated to be involved in the signaling (Bucher et al., 2009; Drissner et al., 2007). On the other hand, a couple of gene products were reported to be involved in nodulation (Fig. 1.1). This is mainly because it is much more laborious and difficult to find AM-impaired (myc^-) mutants than ones unable to form nodules (nod^-). If a number of mutants that show the myc^-nod^+ phenotype, for example, become available in the future, genetic dissection of the upstream and downstream parts of the CSP for AM symbiosis will progress significantly. In this regard, the recent isolation of a $myc^{++}nod^-$ mutant of *M. truncatula* may provide a clue for solving this problem (Morandi et al., 2009). In addition, if the above-described Myc factors are identified and sufficient amounts become available for our experiments, the initial events of AM fungal infection will be revealed at the cellular level.

2.1.4. Transcriptome profiling

Although the genes involved in the CSP play indispensable roles in the establishment of AM symbiosis, their expression is rather constitutive, their transcript levels not changing so much. Transcriptome profiling may shed light on the process of AM symbiosis. Analysis with the aid of DNA arrays has been an especially powerful method for identifying differentially regulated genes in tissues or during biological development. Because AM colonization is not synchronous, however, application of this method sometimes needs careful experimental design to analyze the initial stage of AM fungal infection. Liu et al. (2003) and Deguchi et al. (2007) reported the first DNA array analyses of AM colonization of *M. truncatula* and *L. japonicus* roots, respectively. Both studies revealed that the genes encoding the enzymes involved in defense-related secondary metabolism and the pathogen response were transiently and moderately upregulated at the initial stage. These results are in accord with former reports on gene expression (Blee and Anderson, 1996; Bonanomi et al., 2001; Gao et al., 2004; Harrison and Dixon, 1993, 1994), proteome analysis (Amiour et al., 2006), and biochemistry (Volpin et al., 1994, 1995). A similar observation was also made for rhizobial infection at the initial stage of root nodule formation (Kouchi et al., 2004). Therefore, host plants seem to guard themselves to some extent against unidentified microbes, and then invite some after recognizing that they are symbionts. Recently, Guether et al. (2009a) reported very different results from the above-described ones. However, the physiological meaning of the differential regulation of the newly reported genes has not been discussed. Comparison between the newly reported *L. japonicus* genes (Guether et al., 2009a) and previously reported *M. truncatula* genes, especially the *expansin-like B* gene, by the same

group (Genre et al., 2009; Siciliano et al., 2007), seems not enough, either. It would be natural to expect that the reproducibility of the transcriptional response of *L. japonicus* to salt stress, an abiotic stress, would be much more reproducible than the response to microbe infection, a biotic stress. Since even the reproducibility in the former case is very low (Sanchez et al., 2010), it may not be so unusual that the results of transcriptome analyses of plant–microbe interactions vary from experiment to experiment if the conditions for plant growth and fungus inoculation are different. Grunwald et al. (2009) also reported that very few plant genes were reported to be commonly regulated, depending on the AM fungal species.

2.2. The endosymbiotic phase

2.2.1. Aspects of nutrient trading

After penetration into plant cortical cells, fungal hyphal branches form the main trunks of arbuscules. Then, the trunks undergo repeated dichotomous branching to form mature arbuscules in the intracellular apoplast. Morphometric techniques have shown that the growing and mature stages of arbuscules usually continue for only 2–3 days (Alexander et al., 1989; Smith and Read, 2008). Then, the arbuscules shrink all of a sudden, the fungus forming many septa in the collapsing branches (Harrison, 2005; Javot et al., 2007a). The collapse of arbuscules results in clumps and finally the clumps disappear. The whole arbuscule cycle was estimated to be 7–8 days (Alexander et al., 1989; Smith and Read, 2008).

The metabolic flux of nutrients in AM symbiosis is well summarized in the excellent review of Parniske (2008). Briefly, inorganic or organic nutrients are absorbed by extraradical hyphae from soil through fungal specific transporters of phosphate (Harrison and van Buuren, 1995; Maldonado-Mendoza et al., 2001), ammonium (López-Pedrosa et al., 2006), amino acids (Cappellazzo et al., 2008), and zinc (González-Guerrero et al., 2005). Other micronutrients are also absorbed although the fungal transporters for them have not yet been characterized. Especially in the case of phosphate, plant roots often create a phosphate-depleted zone close to the root surface, because the rate of uptake is much higher than the rate of diffusion in the soil (Bucher, 2007; Karandashov and Bucher, 2005; Marschner, 1995). However, it is the great advantage of AM symbiosis that extraradical hyphae elongate beyond the depleted zone to reach a fresh phosphate pool. Then, the absorbed phosphate and nitrogen nutrients are converted to polyphosphate and arginine, respectively, in the extraradical hyphae (Cox et al., 1980; Govindarajulu et al., 2005; Tani et al., 2009). Polyphosphate forms granules, which moves to the intraradical hyphae and arbuscules (Cox et al., 1980; Kuga et al., 2008). Positively charged arginine and metal ions are thought to be transported with the negatively charged polyphosphate granules. Within (or around) arbuscules, the polyphosphate

granules are hydrolyzed to orthophosphate (Funamoto et al., 2007; Javot et al., 2007a; Solaiman et al., 1999) and arginine is decomposed to ammonium through the urea cycle (Cruz et al., 2007; Govindarajulu et al., 2005; Jin et al., 2005). Then, phosphate and ammonium are exported into the periarbuscular space. On the other hand, carbon is not released from AM fungi (Govindarajulu et al., 2005), probably because it is a precious element for them.

As mentioned before, AM fungi totally depend on the host plants for their carbon sources. Sucrose, which is the most common photosynthate form transported from shoots to AM roots, is hydrolyzed mainly in the periarbuscular space by either sucrose synthase (Hohnjec et al., 2003) or invertase (Schaarschmidt et al., 2006, 2007). The resulting hexoses (mainly glucose) are thought to be imported into AM fungi primarily through arbuscules, although there has been a report that intraradical hyphae also play some role (Solaiman and Saito, 1997). Then, the hexoses are converted to lipid bodies mainly composed of triacylglycerol or polysaccharides such as glycogen for long-distance translocation and storage (Bago et al., 2002, 2003). The lipids and polysaccharides are digested to supply energy and the carbon skeletons of organic compounds where needed.

2.2.2. The nutrient transporters around arbuscules

As described above, fungal arbuscules, the periarbuscular space, and plant periarbuscular membranes are the main sites for nutrient exchange between AM fungi and host plants. Among the nutrients, phosphate is thought to be the most important one that affects the growth of the host plants (Smith and Read, 2008). Phosphate is released from fungal arbuscules, but the fungal phosphate transporter(s) involved in the process has not yet been identified. The ammonium transporter(s) that exports ammonium through the fungal membrane is not known, either. On the other hand, there is a clue as to the import of carbon into fungi. *Geosiphon pyriformis*, a member of the phylum Glomeromycota, establishes symbiosis with photosynthetic cyanobacterium *Nostoc punctiforme* and performs nutrient exchange. Since a fungal gene encoding a unique hexose transporter that probably acts in carbon import from bacteria was identified (Schüßler et al., 2006), AM fungi may express similar hexose transporters on the surface of their arbuscules.

Phosphate transporters that are localized on plant plasma membranes belong to the Pht1 family (Bucher, 2007; Javot et al., 2007b). The Pht1 family belongs further to a major facilitator superfamily, each member of which has 12 transmembrane domains and functions basically as a monomer (Guan and Kaback, 2006). In 2002, Harrison et al. identified an AM-inducible phosphate transporter gene, *MtPT4*, by examining EST databases for *M. truncatula*. Immunolocalization of the protein product demonstrated that MtPT4 resides exclusively on the intracellular membrane closely

surrounding the fine branches of mature arbuscules. This important finding was confirmed later using fluorescent protein fusions (Pumplin and Harrison, 2009). Since members of the Pht1 family are symporters of phosphate and protons (Bucher, 2007; Smith, 2002), the driving force of MtPT4 activity would be a proton gradient generated across the periarbuscular membrane, for example, by an AM-inducible H^+-ATPase (Krajinski et al., 2002). Therefore, the acidic nature of the periarbuscular space is of pivotal importance for phosphate transfer and, actually, the pH was reported to be 4.25–4.8 (Guttenberger, 2000; Smith et al., 2001). Five members of the Pht1 family in *M. truncatula* have thus far been reported (Liu et al., 2008), *MtPT4* being the only AM-inducible phosphate transporter gene. Although phosphate transporters are often divided into high- and low-affinity transporters for convenience (Furihata et al., 1992), it should be kept in mind that some protein modifications may change the characteristics of the transporters. The major nitrate transporter of *Arabidopsis*, for example, exhibits both high- and low-affinity activities depending on its phosphorylation and dephosphorylation states (Ho et al., 2009). Thus, it is called a ''transceptor'' (i.e., transporter and receptor).

As for *L. japonicus*, Maeda et al. (2006) amplified three genes for Pht1 phosphate transporters by PCR and identified an AM-inducible phosphate transporter gene, *LjPT3*, for the first time. Strangely at that time, *MtPT4* and *LjPT3* were not thought to be orthologous, *MtPT4* being a member of divergent subfamily I of the Pht1 family, and *LjPT3* belonging to common subfamily III (Harrison et al., 2002; Javot et al., 2007b; Maeda et al., 2006). Nonetheless, Maeda et al. (2006) claimed that *LjPT3* was likely to be the major AM-inducible phosphate transporter gene in *L. japonicus*. Recently, using a newly prepared OligoChip or improved genomic information on *L. japonicus*, Guether et al. (2009a) and Takeda et al. (2009) found another novel AM-inducible phosphate transporter gene, *LjPT4*, the protein product of which belongs to subfamily I of the Pht1 family. Unfortunately, our classical cDNA arrays did not contain either *LjPT3* or *LjPT4* (Deguchi et al., 2007). Therefore, although somewhat preliminary, we carried out a confirmatory experiment involving inoculation of *Glomus mosseae* and *Gigaspora margarita*, which were used by Maeda et al. (2006) and Guether et al. (2009a), respectively, onto *L. japonicus* roots. As shown in Fig. 1.2, *LjPT3* was AM-inducible, but the extent of its induction in AM roots was low and varied. The inoculation of *G. mosseae*, as in the previous study (Maeda et al., 2006), caused significant upregulation in one plant but not in others. The reason for this discrepancy is unclear, but small differences in growth conditions may have resulted in great differences in gene expression. The extent of *LjPT3* induction was also influenced by the AM fungal species, as Feddermann et al. (2008) pointed out. At 3 weeks after inoculation, *G. margarita* did not exhibit a significant change, as reported by Guether et al. (2009a). At 7 weeks after inoculation, however, the gene

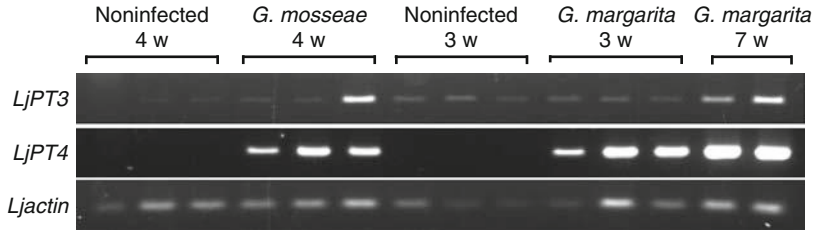

Figure 1.2 Detection of RT-PCR products of *LjPT3*, *LjPT4*, and an actin gene (*Ljactin*) in AM-colonized roots or uninfected control roots of *L. japonicus*. The plants were inoculated with *G. mosseae* (Idemitsu Kosan Co., Tokyo) or *G. margarita* (Central Glass Co., Tokyo) and grown on Kanuma soil, a volcanic ash subsoil, including a half strength of Hoagland medium containing 200 μM phosphate on a growth shelf at 25 °C for the indicated periods. The colonization of fungi was good enough in AM roots, while no colonization was detected in noninfected roots. RNA preparations were extracted from the roots, but it was impossible to recover RNA from 7-week-old noninfected roots, probably because of the phosphate deficiency. Then, cDNAs were synthesized with oligo(dT) and reverse transcriptase, and PCR was carried out using the same primers as for *LjPT3* reported (Maeda et al., 2006). After agarose gel electrophoresis, the bands of expected size (ca. 260, 290, and 90 bp for *LjPT3*, *LjPT4*, and *Ljactin*, respectively) were visualized with ethidium bromide under UV light. Each lane represents an individual biological replicate.

seemed to be upregulated (Fig. 1.2). On the other hand, *LjPT4* was more strongly, steadily, and specifically induced (Fig. 1.2), confirming recent reports (Guether et al., 2009a; Takeda et al., 2009). Obviously, therefore, the claim of Maeda et al. (2006) must be changed as follows: The major AM-inducible phosphate transporter in *L. japonicus* is *LjPT4*, not *LjPT3*. In the previous work, Maeda et al. (2006) designed degenerate primers expecting the exact amino acid sequence that is present in *LjPT4*, but unfortunately the corresponding cDNA fragment was not amplified on PCR for an unknown reason. In addition, they were not aware that real-time RT-PCR tends to exaggerate differences in expression levels compared to hybridization analyses or regular RT-PCR, like in Fig. 1.2 (Guether et al., 2009a; Liu et al., 2007). S. Hata, an author responsible for that paper, hereby expresses his regret for any inconvenience to researchers on AM symbiosis. Because we can now imagine that the result of knockdown or knockout of *LjPT4* would be severer than that in the case of *LjPT3*, like the knockout of *MtPT4* (Javot et al., 2007a), the next question would be why the effect of knockdown of minor *LjPT3* was obvious (Funamoto et al., 2007; Maeda et al., 2006). The reason is unclear again, but one possible explanation would be that *LjPT3* and *LjPT4* have slightly different biological roles. Regarding this point, apoplastic sucrose synthase and invertase, for example, function complementarily. Either knockdown of the sucrose synthase gene (Baier et al., 2010) or inhibition of invertase activity (Schaarschmidt and

Hause, 2008; Schaarschmidt et al., 2007) resulted in evidently defective AM symbiosis, although different plant materials were used in these works. Also notably, both AM symbiosis (Baier et al., 2010) and nodulation (Baier et al., 2007) were impaired on knockdown of the sucrose synthase gene of *M. truncatula*, as reported for *LjPT3* of *L. japonicus* (Maeda et al., 2006). The relationship between *LjPT3* and *LjPT4* remains to be studied more.

In plants, animals, fungi, and bacteria, ammonium is transported across the plasma membrane by members of the Ammonium Transporter/Methylammonium Permease/Rhesus family. Transporters of this family have 11 transmembrane domains and form a homotrimer structure in the membrane (Khademi et al., 2004; Zheng et al., 2004), their carboxyl termini acting as regulatory domains (Neuhäuser et al., 2007). Whether ammonium transport proteins are channels or well-coupled transporters is not yet clear (Mayer et al., 2006). *Arabidopsis*, for example, has six members of this family, five belonging to the AMT1 subfamily and one to the AMT2 subfamily. The AMT1 and AMT2 subfamilies are rather distantly related to each other. In 2009, there was a breakthrough as to ammonium transporters, which function on the periarbuscular membrane. Gomez et al. (2009) and Guether et al. (2009a) found novel highly upregulated genes in AM roots of *M. truncatula* and *L. japonicus*, respectively. Among them, IMGAG/1723.m00046 and *LjAMT2;2* encode putative AMT2-type ammonium transporters. Almost specific expression of these genes in arbuscule-containing cortical cells was also revealed (Gomez et al., 2009; Guether et al., 2009a). Two technical improvements contributed to the findings. One was the adoption of genome-wide GeneChips. This enabled the finding of a number of differentially expressed genes, including *Vapyrin* gene of *M. truncatula* that encode a cytoplasmic protein required for arbuscule formation and efficient epidermal penetration by AM fungi (Pumplin et al., 2010). The other was laser microdissection followed by RT-PCR (Balestrini et al., 2007). This approach allowed very sensitive detection of differential gene expression in arbuscule-containing cells and surrounding noninfected ones. Furthermore, Guether et al. (2009b) demonstrated the functionality of LjAMT2;2 by complementation of a yeast mutant. Intriguingly, it was also shown that the transporter binds the ammonium cations in the periarbuscular space and releases uncharged ammonia into the plant cells (Guether et al., 2009b). This appears in sharp contrast to members of the AMT1 subfamily, which catch and release the ammonium cations (Ludewig et al., 2002; Mayer et al., 2006; Neuhäuser et al., 2007). Recently, AtAMT1;1, a representative member of the *Arabidopsis* AMT1 subfamily, was postulated to be a ''transceptor,'' because its regulatory phosphorylation at T460 is triggered by the extracellular ammonium level (Lanquar et al., 2009). LjAMT2;2 seems to have a distinct regulatory mechanism, because it does not contain a Thr residue at the site corresponding to T460 in AtAMT1;1.

In short, we are now establishing a whole image of the transfer of phosphate and ammonium, the major nutrients, from AM fungi to plants. In the future, our research will extend to the transfer of minor nutrients such as sulfate, mineral ions, etc.

3. Studies on Other Plants

3.1. Bryophytes

Clarification of the process of colonization of the land by green plants is a challenging and romantic work. It is generally accepted that bryophytes, which lack true roots, were the pioneer green plants that advanced to the land. Under harsh conditions, bryophyte–fungus symbiosis, if it occurred, must have been of great advantage for the collection of nutrients, water, etc.

The extant bryophytes comprise three phyla, liverworts, hornworts, and mosses, and the relationship among them has long been ambiguous (Nishiyama et al., 2004). Recently, however, it was suggested that hornworts and mosses belong to sister clades of primitive vascular plants, liverworts being the most ancestral land plants (Dombrovsk and Qiu, 2004; Groth-Malonek et al., 2005). Actually, the earliest land plant fossils of the Ordovician (ca. 475 million years ago) look like ancient liverworts (Wellman et al., 2003). Among the three phyla, liverworts (Bonfante and Genre, 2008; Carafa et al., 2003; Fonseca et al., 2006; Ligrone et al., 2007; Read et al., 2000; Russell and Bulman, 2005) and hornworts (Schüßler, 2000) often include AM fungi, whereas mosses including *Physcomitrella patens* lack such an association (Read et al., 2000; Smith and Read, 2008). Because bryophytes do not have roots, mycorrhizoids and mycothalli are more precise names for fungus-containing bryophyte tissues. Figure 1.3 shows mycorrhizoids and mycothalli of liverworts, *Marchantia paleacea*, also called *Marchantia foliacea* (Campbell, 1965; Ligrone et al., 2007), and *Glomus intraradices* formed under sterile conditions. *G. intraradices* first infects the rhizoids of *Merchantia*, extends its hyphae intracellularly, and then forms arbuscule-like structures in thalli. Therefore, although the first arbuscule fossils were found in *Aglaophyton major*, an Early Devonian (ca. 400 million years ago) primitive vascular plant (Remy et al., 1994; Taylor et al., 1995), it is likely that the ancestors of AM fungi were associated with liverworts in former times. However, it was pointed out by Selosse (2005) that the extant liverworts are usually colonized by *Glomus* group A fungi, which are thought to have appeared later than early land plants (Schüßler et al., 2001). Now, it is thought that the association of extant liverworts and *Glomus* is likely a result of a host shift from vascular plants to liverworts (Ligrone et al., 2007; Selosse, 2005). It is also noteworthy that gain and loss

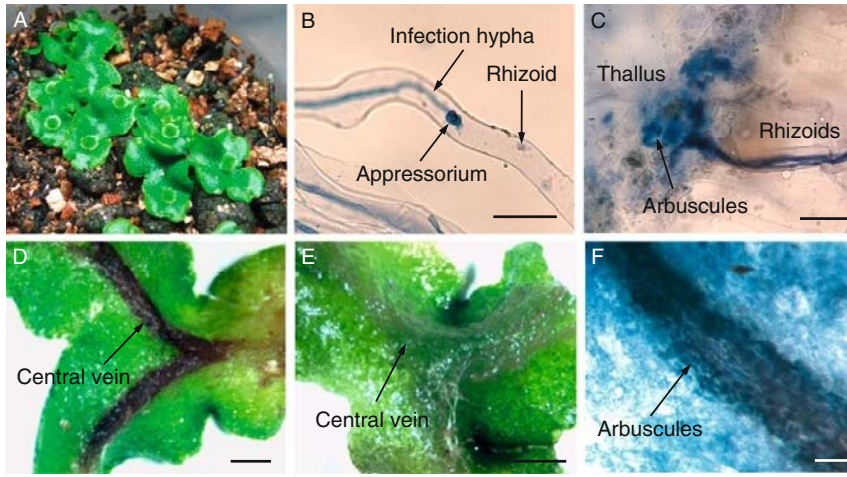

Figure 1.3 Colonization of a liverwort with an AM fungus. (A) Photograph of *Marchantia paleacea* var. *diptera* (a gift from Prof. H. Takano, Kumamoto University), which had been inoculated with spores of *Glomus intraradices*. (B) Trypan blue-staining shows that fungal hyphae formed an appressorium on the surface of the rhizoids, penetrated into the cells, and extended to the thallus. (C) Arbuscules developed in the thallus (40 dpi). (D) AM fungi mainly colonized the central vein of the thallus of *M. paleacea* and brown to red pigments were accumulated around the colonized area. (E) In contrast to in panel (D), coloration was not observed in a noninoculated control. (F) Trypan blue-staining indicates that arbuscules were densely formed in the central vein (60 dpi). Bar = 50 μm (B and C), 2 mm (D and E), and 0.5 mm (F).

of mycorrhiza-like associations occurred repeatedly during the evolution of land plants (Smith and Read, 2008).

We believe that it is still very useful to investigate the mycorrhiza-like associations of liverworts and *Glomus* group A fungi, even if a host shift has occurred. Interpretation of fossils regarding the evolution of ancient plant–microbe associations remains speculative, and so verification is only possible by means of experiments involving extant bryophytes and AM fungi. It would be a very interesting research topic as to whether or not the extant liverworts retain ancient association systems involving fungi, for example, signaling molecules such as strigolactones, signaling pathways that correspond to the CSP and nutrient transporters. Unfortunately, however, even classical experiments on nutrient exchange between liverworts and AM fungi have not been carried out (Smith and Read, 2008). Thus, strictly speaking, it is unclear if the association of liverworts and *Glomus* is symbiotic, parasitic, or something else.

The authors strongly feel that it is the time for researchers of bryophyte–fungus associations, including taxonomists, fossilologists, and molecular biologists, to form an international consortium. This consortium should

define a model bryophyte, to improve genome projects, to establish a transformation system, and to exchange other any information, just like in the cases of *Arabidopsis* and other model plants. We, plant physiologists not familiar with bryophytes, hope that we do not cause any misunderstanding. Incidentally, it is a pity that the most famous variety of *Marchantia polymorpha*, of which the transformation has been established (Ishizaki et al., 2008) and the genome sequence is being determined (Yamato et al., 2007), lacks mycorrhizal associations. Since the methodology of DNA sequencing is progressing fast, determination of the genome sequence of the ''model bryophyte'' will not be difficult. Elucidation of the process of colonization of the land by green plants is not only interesting from the viewpoint of basic research but also important for maintaining a comfortable terrestrial environment filled by green plants in the future.

3.2. Lessons from *Arabidopsis*

Although *Arabidopsis* does not perform symbiosis with microbes, the molecular mechanism underlying regulation of phosphate homeostasis was recently clarified using this leading model plant. Here we will describe an important concept briefly. Doerner (2008) also produced a nice and compact review on phosphate starvation signaling.

In contrast to its extremely slow movement in soil, phosphate moves smoothly in plant bodies. Normally, shoots accumulate more phosphate, which is transferred through the xylem, than roots. With a sufficient phosphate supply in the soil, *Arabidopsis* suppresses the expression of *Pht1;8* and *Pht1;9*, the main phosphate transporter genes in roots, so as to prevent overaccumulation of phosphate to a toxic level. This suppression occurs through the indirect action of a PHO2/UBC24 ubiquitin-conjugating enzyme, which degrades unidentified target proteins involved in the expression of the phosphate transporter genes (Doerner, 2008). Under these conditions, PHR1, a MYB transcription factor that positively regulates the expression of phosphate starvation-induced genes, does not function. *IPS/At4*, a nonprotein coding marker gene of phosphate starvation, is not induced, either. With a limited phosphate supply in the soil, on the other hand, plants not only remobilize internal phosphate but also try to acquire external phosphate. Upon phosphate starvation, PHR1 directs the upregulation of a family of nonprotein coding microRNAs, *miR399a–f*, in shoots (Aung et al., 2006; Bari et al., 2006; Chiou et al., 2006; Fujii et al., 2005). miR399 molecules move from shoots to roots through the phloem (Lin et al., 2008; Pant et al., 2008). Then, around the vascular cylinders of roots, miR399-charged complexes act on the 5′-untranslated regions of *PHO2/UBC24* transcripts that have sequences complementary to miR399, resulting in degradation of the transcripts and low levels of PHO2/UBC24 proteins (Aung et al., 2006; Bari et al., 2006). Now, phosphate transporters encoded

by *Pht1;8* and *Pht1;9* are accumulated in the roots to increase phosphate uptake from the soil. At this time, *IPS/At4*, a noncoding transcript, is also induced. The *IPS/At4* transcript has a sequence partially complementary to miR399, so it mimics the *PHO2/UBC24* transcript and impedes the action of miR399 (Shin et al., 2006). Importantly, *IPS/At4* is not degraded by the miR399-charged complex (Franco-Zorrilla et al., 2007). Thus, *IPS/At4* prevents overaction of Pht1;8 and Pht1;9 transporters. This recently found beautiful regulatory circuit seems to be slightly complicated. For example, the small sequence variation among *miR399a–f* may play a differential role (Lin and Chiou, 2008). It was also pointed out that miR399* may assist the long-distance movement of miR399 or exhibit a buffering effect on the action of miR399 by forming an miR399/miR399* duplex (Hsieh et al., 2009). Besides the above "threesome," SPX (SYG, Pho81, and XPR1) domain-containing proteins are also related to phosphate-starvation signaling. AtSPX1 is rapidly induced by phosphate starvation and may be involved in transcriptional activation of phosphate-mobilization genes, while AtSPX3 plays a role in negative feedback control of gene expression (Duan et al., 2008). In summary, an interaction between both positive and negative regulators of phosphate accumulation controls balanced phosphate homeostasis under phosphate-limiting conditions.

Pant et al. (2009) showed that miR399 is one of the microRNAs induced by phosphorus limitation, as expected, and also that miR169 is induced by nitrogen limitation in *Arabidopsis*. Regarding miR169, Combier et al. (2006) reported that miR169 in *M. truncatula* controls the level of a transcription factor, MtHAP2-1, which plays an important role in nodule formation. Thus, miR169 seems to be involved not only in the response to nitrogen starvation but also in nodulation. That paper was the beginning of research on microRNAs in this model legume. Since then, miR166 and other miRNAs of *M. truncatula* have been reported to be involved in root and root nodule formation (Boualem et al., 2008), and the response to heavy metal stress (Zhou et al., 2008), respectively. Additional novel miRNAs are also present, suggesting complex posttranscriptional gene regulation in *M. truncatula* (Jagadeeswaran et al., 2009). Strangely, microRNAs in *L. japonicus* have been rarely investigated, except that it has been found that miR399, miR169, miR166, and other conserved families are present, like in other plants (Sunkar and Jagadeeswaran, 2008).

The CLE (CLAVATA/ESR-related) peptides originally identified in *Arabidopsis* are 12-amino acid peptides that exhibit various physiological effects as ligands of LRR (leucine-rich repeat) receptor kinases (Cock and McCormick, 2001; Ito et al., 2006; Kondo et al., 2006; Sharma et al., 2003). Okamoto et al. (2009) clearly showed that two specific CLE peptides of *L. japonicus* are involved in regulation of the nodule number, acting as signal molecules from roots to shoots. Small peptides are also thought to be

involved in nodulation by *M. truncatula*, although they are not CLE peptides (Combier et al., 2008a,b). Since CLE peptide-related hypernodulation mutants of *L. japonicus* and other plants are also more heavily colonized by AM fungi than the wild types (Meixner et al., 2005; Solaiman et al., 2000), these small peptides may be involved in regulation of the extent of colonization by AM fungi.

3.3. Crops

Rice, wheat, and maize are the three major cereal crops in the world, the production of each being around 600 million tons per year (FAO, http://www.fao.org/). These are consumed as human food, forage for domestic animals, etc; rice, wheat, and maize providing about 20%, 19%, and 5% of the world energy supply for humans, respectively. On the other hand, soybeans are the most important leguminous crop, about 220 million tons per year being consumed as oils, forage for domestic animals, and human food (Clemente and Cahoon, 2009). Because it is out of the scope of this review to cover many crops, we will discuss mainly about rice and soybeans in the following sections.

3.3.1. Rice

Rice (*Oryza sativa*) is not only a major cereal but also a model monocotyledonous plant. The transformation of rice is relatively easy (Hiei et al., 1994) and the DNA sequence of its rather small genome has been completely determined (International Rice Genome Project, 2005). In rice, all seven CSP orthologs are present in the genome (Banba et al., 2008; Chen et al., 2007, 2008, 2009; Gutjahr et al., 2008), and that is why rice performs AM symbiosis. AM fungi preferentially colonize large lateral roots that contain cortical cells (Gutjahr et al., 2009a). The initiation of the growth of large lateral roots is induced upon colonization by AM fungi, although the architecture of rice roots is somewhat different from that of dicots (Gutjahr et al., 2009a).

Studies on the presymbiotic phase of rice AM symbiosis have been basically lacking, except that it has been found that rice produces strigolactones like all other plants (Umehara et al., 2008). On the other hand, the endosymbiotic phase has been investigated well because of the ample genome information and cDNA array experiments. Paszkowski et al. (2002) identified *OsPT11* as the major AM-inducible phosphate transporter gene among 13 genes for Pht1 phosphate transporters. Later, *OsPT13* was also reported to be AM-inducible (Güimil et al., 2005). Slightly different expression patterns of the two genes were observed (Glassop et al., 2007). Although rice AM-inducible ammonium transporters have not yet been identified, we expect this in the very near future. Research on microRNAs

of rice has been conducted (Sunkar et al., 2005, 2008), but their functions are unclear except for that of the rice ortholog of miR399 (Bari et al., 2006). Recently, OsSPX1 was reported to act via a negative feedback loop to optimize rice growth under phosphate-limited conditions (Wang et al., 2009a), like AtSPX3 in *Arabidopsis* (Duan et al., 2008).

Compared to the roots of other plants such as legumes, rice roots exhibit very low autofluorescence. Making use of this characteristic, we succeeded in real-time observation of pariarbuscular membranes in rice roots as follows (Kobae and Hata, 2010). Since arbuscules are temporal organs and develop mainly in the inner cortical cells of roots, they are optically and physically inaccessible. Therefore, if this difficulty is overcome because fluorescent marker protein-mediated *in planta* imaging becomes feasible, it would be an ideal method for investigating these dynamic organs. We prepared transgenic rice (*O. sativa*) plants that express a fusion, that is, rice AM-inducible phosphate transporter OsPT11-GFP, and grew them with AM fungi. The OsPT11-GFP fusion resides exclusively on the periarbuscular membranes closely surrounding the fine branches of mature arbuscules, this area being called the ''arbuscule branch domain'' (Pumplin and Harrison, 2009). We also established a simple method for visualizing OsPT11-GFP fluorescence in the rhizosphere (Fig. 1.4). The T1 seeds of the transgenic rice were grown in 35 mm petri dishes with 27 mm coverslip windows at the bottom. As the glass bottom was covered with AM fungi inoculant, roots that extended and reached the bottom were effectively infected by AM fungi just above the coverslip window. Consequently, real-time OsPT11-GFP

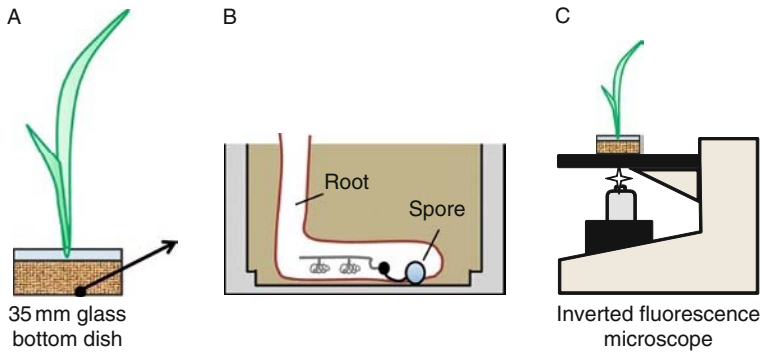

Figure 1.4 A simple device for real-time *in planta* imaging of GFP fluorescence. (A) T1 seeds of transgenic rice that express a fusion protein comprising AM-inducible phosphate transporter and GFP were grown in 35 mm petri dishes with 27 mm coverslip windows at the bottom. (B) Because the glass bottom was covered with spores, the elongated root system spread just above the coverslip window, being effectively colonized by the AM fungus. (C) The GFP fluorescence was observed using an inverted fluorescence microscope. The roots were illuminated and observed from the underside.

fluorescence can be successfully performed around 10 days after seed germination using an inverted fluorescence microscope. In cortical cells, arbuscules seem to be functional for only a couple of days, confirming morphometric studies performed long ago (Alexander et al., 1989; Smith and Read, 2008). Then, time-lapse imaging enabled pinpointing of the beginning of arbuscule degeneration by capturing of images for a period of 220 min (Fig. 1.5A). The images revealed a series of early-stage degeneration events, from the early symptom of arbuscules to the disappearance of OsPT11-GFP. The initial morphological change of collapsing arbuscules comprised rapid shrinkage of arbuscule branches (Fig. 1.5A). It seems likely that the arbuscule branches suddenly became plastic or fragile, and then gradually but rapidly shrank, and, as a result, the periarbuscular membranes might have become stacked and the OsPT11-GFP signals might have

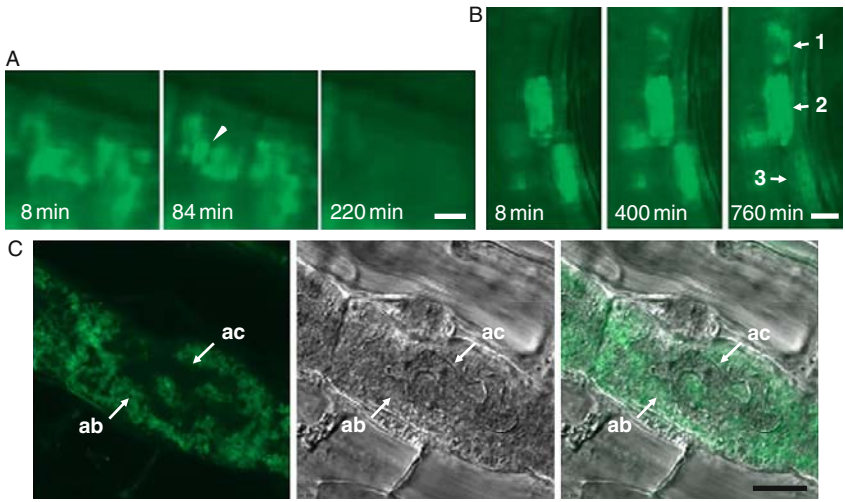

Figure 1.5 Localization and dynamics of AM-inducible nutrient transporters. (A) *In planta* time-lapse imaging of transgenic rice roots that express an AM-inducible phosphate transporter-GFP fusion under the control of its natural promoter. The roots were inoculated with *Gigaspora rosea* 9 days before the observation. The arbuscules showed dynamic collapse. The arrowhead indicates the densely accumulated fusion protein on the periarbuscular membranes. In 220 min, GFP fluorescence almost completely disappeared. (B) Imaging of transgenic roots inoculated with *Glomus mosseae* 12 days before the observation. Arrowheads indicate: 1, a GFP fluorescence-accumulating cell; 2, a GFP signal-stable cell; and 3, a GFP fluorescence-decreasing and collapsing arbuscule-containing cell. (C) Localization of GmAMT4;1-GFP in a mycorrhizal root transformed with *GmAMT4;1 promoter-GmAMT4;1-GFP*. Left: GFP signals were observed specifically in cortical cells containing arbuscules (ab), especially in arbuscule branch domains but not around the arbusculated coil (ac). Center: differential interference contrast (DIC) bright-field image of the left panel. Right: merged image of the left and center panels. A and B, From Kobae and Hata (2010) with modification.

become densely accumulated (Fig. 1.5A). The collapsed state of arbuscules was visible for approximately 2.5 h, and then the GFP fluorescence became undetectable. Therefore, it is probable that the constituents of periarbuscular membrane proteins were promptly digested or realigned during this short time period. Notably, the arbuscule shrinkage preceded the degradation of OsPT11-GFP. It seems likely that withdrawal or autolysis of the fungus induces the degradation event within the plant cells. The collapse of arbuscules occurred in the subsequent several days. Another example, showing that differentially fluorescent cells were present within a single colonization unit, is shown in Fig. 1.5B. It is notable that some arbuscules remained for over 24 h, but others formed and collapsed within 24 h. The images indicate that the OsPT11-GFP expression and the protein turnover in the periarbuscular membrane comprise a cell-autonomous process. In conclusion, the real-time imaging of OsPT11-GFP revealed one of the dynamic aspects of AM symbiosis, namely a period of nutrient exchange. This simple method can be applicable not only for observation of AM symbiosis but also for revealing dynamic aspects of any root proteins of interest, if fluorescent protein fusions are available.

Since AM fungi are basically aerobic microorganisms, they are generally believed to colonize rice plants only under aerobic conditions, that is, not on continuous submersion (Vallino et al., 2009). On the contrary, Secilia and Bagyaraj (1992, 1994) inoculated young rice seedlings with AM fungi in well-drained nursery boxes, transplanted the colonized seedlings to larger pots filled with well-puddled soil and then grew the rice plants for 145 days until harvest under flooded conditions with 5 cm of standing water. They reported that the rice roots were colonized, although the percent of AM colonization of roots was not very high, and that colonization by AM fungi increases the phosphorus absorption by plant bodies and the grain yields. Later, Solaiman and Hirata (1997, 1998) performed similar experiments and confirmed the above results. Moreover, they pointed out that AM colonization increased the absorption of not only phosphorus but also nitrogen from paddy soil by rice plants. We tried to infect rice roots with an AM fungus under water. Surprisingly, infection and colonization occurred even under flooded conditions (Fig. 1.6A and B). As the aerenchyma is formed through programmed death of cortical cells and AM fungi only colonize cortical cells (Gutjahr et al., 2009a), arbuscules were formed in the remaining cortical cells along with the aerenchyma (Fig. 1.6B). The root aerenchyma is connected to those in culms and leaves, enabling efficient air passage from the shoots to the roots. This unique characteristic of rice roots for overcoming the anaerobic and reduced conditions in paddy soil may make the microaerophillic region around the roots a comfortable area for AM fungi. To our knowledge, however, investigations as to how commonly AM fungi live in paddy fields have not yet been performed.

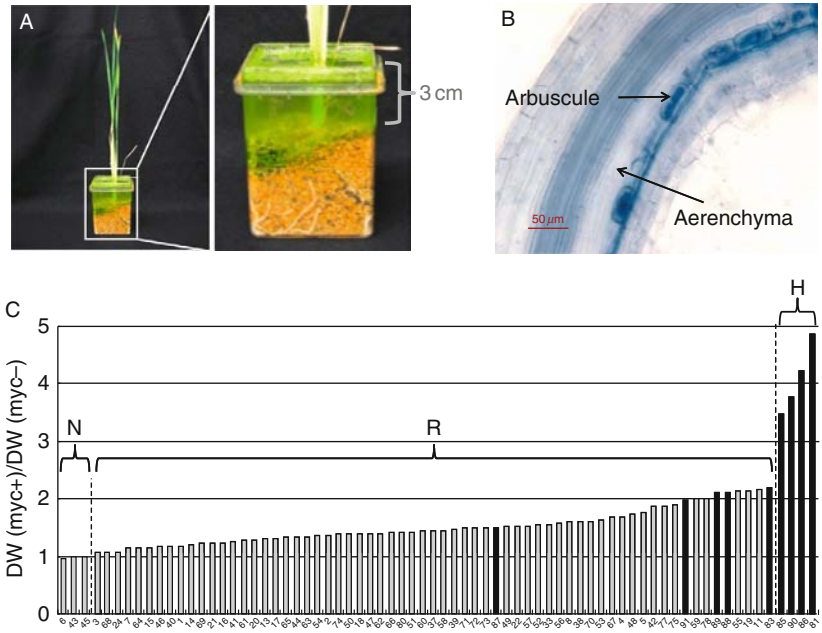

Figure 1.6 (A) Growth of a rice (*Oryza sativa* cv. Nipponbare) seedling in the presence of an AM fungus under flooded conditions. A small seedling was transferred to Kanuma soil, a volcanic ash subsoil, containing a *Glomus mosseae* inoculant, a medium with low concentrations of phosphate was immediately poured into the magenta box, and then the seedling was grown for 4 weeks under fluorescent light. The water surface was kept 3–4 cm above the top of the soil throughout the growth. (B) Trypan blue-staining of the rice root revealed that an intracellular hypha elongated along with the aerenchyma, forming arbuscules in cortical cells. (C) Effects of colonization of *G. mosseae* on the growth of rice seedlings of 72 varieties under natural light and well-drained conditions. The shoot dry weight ratios, AM+/AM−, after 4 weeks of inoculation are shown. N, nonresponsive varieties; R, responsive ones, but the extent is slight; and H, highly responsive ones. Gray bars, cultivated *O. sativa*; and black bars, wild rice varieties.

3.3.2. Soybeans

A draft assembly of the soybean (*Glycine max*) genome was recently released by the DOE Joint Genome Institute (http://www.jgi.doe.gov/). Thus, soybeans have become the third model legume (Cannon et al., 2009).

Research on nitrogen-fixing root nodules of soybeans has a long history (Carroll et al., 1985; Kouchi and Hata, 1993; Tajima and LaRue, 1982). In contrast, little about the molecular mechanism of soybean AM symbiosis, neither the presymbiotic phase nor the endosymbiotic phase, is known. We conducted an *in silico* examination and found 16 genes encoding ammonium transporters in the soybean genome (Kobae et al., submitted). Gene-specific reverse transcription (RT)-PCR indicated that five genes (*GmAMT1;4*,

GmAMT3;1, *GmAMT4;1*, *GmAMT4;3*, and *GmAMT4;4*) were upregulated in AM roots. The detailed transport mechanisms of their protein products remain to be elucidated. Interestingly, most of these soybean AM-inducible ammonium transporters, the exception being GmAMT1;4, do not have the regulatory phosphorylation site, T460, in AtAMT1;1 (Lanquar et al., 2009). Among the transcripts of the five AM-inducible genes, the major one is *GmAMT4;1*, an ortholog of *LjAMT2;2* (Guether et al., 2009b), the intron–exon structures being similar to each other. The transport ability of GmAMT4;1 was confirmed using a yeast mutant that is defective in the three endogenous AMTs (Marini et al., 1997). Promoter–reporter analysis indicated that the strongest *GmAMT4;1* showed limited expression only in arbuscule-containing cortical cells. Moreover, specific localization of a fusion protein of GmAMT4;1 and GFP in the branch domain of periarbuscular membranes was demonstrated for the first time (Kobae et al., submitted; Fig. 1.5C). Thus, it was demonstrated that a specific region of the periarbuscular membrane, called the "arbuscule branch domain" (Pumplin and Harrison, 2009), is the active site of transfer of both phosphate and ammonium. Soybean microRNAs have been reported in relation with root nodule formation (Subramanian et al., 2008; Wang et al., 2009c), but their functions remain to be elucidated.

3.3.3. Other crops

We cite arbitrarily chosen documents, not complete ones. Research on maize (*Zea mays*) AM symbiosis began decades ago. Disturbance of the soil reduces nutrient absorption by maize AM roots (Evans and Miller, 1988). Ammonium assimilation in maize via AM fungi was described early on (Cliquet and Stewart, 1993) and recently (Tanaka and Yano, 2005). A draft DNA sequence of the 2.3-gigabase genome of maize was published just before this review was written (Schnable et al., 2009). As for wheat (*Triticum aestivum*), inoculation of AM fungi increased phosphorus uptake from rock phosphate (Kucey, 1987). However, AM fungi often cause growth depression of wheat (Li et al., 2008). This problem will be discussed in the next section. Solanaceae crops such as potato (*Solanum tuberosum*) and tomato (*Solanum lycopersicum*, formerly *Lycopersicon esculentum*) have been good materials for AM research. In potato, the first AM-inducible phosphate transporter gene, *StPT3*, was identified (Rausch et al., 2001). Subsequently, stronger AM-inducible genes, *StPT4* and *StPT5*, were found (Nagy et al., 2005). This process of finding is very similar to that of *L. japonicus* (see Section 2.2.2), because StPT3 belongs to common subfamily III of the Pht1 family while StPT4 and StPT5 are members of diverged subfamily I. The function of lysophosphatidylchorine in induction of phosphate transporter genes was discovered using potato (Drissner et al., 2007). In tomato, *LePT3*, *LePT4*, and *LePT5* are orthologs of *StPT3*, *StPT4*, and *StPT5*, respectively, and all of them are AM-inducible (Nagy et al., 2005; Poulsen et al., 2005).

AM symbiosis-defective mutant tomato lines have been useful (David-Schwartz et al., 2001, 2003; Gadkar et al., 2003; Nagy et al., 2009). The synthesis of strigolactone and apocarotenoids in tomato has also been investigated in relation to AM symbiosis (Vogel et al., 2009). Very recently, Gu et al. (2010) reported changes of tomato microRNA expression on AM symbiosis. To our knowledge, that is the first publication describing possible correlations between microRNAs and AM symbiosis. Interestingly, among a number of miRNAs that show variable expression according to phosphate availability, the authors found that four miRNAs were specifically induced in shoots of AM plants independently to phosphate levels (Gu et al., 2010). Leguminous crops such as pea (*Pisum sativum*) and alfalfa (*Medicago sativa*) have also been used (Gianinazzi-Pearson, 1996; Harrison and Dixon, 1993), but the basic research on them has tended to shift to that on model legumes.

3.4. Variability of plant responses as to AM colonization

The benefits of AM symbiosis regarding growth stimulation and/or phosphate absorption in phosphorus-depleted soil are well known or well advertised. However, there are not only ''responsive plants'' that show a positive growth response but also ''nonresponsive plants'' that show a negligible or even negative growth increase (Smith and Read, 2008). For example, Fabaceae, such as soybean (*G. max*) and common bean (*Phaseolus vulgaris*), and Liliaceae, such as *Allium* and *Lilium*, have neither ample root hairs nor dense roots. These crops generally depend much on AM fungi for the absorption of nutrients, resulting in a positive growth response. In contrast, a single cultivar of tomato shows responsive (Poulsen et al., 2005) and nonresponsive (Smith et al., 2004) characteristics, probably depending on small differences in the growth conditions. Cereal crops can be roughly divided into two groups, maize and sorghum are positively responsive, while wheat and barley are negatively responsive in general (Tawaraya, 2003). Rice is thought to be a nonresponsive crop, because the growth responses of most cultivated varieties are not strong, if any (Fig. 1.6C). Plant responsiveness varies extensively according to the combination of plants and AM fungi (Klironomos, 2003). Diverse effects of AM fungal species on the growth and phosphorus nutrition of a single cucumber (*Cucumis sativus*) cultivar were reported (Munkvold et al., 2004). Conversely, with a single species of AM fungus, positive, neutral, and negative responses were all observed depending on the wheat cultivar (Hetrick et al., 1996). The reason for this variation is unclear. We obtained seeds of 72 varieties of rice from the National Institute of Genetics (http://www.shigen.nig.ac.jp/rice/oryzabase/wild/coreCollection.jsp) and the National Institute of Agrobiological Sciences (Kojima et al., 2005), and examined the effects of colonization by an AM fungus (*G. mosseae*) on the growth of the seedlings (Fig. 1.6C). When the shoot dry weight ratios, AM+/AM−, after

4 weeks of inoculation were compared, great variation, 0.9–4.8-fold, was found among the varieties (unpublished data). Variation in responsiveness among cultivars of wheat and barley has also been reported, the relation with phosphorus utilization efficiency (i.e., dry matter yield per unit of phosphorus taken up) having been discussed, but the reason is not necessarily clear (Baon et al., 1993; Hetrick et al., 1996; Li et al., 2005; Zhu et al., 2003).

The plant growth response to AM fungi has been explained mainly in terms of phosphate transfer from soil to plants. This is probably because there have been many more studies on phosphorus in connection with AM symbiosis than on nitrogen and other nutrients, and because the former older. Anyhow, it is reasonable to dissect phosphate absorption to plants into the following two pathways: the AM fungal pathway, which is described above in detail, and the direct pathway via root hairs and epidermis. Of course, nonmycorrhizal roots have only the latter one. In AM roots, the fungal and direct pathways have generally been thought to be additive. The traditional explanation for the nonresponsiveness of some host plants is the balance between costs and benefits. When AM fungi supply little or no phosphate to their hosts, the fungal demand for carbon from plants would surpass the benefit of plants caused by phosphorus transfer via AM fungi (Fitter, 1991; Stribley et al., 1980). It turns out, however, that a simple cost–benefit explanation is not applicable (Graham and Abbott, 2000). This is because a significant amount (occasionally 100%) of phosphate is transported via the AM fungal pathway even when there is a negative growth response by the host plants (Li et al., 2006; Smith et al., 2004). Using barley as the plant material and two differently colonizing *Glomus* fungi, Grace et al. (2009) showed that (1) the total phosphorus content and total dry weight of barley are nearly proportional, (2) both a highly colonizing AM fungus and a minimally colonizing one cause similar growth depression and similar inhibition of phosphorus absorption, (3) phosphate is absorbed through the AM fungus pathway according to the different colonization by the two fungi, and (4) the upregulation of a barley gene for an AM-inducible phosphate transporter (Glassop et al., 2005) is roughly proportional to the fungal colonization. From these findings, the authors concluded that (1) AM colonization results in severe growth depression irrespective of the extent of colonization, (2) the AM fungus pathway works well according to the colonization but was not quantitatively related to growth depression, and (3) the contribution of the direct phosphate uptake pathway is markedly reduced by either a highly colonizing or a minimally colonizing AM fungus. According to the last conclusion, Grace et al. (2009) claimed that the genes encoding phosphate transporters involved in the direct pathway are constitutively expressed, despite the apparent shut down of phosphate uptake. Nagy et al. (2005) obtained similar results to those of Grace et al. (2009) using tomato. On the contrary, however, another paper reported

downregulation of these barley genes on AM colonization (Glassop et al., 2005). In any case, a small extent of AM fungal infection appears to shut down the direct phosphate uptake pathway. The molecular mechanism underlying the reduction of the direct pathway must be a clue for converting nonresponding crops to responding ones and will be the subject of intensive investigation in the future (Smith et al., 2009).

3.5. Toward sustainable agriculture

3.5.1. Agricultural resource crisis

The distribution of resources in the world such as fresh water and phosphorus is highly biased. Areas with enough water for agricultural irrigation are limited, highly water-stressed areas being much greater (Oki and Kanae, 2006). AM symbiosis is generally thought to help crops to be drought resistant (Evelin et al., 2009; Smith and Read, 2008). Although a review questioned the dramatic effects of AM fungi (Augé, 2001), another one seemed more optimistic (Ruiz-Lozano, 2003). Since water problems, the competition as to industrial and agricultural use for example, are out of the scope of this review, we would like to discuss them elsewhere. As for phosphorus, the global production per year is estimated to be 40–50 million metric tons of P_2O_5, which is derived from 167 million tons of phosphate rock. Notably, two-thirds of the phosphate rock in the world is mined in only three countries, China, the United States, and Morocco (U.S. Geological Survey (USGS), 2009, http://minerals.usgs.gov/minerals/pubs/commodity/phosphate_rock/mcs-2009-phosp.pdf). Thus, most countries must import phosphorus, because there are no substitutes for this essential element for agriculture. Most crops, cereals, for example, concentrate phosphorus in their seeds as phytate, a very stable compound. On germination, the phytate is hydrolyzed by a special enzyme, phytase, into phosphate. When ruminants eat the seeds, they can make use of phosphate derived from phytate, because bacteria in their rumens degrade a portion of the phytate. However, nonruminants including swine, poultry, fish, and man just excrete phytate, contributing to water pollution. According to Steen (1998, http://www.nhm.ac.uk/research-curation/research/projects/phosphate-recovery/p&k217/steen.htm), phosphate rock of high quality will be exhausted around the end of this century. In addition, the price of phosphate rock in 2008 increased to 4.1-fold of that in 2004 (USGS, 2009). To cope with these crises, several trials have been made (Abelson, 1999; Raboy, 2001). For example, phytase was added to fodder both to feed nonruminants and to prevent water pollution. Mutant cereals that accumulate significant amounts of inorganic phosphate instead of phytate in the endosperm have been found as fodder. Technology to recycle phosphate from sewerage has also been developed. However, none of these means is an effective one for saving phosphate resources.

AM fungi are generally expected to be useful for establishing environment-friendly agriculture with a low input of fertilizers or chemicals. At present, however, we have to admit that we cannot apply the results of pot experiments directly to crop production in the field. One reason for this is that indigenous AM fungi are already present in the field in most cases. Therefore, unlike pot experiments, it is impossible to prepare controls without AM fungi. Besides indigenous AM fungi, there are many kinds of pathogens that affect the growth of crops in the field. As described above, the growth response of a host plant depends on the plant and AM fungus combination. Thus, it would be natural to try to inoculate a crop of interest with an appropriate AM fungus. In some fortuitous cases, inoculation of foreign AM fungi resulted in a positive growth response for alfalfa and onion (Owusu-Bennoah and Mosse, 1979), and apple (Plenchette et al., 1981), noninoculated plants being less colonized by indigenous AM fungi. In most cases, however, the indigenous fungi win the competition with the introduced fungi (Abbott et al., 1983). Therefore, making use of indigenous AM fungi would be a valid alternative to inoculation with foreign fungi. Even when indigenous AM fungi colonize crops in the field, the AM pathway instead of the direct one will play the central role in absorption of nutrients. Regarding this assumption, it is interesting that tomato fruit grown with AM fungi contained more phosphorus and zinc than nonmycorrizal controls (Cavagnaro et al., 2006). AM fungi contributed clearly to an increase in the quality of tomato, although the yield was not affected in that case. The hyphal network of AM fungi also protects soil from erosion. Disturbance of the network by tillage reduces nutrient absorption through the AM pathway (Evans and Miller, 1988), depending on the species of AM fungi (McGonigle et al., 2003). Incidentally, it is another problem that we do not have easy methods for classifying indigenous AM fungi and assessing their activity. It is hard to classify AM fungi just on observation of their spores. Additionally, the viability of spores varies greatly, and so counting of them in the soil does not necessarily predict their infectivity and the final effect of AM fungi on the growth of crops.

3.5.2. Tolerance to abiotic and biotic stresses

There is a hope that AM symbiosis will alleviate pollution caused by toxic heavy metals. In Southeast Asia, subterranean water is used not only for drinking but also for irrigation, especially in the dry season, but it is often contaminated by arsenic, a toxic and carcinogenic element. As a result, arsenate (As(V)) and arsenite (As(III)) accumulating in fields are absorbed by crops and accumulated in their grain (Meharg, 2004). Arsenate is a homolog of orthophosphate and actually absorbed through phosphate transporters. It is incorporated into ATP for example, and thereby inhibits energy metabolism. On the other hand, arsenite is absorbed via aquaporins, and then reacts with sulfhydryl groups of proteins and deactivates them (Meharg, 2004). Tens of millions people suffer from arsenic poisoning. Recently, Christophersen et al.

(2009) showed that AM colonization of barley roots reduces arsenate uptake via downregulation of the direct phosphate uptake pathway. The AM fungal pathway seems to work well, transferring a significant amount of phosphate but little or no arsenate. The details of the mechanism of this "filter effect" is not yet known. Unfortunately, because arsenite (As(III)) is the major form under reducing conditions in paddy fields, the effect of AM fungi colonization on lowland rice plants may not be so great as that on barley under aerobic conditions (Christophersen et al., 2009). Thus, more breakthroughs are needed to overcome a disaster in Southeast Asia (Ma et al., 2008; Norton et al., 2008). A mechanism of unloading arsenic into rice grain was recently reported (Carey et al., 2010). Zhang et al. (2005) found that AM colonization of upland rice plants conferred resistance to heavy metals in soil. The translocation of Cu, Zn, Pb, and Cd from roots to shoots was reduced in AM rice compared to in nonmycorrizal controls, but the mechanism was not known at that time. Later, Zhang et al. (2009) reported that AM colonization increases the Cu-binding capacity of the root cell wall and reduces uptake across the plasma membrane into the root cells. The authors showed a difference in Cu-binding between the cell walls of AM and nonmycorrhizal roots, speculating that their chemical compositions differ from each other. The same group also reported that the adverse effects of a fungicide on the growth of upland rice were alleviated (Zhang et al., 2006).

It is not known whether or not the direct uptake of nitrogen into roots is reduced by AM fungus colonization, like that of phosphate. If this is the case, AM symbiosis may prevent the accumulation of nitrate in pastures. The soil in stock farms is generally rich in nitrate because of the cattle excrement. Too much absorption of nitrate via the direct pathway in pastures results ultimately in the death or nitrate poisoning of the cattle. If AM fungi shut down direct absorption, they will contribute to the health of the cattle, because Tanaka and Yano (2005) reported that AM fungi transfer ammonium but not nitrate to host plants.

AM symbiosis has been reported to confer resistance against pathogenic fungi (Cordier et al., 1998; Pozo et al., 2002) and nematodes (Akkopru and Demir, 2005; Berta et al., 2005; Li et al., 2006). Liu et al. (2007) revealed for the first time that a systemic change in gene expression pattern occurs on AM colonization, stress- or defense-related genes being induced in shoots. They also showed that an AM fungus actually makes the shoots resistant to a bacterial pathogen (Liu et al., 2007). That work could be the first step for clarifying the molecular mechanism underlying the action of AM fungi as to tolerance of crops to biotic stress.

3.5.3. Toward higher yields of crops under normal conditions

Commercial AM fungal inoculants are rather costly at the moment, and so it is hard to use them directly in large fields. Transplantation after establishment of AM colonization of seedlings (Plenchette et al., 1981) is a means of

avoiding this problem, although additional labor is needed. In Asia, nearly 100% of rice plants are transplanted from a nursery to the fields. This system may provide an opportunity to make use of commercial AM fungal inoculants in practice. Nevertheless, indigenous AM fungi that are often more competitive than introduced fungi are already present, as described above. To remove the indigenous AM fungi, fumigation, steam sterilization, and/or application of fungicides to the fields are possible. However, such treatments destroy the microbial balance in the soil, sometimes resulting in tremendous increases in pathogens. Therefore, management of indigenous AM fungi would be almost the only realistic way. Regarding this point, the following is an interesting example. Flavonoids present in root exudates were once believed to activate fungal hyphae and their entry into host roots (Gianinazzi-Pearson et al., 1989). A synthetic isoflavone was applied to asparagus fields, resulting in avoidance of root disease caused by *Fusalium* and an increase in stalks per plant (Elmer, 2002). What we want to emphasize with this example is that a clue for solving the above problems will emerge if the mechanism is elucidated. Plant and fungal receptors of strigolactones must be intensively investigated now. If their structures are elucidated, we will be able to design some stable compounds that are recognized only by fungal receptors. Then, we would repeat the above trial (Elmer, 2002) with these new compounds.

How can we increase the yields of nonresponsive crops such as wheat and barley? Ryan et al. (2005) proposed that reduced colonization of autumn-sown wheat by rotation including break crops, such as weakly colonized lupin and nonmycorrhizal canola, will bring about yield enhancement, because AM fungi are ''parasitic'' for wheat. On the other hand, Smith et al. (2009) claimed that the growth depression during vegetative stages can often be reversed, because, depending on the amount of phosphate fertilizer supplied, the growth depression of wheat seedlings by an AM fungus was overcome on grain development (Li et al., 2005). In the latter case, colonization by indigenous AM fungi may even be beneficial for wheat growth since probably less water has to be used than in the absence of the fungi. In any case, repeated long-term field experiments are necessary to resolve this issue. Establishment of entire image of nonresponsiveness is also important. Regarding this point, we have a small concern if barley phosphate transporter, HvPT8, and its wheat counterpart (Glassop et al., 2005; Grace et al., 2009) are the major AM-inducible ones. They are not really orthologous to rice OsPT11, medic MtPT4, etc., forming an independent sister group to that of the major ones (Javot et al., 2007b; Maeda et al., 2006). Not to repeat our previous mistake on LjPT3 (see Section 2.2.2), progress of the genome projects in barley and wheat is awaited.

Targeted breeding could be the greatest outcome. As already mentioned, variations in responsiveness were observed among varieties of wheat and barley (Baon et al., 1993; Hetrick et al., 1996; Li et al., 2005;

Zhu et al., 2003), and rice (Fig. 1.6C). One thing we have to keep in mind is that our aim is not to study the inability of the varieties of interest to grow in the absence of AM colonization (Janos, 2007; Sawers et al., 2008, 2010). Investigations on the posttranscriptional or posttranslational mechanisms that shut down the direct phosphate absorption pathway relating to miR399, for example, must also be promoted. We would like to emphasize again that, if the mechanism is elucidated, a clue for solving the above problems will emerge.

3.5.4. How can we reuse the fertilizer phosphate already applied to fields?

Only 10–20% of the fertilizer phosphate applied to soil is absorbed and utilized by crops (Holford, 1997). Most of the rest becomes immobilized in the inorganic and organic fractions of the soil, which are hardly available to crop roots. The other small portion flows to rivers, ponds, lakes, etc., causing their pollution. In other words, people have paradoxically or ironically stored up great amounts of fertilizer phosphorus in their fields. Inorganic phosphate forms insoluble salts with counter cations such as Fe^{3+}, Al^{3+}, and Ca^{2+}. As a result, the available phosphate concentration is seldom higher than 10 μM (Bieleski, 1973). On the other hand, the dominant form of organic phosphorus is phytate (here we use this term for a group of compounds; also called phytin or inositol hexakisphosphate) (Dalal, 1977), which is principally derived from plants. In plants, phytate is a stock compound of phosphorus with a highly negative charge density. Unlike other organic phosphates like nucleic acids, sugar phosphate, and phospholipids, it is chemically very stable, and forms insoluble salts with Fe^{3+}, Al^{3+}, and Ca^{2+}, or is adsorbed into soil colloids (Shang et al., 1992; Turner et al., 2002). Then, soil microorganisms cannot gain access to the insoluble phytate, while other organic phosphates are easily decomposed by them. That is why phytate occupies 20–80% of total phosphate in the surface layer of the soil. If we could efficiently make use of these ''buried'' inorganic and organic resources, we might be able to grow crops for several decades without any additional phosphate fertilizers.

In order to overcome this phosphorus deficiency, plants exhibit numerous adaptive responses that presumably facilitate acquisition of this essential nutrient (Raghothama, 1999). These responses include secretion of organic acids, such as citrate, malate, and succinate, into the apoplast (Hoffland et al., 1989). The organic acids act as chelators that dissolve precipitated phosphate, increasing the concentration of available phosphate for plants. The other responses include biochemical processes that limit metabolic requirements for phosphate, and the synthesis and secretion of enzymes, such as acid phosphatases and phytases, that enable access to phosphorus contained in organic phosphorus compounds in the soil. Phosphorus limitation also causes morphological responses including attenuated primary root growth,

and increased lateral root development, root/shoot mass ratios, lateral root number and length (López-Bucio et al., 2003), and root hair production (Raghothama, 1999). Phosphate deficiency also induces the expression of genes that facilitate phosphate uptake into roots and distribution in plant bodies (Raghothama, 1999).

Both AM roots and nonmycorrizal roots absorb labile fractions of phosphorus preferentially in the soil (Smith and Read, 2008). Nevertheless, plants in a symbiotic relationship with AM fungi apparently utilize precipitated inorganic phosphate, such as Fe–phosphate, more efficiently than nonmycorrhizal ones. This is probably due to spatial exploitation of the soil by the fine hyphae of AM fungi, not to active solubilization of the precipitated phosphate (Bolan and Robson, 1987; Smith and Read, 2008).

As for phytate, most people believe that the dephosphorylation of this organic molecule is indispensable for its utilization by plant roots. Conversely, this suggests that plants generally lack a system to absorb phytate through epidermis or root hair. Findenegg and Nalemans (1993) found that, when phytate was added to a nutrient solution in quartz sand as the sole phosphorus source, it was hydrolyzed by exogenous phytase and the resulting phosphate was efficiently taken up by maize plants. However, the exogenous phytase did not work well when the plants were grown in soil with the same phytate-containing nutrient solution. They also reported that maize plants assimilated phosphate from phytate when the organic compound was added at higher concentrations, even in the absence of exogenous phytase (Findenegg and Nalemans, 1993). In the latter case, endogenous phytase might have been secreted and acted, since plants secrete phytase from their roots under phosphorus-deficient conditions (Li et al., 1997). However, the possibility that microorganisms in the sand hydrolyzed the phytate cannot be ruled out (Greaves and Webley, 1969). Later, transgenic plants that highly secrete phytases of fungal, bacterial, and plant origin or a synthetic gene-encoded phytase were prepared (Lung et al., 2005; Richardson et al., 2001; Xiao et al., 2005; Zimmermann et al., 2003). As a result, the transgenic plants hydrolyzed phytate in hydroponic or agar media and showed improved growth. In soil, however, they could not utilize phytate in most cases (Lung et al., 2005; Richardson et al., 2001; Xiao et al., 2005) or deformed plants resulted (Zimmermann et al., 2003). This is because not only the substrate phytate but also the secreted phytase enzyme were adsorbed onto the soil solid phase (George et al., 2005, 2007), confirming the early observation of Findenegg and Nalemans (1993). Therefore, our idea is that phytases secreted by plants can only act on the surface of roots. Recently, Wang et al. (2009b) reported that transgenic soybean plants that secrete acid phosphatase derived from *Arabidopsis* utilize phytate in sand cultures. Nevertheless, we think that confirmatory experiments involving soil instead of sand are necessary regarding previous observations (Adams and Pate, 1992; Findenegg and Nalemans, 1993; George et al., 2005, 2007).

Investigations as to whether or not AM roots make use of phytate should be promoted. In a classical paper, Mosse and Phillips (1971) showed that sterile clover seedlings placed on an agar medium that contained calcium phytate as the sole phosphorus source were colonized well by AM fungi, and that the plants grew well. Later, Koide and Kabir (2000) used a monoxenic (two-membered, i.e., carrot roots and AM fungi) culture system, and claimed that the hyphae of AM fungi transferred phytate-derived phosphorus-secreting phosphatase-like enzymes from the hyphae and that the carrot roots actually grew using the resulting phosphate. Importantly, both works were carried out without contaminating microorganisms, thus we can exclude their effects from consideration. We think that the following two possibilities remain regarding the latter work, because the hydrolysis of phytate outside the hyphae was not demonstrated. (1) The AM fungi might have absorbed phytate and passed it directly to host plants through arbuscules. As described above, the nature of the periarbuscular membrane is different from that of the plasma membrane of epidermal cells. Once phytate gets into plant bodies, it will be hydrolyzed by endogenous phytase. (2) The AM fungi might have hydrolyzed phytate in their hyphae and passed on the resulting phosphate to the plants. In any case, phytate forms insoluble complexes in soil so that it cannot be absorbed or hydrolyzed as easily as in agar media. Nevertheless, like in the case of inorganic phosphate complexes, AM fungi may facilitate the use of buried phytate through extensive exploration by their extraradical hyphae. This possibility remains to be examined. Also, to our knowledge, there is no example of the combination of AM symbiosis and transgenic plants that secrete phytases.

4. Concluding Remarks

In the past decade, significant progress in cell and molecular biology of AM symbiosis was made by an increasing number of excellent investigators (Bucher et al., 2009; Harrison, 2005; Parniske, 2008; Smith and Read, 2008). The compounds signaling between host plants and AM fungi are being revealed. The aspects of nutrient exchange are being clarified at the molecular level. In addition, our research is being extended from model plants to crops as plant materials. In fact, the progress of genome projects on crops is remarkable (Paterson et al., 2009; Schnable et al., 2009). Although we have to say that we are at the stage of collecting basic knowledge on symbiosis, this does not mean that the wide application of AM symbiosis to practical agriculture is impossible. We need additional breakthroughs, but we believe that we are on the right track for making use of this beautiful system.

The CSP genes of bryophytes have recently been reported (Wang et al., 2010).

ACKNOWLEDGMENTS

We thank our laboratory members, especially K. Yano, Y. Tamura, D. Nakagawa, S. Suzuki, S. Takai, and C. Sakuma, for the valuable discussions and cooperation in the preparation of the manuscript. Thanks are also due to K. Ashida, D. Maeda, H. Takano, K. Ishizaki, K. Yamato, and T. Kohchi for their encouragement and for providing experimental materials. The National Institute of Genetics and the National Institute of Agrobiological Sciences are also thanked for the rice seed varieties. This work was supported in part by a grant from the Ministry of Agriculture, Forestry and Fisheries of Japan (Genomics for Agricultural Innovation, PMI-0003), and by the Special Coordination Funds for Promoting Science and Technology of the Japanese Ministry of Education, Culture, Sports, Science and Technology.

REFERENCES

Abbott, L.K., Robson, A.D., Hall, I.R., 1983. Introduction of vesicular arbuscular mycorrhizal fungi into agricultural soils. Aust. J. Agric. Res. 34, 741–749.

Abelson, P.H., 1999. A potential phosphate crisis. Science 283, 2015.

Adams, M.A., Pate, J.S., 1992. Availability of organic and inorganic forms of phosphorus to lupins (*Lupinus* spp.). Plant Soil 145, 107–113.

Akiyama, K., Matsuzaki, K., Hayashi, H., 2005. Plant sesquiterpenes induce hyphal branching in arbuscular mycorrhizal fungi. Nature 435, 824–826.

Akkopru, A., Demir, S., 2005. Biological control of *Fusarium* wilt in tomato caused by *Fusarium oxysporum* f. sp. *lycopersici* by AMF *Glomus intraradices* and some rhizobacteria. J. Phytopathol. 153, 544–550.

Alexander, T., Toth, R., Meier, R., Weber, H.C., 1989. Dynamics of arbuscule development and degeneration in onion, bean, and tomato with reference to vesicular–arbuscular mycorrhizae in grasses. Can. J. Bot. 67, 2505–2513.

Amiour, N., Recorbet, G., Robert, F., Gianinazzi, S., Dumas-Gaudot, E., 2006. Mutations in *DMI3* and *SUNN* modify the appressorium-responsive root proteome in arbuscular mycorrhiza. Mol. Plant Microbe Interact. 19, 988–997.

Ané, J.-M., Kiss, G.B., Riely, B.K., Penmetsa, R.V., Oldroyd, G.E.D., Ayax, C., et al., 2004. *Medicago truncatula DMI1* required for bacterial and fungal symbioses in legumes. Science 303, 1364–1367.

Augeé, R.M., 2001. Water relations, drought and vesicular-arbuscular mycorrhizal symbiosis. Mycorrhiza 11, 3–42.

Aung, K., Lin, S.-I., Wu, C.-C., Huang, Y.-T., Su, C.-I., Chiou, T.-J., 2006. *pho2*, a phosphate overaccumulator, is caused by a nonsense mutation in a microRNA399 target gene. Plant Physiol. 141, 1000–1011.

Bago, B., Pfeffer, P.E., Shachar-Hill, Y., 2000. Carbon metabolism and transport in arbuscular mycorrhizas. Plant Physiol. 124, 949–957.

Bago, B., Zipfel, W., Williams, R.M., Jun, J., Arreola, R., Lammers, P.J., et al., 2002. Translocation and utilization of fungal storage lipid in the arbuscular mycorrhizal symbiosis. Plant Physiol. 128, 108–124.

Bago, B., Pfeffer, P.E., Abubaker, J., Jun, J., Allen, J.W., Brouillette, J., et al., 2003. Carbon export from arbuscular mycorrhizal roots involves the translocation of carbohydrate as well as lipid. Plant Physiol. 131, 1496–1507.

Baier, M.C., Barsch, A., Küster, H., Hohnjec, N., 2007. Antisense repression of the *Medicago truncatula* nodule-enhanced sucrose synthase leads to a handicapped nitrogen fixation

mirrored by specific alterations in the symbiotic transcriptome and metabolome. Plant Physiol. 145, 1600–1618.
Baier, M.C., Keck, M., Godde, V., Niehaus, K., Kuster, H., Hohnjec, N., 2010. Knockdown of the symbiotic sucrose synthase MtSucS1 affects arbuscule maturation and maintenance in mycorrhizal roots of *Medicago truncatula*. Plant Physiol. 152, 1000–1014.
Balestrini, R., Gómez-Ariza, J., Lanfranco, L., Bonfante, P., 2007. Laser microdissection reveals that transcripts for five plant and one fungal phosphate transporter genes are contemporaneously present in arbusculated cells. Mol. Plant Microbe Interact. 20, 1055–1062.
Banba, M., Gutjahr, C., Miyao, A., Hirochika, H., Paszkowski, U., Kouchi, H., et al., 2008. Divergence of evolutionary ways among common sym genes: CASTOR and CCaMK show functional conservation between two symbiosis systems and constitute the root of a common signaling pathway. Plant Cell Physiol. 49, 1659–1671.
Baon, J.B., Smith, S.E., Alston, A.M., 1993. Mycorrhizal responses of barley cultivars differing in P efficiency. Plant Soil 15, 97–105.
Bari, R., Pant, B.D., Stitt, M., Scheible, W.-R., 2006. PHO2, microRNA399, and PHR1 define a phosphate-signaling pathway in plants. Plant Physiol. 141, 988–999.
Barker, D.G., Bianchi, S., Blondon, F., Dattée, Y., Duc, G., Essad, S., et al., 1990. *Medicago truncatula*, a model plant for studying the molecular genetics of the *Rhizobium*-legume symbiosis. Plant Mol. Biol. Rep. 8, 40–49.
Berta, G., Sampo, S., Gamalero, E., Massa, N., Lemanceau, P., 2005. Suppression of *Rhizoctonia* root-rot of tomato by *Glomus mossae* BEG12 and *Pseudomonas fluorescens* A6RI is associated with their effect on the pathogen growth and on the root morphogenesis. Eur. J. Plant Pathol. 111, 279–288.
Bieleski, R.L., 1973. Phosphate pools, phosphate transport, and phosphate availability. Annu. Rev. Plant Physiol. 24, 225–252.
Blee, K.A., Anderson, A.J., 1996. Defense-related transcript accumulation in *Phaseolus vulgaris* L. colonized by the arbuscular mycorrhizal fungus *Glomus intraradices* Schenck & Smith. Plant Physiol. 110, 675–688.
Bolan, N.S., Robson, A.D., 1987. Effects of vesicular-arbuscular mycorrhiza on the availability of iron phosphates to plants. Plant Soil 99, 401–410.
Bonanomi, A., Oetiker, J.H., Guggenheim, R., Boller, T., Wiemken, A., Vögeli-Lange, R., 2001. Arbuscular mycorrhiza in mini-mycorrhizotrons: first contact of *Medicago truncatula* roots with *Glomus intraradices* induces chalcone synthase. New Phytol. 150, 573–582.
Bonfante, P., Genre, A., 2008. Plants and arbuscular mycorrhizal fungi: an evolutionary-developmental perspective. Trends Plant Sci. 13, 492–498.
Bonfante, P., Genre, A., Faccio, A., Martini, I., Schauser, L., Stougaard, J., et al., 2000. The *Lotus japonicus LjSym4* gene is required for the successful symbiotic infection of root epidermal cells. Mol. Plant Microbe Interact. 13, 1109–1120.
Boualem, A., Laporte, P., Jovanovic, M., Laffont, C., Plet, J., Combier, J.-P., et al., 2008. MicroRNA166 controls root and nodule development in *Medicago truncatula*. Plant J. 54, 876–887.
Bucher, M., 2007. Functional biology of plant phosphate uptake at root and mycorrhiza interfaces. New Phytol. 173, 11–26.
Bucher, M., Wegmüller, S., Drissner, D., 2009. Chasing the structures of small molecules in arbuscular mycorrhizal signaling. Curr. Opin. Plant Biol. 12, 1–8.
Buee, M., Rossignol, M., Jauneau, A., Ranjeva, R., Bécard, G., 2000. The pre-symbiotic growth of arbuscular mycorrhizal fungi is induced by a branching factor partially purified from plant root exudates. Mol. Plant Microbe Interact. 13, 693–698.
Campbell, E.O., 1965. Marchantia species of New Zealand. http://www.nzetc.org/tm/scholarly/tei-Bio13Tuat02-t1-body-d6.html. Tuatara 13, 122–136.

Cannon, S.B., May, G.D., Jackson, S.A., 2009. Three sequenced legume genomes and many crop species: rich opportunities for translational genomics. Plant Physiol. 151, 970–977.
Cappellazzo, G., Lanfranco, L., Fitz, M., Wipf, D., Bonfante, P., 2008. Characterization of an amino acid permease from the endomycorrhizal fungus *Glomus mosseae*. Plant Physiol. 147, 429–437.
Carafa, A., Duckett, J.G., Ligrone, R., 2003. Subterranean gametophytic axes in the primitive liverwort *Haplomitrium* harbour a unique type of endophytic association with aseptate fungi. New Phytol. 160, 185–197.
Carey, A.-M., Scheckel, K.G., Lombi, E., Newville, M., Choi, Y., Norton, G.J., et al., 2010. Grain unloading of arsenic species in rice (*Oryza sativa* L.). Plant Physiol. 152, 309–316.
Carroll, B.J., McNeil, D.L., Gresshoff, P.M., 1985. A supernodulation and nitrate-tolerant symbiotic (*nts*) soybean. Plant Physiol. 78, 34–40.
Cavagnaro, T.R., Jackson, L.E., Six, J., Ferris, H., Goyal, H., Asami, D., et al., 2006. Arbuscular mycorrhizas, microbial communities, nutrient availability, and soil aggregates in organic tomato production. Plant Soil 282, 209–225.
Chabaud, M., Venard, C., Defaux-Petras, A., Bécardand, G., Barker, D.G., 2002. Targeted inoculation of *Medicago truncatula in vitro* root cultures reveals *MtENOD11* expression during early stages of infection by arbuscular mycorrhizal fungi. New Phytol. 156, 265–273.
Chalot, M., Blaudez, D., Brun, A., 2006. Ammonia: a candidate for nitrogen transfer at the mycorrhizal interface. Trends Plant Sci. 11, 263–266.
Charpentier, M., Bredemeier, R., Wanner, G., Takeda, N., Schleiff, E., Parmiske, M., 2008. *Lotus japonicus* CASTOR and POLLUX are ion channels essential for perinuclear calcium spiking in legume root endosymbiosis. Plant Cell 20, 3467–3479.
Chen, C., Gao, M., Liu, J., Zhu, H., 2007. Fungal symbiosis in rice requires an ortholog of a legume common symbiosis gene encoding a Ca^{2+}/calmodulin-dependent protein kinase. Plant Physiol. 145, 1619–1628.
Chen, C., Ané, J.-M., Zhu, H., 2008. OsIPD3, an ortholog of the *Medicago truncatula* DMI3 interacting protein IPD3, is required for mycorrhizal symbiosis in rice. New Phytol. 180, 311–315.
Chen, C., Fan, C., Gao, M., Zhu, H., 2009. Antiquity and function of *CASTOR* and *POLLUX*, the twin ion channel-encoding genes key to the evolution of root symbioses in plants. Plant Physiol. 149, 306–317.
Chiou, T.-J., Aung, K., Lin, S.-I., Wu, C.-C., Chiang, S.-F., Su, C.-I., 2006. Regulation of phosphate homeostasis by microRNA in *Arabidopsis*. Plant Cell 18, 412–421.
Christophersen, H.M., Smith, F.A., Smith, S.E., 2009. Arbuscular mycorrhizal colonization reduces arsenate uptake in barley via downregulation of transporters in the direct epidermal phosphate uptake pathway. New Phytol. 184, 962–974.
Clemente, T.E., Cahoon, E.B., 2009. Soybean oil: genetic approaches for modification of functionality and total content. Plant Physiol. 151, 1030–1040.
Cliquet, J.-B., Stewart, G.R., 1993. Ammonia assimilation in *Zea mays* L. infected with a vesicular-arbuscular mycorrhizal fungus *Glomus fasciculatum*. Plant Physiol. 101, 865–871.
Cock, J.M., McCormick, S., 2001. A large family of genes that share homology with *CLAVATA3*. Plant Physiol. 126, 939–942.
Combier, J.P., Frugier, F., de Billy, F., Boualem, A., El-Yahyaoui, F., Moreau, S., et al., 2006. *MtHAP2-1* is a key transcriptional regulator of symbiotic nodule development regulated by microRNA169 *in Medicago truncatula*. Genes Dev. 20, 3084–3088.
Combier, J.P., de Billy, F., Gamas, P., Niebel, A., Rivas, S., 2008a. *Trans*-regulation of the expression of the transcription factor *MtHAP2-1* by a uORF controls root nodule development. Genes Dev. 22, 1549–1559.

Combier, J.-P., Küster, H., Journet, E.-P., Hohnjec, N., Gamas, P., Niebel, A., 2008b. Evidence for the involvement in nodulation of the two small putative regulatory peptide-encoding genes *MtRALFL1* and *MtDVL1*. Mol. Plant Microbe Interact. 21, 1118–1127.

Cook, D.R., 1999. *Medicago truncatula*—a model in the making!. Curr. Opin. Plant Biol. 2, 301–304.

Cordier, C., Pozo, M.J., Barea, J.M., Gianinazzi, S., Gianinazzi-Pearson, V., 1998. Cell defense responses associated with localized and systemic resistance to *Phytophthora parasitica* induced in tomato by an arbuscular mycorrhizal fungus. Mol. Plant Microbe Interact. 11, 1017–1028.

Cox, G., Moran, K.J., Sanders, F., Nockolds, C., Tinker, P.B., 1980. Translocation and transfer of nutrients in vesicular-arbuscular mycorrhizas. III. Polyphosphate granules and phosphorus translocation. New Phytol. 84, 649–659.

Cruz, C., Egsgaard, H., Trujillo, C., Ambus, P., Requena, N., Martins-Loução, M.A., et al., 2007. Enzymatic evidence for the key role of arginine in nitrogen translocation by arbuscular mycorrhizal fungi. Plant Physiol. 144, 782–792.

Dalal, R.C., 1977. Soil organic phosphorus. Adv. Agron. 29, 83–117.

David-Schwartz, R., Badani, H., Smadar, W., Levy, A.A., Galili, G., Kapulnik, Y., 2001. Identification of a novel genetically controlled step in mycorrhizal colonization: plant resistance to infection by fungal spores but not extra-radical hyphae. Plant J. 27, 561–569.

David-Schwartz, R., Gadkar, V., Wininger, S., Bendov, R., Galili, G., Levy, A.A., et al., 2003. Isolation of a premycorrhizal infection (*pmi2*) mutant of tomato, resistant to arbuscular mycorrhizal fungal colonization. Mol. Plant Microbe Interact. 16, 382–388.

Deguchi, Y., Banba, M., Shimoda, Y., Chechetka, S.A., Suzuri, R., Okusako, Y., et al., 2007. Transcriptome profiling of *Lotus japonicus* roots during arbuscular mycorrhiza development and comparison with that of nodulation. DNA Res. 14, 117–133.

Doerner, P., 2008. Phosphate starvation signaling: a threesome controls systemic P_i homeostasis. Curr. Opin. Plant Biol. 11, 536–540.

Dombrovsk, O., Qiu, Y.-L., 2004. Distribution of introns in the mitochondrial gene nad1 in land plants: phylogenetic and molecular evolutionary implications. Mol. Phylogen. Evol. 32, 246–263.

Drissner, D., Kunze, G., Callewaert, N., Gehrig, P., Tamasloukht, M., Boller, T., et al., 2007. Lyso-phosphatidylcholine is a signal in the arbuscular mycorrhizal symbiosis. Science 318, 265–268.

Duan, K., Yi, K., Dang, L., Huang, H., Wu, W., Wu, P., 2008. Characterization of a sub-family of *Arabidopsis* genes with the SPX domain reveals their diverse functions in plant tolerance to phosphorus starvation. Plant J. 54, 965–975.

Ehrhardt, D.W., Wais, R., Long, S.R., 1996. Calcium spiking in plant root hairs responding to Rhizobium nodulation signals. Cell 85, 673–681.

Elmer, W.H., 2002. Influence of formononetin and NaCl on mycorrhizal colonization and fusarium crown and root rot of asparagus. Plant Dis. 86, 1318–1324.

Endre, G., Kereszt, A., Kevei, Z., Mihacea, S., Kaló, P., Kiss, G.B., 2002. A receptor kinase gene regulating symbiotic nodule development. Nature 417, 962–966.

Evans, D.G., Miller, M.H., 1988. Vesicular–arbuscular mycorrhizas and the soil-disturbance-induced reduction of nutrient absorption in maize. New Phytol. 110, 67–74.

Evelin, H., Kapoor, R., Giri, B., 2009. Arbuscular mycorrhizal fungi in alleviation of salt stress: a review. Ann. Bot. 104, 1263–1280.

Feddermann, N., Boller, T., Salzer, P., Elfstrand, S., Wiemken, A., Elfstrand, M., 2008. *Medicago truncatula* shows distinct patterns of mycorrhiza-related gene expression after inoculation with three different arbuscular mycorrhizal fungi. Planta 227, 671–680.

Findenegg, G.R., Nalemans, J.A., 1993. The effect of phytase on the availability of P from myo-inositol hexaphosphate (phytate) for maize roots. Plant Soil 154, 189–196.

Fitter, A.H., 1991. Costs and benefits of mycorrhizas: implications for functioning under natural conditions. Experientia 47, 350–355.

Fonseca, H.M.A.C., Berbara, R.L.L., Pereira, M.L., 2006. *Lunularia cruciata*, a potential *in vitro* host for *Glomus proliferum* and *G. intraradices*. Mycorrhiza 16, 503–508.

Franco-Zorrilla, J.M., Valli, A., Todesco, M., Mateos, I., Puga, M.I., Rubio-Somoza, I., et al., 2007. Target mimicry provides a new mechanism for regulation of MicroRNA activity. Nat. Genet. 39, 1033–1037.

Fujii, H., Chiou, T.-J., Lin, S.-I., Aung, K., Zhu, J.-K., 2005. A miRNA involved in phosphate-starvation response in *Arabidopsis*. Curr. Biol. 15, 2038–2043.

Funamoto, R., Saito, K., Oyaizu, H., Saito, M., Aono, T., 2007. Simultaneous *in situ* detection of alkaline phosphatase activity and polyphosphate in arbuscules within arbuscular mycorrhizal roots. Funct. Plant Biol. 34, 803–810.

Furihata, T., Suzuki, M., Sakurai, H., 1992. Kinetic characterization of two phosphate uptake systems with different affinities in suspension-cultured *Catharanthus roseus* protoplasts. Plant Cell Physiol. 33, 1151–1157.

Gadkar, V., David-Schwartz, R., Nagahashi, G., Douds, D.D., Wininger, S., Kapulnik, Y., 2003. Root exudate of *pmi* tomato mutant M161 reduces AM fungal proliferation *in vitro*. FEMS Microbiol. Lett. 223, 193–198.

Gao, L.-L., Knogge, W., Delp, G., Smith, F.A., Smith, S.E., 2004. Expression patterns of defense-related genes in different types of arbuscular mycorrhizal development in wild-type and mycorrhiza-defective mutant tomato. Mol. Plant Microbe Interact. 17, 1103–1113.

Genre, A., Chabaud, M., Timmers, T., Bonfante, P., Barker, D.G., 2005. Arbuscular mycorrhizal fungi elicit a novel intracellular apparatus in *Medicago truncatula* root epidermal cells before infection. Plant Cell 17, 3489–3499.

Genre, A., Chabaud, M., Faccio, A., Barker, D.G., Bonfante, P., 2008. Prepenetration apparatus assembly precedes and predicts the colonization patterns of arbuscular mycorrhizal fungi within the root cortex of both *Medicago truncatula* and *Daucus carota*. Plant Cell 20, 1407–1420.

Genre, A., Ortu, G., Bertoldo, C., Martino, E., Bonfante, P., 2009. Biotic and abiotic stimulation of root epidermal cells reveals common and specific responses to arbuscular mycorrhizal fungi. Plant Physiol. 149, 1424–1434.

George, T.S., Richardson, A.E., Simpson, R.J., 2005. Behaviour of plant-derived extracellular phytase upon addition to soil. Soil Biol. Biochem. 37, 977–988.

George, T.S., Simpson, R.J., Gregory, P.J., Richardson, A.E., 2007. Differential interaction of *Aspergillus niger* and *Peniophora lycii* phytases with soil particles affects the hydrolysis of inositol phosphates. Soil Biol. Biochem. 39, 793–803.

Gherbi, H., Markmann, K., Svistoonoff, S., Estevan, J., Autran, D., Giczey, G., et al., 2008. SymRK defines a common genetic basis for plant root endosymbioses with arbuscular mycorrhiza fungi, rhizobia, and Frankia bacteria. Proc. Natl. Acad. Sci. USA 105, 4928–4932.

Gianinazzi-Pearson, V., 1996. Plant cell responses to arbuscular mycorrhizal fungi: getting to the roots of the symbiosis. Plant Cell 8, 1871–1883.

Gianinazzi-Pearson, V., Branzanti, B., Gianinazzi, S., 1989. *In vitro* enhancement of spore germination and early hyphal growth of a vesicular-arbuscular mycorrhizal fungus by host root exudates and plant flavonoids. Symbiosis 7, 243–255.

Glassop, D., Smith, S.E., Smith, F.W., 2005. Cereal phosphate transporters associated with the mycorrhizal pathway of phosphate uptake into roots. Planta 222, 688–698.

Glassop, D., Godwin, R.M., Smith, S.E., Smith, F.W., 2007. Rice phosphate transporters associated with phosphate uptake in rice roots colonised with arbuscular mycorrhizal fungi. Can. J. Bot. 85, 644–651.

Gleason, C., Chaudhuri, S., Yang, T., Muñoz, A., Poovaiah, B.W., Oldroyd, G.E.D., 2006. Nodulation independent of rhizobia induced by a calcium-activated kinase lacking autoinhibition. Nature 441, 1149–1152.

Gomez, S.K., Javot, H., Deewatthanawong, P., Torres-Jerez, I., Tang, Y., Blancaflor, E.B., et al., 2009. *Medicago truncatula* and *Glomus intraradices* gene expression in cortical cells harboring arbuscules in the arbuscular mycorrhizal symbiosis. BMC Plant Biol. 9, 10. doi:10.1186/1471-2229-9-10.

Gomez-Roldan, V., Fermas, S., Brewer, P.B., Puech-Pagès, V., Dun, E.A., Pillot, J.-P., et al., 2008. Strigolactone inhibition of shoot branching. Nature 455, 189–195.

González-Guerrero, M., Azcón-Aguilar, C., Mooney, M., Valderas, A., MacDiarmid, C.W., Eide, D.J., et al., 2005. Characterization of a *Glomus intraradices* gene encoding a putative Zn transporter of the cation diffusion facilitator family. Fungal Genet. Biol. 42, 130–140.

Govindarajulu, M., Pfeffer, P.E., Jin, H., Abubaker, J., Douds, D.D., Allen, J.W., et al., 2005. Nitrogen transfer in the arbuscular mycorrhizal symbiosis. Nature 435, 819–823.

Grace, E.J., Cotsaftis, O., Tester, M., Smith, F.A., Smith, S.E., 2009. Arbuscular mycorrhizal inhibition of growth in barley cannot be attributed to extent of colonization, fungal phosphorus uptake or effects on expression of plant phosphate transporter genes. New Phytol. 181, 938–949.

Graham, J.H., Abbott, L.K., 2000. Wheat responses to aggressive and non-aggressive arbuscular mycorrhizal fungi. Plant Soil 220, 207–218.

Greaves, M.P., Webley, D.M., 1969. The hydrolysis of myoinositol hexaphosphate by soil microorganisms. Soil Biol. Biochem. 1, 37–43.

Grimsrud, P.A., den Os, D., Wenger, C.D., Swaney, D.L., Schwartz, D., Sussman, M.R., et al., 2010. Large-scale phosphoprotein analysis in *Medicago truncatula* roots provides insight into *in vivo* kinase activity in legumes. Plant Physiol. 152, 19–28.

Groth-Malonek, M., Pruchner, D., Grewe, F., Knoop, V., 2005. Ancestors of *trans*-splicing mitochondrial introns support serial sister group relationships of hornworts and mosses with vascular plants. Mol. Biol. Evol. 22, 117–125.

Grunwald, U., Guo, W., Fischer, K., Isayenkov, S., Ludwig-Müller, J., Hause, B., et al., 2009. Overlapping expression patterns and differential transcript levels of phosphate transporter genes in arbuscular mycorrhizal, P_i-fertilised and phytohormone-treated *Medicago truncatula* roots. Planta 229, 1023–1034.

Gu, M., Xu, K., Chen, A., Zhu, Y., Tang, G., Xu, G., 2010. Expression analysis suggests potential roles of microRNAs for phosphate and arbuscular mycorrhizal signaling in *Solanum lycopersicum*. Physiol. Plant. 138, 226–237.

Guan, L., Kaback, H.R., 2006. Lessons from lactose permease. Annu. Rev. Biophys. Biomol. Struct. 35, 67–91.

Guether, M., Balestrini, R., Hannah, M., He, J., Udvardi, M.K., Bonfante, P., 2009a. Genome-wide reprogramming of regulatory networks, transport, cell wall and membrane biogenesis during arbuscular mycorrhizal symbiosis in *Lotus japonicus*. New Phytol. 182, 200–212.

Guether, M., Neuhäuser, B., Balestrini, R., Dynowski, M., Ludewig, U., Bonfante, P., 2009b. A mycorrhizal-specific ammonium transporter from *Lotus japonicus* acquires nitrogen released by arbuscular mycorrhizal fungi. Plant Physiol. 150, 73–83.

Güimil, S., Chang, H.-S., Zhu, T., Sesma, A., Osbourn, A., Roux, C., et al., 2005. Comparative transcriptomics of rice reveals an ancient pattern of response to microbial colonization. Proc. Natl. Acad. Sci. USA 102, 8066–8070.

Gutjahr, C., Banba, M., Croset, V., An, K., Miyao, A., An, G., et al., 2008. Arbuscular mycorrhiza-specific signaling in rice transcends the common symbiosis signaling pathway. Plant Cell 20, 2989–3005.

Gutjahr, C., Casieri, L., Paszkowski, U., 2009a. *Glomus intraradices* induces changes in root system architecture of rice independently of common symbiosis signaling. New Phytol. 182, 829–837.

Gutjahr, C., Novero, M., Guether, M., Montanari, O., Udvardi, M., Bonfante, P., 2009b. Presymbiotic factors released by the arbuscular mycorrhizal fungus *Gigaspora margarita* induce starch accumulation in *Lotus japonicus* roots. New Phytol. 183, 53–61.

Guttenberger, M., 2000. Arbuscules of vesicular-arbuscular mycorrhizal fungi inhabit an acidic compartment within plant roots. Planta 211, 299–304.

Handberg, K., Stougaard, J., 1992. *Lotus japonicus*, an autogamous, diploid legume species for classical and molecular genetics. Plant J. 2, 487–496.

Harrison, M.J., 2005. Signaling in the mycorrhizal symbiosis. Annu. Rev. Microbiol. 59, 19–42.

Harrison, M.J., Dixon, R.A., 1993. Isoflavonoid accumulation and expression of defense gene transcripts during the establishment of vesicular-arbuscular mycorrhizal associations in roots of *Medicago truncatula*. Mol. Plant Microbe Interact. 6, 643–654.

Harrison, M.J., Dixon, R.A., 1994. Spatial patterns of expression of flavonoid/isoflavonoid pathway genes during interactions between roots of *Medicago truncatula* and the mycorrhizal fungus *Glomus versiforme*. Plant J. 6, 9–20.

Harrison, M.J., van Buuren, M.L., 1995. A phosphate transporter from the mycorrhizal fungus *Glomus versiforme*. Nature 378, 626–629.

Harrison, M.J., Dewbre, G.R., Liu, J., 2002. A phosphate transporter from *Medicago truncatula* involved in the acquisition of phosphate released by arbuscular mycorrhizal fungi. Plant Cell 14, 2413–2429.

Hetrick, B.A.D., Wilson, G.W.T., Todd, T.C., 1996. Mycorrhizal response in wheat cultivars: relationship to phosphorus. Can. J. Bot. 74, 19–25.

Hiei, Y., Ohta, S., Komari, T., Kumashiro, T., 1994. Efficient transformation of rice (*Oryza sativa* L.) mediated by *Agrobacterium* and sequence analysis of the boundaries of the T-DNA. Plant J. 6, 271–282.

Ho, C.-H., Lin, S.-H., Hu, H.-C., Tsay, Y.-F., 2009. CHL1 functions as a nitrate sensor in plants. Cell 138, 1184–1194.

Hoffland, E., Findenegg, G.R., Nelemans, J.A., 1989. Solubilization of rock phosphate by rape II. Local root exudation of organic acids as a response to P-starvation. Plant Soil 113, 161–165.

Hohnjec, N., Perlick, A.M., Pühler, A., Küster, H., 2003. The *Medicago truncatula* sucrose synthase gene *MtSucS1* is activated both in the Infected region of root nodules and in the cortex of roots colonized by arbuscular mycorrhizal fungi. Mol. Plant Microbe Interact. 16, 903–915.

Holford, I.C.R., 1997. Soil phosphorus: its measurement, and its uptake by plants. Aust. J. Soil Res. 35, 227–239.

Horvath, B., Bachem, C.W.B., Schell, J., Kondorosi, A., 1987. Host-specific regulation of nodulation genes in *Rhizobium* is mediated by a plant-signal, interacting with the *nodD* gene product. EMBO J. 6, 841–848.

Hsieh, L.-C., Lin, S.-I., Shih, A.C.-C., Chen, J.-W., Lin, W.-Y., Tseng, C.-Y., et al., 2009. Uncovering small RNA-mediated responses to phosphate deficiency in *Arabidopsis* by deep sequencing. Plant Physiol. 151, 2120–2132.

Imaizumi-Anraku, H., Takeda, N., Charpentier, M., Perry, J., Miwa, H., Umehara, Y., et al., 2005. Plastid proteins crucial for symbiotic fungal and bacterial entry into plant roots. Nature 433, 527–531.

International Rice Genome Sequencing Project, 2005. The map-based sequence of the rice genome. Nature 436, 793–800.

Ishizaki, K., Chiyoda, S., Yamato, K.T., Kohchi, T., 2008. Agrobacterium-mediated transformation of the haploid liverwort *Marchantia polymorpha* L., an emerging model for plant biology. Plant Cell Physiol. 49, 1084–1091.

Ito, Y., Nakanomyo, I., Motose, H., Iwamoto, K., Sawa, S., Dohmae, N., et al., 2006. Dodeca-CLE peptides as suppressors of plant stem cell differentiation. Science 313, 842–845.

Jagadeeswaran, G., Zheng, Y., Li, Y.-F., Shukla, L.I., Matts, J., Hoyt, P., et al., 2009. Cloning and characterization of small RNAs from *Medicago truncatula* reveals four novels legume-specific microRNA families. New Phytol. 184, 85–98.

Janos, D.P., 2007. Plant responsiveness to mycorrhizas differs from dependence upon mycorrhizas. Mycorrhiza 17, 75–91.

Javot, H., Penmetsa, R.V., Terzaghi, N., Cook, D.R., Harrison, M.J., 2007a. A *Medicago truncatula* phosphate transporter indispensable for the arbuscular mycorrhizal symbiosis. Proc. Natl. Acad. Sci. USA 104, 1720–1725.

Javot, H., Pumplin, N., Harrison, M.J., 2007b. Phosphate in the arbuscular mycorrhizal symbiosis: transport properties and regulatory roles. Plant Cell Environ. 30, 310–322.

Jin, H., Pfeffer, P.E., Douds, D.D., Piotrowski, E., Lammers, P.J., Shachar-Hill, Y., 2005. tThe uptake, metabolism, transport and transfer of nitrogen in an arbuscular mycorrhizal symbiosis. New Phytol. 168, 687–696.

Kanamori, N., Madsen, L.H., Radutoiu, S., Frantescu, M., Quistgaard, E.M.H., Miwa, H., et al., 2006. A nucleoporin is required for induction of Ca^{2+} spiking in legume nodule development and essential for rhizobial and fungal symbiosis. Proc. Natl. Acad. Sci. USA 103, 359–364.

Karandashov, V., Bucher, M., 2005. Symbiotic phosphate transport in arbuscular mycorrhizas. Trends Plant Sci. 10, 22–29.

Khademi, S., O'Connell III, J., Remis, J., Robles-Colmenares, Y., Miercke, L.J.W., Stroud, R.M., 2004. Mechanism of ammonia transport by Amt/MEP/Rh: structure of AmtB at 1.35 Å. Science 305, 1587–1594.

Kistner, C., Parniske, M., 2002. Evolution of signal transduction in intracellular symbiosis. Trends Plant Sci. 7, 511–518.

Kistner, C., Winzer, T., Pitzschke, A., Mulder, L., Sato, S., Kaneko, T., et al., 2005. Seven *Lotus japonicus* genes required for transcriptional reprogramming of the root during fungal and bacterial symbiosis. Plant Cell 17, 2217–2229.

Klironomos, J.N., 2003. Variation in plant response to native exotic arbuscular mycorrhizal fungi. Ecology 84, 2292–2301.

Kobae, Y., Hata, S., 2010. Dynamics of periarbuscular membranes visualized with a fluorescent phosphate transporter in arbuscular mycorrhizal roots of rice. Plant Cell Physiol. 51, 341–353.

Koide, R.T., Kabir, Z., 2000. Extraradical hyphae of the mycorrhizal fungus *Glomus intraradices* can hydrolyse organic phosphate. New Phytol. 148, 511–517.

Kojima, Y., Ebana, K., Fukuoka, S., Nagamine, T., Kawase, M., 2005. Development of an RFLP-based rice diversity research set of germplasm. Breed. Sci. 55, 431–440.

Kondo, T., Sawa, S., Kinoshita, A., Mizuno, S., Kakimoto, T., Fukuda, H., et al., 2006. A plant peptide encoded by *CLV3* identified by in situ MALDI-TOF MS analysis. Science 313, 845–848.

Kosuta, S., Chabaud, M., Lougnon, G., Gough, C., Dénarié, J., Barker, D.G., et al., 2003. A diffusible factor from arbuscular mycorrhizal fungi induces symbiosis-specific *MtENOD11* expression in roots of *Medicago truncatula*. Plant Physiol. 131, 952–962.

Kosuta, S., Hazledine, S., Sun, J., Miwa, H., Morris, R.J., Downie, J.A., et al., 2008. Differential and chaotic calcium signatures in the symbiosis signaling pathway of legumes. Proc. Natl. Acad. Sci. USA 105, 9823–9828.

Kouchi, H., Hata, S., 1993. Isolation and characterization of novel nodulin cDNAs representing genes expressed at early stages of soybean nodule development. Mol. Gen. Genet. 238, 106–119.

Kouchi, H., Shimomura, K., Hata, S., Hirota, A., Wu, G.-J., Kumagai, H., et al., 2004. Large-scale analysis of gene expression profiles during early stages of root nodule formation in a model Legume, *Lotus japonicus*. DNA Res. 11, 263–274.

Krajinski, F., Hause, B., Gianinazzi-Pearson, V., Franken, P., 2002. *Mtha*1, a plasma membrane H^+-ATPase gene from *Medicago truncatula*, shows arbuscule-specific induced expression in mycorrhizal tissue. Curr. Opin. Plant Biol. 4, 754–761.

Kucey, R.M.N., 1987. Increased phosphorus uptake by wheat and field beans inoculated with a phosphorus-solubilizing *Penicillium bilaji* strain and with vesicular-arbuscular mycorrhizal fungi. Appl. Environ. Microbiol. 53, 2699–2703.

Kuga, Y., Saito, K., Nayuki, K., Peterson, R.L., Saito, M., 2008. Ultrastructure of rapidly frozen and freeze-substituted germ tubes of an arbuscular mycorrhizal fungus and localization of polyphosphate. New Phytol. 178, 189–200.

Kuhn, H., Kuster, H., Requena, N., 2010. Membrane steroid-binding protein 1 induced by a diffusible fungal signal is critical for mycorrhization in *Medicago truncatula*. New Phytol. 185, 716–733.

Lanquar, V., Loqué, D., Hörmann, F., Yuan, L., Bohner, A., Engelsberger, W.R., Lalonde, W.X., Schulze, W.X., von Wirén, N., Frommer, W.B., 2009. Feedback inhibition of ammonium uptake by a phospho-dependent allosteric mechanism in *Arabidopsis*. Plant Cell 21, 3610–3622.

Lévy, J., Bres, C., Geurts, R., Chalhoub, B., Kulikova, O., Duc, G., et al., 2004. A putative $Ca2^+$ and calmodulin-dependent protein kinase required for bacterial and fungal symbioses. Science 303, 1361–1364.

Li, M., Osaki, M., Honma, M., Tadano, T., 1997. Purification and characterization of phytase induced in tomato roots under phosphorus-deficient conditions. Soil Sci. Plant Nutr. 43, 179–190.

Li, H.Y., Zhu, Y.G., Marschner, P., Smith, F.A., Smith, S.E., 2005. Wheat responses to arbuscular mycorrhizal fungi in a highly calcareous soil differ from those of clover, and change with plant development and P supply. Plant Soil 277, 221–232.

Li, H., Smith, S.E., Holloway, R.E., Zhu, Y., Smith, F.A., 2006. Arbuscular mycorrhizal fungi contribute to phosphorus uptake by wheat grown in a phosphorus-fixing soil even in the absence of positive growth responses. New Phytol. 172, 536–543.

Li, H., Smith, F.A., Dickson, S., Holloway, R.E., Smith, S.E., 2008. Plant growth depressions in arbuscular mycorrhizal symbioses: not just caused by carbon drain? New Phytol. 178, 852–862.

Ligrone, R., Carafa, A., Lumini, E., Bianciotto, V., Bonfante, P., Duckett, J.G., 2007. Glomeromycotean associations in liverworts: a molecular, cellular, and taxonomic analysis. Am. J. Bot. 94, 1756–1777.

Lin, S.-I., Chiou, T.-J., 2008. Long-distance movement and differential targeting of microRNA399s. Plant Signal. Behav. 3, 730–732.

Lin, S.-I., Chiang, S.-F., Lin, W.-Y., Chen, J.-W., Tseng, C.-Y., 2008. Regulatory network of microRNA399 and *PHO2* by systemic signaling. Plant Physiol. 147, 732–746.

Liu, J., Blaylock, L.A., Endre, G., Cho, J., Town, C.D., VandenBosch, K.A., et al., 2003. Transcript profiling coupled with spatial expression analyses reveals genes involved in distinct developmental stages of an arbuscular mycorrhizal symbiosis. Plant Cell 15, 2106–2123.

Liu, J., Maldonado-Mendoza, I., Lopez-Meyer, M., Cheung, F., Town, C.D., Harrison, M.J., 2007. Arbuscular mycorrhizal symbiosis is accompanied by local and systemic alterations in gene expression and an increase in disease resistance in the shoots. Plant J. 50, 529–544.

Liu, J., Versaw, W.K., Pumplin, N., Gomez, S.K., Blaylock, L.A., Harrison, M.J., 2008. Closely related members of the *Medicago truncatula* PHT1 phosphate transporter gene family encode phosphate transporters with distinct biochemical activities. J. Biol. Chem. 283, 24673–24681.

Logi, C., Sbrana, C., Giovannetti, M., 1998. Cellular events involved in survival of individual arbuscular mycorrhizal symbionts growing in the absence of the host. Appl. Environ. Microbiol. 64, 3473–3479.

López-Bucio, J., Cruz-Ramıirez, A., Herrera-Estrella, L., 2003. The role of nutrient availability in regulating root architecture. Curr. Opin. Plant Biol. 6, 280–287.

López-Pedrosa, A., González-Guerrero, M., Valderas, A., Azcón-Aguilar, C., Ferrol, N., 2006. *GintAMT1* encodes a functional high-affnity ammonium transporter that is expressed in the extraradical mycelium of *Glomus intraradices*. Fungal Genet. Biol. 43, 102–110.

Ludewig, U., von Wirén, N., Frommer, W.B., 2002. Uniport of NH_4^+ by the root hair plasma membrane ammonium transporter LeAMT1;1. J. Biol. Chem. 277, 13548–13555.

Lung, S.-C., Chan, W.-L., Yip, W., Wang, L., Yeung, E.C., Lim, B.L., 2005. Secretion of beta-propeller phytase from tobacco and *Arabidopsis* roots enhances phosphorus utilization. Plant Sci. 169, 341–349.

Ma, J.F., Yamaji, N., Mitani, N., Xu, X.-Y., Su, Y.-H., McGrath, S.P., et al., 2008. Transporters of arsenite in rice and their role in arsenic accumulation in rice grain. Proc. Natl. Acad. Sci. USA 105, 9931–9935.

Madsen, E.B., Madsen, L.H., Radutoiu, S., Olbryt, M., Rakwalska, M., Szczyglowski, K., et al., 2003. A receptor kinase gene of the LysM type is involved in legume perception of rhizobial signals. Nature 425, 637–640.

Maeda, D., Ashida, K., Iguchi, K., Chechetka, S.A., Hijikata, A., Okusako, Y., et al., 2006. Knockdown of an arbuscular mycorrhiza-inducible phosphate transporter gene of *Lotus japonicus* suppresses mutualistic symbiosis. Plant Cell Physiol. 47, 807–817.

Maldonado-Mendoza, I.E., Dewbre, G.R., Harrison, M.J., 2001. A phosphate transporter gene from the extra-radical mycelium of an arbuscular mycorrhizal fungus *Glomus intraradices* is regulated in response to phosphate in the environment. Mol. Plant Microbe Interact. 14, 1140–1148.

Marini, A.-M., Soussi-Boudekou, S., Vissers, S., Andre, B., 1997. A family of ammonium transporters in *Saccharomyces cerevisiae*. Mol. Cell. Biol. 17, 4282–4293.

Markmann, K., Giczey, G., Parniske, M., 2008. Functional adaptation of a plant receptor-kinase paved the way for the evolution of intracellular root symbioses with bacteria. PLoS Biol. 6, 497–506.

Marschner, H., 1995. Mineral Nutrition in Higher Plants, second ed. Academic Press, San Diego, CA, pp. 537–595.

Matzke, M., Weiger, T.M., Papp, I., Matzke, A.J.M., 2009. Nuclear membrane ion channels mediate root nodule development. Trends Plant Sci. 14, 295–298.

Mayer, M., Dynowski, M., Ludewig, U., 2006. Ammonium ion transport by the AMT/Rh homologue LeAMT1;1. Biochem. J. 396, 431–437.

McGonigle, T.P., Yano, K., Shinhama, T., 2003. Mycorrhizal phosphorus enhancement of plants in undisturbed soil differs from phosphorus uptake stimulation by arbuscular mycorrhizae over non-mycorrhizal controls. Biol. Fertil. Soils 37, 268–273.

Meharg, A.A., 2004. Arsenic in rice—understanding a new disaster for South-East Asia. Trends Plant Sci. 9, 415–417.

Meixner, C., Ludwig-Müller, J., Miersch, O., Gresshoff, P., Staehelin, C., Vierheilig, H., 2005. Lack of mycorrhizal autoregulation and phytohormonal changes in the super-nodulating soybean mutant *nts1007*. Planta 222, 709–715.

Messinese, E., Mun, J.-H., Yeun, L.H., Jayaraman, D., Rougé, P., Barre, A., et al., 2007. A novel nuclear protein interacts with the symbiotic DMI3 calcium- and calmodulin-dependent protein kinase of *Medicago truncatula*. Mol. Plant Microbe Interact. 20, 912–921.

Mitra, R.M., Gleason, C.A., Edwards, A., Hadfield, J., Downie, J.A., Oldroyd, G.E.D., et al., 2004. A Ca^{2+}/calmodulin-dependent protein kinase required for symbiotic nodule development: gene identification by transcript-based cloning. Proc. Natl. Acad. Sci. USA 101, 4701–4705.

Miwa, H., Sun, J., Oldroyd, G.E.D., Downi, J.A., 2006. Analysis of Nod-factor-induced calcium signaling in root hairs of symbiotically defective mutants of *Lotus japonicus*. Mol. Plant Microbe Interact. 19, 914–923.

Morandi, D., le Signor, C., Gianinazzi-Pearson, V., Duc, G., 2009. A *Medicago truncatula* mutant hyper-responsive to mycorrhiza and defective for nodulation. Mycorrhiza 19, 435–441.

Mosse, B., 1959. The regular germination of resting spores and some observations on the growth requirements of an *Endogone* sp. causing vesicular-arbuscular mycorrhiza. Trans. Br. Mycol. Soc. 42, 274–286.

Mosse, B., Phillips, J.M., 1971. The influence of phosphate and other nutrients on the development of vesicular-arbuscular mycorrhiza in culture. J. Gen. Microbiol. 69, 157–166.

Munkvold, L., Kjøller, R., Vestberg, M., Rosendahl, S., Jakobsen, I., 2004. High functional diversity within species of arbuscular mycorrhizal fungi. New Phytol. 164, 357–364.

Nagahashi, G., Douds Jr., D.D., 1997. Appressorium formation by AM fungi on isolated cell walls of carrot roots. New Phytol. 136, 299–304.

Nagy, R., Karandashov, V., Chague, V., Kalinkevich, K., Tamasloukht, M., Xu, G., et al., 2005. The characterization of novel mycorrhiza-specific phosphate transporters from *Lycopersicon esculentum* and *Solanum tuberosum* uncovers functional redundancy in symbiotic phosphate transport in solanaceous species. Plant J. 42, 236–250.

Nagy, R., Drissner, D., Amrhein, N., Jakobsen, I., Bucher, M., 2009. Mycorrhizal phosphate uptake pathway in tomato is phosphorus-repressible and transcriptionally regulated. New Phytol. 181, 950–959.

Navazio, L., Moscatiello, R., Genre, A., Novero, M., Baldan, B., Bonfante, P., et al., 2007. A diffusible signal from arbuscular mycorrhizal fungi elicits a transient cytosolic calcium elevation in host plant cells. Plant Physiol. 144, 673–681.

Neuhäuser, B., Dynowski, M., Mayer, M., Ludewig, U., 2007. Regulation of NH_4^+ transport by essential cross talk between AMT monomers through the carboxyl tails. Plant Physiol. 143, 1651–1659.

Nishiyama, T., Wolf, P.G., Kugita, M., Sinclair, B.R., Sugita, M., Sugiura, C., et al., 2004. Chloroplast phylogeny indicates that bryophytes are monophyletic. Mol. Biol. Evol. 21, 1813–1819.

Norton, G.J., Nigar, M., Williams, P.N., Dasgupta, T., Meharg, A.A., Price, A.H., 2008. Rice–arsenate interactions in hydroponics: a three-gene model for tolerance. J. Exp. Bot. 59, 2277–2284.

Okamoto, S., Ohnishi, E., Sato, S., Takahashi, H., Nakazono, M., Tabata, S., et al., 2009. Nod factor/nitrate-induced *CLE* genes that drive HAR1-mediated systemic regulation of nodulation. Plant Cell Physiol. 50, 67–77.

Oki, T., Kanae, S., 2006. Global hydrological cycles and world water resources. Science 313, 1068–1072.

Olah, B., Briere, C., Becard, G., Denarie, J., Gough, C., 2005. Nod factors and a diffusible factor from arbuscular mycorrhizal fungi stimulate lateral root formation in *Medicago truncatula* via the DMI1/DMI2 signalling pathway. Plant J. 44, 195–207.

Owusu-Bennoah, E., Mosse, B., 1979. Plant growth responses to vesicular-arbuscular mycorrhiza. New Phytol. 83, 671–679.

Pant, B.D., Buhtz, A., Kehr, J., Scheible, W.-R., 2008. MicroRNA399 is a long-distance signal for the regulation of plant phosphate homeostasis. Plant J. 53, 731–738.

Pant, B.D., Musialak-Lange, M., Nuc, P., May, P., Buhtz, A., Kehr, J., et al., 2009. Identification of nutrient-responsive *Arabidopsis* and rapeseed microRNAs by comprehensive real-time PCR profiling and small RNA sequencing. Plant Physiol. 150, 1541–1555.

Parniske, M., 2000. Intracellular accommodation of microbes by plants: a common developmental program for symbiosis and disease? Curr. Opin. Plant Biol. 3, 320–328.
Parniske, M., 2005. Cue for the branching connection. Nature 435, 750–751.
Parniske, M., 2008. Arbuscular mycorrhiza: the mother of plant root endosymbioses. Nat. Rev. Mycrobiol. 6, 763–775.
Paszkowski, U., Kroken, S., Roux, C., Briggs, S.P., 2002. Rice phosphate transporters include an evolutionarily divergent gene specifically activated in arbuscular mycorrhizal symbiosis. Proc. Natl. Acad. Sci. USA 99, 13324–13329.
Paterson, A.H., Bowers, J.E., Bruggmann, R., Dubchak, I., Grimwood, J., Gundlach, H., et al., 2009. The Sorghum bicolor genome and the diversification of grasses. Nature 457, 551–556.
Pirozynski, K.A., Malloch, D.W., 1975. The origin of land plants: a matter of mycotrophism. BioSystems 6, 153–164.
Plenchette, C., Furlan, V., Fortin, J.A., 1981. Growth stimulation of apple trees in unsterilized soil under field conditions with VA mycorrhiza inoculation. Can. J. Bot. 59, 2003–2008.
Poulsen, K.H., Nagy, R., Gao, L.-L., Smith, S.E., Bucher, M., Smith, F.A., et al., 2005. Physiological and molecular evidence for Pi uptake via the symbiotic pathway in a reduced mycorrhizal colonization mutant in tomato associated with a compatible fungus. New Phytol. 168, 445–454.
Pozo, M.J., Cordier, C., Dumas-Gaudot, E., Gianinazzi, S., Barea, J.M., Azcon-Aguilar, C., 2002. Localized versus systemic effect of arbuscular mycorrhizal fungi on defence responses to *Phytophthora* infection in tomato plants. J. Exp. Bot. 53, 525–534.
Pumplin, N., Harrison, M.J., 2009. Live-cell imaging reveals periarbuscular membrane domains and organelle location in *Medicago truncatula* roots during arbuscular mycorrhizal symbiosis. Plant Physiol. 151, 809–819.
Pumplin, N., Mondo, S.J., Topp, S., Starker, C.G., Gantt, J.S., Harrison, M.J., 2010. *Medicago truncatula* Vapyrin is a novel protein required for arbuscular mycorrhizal symbiosis. Plant J. 61, 482–494.
Raboy, V., 2001. Seeds for a better future: 'low phytate' grains help to overcome malnutrition and reduce pollution. Trends Plant Sci. 6, 458–462.
Radutoiu, S., Madsen, L.H., Madsen, E.B., Felle, H.H., Umehara, Y., Grønlund, M., et al., 2003. Plant recognition of symbiotic bacteria requires two LysM receptor-like kinases. Nature 425, 585–592.
Raghothama, K.G., 1999. Phosphate acquisition. Annu. Rev. Plant Physiol. Plant Mol. Biol. 50, 665–693.
Rausch, C., Daram, P., Brunner, S., Jansa, J., Laloi, M., Leggewie, G., et al., 2001. A phosphate transporter expressed in arbuscule-containing cells in potato. Nature 414, 462–466.
Read, D.J., Duckett, J.G., Francis, R., Ligrone, R., Russell, A., 2000. Symbiotic fungal associations in 'lower' land plants. Philos. Trans. R. Soc. Lond. B 355, 815–831.
Redecker, D., Kodner, R., Graham, L.E., 2000. Glomalean fungi from the Ordovician. Science 289, 1920–1921.
Remy, W., Taylor, T.N., Hass, H., Kerp, H., 1994. Four hundred-million-year-old vesicular arbuscular mycorrhizae. Proc. Natl. Acad. Sci. USA 91, 11841–11843.
Richardson, A.E., Hadobas, P.A., Hayes, J.E., 2001. Extracellular secretion of *Aspergillus* phytase from *Arabidopsis* roots enables plants to obtain phosphorus from phytate. Plant J. 25, 641–649.
Ruiz-Lozano, J.M., 2003. Arbuscular mycorrhizal symbiosis and alleviation of osmotic stress. New perspectives for molecular studies. Mycorrhiza 13, 309–317.
Russell, J., Bulman, S., 2005. The liverwort *Marchantia foliacea* forms a specialized symbiosis with arbuscular mycorrhizal fungi in the genus *Glomus*. New Phytol. 165, 567–579.

Ryan, M.H., van Herwaarden, A.F., Angus, J.F., Kirkegaard, J.A., 2005. Reduced growth of autumn-sown wheat in a low-P soil is associated with high colonisation by arbuscular mycorrhizal fungi. Plant Soil 270, 275–286.
Saito, K., Yoshikawa, M., Yano, K., Miwa, H., Uchida, H., Asamizu, E., et al., 2007. NUCLEOPORIN85 is required for calcium spiking, fungal and bacterial symbioses, and seed production in *Lotus japonicus*. Plant Cell 19, 610–624.
Sanchez, D.H., Szymanski, J., Erban, A., Udvardi, M.K., Kopka, J., 2010. Mining for robust transcriptional and metabolic responses to long-term salt stress: a case study on the model legume *Lotus japonicus*. Plant Cell Environ. 33, 468–480.
Sawers, R.J.H., Gutjahr, C., Paszkowski, U., 2008. Cereal mycorrhiza: an ancient symbiosis in modern agriculture. Trends Plant Sci. 13, 93–97.
Sawers, R.J.H., Gebreselassie, M.N., Janos, D.P., Paszkowski, U., 2010. Characterizing variation in mycorrhiza effect among diverse plant varieties. Theor. Appl. Genet. 120, 1029–1039.
Schaarschmidt, S., Hause, B., 2008. Apoplastic invertases: multi-faced players in the arbuscular mycorrhization. Plant Signal. Behav. 3, 317–319.
Schaarschmidt, S., Roitsch, T., Hause, B., 2006. Arbuscular mycorrhiza induces gene expression of the apoplastic invertase LIN6 in tomato (*Lycopersicon esculentum*) roots. J. Exp. Bot. 57, 4015–4023.
Schaarschmidt, S., González, M.-C., Roitsch, T., Strack, D., Sonnewald, U., Hause, B., 2007. Regulation of arbuscular mycorrhization by carbon. The symbiotic interaction cannot be improved by Increased carbon availability accomplished by root-specifically enhanced invertase activity. Plant Physiol. 143, 1827–1840.
Schnable, P.S., Ware, D., Fulton, R.S., Stein, J.C., Wei, F., Pasternak, S., et al., 2009. The B73 maize genome: complexity, diversity, and dynamics. Science 326, 1112–1115.
Schüßler, A., 2000. *Glomus claroideum* forms an arbuscular mycorrhiza-like symbiosis with the hornwort *Anthoceros punctatus*. Mycorrhiza 10, 15–21.
Schüßler, A., Schwarzott, D., Walker, C., 2001. A new fungal phylum, the *Glomeromycota*: phylogeny and evolution. Mycol. Res. 105, 1413–1421.
Schüßler, A., Martin, H., Cohen, D., Fitz, M., Wipf, D., 2006. Characterization of a carbohydrate transporter from symbiotic glomeromycotan fungi. Nature 444, 933–936.
Secilia, J., Bagyaraj, D.J., 1992. Selection of efficient vesicular-arbuscular mycorrhizal fungi for wetland rice (*Oryza sativa* L.). Biol. Fertil. Soils 13, 108–111.
Secilia, J., Bagyaraj, D.J., 1994. Selection of efficient vesicular-arbuscular mycorrhizal fungi for wetland rice—a preliminary screen. Mycorrhiza 4, 265–268.
Selosse, M.-A., 2005. Are liverworts imitating mycorrhizas? New Phytol. 165, 345–349.
Shang, C., Stewart, J.W.B., Huang, P.M., 1992. pH effect on kinetics of adsorption of organic and inorganic phosphates by short-range ordered aluminum and iron precipitates. Geoderma 53, 1–14.
Sharma, V.K., Ramirez, J., Fletcher, J.C., 2003. The *Arabidopsis CLV3*-like (*CLE*) genes are expressed in diverse tissues and encode secreted proteins. Plant Mol. Biol. 51, 415–425.
Shin, H., Shin, H.-S., Chen, R., Harrison, M.J., 2006. Loss of *At4* function impacts phosphate distribution between the roots and the shoots during phosphate starvation. Plant J. 45, 712–726.
Siciliano, V., Genre, A., Balestrini, R., Cappellazzo, G., deWit, P.J.G.M., Bonfante, P., 2007. Transcriptome analysis of arbuscular mycorrhizal roots during development of the prepenetration apparatus. Plant Physiol. 144, 1455–1466.
Simon, L., Bousquet, J., Lévesque, R.C., Lalonde, M., 1993. Origin and diversification of endomycorrhizal fungi and coincidence with vascular land plants. Nature 363, 67–69.
Smith, F.W., 2002. The phosphate uptake mechanism. Plant Soil 245, 105–114.
Smith, S.E., Read, D.J., 2008. Mycorrhizal Symbiosis, third ed. Academic Press, San Diego, CA.

Smith, S.E., Dickson, S., Smith, F.A., 2001. Nutrient transfer in arbuscular mycorrhizas: how are fungal and plant processes integrated? Aust. J. Plant Physiol. 28, 683–694.
Smith, S.E., Smith, F.A., Jakobsen, I., 2004. Functional diversity in arbuscular mycorrhizal (AM) symbioses: the contribution of the mycorrhizal P uptake pathway is not correlated with mycorrhizal responses in growth or total P uptake. New Phytol. 162, 511–524.
Smith, F.A., Grace, E.J., Smith, S.E., 2009. More than a carbon economy: nutrient trade and ecological sustainability in facultative arbuscular mycorrhizal symbioses. New Phytol. 182, 347–358.
Solaiman, M.Z., Hirata, H., 1997. Responses of directly seeded wetland rice to arbuscular mycorrhizal fungi inoculation. J. Plant Nutr. 20, 1479–1487.
Solaiman, M.Z., Hirata, H., 1998. *Glomus*-wetland rice mycorrhizas influenced by nursery inoculation techniques under high fertility soil conditions. Biol. Fertil. Soils 27, 92–96.
Solaiman, M.Z., Saito, M., 1997. Use of sugars by intraradical hyphae of arbuscular mycorrhizal fungi revealed by radiorespirometry. New Phytol. 136, 533–538.
Solaiman, M.Z., Ezawa, T., Kojima, T., Saito, M., 1999. Polyphosphates in intraradical and extraradical hyphae of an arbuscular mycorrhizal fungus, *Gigaspora margarita*. Appl. Environ. Microbiol. 65, 5604–5606.
Solaiman, M.Z., Senoo, K., Kawaguchi, M., Imaizumi-Anraku, H., Akao, S., Tanaka, A., et al., 2000. Characterization of mycorrhizas formed by *Glomus* sp. on roots of hyper-nodulating mutants of *Lotus japonicus*. J. Plant Res. 113, 443–448.
Spaink, H.P., 2000. Root nodulation and infection factors produced by rhizobial bacteria. Annu. Rev. Microbiol. 54, 257–288.
Spaink, H.P., Wijffelaman, A., Pees, E., Okker, R.J.H., Lugtenberg, B.J.J., 1987. *Rhizobium* nodulation gene *nodD* as a determinant of host specificity. Nature 328, 337–340.
Stracke, S., Kistner, C., Yoshida, S., Mulder, L., Sato, S., Kaneko, T., et al., 2002. A plant receptor-like kinase required for both bacterial and fungal symbiosis. Nature 417, 959–962.
Stribley, D.P., Tinker, P.B., Rayner, J.H., 1980. Relation of internal phosphorus concentration and plants infected by vesicular-arbuscular mycorrhizas. New Phytol. 86, 261–266.
Subramanian, S., Fu, Y., Sunkar, R., Barbazuk, W.B., Zhu, J.-K., Yu, O., 2008. Novel and nodulation-regulated microRNAs in soybean roots. BMC Genomics 9, 160–173.
Sunkar, R., Jagadeeswaran, G., 2008. *In silico* identification of conserved microRNAs in large number of diverse plant species. BMC Plant Biol. 8, 37–49.
Sunkar, R., Girke, T., Jain, P.K., Zhu, J.-K., 2005. Cloning and characterization of microRNAs from rice. Plant Cell 17, 1397–1411.
Sunkar, R., Zhou, X., Zheng, Y., Zhang, W., Zhu, J.-K., 2008. Identification of novel and candidate miRNAs in rice by high throughput sequencing. BMC Plant Biol. 8, 25–41.
Tajima, S., LaRue, T.A., 1982. Enzymes for acetaldehyde and ethanol formation in legume nodules. Plant Physiol. 70, 388–392.
Takeda, N., Sato, S., Asamizu, E., Tabata, S., Parniske, M., 2009. Apoplastic plant subtilases support arbuscular mycorrhiza development in *Lotus japonicus*. Plant J. 58, 766–777.
Tamasloukht, M., Séjalon-Delmas, N., Kluever, A., Jauneau, A., Roux, C., Bécard, G., et al., 2003. Root factors induce mitochondrial-related gene expression and fungal respiration during the developmental switch from asymbiosis to presymbiosis in the arbuscular mycorrhizal fungus *Gigaspora rosea*. Plant Physiol. 131, 1468–1478.
Tanaka, Y., Yano, K., 2005. Nitrogen delivery to maize via mycorrhizal hyphae depends on the form of N supplied. Plant Cell Environ. 28, 1247–1254.
Tani, C., Ohtomo, R., Osaki, M., Kuga, Y., Ezawa, T., 2009. ATP-Dependent but proton gradient-independent polyphosphate-synthesizing activity in extraradical hyphae of an arbuscular mycorrhizal fungus: ATP-dependent but proton gradient-independent synthesis. Appl. Environ. Microbiol. 75, 7044–7050.

Tawaraya, K., 2003. Arbuscular mycorrhizal dependency of different plant species and cultivars. Soil Sci. Plant Nutr. 49, 655–668.
Taylor, T.N., Remy, W., Hass, H., Kerp, H., 1995. Fossil arbuscular mycorrhizae from the Early Devonian. Mycologia 87, 560–573.
Tirichine, L., Imaizumi-Anraku, H., Yoshida, S., Murakami, Y., Madsen, L.H., Miwa, H., et al., 2006. Deregulation of a Ca^{2+}/calmodulin-dependent kinase leads to spontaneous nodule development. Nature 441, 1153–1156.
Turner, B.L., Paphazy, M.J., Haygarth, P.M., McKelvie, I.D., 2002. Inositol phosphates in the environment. Philos. Trans. R. Soc. Lond. B 357, 449–469.
Umehara, M., Hanada, A., Yoshida, S., Akiyama, K., Arite, T., Takeda-Kamiya, N., et al., 2008. Inhibition of shoot branching by new terpenoid plant hormones. Nature 455, 195–201.
Vallino, M., Greppi, D., Novero, M., Bonfante, P., Lupotto, E., 2009. Rice root colonisation by mycorrhizal and endophytic fungi in aerobic soil. Ann. Appl. Biol. 154, 195–204.
Vogel, J.T., Walter, M.H., Giavalisco, P., Lytovchenko, A., Kohlen, W., Charnikhova, T., et al., 2010. SlCCD7 controls strigolactone biosynthesis, shoot branching and mycorrhiza-induced apocarotenoid formation in tomato. Plant J. 61, 300–311.
Volpin, H., Elkind, Y., Okon, Y., Kapulnik, Y., 1994. A vesicular arbuscular mycorrhizal fungus (*Glomus intraradix*) induces a defense response in alfalfa roots. Plant Physiol. 104, 683–689.
Volpin, H., Phillips, D.A., Okon, Y., Kapulnik, Y., 1995. Suppression of an isoflavonoid phytoalexin defense response in mycorrhizal alfalfa roots. Plant Physiol. 108, 1449–1454.
Wang, C., Ying, S., Huang, H., Li, K., Wu, P., Shou, H., 2009a. Involvement of *OsSPX1* in phosphate homeostasis in rice. Plant J. 57, 895–904.
Wang, X., Wang, Y., Tian, J., Lim, B.L., Yan, X., Liao, H., 2009b. Overexpressing *AtPAP15* enhances phosphorus efficiency in soybean. Plant Physiol. 151, 233–240.
Wang, Y., Li, P., Cao, X., Wang, X., Zhang, A., Li, X., 2009c. Identification and expression analysis of miRNAs from nitrogen-fixing soybean nodules. Biochem. Biophys. Res. Commun. 378, 799–803.
Wang et al., 2010. New Phytol. doi: 10.1111/j.1469-8137.2009.03137.x (in press).
Wegel, E., Schauser, L., Sandal, N., Stougaard, J., Parniske, M., 1998. Mycorrhiza mutants of *Lotus japonicus* define genetically independent steps during symbiotic infection. Mol. Plant Microbe Interact. 11, 933–936.
Wellman, C.H., Osterloff, P.L., Mohiuddin, U., 2003. Fragments of the earliest land plants. Nature 425, 282–285.
Xiao, K., Harrison, M.J., Wang, Z.-Y., 2005. Transgenic expression of a novel *M. truncatula* phytase gene results in improved acquisition of organic phosphorus by *Arabidopsis*. Planta 222, 27–36.
Yamato, K.T., Ishizaki, K., Fujisawa, M., Okada, S., Nakayama, S., Fujishita, M., et al., 2007. Gene organization of the liverwort Y chromosome reveals distinct sex chromosome evolution in a haploid system. Proc. Natl. Acad. Sci. USA 104, 6472–6477.
Yano, K., Yoshida, S., Müller, J., Singh, S., Banba, M., Vickers, K., et al., 2008. CYCLOPS, a mediator of symbiotic intracellular accommodation. Proc. Natl. Acad. Sci. USA 105, 20540–20545.
Yoder, J.I., 1999. Parasitic plant responses to host plant signals: a model for subterranean plant–plant interactions. Curr. Opin. Plant Biol. 2, 65–70.
Zhang, X.H., Zhu, Y.-G., Chen, B.D., Lin, A.J., Smith, S.E., Smith, F.A., 2005. Arbuscular mycorrhizal fungi contribute to resistance of upland rice to combined metal contamination of soil. J. Plant Nutr. 28, 2065–2077.
Zhang, X.-H., Zhu, Y.-G., Lin, A.-J., Chen, B.-D., Smith, S.E., Smith, F.A., 2006. Arbuscular mycorrhizal fungi can alleviate the adverse effects of chlorothalonil on *Oryza sativa* L. Chemosphere 64, 1627–1632.

Zhang, X.-H., Lin, A.-J., Gao, Y.-L., Reid, R.J., Wong, M.-H., Zhua, Y.-G., 2009. Arbuscular mycorrhizal colonisation increases copper binding capacity of root cell walls of *Oryza sativa* L. and reduces copper uptake. Soil Biol. Biochem. 41, 930–935.

Zheng, L., Kostrewa, D., Bernèche, S., Winkler, F.K., Li, X.-D., 2004. The mechanism of ammonia transport based on the crystal structure of AmtB of *Escherichia coli*. Proc. Natl. Acad. Sci. USA 101, 17090–17095.

Zhou, Z.S., Huang, S.Q., Yang, Z.M., 2008. Bioinformatic identification and expression analysis of new microRNAs from *Medicago truncatula*. Biochem. Biophys. Res. Commun. 374, 538–542.

Zhu, Y.-G., Miller, R.M., 2003. Carbon cycling by arbuscular mycorrhizal fungi in soil–plant systems. Trends Plant Sci. 8, 407–409.

Zhu, Y.-G., Smith, F.A., Smith, S.E., 2003. Phosphorus efficiencies and responses of barley (*Hordeumvulgare* L.) to arbuscular mycorrhizal fungi grown in highly calcareous soil. Mycorrhiza 13, 93–100.

Zimmermann, P., Zardi, G., Lehmann, M., Zeder, C., Amrhrein, N., Frossard, E., et al., 2003. Engineering the root–soil interface via targeted expression of a synthetic phytase gene in trichoblasts. Plant Biotechnol. J. 1, 353–360.

CHAPTER TWO

Barley Grain Development: Toward an Integrative View

Nese Sreenivasulu,* Ljudmilla Borisjuk,* Björn H. Junker,* Hans-Peter Mock,* Hardy Rolletschek,* Udo Seiffert,† Winfriede Weschke,* *and* Ulrich Wobus*

Contents

1. Introduction 50
2. Barley Grain Development 51
3. 3-D/4-D Models of Developing Barley Grains 55
   3.1. Caryopsis high-resolution 3-D models from serial sections and data integration 55
   3.2. Magnetic resonance-based modeling 57
4. Omics Technologies and Molecular-Physiological Events During Grain Development 59
   4.1. Transcriptome data revisited 59
   4.2. Maternal influences on grain development 60
   4.3. Programmed cell death in maternal tissues and endosperm 64
   4.4. Endosperm transfer cells 66
   4.5. Transcriptional reprograming in endosperm differentiation, seed filling, and sink strength 67
   4.6. Energy provision for storage metabolism 69
   4.7. Roles of hormones and transcriptional networks in differentiation and maturation of endosperm and embryo 72
5. Systems Biology View of Barley Grain Development 77
   5.1. Data generation, storage, integration, and visualization for systems biology 77
   5.2. Modeling 78
6. Concluding Remarks 79
Acknowledgments 81
References 81

* Leibniz Institute of Plant Genetics and Crop Plant Research, Gatersleben, Germany
† Fraunhofer Institute for Factory Operation and Automation IFF, Magdeburg, Germany

International Review of Cell and Molecular Biology, Volume 281
ISSN 1937-6448, DOI: 10.1016/S1937-6448(10)81002-0

Abstract

Seeds are complex structures composed of several maternal and filial tissues which undergo rapid changes during development. In this review, the barley grain is taken as a cereal seed model. Following a brief description of the developing grain, recent progress in grain development modeling is described. 3-D/4-D models based on histological sections or nondestructive NMR measurements can be used to integrate a variety of datasets. Extensive transcriptome data are taken as a frame to augment our understanding of various molecular-physiological processes. Discussed are maternal influences on grain development and the role of different tissues (pericarp, nucellus, nucellar projection, endosperm, endosperm transfer cells). Programmed cell death (PCD) is taken to pinpoint tissue specificities and the importance of remobilization processes for grain development. Transcriptome data have also been used to derive transcriptional networks underlying differentiation and maturation in endosperm and embryo. They suggest that the "maturation hormone" ABA is important also in early grain development. Massive storage product synthesis during maturation is dependent on sufficient energy, which can only be provided by specific metabolic adaptations due to severe oxygen deficiencies within the seed. To integrate the great variety of data from different research areas in complex, predictive computational modeling as part of a systems biology approach is an important challenge of the future. First attempts of modeling barley grain metabolism are summarized.

Key Words: Barley grain development, 3-D/4-D grain models, Maternal tissues, Programmed cell death, Abscisic acid, Seed maturation, Transcriptome, Metabolic modeling, Systems biology.

1. Introduction

Seeds are complex structures to aid plant dispersal and hold developmental processes to withstand severe environmental conditions. They are at the same time our most important food and feed mainly derived from cereals. Among the cereals, barley is both an important crop (Baik and Ullrich, 2008) and a model for cereal genetics and genomics (Sreenivasulu et al., 2008a). Due to the economic importance and the central role in plant reproduction, numerous studies have dealt with grain development under controlled and different environmental conditions. Recent rapid development of new techniques from high-throughput genomics and post-genomics technologies to nondestructive imaging provides numerous additional data and paves the way for a much deeper understanding of the developing seed in which parallel or time-shifted interconnected physiological processes occur in different tissues. Especially, the omics

technologies became the data-generating workhorses of a more holistic systems approach to seed biology. However, the exploration of cereal seed development with the new technologies is still inadequately advanced; most studies have focused on the model plant *Arabidopsis*. Nevertheless, we can already start to integrate genetic, molecular, biochemical, physiological, and histological data with the help of various computing tools. One tool for global data integration is the recently developed 3-D morphological grain models, extended to the fourth, the time dimension (Section 3). Such models are especially helpful since a major obstacle in the analysis of grain development is the complex nature of a grain. A detailed histological study of barley caryopsis development between anthesis and early maturation revealed at least 18 different tissues and tissue complexes (Gubatz et al., 2007) but even within a single tissue such as the endosperm biochemical and physiological gradients have been detected (Rolletschek et al., 2004). Therefore, we will place special emphasis on spatial aspects whenever data are available. Manually dissected maternal and filial barley grain tissues (Sreenivasulu et al., 2006) as well as two laser-microdissected transport-related tissues, nucellar projection (NP) and endosperm transfer cells (ETC) (Thiel et al., 2008), revealed not only extensive tissue-specific transcriptome but also biochemical data, and an *in silico* comparison with *Arabidopsis* seed tissue-specific transcriptome data (Section 4.7.3) underlined the importance of a spatially differentiated view.

Transcriptome studies unfolded a considerable potential to integrate a multitude of observations due to its global character even if the evidence provided for specific processes and regulatory networks is generally only of correlative nature. Since a single review cannot cover all relevant areas, we had to restrict ourselves to certain aspects, and we chose those that the authors have worked on during recent years with the goal to integrate molecular, biochemical, physiological, histological, and cell biology data. Besides model development, special emphasis is also placed on the molecular mechanisms and regulatory cascades influencing programmed cell death (PCD) events in different grain tissues and on processes involved in seed filling. Furthermore, first attempts to develop predictive models for barley grain metabolism are summarized. Although this review is devoted to barley grain development, we will often refer to studies on other cereals and sometimes also to evolutionary less-related plants if these data significantly broaden our view.

2. Barley Grain Development

The barley grain is a fruit in which pericarp and seed coat (testa) are fused to form a caryopsis. Its development is usually divided into three to four stages: prestorage (or cell division or morphogenesis) phase, storage

(or maturation) phase, and desiccation (or late maturation) phase. Based on the massive transcriptional reprograming between prestorage and storage phase, this time span has been defined as a distinct transition or intermediate phase (Sreenivasulu et al., 2004). Gross morphological and histological changes during development of the barley grain have been described (Bethke et al., 2000; Evers and Millar, 2002; Wobus et al., 2005) and are illustrated in Fig. 2.1. In the following, we delineate grain development from fertilization to the early storage phase in some detail to better understand tissue interactions and respective molecular-physiological processes discussed later.

At the time of double fertilization, the diploid zygote together with the triploid nucleus of the central cell, the antipodal cells, and the synergids are surrounded by the maternal nucellus and embedded into the embryo sac demarcated by the inner and outer integument. At anthesis, style and pericarp/testa (for simplicity abbreviated ''pericarp'') represent more than 90% of the maternal gametophyte; cells of the style contain high amounts of starch (Weschke et al., 2000). Continuous cell division in the absence of cell wall formation leads to the endosperm coenocyte (Olsen, 2001, 2004). Under defined conditions, the coencytic phase lasts for about 60 h (Engell, 1989). Between anthesis and beginning endosperm cellularization, style volume scales down and pericarp grows in most of its parts by cell division and elongation. In cells surrounding the lateral vascular bundles, storage product accumulation takes place (Weschke et al., 2000). The most endosperm-near parts of the maternal nucellus undergo PCD (D. Weier, unpublished results) followed by cellular disintegration. Only the nucellus parts facing the main vascular tissue do not disintegrate but differentiate into the NP, that maternal tissue releases nutrients into the apoplastic space between the maternal and the filial seed part. At 3 days after flowering (DAF), when cellularization of the endosperm coenocyte starts in the middle of the caryopsis opposite NP (Fig. 2.1B), cells of that region differentiate into the ETC. The process of endosperm cellularization spreads into lateral as well as central parts and is finished at about 4–5 DAF (Fig. 2.1C). Typically, endosperm cellularization is accompanied by pericarp elongation, but at the same time remobilization processes take place in dorsal cell rows adjacent to the endosperm (Radchuk et al., 2009).

Cellularization and increasing sink strength of the endosperm are tightly coupled to differentiation and function of the transfer tissues, that is, NP and ETC (Fig. 2.2). Predetermination to become ETC of that region adjacent to the developing NP starts during the syncytial stage (Olsen, 2004). Completed endosperm cellularization coincides with the end of the prestorage phase and represents the beginning of the transition from cell division/elongation into storage product accumulation (Sreenivasulu et al., 2006). This transition phase (7 DAF in Fig. 2.1D) is characterized by internal cell divisions and starch accumulation beginning within the central

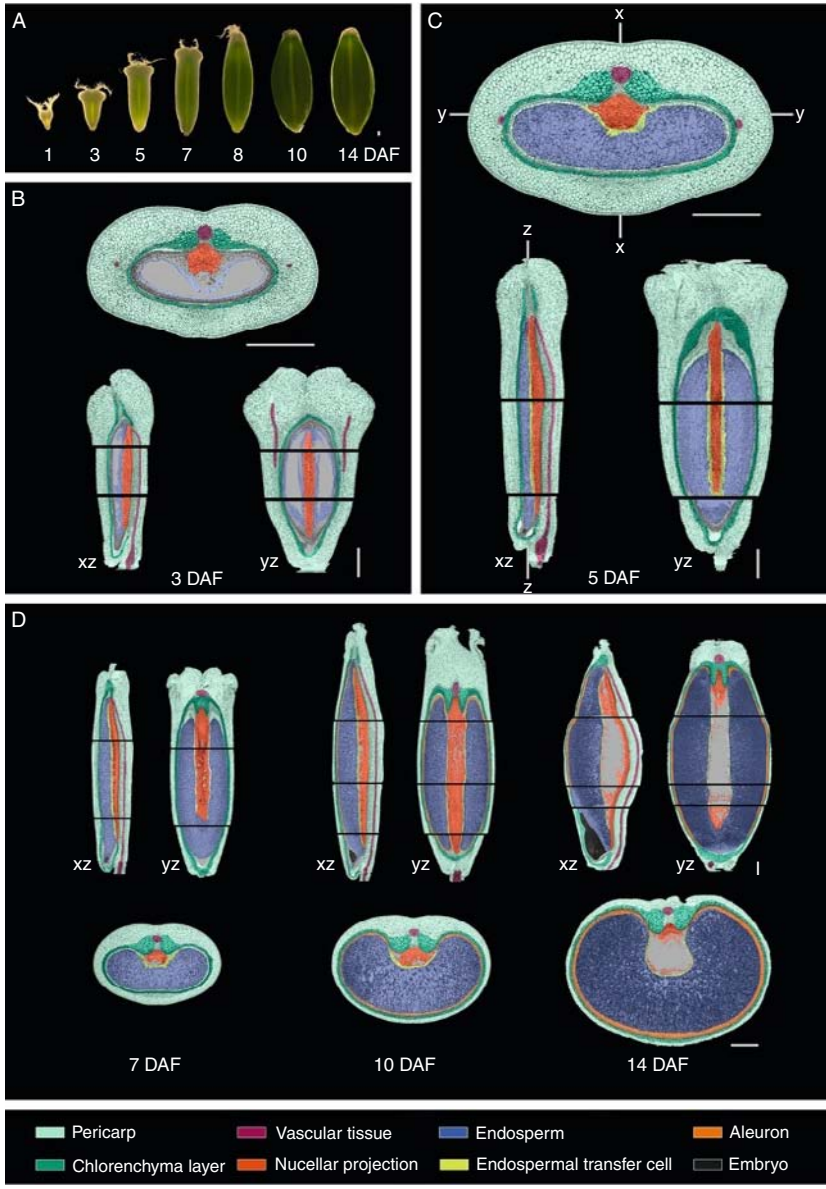

Figure 2.1 The developing barley grain. (A) Barley grains at different developmental stages. Glumes and awn were removed before taking photographs. (B)–(D) Median transverse, longitudinal (xz), and saggital (yz) sections of barley grains at different developmental stages. The x, y, and z position of the sections is given in (C). Longitudinal and saggital sections are created from simulated artificial grains generated by a combination of thin transverse sections from plastic-embedded material. Black bars dividing the longitudinal and saggital sections into pieces result from cutting of the native caryopses necessary for optimal fixation and embedding. Colors representing individual tissues are shown at the bottom panel of the figure. The white patches within the nucellar projection in (D) indicate degeneration of tissue resulting into the endosperm cavity. Bars, 500 μm. DAF, days after flowering.

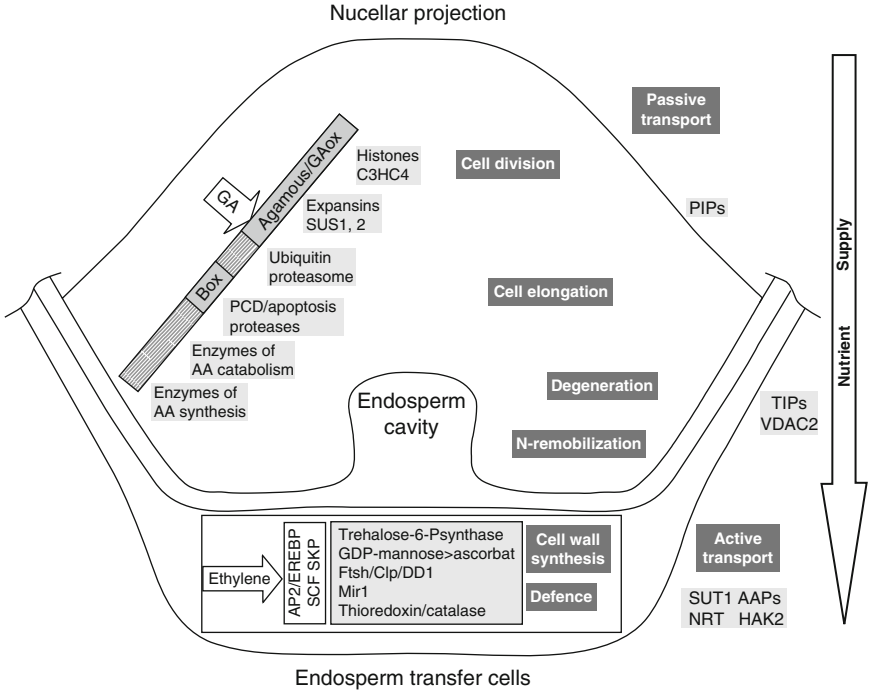

Figure 2.2 Scheme of cellular processes in nucellar projection (NP) and endosperm transfer cells (ETC) at 8 DAF as deduced from transcriptome analysis. NP consists of three different zones reflecting a differentiation gradient (cell division, cell elongation, and degeneration). Light gray left side boxes indicate upregulated gene sets whereas dark gray right side boxes indicate molecular-physiological events. Transcriptome analysis suggests a role for gibberellins (GA) in the establishment of this gradient. Genes involved in cell death-related proteolysis coupled to nitrogen (N) remobilization may be related to the disintegrating part facing the endosperm cavity. Ethylene-related processes in ETC are potentially controlled by trehalose-6-phosphate signaling. Upregulation of transport protein genes indicates nutrient uptake from the apoplastic space into the endosperm (based on Thiel et al., 2008; see text for further explanations). AAP, amino acid permease; HAK, Na^+-sensitive K^+ transporter; NRT, nitrate transporter; PIPs, plasma membrane intrinsic proteins; SUT, sucrose transporter; TIPs, tonoplast intrinsic proteins; VDAC, voltage-dependent anion channels.

part of the starchy endosperm, by differentiation of the outermost cell rows of the endosperm into aleurone cells and by massive remobilization and degeneration processes in the pericarp. During further development, cellular disintegration diminishes nearly the complete pericarp except (i) those regions flanking the main vascular bundle and (ii) the chlorenchyma represented by the innermost green cell rows of the pericarp (Fig. 2.1D). From 10 DAF onward, caryopsis volume increases mainly by thickening of the starchy endosperm (compare 10 DAF to 14 DAF; Fig. 2.1D). Correspondingly,

pericarp disintegrates further, giving space to the filling endosperm. Persisting epidermal cell rows and the inner integument become main parts of the husk of the ripe grain. Following a differentiation gradient spreading against the outer cell rows, cells of the starchy endosperm (for simplicity abbreviated ''endosperm'') accumulate large quantities of starch but also a variety of storage proteins (prolamins, α-globulins, and 11S legumin; Weber et al., 2010). High storage capacity of endosperm cells might be coupled to endoreduplication (Edgar and Orr-Weaver, 2001; Larkins et al., 2001). Like in wheat (Chojecki et al., 1986), barley endosperm undergoes four rounds of endoreduplication reaching a 48 C ploidy level (Our unpublished results). During early- and mid-storage phase, the endosperm grows rapidly but eventually undergoes PCD with the exception of the aleurone (Buckner et al., 2000). Aleurone, like the embryo, acquires desiccation tolerance. Both tissues ensure continuation of the life cycle through the onset of germination under favorable conditions.

3. 3-D/4-D Models of Developing Barley Grains

Proper understanding of organ development is only possible on the basis of detailed morphological and histological studies. Hence, 3-D reconstructions are especially helpful. With respect to barley grains, first efforts were made to model grain development in 3-D based on ^{1}H NMR studies (Glidewell, 2006) and serial sections (Gubatz et al., 2007). A 4-D atlas comparable to that existing for mammals is under development and will be described below.

3.1. Caryopsis high-resolution 3-D models from serial sections and data integration

High-resolution 3-D models from serial section data are available for anthesis, 3 DAF, and 7 DAF representing the maternal gynoecium before pollination, the developing grain at the beginning of endosperm cellularization, and the transition between the prestorage and storage product accumulation phase, respectively (Gubatz et al., 2007; http://3d-barley.ipk-gatersleben.de/). These models are carefully and extensively segmented to show anatomic details of the developing grain. However, the highly laborious and time-consuming process of model generation needed automation to be viable for the establishment of a 4-D atlas that necessarily has to cover all phases of grain development and to take into account individual variations at specific developmental phases.

The hereupon developed automated tool mainly comprises two modules: (1) automated segmentation, that is, the assignment of a logical

entity, such as a particular tissue, to each spatial location and (2) 3-D registration of all separately acquired (2-D) image slices, that is required in case of nonnative 3-D imaging (Bollenbeck and Seiffert, 2008). Histological sectioning along with light microscopy provides at least about 1 order of magnitude higher spatial resolution than typical 3-D imaging technologies that are commonly utilized in medical applications.

Of particular importance in this context is the transfer of available histological knowledge from the biological expert into an automated modeling procedure. Since this knowledge is usually not given explicitly, for example, in terms of mathematical equations, but rather by means of a limited number of manually created sample references, methods of computational intelligence, such as machine learning and artificial neural networks, can beneficially be utilized here (Bollenbeck and Seiffert, 2009). Moreover, biological variability of different individuals needs to be incorporated in the modeling procedure by means of a statistical assessment (Bollenbeck et al., 2009c) in order to turn an individual model into an interindividual atlas. As one result of this assessment, traditional crisp segmentation (Gubatz et al., 2007) is extended to fuzzy segmentation (Seiffert and Bollenbeck, 2008) in a way that each spatial or spatiotemporal position is assigned to a vector containing the probability of belonging to a particular tissue. The resulting interindividual model now also contains, in addition to the spatial distribution of relevant tissues, a statistical measure of interindividual variation.

Such anatomical models now cover barley grain development from anthesis up to the linear increase of storage product accumulation representing specifically the developmental stages anthesis, 3, 5, 7, 10, and 14 DAF. The resulting time-discrete 4-D atlas contains anatomical and histological details and represents a basic framework for data integration (Bollenbeck et al., 2009b). Detailed knowledge about ratios of tissue volumes and their changes during development allows calculation of developmental gradients of gene product distribution, for instance, from qRT-PCR data generated from cellular regions extracted by microdissection (Thiel et al., 2008).

At present, especially 2-D *in situ* gene expression or immunolocalization patterns are targets for integration into 3-D/4-D models (Gubatz et al., 2007; Lee et al., 2006). An especially rich dataset is available for wheat caryopsis development; gene expression patterns of several hundred genes have been determined by *in situ* hybridization (Drea et al., 2005). A method upcoming now called MALDI imaging (Cornett et al., 2007) can generate 2-D molecular mass distribution patterns of hundreds of molecular species in frozen sections in which histological structures are preserved to a certain extent. It complements and vastly extends methods based on bioluminescence single photon counting (Borisjuk et al., 2002; Rolletschek et al., 2004). MALDI imaging patterns have already been integrated into structural 3-D models of barley caryopses (Bollenbeck et al., 2009a; Fig. 2.3).

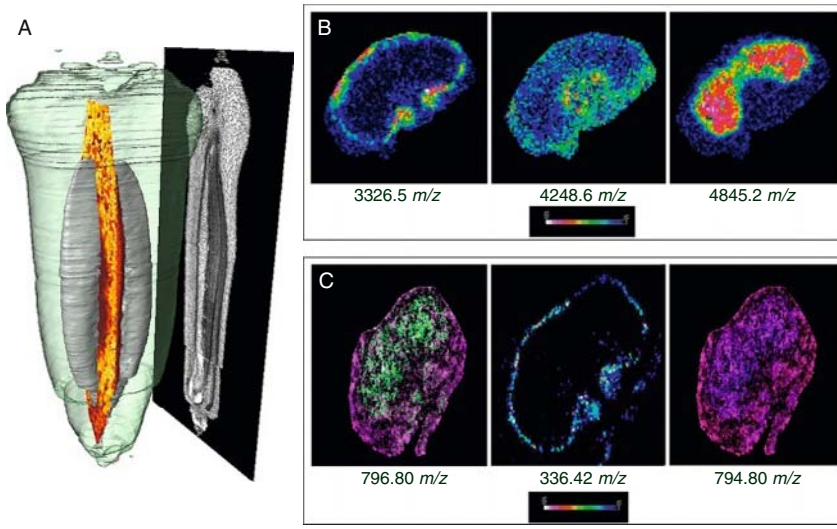

Figure 2.3 Model of an individual barley grain at 7 DAF with an integrated matrix-assisted laser desorption/ionization imaging mass spectrometry (MALDI-IMS) median section visualizing the distribution of an unidentified substance of a mass of $m/z = 9.595$ and a simulated median section (A) and MALDI-IMS cross sections depicting yet unidentified peptides (B) or low-molecular-weight compounds (C). Images were taken with spatial resolutions of 50 μm (B) or 15 μm (C).

3.2. Magnetic resonance-based modeling

4-D modeling based on 3-D images of caryopses needs fine-tuned developmental resolution, especially for early stages when tremendous changes have to be considered in particular for the filial grain part. The necessary high amount of individual 3-D images speaks against usage of serial section data models. Furthermore, chemical influences from fixation and embedding change internal structures as well as outer contours of the young caryopses. High-resolution ^{1}H NMR images reflect the *in vivo* situation and can be established within hours. To mimic the growing barley grain, 16 ^{1}H NMR volumes were acquired, covering development from anthesis to beginning desiccation, and combined to get a virtual impression of the growing grain (Pielot et al., 2008).

^{1}H NMR measurements provide 3-D information of living material in a nondestructive manner, but are of no relevance for any scientific interpretation without precise 3-D structural information that they can be referred to. Therefore, matching of anatomical 3-D models into the virtually growing NMR grain is highly desirable. First, development of the respective tools will visualize changing patterns of proton distribution in the developing

caryopsis. Considering proton/water distribution as signal labeled cellular structures/tissues might be interpreted as being in tight relation to changing metabolite distribution, and therefore, highly relevant for barley grain development. Secondly, available tools can also bring distribution patterns of key metabolites, determined by NMR or other nondestructive methods, into the precise histological context. Such patterns are just becoming available (Melkus et al., 2009; Neuberger et al., 2008, 2009). Notably, the first noninvasive quantitative visualization of lipid using NMR was performed on living barley seeds (Neuberger et al., 2008; Fig. 2.4). Steep gradients in local oil storage were defined at organ- and tissue-specific scales and at a variety of stages. These gradients were closely coordinated with tissue differentiation and seed maturation, as revealed by electron microscopy and biochemical and gene expression analysis. The method can be used to follow the fate of storage lipids during deposition and subsequent mobilization (Neuberger et al., 2008, 2009). Technical advance will result in higher resolution and sensitivity allowing in future visualization of distribution patterns of many substances in biological objects in a noninvasive way *in vivo* without interrupting growth and development.

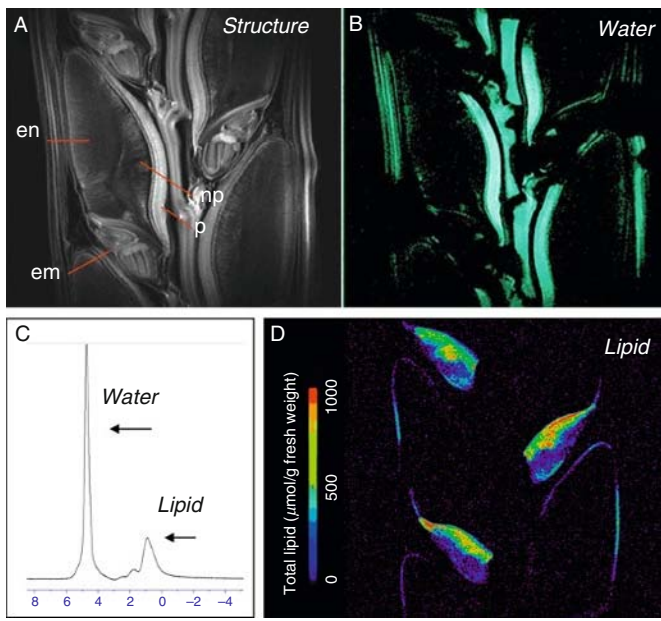

Figure 2.4 Noninvasive visualization of a barley spike section using nuclear magnetic resonance (NMR). (A) Internal grain structure *in vivo* at 35 μm resolution; (B) visualization of the *in vivo* water distribution; (C) water and lipid peaks in the NMR spectrum; (D) quantitative map representing the *in vivo* lipid deposition within grains (mainly within the embryo and the aleuron layer). Lipid content is color-coded. Abbreviations: em, embryo; en, endosperm; np, nucellar projection; p, pericarp.

4. Omics Technologies and Molecular-Physiological Events During Grain Development

Recent advances in high-throughput technologies offered new prospects to study developmental and molecular-physiological processes such as seed development. With respect to barley, first an expressed sequence tags (EST) resource was established (>501,000 as of December 2009, http://www.ncbi.nlm.nih.gov/dbEST/dbEST_summary.html). More than 156,000 of these sequences were generated from developing and mature seeds represented in 38 cDNA libraries. Using an EST dataset generated from different tissues covering the plant's life cycle from cultivar ''Barke,'' genes preferentially expressed in seed tissues were identified (Zhang et al., 2004). These ESTs together with other available unigene sets from ''HarvEST:barley'' assemblies (www.harvest-web.org) have been anchored to a physical map to identify gene-rich regions. Currently, the identified BAC-based gene-rich regions are subjected to sequencing in a coordinated effort of the International Barley Sequencing Consortium (Schulte et al., 2009). A recent update on barley genomics and available genomic resources has been published by Sreenivasulu et al. (2008a).

The rich EST resource allowed the establishment of transcriptome platforms such as cDNA-based macro arrays (e.g., a 12K macro array) mainly representing sequences from developing seed tissues (Sreenivasulu et al., 2004, 2006) as well as oligonucleotide-based 22K Affymetrix arrays (Druka et al., 2006; Sreenivasulu et al., 2008b; Wan et al., 2008) to study global gene expression. Extensive analyses on barley seeds at the proteome level including different seed tissues (Finnie and Svensson, 2003) have also been carried out (Finnie and Svensson, 2009). However, in-depth studies on the same plant material to correlate in detail transcriptome with proteome and additionally metabolome data as published for maize (Prioul et al., 2008) are still lacking.

4.1. Transcriptome data revisited

The complex tissue composition described above suggests cross talk between maternal and filial tissues during development. To gain first insights into underlying mechanisms, transcription profiling data of five major grain tissues were explored to identify parallel and time-shifted molecular-physiological events reflected in the transcriptome. All transcriptome data obtained from a total of 34 experiments using hand-isolated maternal pericarp, filial endosperm, and embryo (Sreenivasulu et al., 2006) as well as microdissected NP and ETC (Thiel et al., 2008) were

reanalyzed and used to derive tissue-specific coexpression networks and to identify overrepresented functional categories of genes thought to mirror characteristic molecular-physiological events. The results are summarized in Fig. 2.5. These data together with histological details (Gubatz et al., 2007), spatial gene expression patterns (Radchuk et al., 2009; Weschke et al., 2000, 2003) as well as spatial information regarding ATP distribution, O_2 gradients, starch accumulation (Rolletschek et al., 2004), and lipid concentration patterns detected by NMR (Neuberger et al., 2008) allowed to address the following four major questions: (i) What are the maternal influences on grain development? (ii) How does PCD operate in maternal seed tissues and endosperm and what are the connected signaling events? (iii) What metabolic, hormonal, and regulatory networks are connected to storage processes in endosperm and embryo? and (iv) What can one learn from such studies about seed energy metabolism as related to storage events?

4.2. Maternal influences on grain development

4.2.1. Role of pericarp

During early development (anthesis until complete endosperm cellularization around 4 DAF), pericarp dominates the young grain and acts as the major sink (Radchuk et al., 2009; Weschke et al., 2003). It consists of several layers of parenchymatic cells including the inner chlorenchyma and the vascular tissues (Gubatz et al., 2007). Nutrients are supplied to the pericarp via the main vascular tissue and the minor lateral and dorsal vascular bundles. At 0–4 DAF, genes connected to sucrose partitioning, transient starch accumulation, and photosynthesis as well as mitochondrial mediated ATP production pathways are preferentially expressed in pericarp tissue (Fig. 2.5). Sucrose cleavage and channeling is mainly mediated by cell wall invertase HvCWINV2 and two enzymes involved in fructan biosynthesis (Hv1-SST, Hv6-SST), which are closely related to vacuolar invertases. Along with them, the hexose transporter HvSTP2 was found to be preferentially expressed throughout the pericarp, whereas *HvSTP1* transcripts were distinctly localized in the syncytium and later also in the NP (Weschke et al., 2003). This scenario suggests that sucrose coming into the developing grain is first used to create hexose gradients promoting cell division events (Weber et al., 2005; Wobus et al., 2005). Eventually, hexoses will also be used for fructan and transient starch biosynthesis in pericarp cells. Starch synthesized and transiently stored near the lateral and main vascular bundles will be mobilized from 4 DAF onward when starch accumulation starts in the central regions of the endosperm (Radchuk et al., 2009; Sreenivasulu et al., 2004; Weschke et al., 2000; Wobus et al., 2005). Starch degradation in the pericarp is due to an activation of α-amylases, AMY1 and AMY4, as deduced from transcript studies (Radchuk et al.,

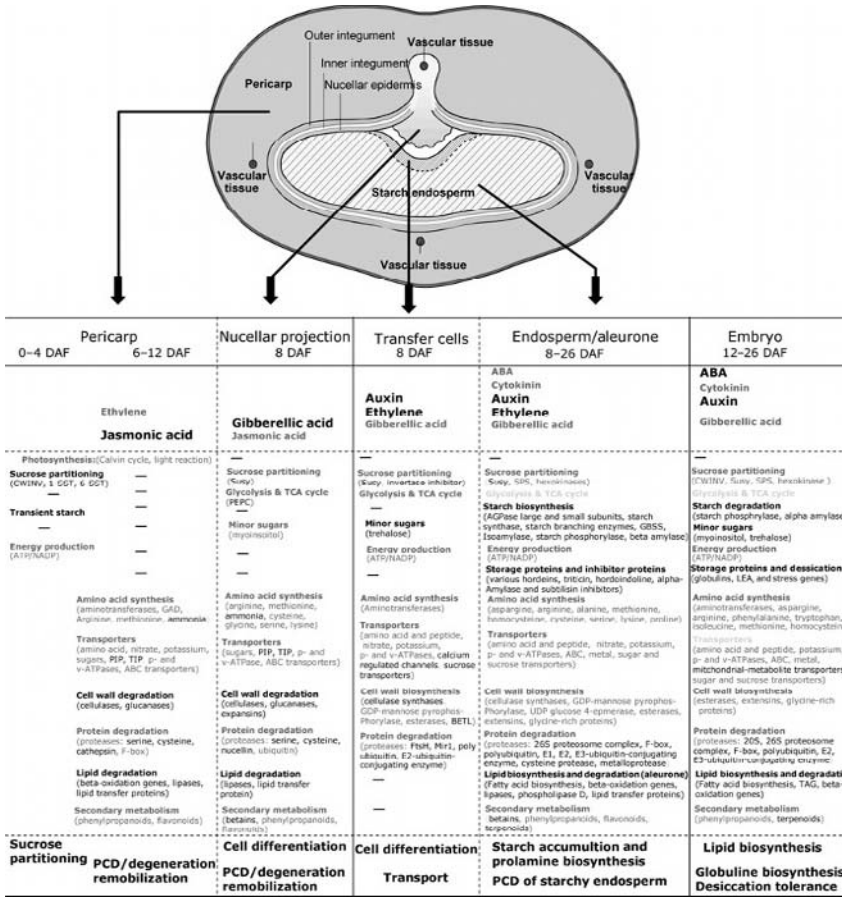

Figure 2.5 Major molecular-physiological events reflected in different grain tissues during barley caryopsis development (0–26 days after flowering; DAF) as revealed by transcriptome analysis. In the upper panel, a schematic representation of a barley caryopsis cross section at 6 DAF is used to show different grain tissues. The tissue-specific processes as well as parallel/time-shifted molecular-physiological events revealed by reanalyzing the transcriptome data of three major tissues (hand-dissected pericarp during 0–12 DAF, endosperm/aleurone fraction during 8–26 DAF, and embryo from 12 to 26 DAF from Sreenivasulu et al. (2006)) and two transport-related tissues (laser capture microdissected probes from nucellar projection and endosperm transfer cells of 8 DAF from Thiel et al. (2008)). The data from all five tissues were first quantile normalized and low-expressed genes were eliminated. Eventually, coexpression patterns were revealed, the enrichment of functional categories derived and assigned to known processes. Functional categories specific for a certain tissue and/or developmental phase are highlighted in bold black and the common subsets of functional categories/genes are shown in gray. The upper panel indicates hormone biosynthesis, the middle panel indicators of primary and secondary metabolism, and the bottom panel summarizes major molecular-physiological events for a given tissue and/or developmental stage.

2009). In addition, proteins are mobilized by specific C1 cysteine proteases (SAG12, Cys-EP, RD19A, γ-VPE), cathepsin, and serine as well as F-box COI1 and FBL3 proteases (Sreenivasulu et al., 2006; Fig. 2.5). Also δ-VPE, a specific vacuolar-processing enzyme related to PCD (Nakaune et al., 2005), is expressed in the pericarp, namely, in that part where tissues of the main vascular bundle differentiate first (D. Weier and W. Weschke, unpublished). In general, the relative amount of assimilates uploaded from the pericarp after remobilization should be rather small and of minor influence on grain development. However, careful analyses of the percentage of compounds imported from different tissues into the developing endosperm are missing.

4.2.2. Role of nucellus

During early grain development, the lack of a fully differentiated main vascular bundle, missing functional transfer tissues connecting the main vascular bundle with the filial grain part, and the presence of cuticular layers between pericarp and filial tissues hinder direct cell-to-cell nutrient transfer. This raises a major question: what feeds syncytial and cellularizing endosperm? The answer could be the nucellus, a tissue of maternal origin located between integuments and plasma membrane of the embryo sac mother cell. Already at anthesis, starch granules are detectable in nucellus cells. Those granules undergo rapid degradation, as indicated by α-amylase AMY4 transcripts, localized there at 2 DAF (Radchuk et al., 2009). Nucellin, an aspartase protease-like protein, has been linked to nucellus degradation (Chen and Foolad, 1997) and its mRNA labels only nucellar tissue in a specific pattern (Gubatz et al., 2007). In a transcriptome study, nucellin mRNA clustered during 0–4 DAF together with three different members of γ-VPE-type cysteine proteases and a subtilisin-like serine protease, all possibly involved in nucellus PCD-like degradation processes. These genes are all related but different from similar genes involved in pericarp PCD (Sreenivasulu et al., 2006). Jekyll, a protein involved in degradation processes in the NP (Radchuk et al., 2006), is also expressed in the nucellus together with nucellain (Linnestadt et al., 1998) and other γ-VPE proteases. These observations point to fine-tuned developmental regulation of the nucellar disintegration process. Nutrients originating by this process might be directly uptaken by transporters present in the plasma membrane of the embryo sac mother cell (Weschke et al., 2003).

Because of its basic importance for nourishment of the early endosperm, nucellus tissue might be the most presumable source of gametophytic influences on grain development, a conclusion backed by histological data. The cell rows of the inner and outer integument are connected only to the nucellus and later on, the NP (Gubatz et al., 2007). Hence, division and elongation of integument cells between anthesis and 4 DAF depend exclusively on remobilized nutrients of the disintegrating nucellus and

subsequent direct cell-to-cell nutrient transfer from the NP. The number and size of nucellus cells, that is, the respective amount of compounds accumulating before fertilization and becoming remobilized between anthesis and completed endosperm cellularization (4 DAF), might predetermine the number of nuclei produced in the syncytial endosperm and the number of primary endosperm cells. They thus could be an important determinant of seed sink strength.

4.2.3. Role of nucellar projection

The NP is a heterogeneous tissue consisting of three different zones and at least four different cell types: an upper zone with meristematic cells undergoing active cell division, a middle zone with differentiating/elongating cells, and the bottom zone with cells showing wall ingrowths and autolysing cells positioned adjacent to the endosperm cavity (Fig. 2.2). NP shows remarkable alterations in shape during development. It is roundish at the end of the prestorage phase (5 DAF). Preferred cellular disintegration of the middle part starting during the transition phase (7 DAF) produces a two-lobe structure resulting in a huge endosperm cavity and only a thin seam of cells at the NP edges (14 DAF in Fig. 2.1D) that might be responsible for nutrient transfer at the end of the filling phase. Whether shape alterations are accompanied by changes of the regulatory programs and nutrient release adapted to the development-specific nutrient demand of the growing grain is unknown.

Establishment of NP functionality is tightly linked to an increasing nutrient demand of the endosperm at the beginning of storage product accumulation around 7 DAF (Weschke et al., 2000). Details of the role of this tissue have been deduced from functional as well as laser-microdissection and subsequent transcript profiling studies (Radchuk et al., 2006; Thiel et al., 2008, 2009). Like in pericarp, genes related to cell wall, protein, and lipid degradation are activated in the NP. High expression, especially of genes encoding different members of the ubiquitin proteasome system, points to early proteolytic processes, which are rather coupled to cellular differentiation than PCD. The high transcriptional activity of gibberellic acid (GA) metabolism genes suggests a role in establishing and maintaining differentiation of mitotically active into elongating cells. In addition, expression of aspartic proteinase (nucellin), C13 cysteine proteinase VPE (nucellain), and cysteine proteinase RD19A were noticed (Fig. 2.5). As discussed for nucellus tissue these proteases are indicators for PCD. In parallel, activation of amino acid biosynthesis and catabolism genes takes place, hinting at the importance of nitrogen remobilization events coupled to PCD (Fig. 2.5). In this context, preferential expression of glutamine synthetase, phosphoenol pyruvate decarboxylase (PEPC), important TCA cycle genes such as aconitate hydrolase and NADP-malic enzyme was found indicating refixation of ammonia into

glutamate and glutamine, major sources of nitrogen, which can be easily taken up by the developing endosperm. Most of the transport proteins expressed in NP belong to the aquaporin family. This points to rather passive than to proton-coupled active processes. Plasma membrane intrinsic protein (PIP), tonoplast intrinsic protein (TIP), and voltage-dependent anion-selective channels (VDAC) are expected to facilitate the transport of remobilized compounds from the lytic cells as well as anions across mitochondrial membranes during apoptosis (Thiel et al., 2008). NP cells also function as metabolic interface to precondition amino acid supply of the endosperm as suggested by transcript profiling data and amino acid measurements (Thiel et al., 2009; Fig. 2.2).

4.3. Programmed cell death in maternal tissues and endosperm

According to present knowledge, PCD occurs in various grain tissues with the exception of ETC, aleurone, and embryo. Comprehensive reviews on PCD events during reproductive development and in developing seeds were published by Riggs (2004) and Gallie (2004). As briefly described above, maternal grain tissues undergo developmental PCD sequentially first in the nucellus immediately after the onset of fertilization and then in both NP and pericarp. In all these maternal tissues, PCD leads to degeneration of an entire tissue by the disappearance of cell walls and the remobilization of the cellular content. However, initiation and regulation of these processes seems to be rather tissue-specific and needs further investigation. By contrast, PCD initiated in the filial endosperm upon seed filling is quite different since the cell constituents remain intact after cell death (Young and Gallie, 2000b).

Based on transcriptome studies, degeneration of maternal tissues is tightly coupled to the activation of hydrolases as α-amylase, various cellulases, and glucanases involved in cell wall degradation, lipases, and PCD marker genes of the proteolytic machinery (serine, cysteine, cathepsin, and nucellin/aspartic proteases) in the nucellus during 2–3 DAF (Sreenivasulu et al., 2006), pericarp during 8–12 DAF, and in NP during 8 DAF (Fig. 2.5). Instead, PCD processes in the starchy endosperm are rather characterized by selective proteolysis executed mainly by the proteosome complex, ubiquitin pathway, and F-box protein machinery (Sreenivasulu et al., 2006). One of the primal causes of the persistence of endosperm tissue during seed maturation might be connected to the suppression of α-amylase activity by preferentially expressed α-amylase inhibitors. The assumption of an important role of α-amylase in cell death is supported by the observation that in the aleurone of wheat genotypes with premature α-amylase activity, pockets of dying cells are already observed during grain maturation (Mrva et al., 2006). The same lines

exhibit a premature sprouting phenotype. Normally, the enzyme is activated in the aleurone during imbibition. Based on these correlative evidences, we hypothesize that α-amylase does not only mediate mobilization of stored starch granules but might also trigger lytic events during PCD resulting in tissue degradation during seed development and germination.

Which signals (hormones and connected regulators) are responsible for the onset of PCD in the different maternal tissues and the distinct PCD events in the endosperm? Based on the available tissue-specific transcriptome data, we can tackle these questions by the ''guilty-by-association'' approach considering mostly the two maternal tissues pericarp and NP and the endosperm. Transcript profiling and hormone measurements showed that in the degenerating pericarp during 8–14 DAF together with lipolysis the jasmonic acid (JA) pathway is activated with correspondingly high levels of OPDA (12-oxo-phytodienoic acid) and JA. Precursors of JA biosynthesis are seemingly provided by lipoxygenases as part of the lipid degradation machinery both in degenerating pericarp and NP. In addition to JA biosynthesis genes, genes of the ethylene biosynthetic pathway and ethylene signal transduction pathways are operative in degenerating pericarp (Sreenivasulu et al., 2006). Interestingly, the same preferential activation of lipolysis and JA as well as ethylene pathways was found in degenerating NP tissue (Fig. 2.5), hinting at certain commonalities between disintegration processes in pericarp and NP. Besides the quite abundant JA, several fatty acids resulting from lipolysis might be involved in signaling in degenerating seed tissues as proposed for leaf senescence (Berger et al., 2001; Overmyer et al., 2003). Taken together, the discussed results suggest that both JA and ethylene are involved in regulating PCD in pericarp and NP. With respect to key transcription factors, we noticed coexpression of an agamous MIKC-type MADS-box TF and TF FBP7 together with nine MADS-box TF in both pericarp and NP tissues undergoing PCD. In maize, MIKC-type ZmMADS2 has been shown to be involved in PCD during anther dehiscence (Schreiber et al., 2004), and in petunia TF FBP7 and 11 were found to be expressed in ovules. Their suppression leads to degeneration of the endosperm (Colombo et al., 1997), suggesting a function in regulating maternal–filial growth relationship.

Contrary to maternal PCD, endosperm PCD is accompanied by the expression of ethylene biosynthesis and signal transduction components and a clear suppression of genes involved in lipolysis and JA biosynthesis. However, the ethylene biosynthesis and signaling gene family members expressed in pericarp are distinct from the ones expressed in endosperm tissue (Sreenivasulu et al., 2006). Together with ethylene-related genes, abscisic acid (ABA) and auxin biosynthesis genes are activated in the endosperm. ABA may modulate ethylene production as deduced from experiments in maize. Also the *vp1* (ABA-insensitive) and *vp9* (deficient in ABA biosynthesis) maize mutants lead to a two- to fourfold increase in

ethylene production coinciding with the premature onset of internucleosomal fragmentation and PCD (Young and Gallie, 2000a,b). Therefore, a fine-tuned balance of ABA and ethylene seems to orchestrate the timing of PCD in endosperm.

4.4. Endosperm transfer cells

Coordinated establishment and differentiation of filial endospermal transfer cells (ETC), which critically influence grain filling (Royo et al., 2007), starts opposite to the developing NP already during the syncytial stage (Olsen, 2004). A scheme of the NP/ETC ''complex'' with indicated functions is given in Fig. 2.2.

ET cells become functional concomitant with the development of cell wall ingrowth to increase transport active surfaces in accordance with their role in nourishment and solute supply (Offler et al., 2003; Thompson et al., 2001; Weschke et al., 2000). Regulation of ETC differentiation was not analyzed so far. However, ectopic expression of the transfer cell-specific transcriptional activator Myb-related protein-1 (MRP-1) is sufficient to temporally transform epidermal cells of the maize endosperm into transfer cells (Gómez et al., 2009).

Laser microdissection followed by transcript profiling of barley ETC at 8 DAF identified key processes active in ETC at the beginning of storage product accumulation in the barley endosperm (Thiel et al., 2008). As suggested by these data, sucrose is taken up by an H^+-dependent sucrose transporter as well as various kinds of nitrogen compounds (amino acids and nitrate) by various amino acid, peptide, and nitrate transporters (Fig. 2.5). In addition, calcium-regulated channels and Na^+-sensitive K^+ transporter are preferentially activated in ETC. As proposed by Zhang et al. (2000, 2002), these cation transporters may help to coordinate the sucrose influx via pH within the transfer cells by taking up the sucrose from the endosperm cavern. Interestingly, in legume seed coats, two types of sucrose transporters are expressed: (a) the well-known sucrose/H^+ symporter highly dependent on energy as PvSUT1 and (b) transporters facilitating the pH- and energy-independent bidirectional diffusion of sucrose as, for instance, PvSUF1 (Zhou et al., 2007). Whether such a system also exists in barley has yet to be revealed.

Upregulation of sucrose synthase (Fig. 2.5) provides UDP-D-glucose, the prerequisite substrate for cellulose synthase. Among genes preferentially expressed in ETC are specific members of cellulose synthase (homologous to AtCslA02, AtCslA03, AtCslA09), GDP-mannose pyrosphosphorylase, esterases, and polygalacturonase genes active in cell wall biosynthesis. These gene family member genes are distinct from those expressed in the endosperm, as for instance, cellulose synthase members homologous to AtCesA05 and AtCslD2. The discussed findings highlight the importance

of specific gene family members in promoting the differentiation of the specialized cell walls of ETC. Barley ETC also express specific genes such as BETL (cysteine-rich cell wall polypeptides) and invertase inhibitor genes as known from maize (Costa et al., 2003) and wheat (Drea et al., 2005).

Of special interest is the prominent expression of sequences related to type II trehalose-6-phosphate synthase/phosphatase genes (*TPS/TPP*). The respective enzyme/s produce trehalose by converting Glc-6-P into trehalose-6-P, which is subsequently dephosphorylated. Thiel et al. (2008) speculated about a regulatory role of TPS/TPPs in the turnover of cell wall components and/or pectins. Other functions have been described in other tissues, for example, a role as signal molecule in sensing carbohydrates and regulating starch breakdown as recently demonstrated in the starch-deficient *pgm* mutant of *Arabidopsis* during the diurnal cycle (Usadel et al., 2008). Notably, the transfer cells do not accumulate starch during the main course of storage events, thus allowing a continuous symplastic transport. Among the five studied tissues, pericarp, NP, and endosperm accumulate persistent or transient starch and undergo PCD, whereas ETC and embryo prevent PCD and do not prominently store starch but express transcripts connected to trehalose biosynthesis. Concomitantly, senescence marker genes encoding, for instance, serine, cysteine, and cathepsin proteases as well as lipases coupled to lipid degradation and secondary metabolism genes are not expressed in ETC (Fig. 2.5). Overall, the specialized ETC are characterized by a unique metabolism directed to transport functions (Fig. 2.2) and the simultaneous absence of storage events and PCD.

4.5. Transcriptional reprograming in endosperm differentiation, seed filling, and sink strength

When endosperm cellularization is completed, endoreduplication and storage product synthesis is initiated, and thus, seed filling and the creation of sink strength accompanied by massive transcriptional reprograming (Sreenivasulu et al., 2004). Also, energy metabolism is dramatically influenced as detailed in Section 4.6. Seed filling is preceded by a strongly increased sucrose flux leading at first to starch biosynthesis and storage and subsequently to storage protein accumulation (mainly hordeins) in the starchy endosperm. During the intermediate stage, incoming sucrose is cleaved by sucrose synthase. The resultant UDP-glucose is used for the production of UDP-sugars for cell wall biosynthesis and modification (as suggested by data in Fig. 2.5) as well as for the production of glucose-1-phosphate and subsequently ADP-glucose (ADP-glc), which is the key precursor of starch biosynthesis. Between 8 and 16 DAF, transcript profiling revealed preferential activation of genes involved in ADP-glc biosynthesis whereas the following steps toward starch as branching and debranching events seem to take place between 16 and 26 DAF (Fig. 2.5;

Radchuk et al., 2009). AGPase regulates starch biosynthesis and is probably the most important determinant of seed sink strength and yield (Smidansky et al., 2002). In barley (Johnson et al., 2003) and other graminaceous plants (Denyer et al., 1996; Tetlow et al., 2003; Thorbjørnsen et al., 1996), cytosolic and not plastidic ADP-glc-pyrophosphorylase (AGPase) is responsible for the majority of starch.

ADP-glc transporter (*AGT*) transcripts are specifically and strongly accumulated in endosperm between 6 and 16 DAF (Radchuk et al., 2009). These results support the above conclusion that cytosolic AGPase produces ADP-glc, which is further transported into plastids by AGT to be used in starch synthesis (Patron et al., 2004). Although the cytosolic ADP-glc pathway feeds the major route of starch biosynthesis in endosperm, detection of basal levels of two glucose-6-phosphate/phosphate translocator (*GPT*) gene transcripts in the developing endosperm (Radchuk et al., 2009) underlines that the plastidic pathway is still operative. This had already been proven by analyzing the barley mutant Risø16, which is free of cytosolic AGPase activity but still synthesizes starch (both A- and B-type granules) albeit at a reduced amount (Johnson et al., 2003).

Starch biosynthesis driven by sucrose synthase and AGPase activity is a major determinant of sink strength together with factors established earlier during development such as, for instance, cell number and cell size, as well as metabolic activities in the sink tissue (Herbers and Sonnewald, 1998). Factors influencing the cell cycle during endosperm establishment and events connected to endoreduplication in cereals have been summarized by Sabelli and Larkins (2009). In this respect, links between glucose levels and cell division and growth are of special interest (LeClere et al., 2008; Rolland et al., 2002; Weber et al., 1997), processes which are controlled by sugar metabolism (e.g., invertases) and at hormonal levels (e.g., gibberellins (Ozga et al., 2002; Swain et al., 1997) and cytokinin (Emery and Atkins, 2006)). Analysis of sugar signaling mutants in *Arabidopsis* revealed a complex signaling network that links sugar responses to ABA and ethylene (Kim et al., 2004; Yanagisawa et al., 2003). Related signaling and metabolic pathways in barley grains will be discussed in Section 4.7.

Storage protein transcripts encoding B and γ-hordeins (sulfur-rich prolamins), C hordeins (sulfur-poor hordeins), and D hordeins (high-molecular-weight subunits) start to appear around 12 DAF and reach highest levels from 16 DAF onward in the endosperm/aleurone fraction (Sreenivasulu et al., 2006, 2008b). Further details about synthesis, distribution, and gradients of different cereal prolamin fractions have been reviewed by Shewry and Halford (2002). The regulation of prolamin gene expression is presumably under the control of both CpG methylation and the action of specific prolamin-box binding TF complexes (Diaz et al., 2005; Weber et al., 2010). Coinciding with the accumulation peak of hordein transcripts after 16 DAF is a general reduction in expression levels of genes of the

sucrose to starch pathway followed by an activation of aspartate amino acid metabolism genes leading to asparagine, methionine, lysine, homoserine, and homocysteine, and genes of proline biosynthesis starting with glutamate (Fig. 2.5). During the maturation period (20–30 DAF), activation of minor carbohydrate metabolism genes leading to sugars such as raffinose, trehalose, and aldose was noticed in the endosperm/aleurone fraction as well as in the embryo. In the latter, levels continue to increase until 24 h after imbibition (Sreenivasulu et al., 2008b). The data suggest that the synthesized sugar alcohols not only protect aleurone and embryo cells during seed maturation from desiccation but also help to stabilize proteins which are activated during early seed germination.

While imported nitrogen is mainly used for seed storage protein biosynthesis in cereals (Balconi et al., 1991; Müller and Knudsen, 1993) and legumes (Salon et al., 2001), imported sucrose also provides carbon skeletons through glycolysis and the TCA cycle for the synthesis of amino acids but also functions as signal molecule (Koch, 2004). Furthermore, seed protein content is partially increased by the increased availability of carbon acceptors in the form of organic acids (Miflin and Lea, 1977), indicating a general carbon limitation for amino acid/seed protein synthesis at least if sufficient nitrogen is available (Weigelt et al., 2008). Thus, an increased sucrose uptake into the seed should increase sink strength and perhaps subsequently also seed protein synthesis. This concept was validated in wheat. By expressing in developing wheat grains the transfer cell-specific sucrose transporter HvSUT1 from barley (Weschke et al., 2000) under the control of the endosperm-specific hordein B1 promoter an increased sucrose uptake was achieved, but no increase in sucrose steady state levels, suggesting alterations of sucrose flux in the developing transgenic seeds. Analysis of transgenic plants grown under field-near conditions revealed an increase of both thousand-grain-weight and grain protein content as compared to nontransgenic control seeds and an unaltered starch content (Weichert et al., 2010). The results indicate a possibility to overcome the well-known negative correlation between yield and grain protein content in cereal breeding (Barneix, 2007) by a transgenic approach.

4.6. Energy provision for storage metabolism

Like seeds of most plants, the developing barley caryopsis relies mainly on metabolite delivery from the maternal part. Sucrose, amino acids, and other nutrients, delivered via phloem, are utilized for biosynthetic and energetic purposes. Since the photosynthetically active tissue in the caryopsis, the chlorenchyma, is confined to a few cell layers within the pericarp, the photosynthetic input to energy delivery is likely restricted to the maternal tissue (Caley et al., 1990; Nutbeam and Duffus, 1978). This is in contrast to dicot seeds, where the green embryo gains a significant amount of energy

via its own photosynthesis (Goffman et al., 2005). In barley, the filial storage organs (endosperm and embryo) are nongreen and drive exclusively heterotrophic metabolism, mainly based on respiration. Under *in vivo* conditions, the endogenous oxygen concentration can limit mitochondrial respiration, and causes a minor induction of fermentative pathways. Alcoholic fermentation takes place from the by-product of glycolytic pathway generating ATP without the consumption of oxygen (Tadege et al., 1999). The ratio of respiration to fermentation changes during the course of seed development and strongly depends on the topography (localization of specific tissues within the seed).

During early stages of seed development, gene expression analysis shows preferred expression of genes encoding enzymes of the respiratory pathway (Zhang et al., 2004). Transcripts of four different ADH isoforms and lactate dehydrogenase are apparent at low levels (Sreenivasulu et al., 2004). The seed is characterized by a relatively high hexose/sucrose ratio, favoring respiratory fluxes. The analysis of the adenine nucleotide pool shows constant levels of AMP, ADP, and ATP during early seed development. The adenylate energy charge (AEC) reflecting the amount of available energy (defined as $[ATP + 0.5 \times ADP]/[ATP + ADP + AMP]$; Pradet and Raymond, 1983) in the seed tissue is correspondingly high. It is assumed that the relative respiratory activity is quite high during early development as a necessity to provide the growing young filial tissues with ATP. Neither sugar nor oxygen supply are limiting factors for respiration in young seeds.

However, the increasing storage activity in the starchy endosperm is coupled with elevated starch accumulation rates and with an overall increase of metabolite levels in the starch biosynthesis pathway (Rolletschek et al., 2004). EST analysis indicated an increasing expression of fermentative enzymes during the switch to the storage phase (Zhang et al., 2004). The levels of several metabolites of the glycolytic pathway and the tricarboxylic acid (TCA) cycle also start to increase several-fold and remain high toward maturation (Rolletschek et al., 2004). The elevated biosynthetic flux is coupled with decreases in AEC, mainly due to both lower ATP and higher AMP levels. This decline is especially apparent during darkness when photosynthetic inputs (oxygen delivery) are lacking. Also expression of fermentative enzymes increases during the storage phase (Zhang et al., 2004). Based on data from transcript and metabolite analysis as well as oxygen mapping, a limitation of the respiratory pathway is expected especially in some interiorly located parts of the caryopsis, leading to partial activation of fermentative processes. The main storage phase becomes increasingly energy-limited. This limitation is a result of (i) the elevated metabolic activity that leads to an increased energy demand and (ii) the developmental decline in oxygen delivered by diffusive gas exchange and produced by photosynthesis in the pericarp. Finally, alanine and malate are

accumulated to some degree during the storage phase (indicative of fermentation; Macnicol and Jacobsen, 1992) and ratios of lactate to pyruvate are significantly higher, especially during the night (indicative of a strongly reduced NAD^+ system; Rolletschek et al., 2003). This implies an O_2-limited respiration *in vivo*, reflected by the induction of fermentation enzymes (Macnicol and Jacobsen, 2001). A joint transcriptomic, proteomic, and metabolomic analysis of developing maize endosperm demonstrated a clear relationship between energy metabolism and storage compound synthesis (Prioul et al., 2008). Furthermore, a switch from central carbon metabolism/respiration to glycolysis and fermentation was observed during starch storage (maize: Prioul et al., 2008; rice: Xu et al., 2008). The mechanism regulating this switch remains poorly understood. In order to examine the relationship between energy metabolism and storage compound synthesis, we investigated oxygen distribution within the barley caryopsis and compared it with ATP and storage patterns on a topographical level as follows.

Detailed mapping of oxygen distribution within the caryopsis demonstrates the existence of steep gradients in oxygen concentrations within the cereal grain. The shape of the gradients indicates that (i) oxygen is produced at high rates within the chlorophyll-containing cell layers of the pericarp and (ii) oxygen flows toward both the endosperm and the outer pericarp. Lateral and peripheral regions of endosperm are favorably supplied with oxygen. Oxygen supply to the endosperm is therefore inherent in the chlorophyll pattern. The sharp decline in oxygen concentration within the endosperm during the storage phase points to a strong consumption due to high metabolic activity. Integuments attached to the endosperm (except at the creased vein area) obviously allow O_2 diffusion as derived from O_2 concentration gradients (Rolletschek et al., 2004). Nevertheless, their suberine layers may impede gas exchange (Chochrane and Duffus, 1979). One might speculate that the role of pericarp photosynthesis for the storage process consists more of oxygen supply to the endosperm than of energy supply or CO_2 fixation (only 2% of final starch are derived from grain photosynthesis; Watson and Duffus, 1988).

Under oxygen limitation, oxygen delivery driven by pericarp photosynthesis is crucial for respiratory ATP synthesis until the intermediate stage of seed development. High ATP concentrations were associated with endosperm differentiation and the local onset of starch storage within the distal parts of the endosperm, while low ATP overlapped with the most hypoxic regions. Building of steep gradients in ATP within the endosperm coincided with overall elevated metabolite levels, specific changes in metabolite profiles (glycolysis and TCA cycle) and channeling of metabolic fluxes toward storage (increased starch accumulation rate) (Rolletschek et al., 2004). These findings implicate an inhomogeneous spatial arrangement of metabolic activity within the caryopsis. It is suggested that the local onset of

starch storage is coupled with the accumulation of ATP and elevated overall metabolic activity. The local ATP level probably reflects the metabolic state of storage tissue. High ATP/energy state might even be necessary to fuel the elevated metabolic fluxes (Rolletschek et al., 2003). Although possibly coincidental, accumulation of storage products with a high energy demand during synthesis (lipids and proteins) occurs in regions with favorable oxygen supply (Neuberger et al., 2008); both embryo (strong lipid biosynthesis) and aleurone (strong protein biosynthesis) are located next to the photosynthetic chlorenchyma during late seed maturation. Conversely, biosynthesis of starch, which requires much less energy, is localized mainly in central regions of endosperm, known as most oxygen-depleted.

Detailed studies on the flux of isotope-labeled sucrose into starch, protein, and lipid in seeds of both maize (Rolletschek et al., 2005) and barley (own unpublished data) clearly demonstrate that under conditions favoring mitochondrial respiration (via increasing oxygen supply), distribution of ATP is shifted within the seed and the energy status (ATP/ADP ratio) increases. However, elevated respiration/oxygen supply did not affect the steady state level of ADP-glc, the activity of AGPase and the flux from sucrose into ADP-glc as well as into starch. In contrast, elevated respiration/oxygen supply stimulates sucrose uptake into the embryo, flux of sucrose into acetyl-coenzyme A (precursor for fatty acid biosynthesis) as well as into lipids. Lipid accumulation in the embryo appeared highest in regions with high ATP. Consistent with the above data, a decrease in respiration/oxygen supply most strongly affected lipid storage in the embryo as well as protein storage (embryo and aleurone). Higher O_2 supply expanded the ATP-rich zones toward the starchy endosperm and the scutellar part of the embryo. The latter might be responsible for higher sucrose uptake into the embryo. Similar studies on legume seeds confirmed the view that the energy state of tissues is related to the local distribution of storage activity as well as to the partitioning of assimilates into different storage product classes (Borisjuk et al., 2003; Rolletschek et al., 2003; Weber et al., 2005).

Taken together, the available data suggest a role of the energy status in the regulation of local storage activity within the seeds. This regulation is probably mediated on a both transcriptional and posttranscriptional level. Independent of specific morphophysiological features and photosynthetic capabilities, seeds have to cope with a limitation of energy availability.

4.7. Roles of hormones and transcriptional networks in differentiation and maturation of endosperm and embryo

Hormones play decisive roles during grain development. Our knowledge on plant hormone biosynthesis, degradation, transport, signaling, and interactions has increased dramatically during recent years but most data were obtained using *Arabidopsis* due to a wealth of mutants and sophisticated

genomics methods (Gutierrez et al., 2007; Holdsworth et al., 2008; To et al., 2006; Verdier and Thompson, 2008). Cereal grain hormone studies were of more general nature or focused on the barley aleurone and its role in germination (Fath et al., 2001; Ho et al., 2003; Ritchie et al., 2000, 2002). Here we will focus on the endosperm and the ETC. In the endosperm, cytokinins stimulate cell division and GA are involved in cell differentiation events (summarized in Nguyen et al., 2007) and thus regulate sink size whereas ABA levels correlate with the grain filling rate (Yang et al., 2006). Although ABA is well known to regulate seed maturation, desiccation tolerance, and dormancy (Finkelstein et al., 2002), knowledge about its role in early seed development is scarce.

4.7.1. ABA-influences on endosperm cellularization and endopolyploidization

ABA is known to be translocated from leaves to seeds via phloem, and this maternally derived ABA is inhibiting cell division and inducing maturation (Ober and Setter, 1990). Early ABA deficiency resulted in a reduction of endosperm and delayed seed development in *Nicotiana plumbaginifolia* (Frey et al., 2004). In barley, at the time of fertilization, high levels of ABA were measured which decrease dramatically after 4 DAF (our unpublished results). The levels of this most probably maternal ABA are comparable in both pericarp and embryo sac fractions during early seed development. Analyses of *seg8* mutant grains (our unpublished results) revealed deregulated ABA levels, which are lower compared to the wild type during the prestorage phase but higher during the transition phase. Ploidy levels and ABA amounts were inversely correlated in the developing endosperm of both mutant and wild type, suggesting a potential influence of ABA on cell cycle regulation. Low ABA amounts and higher endosperm ploidy levels during early development result not only in abnormal cellularization patterns especially in transfer cells but also in the endosperm. Increased ABA levels and lower ploidy levels during the transition phase result in a strong decrease of accumulated starch reflected by the low thousand grain weight of *seg8* grains (27% of the wild type; Röder et al., 2006). Correspondingly, the increased ABA levels found during the transition phase were reflected in upregulation of HvKRP1 (kinase inhibitor protein-related protein 1) gene expression in *seg8* endosperm, suggesting a direct influence of ABA on KRP1 expression as reported for *Arabidopsis* and maize (Coelho et al., 2005; Wang et al., 1998). Involvement of ABA in cell cycle control could be realized by inducing expression of KRP1, which decreases cyclin-dependent kinase (CDK) activities (Wang et al., 1998) and thus alters cell cycle progression and DNA content as shown in maize (Coelho et al., 2005) as well as endoreduplication in endosperm and seed filling in rice (Barrôco et al., 2006). Accordingly, endosperm cell division, and, to a lesser degree, endoreduplication in early maize kernels is inhibited by exogenously

applied ABA (Mambelli and Setter, 1998; Myers et al., 1990). Furthermore, reduced transcript amounts of the plastid division gene *FtsZ* as well as general transcriptional downregulation of the starch biosynthesis pathway in developing *seg8* grains hint to relations between ABA, plastid differentiation, and reduced starch accumulation.

4.7.2. ABA-influences on endosperm storage activities and embryo desiccation

ABA's role in processes as acquisition of desiccation tolerance, dormancy induction, prevention of precocious germination, and deposition of storage reserves has been studied in some detail especially in *Arabidopsis* and maize favored by the greater number of available mutants (Finkelstein et al., 2002; Holdsworth et al., 2008). There is no doubt that ABA is also the major determinant of dormancy in barley (Jacobsen et al., 2002; Millar et al., 2006) but the precise role in endosperm and embryo tissues during seed maturation is less clear. Endogenous production of ABA in endosperm and embryo is indicated during seed maturation in barley by the preferential activation of distinct ABA aldehyde oxidase (*AAO*) gene family members (Sreenivasulu et al., 2006), which catalyze the final step of ABA biosynthesis. In *Arabidopsis*, AAO3 has been shown to play a major role in the production of ABA in seeds (Seo et al., 2004). A similar situation seems to exist in maize kernels, where ABA measurements of seeds grown *in vitro* suggested *in situ* synthesis by kernel components (Jones and Brenner, 1987). In barley, distinct ABA biosynthesis signaling gene family members are expressed in endosperm and embryo during seed maturation, suggesting independent synthesis in both tissues and tissue-specific signaling networks (Sreenivasulu et al., 2006). Based on the correlative evidence from transcriptome data and *cis* element predictions, it appears that ABA influences storage product biosynthesis via SNF1 kinase in the endosperm but not in the embryo where ABA most likely participates in the activation of LEA and oleosin genes, thus eventually influencing desiccation tolerance (Sreenivasulu et al., 2006).

Along with ABA, ethylene and auxin biosynthesis genes are strongly induced during seed maturation within the endosperm fraction. As discussed in Section 4.3, the ABA and ethylene ratio seems to modulate the timing of PCD in endosperm. Auxin biosynthesis in the endosperm during 12–26 DAF is assumed to be involved in the induction of endoreduplication as recently summarized by Nguyen et al. (2007). The possible cross talk between ABA and auxin during endosperm maturation remains unexplored.

4.7.3. Regulators conserved between *Arabidopsis* and barley operating during seed maturation

The overall picture of regulatory networks integrating hormonal and metabolic signals with genetic programs has been worked out in *Arabidopsis* and can be briefly summarized as follows. A network of LEC1/AFL

(*A*BI3/*F*US3/*L*EC2) B3 domain transcription factors tightly connected with hormone signaling pathways controls embryo maturation and the transition to dormancy whereas VAL B3 factors repress the ALF B3 network and thus allow germination and vegetative development (Suzuki and McCarty, 2008). Chromatin remodeling factors as parts of epigenetic mechanisms are also involved (Chinnusamy et al., 2008; Zhang and Ogas, 2009). The relationship between LEC TFs and hormones during maturation seems to involve a feedback loop (Braybrook and Harada, 2008). Since little is known about the role of these regulators in the *Arabidopsis* endosperm, we analyzed the available transcript data with respect to spatial and temporal differences. Figure 2.6 highlights the results and enables a comparison with similar data from barley. First, it is worth mentioning that the five analyzed genes *LEC1*, *LEC2*, *FUS3*, *ABI3*, and *ABI6* in *Arabidopsis* are not only expressed in the embryo but also in the endosperm in a rather specific manner. The function there is widely unknown. In the seed coat, only *ABI5* is present during development, *FUS3* is restricted to the mature state and *LEC1*, *LEC2*, and *ABI3* transcripts are nearly absent. *In situ* localization data showed that the *FUS3* gene is preferentially expressed in the protoderm of the embryo, *LEC2* in the embryo axis, and *ABI3* as well as *LEC1* throughout the embryo (Santos-Mendoza et al., 2008). Altogether the data implicate that each tissue/cell type may be characterized by its own qualitative and quantitative combination of main regulators and that the commonly described interaction networks are just a generalization for the embryo. In barley grains, the analyzed regulator transcripts are also present in both embryo and endosperm and again spatially and temporally differentiated (Fig. 2.6). Interestingly, HvLEC2 is more specific for the endosperm and especially expressed during 8 and 16 DAF whereas the B3-type HvABI3/VP1 and HvFUS3 TFs are abundantly expressed in the embryo and moderately in the endosperm during maturation (Fig. 2.6). HvFUS3 is absent from the maternal testa/pericarp (Moreno-Risueno et al., 2008; Fig. 2.6), whereas AtFUS3 is heavily expressed in the seed coat during maturation (Fig. 2.6). The functional equivalence of HvFUS3 with the *Arabidopsis* ortholog AtFUS3 is underlined by the observation that HvFUS3 complements the loss-of-function mutant *Atfus3*. It also binds to the well-defined RY-motif in the promoters of endosperm-specifically expressed barley genes such as B-hordein Hor-2 and trypsin inhibitor BTI-CMe (Moreno-Risueno et al., 2008). Although the role of individual TF members of AFL seems to be conserved between dicot and monocot species, it is unclear how in cereals the AFL complex functions in the two tissues endosperm and embryo to control the whole spectrum of events: differentiation, seed storage protein gene regulation, desiccation, and dormancy breaking.

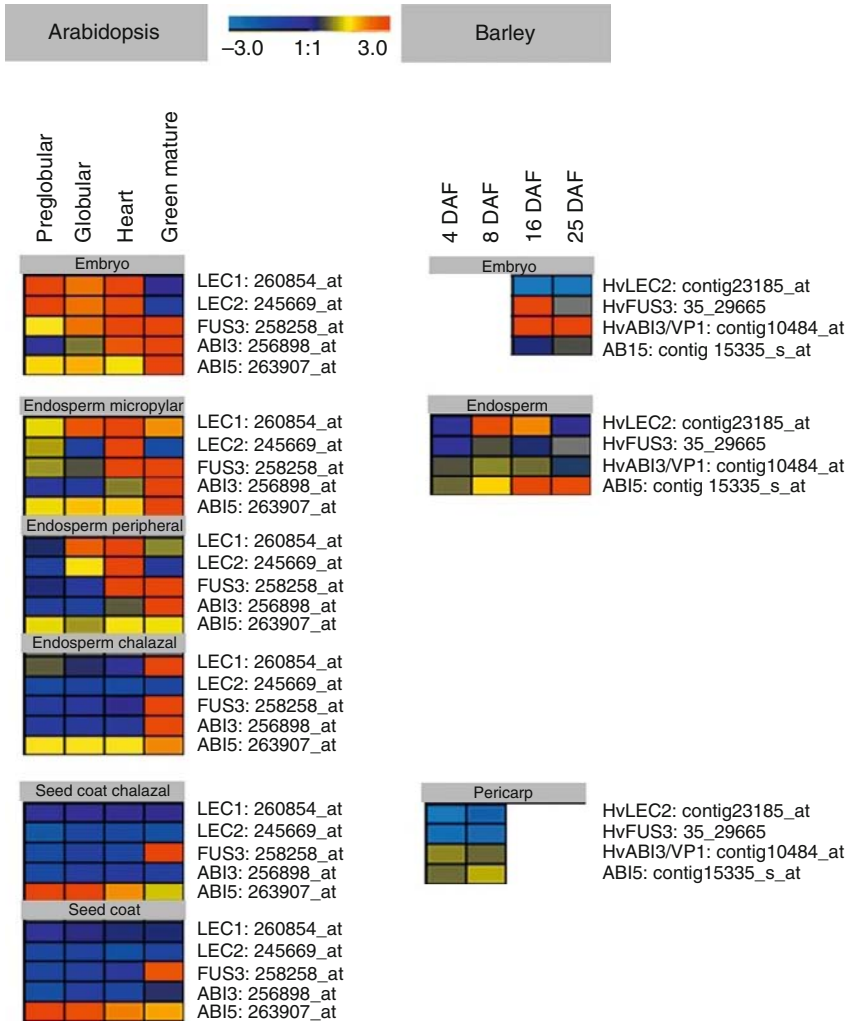

Figure 2.6 Tissue-specific expression patterns of key seed maturation regulatory genes in *Arabidopsis* and barley. First, the barley sequences homologs to the *Arabidopsis* genes *LEC1*, *LEC2*, *FUS3*, *ABI3*, and *ABI5* were defined. Second, publicly available Affymetrix expression data of microdissected *Arabidopsis* seed tissues (Series GSE12402, GSE11262, GSE15160, GSE15165) and our own data obtained from manually dissected tissues of three major barley grain tissues (Series GSE9365) were subjected to Robust Multiarray normalization, and the expression patterns of the key regulators are shown as heat maps. Signal intensities are color coded: red, high expression; yellow, moderate expression; dark blue, low expression; light blue, very low expression. LEC, leafy cotyledon; FUS3, FUSCA3; ABI, abscisic acid insensitive.

5. Systems Biology View of Barley Grain Development

Barley, and especially the barley grain, has been deeply characterized on many levels of biological organization. Large EST collections are available (Künne et al., 2005 and above), different transcriptome and proteome profiling methods have been applied (Section 4) and genome sequencing programs are under way (Schulte et al., 2009). Furthermore, large amounts of metabolic and other physiological data have been generated. These extensive datasets ask for a systems biology approach to allow proper data integration and more proper data interpretation. We have started to apply this approach, which relies on an iterative cycle of data acquisition and model building, to developing barley seeds.

5.1. Data generation, storage, integration, and visualization for systems biology

Model construction needs the most precise and most comprehensive parameterization that is possible. For example, to characterize the state of a metabolic system, we need information about metabolite concentrations, enzyme activities, and metabolic fluxes at this state. To date, the most comprehensive metabolite determinations in barley seeds have been obtained in targeted approaches by liquid chromatography coupled to mass spectrometry (Rolletschek et al., 2004). Besides the determination of the components itself, interactions between components and processes mediated by different compounds are of major importance. To this end, a method for the medium-throughput determination of about 30 enzyme activities (Gibon et al., 2004) has recently been adapted to barley seeds (K. Merx and H.-P. Mock, unpublished). Furthermore, methods for measurements of steady state metabolic fluxes are under development (B.H. Junker, unpublished).

The large size of datasets used in systems biology demands storage in databases, evaluation by the help of statistics software, and visualization by specialized software packages. For barley, there is a variety of databases on various aspects of genomics, which have been reviewed recently (Sreenivasulu et al., 2008a). One example is MetaCrop (Grafahrend-Belau et al., 2008), which is a metabolic pathway database for crops and model plants, currently containing information on 412 reactions from barley, including stoichiometry, tissue and organelle specificity, and in some cases, kinetic information. Furthermore, MetaCrop allows the collection and export of metabolic models in the standardized data format SBML (Systems Biology Markup Language; Hucka et al., 2003).

For the visualization of omics datasets, there are two tools especially interesting to the plant and especially barley community: MapMan (Sreenivasulu et al., 2008b; Thimm et al., 2004) and Vanted (Junker et al., 2006). MapMan is a tool for the display of large transcriptome and metabolome datasets onto diagrams of metabolic pathways or other processes. A particular strength of MapMan is that mappings of genes to functional categories have been manually generated for a variety of plants, among them barley (Sreenivasulu et al., 2008b). Vanted, which stands for ''visualization and analysis of networks containing experimental data,'' is a tool that enables the visualization of transcriptomics, proteomics, metabolomics, and other high-throughput data on the underlying networks (e.g., metabolic pathways) or hierarchies such as the gene ontology categories (Junker et al., 2006). Vanted also contains various tools for statistical evaluation of the data, such as correlation analysis and clustering methods. It is constantly extended by other tools via a plug-in mechanism.

5.2. Modeling

In barley, different types of computational models covering large ranges of detail have been constructed and analyzed. Examples for spatial or spatiotemporal models are the 3-D/4-D models of barley grains described in Section 3. Another type of models that have been constructed for barley are functional–structural plant models (FSPMs; Vos et al., 2007). FSPMs are combinations of process-based models, which are quantitatively describing the growth of single crops or populations in relation to environmental conditions, and structural models, which are models for the architecture and morphology of plants. The virtual crop-modeling system ''VICA'' has recently been specified for barley plants and considers organ initiation, organ growth and senescence, photon transfer, photosynthesis, basic features of the carbon- and nitrogen-metabolism, and mass fluxes between the objects (Wernecke et al., 2007).

Models of metabolic networks concentrate on one aspect of the organism's biology. Metabolism can be described mathematically on various levels of detail. The easiest way is to consider the network structure only, which can then be enriched by the stoichiometries of the reactions to perform algebraic operations on the stoichiometric matrix of the metabolic network, for example, elementary mode analysis, which yields information on feasible paths through the network. After adding quantitative information about input fluxes of substrates and the biomass composition, flux balance analysis (FBA) can be applied to predict flux distributions, essentialities of enzymes, metabolic behavior at different growth conditions, and metabolic yield. Such a model has recently been constructed for the barley grain and contains 234 metabolites, 192 enzymes, and 65 transporters distributed between four compartments (Grafahrend-Belau et al., 2009). With this model it was possible to predict

growth rates of grains and patterns of active metabolic pathways under anoxic, hypoxic, and aerobic conditions. The predictions were in accordance with experimental results described in the literature. Furthermore, the predictions gave insight into the potential role of pyrophosphate metabolism to maintain seed metabolism under oxygen deprivation.

While an FBA model predicts fluxes based on an underdetermined linear equation system by using an objective function, steady-state ^{13}C metabolic flux analysis (MFA) adds the necessary biochemical and experimental constraints so that the equation system becomes overdetermined and thus we can speak of ''measurements'' rather than ''predictions.'' This methodology has been applied with success to seeds of several dicotyledonous plants (e.g., canola; Schwender et al., 2004), but maize so far is the only monocotyledonous plant to which this approach has been applied (Glawischnig et al., 2001). Before this method can be applied to barley, a suitable protocol for the *in vitro* cultivation of barley grains or spikes has to be developed.

The most detailed metabolic models are kinetic models that quantitatively simulate the dynamics of metabolic networks (Steuer and Junker, 2009). Besides the stoichiometric matrix, kinetic models are characterized by rate equations that quantitatively describe the conversion rate (*in vivo* this means the metabolic flux) mediated by a reaction in response to several parameters such as the maximal catalytic activity of the respective enzyme and binding constants for substrates or inhibitors. Only with the help of kinetic models is it possible to relate metabolic fluxes, enzyme activities, and metabolite concentrations to each other with one set of differential equations. However, most probably due to an insufficient availability of suitable datasets, only a limited number of kinetic models for metabolic networks have been constructed, among them models for carbohydrate metabolism in sugar cane (Rohwer and Botha, 2001; Uys et al., 2007) and potato (Junker, 2004), which may be adapted to barley. A comparison of barley and potato models might throw some light, especially on the role of the predominantly cytosolic AGPase (discussed in Section 4.5) in cereals, which is absent in potato.

However, ''systems biology, if only rooted in the 'omics' area, will result in an ever-increasing gap between genotypes and crop phenotypes.'' Therefore, in a following step, the next organizational level, the whole plant, has to be involved to converge functional genomics with crop physiology in an approach called crop systems biology (Yin and Struik, 2008).

6. Concluding Remarks

In the present review, grain development in barley is taken as an example to show how a multitude of different techniques and approaches have added many pieces to a puzzle that is still far from being complete.

Rapid development of throughput technologies in the field of genomics resulted in defining gene-regulatory and biochemical networks inferring correlative relationships between sets of coexpressed genes and a biological phenomenon. Such methods represent part of a ''top-down systems approach,'' leading to hints as of ''what to look for'' in a given biology and to new hypothesis-driven research. As an example, the conserved regulatory networks defining canonical steps of PCD in complex maternal tissues were revealed by using coexpression analysis of tissue-specific transcriptome data. The results point to the importance of fine-tuned and interrelated PCD processes in the different maternal tissues during development, which regulate maternal tissue growth relative to filial ones and at the same time provide space and nutrients to build filial sink strength. Global transcriptome data can also be related to diverse sets of molecular-physiological data as exemplified by the established link between ABA and endosperm cellularization and endoreduplication. However, the derived conclusions are mostly based on only correlative evidence and therefore need careful additional studies. Moreover, epigenetic processes form an integral part of, for instance, ABA-regulated processes (Chinnusamy et al., 2008) and generally need increasing attention. The recent identification of definite ABA receptors at the plasma membrane (Pandey et al., 2009) and in the cytosol (Ma et al., 2009; Park et al., 2009), the reconstruction of respective ABA complexes (Melcher et al., 2009; Nishimura et al., 2009; Santiago et al., 2009), and the elucidation of its role in the phosphatase (PP2C)- and kinase (SnRK2.6)-mediated signal transduction to a transcription factor (ABF2/AREB1) (Fujii et al., 2009) will open up new horizons of understanding ABA's relevance in seeds and new avenues for application.

In spite of the substantial recent increase in knowledge, there are still important technical limitations to overcome. Cell- and tissue-specific studies are still scarce. Even less advanced are methods to study metabolism at the cellular and subcellular level through kinetics and flux studies as a ''bottom-up systems approach.'' However, without the respective data predictive modeling as strived for in systems, biology will not reach the necessary precision.

Eventually, systems biology will provide a way to integrate all data in a complex predictive model of grain development. One prerequisite is a 3-D/4-D model, which represents grain morphology down to the histological level and its changes in time. The enormous progress made in this field is summarized here together with first steps to integrate biochemical and molecular data. Such integration needs massive bioinformatics input and will at the same time close large gaps in our available datasets. Evident gaps may be closed by new high resolution, noninvasive, MALDI-based methods (Sinha et al., 2008) to localize in 3-D nearly any substance of reasonable concentration as well as the allocation of substances under close to natural conditions in space and time (Jahnke et al., 2009). It is very

exciting to envision that in the time to come, most relevant data can be measured noninvasively with a hand-held device directly in the field.

We have only regarded processes within the developing grain and neglected the whole plant context, which is, of course, of eminent importance. For instance, manipulations of the brassinosteroid hormone pathway in rice nonseed tissues increased grain yield per plant in greenhouse- and field-grown plants by roughly 15–40% underlining the importance of the assimilate flow from source to sink (Wu et al., 2008). All in all, seeds will remain an important and fascinating object to study with the intention to help feed an ever increasing number of people.

ACKNOWLEDGMENTS

The authors thank Dr. Diana Weier for preparing Fig. 2.1, Felix Bollenbeck for contributing to Fig. 2.3, and all our colleagues for helpful discussions. Financial support was kindly provided by IPK and the Bundesministerium für Forschung und Technologie (BMBF) within its GABI program.

REFERENCES

Baik, B.-K., Ullrich, S.E., 2008. Barley for food: characteristics, improvement, and renewed interest. J. Cereal Sci. 48, 233–242.

Balconi, C.E., Rizzi, E., Manzocchi, L., Soave, C., Motto, M., 1991. Analysis of in vivo and in vitro grown endosperms of high and low protein strains in maize. Plant Sci. 73, 9–18.

Barneix, A.J., 2007. Physiology and biochemistry of source-regulated protein accumulation in the wheat grain. J. Plant Physiol. 164, 581–590.

Barrôco, R.M., Peres, A., Droual, A.-M., De Veylder, L., Nguyen, L.S.L., De Wolf, J., et al. 2006. The cyclin-dependent kinase inhibitor Orysa; KRP1 plays an important role in seed development of rice. Plant Physiol. 142, 1053–1064.

Berger, S., Weichert, H., Porzel, A., Wasternack, C., Kühn, H., Feussner, I., 2001. Enzymatic and non-enzymatic lipid peroxidation in leaf development. Biochim. Biophys. Acta 1533, 266–276.

Bethke, P.C., Jacobsen, J.V., Jones, R.L., 2000. Barley biotechnology. In: Black, M., Bewley, J.D. (Eds.), Seed Technology and Its Biological Basis. Sheffield Academic Press, CRC Press, Boca Raton, FL, pp. 184–225.

Bollenbeck, F., Seiffert, U., 2008. Fast registration-based automatic segmentation of serial section images for high-resolution 3-D plant seed modelling. In: IEEE International Symposium on Biomedical Imaging (ISBI), pp. 352–355.

Bollenbeck, F., Seiffert, U., 2009. Computational intelligence in biomedical image processing. In: Abraham, A. et al. (Ed.), Foundations of Computational Intelligence, vol. 5. Springer, Berlin, Heidelberg, pp. 197–222.

Bollenbeck, F., Kaspar, S., Mock, H.-P., Weier, D., Seiffert, U., 2009a. Three-dimensional multimodality modelling by integration of high-resolution interindividual atlases and functional MALDI-IMS data. Lect.Notes Bioinform. (LNBI) 5462, 126–139.

Bollenbeck, F., Pielot, R., Weier, D., Weschke, W., Seiffert, U., 2009b. Inter-modality registration of NMRi and histological section images using neural networks registration

in gabor feature space. In: IEEE Symposium on Computational Intelligence for Image Processing (CIIP) 2009, pp. 27–34.

Bollenbeck, F., Weier, D., Schoor, W., Seiffert, U., 2009c. From individual intesity voxel data to inter-individual probabilistic atlases of biological objects by an interleaved registration-segmentation approach. In: Proceedings of 4th International Conference on Computer Vision and Applications VISAPP 2009, 125–129.

Borisjuk, L., Walenta, S., Rolletschek, H., Mueller-Klieser, W., Wobus, U., Weber, H., 2002. Spatial analysis of plant metabolism: sucrose imaging within *Vicia faba* cotyledons reveals specific developmental patterns. Plant J. 29, 521–530.

Borisjuk, L., Rolletschek, H., Walenta, S., Panitz, R., Wobus, U., Weber, H., 2003. Energy status and its control on embryogenesis of legumes: ATP distribution within *Vicia faba* embryos is developmentally regulated and correlated with photosynthetic capacity. Plant J. 36, 318–329.

Braybrook, S.A., Harada, J.J., 2008. LECs go crazy in embryo development. Trends Plant Sci. 13, 624–630.

Buckner, B., Johal, G.S., Janick-Buckner, D., 2000. Cell death in maize. Physiol. Plant. 108, 231–239.

Caley, C.Y., Duffus, C.M., Jeffcoat, B., 1990. Photosynthesis in the pericarp of developing wheat grains. J. Exp. Bot. 41, 303–307.

Chen, F., Foolad, M.R., 1997. Molecular organization of a gene in barley which encodes a protein similar to aspartic protease and its specific expression in nucellar cells during degeneration. Plant Mol. Biol. 35, 821–831.

Chinnusamy, V., Gong, Z., Zhu, J.-K., 2008. Abscisic acid-mediated epigenetic processes in plant development and stress responses. J. Integr. Plant Biol. 50, 1187–1195.

Chochrane, M.P., Duffus, C.M., 1979. Morphology and ultrastructure of immature cereal grains in relation to transport. Ann. Bot. 44, 67–72.

Chojecki, A.J.S., Bayliss, M.W., Gale, M.D., 1986. Cell production and DNA accumulation in the wheat endosperm, and their association with grain weight. Ann. Bot. 58, 809–817.

Coelho, C.M., Dante, R.A., Sabelli, P.A., Sun, Y., Dilkes, B.P., Gordon-Kamm, W.J., et al. 2005. Cyclin-dependent kinase inhibitors in maize endosperm and their potential role in endoreduplication. Plant Physiol. 138, 2323–2336.

Colombo, L., Franken, J., van der Krol, A.R., Wittich, P.E., Dons, H.J.M., Angenent, G.C., 1997. Downregulation of ovule-specific MADS box genes from petunia results in maternally controlled defects in seed development. Plant Cell 9, 703–715.

Cornett, D.S., Reyzer, M.L., Chaurand, P., Caprioli, R.M., 2007. MALDI imaging mass spectrometry: molecular snapshots of biochemical systems. Nat. Methods 4, 828–833.

Costa, L.M., Gutiérrez-Marcos, J.F., Brutnell, T.P., Greenland, A.J., Dickinson, H.G., 2003. The globby1-1 (glo1-1) mutation disrupts nuclear and cell division in the developing maize seed causing alterations in endosperm cell fate and tissue differentiation. Development 130, 5009–5017.

Denyer, K., Dunlap, F., Thorbjornsen, T., Keeling, P., Smith, A.M., 1996. The major form of ADP-glucose pyrophosphorylase in maize endosperm is extra-plastidial. Plant Physiol. 112, 779–785.

Diaz, I., Martinez, M., Isabel-LaMoneda, I., Rubio-Somoza, I., Carbonero, P., 2005. The DOF protein, SAD, interacts with GAMYB in plant nuclei and activates transcription of endosperm-specific genes during barley seed development. Plant J. 42, 652–662.

Drea, S., Leader, D.J., Arnold, B.C., Shaw, P., Dolan, L., Doonan, J.H., 2005. Systematic spatial analysis of gene expression during wheat caryopsis development. Plant Cell 17, 2172–2185.

Druka, A., Muehlbauer, G., Druka, I., Caldo, R., Baumann, U., Rostoks, N., et al. 2006. An atlas of gene expression from seed to seed through barley development. Funct. Integr. Genomics 6, 202–211.

Edgar, B.A., Orr-Weaver, T.L., 2001. Endoreplication cell cycles: more for less. Cell 105, 297–306.
Emery, R.J.N., Atkins, C.A., 2006. Cytokinins and seed development. In: Basra, A.S. (Ed.), Seed Science and Technology: Trends and Advances. Haworth Press Inc., Binghamton, NY, pp. 63–93.
Engell, K., 1989. Embryology of barley: time course and analysis of controlled fertilization and early embryo formation based on serial sections. Nord. J. Bot. 9, 265–280.
Evers, T., Millar, S., 2002. Cereal grain structure and development. Some implications for quality. J. Cereal Sci. 36, 261–284.
Fath, A., Bethke, P.C., Belligni, M.V., Spiegel, Y.N., Jones, R.L., 2001. Signalling in the cereal aleurone: hormones, reactive oxygen and cell death. New Phytol. 151, 99–107.
Finkelstein, R.R., Gampala, S.S.L., Rock, C.D., 2002. Abscisic acid signaling in seeds and seedlings. Plant Cell (Suppl.), S15–S45.
Finnie, C., Svensson, B., 2003. Feasibility study of a tissue-specific approach to barley proteome analysis: aleurone layer, endosperm, embryo and single seeds. J. Cereal Sci. 38, 217–227.
Finnie, C., Svensson, B., 2009. Barley seed proteomics from spots to structures. J. Proteomics 72, 315–324.
Frey, A., Godin, B., Bonnet, M., Sotta, B., Marion-Poll, A., 2004. Maternal synthesis of abscisic acid controls seed development and yield in *Nicotiana plumbaginifolia*. Planta 218, 958–964.
Fujii, H., Chinnusamy, V., Rodrigues, A., Rubio, S., Antoni, R., Park, S.Y., et al. 2009. In vitro reconstitution of an abscisic acid signalling pathway. Nature 462, 660–664.
Gallie, D.R., 2004. Programmed cell death during seed development and germination. In: Gray, J. (Ed.), Programmed Cell Death in Plants. Blackwell, CRC Press, Oxford, UK; Boca Raton, FL, USA, pp. 44–70.
Gibon, Y., Blaesing, O.E., Hannemann, J., Carillo, P., Höhne, M., Hendriks, J.H., et al. 2004. A robot-based platform to measure multiple enzyme activities in *Arabidopsis* using a set of cycling assays: comparison of changes of enzyme activities and transcript levels during diurnal cycles and in prolonged darkness. Plant Cell 16, 3304–3325.
Glawischnig, E., Gierl, A., Tomas, A., Bacher, A., Eisenreich, W., 2001. Retrobiosynthetic nuclear magnetic resonance analysis of amino acid biosynthesis and intermediary metabolism. Metabolic flux in developing maize kernels. Plant Physiol. 125, 1178–1186.
Glidewell, S.M., 2006. NMR imaging of developing barley grains. J. Cereal Sci. 43, 70–78.
Goffman, F.D., Alonso, A.P., Schwender, J., Ohlrogge, J.B., Shachar-Hill, Y., 2005. Light enables a very high efficiency of carbon storage in developing embryos of *Brassica napus*. Plant Physiol. 138, 2269–2279.
Gómez, E., Royo, J., Muñiz, L.M., Sellam, O., Paul, W., Gerentes, D., et al. 2009. The maize transcription factor myb-related protein-1 is a key regulator of the differentiation of transfer cells. Plant Cell 21, 2022–2035.
Grafahrend-Belau, E., Weise, S., Koschützki, D., Scholz, U., Junker, B.H., Schreiber, F., 2008. MetaCrop: a detailed database of crop plant metabolism. Nucleic Acids Res. 36, D954–D958.
Grafahrend-Belau, E., Schreiber, F., Koschützki, D., Junker, B.H., 2009. Flux balance analysis of barley seeds: a computational approach to study systemic properties of central metabolism. Plant Physiol. 149, 585–598.
Gubatz, S., Dercksen, V.J., Brüß, C., Weschke, W., Wobus, U., 2007. Analysis of barley (*Hordeum vulgare*) grain development using three-dimensional digital models. Plant J. 52, 779–790.
Gutierrez, L., Van Wuytswinkel, O., Castelain, M., Bellini, C., 2007. Combined networks regulating seed maturatiom. Trends Plant Sci. 12, 294–300.

Herbers, K., Sonnewald, U., 1998. Molecular determinants of sink strength. Curr.Opin. Plant Biol. 1, 207–216.

Ho, T.D., Gomez-Cadenas, A., Zentella, R., Casaretto, J., 2003. Crosstalk between gibberellin and abscisic acid in cereal aleurone. J. Plant Growth Regul. 22, 185–194.

Holdsworth, M.J., Bentsink, L., Soppe, W.J.J., 2008. Molecular networks regulating Arabdidopsis seed maturation, afterripening, dormancy and germination. New Phytol. 179, 33–54.

Hucka, M., Finney, A., Sauro, H.M., Bolouri, H., Doyle, J.C., Kitano, H., et al. 2003. The systems biology markup language (SBML): a medium for representation and exchange of biochemical network models. Bioinformatics 19, 524–531.

Jacobsen, J.V., Pearce, D.W., Poole, A.T., Pharis, R.P., Mander, L.N., 2002. Abscisic acid, phaseic acid and gibberillin contents associated with dormancy and germination in barley. Physiol. Plant. 115, 428–441.

Jahnke, S., Menzel, M.I., van Dusschoten, D., Roeb, G.W., Bühler, J., Minwuyelet, S., et al. 2009. Combined MRI-PET dissects dynamic changes in plant structures and functions. Plant J. 59, 634–644.

Johnson, P.E., Patron, N.J., Bottrill, A.R., Dinges, J.R., Fahy, B.F., Parker, M.L., et al. 2003. A low-starch barley mutant, Risø 16, lacking the cytosolic small subunit of ADP-glucose pyrophosphorylase, reveals the importance of the cytosolic isoform and the identity of the plastidial small subunit. Plant Physiol. 131, 684–696.

Jones, R.J., Brenner, M.L., 1987. Distribution of abscisic acid in maize kernels during grain filling. Plant Physiol. 83, 905–909.

Junker, B.H., 2004. Sucrose breakdown in the potato tuber. PhD thesis, Potsdam University, Germany.

Junker, B.H., Klukas, C., Schreiber, F., 2006. VANTED: a system for advanced data analysis and visualization in the context of biological networks. BMC Bioinform. 7, e109.

Kim, S., Kang, J.Y., Cho, D.I., Park, J.H., Kim, S.Y., 2004. ABF2, an ABRE-binding bZIP factor, is an essential component of glucose signaling and its overexpression affects multiple stress tolerance. Plant J. 40, 75–87.

Koch, K., 2004. Sucrose metabolism: regulatory mechanisms and pivotal roles in sugar sensing and plant development. Curr. Opin. Plant Biol. 7, 235–246.

Künne, C., Lange, M., Funke, T., Miehe, H., Thiel, T., Grosse, I., et al. 2005. CR-EST: a resource for crop ESTs. Nucleic Acids Res. 33, D619–D621.

Larkins, B.A., Dilkes, B.P., Dante, R.A., Coelho, C.M., Woo, Y.M., Liu, Y., 2001. Investigating the hows and whys of DNA endoreduplication. J. Exp. Bot. 52, 183–192.

LeClere, S., Schmelz, E.A., Chourey, P.S., 2008. Cell wall invertase-deficient miniature*1* kernels have altered phytohormone levels. Phytochemistry 69, 692–699.

Lee, K., Avondo, J., Morrison, H., Blot, L., Stark, M., Sharpe, J., et al. 2006. Visualizing plant development and gene expression in three dimensions using optical projection tomography. Plant Cell 18, 2145–2156.

Linnestadt, C., Doan, D.N., Brown, R.C., Lemmon, B.E., Meyer, D.J., Jung, R., et al. 1998. Nucellain, a barley homolog of the dicot vacuolar-processing protease, is localized in nuclear cell walls. Plant Physiol. 118, 1169–1180.

Ma, Y., Szostkiewicz, I., Korte, A., Moes, D., Christmann, A., Grill, E., 2009. Regulators of PP2C phosphatase activity function as abscisic acid sensors. Science 324, 1064–1068.

Macnicol, P.K., Jacobsen, J.V., 1992. Endosperm acidification and related metabolic processes in the developing barley grain. Plant Physiol. 98, 1098–1104.

Macnicol, P.K., Jacobsen, J.V., 2001. Regulation of alcohol dehydrogenase gene expression in barley aleurone by gibberellin and abscisic acid. Physiol. Plant 111, 533–539.

Mambelli, S., Setter, T.L., 1998. Inhibition of maize endosperm cell division and endoreduplication by exogenously applied abscisic acid. Physiol. Plant 104, 266–272.

Melcher, K., Ng, L.M., Zhou, X.E., Soon, F.F., Xu, Y., Suino-Powell, K.M., et al. 2009. A gate-latch-lock mechanism for hormone signalling by absicic acid receptors. Nature 462, 602–608.

Melkus, G., Rolletschek, H., Radchuk, R., Fuchs, J., Rutten, T., Wobus, U., et al. 2009. The metabolic role of the legume endosperm: a non-invasive imaging study. Plant Physiol. 151, 1139–1154.

Miflin, B.J., Lea, P.J., 1977. Amino acid metabolism. Annu. Rev. Plant Physiol. 28, 299–329.

Millar, A.A., Jacobsen, J.V., Ross, J.J., Helliwell, C.A., Poole, A.T., Scofield, G., et al. 2006. Seed dormancy and ABA metabolism in *Arabidopsis* and barley: the role of ABA 8'-hydroxylase. Plant J. 45, 942–954.

Moreno-Risueno, M.A., González, N., Díaz, I., Parcy, F., Carbonero, P., Vicente-Carbajosa, J., 2008. FUSCA3 from barley unveils a common transcriptional regulation of seed-specific genes between cereals and *Arabidopsis*. Plant J. 53, 882–894.

Mrva, K., Wallwork, M., Mares, D.J., 2006. α-Amylase and programmed cell death in aleurone of ripening wheat grains. J. Exp. Bot. 57, 877–885.

Müller, M., Knudsen, S., 1993. The nitrogen response of a barley C-hordein promoter is controlled by positive and negative regulation of the GCN4 and endosperm box. Plant J. 4, 343–355.

Myers, P.N., Setter, T.L., Madison, J.T., Thompson, J.F., 1990. Abscisic acid inhibition of endosperm cell division in cultured maize kernels. Plant Physiol. 94, 1330–1336.

Nakaune, S., Yamada, K., Kondo, M., Kato, T., Tabata, S., Nishimura, M., et al. 2005. A vacuolar processing enzyme, deltaVPE, is involved in seed coat formation at the early stage of seed development. Plant Cell 17, 876–887.

Neuberger, T., Sreenivasulu, N., Rokitta, M., Rolletschek, H., Göbel, C., Rutten, T., et al. 2008. Quantitative imaging of oil storage in developing crop seeds. Plant Biotechnol. J. 6, 31–45.

Neuberger, T., Rolletschek, H., Webb, A., Borisjuk, L., 2009. Non-invasive mapping of lipids in plant tissue using magnetic resonance imaging. In: Armstrong, D. (Ed.), Lipidomics, Vol. 1. Methods and Protocols. Humana Press, Springer, New York, pp. 485–496.

Nguyen, H.N., Sabelli, P.A., Larkins, B.A., 2007. Endoreduplication and programmed cell death in the cereal endosperm. In: Olsen, O.-A. (Ed.), Endosperm—Development and Molecular Biology. Plant Cell Monographs, Vol. 8. Springer, Berlin, Heidelberg, pp. 21–43.

Nishimura, N., Hitomi, K., Arvai, A.S., Rambo, R.P., Hitomi, C., Cutler, S.R., et al. 2009. Structural mechanism of abscisic acid binding and signalling by dimeric Pyr1. Science 326, 1356–1357.

Nutbeam, A.R., Duffus, C.M., 1978. Oxygen exchange in the pericarp green layer of immature cereal grains. Plant Physiol. 62, 360–362.

Ober, E.S., Setter, T.L., 1990. Timing of kernel development in water stressed maize: water potentials and ABA concentrations. Ann. Bot. 66, 665–672.

Offler, C.E., McCurdy, D.W., Patrick, J.W., Talbot, M.J., 2003. Transfer cells: cells specialized for a special purpose. Annu. Rev. Plant Biol. 54, 431–454.

Olsen, O.A., 2001. Endosperm development: cellularization and cell fate specification. Annu. Rev. Plant Physiol. Plant Mol. Biol. 52, 233–267.

Olsen, O.A., 2004. Nuclear endosperm development in cereals and *Arabidopsis thaliana*. Plant Cell 16, S214–S227.

Overmyer, K., Brosché, M., Kangasjärvi, J., 2003. Reactive oxygen species and hormonal control of cell death. Trends Plant Sci. 8, 335–342.

Ozga, J.A., van Huizen, R., Reinecke, D.M., 2002. Hormone and seed-specific regulation of pea fruit growth. Plant Physiol. 128, 1379–1389.

Pandey, S., Nelson, D.C., Assmann, S.M., 2009. Two novel GPCR-type G proteins are abscisic acid receptors in *Arabidopsis*. Cell 136, 136–148.

Park, S.Y., Fung, P., Nishimura, N., Jensen, D.R., Fujii, H., Zhao, Y., et al. 2009. Abscisic acid inhibits type 2C protein phosphatases via the PYR/PYL family of START proteins. Science 324, 1068–1071.

Patron, N.J., Greber, B., Fahy, B.F., Laurie, D.A., Parker, M.L., Denyer, K., 2004. The lys5 mutations of barley reveal the nature and importance of plastidial ADP-Glc transporters for starch synthesis in cereal endosperm. Plant Physiol. 135, 2088–2097.

Pielot, R., Manz, B., Weiter, D., Volke, F., Weschke, W., Seiffert, U., 2008. 4D warping for analysing morphological changes in seed development of barley grains. In: VISAPP 2008, pp. 335–340.

Pradet, A., Raymond, A., 1983. Adenine nucleotide rations and adenylate energy charge in energy metabolism. Annu. Rev. Plant Physiol. 34, 199–224.

Prioul, J.L., Méchin, V., Lessard, P., Thévenot, C., Grimmer, M.K., Chateau-Joubert, S., et al. 2008. A joint transcriptomic, proteomic and metabolic analysis of maize endosperm development and starch filling. Plant Biotechnol. J. 6, 855–869.

Radchuk, V., Borisjuk, L., Radchuk, R., Steinbiss, H.-H., Rolletschek, H., Broeders, S., et al. 2006. *Jekyll* encodes a novel protein involved in the sexual reproduction of barley. Plant Cell 18, 1652–1666.

Radchuk, V., Borisjuk, L., Sreenivasulu, N., Merx, K., Mock, H.-P., Rolletschek, H., et al. 2009. Spatio-temporal profiling of starch biosynthesis and degradation in the developing barley grain. Plant Physiol. 150, 190–204.

Riggs, C.D., 2004. Programmed cell death events during reproductive development. In: Gray, J. (Ed.), Programmed Cell Death in Plants. Blackwell, CRC Press, Oxford, UK; Boca Raton, FL, USA, pp. 71–105.

Ritchie, S., Swanson, S.J., Gilroy, S., 2000. Physiology of the aleurone layer and starchy endosperm during grain development and early seedling growth: new insights from cell and molecular biology. Seed Sci. 10, 193–212.

Ritchie, S., Swanson, S.J., Gilroy, S., 2002. From common signaling components to cell specific responses: insights from the cereal aleurone. Plant Physiol. 115, 342–351.

Röder, M.S., Kaiser, C., Weschke, W., 2006. Molecular mapping of the shrunken endosperm genes seg8 and sex1 in barley (*Hordeum vulgare* L.). Genome 49, 1–6.

Rohwer, J.M., Botha, F.C., 2001. Analysis of sucrose accumulation in the sugar cane culm on the basis of in vitro kinetic data. Biochem. J. 358, 437–445.

Rolland, F., Moore, B., Sheen, J., 2002. Sugar sensing and signaling in plants. Plant Cell 14 (Suppl.), S185–S205.

Rolletschek, H., Weber, H., Borisjuk, L., 2003. Energy status and its control on embryogenesis of legumes. Embryo photosynthesis contributes to oxygen supply and is coupled to biosynthetic fluxes. Plant Physiol. 132, 1196–1206.

Rolletschek, H., Weschke, W., Weber, H., Wobus, U., Borisjuk, L., 2004. Energy state and its control on seed development: starch accumulation is associated with high ATP and steep oxygen gradients within barley grains. J. Exp. Bot. 55, 1351–1359.

Rolletschek, H., Koch, K., Wobus, U., Borisjuk, L., 2005. Positional cues for the starch/lipid balance in maize kernels and resource partitioning to the embryo. Plant J. 42, 69–83.

Royo, J., Gomez, E., Hueros, G., 2007. Transfer cells. In: Olsen, O.-A. (Ed.), Endosperm—Development and Molecular Biology. Plant Cell Monographs, Vol. 8. Springer, Berlin, Heidelberg, pp. 73–89.

Sabelli, P.A., Larkins, B.A., 2009. The development of endosperm in grasses. Plant Physiol. 149, 14–26.

Salon, C., Munier-Jolain, N.G., Duc, G., Voisin, A.S., Grandgirard, D., Larmure, A., et al. 2001. Grain legume seed filling in relation to nitrogen acquisition: a review and prospects with particular reference to pea. Agronomie 21, 539–552.

Santiago, J., Dupeux, F., Round, A., Antoni, R., Park, S.Y., Jamin, M., 2009. The abscisic acid receptor PYR1 in complex with abscisic acid. Nature 462, 665–668.

Santos-Mendoza, M., Dubreucq, B., Baud, S., Parcy, F., Caboche, M., Lepiniec, L., 2008. Deciphering gene regulatory networks that control seed development and maturation in *Arabidopsis*. Plant J. 54, 608–620.

Schreiber, D.N., Bantin, J., Dresselhaus, T., 2004. The MADS box transcription factor ZmMADS2 is required for anther and pollen maturation in maize and accumulates in apoptotic bodies during anther dehiscence. Plant Physiol. 134, 1069–1079.

Schulte, D., Close, T.J., Graner, A., Langridge, P., Matsumoto, T., Muehlbauer, G., 2009. The international barley sequencing consortium—at the threshold of efficient access to the barley genome. Plant Physiol. 149, 142–147.

Schwender, J., Goffman, F., Ohlrogge, J.B., Shachar-Hill, Y., 2004. Rubisco without the Calvin cycle improves the carbon efficiency of developing green seeds. Nature 432, 779–782.

Seiffert, U., Bollenbeck, F., 2008. Fuzzy image segmentation by potential fields. In: IEEE World Congress on Computational Intelligence (WCCI), 1118–1123.

Seo, M., Aoki, H., Koiwai, H., Kamiya, Y., Nambara, E., Koshiba, T., 2004. Comparative studies on the *Arabidopsis* aldehyde oxidase (*AAO*) gene family revealed a major role of *AAO3* in ABA biosynthesis in seeds. Plant Cell Physiol. 45, 1694–1703.

Shewry, P.R., Halford, N.G., 2002. Cereal seed storage proteins: structures, properties and role in grain utilization. J. Exp. Bot. 53, 947–958.

Sinha, T.K., Khatib-Shahidi, S., Yankeelov, T.E., Mapara, K., Ehtesham, M., Cornett, D.S., et al. 2008. Integrating spatially resolved three-deminsional MALDI IMS with in vivo magnetic resonance imaging. Nat. Methods 5, 57–59.

Smidansky, E.D., Clancy, M., Meyer, F.D., Lanning, S.P., Blake, N.K., Talbert, L.E., et al. 2002. Enhanced ADP-glucose pyrophosphorylase activity in wheat endosperm increases seed yield. Proc. Natl. Acad. Sci. USA 99, 1724–1729.

Sreenivasulu, N., Altschmied, L., Radchuk, V., Gubatz, S., Wobus, U., Weschke, W., 2004. Transcript profiles and deduced changes of metabolic pathways in maternal and filial tissues of developing barley grains. Plant J. 37, 539–553.

Sreenivasulu, N., Radchuk, V., Strickert, M., Miersch, O., Weschke, W., Wobus, U., 2006. Gene expression patterns reveal tissue-specific signaling networks controlling programmed cell death and ABA-regulated maturation in developing barley seeds. Plant J. 47, 310–327.

Sreenivasulu, N., Graner, A., Wobus, U., 2008a. Barley genomics: an overview. Int. J. Plant Genomics Article ID 486258, 13pp.

Sreenivasulu, N., Usadel, B., Winter, A., Radchuk, V., Scholz, U., Stein, N., 2008b. Barley grain maturation and germination: metabolic pathway and regulatory network commonalities and differences highlighted by new MapMan/PageMan profiling tools. Plant Physiol. 146, 1738–1758.

Steuer, R., Junker, B.H., 2009. Computational models of metabolism: stability and regulation in metabolic networks. Adv. Chem. Phys. 142, 105–251.

Suzuki, M., McCarty, D.R., 2008. Functional symmetry of the B3 network controlling seed development. Curr. Opin. Plant Biol. 11, 548–553.

Swain, S.M., Reid, J.B., Kamiya, Y., 1997. Gibberellins are required for embryo growth and seed development in pea. Plant J. 12, 1329–1338.

Tadege, M., Dupuis, I., Kuhlemeier, C., 1999. Ethanolic fermentation: new functions for an old pathway. Trends Plant Sci. 4, 320–325.

Tetlow, I.J., Davies, E.J., Vardy, K.A., Bowsher, C.G., Burrell, M.M., Emes, M.J., 2003. Subcellular localisation of ADPglucose pyrophosphorylase in developing wheat endosperm and analysis of the properties of a plastidial isoform. J. Exp. Bot. 54, 715–725.

Thiel, J., Weier, D., Sreenivasulu, N., Strickert, M., Weichert, N., Melzer, M., et al. 2008. Differential hormonal regulation of cellular differentiation and function in nucellar projection and endosperm transfer cells: a microdissection-based transcriptome study of young barley grains. Plant Physiol. 148, 1436–1452.

Thiel, J., Müller, M., Weschke, W., Weber, H., 2009. Amino acid metabolism at the maternal-filial boundary of young barley seeds: a microdissection-based study. Planta 230, 205–213.

Thimm, O., Bläsing, O., Gibon, Y., Nagel, A., Meyer, S., Krüger, P., et al. 2004. MAPMAN: a user-driven tool to display genomics data sets onto diagrams of metabolic pathways and other biological processes. Plant J. 37, 914–939.

Thompson, R.D., Hueros, G., Becker, H., Maitz, M., 2001. Development and functions of seed transfer cells. Plant Sci. 160, 775–783.

Thorbjørnsen, T., Villand, P., Denyer, K., Olsen, O.-A., Smith, A.M., 1996. Distinct isoforms of ADPglucose pyrophosphorylase occur inside and outside the amyloplasts in barley endosperm. Plant J. 10, 243–250.

To, A., Valon, C., Savino, G., Guilleminot, J., Devic, M., Giraudat, J., et al. 2006. A network of local and redundant gene regulation governs *Arabidopsis* seed maturation. Plant Cell 18, 1642–1651.

Usadel, B., Bläsing, O.E., Gibon, Y., Retzlaff, K., Höhne, M., Günther, M., et al. 2008. Global transcript levels respond to small changes of the carbon status during progressive exhaustion of carbohydrates in *Arabidopsis* rosettes. Plant Physiol. 146, 1834–1861.

Uys, L., Botha, F.C., Hofmeyr, J.H., Rohwer, J.M., 2007. Kinetic model of sucrose accumulation in maturing sugarcane culm tissue. Phytochemistry 68, 2375–2392.

Verdier, J., Thompson, R.D., 2008. Transcriptional regulation of storage protein synthesis during dicotyledon seed filling. Plant Cell Physiol. 49, 1263–1271.

Vos, J., Marcelis, L.F.M., Evers, J.B., 2007. Functional–structural plant modelling in crop production—adding a dimension. In: Vos, J., Marcelis, L.F.M., de Visser, P.H.B., Struik, P.C., Evers, J.B. (Eds.), Functional–Structural Plant Modelling in Crop Production. Springer, Berlin, pp. 1–12.

Wan, Y., Poole, R.L., Huttly, A.K., Toscano-Underwood, C., Feeney, K., Welham, S., et al. 2008. Transcriptome analysis of grain development in hexaploid wheat. BMC Genomics 9, 121.

Wang, H., Qi, Q., Schorr, P., Cutler, A.J., Crosby, W.L., Fowke, L.C., 1998. ICK1, a cyclin-dependent protein kinase inhibitor from *Arabidopsis thaliana* interacts with both Cdc2a and CycD3, and its expression is induced by abscisic acid. Plant J. 15, 501–510.

Watson, P.A., Duffus, C.M., 1988. Carbon dioxide fixation by detached cereal caryopses. Plant Physiol. 87, 504–509.

Weber, H., Borisjuk, L., Wobus, U., 1997. Sugar import and metabolism during seed development. Trends Plant Sci. 2, 169–174.

Weber, H., Borisjuk, L., Wobus, U., 2005. Molecular physiology of legume seed development. Annu. Rev. Plant Biol. 56, 253–279.

Weber, H., Sreenivasulu, N., Weschke, W., 2010. The molecular physiology of seed maturation and seed storage protein biosynthesis. In: Pua, E.-C., Davey, M. (Eds.), Plant Developmental Biology—Biotechnological Perspectives, vol. 2. Springer, Heidelberg.

Weichert, N., Saalbach, I., Weichert, H., Kohl, S., Erban, A., Kopka, J., et al. 2010. Increasing sucrose uptake capacity of wheat grains stimulates storage protein synthesis. Plant Physiol. 152, 698–710.

Weigelt, K., Küster, H., Radchuk, R., Müller, M., Weichert, H., Fait, A., et al. 2008. Increasing amino acid supply in pea embryos reveals specific interactions of N and C metabolism, and highlights the importance of mitochondrial metabolism. Plant J. 55, 909–926.

Wernecke, P., Müller, J., Dornbusch, T., Wernecke, A., 2007. The virtual crop-modelling system 'VICA' specified for barley. In: Vos, J., Marcelis, L.F.M., de Visser, P.H.B., Struik, P.C., Evers, J.B. (Eds.), Functional–Structural Plant Modelling in Crop Production. Springer, Berlin, pp. 53–64.

Weschke, W., Panitz, R., Sauer, N., Wang, Q., Neubohn, B., Weber, H., et al. 2000. Sucrose transport into barley seeds: molecular characterization and implications for seed development and starch accumulation. Plant J. 21, 455–467.

Weschke, W., Panitz, R., Gubatz, S., Wang, Q., Radchuk, R., Weber, H., et al. 2003. The role of invertases and hexose transporters in controlling sugar ratios in maternal and filial tissues of barley caryopses during early development. Plant J. 33, 395–411.

Wobus, U., Sreenivasulu, N., Borisjuk, L., Gubatz, S., Rolletschek, H., Panitz, R., et al. 2005. Molecular physiology and genomics of developing barley grains. In: Pandalai, S.G. (Ed.), Recent Research Developments in Plant Molecular Biology, vol. 2. Research Signpost, Trivandrum/Kerala, India, pp. 1–29.

Wu, C.-Y., Trieu, A., Radhakrishnan, P., Kwok, S.F., Harris, S., Zhang, K., et al. 2008. Brassinosteroids regulate grain filling in rice. Plant Cell 20, 2130–2145.

Xu, S.B., Li, T., Deng, Z.Y., Chong, K., Xue, Y., Wang, T., 2008. Dynamic proteomic analysis reveals a switch between central carbon metabolism and alcoholic fermentation in rice filling grains. Plant Physiol. 148, 908–925.

Yanagisawa, S., Yoo, S.-D., Sheen, J., 2003. Differential regulation of EIN3 stability by glucose and ethylene signalling in plants. Nature 425, 521–525.

Yang, J., Zhang, J., Liu, K., Wang, Z., Liu, L., 2006. Abscisic acid and ethylene interact in wheat grains in response to soil drying during grain filling. New Phytol. 171, 293–303.

Yin, X., Struik, P.C., 2008. Applying modelling experiences from the past to shape crop systems biology: the need to converge crop physiology and functional genomics. New Phytol. 179, 629–642.

Young, T.E., Gallie, D.R., 2000a. Regulation of programmed cell death in maize endosperm by abscisic acid. Plant Mol. Biol. 42, 397–414.

Young, T.E., Gallie, D.R., 2000b. Programmed cell death during endosperm development. Plant Mol. Biol. 44, 283–301.

Zhang, H., Ogas, J., 2009. An epigenetic perspective on developmental regulation of seed genes. Mol. Plant 2, 610–627.

Zhang, W.H., Walker, N.A., Tyerman, S.D., Patrick, J.W., 2000. Fast activation of a time-dependent outward current in protoplasts derived from coats of developing *Phaseolus vulgaris* seeds. Planta 211, 894–898.

Zhang, W.H., Skerret, M., Walker, N.A., Patrick, J.W., Tyerman, S.D., 2002. Nonselective currents and channels in plasma membranes of protoplasts from coats of developing seeds of bean. Plant Physiol. 128, 388–399.

Zhang, H., Sreenivasulu, N., Weschke, W., Stein, N., Rudd, S.D., Radchuk, V., et al. 2004. Large-scale analysis of the barley transcriptome based on expressed sequence tags. Plant J. 40, 276–290.

Zhou, Y., Qu, H., Dibley, K.E., Offler, C.E., Patrick, J.W., 2007. A suite of sucrose transporteres expressed in coats of developing legume seeds includes novel pH-independent facilitators. Plant J. 49, 750–764.

This page intentionally left blank

CHAPTER THREE

New Insights into the Regulation of the Actin Cytoskeleton by Tropomyosin

C.-L. Albert Wang *and* Lynne M. Coluccio

Contents

1. Introduction 92
2. Biochemical and Biophysical Properties of Tropomyosin 92
   2.1. Gene structure 92
   2.2. Protein structure 95
   2.3. Biochemical properties 98
3. Roles of Tropomyosin in Muscle and Nonmuscle Cells 99
   3.1. Striated muscle contraction 99
   3.2. Smooth muscle 101
   3.3. Tropomyosin in nonmuscle cells 102
4. Intracellular Distribution of Tropomyosin Isoforms 105
   4.1. Distribution of tropomyosin isoforms 105
   4.2. Interaction of actin–tropomyosin with myosin II 107
   4.3. Class I myosins and tropomyosins at the cell membrane 108
5. Caldesmon and Tropomyosins 108
   5.1. Relationship between tropomyosin and caldesmon 108
   5.2. Phosphorylation of tropomyosin and caldesmon in cells 110
   5.3. How caldesmon and tropomyosins affect actin dynamics 112
6. Potential Roles of Tropomyosin in Cancer Metastasis 114
7. Concluding Remarks 116
Acknowledgments 116
References 117

Abstract

The actin cytoskeleton is regulated by a variety of actin-binding proteins including those constituting the tropomyosin family. Tropomyosins are coiled-coil dimers that bind along the length of actin filaments. In muscles, tropomyosin regulates the interaction of actin-containing thin filaments with myosin-containing thick filaments to allow contraction. In nonmuscle cells where multiple tropomyosin isoforms are expressed, tropomyosins participate in a number of cellular events

Boston Biomedical Research Institute, Watertown, Massachusetts, USA

International Review of Cell and Molecular Biology, Volume 281
ISSN 1937-6448, DOI: 10.1016/S1937-6448(10)81003-2

involving the cytoskeleton. This chapter reviews the current state of the literature regarding tropomyosin structure and function and discusses the evidence that tropomyosins play a role in regulating actin assembly.

Key Words: Tropomyosin, Actin dynamics, Cytoskeleton, Muscle, Caldesmon.

1. Introduction

Tropomyosins (Tms) constitute a family of actin-binding proteins that are important in both muscle and nonmuscle cells. In skeletal muscles where it was first identified (Bailey, 1948), Tm plays a pivotal role in conjunction with troponin in regulating the interaction of actin-containing thin filaments with myosin-containing thick filaments to effect muscle contraction. Tm was subsequently identified as a component of nonmuscle cells (Cohen and Cohen, 1972; Lazarides, 1975). In fact, there are >40 mammalian Tm isoforms, 18 of which are expressed in nonmuscle cells (Gunning et al., 2008). Why so many isoforms exist, how they differ in structure and function, and what roles they play in regulating the actin cytoskeleton, are a few of the most important outstanding questions in the biology of Tms. The generally accepted role of Tms in nonmuscle cells is to stabilize actin filaments particularly against severing proteins; however, Tms have also been identified in lamellipodia of migrating cells where actin is thought to be highly dynamic, suggesting that this notion must be reevaluated. Indeed, it is possible that Tms have multiple effects on the dynamics of actin assembly and this idea will be discussed here. Tms have been the subject of many studies and recent reviews exist (Gunning et al., 2008; O'Neill et al., 2008; Perry, 2001). In particular, chapters devoted to Tms constitute a recent volume (644) in *Advances in Experimental Medicine and Biology*. In this review, we summarize the current status of Tm research with an emphasis on the interaction between Tm and other actin-binding proteins with respect to the actin cytoskeleton.

2. Biochemical and Biophysical Properties of Tropomyosin

2.1. Gene structure

In mammals there are four genes that code for Tm: α, β, γ, and δ, also referred to as *TPM1*, *TPM2*, *TPM3*, and *TPM4*, respectively (Lin et al., 2008; Pittenger et al., 1994; Vrhovski et al., 2008) (Fig. 3.1). Alternative splicing of these four genes, the use of multiple promoters, and the choice of

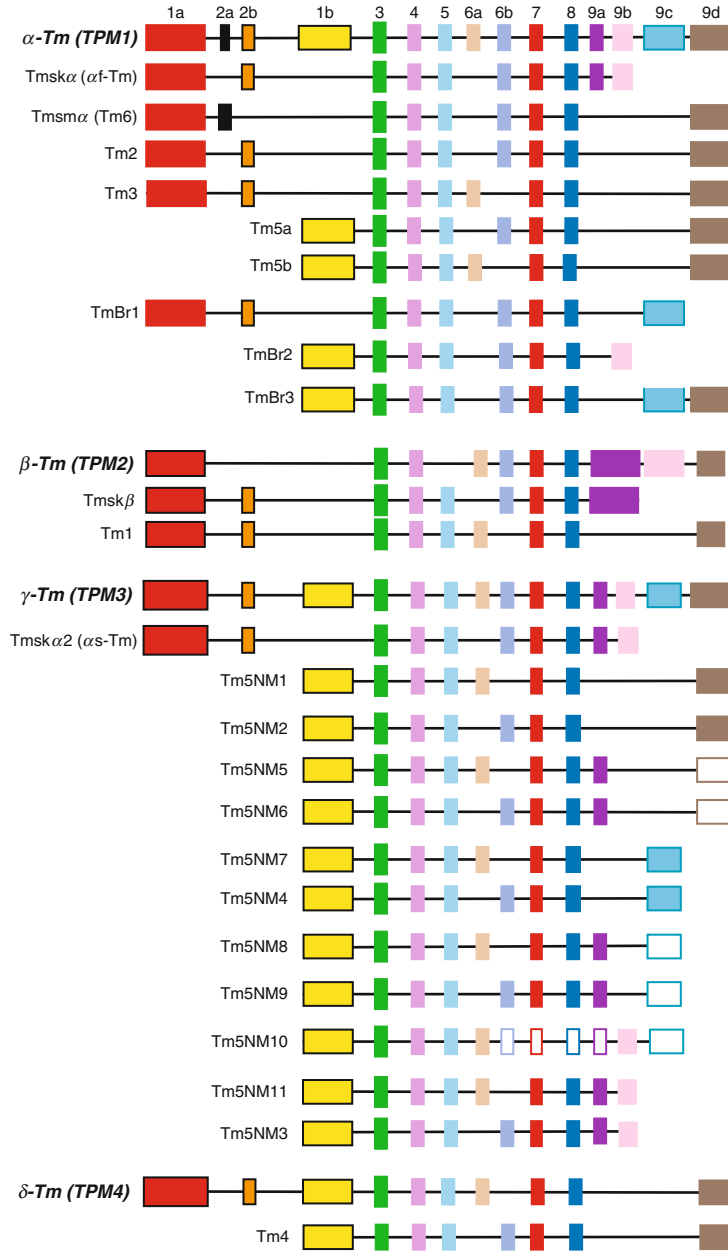

Figure 3.1 Schematic of exon organization of the four tropomyosin genes in mammals where exons are represented by boxes and introns are represented by solid lines. Isoform variation is primarily at the amino and carboxyl ends and a result, for example, of the alternative use of exon 2a versus 2b in TPM1 and one of the four exons (9a, 9b, 9c, and 9d) at the C-terminus. The figure is based on previously published figures (Gunning et al., 2008; Lin et al., 2008; Vrhovski et al., 2008).

polyadenylation site (Helfman et al., 1986; Ruiz-Opazo and Nadal-Ginard, 1987) lead to expression of at least 22 different Tms in humans (Lin et al., 2008). As a result of alternative 5′- end exons, two types of Tms are generated by different promoters: high molecular weight (HMW) isoforms, which are 284 amino acids in length, and contain seven actin-binding regions; and low molecular weight (LMW) isoforms, which are ~248 amino acids in length, and contain six actin-binding motifs. In *TPM1-3*, there are alternative 3′ exons that result in different C-termini and 3′-untranslated regions. And, there is mutual exclusive splicing of exons leading to different sequences at the N-termini (*TPM1*) and within the molecule (*TPM1-3*).

α-*Tm* is perhaps the best studied Tm gene. It is ~28 kb in size and contains 15 exons; and has two alternative promoters, two mutually exclusive exons (2a/2b and 6a/6b), and four alternatively spliced 3′ exons (9a/9b/9c/9d) resulting in different C-termini. It codes for skeletal (Tmskα), smooth (Tmsmα), and several nonmuscle Tms (Tm2, Tm3, Tm5a, and Tm5b) including three brain-specific isoforms (TmBr1, TmBr2, TmBr3) (Lees-Miller et al., 1990a; Lewis and Smillie, 1980; Lin et al., 2008; Vrhovski et al., 2008). Curiously, the sequences of the alternative exons, such as 1a versus 1b, are quite different; however, the exons in one gene are similar to the corresponding exons in the different genes. *β-Tm* is 8–10 kb depending on the source, has 11 exons and a single promoter, a mutually exclusive internal exon (6a/6b), and two different C-terminal exons (9a/9d). It produces skeletal muscle β-Tm; and smooth muscle β-Tm, which is the same as cytoskeletal Tm1, all of which have 284 amino acids. In humans a second cytoskeletal form is found, hTm1-1 (Lin et al., 2008). γ-*Tm* spans 42 kb of DNA, and has at least 13 exons, two alternative exons (6a/6b), and four carboxyl-terminal exons (9a–d) (Clayton et al., 1988; Dufour et al., 1998). It codes for the slow twitch isoform of skeletal muscle α-Tm (TMskα2) as well as at least 11 nonmuscle forms in mouse: TmNM-1, TmNM-2, TmNM-5, TmNM-6, TmNM-7, TmNM-4, TmNM-8, TmNM-9, TmNM-11, TmNM-3, and TmNM-10 (Beisel and Kennedy, 1994; Dufour et al., 1998; Vrhovski et al., 2008). *δ-Tm*, which codes for nonmuscle TM4, spans 16–18 kb and unlike the other Tm genes is not alternatively spliced in rat and mouse (Lees-Miller et al., 1990b). Interestingly, the molecule contains two case sequences similar to exons from the other Tm genes; however, they contain mutations that make these regions nonfunctional as coding exons (Lees-Miller et al., 1990b). The human γ-*Tm* gene spans 35 kb and in addition to LMW Tm4, codes for a HMW isoform similar to smooth muscle Tm (hTm4HMW) (Lin et al., 2008; Vrhovski et al., 2008).

In striated muscle, the main isoforms are α-fast tropomyosin (αf-Tm or Tmskα1) from α-*Tm*, β-tropomyosin (β-Tm or hTmskβ) from the *β-Tm* gene, and α-slow tropomyosin (αs-Tm) from the γ-*Tm* gene. Heart contains

hTmskα1 and hTmskα1-1 from the α-*Tm* gene. Smooth muscle contains hTmsmα and hTmsmα-1 from the α-*Tm* gene, hTm1 from *β-Tm*, and hTm5 from *γ-Tm*.

2.2. Protein structure

Tms consist of heptapeptide repeats of the form *a-b-c-d-e-f-g* characteristic of a coiled-coil structural motif, where *a* and *d* are generally apolar residues. Two right-handed helices wind around each other to form a left-handed coiled coil. The stability of the coiled coil depends on hydrophobic interactions within the core and ionic bonds between the side chains. In some places alanines are at these positions, which serve to destabilize the coiled coil (Nitanai et al., 2007; Sumida et al., 2008; Whitby and Phillips, 2000). These variations and others including acidic residues, Asp^{137} and Glu^{218}, at positions *d* and *a*, respectively, are believed to account for its flexibility (Sumida et al., 2008), which is observed in both low- resolution crystal structures of full-length cardiac Tm (Whitby and Phillips, 2000) and higher resolution images of the N- (Brown et al., 2001) and C-ends (Li et al., 2002). In particular, the fact that Tm is preferentially cleaved at Arg^{133} as a consequence of Asp^{137}, which destabilizes the middle of the molecule (Sumida et al., 2008), and that substitution of Asp with Leu at this position results in an increase in myosin ATPase activity (Sumida et al., 2008) indicate that differences in flexibility of Tms might be responsible for the different cellular functions of various Tm isoforms.

Tms are long α-helical dimers that polymerize head-to-tail. In skeletal muscle Tm is present predominantly as a mixture of αβ heterodimers and αα homodimers, which are more thermodynamically stable than ββ homodimers (Bronson and Schachat, 1982). Correct dimer formation is critical as evidenced by the finding that mutation in Tm leading to the formation of αα dimers rather than αβ dimers results in nemaline myopathy (Corbett et al., 2005), a human genetic disease characterized by muscle weakening (Kee and Hardeman, 2008). In mice both α- and β-Tm are expressed in cardiac muscle during embryogenesis and fetal development; however, soon after birth the expression of β-Tm decreases leaving the αα chain as the predominant Tm (Muthuchamy et al., 1993). Substitution of α-Tm for β-Tm in the mouse heart has a significant effect on diastolic function (Muthuchamy et al., 1995).

Seven nonmuscle Tm isoforms are expressed at the same time in rat liver fibroblasts, which suggests that a mechanism must be in place to ensure that proper pairing occurs. Studies of epitope-tagged Tms in living cells showed that the HMW nonmuscle isoforms, Tm1, Tm2, and Tm3, form homodimers; whereas the LMW Tms, Tm4, Tm5NM1, Tm5a, and Tm5b, form both homo- and heterodimers (Gimona, 2008; Gimona et al., 1995; Pittenger and Helfman, 1992; Temm-Grove et al., 1998). HMW and

LMW Tms do not form stable dimers together. Studies indicate that specificity of dimer formation is contained within the amino acid sequence of the Tms themselves and is influenced by alternatively spliced exons (Gimona et al., 1995). Curiously, Tm5a and Tm5b, which differ only in exon 6, are not able to form heterodimers *in vitro*; whereas Tm2 and Tm3, which also differ in their use of exon 6, form heterodimers. Studies *in vitro* have indicated that for frog skeletal and gizzard smooth muscle Tm, heterodimers are preferentially formed to minimize overall thermodynamic dissociation (Lehrer and Qian, 1990; Lehrer et al., 1989).

Tm dimers bind along the length of actin filaments and wind around the actin helix (Hanson and Lowy, 1963; Lin et al., 1997; Moore et al., 1970; Phillips et al., 1986). In skeletal muscle each Tm binds to seven successive actin subunits (38 nm). Although binding of monomeric Tm to actin is weak (Wegner, 1979), the head-to-tail interactions of multiple Tms increases binding. There is an overlap of ~4–18 amino acids in the N- and C-termini of adjacent Tms depending on the isoform (Heeley et al., 1989; Tobacman, 2008). One would think that the length of the overlap has implications for Tm binding to actin with a long overlap correlating with more cooperative binding to actin, but yeast Tms have an overlap of only four amino acids and bind to actin with the same cooperativity as seen for muscle Tms, suggesting that other factors are at work (Strand et al., 2001; Tobacman, 2008). The overlap regions share similar axial positions on actin (Tobacman, 2008).

Structural studies have suggested that Tm is a highly flexible molecule in which regions of destabilizing residues are interspersed with more stable coiled-coil regions (Brown et al., 2001, 2005; Phillips and Chacko, 1996; Smith and Geeves, 2003; Smith et al., 2003). The joint between successive Tm molecules has been considered flexible allowing Tm to act like a flexible cable along the length of the actin filament and adjust its position in response to myosins and troponin (Greenfield et al., 2006). A recent report using electron microscopy and molecular dynamic simulations suggests that Tm has a curved conformation that matches the helical shape of F-actin and rather than being flexible is actually semirigid (Li et al., 2009). This would allow Tm to move more easily as a cooperative unit as previously suggested (Geeves and Lehrer, 1994). Alternatively, local destabilization rather than segmental bending allows Tm to conform to the actin filament (Singh and Hitchcock-DeGregori, 2003, 2009).

The polypeptide chains contain multiple quasi-equivalent domains of approximately 40 amino acids each of which interacts with an actin subunit when bound to an actin filament. There is, however, no repeated consensus sequence for actin binding. Deletion analyses showed that an uninterrupted coiled coil is required for actin binding (Hitchcock-DeGregori and Varnell, 1990), and that the seven periodic repeats are not equivalent. For example, deletion of period 2 has little effect on actin binding or actomyosin ATPase activity, whereas deletion of period 5 severely reduces actin affinity and

myosin binding to actin (Hitchcock-DeGregori et al., 2002). One idea based on mutagenesis studies is that the Tm coiled coil is locally destabilized where it binds actin and that these regions are able to reorient to maximize their interactions (Singh and Hitchcock-DeGregori, 2009). In addition to actin-binding sites, there are two troponin T-binding sites on skeletal muscle Tm, one near the C-terminus and the other near Cys-190 (Lamkin et al., 1983), a region in which the sequences of fibroblast and skeletal muscle Tm differ (Helfman et al., 1986).

Skeletal and smooth muscle Tms require acetylation of the N-terminal methionine for strong binding to actin. Lack of an acetyl group destabilizes the N-terminal coiled coil and reduces the affinity of striated muscle Tm for actin (Greenfield et al., 1994; Palm et al., 2003). The likely role of acetylation is to facilitate end-to-end binding of Tms. Structural data showed that the region of Tm containing the C-terminal 11 amino acids is splayed whereas the N-terminus is not, provided that it is acetylated (Brown et al., 2001). This allows the N-terminus to fit inside the C-terminus facilitating assembly of Tms into filaments; the N-terminus is rotated $\sim 90^{\circ}$ relative to the C-terminus (Greenfield et al., 2006). The addition of a di- or tripeptide at the N-terminus of expressed Tm substitutes for the *N*-acetyl group of muscle Tms and allows binding to actin (Monteiro et al., 1994).

Crystal structures of native Tm are available, although at low resolution, whereas the structures of several fragments have been solved at high resolution. The structure of the N-terminal 81 amino acids of chicken skeletal α-Tm, solved to 2.0 Å (Brown et al., 2001), is almost entirely α-helical with the exception of the first two residues, which are in an extended conformation. Because the fragment used was expressed in bacteria the amino terminus was unacetylated, which might account for the extended conformation of the first two residues. A previous NMR study of the acetylated first 14 amino acids of Tm showed the structure to be completely α-helical (Greenfield et al., 1998). The crystal structure revealed that the core has an unusually high content of alanines that might be responsible for a small axial shift that breaks the symmetry and causes bending of the molecule, which supports the winding of Tm around the actin filament (Brown et al., 2001). The mid-region also exhibits specific bends of the coiled coil and apolar patches representing actin-binding sites (Brown et al., 2005). Other crystallographic studies showed that rather than forming a coiled coil, the α-helices that comprise the C-terminal 22 amino acids of skeletal muscle α-Tm splay apart; this region is critical to troponin binding (Li et al., 2002). Studies of a C-terminal fragment comprising more than 40% of α-Tm suggest that the structure of Tm best resembles a ''rubber rod with ... flexible regions'' because they observed that the hydrophobic core has holes that contain water molecules (MInakata et al., 2008).

Three-dimensional reconstructions of both native and reconstituted thin filaments show densities attributable to Tm in one of two equilibrium

positions: on the inner edge of the outer domain of the actin filament in the absence of Ca^{2+} and on the outer edge of the inner domain of the actin filament when Ca^{2+} is present (Lehman et al., 2000; Vibert et al., 1997; Xu et al., 1999). These studies demonstrate the Ca^{2+}-sensitive movement of Tm on actin filaments that is critical to muscle contraction when troponin is present. Similar studies performed with various Tm isoforms, although in the absence of troponin, show that the position that Tm adopts on actin filaments is a function of the specific actin or Tm isoform being studied (Lehman et al., 2000). For example, although skeletal ($\alpha\alpha$ and $\alpha\beta$) Tm and nonmuscle Tm5a prefer to bind to the outer edge of the inner domain of actin (the same so-called C-state that Tm adopts on reconstituted filaments in the presence of Ca^{2+}; Section 3.1), cardiac ($\alpha\alpha$) Tm and smooth ($\alpha\beta$) Tm under the same conditions bind to the inner part of the outer domain. The studies support the notion that troponin acts as an off switch that keeps Tm at the outer domain in the absence of Ca^{2+}. These Tms bind at one of two possible sites on the inner domain of skeletal muscle F-actin, but, on the outer domain of actin isolated from yeast (Lehman et al., 2000) emphasizes the importance of investigating the interaction of nonmuscle Tms with nonmuscle actin.

2.3. Biochemical properties

The LMW Tms Tm4, Tm5NM1, Tm5a, and Tm5b and the HMW Tms Tm1, Tm2, Tm3, and Tm6 are expressed in nonmuscle cells. Tm1, Tm2, and Tm3 along with Tm4 are the major isoforms expressed in untransformed cells (Helfman et al., 2008). The large number of Tm isoforms expressed in cells might represent how Tms play a variety of functions in different cell types. These different Tm isoforms display different biochemical properties, and are not redundant in function, support this notion. For example, both HMW and LMW Tms bind actin simultaneously *in vitro*; however, the LMW Tm, Tm5b, readily displaces other Tms from actin, including Tm5a which differs from Tm5b only in the use of exon 6a (Tm5b) versus 6b (Tm5a), a difference of some 24 amino acids (Pittenger and Helfman, 1992). Other studies showed that although γ-gene product, Tm5, binds F-actin more strongly than α-gene product, Tm3, the latter has a higher cooperativity of binding than Tm5; and Tm5/Tm3 chimeras have even stronger actin binding than Tm3 (Novy et al., 1993). A study using bacterially expressed chimeras representing α-Tm isoforms with different N- and C-termini indicated that the ends of Tm determine Tm's affinity for actin, which has a direct effect on the cooperativity of myosin in inducing Tm binding to actin. When actin affinity is high, fewer myosin molecules are necessary to activate the filament (Moraczewska et al., 1999).

Tms are not equal in their interactions with myosin. Rabbit skeletal Tm activates or inhibits the myosin II S1 ATPase activity depending on the S1

concentration (Lehrer and Morris, 1982); whereas nonmuscle cytoskeletal Tms and smooth muscle Tm stimulate the myosin II ATPase activity, although not equivalently. This can now be understood in terms of the different cooperativities due to end-to-end interactions of different Tm isoforms. Tm5, product of the human γ gene, stimulates the actin-activated myosin ATPase activity threefold greater than α-gene product, Tm3 (Novy et al., 1993).

Tms bind along the length of actin filaments and protect them from actin-severing proteins such as gelsolin, villin, and ADF/cofilin (Bernstein and Bamburg, 1982; Burgess et al., 1987; DesMarais et al., 2002) and depolymerization of actin from the pointed end (Broschat, 1990). There is evidence from cellular studies that some LMW Tms protect actin filaments from severing better than HMW Tms (Creed et al., 2008). Tms inhibit branching and nucleation of actin in the leading edge of motile cells by the Arp2/3 complex activated by the C-terminus of the Wiskott–Aldrich syndrome protein, WASp-WA (Blanchoin et al., 2001). In particular, Tm5a inhibits actin assembly stimulated by the Arp2/3 complex and WASp-WA to a greater extent than Tm2 (Blanchoin et al., 2001). Tms also prevent bundling of actin filaments by villin (Burgess et al., 1987) and in the case of skeletal muscle Tm alone, but not nonmuscle Tm (Section 5.2.3), bundling by fascin (Bryan et al., 1993; Matsumura and Yamashiro-Matsumura, 1986). Tms interact with tropomodulin, which binds at the pointed ends of actin filaments, to prevent the disassembly of actin subunits (Fowler, 1996; Kostyukova, 2008).

3. Roles of Tropomyosin in Muscle and Nonmuscle Cells

3.1. Striated muscle contraction

Tm was first identified in skeletal muscle (Bailey, 1948) where it was found to extract from the I bands along with actin (Corsi and Perry, 1958). In concert with the Ca^{2+}-binding protein, troponin, Tm mediates the interaction of thin filaments with myosin-containing thick filaments (Greaser and Gergely, 1971). The association of mutations in both Tm and troponin with cardiac myopathies and hypertension as well as respiratory and other diseases testifies to their importance (Ochala, 2008).

Troponin, which consists of a globular region and an extended tail (Flicker et al., 1982), is a complex of three subunits: troponin-I (TnI), which inhibits the myosin ATPase activity; troponin-T (TnT), which binds the troponin complex to Tm; and troponin-C (TnC), which binds calcium ions (Greaser and Gergely, 1971; Potter and Gergely, 1974). Because troponin is positioned at every seventh actin, there has been little

information regarding its structure on actin because it is averaged out with available reconstruction methods. New single-particle analyses suggest that in low Ca^{2+} troponin is tapered with the widest point toward the barbed end of the thin filament (Paul et al., 2009). This is opposite to that proposed in an earlier and more generally accepted model (Ohtsuki, 1979), and calls for a reevaluation of how TnT and Tm interact. Further structural studies done in the presence of Ca^{2+} are likely to shed more light on exactly where Tn binds actin and its relationship to Tm.

Muscle contraction involves the sliding of actin-containing thin filaments past myosin-containing thick filaments in the presence of ATP. Myosin heads, which form crossbridges that extend out from the thick filament, interact with actin subunits in the thin filaments and through a conformational change associated with ATP hydrolysis push the actin filament relative to the thick filament effecting contraction. It is generally believed that in striated muscle filaments, Tm and troponin lie on the outer domain of the long grooves of F-actin obscuring the myosin-binding site on actin (Hanson and Lowy, 1964; Moore et al., 1970). This has been referred to as the *blocked* (no myosin binding, or the B-) state, one of three states that Tm assumes on actin; the others are referred to as the *closed* (Ca^{2+}-induced; or the C-) and *open* (myosin-induced; or the O-) states (Geeves and Lehrer, 1994; Maytum et al., 2001; McKillop and Geeves, 1993), both of which are more toward the inner domain of actin. The presence of three Tm states is well supported by kinetic evidence. As a consequence of Ca^{2+} signaling through troponin, Tm is shifted to the closed state by moving laterally and uncovering myosin-binding sites on actin to allow myosin to isomerize to produce the force-generating, or *open*, state. This permits the interaction of myosin heads with actin allowing sliding of the thick filaments relative to the thin filaments and muscle contraction. Ca^{2+}-dependent shifts in position of Tm on thin filaments isolated from vertebrate muscle or actin filaments reconstituted with actin and Tm are observable in three-dimensional reconstructions of electron micrographs (Lehman and Craig, 2008; Lehman et al., 1995, 2000).

α- and β- striated muscle Tms are the predominant forms in mammalian striated muscle. αTm is found predominantly in fast twitch skeletal muscle, whereas β and γ Tms predominate in slow twitch skeletal muscle (Lees-Miller and Helfman, 1991; Schevzov and O'Neill, 2008). Each Tm gene has its own pattern of transcript accumulation in adult muscle and during myogenesis (Gunning et al., 1990). In mouse cardiac muscle only a single α isoform exists (Muthuchamy et al., 1993; Schevzov and O'Neill, 2008). Knockout of α-Tm by homologous recombination is lethal leading to death at embryonic day 10–14 in mice, which corresponds to development of the myocardium (Blanchard et al., 1997; Rethinasamy et al., 1998). New studies show that substituting the α isoform with β- or γ-Tm leads to functional differences in the heart in the rates of relaxation and contraction

(Jagatheesan et al., 2009). Mutations in two Tm genes, *β-Tm* and *γ-Tm*, are responsible for congenital muscle diseases and disorders including nemaline myopathy (*β-Tm* and *γ-Tm*), distal arthrogryposis (*β-Tm*), cap disease (*β-Tm*), and congenital fiber-type disproportion (*γ-Tm*) (Kee and Hardeman, 2008).

Cytoskeletal Tms are also expressed in muscle tissues. Tm5NM1 is associated with the sarcolemma and is found adjacent to the Z-line consistent with the localization of T-tubules (Kee et al., 2004). Myofibers from mice in which Tm5NM1 expression is ablated display an altered excitation–contraction coupling (Vlahovich et al., 2009). The cytoskeletal Tm, Tm4, also associates with a Z-line-associated cytoskeleton and during myofiber growth and repair with longitudinal filaments that are oriented parallel to the sarcoplasmic reticulum (Vlahovich et al., 2008). When Tm3 is expressed in mice, rather than associating with the thin filaments in the sarcomere of skeletal muscle, it becomes associated with regions where endogenous cytoplasmic Tms are found, that is, adjacent to the Z-lines in muscle. Expression of this Tm, which is not normally found in skeletal muscle, leads to late onset muscular dystrophy probably by compromising the structural integrity of the muscle (Kee et al., 2004, 2009). During myogenesis, muscle-specific isoforms are induced and cytoskeletal forms are repressed. The function of these nonmuscle Tms in muscle tissues remains to be elucidated.

3.2. Smooth muscle

The main proteins in thin filaments of smooth muscle are actin, Tm, caldesmon (h-CaD), and calmodulin, but no troponin (Smith and Marston, 1985). Smooth muscle Tm isoforms derive from splicing of the *α-Tm* gene and *β-Tm* gene; most of the Tm is present as *α*/*β* heterodimers. Smooth muscle *β* Tm is the same as nonmuscle Tm1.

Tm and h-CaD in smooth muscle act on the actomyosin ATPase activity in an opposite manner. Unlike striated muscle Tm, smooth muscle Tm by itself "potentiates" the enzymatic activity of actomyosin (except at low S1 concentration and high Mg^{2+}) (Chacko and Eisenberg, 1990; Chacko et al., 1977; Dabrowska et al., 1996; Lehrer and Morris, 1984). This is because of the stronger end-to-end interactions between smooth muscle Tms that facilitate the movement from the blocked to the open position (Lehrer et al., 1997). CaD alone, on the other hand, inhibits the actomyosin ATPase (Dabrowska et al., 1985; Sobue et al., 1985). Such inhibition is enhanced by the presence of Tm, thus from the viewpoint of CaD, the two proteins have a synergistic effect (Ngai and Walsh, 1984). Notably, the fact that smooth muscle Tm can further activate myosin beyond the level of actin alone (Lehrer and Morris, 1984; Lehrer et al., 1997) suggests that Tm does not simply remove some inhibitory factors, but may also change the

structure of actin filaments so that myosin binding is enhanced or the myosin ATPase activity is more effectively activated.

The precise mechanism of the inhibitory action of CaD–Tm has been under extensive study, but still remains controversial. In one model (*cooperative allosteric model*) smooth muscle CaD–Tm is thought to work in a mechanism similar to that of the troponin–Tm system in striated muscles. Unlike skeletal muscle, in smooth muscle there appears to be only two possible positions of Tm on the actin filament relative to the myosin-binding site(s): *open* (or activated) and *blocked* (or inhibited) positions (Lehman et al., 2000). By pushing the bound Tm from the *blocked* position to the *open* position, myosin cooperatively activates the filament upon strong binding (e.g., in the absence of ATP). In contrast, h-CaD preferentially binds to actin–Tm at its off state (Ansari et al., 2008) as evidenced by a fluorescence change (Ishii and Lehrer, 1987), thus preventing it from being activated.

Although the switching off of the filament by h-CaD does not necessarily dissociate the bound myosin (e.g., when Tm is at the *closed* position), displacement does occur when the concentration of h-CaD is sufficiently high. Under this condition the mechanism is described by the *competition model* (Yan et al., 2003). Biochemical data suggest that h-CaD directly competes with myosin for actin binding in the presence of ATP, the so-called weak binding state (Chalovich et al., 1987; Hemric et al., 1993; Horiuchi et al., 1991). The binding sites on the actin surface for myosin and h-CaD overlap (Lehman et al., 1997); however, since the typical physiological concentration of h-CaD is low compared to that of actin (i.e., less than 1/20 of the actin concentration; Haeberle et al., 1992; Lehman et al., 1993), a level at which inhibition of the actomyosin ATPase activity can still be attained but not myosin displacement (Alahyan et al., 2006), it is generally assumed that h-CaD works *in vivo* by the cooperative allosteric mechanism (Ansari et al., 2008). Nevertheless, it should be noted that h-CaD is not evenly distributed in smooth muscle cells (Mabuchi et al., 2001). Although the overall content is low, there may be regions in the cell that contain relatively high concentrations of h-CaD. Whether such local concentrations of h-CaD would allow competition with myosin remains to be investigated.

3.3. Tropomyosin in nonmuscle cells

Major cellular events ranging from cell locomotion to intracellular transport are mediated by the actin cytoskeleton. Actin behavior in turn is regulated by the plethora (>165) of actin-binding proteins including Tm (Dos Remedios et al., 2003; Ono, 2007). There is growing evidence that different populations of actin filaments distinguished by the composition of their actin-binding proteins are spatially organized in distinct regions within cells where they perform specific functions (Gunning et al., 2008; Stehn et al., 2006).

Although the functions of various Tm isoforms expressed in nonmuscle cells are not completely understood, there is substantial evidence that Tm isoforms are critical for cytoskeletal function (Lin et al., 2008). This is likely due as described above to the protection that Tm confers on actin filaments from actin-severing proteins such as gelsolin, villin, and ADF/cofilin (Bernstein and Bamburg, 1982; Burgess et al., 1987; DesMarais et al., 2002), branching induced by the Arp2/3 complex (Blanchoin et al., 2001), and bundling (Bryan et al., 1993; Burgess et al., 1987; Matsumura and Yamashiro-Matsumura, 1986). In fact, different Tms confer different properties on cells, for example, stress fibers in cells expressing LMW Tm5 (NM1) are more resistant to latrunculin A and cytochalasin D treatment than those in cells expressing HMW Tm3 (Creed et al., 2008).

Cell biological experiments indicate that Tms participate in organelle transport. Microinjection into chick embryo fibroblasts of antibodies against Tm1 and Tm3 slows vesicle transport (Hegmann et al., 1989). On the other hand, microinjection of bacterially expressed hTm3, but not hTm5, into normal rat kidney epithelial cells induces retrograde movement of mitochondria and lysosomes into the perinuclear region (Pelham et al., 1996). Apparently, only particular Tm isoforms associate with Golgi-derived vesicles: For example, Tm5NM-1 and Tm5NM-2 derived from the *TPM3* gene are found on Golgi membranes in fibroblasts, but Tms2, 3, 5a, and 5b from *TPM1* (αTm_f), and Tm1 from *TPM2* (β-Tm) are not (Heimann et al., 1999). These data further support the notion that different Tm isoforms support different functions.

In dividing cells, Tms are found around the cell equator and near the cell poles (Eppinga et al., 2006). Studies with cells engineered to express mutant Tms show a correlation between speed of cell division and actomyosin-II ATPase activity. Tm mutations that increase the actomyosin-II ATPase activity show an increase in the rate at which they reach 50% cytokinesis (Eppinga et al., 2006). Thus, Tms also play a role in cell division.

Tms, which localize prominently to stress fibers, were originally thought to be associated in large part with stable actin filaments; however, both HMW and LMW Tms have now been found in regions of the cell where actin is dynamic (Hillberg et al., 2006) bringing into question whether the sole function of Tms in nonmuscle cells is to stabilize actin filaments. At the leading edge of migrating cells, two distinct regions in regards to actin filament organization and behavior have been described, the lamellipodium and the lamellum, using speckle microscopy, a technique in which a small amount of labeled actin microinjected into cells is tracked and analyzed (Gupton et al., 2005; Ponti et al., 2004). The lamellipodium is a 2–4 μm wide region adjacent to the cell membrane in which actin filaments rapidly assemble and disassemble in response to the regulatory proteins ADF/cofilin and the Arp2/3 complex (Svitkina and Borisy, 1999). The lamellum, on the other hand, is a region 3–15 μm

from the cell membrane and is characterized by discrete foci of actin assembly and myosin II- and Tm-mediated slow retrograde flow (Ponti et al., 2004).

Although Tm is found primarily in the lamellum (Ponti et al., 2004), there is evidence that LMW Tm5a/b are specifically located in ruffling membranes in mouse primary fibroblasts (Schevzov et al., 2005a). Furthermore, HMW Tms reach out into the lamellipodia of migrating fibroblasts and both expressed HMW Tm1 and Tm2 and LMW Tm4 and Tm5 localize out to the edge of the lamellipodium (Hillberg et al., 2006). Experimental data support the notion that Tms play a role in lamellipodia. Microinjection of skeletal muscle α-Tm into epithelial cells results in mislocalization of Tm and myosin II to the leading edge (Gupton et al., 2005). As a result, formation of lamellipodia is inhibited while rapid cell movement persisted, suggesting that Tms are major regulators of cell migration. Similarly, in an *in vitro* reconstituted motility assay involving actin and bead-immobilized N-WASP, Arp2/3, capping protein, ADF, and profilin, the addition of skeletal muscle Tm causes changes in propulsion of the beads and morphology of the Arp2/3-branched actin filaments, presumably due to inhibition by Tm of actin capping activity by ADF and branching by Arp2/3 (Bugyi et al., 2009).

Together, these results indicate that a role for Tm must be incorporated into models of actin dynamics at the leading edge of cells. One idea is that only specific isoforms are found in lamellipodia and that Tms found in lamellipodia have distinct roles from those associated with stable actin structures such as stress fibers. Indeed, as will be discussed in a subsequent section, there is new evidence that Tms might regulate actin assembly in cells by spatially and temporally modulating actin dynamics. These exciting results indicate that Tms play an important role in actin filament dynamics and challenge the current dogma regarding the primary role of Tms as stabilizers of formed actin filaments.

Ultimately, the different cellular properties of Tms will be a consequence of their differences in length and/or N-terminal sequence. Tm2, a HMW Tm and Tm5a, a LMW Tm, interact with 7 and 6 actin subunits, respectively. In both α-gene products, Tm2 differs from Tm5a at the N-terminus. Tm5a is missing the sequence coded for by exon 2b and uses exon 1b instead of 1a. One reasonable hypothesis is that actin–Tm5a filaments and actin–Tm2 filaments have different physical properties. For example, due to their end-to-end interactions or length, one filament might be more or less flexible than the other. This would have serious implications in the cell as filaments that are more flexible, for example, would be more dynamic than those that are less flexible. Similarly, the properties of the filaments would differ depending on whether a mixture of Tms is located on one filament.

4. Intracellular Distribution of Tropomyosin Isoforms

4.1. Distribution of tropomyosin isoforms

Expression of Tm is required for embryonic development as demonstrated by the finding that mice lacking a functional α-Tm gene die between embryonic day 9.5 and 13.5 (Blanchard et al., 1997). Expression is also developmentally regulated. Changes in isoform expression correlate with organ and tissue differentiation in early embryogenesis (Gunning et al., 2005). In muscle, muscle-specific isoforms are induced and cytoskeletal forms are repressed during myogenesis. α- and β- striated muscle Tms are the predominant forms in mammalian striated muscle. αTm is found predominantly in fast twitch skeletal muscle, whereas β and γ Tms predominate in slow twitch skeletal muscle (Lees-Miller and Helfman, 1991; Schevzov and O'Neill, 2008). Each Tm gene has its own pattern of transcript accumulation in adult muscle and during myogenesis (Gunning et al., 1990). There are widespread changes in isoform expression in brain. Expression of some isoforms, such as neuronal TmBr1 and TmBr3, is confined to specific cell types (Gunning et al., 2005; Lees-Miller and Helfman, 1991; Stamm et al., 1993). In addition, the levels of different Tms differ among different cell types. In a study of 10 different Tm isoforms, it was determined that no two tissues in mouse have the same levels of the same Tm isoforms (Schevzov et al., 2005b).

One of the most prominent features of transformed cells is an altered cytoskeleton due in part to the suppression of Tm expression (Bharadwaj et al., 2005; Pawlak and Helfman, 2001). Cell transformation is accompanied by highly reproducible changes in Tm expression. In particular, there is a decrease in the expression of HMW Tm in fibroblasts transformed by various oncogenes, chemical carcinogens, and DNA and RNA tumor viruses (Helfman et al., 2008; Pawlak and Helfman, 2001). The decrease in expression of HMW Tms correlates with a disruption in both stress fibers and focal adhesions. *In vitro* expression of HMW Tm1 and Tm2 in Ras- and Src-transformed fibroblasts reverts the tumorigenic phenotype by restoring stress fibers and reducing cell motility (Gimona et al., 1996; Helfman et al., 2008; Prasad et al., 1993, 1999). Expression of both Tm2 and Tm3 was found to rescue stress fiber organization in virally transformed cells; however, rescue was better with Tm2 even though both Tm2 and Tm3 are found in stress fibers (Gimona et al., 1996). In another study, Tm1, but not Tm2, rescued a transformed phenotype suggesting that Tm1 is a tumor suppressor (Prasad et al., 1999). Thus, transformed cells that are rescued by expression of specific isoforms indicate that Tm isoforms do not overlap in function. In fact, studies with Tm5NM1 and TmBr3 in a neuroepithelial

cell line demonstrated that expression of the two different isoforms in the same cell type produces drastically different results. Tm5NM1 promoted stress fiber formation and decreased cell motility; whereas TmBr5 reduced stress fiber formation and increased cell motility (Bryce et al., 2003). These studies suggest that specific Tms are required for specific functions of the actin cytoskeleton. Such notions are supported by mammalian gene knockout experiments in which coexpressed Tm genes do not compensate for elimination of the γ-Tm gene (Hook et al., 2004). In some cases such as with RIE-1 epithelial cells (Shields et al., 2002) and neuroblastoma cells (Yager et al., 2003), ectopic expression of Tms did not reverse the transformed phenotype suggesting that the situation is more complex in these cells. In addition to studies on cells in culture, there are changes in expression of Tm isoforms in several different human tumors (Pawlak and Helfman, 2001). HMW Tms are reduced in malignant breast cancer (Franzén et al., 1996; Raval et al., 2003), prostate cancer (Pelham et al., 1996), CNS tumors (Hughes et al., 2003), and carcinoma of the urinary bladder (Pawlak et al., 2004).

There is evidence that Tms sort to different intracellular sites suggesting that specific Tms act as interpreters of the local signaling environment (Martin and Gunning, 2008; O'Neill et al., 2008). In chick embryo fibroblasts and human bladder carcinoma cells, both HMW and LMW Tms associate with stress fibers as shown by indirect immunofluorescence microscopy with isoform-specific antibodies; however, only the LMW isoforms are also associated with membrane ruffles (Lin et al., 1988). In NIH 3T3 cells, Tm isoforms are differentially localized during the G1 phase of the cell cycle (Percival et al., 2000). For example, Tm5NM1 and Tm5NM2 are not incorporated into stress fibers, but are present in the perinuclear region, whereas Tm5NM3-11 is incorporated in stress fibers. Furthermore, Tm1, 2, 3, 6, 5a, and 5b are enriched at the cell edge when compared to Tm5aNM1 and Tm5NM2. In epithelial cells, the α-isoforms LMW Tm5a and Tm5b are found at the apical membrane and HMW Tm2 and Tm3 are found at the basolateral membrane, whereas the γ-Tm gene products are found in the cytoplasm (Dalby-Payne et al., 2003). In addition, LMW Tm5a/5b, but not HMW Tm2 from the same gene, is found associated with stress fibers at the cell periphery and in ruffling membranes (Schevzov et al., 2005a). What is responsible for Tm isoform sorting is unknown. Sorting information is not conserved in the same exon across the Tm genes. Isoforms containing exon 9c from the α- and γ-Tm genes do not colocalize in neurons; and those containing exon 9d from the α- and γ-Tm genes do not colocalize in fibroblasts (Vrhovski et al., 2003; Weinberger et al., 1996). There is evidence, however, that alternative exons play a role in sorting because Tm5b and Tm3 differ only in their N-terminus, yet Tm5b associates with the apical region of epithelial cells and Tm3 associates with the basolateral region (Dalby-Payne et al., 2003; Percival et al., 2000).

Overall, the distribution of various isoforms of Tm is rather complicated, and does not appear to follow simple rules. Additional factors, for example, the presence of other protein components, must therefore be taken into consideration.

4.2. Interaction of actin–tropomyosin with myosin II

Myosins are molecular motors that translocate actin filaments (Coluccio, 2008a). There are >30 classes of myosins (Foth et al., 2006; Odronitz and Kollmar, 2007); 12 phylogenetically distinct families are found in humans (Berg et al., 2001). All myosins contain an actin-binding site and an ATP-binding site in their amino terminal or ''motor'' domain. The motor domain is often followed by the neck or light-chain-binding region, which binds light chains or calmodulin. The C-terminus of myosins can be involved in a variety of functions including filament formation, membrane binding, and/or cargo binding. Myosins are widely expressed and in addition to a role in muscle contraction (mediated by two-headed myosin II), myosins function in various cellular activities such as organelle transport, signal transduction, cell adhesion, membrane events, and generation of tension (Mooseker and Foth, 2008).

Myosin II motors, which function in cell migration in nonmuscle cells, are differentially regulated by the Tm composition of the actin filaments. The interaction of the ends of Tm filaments with neighboring Tms can have dramatic effects on regulation. If end-to-end interactions are weak, cooperativity is low whereas if end-to-end interactions are strong then the movement of one Tm can result in activation of a large area of the actin filament. Tms that differ primarily in the amino acid sequences at their N- and C-termini have different equilibria between the *closed* and *open* states. Using a series of bacterially expressed α-Tm variants that differ in sequence at the ends, it was found that both the N- and C-termini determine actin affinity (Moraczewska et al., 1999). It is likely that regions of Tm other than the ends also contribute to thin filament activation. Although originally believed to be so, there is not a simple relationship between Tm size and actin affinity (Gunning et al., 2005). Whether different Tms by virtue of their terminal amino acid sequences confer different actin-binding and myosin II-activation properties is largely unknown.

Bryce and colleagues showed that LMW Tm5NM1 recruits myosin II into stress fibers resulting in a decrease in lamellipodia and cell migration (Bryce et al., 2003). In contrast, expression of HMW Tm3, which differs at the N-terminus from Tm5NM1, induces lamellipodial formation, increases cell migration, and reduces stress fiber formation (Bryce et al., 2003). Neuronal cells overexpressing Tm5NM1 have significantly enlarged growth cones, which are enriched for myosin II, while overexpression of TmBr3 inhibits neurite growth (Schevzov et al., 2005a). Lehman and

colleagues have shown that these two LMW Tms occupy different sites on actin, which might account for differential myosin binding (Lehman et al., 2000).

4.3. Class I myosins and tropomyosins at the cell membrane

In contrast to myosin II, class I myosins are single-headed myosins that do not form filaments. Myosins I are involved in such diverse functions as intestinal microvillar structure and function, adaptation in the specialized hair cells of the inner ear and insulin-mediated GLUT4 recycling in adipocytes (Coluccio, 2008b). Class I myosins, like mammalian Myo1b, are frequently found in association with membranes. Tm2 inhibits the actin-activated ATPase activity of Myo1b (Lieto-Trivedi et al., 2007). The molecular mechanism is not completely known, although it appears that Myo1b binds to actin–Tm, but is prevented from carrying out its power stroke. In this case, Myo1b could bind to actin–Tm filaments in cells and hold them in place at the membrane. The inhibition of Myo1b activity observed in the presence of Tm is reversed with Myo1b mutants in which a flexible loop at the actin-binding site, loop 4, is mutated (Lieto-Trivedi et al., 2007). These studies give insight into the structural relationship among actin, Tm, and Myo1b.

5. Caldesmon and Tropomyosins

5.1. Relationship between tropomyosin and caldesmon

In nonmuscle cells a shorter isoform of CaD (l-CaD) is expressed. l-CaD differs from h-CaD only by missing a central helical region through alternative splicing (Fig. 3.2). Both Tm and CaD are integral components of the contractile apparatus; each binds to actin filaments on the side and stabilizes the filamentous structure. As a result they are intimately involved in the regulation of assembly and organization of the actin cytoskeleton (Pollard and Borisy, 2003; Winder, 2003). As described in Section 3.2 above, Tm and h-CaD work together in smooth muscle cells to regulate the actomyosin ATPase activity. Although the precise function of l-CaD in nonmuscle cells has not yet been determined, a mechanism similar to that in smooth muscle cells may very well be operative.

Not only is Tm related to CaD functionally, the expression of the two proteins may also be under control of the same signaling pathways. For example, upon culturing, smooth muscle cells quickly lose their contractile phenotype and become dedifferentiated, fibroblast-like cells. At the same time, h-CaD undergoes a differentiation-dependent isoform switchover to l-CaD (Dingus et al., 1986; Owada et al., 1984). This process is accompanied by changes in several other smooth muscle-specific proteins including actin

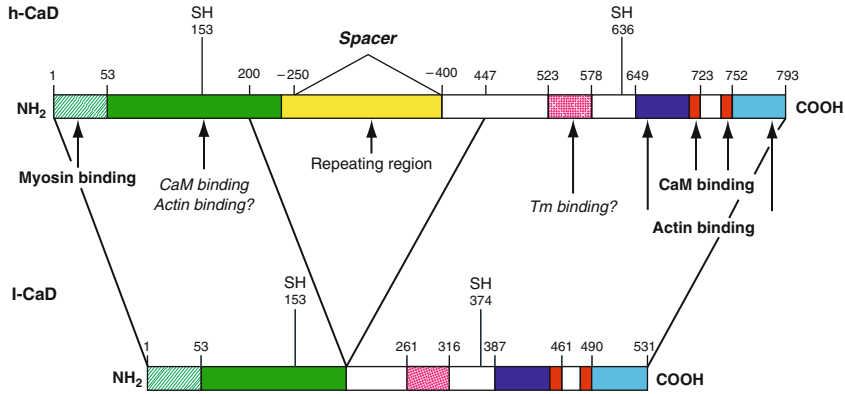

Figure 3.2 Domain structures of smooth muscle-specific CaD (h-CaD) and nonmuscle CaD (l-CaD). Both isoforms are derived from the same gene via alternative splicing. In l-CaD a highly charged repeating sequence, which forms a helical stretch in the middle of the h-CaD molecule, is missing, while the other functional domains are identical for the two isoforms.

(Owens et al., 1986), myosin heavy chain (Rovner et al., 1986), Tm (Kashiwada et al., 1997), calponin (Shanahan et al., 1993), and vinculin (Volberg et al., 1986). Among all these proteins the expression of CaD and Tm may be most closely related to each other. It has been shown that the two α-Tm isoforms (Tm6 and Tm2) are expressed in a tightly coordinated fashion with the two isoforms of CaD both *in vivo* and *in vitro* (Kashiwada et al., 1997; Sobue et al., 1999). Thus, the same splicing machinery might work on both CaD and Tm. Interestingly, when cells are forced to express Tm1, there is also an upregulation of CaD expression (Shah et al., 2001). A serum response factor is necessary, albeit not sufficient, to transactivate the CaD promoter (Momiyama et al., 1998). It remains to be seen whether the same or additional factors are recruited for the Tm promoter. Finally, CaD (Cerda-Nicolas et al., 2006; Yoshio et al., 2007) and Tm (Leonardi et al., 1982; Ryan and Higgins, 1988) are also simultaneously downregulated in transformed cells and in certain types of cancer cells so that the two actin-binding proteins are thought to be tumor suppressors.

Like the HMW Tms1, 2, 3, and 6 (Gunning et al., 2005), l-CaD is normally present in stress fibers of nonmuscle cells, but characteristically excluded from stable focal adhesions. On the other hand, both proteins as well as myosin II are found in nascent focal contacts and more dynamic structures such as podosomes (Tanaka et al., 1993) and neuronal growth cones (Kira et al., 1995). Since these contractile proteins are involved in the regulation of actomyosin activities, their presence, therefore, indicates loci of cellular contraction. In activated fibroblasts, l-CaD is primarily associated with short actin filaments in the core of podosomes (Tanaka et al., 1993) as

well as ruffling membranes (Bretscher and Lynch, 1985). Curiously, LMW Tms (Lin et al., 1988) along with other cytoskeletal proteins including myosin I (Fukui et al., 1989; Ruppert et al., 1995; Tang and Ostap, 2001), but not HMW Tm and myosin II, are also found at the leading edge and growth cones. It has been reported that in osteoclasts, LMW Tms are present in podosomes with Tm4 in the actin core where unphosphorylated l-CaD resides, while Tm5a/5b is present in the ring that encircles the podosome core (McMichael et al., 2006), where phosphorylated l-CaD is localized (Gu et al., 2007). It appears that l-CaD and LMW Tm target two separate pools of actin filaments and regulate different types of contractile activities. This intriguing possibility remains to be investigated.

5.2. Phosphorylation of tropomyosin and caldesmon in cells

5.2.1. Regulation of CaD by phosphorylation

Both h- and l-CaD can be phosphorylated by a number of kinases, including MAP kinase, PAK (Van Eyk et al., 1998), PKC, CamKII, and CKII. Phosphorylation of CaD by ERK1/2, in particular, was detected in cultured smooth muscle cells upon serum stimulation (D'Angelo et al., 1999). Earlier, Matsumura and his associates had shown that l-CaD is transiently dissociated from actin filaments during mitosis (Yamashiro et al., 1990) and that the kinase $p34^{cdc2}$ regulates this process (Yamashiro et al., 1991). It was postulated that l-CaD inhibits the activation of the contractile ring by blocking the actomyosin interaction or severing activities of gelsolin; phosphorylation alleviates the blockage during cytokinesis. On the other hand, a dynamic change in the level of l-CaD phosphorylation was observed throughout the progression of the cell cycle opposite to the change in the amount of actin stress fibers (Kordowska et al., 2006). These results indicate that phosphorylation of l-CaD is involved in cell shape changes during both cell division and postmitotic spreading. Indeed, the same residues phosphorylated in mitotic cells (Yamashiro et al., 1995) are phosphorylated when cultured smooth muscle cells are stimulated to migrate (Goncharova et al., 2002; Yamboliev and Gerthoffer, 2001).

l-CaD is also phosphorylated by PAK, which is a downstream effector in the Rac1/Cdc42 signaling pathways (Vidal et al., 2002). Like that by ERKs, PAK-mediated phosphorylation modulates CaD's action in podosome dynamics (Morita et al., 2007). The phosphorylation sites on l-CaD for both enzymes are all in the C-terminal region near the actin-binding sites (Fig. 3.3). Curiously, in both cases the two phosphorylatable serines are 30 residues apart from each other. It is thus likely that upon phosphorylation by either ERK or PAK, CaD's ability to bind actin is weakened, thus permitting severing proteins (e.g., gelsolin and ADF/cofilin) to disassemble the actin cytoskeleton, freeing l-CaD to move to the cell periphery where the cytoskeleton is reassembling. This dynamic process is essential for cells to

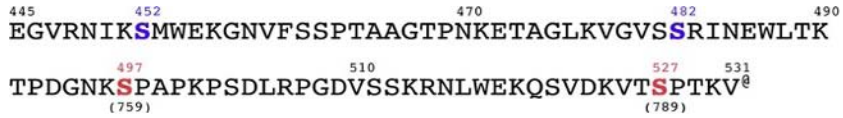

Figure 3.3 Major phosphorylation sites in the C-terminal actin-binding region of CaD. The sequence near the C-terminal end of CaD encompasses the sites for ERK (497, 527)- and PAK (452, 482)- mediated phosphorylation. The numbers for the residues in the human l-CaD sequence are shown here. The numbers in parentheses relate to the corresponding residues in the h-CaD sequence. Note that the two phosphorylation sites in each set are separated by the same number (30) of residues.

change shape, for example, during migration. In prostate cancer cells, cotransfection of cdc2 kinase and l-CaD, but not l-CaD alone, results in a higher level of cell migration than transfection of cdc2 kinase alone (Manes et al., 2003). This would suggest that phosphorylated l-CaD does not just passively dissociate from actin filaments, but instead, is involved in other cellular processes at the cell periphery.

It has been suggested that the function of focal adhesions involves actomyosin-based contractility (Grosheva et al., 2006). The focal adhesions in cells overexpressing l-CaD were found to be either unchanged (Jiang et al., unpublished observations), disrupted (Gabelt et al., 2006; Helfman et al., 1999), or variable, depending on the level of expression (Eves et al., 2006). The observation that phosphorylated, but not unphosphorylated, l-CaD colocalizes with vinculin (Kordowska et al., 2006) supports the notion that phospho-CaD recruits essential partners to early focal contacts. This process might be blocked by unphosphorylated l-CaD when expressed in large quantities. Thus, the apparently conflicting results in the literature might very well be consequences of differential kinase activity.

5.2.2. Tropomyosin phosphorylation

Tm is reportedly phosphorylated, although the properties of phosphorylated Tm are not yet fully characterized. Both cardiac and skeletal muscle Tms (primarily the α-form) are subjected to phosphorylation regulation at Ser^{283} near the C-terminus (Mak et al., 1978). Phosphorylated Tm appears to support stronger end-to-end interactions (Heeley et al., 1989) and enhanced binding to TnT (Heeley, 1994). More recently, it was shown that phosphorylated α-Tm increases the cooperative activation by myosin and generates stronger force (Rao et al., 2009). Smooth muscle Tm can also be phosphorylated, which might modify the interactions of smooth muscle Tm with h-CaD and Hsp27 (Somara et al., 2005). Several kinases have been suggested as being responsible for Tm phosphorylation *in vivo*. Protein kinase C-ζ, for example, is thought to regulate cardiac Tm (Wu and Solaro, 2007). Phosphoinositide 3-kinase, which is activated by the β-adrenergic receptor, can also lead to phosphorylation of Tm and internalization of the receptor (Praasad et al.,

2005). Tm-1 in endothelial cells is phosphorylated under oxidative stress (Houle et al., 2003). Since the MEK inhibitor (PD098059) blocks this process, the phosphorylation was thought to be mediated by ERKs. Subsequently, it was found that death-associated protein kinase-1 (DAPK-1), which is downstream of ERK, directly acts on this HMW Tm and that the site of modification is also Ser^{283} (Houle et al., 2007). Phosphorylation of Tm-1 is accompanied by the formation of stress fibers and focal adhesions, suggesting that binding of Tm-1 to actin filaments is strengthened upon phosphorylation; however, *in vitro* experiments showed that binding of Tm to actin is not affected by phosphorylation (Heeley et al., 1989). This may indicate that additional properties of phosphorylated Tm remain to be defined. Other intriguing questions include whether some LMW Tms that contain the homologous residue of Ser^{283} (such as Tm5a/b and Tm4) are also under the same phosphorylation regulation, and whether other kinases act on Tm isoforms that do not contain such a residue.

5.2.3. Direct interaction between CaD and tropomyosin

The direct interaction between CaD and Tm has been shown by binding studies (Smith et al., 1987) and by the salt-dependent enhancement in viscosity of gizzard Tm (Graceffa, 1987). This direct interaction might conceivably contribute to the observed increase in the inhibitory effect of CaD by Tm, although a more indirect route through actin cannot be ruled out (Nomura et al., 1987). The affinity between CaD and Tm at physiological ionic strength is estimated to be $2.5 \times 10^{-5}\ M^{-1}$ and is enhanced by actin (Horiuchi and Chacko, 1988). A model was proposed in which CaD binds Tm in an antiparallel manner at sites near Cys^{190} (residue 201–227) (Watson et al., 1990). This region also interacts with calponin (Childs et al., 1992). CaD and Tm enhance each other's affinity for actin. They also act synergistically on other actin-binding proteins. For example, as mentioned in Section 2.3, CaD and Tm together, but not separately, inhibit the actin-binding and actin-bundling activity of fascin, a protein involved in the formation of microspikes in cultured cells (Ishikawa et al., 1998). The interaction between l-CaD and Tm is likely to play a role in this effect, but the detailed mechanism is unclear. For example, the affinity of phosphorylated l-CaD for different Tm isoforms is unknown. Future investigations along this direction should prove to be useful. In particular, the complicated distribution of Tm isoforms may be explained by preferred interactions with respective forms of l-CaD.

5.3. How caldesmon and tropomyosins affect actin dynamics

The fact that phosphorylated CaD moves to the cell periphery where actin is undergoing rapid assembly and disassembly suggests that phosphorylated CaD plays a role in actin dynamics. It is known that CaD promotes actin nucleation, bundles actin filaments, and interacts directly with cortactin

(Huang et al., 2006), a cortical actin-binding protein. Moreover, CaD competes with Arp2/3 for actin binding (Yamakita et al., 2003); however, the effects of CaD on polymerizing actin remain unclear. To address this problem, we have recently performed *in vitro* actin polymerization experiments using pyrene-labeled actin and CaD (Huang et al., 2010). We found that CaD produces different pyrene fluorescence changes depending on when it is added. If CaD or its C-terminal actin-binding fragment is added at the beginning of actin polymerization, the typical enhancement of pyrene fluorescence reflecting actin polymerization is severely suppressed. Inclusion of CaM in the presence of Ca^{2+} recovers the pyrene fluorescence intensity. As suggested by Huang et al. (2003), CaM causes the entire C-terminal region of CaD to dissociate from actin filaments. The reversibility of CaD-induced changes by CaM indicates that the lower fluorescence results from binding of CaD to actin filaments. On the other hand, when CaD is added *after* polymerization has started, it no longer inhibits pyrene fluorescence enhancement. Instead, CaD accelerates the pyrene fluorescence enhancement after an initial decrease in intensity of pyrene emission. Both the initial drop in pyrene fluorescence and the slope of recovery of pyrene fluorescence are proportional in magnitude to the level of polymerized actin at the time of addition. Thus, these observations indicate that once polymerization starts, it is actually promoted by CaD.

The same amount of sedimentable actin is observed in samples containing actin alone, actin with CaD added before initiation of polymerization, and actin with CaD added after actin polymerization. There are several important implications: (i) The observed increase in pyrene fluorescence reports a conformational change associated with actin polymerization, rather than polymerization itself. (ii) Actin polymerization is not inhibited by CaD fragment. (iii) Instead, the apparent suppression of the pyrene–actin fluorescence enhancement reflects a different conformational state of the filament. These data can be best explained by the hypothesis that actin filaments undergo a ''maturation'' process, and that CaD arrests actin filaments at a ''young'' stage if present before this process, but further stabilizes filaments once they have matured (Huang et al., 2010). This phenomenon provides evidence for a novel mechanism by which CaD regulates assembly of the actin cytoskeleton both spatially and temporally.

The idea of actin filament maturation has been postulated previously based on imaging (Millonig et al., 1988; Orlova et al., 2004), biochemical (Galinska-Rakoczy et al., 2009), and kinetic studies (Kueh and Mitchison, 2009; Kueh et al., 2008). It is possible that the ''ragged'' morphology of nascent actin filaments represents the state before maturation, which may be the preferred configuration for interacting with accessory proteins (such as Arp2/3, cofilin, cortactin, etc.) during rapid actin assembly and disassembly. Phosphorylated l-CaD, which coexists with polymerizing actin in the cell, can therefore stabilize this configuration and promote actin dynamics.

Preliminary experiments with nonmuscle Tm5a and Tm5b indicate that these LMW Tms exhibit behavior similar to l-CaD (Huang and Wang, 2009). Depending on when they bind actin relative to the initiation of actin polymerization, they, too, either arrest actin filaments at an intermediate and more dynamic "young" state, or stabilize actin filaments at a more static, matured state. Whether this is a property unique to LMW Tms awaits further investigation.

The combined effect of CaD and Tm on actin assembly was also tested. CaD (or its C-terminal fragment) and Tm (e.g., Tm5a) were incubated with actin before polymerization was initiated. Next, CaM was added to dissociate CaD. Under this condition, F-actin is normally allowed to mature; however, since Tm5a is sufficient to inhibit the maturation process, no change in the pyrene–actin emission was observed. Thus, CaD and Tm5a could synergistically modulate the conformation of actin during polymerization and maintain actin filaments in a less static configuration by binding to nascent actin filaments as they assemble. Importantly, both phosphorylated CaD and LMW Tms, including Tm5a, are indeed found at the leading edge of cells (and similar structures such as podosomes). The possibility that Tm isoforms work with other actin-binding proteins to modulate actin dynamics undoubtedly opens up a new direction for investigation.

6. Potential Roles of Tropomyosin in Cancer Metastasis

Cell migration is critically related to cancer metastasis. Metastatic cells such as human breast cancer cell line, MDA-MB231, migrate faster than the nonmetastatic counterpart cell line MCF-7. Since the migratory activity of cells includes both a cellular extension step, which depends on dynamic assembly of the actin cytoskeleton, and a contraction step, which requires a stable actin cytoskeleton, it is conceivable that the process involves the actin-binding proteins, CaD and Tm. It was shown previously that CaD phosphorylation by cdc2 is *sufficient* to increase migration of prostate cancer cells (Manes et al., 2003). We (Jiang et al., 2009) and others (Eppinga et al., 2006) have demonstrated that phosphorylation of CaD at the ERK and PAK sites is also *necessary* for maintaining enhanced cell migration. Therefore, the ERK/PAK signaling via CaD could play a key role in controlling cell migration.

Our results further establish that compared to the nonmetastatic cell line, MCF-7, the metastatic cell line, MDA-MB231, not only has a significant higher amount of l-CaD, but the ERK-mediated CaD phosphorylation is also very extensive. This may be because MDA-MB231 cells carry the K-ras mutation (Davidson et al., 1987; Ennis et al., 1991; Kato et al., 1998; Toulany

et al., 2005), and as a consequence exhibit more migration (Price et al., 1999). Interestingly, several other aggressive tumor cell lines, such as HS578T (human breast cancer; Lakka et al., 2000) and SNB-19 (human glioblastoma; Kraus et al., 1984), were also found to have high levels of CaD as well as constitutively activated ERK and/or PAK pathways. The combination of elevated CaD levels and kinase activity may be critical factors for the highly invasive and migratory behaviors of metastatic tumor cells. Phosphorylated CaD, in particular, at the leading edge of the cell stabilizes nascent actin filaments and thereby promotes actin dynamics (Huang and Wang, 2009).

The relationship between Tm and tumor metastasis has not been explored. Interestingly, we have found that the metastatic cells, MDA-MB231, contain a different form of Tm from nonmetastatic MCF-7 cells. When extracts of these two kinds of tumor cells were probed with anti-(pan)Tm, two different bands were detected. MDA-MB231 cells contain a Tm species that migrates on the gel more slowly than the species in MCF-7 cells (Fig. 3.4). Whether such a difference can be generalized to other types of tumor cells is not yet known; the nature of this difference also awaits further investigation. Nevertheless, such properties could have important bearings on the functional involvement of both CaD and Tm in tumor

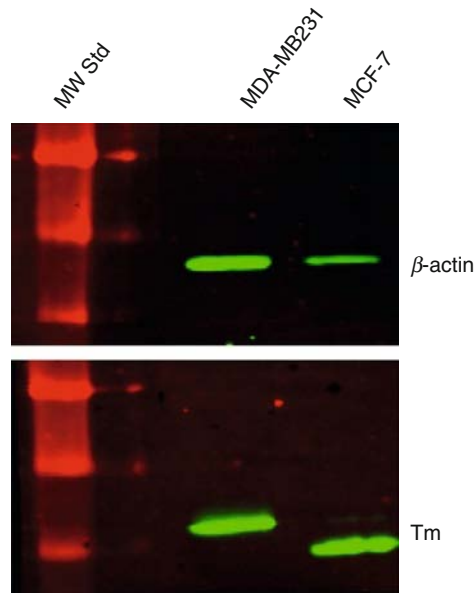

Figure 3.4 Metastatic and nonmetastatic human breast tumor cells contain different Tms. Western blot analysis with Odyssey software showing that the Tm in the two types of tumor cells, MDA-MB231 (metastatic) and MCF-7 (nonmetastatic), exhibit different mobilities on SDS–polyacrylamide gels (lower panel). β-Actin was used as a reference for loading (upper panel).

metastasis. For example, one possibility is that this results from a differential interaction between l-CaD and Tm depending on the phosphorylation state of l-CaD. It will also be interesting to test the level of CaD and Tm expression and the amounts of phosphorylation in other types of malignant tumor cells. The idea that either Tm or CaD mutants might serve as therapeutic agents to battle certain metastatic cancers remains to be tested.

7. Concluding Remarks

Many questions remain regarding the structure and function of Tms beginning with the molecular basis of the interaction of Tm with actin filaments. For example, knowing what controls dimerization and what are the properties of filaments with specific Tm compositions are valuable information for predicting the cellular roles of Tms. Understanding how Tm isoforms are targeted to different pools of actin filaments in the cell is also critical. In fact, the apparent lack of simple rules to account for the localization of Tm isoforms requires consideration of additional players such as other actin-binding proteins. The ongoing studies directed at investigating the effects of Tm on actin dynamics will also spur further work designed to reveal how Tms affect actin assembly and whether the cooperation of Tms with other actin-binding proteins control the rate and extent of actin assembly. The recent recognition of the large size of the Tm family and the availability of DNA sequences coding for the various isoforms should facilitate the generation, for one, of isoform-specific antibodies and other reagents to target individual Tm gene products. Antibodies that allow visualization of specific isoforms in the cell will be of particular importance to understanding where specific isoforms localize in the cell, providing clues to cellular function. In addition, or alternatively, the identification of inhibitors specific for particular Tm isoforms will also be very useful for distinguishing the roles of specific isoforms in the cell. Understanding the role of Tms in cell migration is of particular importance given that changes in expression of Tms accompany transformation. The future holds the promise of developing biomarkers and therapeutic targets based on Tms. The roles of Tms in cardiovascular disease and skeletal muscle disease, in particular how mutations give rise to specific pathologies, also remain to be revealed.

ACKNOWLEDGMENTS

We thank BBRI colleagues, Sam Lehrer, and Zenek Grabarek for helpful comments. Studies in the Wang laboratory are supported by NIH HL092252. Studies in the Coluccio laboratory are supported by NIH DC08793.

REFERENCES

Alahyan, M., Webb, M.R., Marston, S.B., El-Mezgueldi, M., 2006. The mechanism of smooth muscle caldesmon–tropomyosin inhibition of the elementary steps of the actomyosin ATPase. J. Biol. Chem. 281, 19433–19448.

Ansari, S., Alahyan, M., Marston, S.B., El-Mezgueldi, M., 2008. Role of caldesmon in the Ca^{2+} regulation of smooth muscle thin filaments: evidence for a cooperative switching mechanism. J. Biol. Chem. 283, 47–56.

Bailey, K., 1948. Tropomyosin: a new asymmetric protein component of the muscle fibril. Biochem. J. 43, 271–279.

Beisel, K.W., Kennedy, J.E., 1994. Identification of novel alternatively spliced isoforms of the tropomyosin-encoding gene, TMnm, in the rat cochlea. Gene 143, 251–256.

Berg, J.S., Powell, B.C., Cheney, R.E., 2001. A millennial myosin census. Mol. Biol. Cell 12, 780–794.

Bernstein, B.W., Bamburg, J.R., 1982. Tropomyosin binding to F-actin protects the F-actin from disassembly by brain actin-depolymerizing factor (ADF). Cell Motil. 2, 1–8.

Bharadwaj, S., Thanawala, R., Bon, G., Falcioni, R., Prasad, G.L., 2005. Resensitization of breast cancer cells to anoikis by tropomyosin-1: role of Rho kinase-dependent cytoskeleton and adhesion. Oncogene 24, 8291–8303.

Blanchard, E.M., Iizuka, K., Christe, M., Conner, D.A., Geisterfer-Lowrance, A., Schoen, F.J., et al., 1997. Targeted ablation of the murine alpha-tropomyosin gene. Circ. Res. 81, 1005–1010.

Blanchoin, L., Pollard, T.D., Hitchcock-DeGregori, S.E., 2001. Inhibition of the Arp2/3 complex-nucleated actin polymerization and branch formation by tropomyosin. Curr. Biol. 11, 1300–1304.

Bretscher, A., Lynch, W., 1985. Identification and localization of immunoreactive forms of caldesmon in smooth and nonmuscle cells: a comparison with the distributions of tropomyosin and alpha-actinin. J. Cell Biol. 100, 1656–1663.

Bronson, D.D., Schachat, F.H., 1982. Heterogeneity of contractile proteins. Differences in tropomyosin in fast, mixed, and slow skeletal muscles of the rabbit. J. Biol. Chem. 257, 3937–3944.

Broschat, K.O., 1990. Tropomyosin prevents depolymerization of actin filaments from the pointed end. J. Biol. Chem. 265, 21323–21329.

Brown, J.H., Kim, K.-H., Jun, G., Greenfield, N.J., Dominguez, R., Volkmann, N., et al., 2001. Deciphering the design of the tropomyosin molecule. Proc. Natl. Acad. Sci. USA 98, 8496–8501.

Brown, J.H., Zhou, Z., Reshetnikova, L., Robinson, H., Yammani, R.D., Tobacman, L.S., et al., 2005. Structure of the mid-region of tropomyosin: bending and binding sites for actin. Proc. Natl. Acad. Sci. USA 102, 18878–18883.

Bryan, J., Edwards, R., Matsudaira, P., Otto, J., Wulfkuhle, J., 1993. Fascin, an echinoid actin-bundling protein, is a homolog of the Drosophila singed gene product. Proc. Natl. Acad. Sci. USA 90, 9115–9119.

Bryce, N.S., Schevzov, G., Ferguson, V., Percival, J.M., Lin, J.J., Matsumura, F., et al., 2003. Specification of actin filament function and molecular composition by tropomyosin isoforms. Mol. Biol. Cell 14, 1002–1016.

Bugyi, B., Didry, D., Carlier, M.-F., 2009. How tropomyosin regulates lamellipodial actin-based motility: a combined biochemical and reconstituted motility approach. EMBO J. 28, 1–13.

Burgess, D.R., Broshat, K.O., Hayden, J.M., 1987. Tropomyosin distinguishes between the two actin-binding sites of villin and affects actin-binding properties of other brush border proteins. J. Cell Biol. 104, 29–40.

Cerda-Nicolas, M., Lopez-Gines, C., Gil-Benso, R., Benito, R., Pellin, A., Ruiz-Sauri, A., et al., 2006. Solitary fibrous tumor of the orbit: morphological, cytogenetic and molecular features. Neuropathology 26, 557–563.

Chacko, S., Eisenberg, E., 1990. Cooperativity of actin-activated ATPase of gizzard heavy meromyosin in the presence of gizzard tropomyosin. J. Biol. Chem. 265, 2105–2110.

Chacko, S., Conti, M.A., Adelstein, R.S., 1977. Effect of phosphorylation of smooth muscle myosin on actin activation and Ca^{2+} regulation. Proc. Natl. Acad. Sci. USA 74, 129–133.

Chalovich, J.M., Cornelius, P., Benson, C.E., 1987. Caldesmon inhibits skeletal actomyosin subfragment-1 ATPase activity and the binding of myosin subfragment-1 to actin. J. Biol. Chem. 262, 5711–5716.

Childs, T.J., Watson, M.H., Novy, R.E., Lin, J.J., Mak, A.S., 1992. Calponin and tropomyosin interactions. Biochim. Biophys. Acta 1121, 41–46.

Clayton, L., Reinach, F.C., Chumbley, G.M., Macleod, A.R., 1988. Organization of the hTm_{nm} gene: implications for the evolution of muscle and non-muscle tropomyosins. J. Mol. Biol. 201, 507–515.

Cohen, I., Cohen, C., 1972. A tropomyosin-like protein from human platelets. J. Mol. Biol. 68, 383–387.

Coluccio, L.M., 2008a. Myosins: A Superfamily of Molecular Motors. Springer, Dordrecht, The Netherlands.

Coluccio, L. M., 2008b. Myosin I. Proteins and Cell Regulation. 7, 95–124.

Corbett, M.A., Akkari, P.A., Domazetovska, A., Cooper, S.T., North, K.N., Laing, N.G., et al., 2005. An αTropomyosin mutation alters dimer preference in nemaline myopathy. Ann. Neurol. 57, 42–49.

Corsi, A., Perry, S.V., 1958. Some observations on the localisation of myosin, actin and tropomyosin in the rabbit myofibril. Biochem. J. 68, 12–17.

Creed, S.J., Bryce, N., Naumanen, P., Weinberger, R.P., Lappalainen, P., Stehn, J., et al., 2008. Tropomyosin isoforms define distinct microfilament populations with different drug susceptibility. Eur. J. Cell Biol. 87, 709–720.

Dabrowska, R., Goch, A., Galazkiewicz, B., Osinska, H., 1985. The influence of caldesmon on ATPase activity of the skeletal muscle actomyosin and bundling of actin filaments. Biochim. Biophys. Acta 842, 70–75.

Dabrowska, R., Hinssen, H., Galazkiewicz, B., Nowak, E., 1996. Modulation of gelsolin-induced actin-filament severing by caldesmon and tropomyosin and the effect of these proteins on the actin activation of myosin Mg(2+)-ATPase activity. Biochem. J. 315, 753–759.

Dalby-Payne, J.R., O'Loughlin, E.V., Gunning, P., 2003. Polarization of specific tropomyosin isoforms in gastrointestinal epithelial cells and their impact on CFTR at the apical membrane. Mol. Biol. Cell 14, 4365–4375.

D'Angelo, G., Graceffa, P., Wang, C.-L.A., Wrangle, J., Adam, L.P., 1999. Mammal-specific, ERK-dependent, caldesmon phosphorylation in smooth muscle. Quantitation using novel anti-phosphopeptide antibodies. J. Biol. Chem. 274, 30115–30121.

Davidson, N.E., Gelmann, E.P., Lippman, M.E., Dickson, R.B., 1987. Epidermal growth factor receptor gene expression in estrogen receptor-positive and negative human breast cancer cell lines. Mol. Endocrinol. 1, 216–223.

DesMarais, V., Ichetovkin, I., Condeelis, J., Hitchcock-DeGregori, S., 2002. Spatial regulation of actin dynamics: a tropomyosin-free, actin-rich compartment at the leading edge. J. Cell. Sci. 115, 4649–4660.

Dingus, J., Hwo, S., Bryan, J., 1986. Identification by monoclonal antibodies and characterization of human platelet caldesmon. J. Cell Biol. 102, 1748–1757.

Dos Remedios, C.G., Chhabra, D., Kekic, M., Dedova, I.V., Tsubakihara, M., Berry, D.A., et al., 2003. Actin binding proteins: regulation of cytoskeletal microfilaments. Physiol. Rev. 83, 433.

Dufour, C., Weinberger, R.P., Schevzov, G., Jeffrey, P.L., Gunnning, P., 1998. Splicing of two internal and four carboxyl-terminal alternative exons in nonmuscle tropomyosin 5 pre-mRNA is independently regulated during development. J. Biol. Chem. 273, 18547–18555.

Ennis, B.W., Lippman, M.E., Dickson, R.B., 1991. The EGF receptor system as a target for antitumor therapy. Cancer Invest. 9, 553–562.

Eppinga, R.D., Li, Y., Lin, J.L.-C., Lin, J.J.-C., 2006. Tropomyosin and caldesmon regulate cytokinesis speed and membrane stability during cell division. Arch. Biochem. Biophys. 456, 161–174.

Eves, R., Webb, B.A., Zhou, S., Mak, A.S., 2006. Caldesmon is an integral component of podosomes in smooth muscle cells. J. Cell. Sci. 119, 1691–1702.

Flicker, P.F., Phillips Jr., G.N., Cohen, C., 1982. Troponin and its interactions with tropomyosin. An electron microscope study. J. Mol. Biol. 162, 495–501.

Foth, B.J., Goedecke, M.C., Soldati, D., 2006. New insights into myosin evolution and classification. Proc. Natl. Acad. Sci. USA 103, 3681–3686.

Fowler, V., 1996. Regulation of actin filament length in erythrocytes and striated muscle. Curr. Opin. Cell Biol. 8, 86–96.

Franzén, B., Linder, S., Uryu, K., Alaiya, A.A., Hirano, T., Kato, H., et al., 1996. Expression of tropomyosin isoforms in benign and malignant human breast lesions. Br. J. Cancer 73, 909–913.

Fukui, Y., Lynch, T.J., Brzeska, H., Korn, E.D., 1989. Myosin I is located at the leading edges of locomoting *Dictyostelium amoebae*. Nature 341, 328–331.

Gabelt, B.T., Hu, Y., Vittitow, J.L., Rasmussen, C.R., Grosheva, I., Bershadsky, A.D., et al., 2006. Caldesmon transgene expression disrupts focal adhesions in HTM cells and increases outflow facility in organ-cultured human and monkey anterior segments. Exp. Eye Res. 82, 935–944.

Galinska-Rakoczy, A., Wawro, B., Strzelecka-Golaszewska, H., 2009. New aspects of the spontaneous polymerization of actin in the presence of salts. J. Mol. Biol. 387, 869–882.

Geeves, M.A., Lehrer, S.S., 1994. Dynamics of the muscle thin filament regulatory switch: the size of the cooperative unit. Biophys. J. 67, 273–282.

Gimona, M., 2008. Dimerization of tropomyosins. Adv. Exp. Med. Biol. 644, 73–84.

Gimona, M., Watakabe, A., Helfman, D.M., 1995. Specificity of dimer formation in tropomyosins: influence of alternatively spliced exons on homodimer and heterodimer assembly. Proc. Natl. Acad. Sci. USA 92, 9776–9780.

Gimona, M., Kazzaz, J.A., Helfman, D.M., 1996. Forced expression of tropomyosin 2 or 3 in v-Ki-ras-transformed fibroblasts results in distinct phenotypic effects. Proc. Natl. Acad. Sci. USA 93, 9618–9623.

Goncharova, E.A., Vorotnikov, A.V., Gracheva, E.O., Albert, W.C., Panettieri Jr., R.A., Stepanova, V.V., et al., 2002. Activation of p38 MAP-kinase and caldesmon phosphorylation are essential for urokinase-induced human smooth muscle cell migration. Biol. Chem. 383, 115–126.

Graceffa, P., 1987. Evidence for interaction between smooth muscle tropomyosin and caldesmon. FEBS Lett. 218, 139–142.

Greaser, M.L., Gergely, J., 1971. Reconstitution of troponin activity from three protein components. J. Biol. Chem. 246, 4226–4233.

Greenfield, N.J., Stafford, W.S.I., Hitchcock-DeGregori, S.E., 1994. The effect of N-terminal acetylation on the structure of an N-terminal tropomyosin peptide and alpha alpha-tropomyosin. Protein Sci. 3, 402–410.

Greenfield, N., Montelione, G., Farid, R., Hitchcock-DeGregori, S., 1998. The structure of the N-terminus of striated muscle alpha-tropomyosin in a chimeric peptide: nuclear magnetic resonance structure and circular dichroism studies. Biochemistry 37, 7834–7843.

Greenfield, N.J., Huang, Y.J., Swapna, G.V.T., Bhattacharya, A., Rapp, B., Singh, A., et al., 2006. Solution NMR structure of the junction between tropomyosin molecules: implications for actin binding and regulation. J. Mol. Biol. 364, 80–96.

Grosheva, I., Vittitow, J.L., Goichberg, P., Gabelt, B.T., Kaufman, P.L., Borras, T., et al., 2006. Caldesmon effects on the actin cytoskeleton and cell adhesion in cultured HTM cells. Exp. Eye Res. 82, 945–958.

Gu, Z., Kordowska, J., Williams, G.L., Wang, C.L., Hai, C.M., 2007. Erk1/2 MAPK and caldesmon differentially regulate podosome dynamics in A7r5 vascular smooth muscle cells. Exp. Cell Res. 313, 849–866.

Gunning, P., Gordon, M., Wade, R., Gahlmann, R., Lin, C.-S., Hardeman, E., 1990. Differential control of tropomyosin mRNA levels during myogenesis suggests the existence of an isoform competition-autoregulatory compensation control mechanism. Dev. Biol. 138, 443–453.

Gunning, P.W., Schevroz, G., Kee, A.J., Hardeman, E.C., 2005. Tropomyosin isoforms: divining rods for actin cytoskeleton function. Trends Cell Biol. 15, 333–341.

Gunning, P., O'Neill, G., Hardeman, E., 2008. Tropomyosin-based regulation of the actin cytoskeleton in time and space. Physiol. Rev. 88, 1–35.

Gupton, S.L., Anderson, K.L., Kole, T.P., Fischer, R.S., Ponti, A., Hitchcock-DeGregori, S.E., et al., 2005. Cell migration without a lamellipodium: translation of actin dynamics into cell movement mediated by tropomyosin. J. Cell Biol. 168, 619–631.

Haeberle, J.R., Hathaway, D.R., Smith, C.L., 1992. Caldesmon content of mammalian smooth muscles [see comments]. J. Muscle Res. Cell. Motil. 13, 81–89.

Hanson, J., Lowy, J., 1963. The structure of F-actin and actin filaments isolated from muscle. J. Mol. Biol. 6, 46–60.

Hanson, J., Lowy, J., 1964. The structure of actin filaments and the origin of the axial periodicity in the I-substance of vertebrate striated muscle. Proc. R. Soc. Lond., B, Biol. Sci. 160, 449–460.

Heeley, D.H., 1994. Investigation of the effects of phosphorylation of rabbit striated muscle alpha alpha-tropomyosin and rabbit skeletal muscle troponin-T. Eur. J. Biochem. 221, 129–137.

Heeley, D.H., Smillie, L.B., Lohmeier-Vogel, E.M., 1989. Effects of deletion of tropomyosin overlap on regulated actomyosin subfragment 1 ATPase. Biochem. J. 258, 831–836.

Hegmann, T.E., Lin, J.L.-C., Lin, J.J.-C., 1989. Probing the role of nonmuscle tropomyosin isoforms in intracellular granule movement by microinjection of monoclonal antibodies. J. Cell Biol. 109, 1141–1152.

Heimann, K., Percival, J.M., Weinberger, R., Gunning, P., Stow, J.L., 1999. Specific isoforms of actin-binding proteins on distinct populations of Golgi-derived vesicles. J. Biol. Chem. 274, 10743–10750.

Helfman, D.M., Cheley, S., Kuismanen, E., Finn, L., Yamawaki-Kataoka, Y., 1986. Nonmuscle and muscle tropomyosin isoforms are expressed from a single gene by alternative RNA splicing and polyadenylation. Mol. Cell. Biol. 6, 3582–3595.

Helfman, D.M., Levy, E.T., Berthier, C., Shtutman, M., Riveline, D., Grosheva, I., et al., 1999. Caldesmon inhibits nonmuscle cell contractility and interferes with the formation of focal adhesions. Mol. Biol. Cell 10, 3097–3112.

Helfman, D.M., Flynn, P., Khan, P., Saeed, A., 2008. Tropomyosin as a regulator of cancer cell transformation. Adv. Exp. Med. Biol. 644, 124–131.

Hemric, M.E., Freedman, M.V., Chalovich, J.M., 1993. Inhibition of actin stimulation of skeletal muscle (A1)S-1 ATPase activity by caldesmon. Arch. Biochem. Biophys. 306, 39–43.

Hillberg, L., Zhao Rathje, L.-S., Nyåkern-Meazza, M., Helfand, B., Goldman, R.D., Schutt, C.E., et al., 2006. Tropomyosins are present in lamellipodia of motile cells. Eur. J. Cell Biol. 85, 399–409.

Hitchcock-DeGregori, S.E., Varnell, T.A., 1990. Tropomyosin has discrete actin-binding sites with sevenfold and fourteenfold periodicities. J. Mol. Biol. 214, 885–896.

Hitchcock-DeGregori, S.E., Song, Y., Greenfield, N.J., 2002. Functions of tropomyosin's periodic repeats. Biochemistry 41, 15036–15044.

Hook, J., Lemckert, F., Qin, H., Schevzov, G., Gunning, P., 2004. Gamma tropomyosin gene products are enquired for embryonic development. Mol. Cell. Biol. 24, 2318–2323.

Horiuchi, K.Y., Chacko, S., 1988. Interaction between caldesmon and tropomyosin in the presence and absence of smooth muscle actin. Biochemistry 27, 8388–8393.

Horiuchi, K.Y., Samuel, M., Chacko, S., 1991. Mechanism for the inhibition of acto-heavy meromyosin ATPase by the actin/calmodulin binding domain of caldesmon. Biochemistry 30, 712–717.

Houle, F., Rousseau, S., Morrice, N., Luc, M., Mongrain, S., Turner, C.E., et al., 2003. Extracellular signal-regulated kinase mediates phosphorylation of tropomyosin-1 to promote cytoskeleton remodeling in response to oxidative stress: impact on membrane blebbing. Mol. Biol. Cell 14, 1418–1432.

Houle, F., Poirier, A., Dumaresq, J., Huot, J., 2007. DAP kinase mediates the phosphorylation of tropomyosin-1 downstream of the ERK pathway, which regulates the formation of stress fibers in response to oxidative stress. J. Cell. Sci. 120, 3666–3677.

Huang, R., Wang, C.-L.A., 2009. Caldesmon and tropomyosin synergistically regulate actin dynamics. Presented at the 53th Annual Meeting of the Biophysical Society, Boston, Feb 28–Mar 4, 2009, Abstract #1997.

Huang, R., Li, L., Guo, H., Wang, C.-L.A., 2003. Caldesmon binding to actin is regulated by calmodulin and phosphorylation via different mechanisms. Biochemistry 42, 2513–2523.

Huang, R., Cao, G.J., Guo, H., Kordowska, J., Wang, C.-L.A., 2006. Direct interaction between caldesmon and cortactin. Arch. Biochem. Biophys. 456, 175–182.

Huang, R., Grabarek, Z., Wang, C.-L.A., 2010. Differential effects of caldesmon on the intermediate conformational states of polymerizing actin. J. Biol. Chem. 285, 71–79.

Hughes, J., Cook-Yarborough, C.M., Chadwick, N.C., Schevzov, G., Arbuckel, S.M., Gunning, P., et al., 2003. High-molecular-weight tropomyosins localize to the contractile rings of dividing CNS cells but are absent from malignant pediatric and adult CNS tumors. Glia 42, 25–35.

Ishii, Y., Lehrer, S.S., 1987. Fluorescence probe studies of the state of tropomyosin in reconstituted muscle thin filaments. Biochemistry 26, 4922–4925.

Ishikawa, R., Yamashiro, S., Kohama, K., Matsumura, F., 1998. Regulation of actin binding and actin bundling activities of fascin by caldesmon coupled with tropomyosin. J. Biol. Chem. 273, 26991–26997.

Jagatheesan, G., Rajan, S., Wieczorek, D., 2009. Investigations into tropomyosin function using mouse models. J. Mol. Cell. Cardiol. (in press).

Jiang, Q., Huang, R., Wang, C.-L.A., 2009. Regulation of cell migration by caldesmon phosphorylation may control tumor metastasis. Mol. Biol. Cell 20 (10), Abstract No. 1136.

Kashiwada, K., Nishida, W., Hayashi, K., Ozawa, K., Yamanaka, Y., Saga, H., et al., 1997. Coordinate expression of alpha-tropomyosin and caldesmon isoforms in association with phenotypic modulation of smooth muscle cells. J. Biol. Chem. 272, 15396–15404.

Kato, K., Ueoka, Y., Kato, K., Tamura, T., Nishida, J., Wake, N., 1998. Oncogenic Ras modulates epidermal growth factor responsiveness in endometrial carcinomas. Eur. J. Cancer 34, 737–744.

Kee, A.J., Hardeman, E.C., 2008. Tropomyosins in skeletal muscle disease. Adv. Exp. Med. Biol. 644, 143–157.
Kee, A.J., Schevzov, G., Nair-Shalliker, V., Robinson, C.S., Vrhovski, B., Ghoddusi, M., et al., 2004. Sorting of a nonmuscle tropomyosin to a novel cytoskeletal compartment in skeletal muscle results in muscular dystrophy. J. Cell Biol. 166, 685–698.
Kee, A.J., Gunning, P., Hardeman, E., 2009. A cytoskeletal tropomyosin can compromise the structural integrity of skeletal muscle. Cell Motil. Cytoskeleton 66, 710–720.
Kira, M., Tanaka, J., Sobue, K., 1995. Caldesmon and low Mr isoform of tropomyosin are localized in neuronal growth cones. J. Neurosci. Res. 40, 294–305.
Kordowska, J., Hetrick, T., Adam, L.P., Wang, C.-L.A., 2006. Phosphorylated l-caldesmon is involved in disassembly of actin stress fibers and postmitotic spreading. Exp. Cell Res. 312, 95–110.
Kostyukova, A.S., 2008. Tropomodulin/tropomyosin interactions regulate actin pointed end dynamics. Adv. Exp. Med. Biol. 644, 283–292.
Kraus, M.H., Yuasa, Y., Aaronson, S.A., 1984. A position 12-activated H-ras oncogene in all HS578T mammary carcinosarcoma cells but not normal mammary cells of the same patient. Proc. Natl. Acad. Sci. USA 81, 5384–5388.
Kueh, H.Y., Mitchison, T.J., 2009. Structural plasticity in actin and tubulin polymer dynamics. Science 325, 960–963.
Kueh, H.Y., Brieher, W.M., Mitchison, T.J., 2008. Dynamic stabilization of actin filaments. Proc. Natl. Acad. Sci. USA 105, 16531–16536.
Lakka, S.S., Jasti, S.L., Kyritsis, A.P., Yung, W.K., Ali-Osman, F., Nicolson, G.L., et al., 2000. Regulation of MMP-9 (type IV collagenase) production and invasiveness in gliomas by the extracellular signal-regulated kinase and jun amino-terminal kinase signaling cascades. Clin. Exp. Metastasis 18, 245–252.
Lamkin, M., Tao, T., Lehrer, S.S., 1983. Tropomyosin–troponin and tropomyosin–actin interactions: a fluorescence quenching study. Biochemistry 22, 3053–3058.
Lazarides, E., 1975. Tropomyosin antibody: the specific localization of tropomyosin in nonmuscle cells. J. Cell Biol. 65, 549–561.
Lees-Miller, J.P., Helfman, D.M., 1991. The molecular basis for tropomyosin isoform diversity. Bioessays 13, 429–437.
Lees-Miller, J.P., Goodwin, L.O., Helfman, D.M., 1990a. Three novel brain tropomyosin isoforms are expressed from the rat alpha-tropomyosin gene through the use of alternate promoters and alternative RNA processing. Mol. Cell. Biol. 10, 1729–1742.
Lees-Miller, J.P., Yan, A., Helfman, D.M., 1990b. Structure and complete nucleotide sequence of the gene encoding rat fibroblast tropomyosin 4. J. Mol. Biol. 213, 399–405.
Lehman, W., Craig, R., 2008. Tropomyosin and the steric mechanism of muscle contraction. Adv. Exp. Med. Biol. 644, 95–109.
Lehman, W., Denault, D., Marston, S., 1993. The caldesmon content of vertebrate smooth muscle. Biochim. Biophys. Acta 1203, 53–59.
Lehman, W., Vibert, P., Uman, P., 1995. Steric-blocking by tropomyosin visualized in relaxed vertebrate muscle thin filaments. J. Mol. Biol. 251, 191–196.
Lehman, W., Vibert, P., Craig, R., 1997. Visualization of caldesmon on smooth muscle thin filaments. J. Mol. Biol. 274, 310–317.
Lehman, W., Hatch, V., Korman, V., Rosol, M., Thomas, L., Maytum, R., et al., 2000. Tropomyosin and actin isoforms modulate the localization of tropomyosin strands on actin filaments. J. Mol. Biol. 302, 593–606.
Lehrer, S.S., Morris, E.P., 1982. Dual effects of tropomyosin and troponin-tropomyosin on actomyosin subfragment 1 ATPase. J. Biol. Chem. 257, 8073–8080.
Lehrer, S.S., Morris, E.P., 1984. Comparison of the effects of smooth and skeletal tropomyosin on skeletal actomyosin subfragment 1 ATPase. J. Biol. Chem. 259, 2070–2072.

Lehrer, S.S., Qian, Y., 1990. Unfolding/refolding studies of smooth muscle tropomyosin. Evidence for a chain exchange mechanism in the preferential assembly of the native heterodimer. J. Biol. Chem. 265, 1134–1138.
Lehrer, S.S., Qian, Y.D., Hvidt, S., 1989. Assembly of the native heterodimer of Rana esculenta tropomyosin by chain exchange. Science 246, 926–928.
Lehrer, S.S., Golitsina, N.L., Geeves, M.A., 1997. Actin-tropomyosin activation of myosin subfragment 1 ATPase and thin filament cooperativity. The role of tropomyosin flexibility and end-to-end interactions. Biochemistry 36, 13449–13454.
Leonardi, C.L., Warren, R.H., Rubin, R.W., 1982. Lack of tropomyosin correlates with the absence of stress fibers in transformed rat kidney cells. Biochim. Biophys. Acta 720, 154–162.
Lewis, W.G., Smillie, L.B., 1980. The amino acid sequence of rabbit cardiac tropomyosin. J. Biol. Chem. 255, 6854–6859.
Li, Y., Mui, S., Brown, J.H., Strand, J., Reshetnikova, L., Tobacman, L.S., et al., 2002. The crystal structure of the C-terminal fragment of striated-muscle α-tropomyosin reveals a key troponin T recognition site. Proc. Natl. Acad. Sci. USA 99, 7378–7383.
Li, X., Holmes, K.C., Lehman, W., Jung, H., Fischer, S., 2010. The shape and flexibility of tropomyosin coiled coils: implications for actin filament assembly and regulation. J. Mol. Biol. 395, 327–339.
Lieto-Trivedi, A., Dash, S., Coluccio, L.M., 2007. Myosin surface loop 4 modulates inhibition of actomyosin 1b ATPase activity by tropomyosin. Biochemistry 46, 2779–2786.
Lin, J.J., Hegmann, T.E., Lin, J.L., 1988. Differential localization of tropomyosin isoforms in cultured nonmuscle cells. J. Cell Biol. 107, 563–572.
Lin, J.J., Warren, K.S., Wamboldt, D.D., Wang, T., Lin, J.L., 1997. Tropomyosin isoforms in nonmuscle cells. Int. Rev. Cytol. 170, 1–38.
Lin, J.J.-C., Eppinga, R.D., Warren, K.S., McCrae, K.R., 2008. Human tropomyosin isoforms in the regulation of cytoskeleton functions. Adv. Exp. Med. Biol. 644, 201–222.
Mabuchi, K., Li, Y., Carlos, A., Wang, C.L., Graceffa, P., 2001. Caldesmon exhibits a clustered distribution along individual chicken gizzard native thin filaments. J. Muscle Res. Cell. Motil. 22, 77–90.
Mak, A., Smillie, L.B., Bárány, M., 1978. Specific phosphorylation at serine-283 of alpha tropomyosin from frog and rabbit skeletal and cardiac muscle. Proc. Natl. Acad. Sci. USA 75, 3588–3592.
Manes, T., Zheng, D.Q., Tognin, S., Woodard, A.S., Marchisio, P.C., Languino, L.R., 2003. Alpha(v)beta3 integrin expression up-regulates cdc2, which modulates cell migration. J. Cell Biol. 161, 817–826.
Martin, C., Gunning, P., 2008. Isoform sorting of tropomyosins. Adv. Exp. Med. Biol. 644, 187–200.
Matsumura, F., Yamashiro-Matsumura, S., 1986. Modulation of actin-binding activity of 55-kDa protein by multiple isoforms of tropomyosin. J. Biol. Chem. 261, 4655–4659.
Maytum, R., Konrad, M., Lehrer, S.S., Geeves, M.A., 2001. Regulatory properties of tropomyosin effects of length, isoform, and N-terminal sequence. Biochemistry 40, 7334–7341.
McKillop, D.F., Geeves, M.A., 1993. Regulation of the interaction between actin and myosin subfragment 1: evidence for three states of the thin filament. Biophys. J. 65, 693–701.
McMichael, B.K., Kotadiya, P., Singh, T., Holliday, L.S., Lee, B.S., 2006. Tropomyosin isoforms localize to distinct microfilament populations in osteoclasts. Bone 39, 694–705.
Millonig, R., Salvo, H., Aebi, U., 1988. Probing actin polymerization by intermolecular cross-linking. J. Cell Biol. 106, 785–796.
MInakata, S., Maeda, K., Oda, N., Wakabayashi, K., Nitanai, Y., Maéda, Y., 2008. Two-crystal structures of tropomyosin C-terminal fragment 176-273: exposure of the

hydrophobic core to the solvent destabilizes the tropomyosin molecule. Biophys. J. 95, 710–719.
Momiyama, T., Hayashi, K., Obata, H., Chimori, Y., Nishida, T., Ito, T., et al., 1998. Functional involvement of serum response factor in the transcriptional regulation of caldesmon gene. Biochem. Biophys. Res. Commun. 242, 429–435.
Monteiro, P.B., Lataro, R.C., Ferro, J.A., Reinach, F.D.C., 1994. Functional α-tropomyosin produced in *Escherichia coli*. A dipeptide extension can substitute the amino-terminal acetyl group. J. Biol. Chem. 269, 10461–10466.
Moore, P.B., Huxley, H.E., DeRosier, D.J., 1970. Three dimensional reconstruction of F-actin, thin filament and decorated thin filaments. J. Mol. Biol. 50, 2279–2295.
Mooseker, M.S., Foth, B.J., 2008. The structural and functional diversity of the myosin family. Proteins Cell Regul. 7, 1–34.
Moraczewska, J., Nicholson-Flynn, K., Hitchcock-DeGregori, S.E., 1999. The ends of tropomyosin are major determinants of actin affinity and myosin subfragment 1-induced binding to F-actin in the open state. Biochemistry 38, 15885–15892.
Morita, T., Mayanagi, T., Yoshio, T., Sobue, K., 2007. Changes in the balance between caldesmon regulated by p21-activated kinases and the Arp2/3 complex govern podosome formation. J. Biol. Chem. 282, 8454–8463.
Muthuchamy, M., Pajak, L., Howles, P., Doetschman, T., Wieczorek, D.F., 1993. Developmental analysis of tropomyosin gene expression in embryonic stem cells and mouse embyros. Mol. Cell. Biol. 13, 3311–3323.
Muthuchamy, M., Grupp, I.L., Grupp, G., O'Toole, B.A., Kier, A.B., Boivin, G.P., et al., 1995. Molecular and physiological effects of overexpressing striated muscle β-tropomyosin in adult murine heart. J. Biol. Chem. 270, 30593–30603.
Ngai, P.K., Walsh, M.P., 1984. Inhibition of smooth muscle actin-activated myosin Mg^{2+}-ATPase activity by caldesmon. J. Biol. Chem. 259, 13656–13659.
Nitanai, Y., Minakata, S., Maeda, K., Oda, N., Maéda, Y., 2007. Crystal structures of tropomyosin: flexible coiled-coil. Adv. Exp. Med. Biol. 592, 137–151.
Nomura, M., Yoshikawa, K., Tanaka, T., Sobue, K., Maruyama, K., 1987. The role of tropomyosin in the interactions of F-actin with caldesmon and actin-binding protein (or filamin). Eur. J. Biochem. 163, 467–471.
Novy, R.E., Sellers, J.R., Liu, L., Lin, J.J.-C., 1993. *In vitro* functional characterization of bacterially expressed human fibroblast tropomyosin isoforms and their chimeric mutants. Cell Motil. Cytoskeleton 26, 248–261.
Ochala, J., 2008. Thin filament proteins mutations associated with skeletal myopathies: defective regulation of muscle contraction. J. Mol. Med. 86, 1197–1204.
Odronitz, F., Kollmar, M., 2007. Drawing the tree of eukaryotic life based on the analysis of 2,269 manually annotated myosins from 328 species. Genome Biol. 8, R196.
Ohtsuki, I., 1979. Molecular arrangement of troponin-T in the thin filament. J. Biochem. (Tokyo) 86, 491–497.
O'Neill, G.M., Stehn, J., Gunning, P., 2008. Tropomyosins as interpreters of the signalling environment to regulate the local cytoskeleton. Semin. Cancer Biol. 18, 35–44.
Ono, S., 2007. Mechanism of depolymerization and severing of actin filaments and its significance in cytoskeletal dynamics. Int. Rev. Cytol. 258, 1–82.
Orlova, A., Shvetsov, A., Galkin, V.E., Kudryashov, D.S., Rubenstein, P.A., Egelman, E.H., et al., 2004. Actin-destabilizing factors disrupt filaments by means of a time reversal of polymerization. Proc. Natl. Acad. Sci. USA 101, 17664–17668.
Owada, M.K., Hakura, A., Iida, K., Yahara, I., Sobue, K., Kakiuchi, S., 1984. Occurrence of caldesmon (a calmodulin-binding protein) in cultured cells: comparison of normal and transformed cells. Proc. Natl. Acad. Sci. USA 81, 3133–3137.

Owens, G.K., Loeb, A., Gordon, D., Thompson, M.M., 1986. Expression of smooth muscle-specific alpha-isoactin in cultured vascular smooth muscle cells: relationship between growth and cytodifferentiation. J. Cell Biol. 102, 343–352.

Palm, T., Greenfield, N.J., Hitchcock-DeGregori, S.E., 2003. Tropomyosin ends determine the stability and functionality of overlap and troponin T complexes. Biophys. J. 84, 3181–3189.

Paul, D.M., Morris, E.P., Kensler, R.W., Squire, J.M., 2009. Structure and orientation of troponin in the thin filament. J. Biol. Chem. 284, 15007–15015.

Pawlak, G., Helfman, D.M., 2001. Cytoskeletal changes in cell transformation and tumorigenesis. Curr. Opin. Genet. Dev. 11, 41–47.

Pawlak, G., McGarvey, T.W., Nguyen, T.B., Tomaszewski, J.E., Puthiyaveettil, R., Malkowicz, S.B., et al., 2004. Alternations in tropomyosin isoform expression in human transitional cell carcinoma of the urinary bladder. Int. J. Cancer 110, 368–373.

Pelham Jr., R.J., Lin, J.J.-C., Wang, Y.-l., 1996. A high molecular mass non-muscle tropomyosin isoform stimulates retrograde organelle transport. J. Cell. Sci. 109, 981–989.

Percival, J.M., Thomas, G., Cock, T.-A., Gardiner, E.M., Jeffrey, P.L., Lin, J.J.-C., et al., 2000. Sorting of tropomyosin isoforms in synchronised NIH 3T3 fibroblasts: evidence for distinct microfilament populations. Cell Motil. Cytoskeleton 47, 189–208.

Perry, S.V., 2001. Vertebrate tropomyosin: distribution, properties and function. J. Muscle Res. Cell Motil. 22, 5–49.

Phillips Jr., G.N., Chacko, S., 1996. Mechanical properties of tropomyosin and implications for muscle regulation. Biopolymers 38, 89–95.

Phillips Jr., G.N., Fillers, J.P., Cohen, C., 1986. Tropomyosin crystal structure and muscle regulation. J. Mol. Biol. 192, 111–131.

Pittenger, M.F., Helfman, D.M., 1992. *In vitro* and *in vivo* characterization of four fibroblast tropomyosins produced in bacteria: TM-2, TM-3, TM-5a, and TM-5b are co-localized in interphase fibroblasts. J. Cell Biol. 118, 841–858.

Pittenger, M.F., Kazzaz, J.A., Helfman, D.M., 1994. Functional properties of non-muscle tropomyosin isoforms. Curr. Opin. Cell Biol. 6, 96–104.

Pollard, T.D., Borisy, G.G., 2003. Cellular motility driven by assembly and disassembly of actin filaments. Cell 112, 453–465.

Ponti, A., Machacek, S.L., Gupton, C.M., Waterman-Storer, C.M., Danuser, G., 2004. Two distinct actin networks drive the protrusion of migrating cells. Science 305, 1782–1786.

Potter, J., Gergely, J., 1974. Troponin, tropomyosin and actin interaction in the Ca^{2+} regulation of muscle contraction. Biochemistry 13, 2697–2703.

Praasad, S.V.N., Jayatilleke, A., Madamanchi, A., Rockman, H.A., 2005. Protein kinase activity of phosphoinositide 3-kinase regulates β-adrenergic receptor endocytosis. Nat. Cell Biol. 7, 785–796.

Prasad, G.L., Fuldner, R.A., Cooper, H.L., 1993. Expression of transduced tropomyosin 1 cDNA suppresses neoplastic growth of cells transformed by the ras oncogene. Proc. Natl. Acad. Sci. USA 90, 7039–7043.

Prasad, G.L., Masuelli, L., Raj, M.H., Harindranath, N., 1999. Suppression of src-induced transformed phenotype by expression of tropomyosin-1. Oncogene 18, 2027–2031.

Price, J.T., Tiganis, T., Agarwal, A., Djakiew, D., Thompson, E.W., 1999. Epidermal growth factor promotes MDA-MB-231 breast cancer cell migration through a phosphatidylinositol 3'-kinase and phospholipase C-dependent mechanism. Cancer Res. 59, 5475–5478.

Rao, V.S., Marongelli, E.N., Guilford, W.H., 2009. Phosphorylation of tropomyosin extends cooperative binding of myosin beyond a single regulatory unit. Cell Motil. Cytoskeleton 66, 10–23.

Raval, G.N., Bharadwaj, S., Levine, E.A., Willingham, M.C., Geary, R.L., Kute, T., et al., 2003. Loss of expression of tropomyosin-1, a novel class II tumor alerts tumor suppression that induces anoikis, in primary breast tumors. Oncogene 22, 6194–6203.

Rethinasamy, P., Muthuchamy, M., Hewett, T., Boivin, G., Wolska, B.M., Evans, C., et al., 1998. Molecular and physiological effects of alpha-tropomyosin ablation in the mouse. Circ. Res. 82, 134–136.

Rovner, A.S., Murphy, R.A., Owens, G.K., 1986. Expression of smooth muscle and nonmuscle myosin heavy chains in cultured vascular smooth muscle cells. J. Biol. Chem. 261, 14740–14745.

Ruiz-Opazo, N., Nadal-Ginard, B., 1987. α-Tropomyosin gene organization. J. Biol. Chem. 262, 4755–4765.

Ruppert, C., Godel, J., Müller, R.T., Kroschewski, R., Reinhard, J., Bähler, M., 1995. Localization of the rat myosin I molecules myr 1 and myr 2 and *in vivo* targeting of their tail domains. J. Cell. Sci. 108, 3775–3786.

Ryan, M.P., Higgins, P.J., 1988. Cytoarchitecture of Kirsten sarcoma virus-transformed rat kidney fibroblasts: butyrate-induced reorganization within the actin microfilament network. J. Cell. Physiol. 137, 25–34.

Schevzov, G., O'Neill, G., 2008. Tropomyosin gene expression *in vivo* and *in vitro*. Adv. Exp. Med. Biol. 644, 43–59.

Schevzov, G., Bryce, N.S., Almonte-Baldonado, R., Joya, J.E., Lin, J.J.-C., Hardeman, E., et al., 2005a. Specific features of neuronal size and shape are regulated by tropomyosin isoforms. Mol. Biol. Cell 16, 3425–3437.

Schevzov, G., Vrhovski, B., Bryce, N.S., Elmir, S., Qiu, M.R., O'Neill, G.M., et al., 2005b. Tissue-specific tropomyosin isoform composition. J. Histochem. Cytochem. 53, 557–570.

Shah, V., Bharadwaj, S., Kaibuchi, K., Prasad, G.L., 2001. Cytoskeletal organization in tropomyosin-mediated reversion of ras-transformation: evidence for Rho kinase pathway. Oncogene 20, 2112–2121.

Shanahan, C.M., Weissberg, P.L., Metcalfe, J.C., 1993. Isolation of gene markers of differentiated and proliferating vascular smooth muscle cells. Circ. Res. 73, 193–204.

Shields, J.M., Mehta, H., Pruitt, K., Der, C.J., 2002. Opposing roles of the extracellular signal-regulated kinase and p38 mitogen-activated protein kinase cascades in Ras-mediated down regulation of tropomyosin. Mol. Cell. Biol. 22, 2304.

Singh, A., Hitchcock-DeGregori, S.E., 2003. Local destabilization of the tropomyosin coiled coil gives the molecular flexibility required for actin binding. Biochemistry 42, 14114–14121.

Singh, A., Hitchcock-DeGregori, S.E., 2009. A peek into tropomyosin binding and unfolding on the actin filament. PLoS One 4, e6336.

Smith, D.A., Geeves, M.A., 2003. Cooperative regulation of myosin-actin interactions by a continuous flexible chain II: actin-tropomyosin–troponin and regulation by calcium. Biophys. J. 84, 3168–3180.

Smith, C.W.J., Marston, S.B., 1985. Disassembly and reconstitution of the Ca^{2+}-sensitive thin filament of vascular smooth muscle. FEBS Lett. 184, 115–119.

Smith, C.W., Pritchard, K., Marston, S.B., 1987. The mechanism of Ca^{2+} regulation of vascular smooth muscle thin filaments by caldesmon and calmodulin. J. Biol. Chem. 262, 116–122.

Smith, D.A., Maytum, R., Geeves, M.A., 2003. Cooperative regulation of myosin-actin interactions by a continuous flexible chain I: actin-tropomyosin systems. Biophys. J. 84, 3155–3167.

Sobue, K., Takahashi, K., Wakabayashi, I., 1985. Caldesmon150 regulates the tropomyosin-enhanced actin–myosin interaction in gizzard smooth muscle. Biochem. Biophys. Res. Commun. 132, 645–651.

Sobue, K., Hayashi, K., Nishida, W., 1999. Expressional regulation of smooth muscle cell-specific genes in association with phenotypic modulation. Mol. Cell. Biochem. 190, 105–118.

Somara, S., Pang, H., Bitar, K., 2005. Agonist-induced association of tropomyosin with protein kinase Cα in colonic smooth muscle. Am. J. Physiol. Gastrointest. Liver Physiol. 288, G268–G276.

Stamm, S., Casper, D., Lees-Miller, J.P., Helfman, D.M., 1993. Brain-specific tropomyosins TMBr-1 and TMBr-3 have distinct patterns of expression during development in adult brain. Proc. Natl. Acad. Sci. USA 90, 9857–9861.

Stehn, J.R., Schevzov, G., O'Neill, G.M., Gunning, P., 2006. Specialisation of the tropomyosin composition of actin filaments provides new potential targets for chemotherapy. Curr. Cancer Drug Targets 6, 245–256.

Strand, J., Nili, M., Homsher, E., Tobacman, L.S., 2001. Modulation of myosin function by isoform-specific properties of *S. cerevisiae* and muscle tropomyosins. J. Biol. Chem. 276, 34832–34839.

Sumida, J.P., Wu, E., Lehrer, S.S., 2008. Conserved asp-137 imparts flexibility to tropomyosin and affects function. J. Biol. Chem. 283, 6728–6734.

Svitkina, T.M., Borisy, G.G., 1999. Arp2/3 complex and actin depolymerizing factor/cofilin in dendritic organization and treadmilling of actin filament array in lamellipodia. J. Cell Biol. 145, 1009–1026.

Tanaka, J., Watanabe, T., Nakamura, N., Sobue, K., 1993. Morphological and biochemical analyses of contractile proteins (actin, myosin, caldesmon and tropomyosin) in normal and transformed cells. J. Cell. Sci. 104, 595–606.

Tang, N., Ostap, E.M., 2001. Motor domain-dependent localization of myo1b (myr-1). Curr. Biol. 11, 1131–1135.

Temm-Grove, C.J., Jockusch, B.M., Weinberger, R.P., Schevzov, G., Helfman, D.M., 1998. Distinct localizations of tropomyosin isoforms in LLC-PK1 epithelial cells suggests specialized function at cell-cell adhesions. Cell Motil. Cytoskeleton 40, 393–407.

Tobacman, L., 2008. Cooperative binding of tropomyosin to actin. Adv. Exp. Med. Biol. 644, 85–94.

Toulany, M., Dittmann, K., Baumann, M., Rodemann, H.P., 2005. Radiosensitization of Ras-mutated human tumor cells *in vitro* by the specific EGF receptor antagonist BIBX1382BS. Radiother. Oncol. 74, 117–129.

Van Eyk, J.E., Arrell, D.K., Foster, D.B., Strauss, J.D., Heinonen, T.Y., Furmaniak-Kazmierczak, E., et al., 1998. Different molecular mechanisms for Rho family GTPase-dependent, Ca^{2+}- independent contraction of smooth muscle. J. Biol. Chem. 273, 23433–23439.

Vibert, P., Craig, R., Lehman, W., 1997. Steric-model for activation of muscle thin filaments. J. Mol. Biol. 266, 8–14.

Vidal, C., Geny, B., Melle, J., Jandrot-Perrus, M., Fontenay-Roupie, M., 2002. Cdc42/Rac1-dependent activation of the p21-activated kinase (PAK) regulates human platelet lamellipodia spreading: implication of the cortical-actin binding protein cortactin. Blood 100, 4462–4469.

Vlahovich, N., Schevzov, G., Nair-Shaliker, V., Ilkovski, B., Artap, S.T., Joya, J.E., et al., 2008. Tropomyosin 4 defines novel filaments in skeletal muscle associated with muscle remodeling/regeneration in normal and diseased muscle. Cell Motil. Cytoskeleton 65, 73–85.

Vlahovich, N., Kee, A.J., van der Pole, C., Kettle, E., Hernandez-Deviez, D., Lucas, C., et al., 2009. Cytoskeletal tropomyosin Tm5NM1 is required for normal excitation–contraction coupling in skeletal muscle. Mol. Biol. Cell. 20, 400–409.

Volberg, T., Sabanay, H., Geiger, B., 1986. Spatial and temporal relationships between vinculin and talin in the developing chicken gizzard smooth muscle. Differentiation 32, 34–43.

Vrhovski, B., Schevzov, G., Dingle, S., Lessard, J.L., Gunning, P., Weinberger, R.P., 2003. Tropomyosin isoforms from the gamma gene differing at the C-terminus are spatially and developmentally regulated in the brain. J. Neurosci. Res. 72, 373–383.

Vrhovski, B., Thézé, N., Thiébaud, P., 2008. Structure and evolution of tropomyosin genes. Adv. Exp. Med. Biol. 644, 6–26.

Watson, M.H., Kuhn, A.E., Novy, R.E., Lin, J.J., Mak, A.S., 1990. Caldesmon-binding sites on tropomyosin. J. Biol. Chem. 265, 18860–18866.

Wegner, A., 1979. Equilibrium of the actin-tropomyosin interaction. J. Mol. Biol. 131, 839–853.

Weinberger, R., Schevzov, G., Jeffrey, P., Gordon, K., Hill, M., Gunning, P., 1996. The molecular composition of neuronal microfilaments is spatially and temporally regulated. J. Neurosci. 16, 238–252.

Whitby, F.G., Phillips Jr., G.N., 2000. Crystal structure of tropomyosin at 7 Ångstroms. Proteins 38, 49–59.

Winder, S.J., 2003. Structural insights into actin-binding, branching and bundling proteins. Curr. Opin. Cell Biol. 15, 14–22.

Wu, S.C., Solaro, R.J., 2007. Protein kinase C zeta. A novel regulator of both phosphorylation and de-phosphorylation of cardiac sarcomeric proteins. J. Biol. Chem. 282, 30691–30698.

Xu, C., Craig, R., Tobacman, L., Horwitz, R., Lehman, W., 1999. Tropomyosin positions in regulated thin filaments revealed by cryelectron microscopy. Biophys. J. 77, 985–992.

Yager, M., Hughes, J., Lovicu, F., Gunning, P., Weinberger, R., O'Neill, G., 2003. Functional analysis of the actin-binding protein, tropomyosin 1, in neuroblastoma. Br. J. Cancer 89, 860–863.

Yamakita, Y., Oosawa, F., Yamashiro, S., Matsumura, F., 2003. Caldesmon inhibits Arp2/3-mediated actin nucleation. J. Biol. Chem. 278, 17937–17944.

Yamashiro, S., Yamakita, Y., Ishikawa, R., Matsumura, F., 1990. Mitosis-specific phosphorylation causes 83 K non-muscle caldesmon to dissociate from microfilaments. Nature 344, 675–678.

Yamashiro, S., Yamakita, Y., Hosoya, H., Matsumura, F., 1991. Phosphorylation of non-muscle caldesmon by p34cdc2 kinase during mitosis. Nature 349, 169–172.

Yamashiro, S., Yamakita, Y., Yoshida, K., Takiguchi, K., Matsumura, F., 1995. Characterization of the COOH terminus of non-muscle caldesmon mutants lacking mitosis-specific phosphorylation sites. J. Biol. Chem. 270, 4023–4030.

Yamboliev, I.A., Gerthoffer, W.T., 2001. Modulatory role of ERK MAPK-caldesmon pathway in PDGF-stimulated migration of cultured pulmonary artery SMCs. Am. J. Physiol., Cell Physiol. 280, C1680–C1688.

Yan, B., Sen, A., Chalovich, J.M., Chen, Y.D., 2003. Theoretical studies on competitive binding of caldesmon and myosin S1 to actin: prediction of apparent cooperativity in equilibrium and slow-down in kinetics of S1 binding by caldesmon. Biochemistry 42, 4208–4216.

Yoshio, T., Morita, T., Kimura, Y., Tsujii, M., Hayashi, N., Sobue, K., 2007. Caldesmon suppresses cancer cell invasion by regulating podosome/invadopodium formation. FEBS Lett. 581, 3777–3782.

CHAPTER FOUR

Regulation of Sulfate Transport and Assimilation in Plants

Hideki Takahashi

Contents

1. Introduction 130
2. Sulfate Transport Systems 132
   2.1. Uptake of sulfate 132
   2.2. Root-to-shoot transport of sulfate 137
   2.3. Vacuolar transport of sulfate 139
   2.4. Source-to-sink transport of sulfur 140
   2.5. Other transport processes 142
3. Regulation of Sulfate Transport and Metabolism 145
   3.1. Effectors of regulation 145
   3.2. Regulatory elements 148
4. Concluding Remarks 152
Acknowledgments 153
References 153

Abstract

Plants as autotrophic organisms have a set of transporters and enzymes that mediate uptake and assimilation of inorganic sulfate and subsequent metabolic conversion to organic sulfur compounds. Studies in higher plants indicate the individual components of sulfate transport systems and enzymes for sulfate assimilation are consisted of multiple isoforms. Among these isoforms, several essential components are shown to have specific biochemical properties and localize in specific cellular and subcellular compartments. This chapter will describe the functions and regulation of sulfate transport systems and assimilatory enzymes, particularly focusing on the sulfate transporter gene family of a model plant species *Arabidopsis thaliana*. Recent findings provided evidence that the regulatory pathways are highly organized to balance the uptake, storage, and assimilation of sulfate in plants. In addition to the physiological and biochemical functions diversified among the isoforms of sulfate transporters, regulatory elements in transcriptional and posttranscriptional mechanisms

RIKEN Plant Science Center Joint Laboratory, Kihara Institute for Biological Research, Yokohama City University, Maioka-cho, Totsuka-ku, Yokohama, Japan

International Review of Cell and Molecular Biology, Volume 281
ISSN 1937-6448, DOI: 10.1016/S1937-6448(10)81004-4

were suggested to play significant roles in coordinating the assimilatory functions to adapt with varying sulfur nutritional status that fluctuates in the environment.

Key Words: Plants, *Arabidopsis*, Sulfur, Sulfate, Transporter, Metabolism.

1. Introduction

In nature, sulfur is available both in inorganic and organic forms. Sulfate is an oxidized form of sulfur and is present as a divalent anion in aqueous solution. Plants mostly utilize sulfate in the soil solution as the sulfur source to synthesize organic sulfur compounds for vitalization (Leustek et al., 2000; Saito, 2000, 2004). Reduced inorganic forms of sulfur (e.g., elemental sulfur) and organic sulfur in the forms of sulfated or sulfonated compounds exist in the environment, but they are not usually utilized by higher plants in the ecosystem. Within the sulfur cycle in nature, generally microorganisms carry out the hydrolytic degradation of sulfated compounds and decomposition of sulfonated compounds, generating sulfate that is to be incorporated and utilized by plants. Auxotrophic organisms rely on the organic sulfur compounds, and the wastes and remains of higher organisms are degraded by microorganisms to have sulfur recycled back to sulfate. The sulfur cycle in nature therefore stands on a balance between assimilatory and catabolic functions of metabolisms in plants and microorganisms (Crawford et al., 2000; Leustek et al., 2000; Saito, 2000, 2004).

The uptake and assimilation of sulfate are energy-dependent biochemical processes. As will be discussed in the Section 2.1.1, the proton gradient across the plasma membrane is considered as a driving force for the influx of sulfate (Hawkesford et al., 1993; Lass and Ullrich-Eberius, 1984). Since the proton gradient is maintained by proton-ATPase that hydrolyzes ATP and pumps out protons from cytosol to extracellular space, sulfate uptake activity is dependent on the rates of ATP consumption besides the influx of sulfate is largely influenced by the amount of sulfate provided from the environment (Fig. 4.1). Once sulfate is incorporated into the cell and the chloroplast, it goes through consecutive enzymatic reactions utilizing ATP and reducing cofactors for conversion of sulfur from oxidized (+VI) to reduced (−II) states (Fig. 4.1) (Leustek et al., 2000; Saito, 2000, 2004). Sulfide produced from this pathway is an immediate substrate for cysteine biosynthesis. ATP, glutathione, and ferredoxin used for the reduction of sulfate to sulfide are generated through the reactions of photosynthetic electron transfer, thus the pathway of sulfur assimilation is essentially dependent on light energy

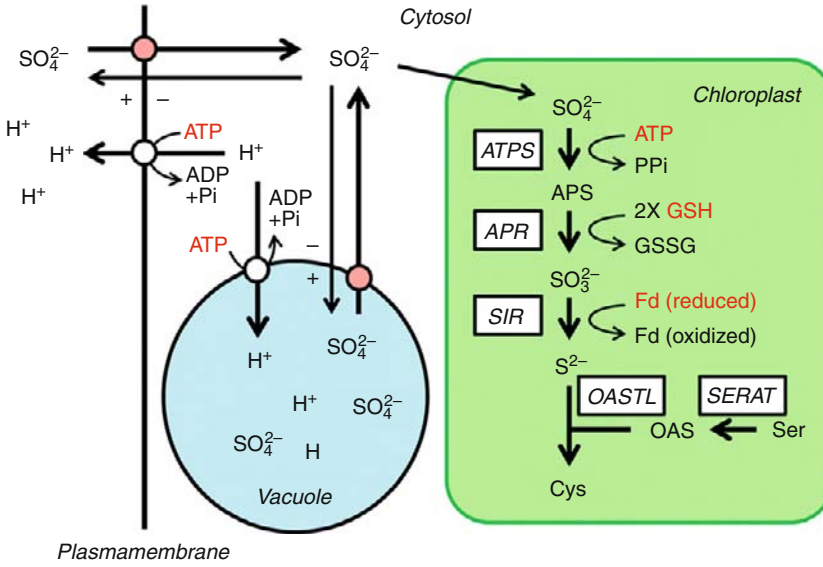

Figure 4.1 Sulfate transport and assimilation. The figure illustrates a simplified scheme of sulfate transport systems across the plasmamembrane and tonoplast, and sulfur metabolism in the chloroplast. Sulfate transporters and ATPases are indicated in pink and white circles, respectively. Abbreviations: *APR*, APS reductase; APS, adenosine-5′-phosphosulfate; *ATPS*, ATP sulfurylase; Cys, cysteine; Fd, ferredoxin; GSH, glutathione; GSSG, oxidized glutathione; OAS, *O*-acetylserine; *OASTL*, OAS (thiol)lyase; Ser, serine; *SERAT*, serine acetyltransferase; *SIR*, sulfite reductase.

harvesting. In nonphotosynthetic tissues, photoassimilates serve as energy sources. These assimilatory functions are the major differences between the sulfur metabolisms of plants and animals.

Sulfate is the favorable sulfur source for higher plants as it can be readily utilized in the assimilatory pathway. Sulfate in the soil is taken up by roots and distributed to various organs where reduction of sulfate takes place. The essentiality of sulfur is evident from its presence in major cellular components and diversified biological activities of sulfur-containing metabolites (Crawford et al., 2000; Leustek et al., 2000; Saito, 2000, 2004). Cysteine and methionine are amino acids containing sulfur in their functional moieties. Particularly, the thiol residue of cysteine forms S–S bonds and is important for protein structure. It also serves as active centers in many enzyme reactions, providing sites for electron transfer. In addition, thiols in glutathione, ferredoxins, and thioredoxins function in redox control (Buchanan and Balmer, 2005). As a cellular constituent other than amino acids and proteins, sulfur is found in sulfolipid which is essential for the maintenance of chloroplast membranes (Benning, 1998). Sulfur is also

present in vitamins and cofactors such as thiamine, biotin, and coenzyme A. Furthermore, many sulfur-containing secondary metabolites are known to have specialized biological functions. Compounds derived from glucosinolates in Brassicaceae plants (Grubb and Abel, 2006; Halkier and Gershenzon, 2006) and *S*-alkylcysteine sulfoxides in Alliaceae plants (Jones et al., 2004) are characteristic of having special odors and pungency. For humans, daily intake of these secondary metabolites is beneficial for health as they induce detoxifying enzymes and prevent tumor formation (Bianchini and Vainio, 2001; Talalay and Fahey, 2001). They are also known as repellants against insects and microorganisms. With respect to plant–microbe interactions, Nod factors are essential for establishment of the symbiosis of nitrogen-fixing rhizobacteria in legumes (Fisher and Long, 1992).

As mentioned above, plant cells synthesize a wide range of sulfur-containing compounds from primary to secondary metabolites. Notwithstanding their biological functions, sulfur in all sulfur-containing metabolites derives from sulfate. The metabolic pathway from the uptake and reduction of sulfate to cysteine biosynthesis is therefore the basis of sulfur metabolism. Roots predominantly function for the acquisition of sulfur source from the soil environment. Accordingly, the rate of initial sulfate uptake in the root subsequently affects the fluxes of sulfur through the processes of internal transport and metabolic conversion. On the other hand, the acquisition of sulfate needs to be controlled depending on requirements of sulfur at the whole plant level. Recent studies unveiled regulatory elements for this highly organized system that necessarily keeps the balances among the input and internal utilization of sulfate in plants. The underlying mechanisms involved both transcriptional and posttranscriptional regulations. This chapter describes how the individual components of sulfate transport systems are regulated and organized as a system to have an optimized control of sulfur use at the whole plant level.

2. Sulfate Transport Systems

2.1. Uptake of sulfate

2.1.1. Mechanism of sulfate uptake

Historically, uptake of sulfate to plant roots has been measured using ^{35}S-labeled sulfate. The activity of sulfate influx to plant roots was initially demonstrated in 1950s (Leggett and Epstein, 1956). Similar to the case in other nutrients, the kinetics of sulfate influx followed the Michealis–Menten equation, indicating a transport protein specific for sulfate mediates the influx. This phase I transport system having high affinity to its substrate sulfate was shown to be induced under sulfur-limited conditions (Clarkson et al., 1983; Deane-Drummond, 1987). With respect to the mechanisms for

the uptake of sulfate at the plasmamembranes, sulfate as a negatively charged ion needs to be transported to the cytosol against the membrane potential and concentration gradient of sulfate itself (Fig. 4.1). A secondary active transport system can be suggested as a membrane-bound facilitator for the inward rectifying movement of sulfate across the plasmamembranes as it may utilize proton as a motive force to pump up sulfate to the cytosol (Fig. 4.1). This mechanism is widely believed based on the evidence that sulfate transport activity is dependent on formation of a proton gradient across the membrane (Hawkesford et al., 1993; Lass and Ullrich-Eberius, 1984). However, as in the case of mammals (Mount and Romero, 2004), there still might be a possibility that anion exchange systems may facilitate the uptake of sulfate to plant cells.

2.1.2. Transporters for sulfate uptake

Molecular biology of plant sulfate transporter is preceded by yeast genetic studies. Yeast mutants lacking sulfate uptake activities were isolated by screening resistance to selenate and chromate, the toxic analogs of sulfate (Cherest et al., 1997; Smith et al., 1995a). The growth of the isolated yeast mutant was recovered when the concentration of sulfate was over 1 mM, suggesting defects are specific to the high-affinity sulfate transport systems. The mutations were found in genes encoding the yeast sulfate transporters, SUL1 and SUL2, both of which were functional and facilitated the influx of sulfate (Cherest et al., 1997; Smith et al., 1995a). Plant sulfate transporters were first identified from leguminous plant *Stylosanthes hamata* by functional complementation of the yeast mutant defective in sulfate transporters (Smith et al., 1995b). The basic structures of plant sulfate transporters were similar to those predicted for the orthologs of yeast and fungus origins (Cherest et al., 1997; Ketter et al., 1991; Smith et al., 1995a). The SHST1, SHST2, and SHST3 proteins encoded by *S. hamata* sulfate transporter genes contained 12 putative membrane-spanning domains predicted to fold their structures anchored in lipid bilayers of the membrane (Smith et al., 1995b). A hydrophilic STAS (sulfate transporter and antisigma factor antagonist) domain in the C-terminus was another structural characteristic (Aravind and Koonin, 2000). Recent studies indicated the STAS domain controls plasmamembrane localization and the function of sulfate transporter (Rouached et al., 2005; Shibagaki and Grossman, 2004, 2006). More importantly, SHST1 and SHST2 showed saturable kinetics of sulfate uptake with micromolar K_m values when they were expressed in yeast mutant (Smith et al., 1995b). These two isoforms were abundantly expressed in the root of sulfur-starved plants, suggesting relevance to the initial sulfate uptake systems. These features of SHST1 and SHST2 were consistent with the induction of high-affinity sulfate uptake activity that is generally observed in the roots of sulfate-starved plants. On the other hand, SHST3 showed a somewhat lower affinity to sulfate and was suggested to be

functional for internal transport of sulfate (Smith et al., 1995b). Following this work, numbers of sulfate transporters that were able to complement the yeast mutant have been isolated from various plant species, many of which were high-affinity sulfate transporters expressed in the root tissues of sulfur-starved plants (Bolchi et al., 1999; Buchner et al., 2004a; Hopkins et al., 2005; Howarth et al., 2003; Smith et al., 1997; Vidmar et al., 1999). For the sequences derived from *Arabidopsis* and rice genomes, 12 distinct sulfate transporter genes can be classified into four groups including both the functional and putative isoforms suggested to play specialized roles in the uptake and translocation of sulfate in plants (Fig. 4.2) (Buchner et al., 2004b; Takahashi et al., 2006).

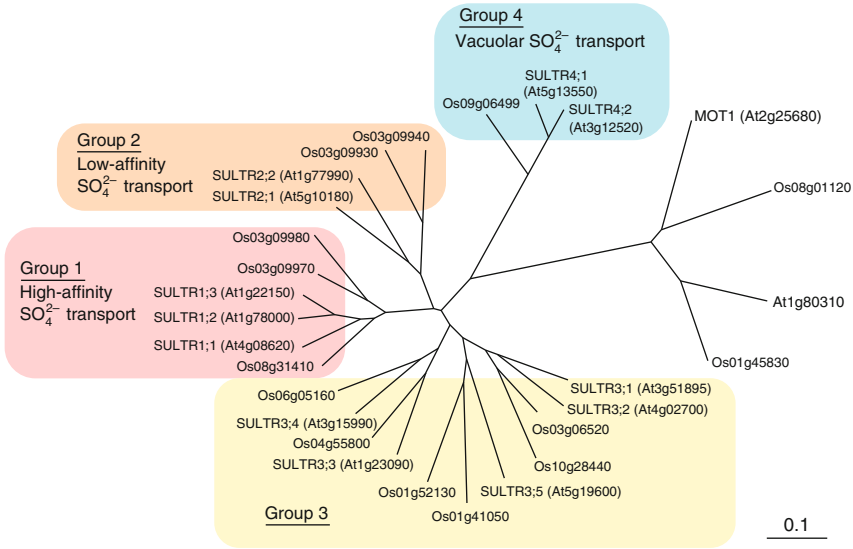

Figure 4.2 Phylogenetic tree of *Arabidopsis* and rice sulfate transporters. *Arabidopsis* genes are indicated by the gene names and AGI code numbers with At prefixes. Rice genes are indicated by MSU locus numbers with Os prefixes. Protein sequences of SULTR (sulfate transporter) and MOT (molybdate transporter) were obtained by BLASTP programs at The Arabidopsis Information Resources (TAIR) (http://www.arabidopsis.org/Blast/), MSU Rice Genome Annotation Project (http://rice.plantbiology.msu.edu/blast.shtml), and Rice Annotation Project (RAP) (http://rapdb.lab.nig.ac.jp/blast/index.html). Protein sequences were aligned by ClustalW (Thompson et al., 1994), and the phylogenetic tree was created by the neighbor-joining method (Saitou and Nei, 1987). Programs at DNA Data Bank of Japan (DDBJ) (http://www.ddbj.nig.ac.jp/search/clustalw-j.html) were used for the alignment of protein sequences. An unrooted phylogenetic tree was created by TreeView (http://taxonomy.zoology.gla.ac.uk/rod/treeview.html) (Page, 1996).

2.1.3. High-affinity sulfate transporters for sulfate uptake in *Arabidopsis*

Precise analyses of the physiological functions of high-affinity sulfate transporters have been carried out in *Arabidopsis*. In *Arabidopsis*, *SULTR1;1* and *SULTR1;2* are the high-affinity sulfate transporters having their main functions in root sulfate uptake systems (Fig. 4.3). They were predominantly localized in the root hairs, epidermis, and cortex of roots, and their transcripts were accumulated in response to sulfur limitation (Shibagaki et al., 2002; Takahashi et al., 2000; Vidmar et al., 2000; Yoshimoto et al., 2002). Both *SULTR1;1* and *SULTR1;2* were expressed in cell layers where

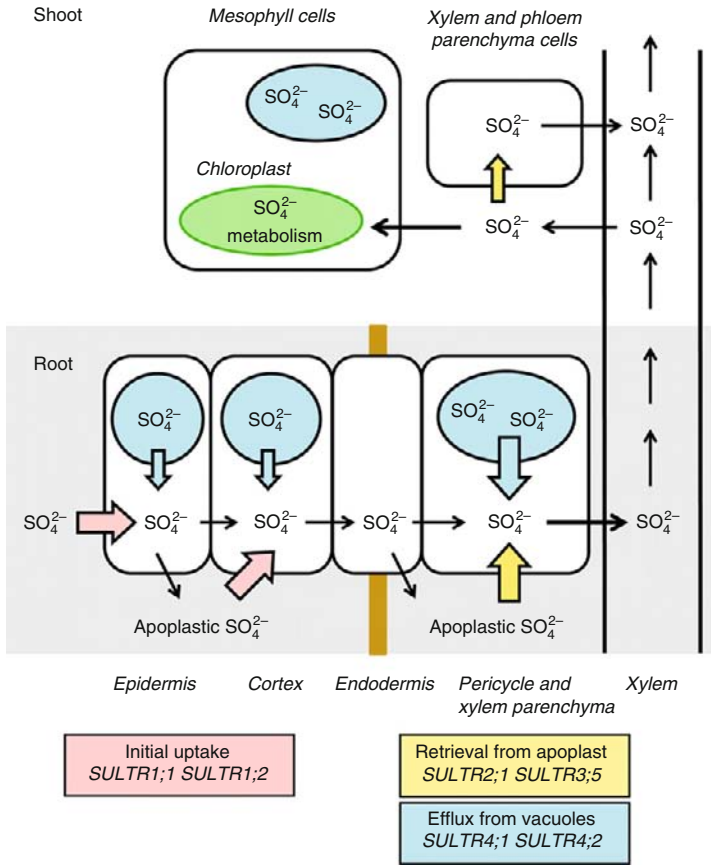

Figure 4.3 Steps for uptake and internal translocation of sulfate in *Arabidopsis*. High-affinity sulfate uptake by SULTR1;1 and SULTR1;2 (pink), low-affinity sulfate transport by SULTR2;1 and SULTR3;5 (yellow), and vacuolar sulfate transport by SULTR4;1 and SULTR4;2 (blue) are indicated by thick arrows.

the acquisition of nutrients generally occurs, and induced at both transcript and protein levels when plants require sulfur source (Yoshimoto et al., 2002, 2007), indicating significance of their functions in the uptake of sulfate. Although *SULTR1;1* and *SULTR1;2* appear to function redundantly for the uptake of sulfate in *Arabidopsis* roots, some differences should be noted between the two isoforms. *SULTR1;2* was more abundantly expressed compared to *SULTR1;1* (Yoshimoto et al., 2002), and disruption of *SULTR1;2* resulted in losing 50–70% of sulfate uptake activities in *Arabidopsis* seedlings (Barberon et al., 2008; Maruyama-Nakashita et al., 2003; Yoshimoto et al., 2007). As in the case of yeast mutant (Cherest et al., 1997; Smith et al., 1995a), the *Arabidopsis sultr1;2* (*sel1*) mutants having defects in sulfate uptake were tolerant to selenate, which allowed identification of the *SULTR1;2* gene function from genetic screening (El Kassis et al., 2007; Shibagaki et al., 2002). Although deletion of *SULTR1;2* affects the sulfur status in *Arabidopsis* seedlings, contribution of *SULTR1;1* to sulfate uptake was not negligible as being overaccumulated compensatory in the *sultr1;2* mutant (El Kassis et al., 2007; Maruyama-Nakashita et al., 2003). When both components of the high-affinity sulfate uptake system were abolished in *sultr1;1 sultr1;2* double mutant, the seedlings first became stunted under the low-sulfur environments (Barberon et al., 2008; Yoshimoto et al., 2007). However, the *sultr1;1 sultr1;2* double mutant was still able to survive when sulfate was adequately supplied, suggesting a bypassing transport system having lower affinity to sulfate can partially substitute the initial sulfate uptake function. The molecular identity of this remaining sulfate uptake activity has not yet been verified.

2.1.4. Distinguishable characteristics of SULTR1;1 and SULTR1;2

According to the present understandings, SULTR1;1 and SULTR1;2 function for the uptake of sulfate when both are present (Barberon et al., 2008; Yoshimoto et al., 2007). A clear difference can be found in the response of their transcripts to sulfur; *SULTR1;1* were more strongly induced by sulfur starvation to accumulate its transcripts in roots, although the *SULTR1;2* transcripts were already abundantly accumulated under sulfur-replete conditions and less modulated by the changes in sulfur conditions compared to *SULTR1;1* (Maruyama-Nakashita et al., 2005; Rouached et al., 2008; Yoshimoto et al., 2002). In addition to these characteristics in transcript regulation, the calculated K_m value for sulfate was slightly lower for SULTR1;1 than SULTR1;2 (Takahashi et al., 2000; Yoshimoto et al., 2002). Although correct interpretation awaits verification of their biochemical properties *in planta*, SULTR1;1 likely possesses a characteristic favorable for stressed conditions where roots are supplied with trace amount of sulfate. SULTR1;1 would take specific actions to the fluctuations of sulfur conditions more sensitive than that of SULTR1;2. Although SULTR1;1 encodes a less-abundant isoform, several lines of

evidence mentioned above strongly suggest its contribution to the high-affinity sulfate uptake system as a more specialized component.

2.2. Root-to-shoot transport of sulfate

2.2.1. Horizontal transport of sulfate from epidermis to central cylinder in roots

Following uptake of sulfate to root hairs and epidermis, sulfate can be transferred horizontally through plasmodesmal connections between the cells to reach the cells adjacent to xylem vessels (Fig. 4.3). Not all sulfate ions will move through this symplastic pathway. Because of the outside positive membrane potential, sulfate can be leaked from cells to extracellular cell wall space (apoplastic space) through an anion permeable ion channel protein (Fig. 4.1). The exact mechanism for this efflux system still remains unverified. In the cortical cell layers of *Arabidopsis* roots, SULTR1;1 and SULTR1;2 will retrieve apoplastic sulfate back to the symplastic pathway (Fig. 4.3) (Shibagaki et al., 2002; Takahashi et al., 2000; Yoshimoto et al., 2002). In addition, this retrieval function seems to be attributable to the function of barley high-affinity sulfate transporter HVST1 whose expression was found not only in epidermis in the root-tip region but also in endodermis, pericycle, and xylem parenchyma cells in the mature zone of sulfur-starved root (Rae and Smith, 2002). Once sulfate is transferred to central cylinder, it may distribute to pericycle and parenchyma cells having symplastic connections to xylem. Although the sulfate loading system is unknown, some family members of sulfate transporters located in the cells of root central cylinder are known to increase the rate of root-to-shoot transfer of sulfate (Kataoka et al., 2004a,b). In *Arabidopsis*, SULTR2;1 and SULTR3;5 were suggested to play important roles in this mechanism (Kataoka et al., 2004b). As described in the following sections, they were suggested to have specific functions in retrieval of sulfate from the apoplast, preventing the loss of sulfate diffused to the apoplastic space of vascular tissues (Fig. 4.3).

2.2.2. Suggested function of low-affinity sulfate transporter SULTR2;1

SULTR2;1 is a low-affinity sulfate transporter identified as a homolog of group 1 high-affinity sulfate transporters (Fig. 4.2). SULTR2;1 was capable of restoring the growth of yeast sulfate transporter mutant and mediated the influx of sulfate, although its kinetic features indicated this transport protein has specific but lower affinity to sulfate (Takahashi et al., 1997, 2000). The *in situ* hybridization of *SULTR2;1* mRNA and promoter-GUS expression indicated predominant function of SULTR2;1 in the vascular tissues particularly in pericycle and xylem parenchyma cells in roots, and in xylem and phloem parenchyma cells in shoots (Takahashi et al., 1997, 2000). Despite the significant similarities of spatial expression

patterns in roots and shoots, *SULTR2;1* mRNA was accumulated in response to sulfur starvation in the root, while strongly repressed by sulfur limitation in the shoot (Takahashi et al., 2000). These differential responses suggest potential functions of SULTR2;1 in facilitating distribution of sulfate to leaf tissues under sulfur-limited conditions: (i) induction of *SULTR2;1* in the root central cylinder prevents leakage of sulfate from the parenchyma cells and will contribute for the maintenance of symplastic sulfate transferred to xylem; (ii) in shoots, repression of *SULTR2;1* will prevent retrieval of sulfate to the parenchyma cells of vascular tissues and allow sulfate to be distributed more efficiently to mesophyll cells distantly located from the vasculature (Fig. 4.3). According to these principles, *SULTR2;1* must be regulated under contrasting mechanisms that may influence the physiological functions of this transport system either in positive or negative ways in roots and shoots, respectively. Regulation of *SULTR2;1* is additionally described in the section of regulatory elements (Section 3.2.3).

2.2.3. Functional interplay in low-affinity sulfate transport

Recent studies indicated that an isoform of group 3 sulfate transporter, SULTR3;5 (Fig. 4.2), is a component that functionally couples with SULTR2;1 low-affinity sulfate transporter (Kataoka et al., 2004b). When expressed in yeast cells, SULTR3;5 barely exhibited sulfate uptake activities. Its activity was only slightly higher than the background level of the yeast mutant strain. However, when both transport proteins were coexpressed in yeast, the capacity of sulfate uptake rate increased about threefolds of the activity of SULTR2;1 without changing the affinity for sulfate (Kataoka et al., 2004b). SULTR3;5 itself is most likely a silent isoform as a sulfate transporter, but seems to activate its counterpart component, SULTR2;1. The significance of the functional interplay between SULTR2;1 and SULTR3;5 is also evidenced in *Arabidopsis* plants. Colocalization of the two isoforms was suggested in root vasculature. *SULTR3;5* was expressed in pericycle and xylem parenchyma cells of root central cylinder (Kataoka et al., 2004b). At least in roots, cells that express *SULTR3;5* overlapped with those accumulating *SULTR2;1* transcripts under sulfur-starved conditions (Takahashi et al., 1997, 2000). However, in contrast to *SULTR2;1*, the transcript levels of *SULTR3;5* were not modulated by sulfur nutrition (Kataoka et al., 2004b). Consistent with these observations, *sultr3;5* mutants showed defects in transferring sulfate from roots to shoots when adequate amount of sulfate was resupplied to the roots of sulfur-starved seedlings (Kataoka et al., 2004b). Under these conditions, SULTR2;1 will carry out low-affinity sulfate uptake to xylem parenchyma cells cooperating with SULTR3;5 (Fig. 4.3). Consequently, the absence of SULTR3;5 can limit root-to-shoot transport of sulfate in sulfur-starved seedlings.

2.3. Vacuolar transport of sulfate

2.3.1. Mechanisms of sulfate transport across tonoplast

Vacuoles serve as storage compartments of sulfate. At the tonoplast membranes, proton-ATPase and proton-pyrophosphatase continuously pump up protons from cytoplasm to vacuolar lumen, providing inside positive electrical potentials (Martinoia et al., 2000, 2007) (Fig. 4.1). Under such circumstances, sulfate can be transported into vacuoles considerably through a tonoplast-localized ion channel or carrier as the electrical gradient is favorable for the incorporation of negatively charged ions. The actual mechanisms or transport proteins mediating the influx of sulfate to vacuoles is still unverified; however, studies with isolated mesophyll vacuoles indicate biphasic kinetics for the influx of sulfate to the vacuoles, suggesting existence of saturable and linear components (Kaiser et al., 1989). With respect to the efflux of sulfate from the vacuoles, the situation can be similar with the uptake of sulfate across the plasmamembrane, as sulfate being transported against the membrane potential, although the concentration of sulfate is normally high in the lumen side. A steep proton gradient generated by proton-ATPase and proton-pyrophosphatase can be used as a motive force for the efflux of sulfate from the vacuoles (Fig. 4.1). Alternatively, anion exchange systems may facilitate the influx and efflux of sulfate across the tonoplast.

2.3.2. Sulfate transporters for remobilization of vacuolar sulfate

When the supplies of sulfur source become limited, the internal storage of sulfate must be remobilized. Under such circumstances, transporters that export sulfate from the vacuoles make significant contribution to remobilization (Fig. 4.1). In *Arabidopsis*, SULTR4;1 and SULTR4;2 were the tonoplast-localizing sulfate transporters that serve for this essential step (Kataoka et al., 2004a). The isoforms of group 4 sulfate transporters formed a distinct group in the *SULTR* gene family (Fig. 4.2). Both SULTR4;1 and SULTR4;2 were expressed in roots and shoots where predominant expression was detected in the vasculature (Kataoka et al., 2004a). Although the cell type- and subcellular-specific localizations of SULTR4;1 and SULTR4;2 were quite similar to each other, slight differences in expression levels and responses to sulfur nutrition were observed like in the case of *SULTR1;1* and *SULTR1;2*. In the case of vacuolar isoforms, *SULTR4;1* was the abundant form in transcript levels and *SULTR4;2* was the less-abundant form that was more strongly induced by sulfur limitation (Kataoka et al., 2004a). Disruption of *SULTR4;1* and *SULTR4;2* by T-DNA insertions further indicated the *in planta* functions of these vacuolar isoforms of sulfate transporters. Following sulfur limitation, vacuoles isolated from the cell culture of the *sultr4;1 sultr4;2* mutant line showed increased accumulation of sulfate compared to the wild type.

The expression of SULTR4;1–GFP fusion protein that localizes in the tonoplast restored the vacuolar sulfate content of *sultr4;1 sultr4;2* double mutant to the wild-type level. These lines of evidence indicated the functions of SULTR4;1 and SULTR4;2 are relevant to the efflux of sulfate from the vacuoles (Kataoka et al., 2004a).

2.3.3. Vacuolar sulfate transporters control transport of sulfate to shoots

Besides the roles in intracellular mobilization of vacuolar sulfate pools, SULTR4;1 and SULTR4;2 were suggested to control the amount of sulfate transferred to xylem from the pericycle and xylem parenchyma cells of roots (Fig. 4.3). In the seedlings of *sultr4;1 sultr4;2* mutant, ^{35}S-sulfate incorporated to roots was retained in the root tissues and its distribution to the shoots was significantly restricted (Kataoka et al., 2004a). This phenomenon was observed under low-sulfur conditions. Accordingly, export of sulfate from the vacuoles is suggested to be necessary for release of vacuolar sulfate pool and to prevent excessive accumulation of sulfate in the vacuoles of root tissues when demands for sulfur are increased in the aerial organs (Kataoka et al., 2004a). This mechanism will substantially contribute to the efficient distribution of sulfate incorporated to *Arabidopsis* seedlings (Fig. 4.3). In addition, labeling of *Brassica napus* plants with ^{34}S-sulfate indicated decrease in ^{34}S contents of old leaves correlates with the increase in *SULTR4;1* and *SULTR4;2* transcript accumulation (Dubousset et al., 2009). The results appear to explain sulfate remobilized from the vacuoles of old senescing leaves contributes to redistribution of sulfur to young leaves. Based on the patterns of sulfur-responsive regulation of *SULTR2;1* in the shoot vascular tissues (Takahashi et al., 2000), translocation of sulfate itself from old to young leaves is suggested to be restricted under low-sulfur conditions (see Section 2.4.1). According to this model, it is more likely that sulfate remobilized from the vacuoles is metabolized to transportable forms of sulfur-containing compounds before entering source-to-sink transport system.

2.4. Source-to-sink transport of sulfur

2.4.1. Sulfate transporters in phloem parenchyma cells

Sulfur is generally categorized as a less-mobile element with respect to translocation from source-to-sink organs, but is known to have a certain extent of mobility in the sieve element of the phloem. *S*-Methylmethionine and glutathione are considered to be the major chemical forms of sulfur transported through the sieve element (Bourgis et al., 1999; Herschbach et al., 2000; Kuzuhara et al., 2000). In addition, sulfate is also found in the phloem sap. With respect to the components of sulfate transport proteins that may affect phloem transport of sulfur source, *SULTR2;1* localizes

in the parenchyma cells surrounding sieve elements and companion cells (Takahashi et al., 2000). As mentioned in the previous section, *SULTR2;1* was expressed in both xylem and phloem parenchyma cells in the shoot. In addition, the level of *SULTR2;1* transcript was decreased in the shoot under low-sulfur conditions (Takahashi et al., 2000). These observations suggest the amount of sulfate delivered to phloem can be decreased when sulfate is limiting. According to the mechanism postulated here for the regulation of *SULTR2;1*, transport of sulfate or other forms of sulfur sources from old to young leaves probably occurs actively through the sieve element when plants are adequately supplied with sulfate. By contrast, when sulfate supply is limited, local distribution of sulfate within the leaf appears to be important rather than delivering sulfur resources distantly to other leaves or sink organs (Fig. 4.3). These mechanisms probably apply to Brassicaceae plants that generally have high demand for sulfur. The less mobility of sulfur in source-to-sink transport may be attributed to the downregulation of *SULTR2;1* in the shoot vascular tissues particularly in the phloem parenchyma cells.

2.4.2. Sulfate transporters in phloem companion cells

Additional evidence has been demonstrated for involvement of sulfate transporter in source-to-sink transport of sulfur in *Arabidopsis*. SULTR1;3 was shown to localize in the companion cells of phloem, and deletion of this high-affinity sulfate transporter restricted transfer of ^{35}S from cotyledons to shoot meristems and roots in *Arabidopsis* (Yoshimoto et al., 2003). The amount of *SULTR1;3* mRNA was increased both in shoots and roots under low-sulfur conditions, suggesting the function of this sulfate transporter is required for the uptake of sulfate and maintenance of sulfur metabolism in the phloem companion cells. Particularly, in the shoot where *SULTR2;1* in phloem parenchyma cells is repressed by sulfur limitation (Takahashi et al., 2000), induction of *SULTR1;3* may become significant for the acquisition of sulfate to the companion cells. In addition to *SULTR1;3*, a low-affinity sulfate transporter *SULTR2;2* is also known to be expressed in the phloem companion cells (Takahashi et al., 2000). Transport and metabolism of sulfate seem to occur actively in the phloem. However, it is not well defined how these two sulfate transporters share their functions in the same or similar cell types.

2.4.3. Transport of sulfur to seeds

Translocation of sulfur source to developing seeds is an important event of nutrient distribution. SULTR2;1 is suggested to function for this purpose (Awazuhara et al., 2005). In the developing siliques of *Arabidopsis*, the expression of *SULTR2;1* was found in the vasculatures and the base of seed pods, and in the funiculus connected to seeds. The amounts of sulfate and thiols in seeds were decreased by antisense suppression of *SULTR2;1*, suggesting the function of this transporter is relevant to delivery of sulfate

or sulfur metabolites to seeds. The low-sulfur status of *SULTR2;1* antisensed plant seeds was further indicated by introducing an indicator construct consisted of a sulfur-responsive promoter sequence of β-conglycinin and GUS reporter (Awazuhara et al., 2005). β-Conglycinin is a soybean seed storage protein that accumulates under low-sulfur conditions and exhibits sulfur deficiency responses when expressed heterologously in *Arabidopsis* (Awazuhara et al., 2002; Hirai et al., 1995). As described previously, *SULTR2;1* is regulated by the sulfur status, displaying contrasting patterns of mRNA accumulation between roots and shoots (Takahashi et al., 2000). It can be hypothesized that SULTR2;1 controls loading of sulfate to xylems in roots and to phloems in shoots (Fig. 4.3), and eventually both would affect the sulfur content of the seeds. In addition, transport of sulfate or sulfur-containing compounds to seeds through the funiculus can be affected under both low- and high-sulfur conditions as apparent insensitivity of *SULTR2;1* transcript control mechanisms to sulfur conditions was indicated for the siliques (Awazuhara et al., 2005). Besides the function of SULTR2;1, sulfur metabolism in developing seeds is suggested to be important for sulfur nutrition. Developing cotyledons of lupin shows significant rates of sulfate assimilation (Tabe and Droux, 2001). In addition, glutathione is shown to be actively synthesized in developing embryo and funiculus of *Arabidopsis* seeds (Cairns et al., 2006). These results suggest organic sulfur compounds are synthesized from sulfate and transported to seeds.

2.5. Other transport processes

2.5.1. Symbiotic sulfate transporter

Among the four groups of sulfate transporter gene family (Fig. 4.2), the members of group 3 are relatively uncharacterized compared to the functional isoforms in groups 1 and 2, and vacuolar specific isoforms in group 4. As described in the previous section of root-to-shoot transport of sulfate (Section 2.2.3), SULTR3;5 exhibited hardly detectable levels of sulfate transport activities but was essential for enhancing the activity of SULTR2;1 low-affinity sulfate transporter (Kataoka et al., 2004b). A postulated function assigned to the group 3 members (Fig. 4.2) could be the one as being a subsidiary component of the partnering functional isoform. Among this enigmatic group, a *Lotus japonicus* gene homologous to *Arabidopsis SULTR3;5* has been identified to encode a symbiosome membrane-localizing sulfate transporter (Krusell et al., 2005). The gene named *SST1* for symbiotic sulfate transporter was a causal gene of a *L. japonicus* mutant defective in nodule development. The function of SST1 was verified by restoration of the growth of yeast sulfate transporter mutant. The finding of SST1 suggests significance of intracellular transport

of sulfate to symbiosomes where *Rhizobia* proliferate for nitrogen fixation (Krusell et al., 2005).

2.5.2. Transport of sulfate in leaf tissues

The major sites of sulfur metabolism are the photosynthetic organs, namely, the cells in leaf tissues. Following transport of sulfate from root to shoot through xylem, sulfate is unloaded from the xylem and needs to be incorporated to mesophyll cells where it undergoes reduction in chloroplasts to synthesize cysteine (Fig. 4.3). There are several sulfate transporter genes expressed in leaf tissues, but none of them has been verified as functional components for these transport processes. How and what types of transporters actually mediate the uptake of sulfate to mesophyll cells and to chloroplasts remain to be elucidated. As for the uptake of sulfate to chloroplasts, biochemical measurements using isolated chloroplasts suggest the influx of sulfate competes with phosphate and triose-phosphate translocation (Gross et al., 1990). Although it is not clear whether the same transport protein is mediating the activity, the K_m value for sulfate was around 2.5 mM, indicating affinity to sulfate is quite low compared to phosphate and triose-phosphate (Gross et al., 1990). The sulfate uptake system is completely different in bacteria. The bacterial-type sulfate transporter complex is consisted of an extracellular sulfate-binding protein, membranous components, and an ATP-binding cassette protein (Laudenbach and Grossman, 1991; Sirko et al., 1990). This transport system is conserved in *Chlamydomonas reinhardii*, mediating uptake of sulfate to the chloroplast (Lindberg and Melis, 2008). However, orthologous proteins for the bacterial-type sulfate transporter complex have not been identified from higher plant species. Within the leaf tissues, hydathodes express high-affinity sulfate transporter *SULTR1;1* which probably functions for retrieval of sulfate from leaf exudates (Takahashi et al., 2000). *SULTR1;1* was additionally expressed in auxiliary buds. Another high-affinity sulfate transporter *SULTR1;2* was found to be expressed in guard cells (Shibagaki et al., 2002; Yoshimoto et al., 2002), suggesting high demands for sulfur at the plant–environment interface where gas exchange occurs. Acquisition of sulfate can profit for the maintenance of redox potentials. Alternatively, the function of this major sulfate uptake facilitator may modulate stomata movement interfering with other ion transport systems.

2.5.3. Transport of other oxyanions by sulfate transporters

Sulfate transport system is capable of mediating uptake of other oxyanions. Selenate is a toxic analog of sulfate, and is transported by plasmamembrane-bound sulfate transporter. This is indicated by the facts that yeast and *Arabidopsis* mutants defective in sulfate transporter genes tolerate on selenate (Cherest et al., 1997; El Kassis et al., 2007; Shibagaki et al., 2002;

Smith et al., 1995a). Molybdate is another anion that may interfere with the sulfate transport system. It is shown that the high-affinity sulfate transporters SULTR1;2 from *Arabidopsis* and SHST1 from *S. hamata* are able to transport molybdate to yeast cells (Fitzpatrick et al., 2008; Tomatsu et al., 2007). More precisely, the molybdate and sulfate influx activities of SHST1 were linearly concentration dependent when the external supplies of substrates were below 1 μM (Fitzpatrick et al., 2008). In addition, the uptake of molybdate by SHST1 was not inhibited by sulfate, tangstenate, or nitrate, under these conditions. These findings indicate that molybdate can be incorporated equally with sulfate by SHST1 and that transport activities are not inhibited each other when substrate concentrations are at a submicromolar range. By contrast, influx of sulfate at the concentration of 25 μM showing saturable kinetics of transport activities was inhibited by the addition of equal amount of molybdate (Fitzpatrick et al., 2008). These biochemical characteristics may require further verification *in planta*, although the results were indicative of its substrate specificity being more strictly controlled to favor the uptake of sulfate and to avoid unnecessary incorporation of excessive molybdate which rarely occurs under the natural environment.

2.5.4. Molybdate transporter

Genes having low sequence similarities to sulfate transporters have been additionally shown to exhibit molybdate transport activities. These were previously called group 5 members of sulfate transporter gene family (Fig. 4.2), although they were structurally distinct from the isoforms of other groups (Buchner et al., 2004b). They appear to lack sulfate transporter signature and hydrophilic regions in both N- and C-terminal ends. The function of an isoform previously named *SULTR5;2* was identified from an *Arabidopsis* ecotype Landsberg *erecta* which was unable to take up molybdate sufficiently hence having low molybdenum content (Baxter et al., 2008; Tomatsu et al., 2007). The gene was renamed *MOT1* after its specific function in molybdate uptake. MOT1 mediated high-affinity molybdate uptake showing saturable kinetics with an extremely low K_m value ($\sim$20 nM) in yeast cells (Tomatsu et al., 2007). These characteristics in substrate specificity and kinetics were contrasting to what has been reported for SHST1 showing linearity in molybdate uptake (Fitzpatrick et al., 2008). As confirmed genetically, MOT1 is suggested to be a component more specific for the uptake of trace amount of molybdate from the environment. In contrast to genetic and biochemical evidence substantiating MOT1's function in molybdate uptake, its subcellular localization remains unsettled as one indicating presence in plasmamembranes and endomembranes (Tomatsu et al., 2007) while another suggesting association with mitochondria (Baxter et al., 2008). An ortholog of *MOT1* has also been identified from *Chlamydomonas*, suggesting this uptake system is conserved among

photosynthetic eukaryotes (Tejada-Jiménez et al., 2007). Close connection of molybdate utilization in nitrate assimilation was shown by the induction of *MOT1* expression by nitrate but not molybdate availability (Tejada-Jiménez et al., 2007). The regulation derives from the fact that nitrate reductase requires molybdopterin as a cofactor to fulfill its function.

3. Regulation of Sulfate Transport and Metabolism

3.1. Effectors of regulation

3.1.1. Feedback regulation

The availability of sulfur source regulates the transcript levels of sulfate transporters in plant roots. When the supply of sulfate is inadequate, the amounts of cysteine, methionine, and glutathione synthesized through primary sulfur metabolism will decrease, and the negative feedback effects of these sulfur-containing metabolites can be released to increase the efficiency of sulfate uptake. The reversal of which may occur when plants receive excess sulfate from the environment. In fact in many plant species, feeding experiments indicate application of cysteine and glutathione to plants will cause drastic decrease in sulfate uptake activity concomitant with repression of sulfate transporters in roots (Bolchi et al., 1999; Herschbach and Rennenberg, 1991; Smith et al., 1997; Vidmar et al., 1999). In *Arabidopsis*, the high-affinity sulfate transporters *SULTR1;1* and *SULTR1;2* mediating the uptake of sulfate in roots were regulated under this feedback mechanism (Maruyama-Nakashita et al., 2004a,b; Shibagaki et al., 2002; Takahashi et al., 2000; Vidmar et al., 2000; Yoshimoto et al., 2002). Sulfate transporters for internal translocation and remobilization of sulfate pools are also regulated under the same scheme (Kataoka et al., 2004a,b; Takahashi et al., 1997; Vidmar et al., 2000). Particularly, for low-affinity sulfate transporter *SULTR2;1*, a repressive signal from distant organs is suggested to be transported through the phloem (Lappartient and Touraine, 1996; Lappartient et al., 1999). The balance of glutathione and sulfate in the phloem sap is suggested to indicate the sulfur status that controls the rate of sulfate acquisition (Herschbach and Rennenberg, 1991; Herschbach et al., 2000). These observations indicate the feedback regulation may work both systemically and locally to control the requirement of sulfur source. Although it appears that any of the end products of sulfur assimilatory pathways mentioned here, namely cysteine or glutathione, may work as negative effectors in regulating the gene expression, the exact sensing and/or signaling mechanism relevant to these metabolites remains to be investigated.

3.1.2. *O*-Acetylserine is a positive effector

Current understanding indicates *O*-acetylserine (OAS), the precursor of cysteine biosynthesis (Fig. 4.1), is involved in the regulation of sulfate assimilation. Primarily, cysteine biosynthesis is controlled by OAS. The cysteine synthase complex is consisted of two enzymes, serine acetyltransferase and OAS(thiol)lyase, and is tightly controlled by the sulfur status (Berkowitz et al., 2002; Droux et al., 1998; Wirtz and Hell, 2006). The cysteine synthase complex can dissociate in the presence of excess OAS. This mechanism will release free OAS(thiol)lyase to synthesize cysteine, while serine acetyltransferase appears to remain inactive for OAS formation. By contrast, excess sulfide reversibly promotes reassociation of the complex which entirely serves as serine acetyltransferase to synthesize OAS. As OAS (thiol)lyase exists in excess amount (Ruffet et al., 1994), cysteine biosynthesis occurs under a condition where the cysteine synthase complex synthesizes OAS and free OAS(thiol)lyase subsequently converts OAS to cysteine (Wirtz and Hell, 2006). Dissociation of the complex by OAS therefore limits OAS synthesis. In addition to the regulation of the complex, the activity of cytosolic serine acetyltransferase is feedback inhibited by cysteine (Kawashima et al., 2005; Noji et al., 1998). The feedback-sensitive isoform of *Arabidopsis* serine acetyltransferase, *SERAT3;2*, significantly accumulated under sulfur-starved conditions, suggesting its specialized role in synthesizing OAS (Kawashima et al., 2005).

The OAS- and sulfide-dependent dissociation and association mechanisms of the cysteine synthase complex suggest a function of this machinery in substrate sensing that could be implicitly interpreted as sensing of sulfur status. In fact, OAS is known to act as a positive effector inducing the expression of high-affinity sulfate transporters (Maruyama-Nakashita et al., 2004b; Smith et al., 1997). In barley roots, the transcript abundance of *HVST1* sulfate transporter was significantly increased after the application of OAS, which resulted in inducing sulfate uptake activities, nevertheless glutathione and cysteine are abundantly accumulated (Smith et al., 1997). Besides the regulation of sulfate transporters, OAS is shown to induce the expression of other genes responsive to sulfur limitation. The most typical example is adenosine-5′-phosphosulfate (APS) reductase whose mRNA level is enhanced by application of OAS to nitrogen-starved plants (Koprivova et al., 2000). The OAS-mediated positive control mechanism appears to be important for the regulation of this flux-controlling enzyme of sulfate assimilation pathway in addition to the feedback regulation by glutathione (Vauclare et al., 2002). Furthermore, the *Arabidopsis osh1* mutant that accumulates high levels of OAS stimulated the activity of sulfur limitation-responsive promoter of β-conglycinin gene (Ohkama-Ohtsu et al., 2004). Microarray studies additionally indicate gene expression profiles of OAS-fed plants and sulfur-starved plants are similar, showing

significant overlaps (Hirai et al., 2003, 2004; Maruyama-Nakashita et al., 2005; Nikiforova et al., 2003). It is generally accepted that application or overaccumulation of OAS may cause accumulation of the transcripts of sulfur limitation responsive genes. However, how this metabolic intermediate triggers or potentiates the signaling cascade awaits further investigation.

3.1.3. Cytokinin participates in repression of sulfate transporters

Besides the signals of sulfur deficiency, a plant hormone, cytokinin, is known to regulate the expression of sulfate transporters in *Arabidopsis* (Maruyama-Nakashita et al., 2004b). To screen active plant hormone signals that may induce or interfere with the expression of sulfate transporters in *Arabidopsis* roots, plants expressing a *SULTR1;2* promoter–GFP fusion gene were grown in the presence of hormones and the fluorescence of GFP was quantified. Among the plant hormones tested, application of cytokinin to the medium effectively downregulated the expression of GFP under sulfur-limited conditions (Maruyama-Nakashita et al., 2004b). The amounts of *SULTR1;1* and *SULTR1;2* transcripts were downregulated under the same condition, indicating regulation occurs generally for high-affinity sulfate transporters that mediate the uptake of sulfate in roots. The *Arabidopsis cre1* mutant was unable to direct this cytokinin-mediated downregulation (Maruyama-Nakashita et al., 2004b). The regulatory pathway is therefore considered to be under the control of a cytokinin receptor histidine kinase encoded by *CRE1* (Inoue et al., 2001). The current understandings indicate the positive signals from sulfur deficiency and the negative signals from cytokinin-mediated pathway may work in parallel, since cytokinin was regulating the amount of *SULTR1;2* transcripts but not the rates of their responsiveness to sulfur limitation (Maruyama-Nakashita et al., 2004b). Signals specific to the plant sulfur status activate the expression of high-affinity sulfate transporters for the acquisition of sulfur source, while cytokinin functions probably as a more general repressive signal that moderates sulfate uptake. Recent study in collection of expression data from various environments indicates *SULTR1;1* is more strongly regulated by sulfur but *SULTR1;2* shows rather general responses to broader conditions (Rouached et al., 2008). Cytokinin might be defined as one of the general factors regulating both transporters. The negative regulation by cytokinin appears to be similar in phosphorus response (Franco-Zorrilla et al., 2002; Martin et al., 2000). This further suggests the generality of cytokinin-mediated regulatory pathway in controlling nutrient uptake. Besides regulation of sulfate transporters, APS reductase has been reported to be positively controlled by cytokinin (Ohkama et al., 2002). The cytokinin response occurred in parallel with the induction of the activity of sulfur limitation-responsive β-conglycinin promoter (Ohkama et al., 2002). Responses to cytokinin were suggested to

be opposite between sulfate transporter and APS reductase, although both induced by sulfur limitation. As the presence of cytokinin significantly repress the amounts of *SULTR1;1* and *SULTR1;2* sulfate transporters and subsequently reduce sulfate uptake, an alternative interpretation could be that cytokinin was inducing sulfur deficiency and hence the expression of sulfur-responsive genes including APS reductase may have been consequently stimulated.

3.2. Regulatory elements

3.2.1. Sulfur-responsive *cis*-acting element

A *cis*-acting element for the sulfur response is reported for the *Arabidopsis SULTR1;1* sulfate transporter gene (Maruyama-Nakashita et al., 2005). The sulfur-responsive region of *SULTR1;1* existed in the 5′-upstream region between −2777 and −2762 of its coding sequence. This region was named SURE after sulfur-responsive element. SURE was shown to direct the induction of reporter gene expression by sulfur limitation and the repression by cysteine and glutathione (Maruyama-Nakashita et al., 2005). Within this 16 bp sequence of SURE, an auxin response factor (ARF) binding site sequence, GAGACA (Hagen and Guilfoyle, 2002; Ulmasov et al., 1999), was included as a potential binding site. The base substitution experiments for SURE indicated GGAGACA as a core site (Maruyama-Nakashita et al., 2005). Although the transcript level of SULTR1;1 was slightly enhanced on auxin medium, SURE itself was not responsive to auxin. It is suggested that transcriptional activation of *SULTR1;1* may involve an ARF-type transcription factor but has no or limited relevance to auxin response. The SURE-binding protein has not yet been identified. Generality of SURE-mediated regulation in plant sulfur response is suggested from microarray analysis of sulfate deprivation response. Among the genes on the array, numbers of GGAGACA, GAGAC, and their complementary sequences were present in the 5′-regions of sulfur-responsive genes (Maruyama-Nakashita et al., 2005). In addition, similar sequences were found in the 5′-region of *NIT3* nitrilase (Kutz et al., 2002) and β-conglycinin promoter (Awazuhara et al., 2002). However, SURE sequences could not be identified in the 5′-region of *SULTR1;2* (Maruyama-Nakashita et al., 2005). As indicated in functional analysis, SULTR1;2 plays a major role in sulfate uptake under both sulfur-replete and -deficient conditions, while SULTR1;1 is suggested to make more specific contribution to the uptake of limited amounts of sulfate under low-sulfur environments (Shibagaki et al., 2002; Takahashi et al., 2000; Yoshimoto et al., 2002, 2007). Differential regulation of gene expression is also suggested from other expression studies (Rouached et al., 2008).

3.2.2. Regulation of sulfate uptake and metabolism by SLIM1

Until quite recently, elements for transcriptional regulation of sulfate uptake system had not been identified from plants. Genetic screening of sulfur limitation response-less mutants identified a key transcription factor, SLIM1, necessary for the induction of sulfur-responsive genes in sulfate uptake and sulfur metabolisms (Maruyama-Nakashita et al., 2006). The *sulfur limitation1* (*slim1*) mutant was first identified using *SULTR1;2* promoter–GFP as a fluorescent indicator to quantitatively analyze sulfur limitation symptoms. The *in vivo* fluorescence of GFP was increased as the transcript of *SULTR1;2* accumulated in response to low sulfur. The *slim1* mutant was identified by isolating nonfluorescent seedlings on low-sulfur medium. In addition to having defects in expression of *SULTR1;2* sulfate transporter, the *slim1* mutant showed reduced sulfate uptake activity and reduced ability to elongate primary roots under sulfur-limited conditions (Maruyama-Nakashita et al., 2006). The causal gene of *slim1* encoded an EIL-family transcription factor, ETHYLENE-INSENSITIVE3-LIKE3 (EIL3). EIL3 was previously reported as a homolog of ETHYLENE-INSENSITIVE3 (EIN3); however, its function in ethylene response had not been confirmed (Chao et al., 1997; Guo and Ecker, 2004). The finding of SLIM1 revealed its function is related to sulfur response (Maruyama-Nakashita et al., 2006). Transcriptome analysis of *slim1* mutant indicated SLIM1 can function as a global regulator of sulfur metabolic pathways. Metabolic pathways regulated by SLIM1 are indicated in Fig. 4.4. In a bird's-eye view of sulfur metabolic networks, genes whose functions were suggested to be essential for sulfate uptake and internal remobilization of sulfur source were generally induced by SLIM1 under sulfur deficiency, while those related to sulfur utilization in secondary metabolism were regulated oppositely (Maruyama-Nakashita et al., 2006).

As for the expression of sulfate transporters, isoforms that contribute to the enhancement of uptake and internal transport of sulfate under sulfur-limited conditions were regulated positively by SLIM1. A serine acetyltransferase SERAT3;1 (Kawashima et al., 2005) was induced by sulfur limitation and was dependent on SLIM1. In the sulfate reduction pathway, APS reductase genes (*APR*) (Gutierrez-Marcos et al., 1996; Setya et al., 1996) was strongly induced by sulfur limitation, although the induction occurred independent of SLIM1. Regarding the pathways for glucosinolate biosynthesis (Grubb and Abel, 2006; Halkier and Gershenzon, 2006), number of enzymes were controlled by SLIM1 positively on high-sulfur but negatively on low-sulfur conditions, suggesting adjustment of sulfur metabolism occurs under the same transcriptional control mechanism. APS kinase (*APK*), which is an enzyme at the branching point of sulfate reduction pathway, was regulated similarly. This enzyme catalyzes formation of 3′-phosphoadenosine-5′-phosphosulfate for sulfation reactions in secondary

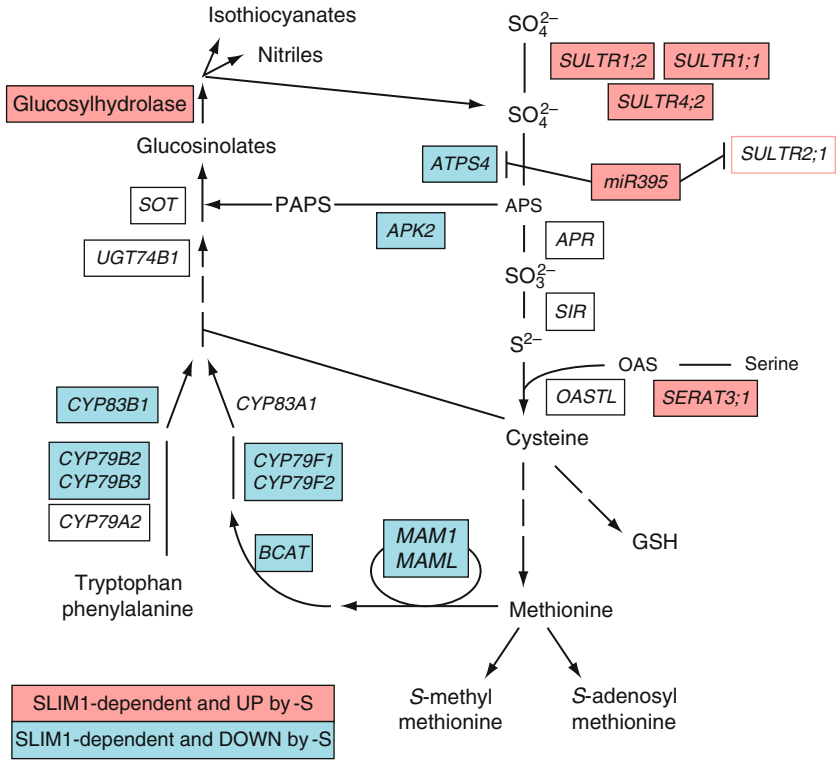

Figure 4.4 SLIM1 controls sulfate uptake and metabolism. SLIM1-dependent genes upregulated by sulfur limitation (pink) or downregulated by sulfur limitation (blue) are highlighted. Lines from miR395 indicate target gene silencing. Abbreviations for genes: *APK*, APS kinase; *APR*, APS reductase; *ATPS*, ATP sulfurylase; *BCAT*, branched-chain amino acid aminotransferase; *CYP*, cytochrome P450; *MAM*, methyl (thio)alkylmalate synthase; *miR395*, microRNA-395; *OASTL*, OAS(thiol)lyase; *SERAT*, serine acetyltransferase; *SIR*, sulfite reductase; *SOT*, desulfoglucosinolate sulfotransferase; *SULTR*, sulfate transporter; *UGT74B1*, UDP-glucose:thiohydroximic acid *S*-glucosyltransferase. Abbreviations for metabolites: APS, adenosine-5′-phosphosulfate; GSH, glutathione; OAS, *O*-acetylserine; PAPS, 3′-phosphoadenosine-5′-phosphosulfate.

sulfur metabolism (Mugford et al., 2009). An isoform of ATP sulfurylase, *ATPS4*, showed the same pattern of expression. ATP sulfurylase mRNA is regulated by microRNA-395 (miR395) as will be mentioned in Section 3.2.3. Reflecting the patterns of gene expression profiles, the *slim1* mutants still accumulated glucosinolates under low-sulfur conditions where the wild-type plants normally reduce the cost of using sulfur for secondary metabolites (Maruyama-Nakashita et al., 2006). More specifically, for the regulation of glucosinolate pathways, DOF and MYB

transcription factors are known to directly stimulate the expression of biosynthetic enzymes (Celenza et al., 2005; Gigolashvili et al., 2007a,b; Hirai et al., 2007; Skirycz et al., 2006). However, the expression of these transcription factors was not significantly modulated by SLIM1. These observations suggest SLIM1 controls sulfate uptake and internal use of sulfur source in secondary metabolism, but its function is different from the direct regulators of the glucosinolate pathways.

3.2.3. microRNA-395

microRNAs are noncoding short RNAs transcribed in general from intergenic regions as precursor forms containing a double-stranded hairpin structure within the molecules (Jones-Rhoades et al., 2006). Processing of the precursor forms generate 21 nucleotide mature microRNAs that are incorporated to RNA-induced silencing complex and hybridize to their specific target mRNAs having complementary sequences. The target mRNAs will be cleaved in the silencing complex and degraded. Among the plant microRNAs reported to present, miR395 is specific for its accumulation under low-sulfur conditions. miR395 has a complementary sequence that can hybridize with low-affinity sulfate transporter *SULTR2;1* and three isoforms of ATP sulfurylase, *ATPS1, ATPS3*, and *ATPS4* (Allen et al., 2005; Jones-Rhoades and Bartel, 2004; Kawashima et al., 2009). More recently, the analysis of *slim1* mutant indicated that the accumulation of miR395 was dependent on SLIM1's function (Kawashima et al., 2009) (Fig. 4.4). Downregulation of *ATPS4* mRNA under sulfur deficiency is suggested to be under this regulatory cascade. The same applies for suppression of *SULTR2;1* mRNA in the shoots of sulfur-starved plant seedlings. However, suppression of *ATPS1* and *ATPS3* by sulfur deficiency was not significant, and more strikingly the *SULTR2;1* mRNA was induced by sulfur limitation in the roots. These discrepancies would raise possibilities that the regulation of *ATPS1*, *ATPS3*, and *SULTR2;1* might involve additional mechanisms that override or interfere with the miR395-meidated regulation.

At least for *SULTR2;1*, an additional regulatory mechanism may dominate over the miR395-meidated regulation in roots to achieve abundant expression of this sulfate transporter in pericycle and xylem parenchyma cells (Takahashi et al., 1997, 2000). As mentioned in Section 2.2.2, the function of SULTR2;1 in roots is suggested to control transfer of sulfate to shoots, possibly by preventing the loss of sulfate from xylem parenchyma cells attached to xylems in the root central cylinder (Fig. 4.3). On the other hand, in leaves, downregulation of *SULTR2;1* in parenchyma cells of xylem and phloem may become necessary under low-sulfur conditions to prevent retrieval of apoplastic sulfate to xylem and to make sulfate more efficiently distributed toward mesophyll cells (Fig. 4.3) (Takahashi et al., 2000). Therefore, it sounds reasonable to have miR395-meidated negative

control mechanism to work dominantly in shoots, but not in roots. How the balance of positive and negative mechanisms is controlled between the root and shoot vascular tissues remains as an open question. In addition, miR395 was expressed in phloem companion cells (Kawashima et al., 2009), while its target gene *SULTR2;1* was predominantly expressed in the parenchyma cells (Takahashi et al., 2000). Movement of miR395 from companion cells to surrounding parenchyma cells or to more distant organs via phloem can be suggested to explain apparent disconnection with the target gene expression sites.

4. Concluding Remarks

Plants have highly organized systems to efficiently utilize the sulfur source in the environment. Sulfate is the form of sulfur which stably exists in the environment. As highlighted in this chapter, incorporation and distribution of sulfate will occur across the membrane barriers of numbers of cell types and organs. A set of sulfate transporters are present in the plant genome, and the individual protein components are assigned to have specific functions. The physiological roles of each sulfate transporters are substantiated by their biochemical properties, cell type-specific expression, and regulation by requirement of sulfur. Responding to the environmental sulfur condition or internal sulfur status, sulfate transport system is controlled both locally and at the whole plant level. It is important to note that the regulatory elements organize the complex transport system to balance the uptake, storage, and assimilation of sulfate in plants. Transcriptional regulation of sulfate transport system is not entirely elucidated, although SLIM1 was suggested as a key regulator. Besides the negative control of sulfate transporter and ATP sulfurylase by miR395, regulatory cascades downstream of SLIM1 need further investigation. Current understanding additionally indicates existence of SLIM1-independent pathway(s) in the regulation. For sulfate reduction, the regulatory pathways are not always identical with those controlling sulfate transporters. Regulations of ATP sulfurylase and sulfate transporter are only partially overlapped under SLIM1 and miR395. APS reductase apparently shows similar responses to sulfur as demonstrated for sulfate transporters; however, its regulation was independent of SLIM1. These lines of evidence indicate complexity of the regulatory pathways, although some are shared among the essential entry steps of sulfur assimilation. The remaining open questions would be how and where sulfate or sulfur-containing compounds are sensed to trigger the regulatory pathways in the cells. Findings of sensory machinery would require further genetic, genomic, and biochemical studies that complement current understandings of the regulatory mechanisms.

ACKNOWLEDGMENTS

The author thanks his colleagues and collaborators for providing excellent results and ideas to create the concept of this review chapter. The research projects have been partly supported by RIKEN Plant Science Center and by the grant supports from the Ministry of Education, Culture, Sports, Science and Technology of Japan, and Bio-oriented Technology Research Advancement Institution of Japan.

REFERENCES

Allen, E., Xie, Z., Gustafson, A.M., Carrington, J.C., 2005. microRNA-directed phasing during trans-acting siRNA biogenesis in plants. Cell 121, 207–221.

Aravind, L., Koonin, E.V., 2000. The STAS domain—a link between anion transporters and antisigma-factor antagonists. Curr. Biol. 10, R53–R55.

Awazuhara, M., Kim, H., Goto, D.B., Matsu, A., Hayashi, H., Chino, M., et al., 2002. A 235-bp region from a nutritionally regulated soybean seed-specific gene promoter can confer its sulfur and nitrogen response to a constitutive promoter in aerial tissues of *Arabidopsis thaliana*. Plant Sci. 163, 75–82.

Awazuhara, M., Fujiwara, T., Hayashi, H., Watanabe-Takahashi, A., Takahashi, H., Saito, K., 2005. The function of SULTR2;1 sulfate transporter during seed development in *Arabidopsis thaliana*. Physiol. Plant. 125, 95–105.

Barberon, M., Berthomieu, P., Clairotte, M., Shibagaki, N., Davidian, J.-C., Gosti, F., 2008. Unequal functional redundancy between the two *Arabidopsis thaliana* high-affinity sulphate transporters *SULTR1;1* and *SULTR1;2*. New Phytol. 180, 608–619.

Baxter, I., Muthukumar, B., Park, H.C., Buchner, P., Lahner, B., Danku, J., et al., 2008. Variation in molybdenum content across broadly distributed populations of *Arabidopsis thaliana* is controlled by a mitochondrial molybdenum transporter (MOT1). PLoS Genet. 4, e1000004.

Benning, C., 1998. Biosynthesis and function of the sulfolipid sulfoquinovosyl diacylglycerol. Annu. Rev. Plant Physiol. Plant Mol. Biol. 49, 53–75.

Berkowitz, O., Wirtz, M., Wolf, A., Kuhlmann, J., Hell, R., 2002. Use of biomolecular interaction analysis to elucidate the regulatory mechanism of the cysteine synthase complex from *Arabidopsis thaliana*. J. Biol. Chem. 277, 30629–30634.

Bianchini, F., Vainio, H., 2001. Allium vegetables and organosulfur compounds: do they help prevent cancer? Environ. Health Perspect. 109, 893–902.

Bolchi, A., Petrucco, S., Tenca, P.L., Foroni, C., Ottonello, S., 1999. Coordinate modulation of maize sulfate permease and ATP sulfurylase mRNAs in response to variations in sulfur nutritional status: stereospecific down-regulation by L-cysteine. Plant Mol. Biol. 39, 527–537.

Bourgis, F., Roje, S., Nuccio, M.L., Fisher, D.B., Tarczynski, M.C., Li, C., et al., 1999. *S*-Methylmethionine plays a major role in phloem sulfur transport and is synthesized by a novel type of methyltransferase. Plant Cell 11, 1485–1498.

Buchanan, B.B., Balmer, Y., 2005. Redox regulation: a broadening horizon. Annu. Rev. Plant Biol. 56, 187–220.

Buchner, P., Stuiver, C.E., Westerman, S., Wirtz, M., Hell, R., Hawkesford, M.J., et al., 2004a. Regulation of sulfate uptake and expression of sulfate transporter genes in *Brassica oleracea* as affected by atmospheric H_2S and pedospheric sulfate nutrition. Plant Physiol. 136, 3396–3408.

Buchner, P., Takahashi, H., Hawkesford, M.J., 2004b. Plant sulphate transporters: co-ordination of uptake, intracellular and long-distance transport. J. Exp. Bot. 55, 1765–1773.

Cairns, N.G., Pasternak, M., Wachter, A., Cobbett, C.S., Meyer, A.J., 2006. Maturation of *Arabidopsis* seeds is dependent on glutathione biosynthesis within the embryo. Plant Physiol. 141, 446–455.

Celenza, J.L., Quiel, J.A., Smolen, G.A., Merrikh, H., Silvestro, A.R., Normanly, J., et al., 2005. The *Arabidopsis* ATR1 Myb transcription factor controls indolic glucosinolate homeostasis. Plant Physiol. 137, 253–262.

Chao, Q., Rothenberg, M., Solano, R., Roman, G., Terzaghi, W., Ecker, J.R., 1997. Activation of the ethylene gas response pathway in *Arabidopsis* by the nuclear protein ETHYLENE-INSENSITIVE3 and related proteins. Cell 89, 1133–1144.

Cherest, H., Davidian, J.-C., Thomas, D., Benes, V., Ansorge, W., Surdin-Kerjan, Y., 1997. Molecular characterization of two high affinity sulfate transporters in *Saccharomyces cerevisiae*. Genetics 145, 627–635.

Clarkson, D.T., Smith, F.W., Vanden Berg, P.J., 1983. Regulation of sulfate transport in a tropical legume, *Macroptilium atropurpureum* cv. Siratro. J. Exp. Bot. 34, 1463–1483.

Crawford, N.M., Kahn, M.L., Leustek, T., Long, S.R., 2000. Nitrogen and sulfur. In: Buchanan, B.B., Gruissem, W., Jones, R.L. (Eds.), Biochemistry & Molecular Biology of Plants. American Society of Plant Biologists, Rockville, MD, pp. 824–849.

Deane-Drummond, C.E., 1987. The regulation of sulfate uptake following growth of *Pisum sativum* L. seedlings in S nutrient limiting conditions. Interaction between nitrate and sulphate transport. Plant Sci. 50, 27–35.

Droux, M., Ruffet, M.L., Douce, R., Job, D., 1998. Interactions between serine acetyltransferase and *O*-acetylserine (thiol) lyase in higher plants—structural and kinetic properties of the free and bound enzymes. Eur. J. Biochem. 255, 235–245.

Dubousset, L., Abdallah, M., Desfeux, A.S., Etienne, P., Meuriot, F., Hawkesford, M.J., et al., 2009. Remobilization of leaf S compounds and senescence in response to restricted sulphate supply during the vegetative stage of oilseed rape are affected by mineral N availability. J. Exp. Bot. 60, 3239–3253.

El Kassis, E., Cathala, N., Rouached, H., Fourcroy, P., Berthomieu, P., Terry, N., et al., 2007. Characterization of a selenate-resistant *Arabidopsis* mutant. Root growth as a potential target for selenate toxicity. Plant Physiol. 143, 1231–1241.

Fisher, R.F., Long, S.R., 1992. *Rhizobium*-plant signal exchange. Nature 357, 655–660.

Fitzpatrick, K.L., Tyerman, S.D., Kaiser, B.N., 2008. Molybdate transport through the plant sulfate transporter SHST1. FEBS Lett. 582, 1508–1513.

Franco-Zorrilla, J.M., Martin, A.C., Solano, R., Rubio, V., Leyva, A., Paz-Ares, J., 2002. Mutations at *CRE1* impair cytokinin-induced repression of phosphate starvation responses in *Arabidopsis*. Plant J. 32, 353–360.

Gigolashvili, T., Berger, B., Mock, H.P., Müller, C., Weisshaar, B., Flügge, U.I., 2007a. The transcription factor HIG1/MYB51 regulates indolic glucosinolate biosynthesis in *Arabidopsis thaliana*. Plant J. 50, 886–901.

Gigolashvili, T., Yatusevich, R., Berger, B., Müller, C., Flügge, U.I., 2007b. The R2R3-MYB transcription factor HAG1/MYB28 is a regulator of methionine-derived glucosinolate biosynthesis in *Arabidopsis thaliana*. Plant J. 51, 247–261.

Gross, A., Brückner, G., Heldt, H.W., Flügge, U.-I., 1990. Comparison of the kinetic properties, inhibition and labelling of the phosphate translocators from maize and spinach mesophyll chloroplasts. Planta 180, 262–271.

Grubb, C., Abel, S., 2006. Glucosinolate metabolism and its control. Trends Plant Sci. 11, 89–100.

Guo, H., Ecker, J.R., 2004. The ethylene signaling pathway: new insights. Curr. Opin. Plant Biol. 7, 40–49.

Gutierrez-Marcos, J.F., Roberts, M.A., Campbell, E.J., Wray, J.L., 1996. Three members of a novel small gene-familiy from *Arabidopsis thaliana* able to complement functionally an *Escherichia coli* mutant defective in PAPS reductase activity encode proteins with a thioredoxin-like domain and "APS reductase" activity. Proc. Natl. Acad. Sci. USA 93, 13377–13382.

Hagen, G., Guilfoyle, T.J., 2002. Auxin-responsive gene expression, genes, promoters and regulatory factors. Plant Mol. Biol. 49, 373–385.

Halkier, B.A., Gershenzon, J., 2006. Biology and biochemistry of glucosinolates. Annu. Rev. Plant Biol. 57, 303–333.

Hawkesford, M.J., Davidian, J.-C., Grignon, C., 1993. Sulphate/proton cotransport in plasma-membrane vescicles isolated from roots of *Brassica napus* L.: increased transport in membranes isolated from sulphur-starved plants. Planta 190, 297–304.

Herschbach, C., Rennenberg, H., 1991. Influence of glutathione (GSH) on sulfate influx, xylem loading and exudation in excised tobacco roots. J. Exp. Bot. 42, 1021–1029.

Herschbach, C., van Der Zalm, E., Schneider, A., Jouanin, L., De Kok, L.J., Rennenberg, H., 2000. Regulation of sulfur nutrition in wild-type and transgenic poplar over-expressing γ-glutamylcysteine synthetase in the cytosol as affected by atmospheric H_2S. Plant Physiol. 124, 461–473.

Hirai, M.Y., Fujiwara, T., Chino, M., Naito, S., 1995. Effects of sulfate concentrations on the expression of a soybean seed storage protein gene and its reversibility in transgenic *Arabidopsis thaliana*. Plant Cell Physiol. 36, 1331–1339.

Hirai, M.Y., Fujiwara, T., Awazuhara, M., Kimura, T., Noji, M., Saito, K., 2003. Global expression profiling of sulfur-starved *Arabidopsis* by DNA macroarray reveals the role of *O*-acetyl-L-serine as a general regulator of gene expression in response to sulfur nutrition. Plant J. 33, 651–663.

Hirai, M.Y., Yano, M., Goodenowe, D.B., Kanaya, S., Kimura, T., Awazuhara, M., et al., 2004. Integration of transcriptomics and metabolomics for understanding of global responses to nutritional stresses in *Arabidopsis thaliana*. Proc. Natl. Acad. Sci. USA 101, 10205–10210.

Hirai, M.Y., Sugiyama, K., Sawada, Y., Tohge, T., Obayashi, T., Suzuki, A., et al., 2007. Omics-based identification of *Arabidopsis* Myb transcription factors regulating aliphatic glucosinolate biosynthesis. Proc. Natl. Acad. Sci. USA 104, 6478–6483.

Hopkins, L., Parmar, S., Blaszczyk, A., Hesse, H., Hoefgen, R., Hawkesford, M.J., 2005. *O*-Acetylserine and the regulation of expression of genes encoding components for sulfate uptake and assimilation in potato. Plant Physiol. 138, 433–440.

Howarth, J.R., Fourcroy, P., Davidian, J.-C., Smith, F.W., Hawkesford, M.J., 2003. Cloning of two contrasting high-affinity sulphate transporters from tomato induced by low sulphate and infection by the vascular pathogen *Verticillium dahlia*. Planta 218, 58–64.

Inoue, T., Higuchi, M., Hashimoto, Y., Seki, M., Kobayashi, M., Kato, T., et al., 2001. Identification of CRE1 as a cytokinin receptor from *Arabidopsis*. Nature 409, 1060–1063.

Jones, M.G., Hughes, J., Tregova, A., Milne, J., Tomsett, A.B., Collin, H.A., 2004. Biosynthesis of the flavour precursors of onion and garlic. J. Exp. Bot. 55, 1903–1918.

Jones-Rhoades, M.W., Bartel, D.P., 2004. Computational identification of plant micro-RNAs and their targets, including a stress-induced miRNA. Mol. Cell 14, 787–799.

Jones-Rhoades, M.W., Bartel, D.P., Bartel, B., 2006. MicroRNAs and their regulatory roles in plants. Annu. Rev. Plant Biol. 57, 19–53.

Kaiser, G., Martinoia, E., Schroppelmeier, G., Heber, U., 1989. Active-transport of sulfate into the vacuole of plant-cells provides halotolerance and can detoxify SO_2. J. Plant Physiol. 133, 756–763.

Kataoka, T., Watanabe-Takahashi, A., Hayashi, N., Ohnishi, M., Mimura, T., Buchner, P., et al., 2004a. Vacuolar sulfate transporters are essential determinants controlling internal distribution of sulfate in *Arabidopsis*. Plant Cell 16, 2693–2704.

Kataoka, T., Hayashi, N., Yamaya, T., Takahashi, H., 2004b. Root-to-shoot transport of sulfate in *Arabidopsis*: evidence for the role of SULTR3;5 as a component of low-affinity sulfate transport system in the root vasculature. Plant Physiol. 136, 4198–4204.

Kawashima, C.G., Berkowitz, O., Hell, R., Noji, M., Saito, K., 2005. Characterization and expression analysis of a serine acetyltransferase gene family involved in a key step of the sulfur assimilation pathway in *Arabidopsis*. Plant Physiol. 137, 220–230.

Kawashima, C.G., Yoshimoto, N., Maruyama-Nakashita, A., Tsuchiya, Y.N., Saito, K., Takahashi, H., et al., 2009. Sulphur starvation induces the expression of microRNA-395 and one of its target genes but in different cell types. Plant J. 57, 313–321.

Ketter, J.S., Jarai, G., Fu, Y.H., Marzluf, G.A., 1991. Nucleotide sequence, messenger RNA stability, and DNA recognition elements of *cys*-14, the structural gene for sulfate permease II in *Neurospora crassa*. Biochemistry 30, 1780–1787.

Koprivova, A., Suter, M., Op den Camp, R., Brunold, C., Kopriva, S., 2000. Regulation of sulfur assimilation by nitrogen in *Arabidopsis*. Plant Physiol. 122, 737–746.

Krusell, L., Krause, K., Ott, T., Desbrosses, G., Krämer, U., Sato, S., et al., 2005. The sulfate transporter SST1 is crucial for symbiotic nitrogen fixation in *Lotus japonicus* root nodules. Plant Cell 17, 1625–1636.

Kutz, A., Müller, A., Hennig, P., Kaiser, W.M., Piotrowski, M., Weiler, E.W., 2002. A role for nitrilase 3 in the regulation of root morphology in sulphur-starving *Arabidopsis thaliana*. Plant J. 30, 95–106.

Kuzuhara, Y., Isobe, A., Awazuhara, M., Fujiwara, T., Hayashi, H., 2000. Glutathione levels in phloem sap of rice plants under sulfur deficient conditions. Soil Sci. Plant Nutr. 46, 265–270.

Lappartient, A.G., Touraine, B., 1996. Demand-driven control of root ATP sulfurylase activity and SO_4^{2-} uptake in intact canola. The role of phloem-translocated glutathione. Plant Physiol. 111, 147–157.

Lappartient, A.G., Vidmar, J.J., Leustek, T., Glass, A.D.M., Touraine, B., 1999. Inetr-organ signaling in plants: regulation of ATP sulfurylase and sulfate transporter genes expression in roots mediated by phloem-translocated compound. Plant J. 18, 89–95.

Lass, B., Ullrich-Eberius, C.L., 1984. Evidence for proton/sulfate cotransport and its kinetics in *Lemna gibba* G1. Planta 161, 53–60.

Laudenbach, D.E., Grossman, A.R., 1991. Characterization and mutagenesis of sulfur-regulated genes in a cyanobacterium: evidence for function in sulfate transport. J. Bacteriol. 173, 2739–2750.

Leggett, J.E., Epstein, E., 1956. Kinetics of sulfate absorption by barley roots. Plant Physiol. 31, 222–226.

Leustek, T., Martin, M.N., Bick, J.A., Davies, J.P., 2000. Pathways and regulation of sulfur metabolism revealed through molecular and genetic studies. Annu. Rev. Plant Physiol. Plant Mol. Biol. 51, 141–165.

Lindberg, P., Melis, A., 2008. The chloroplast sulfate transport system in the green alga *Chlamydomonas reinhardtii*. Planta 228, 951–961.

Martin, A.C., del Pozo, J.C., Iglesias, J., Rubio, V., Solano, R., de la Pena, A., et al., 2000. Influence of cytokinins on the expression of phosphate starvation responsive genes in *Arabidopsis*. Plant J. 24, 559–567.

Martinoia, E., Massonneau, A., Frangne, N., 2000. Transport processes of solutes across the vacuolar membrane of higher plants. Plant Cell Physiol. 41, 1175–1186.

Martinoia, E., Maeshima, M., Neuhaus, H.E., 2007. Vacuolar transporters and their essential role in plant metabolism. J. Exp. Bot. 58, 83–102.

Maruyama-Nakashita, A., Inoue, E., Watanabe-Takahashi, A., Yamaya, T., Takahashi, H., 2003. Transcriptome profiling of sulfur-responsive genes in *Arabidopsis* reveals global effect on sulfur nutrition on multiple metabolic pathways. Plant Physiol. 132, 597–605.

Maruyama-Nakashita, A., Nakamura, Y., Watanabe-Takahashi, A., Yamaya, T., Takahashi, H., 2004a. Induction of SULTR1;1 sulfate transporter in *Arabidopsis* roots involves protein phosphorylation/dephosphorylation circuit for transcriptional regulation. Plant Cell Physiol. 45, 340–345.

Maruyama-Nakashita, A., Nakamura, Y., Yamaya, T., Takahashi, H., 2004b. A novel regulatory pathway of sulfate uptake in *Arabidopsis* roots: implication of CRE1/WOL/AHK4-mediated cytokinin-dependent regulation. Plant J. 38, 779–789.

Maruyama-Nakashita, A., Nakamura, Y., Watanabe-Takahashi, A., Inoue, E., Yamaya, T., Takahashi, H., 2005. Identification of a novel *cis*-acting element conferring sulfur deficiency response in *Arabidopsis* roots. Plant J. 42, 305–314.

Maruyama-Nakashita, A., Nakamura, Y., Tohge, T., Saito, K., Takahashi, H., 2006. *Arabidopsis* SLIM1 is a central transcriptional regulator of plant sulfur response and metabolism. Plant Cell 18, 3235–3251.

Mount, D.B., Romero, M.F., 2004. The SLC26 gene family of multifunctional anion exchangers. Pflugers Arch. 447, 710–721.

Mugford, S.G., Yoshimoto, N., Reichelt, M., Wirtz, M., Hill, L., Mugford, S.T., et al., 2009. Disruption of adenosine-5′-phosphosulfate kinase in *Arabidopsis* reduces levels of sulfated secondary metabolites. Plant Cell 21, 910–927.

Nikiforova, V., Freitag, J., Kempa, S., Adamik, M., Hesse, H., Hoefgen, R., 2003. Transcriptome analysis of sulfur depletion in *Arabidopsis thaliana*: interlacing of biosynthetic pathways provides response specificity. Plant J. 33, 633–650.

Noji, M., Inoue, K., Kimura, N., Gouda, A., Saito, K., 1998. Isoform-dependent differences in feedback regulation and subcellular localization of serine acetyltransferase involved in cysteine biosynthesis from *Arabidopsis thaliana*. J. Biol. Chem. 273, 32739–32745.

Ohkama, N., Takei, K., Sakakibara, H., Hayashi, H., Yoneyama, T., Fujiwara, T., 2002. Regulation of sulfur-responsive gene expression by exogenously applied cytokinins in *Arabidopsis thaliana*. Plant Cell Physiol. 43, 1493–1501.

Ohkama-Ohtsu, N., Kasajima, I., Fujiwara, T., Naito, S., 2004. Isolation and characterization of an *Arabidopsis* mutant that overaccumulates *O*-acetyl-L-Ser. Plant Physiol. 136, 3209–3222.

Page, R.D.M., 1996. TREEVIEW: an application to display phylogenetic trees on personal computers. Comput. Appl. Biosci. 12, 357–358.

Rae, A.L., Smith, F.W., 2002. Localisation of expression of a high-affinity sulfate transporter in barley roots. Planta 215, 565–568.

Rouached, H., Berthomieu, P., El Kassis, E., Cathala, N., Catherinot, V., Labesse, G., et al., 2005. Structural and functional analysis of the C-terminal STAS (sulfate transporter and anti-sigma antagonist) domain of the *Arabidopsis thaliana* sulfate transporter SULTR1.2. J. Biol. Chem. 280, 15976–15983.

Rouached, H., Wirtz, M., Alary, R., Hell, R., Arpat, A.B., Davidian, J.-C., et al., 2008. Differential regulation of the expression of two high-affinity sulfate transporters, SULTR1.1 and SULTR1.2, in *Arabidopsis*. Plant Physiol. 147, 897–911.

Ruffet, M.L., Droux, M., Douce, R., 1994. Purification and kinetic properties of serine acetyltransferase free of *O*-acetylserine(thiol)lyase from spinach chloroplasts. Plant Physiol. 104, 597–604.

Saito, K., 2000. Regulation of sulfate transport and synthesis of sulfur-containing amino acids. Curr. Opin. Plant Biol. 3, 188–195.

Saito, K., 2004. Sulfur assimilatory metabolism. The long and smelling road. Plant Physiol. 136, 2443–2450.

Saitou, N., Nei, M., 1987. The neighbor-joining method: a new method for reconstructing phylogenetic trees. Mol. Biol. Evol. 4, 406–425.

Setya, A., Murillo, M., Leustek, T., 1996. Sulfate reduction in higher plants: molecular evidence for a novel 5′-adenylylsulfate reductase. Proc. Natl. Acad. Sci. USA 93, 13383–13388.

Shibagaki, N., Grossman, A.R., 2004. Probing the function of STAS domains of the *Arabidopsis* sulfate transporters. J. Biol. Chem. 279, 30791–30799.

Shibagaki, N., Grossman, A.R., 2006. The role of the STAS domain in the function and biogenesis of a sulfate transporter as probed by random mutagenesis. J. Biol. Chem. 281, 22964–22973.

Shibagaki, N., Rose, A., Mcdermott, J.P., Fujiwara, T., Hayashi, H., Yoneyama, T., et al., 2002. Selenate-resistant mutants of *Arabidopsis thaliana* identify SULTR1;2, a sulfate transporter required for efficient transport of sulfate into roots. Plant J. 29, 475–486.

Sirko, A., Hryniewicz, M., Hulanicka, D., Böck, A., 1990. Sulfate and thiosulfate transport in *Escherichia coli* K-12: nucleotide sequence and expression of the *cysTWAM* gene cluster. J. Bacteriol. 172, 3351–3357.

Skirycz, A., Reichelt, M., Burow, M., Birkemeyer, C., Rolcik, J., Kopka, J., et al., 2006. DOF transcription factor AtDof1.1 (OBP2) is part of a regulatory network controlling glucosinolate biosynthesis in *Arabidopsis*. Plant J. 47, 10–24.

Smith, F.W., Hawkesford, M.J., Prosser, I.M., Clarkson, D.T., 1995a. Isolation of a cDNA from *Saccharomyces cerevisiae* that encodes a high affinity sulphate transporter at the plasma membrane. Mol. Gen. Genet. 247, 709–715.

Smith, F.W., Ealing, P.M., Hawkesford, M.J., Clarkson, D.T., 1995b. Plant members of a family of sulfate transporters reveal functional subtypes. Proc. Natl. Acad. Sci. USA 92, 9373–9377.

Smith, F.W., Hawkesford, M.J., Ealing, P.M., Clarkson, D.T., Vanden Berg, P.J., Belcher, A.R., et al., 1997. Regulation of expression of a cDNA from barley roots encoding a high affinity sulfate transporter. Plant J. 12, 875–884.

Tabe, L.M., Droux, M., 2001. Sulfur assimilation in developing lupin cotyledons could contribute significantly to the accumulation of organic sulfur reserves in the seed. Plant Physiol. 126, 176–187.

Takahashi, H., Yamazaki, M., Sasakura, N., Watanabe, A., Leustek, T., de Almeida Engler, J., et al., 1997. Regulation of sulfur assimilation in higher plants: a sulfate transporter induced in sulfate starved roots plays a central role in *Arabidopsis thaliana*. Proc. Natl. Acad. Sci. USA 94, 11102–11107.

Takahashi, H., Watanabe-Takahashi, A., Smith, F.W., Blake-Kalff, M., Hawkesford, M.J., Saito, K., 2000. The role of three functional sulfate transporters involved in uptake and translocation of sulfate in *Arabidopsis thaliana*. Plant J. 23, 171–182.

Takahashi, H., Yoshimoto, N., Saito, K., 2006. Anionic nutrient transport in plants: the molecular bases of sulfate transporter gene family. In: Setlow, J.K. (Ed.), Genetic Engineering, Vol. 27. Springer, New York, NY, pp. 67–80.

Talalay, P., Fahey, J.W., 2001. Phytochemicals from cruciferous plants protect against cancer by modulating carcinogen metabolism. J. Nutr. 131, 3027S–3033S.

Tejada-Jiménez, M., Llamas, A., Sanz-Luque, E., Galván, A., Fernández, E., 2007. A high-affinity molybdate transporter in eukaryotes. Proc. Natl. Acad. Sci. USA 104, 20126–20130.

Thompson, J.D., Higgins, D.G., Gibson, T.J., 1994. CLUSTAL W: improving the sensitivity of progressive multiple sequence alignment through sequence weighting, position-specific gap penalties and weight matrix choice. Nucleic Acids Res. 22, 4673–4680.

Tomatsu, H., Takano, J., Takahashi, H., Watanabe-Takahashi, A., Shibagaki, N., Fujiwara, T., 2007. An *Arabidopsis thaliana* high-affinity molybdate transporter required for efficient uptake of molybdate from soil. Proc. Natl. Acad. Sci. USA 104, 18807–18812.

Ulmasov, T., Hagen, G., Guilfoyle, T.J., 1999. Dimerization and DNA binding of auxin response factors. Plant J. 19, 309–319.

Vauclare, P., Kopriva, S., Fell, D., Suter, M., Sticher, L., von Ballmoos, P., et al., 2002. Flux control of sulphate assimilation in *Arabidopsis thaliana*: adenosine 5′-phosphosulphate reductase is more susceptible than ATP sulphurylase to negative control by thiols. Plant J. 31, 729–740.

Vidmar, J.J., Schjoerring, J.K., Touraine, B., Glass, A.D.M., 1999. Regulation of the *hvst1* gene encoding a high-affinity sulfate transporter from *Hordeum vulgare*. Plant Mol. Biol. 40, 883–892.

Vidmar, J.J., Tagmount, A., Cathala, N., Touraine, B., Davidian, J.-C.E., 2000. Cloning and characterization of a root specific high-affinity sulfate transporter from *Arabidopsis thaliana*. FEBS Lett. 475, 65–69.

Wirtz, M., Hell, R., 2006. Functional analysis of the cysteine synthase protein complex from plants: structural, biochemical and regulatory properties. J. Plant Physiol. 163, 273–286.

Yoshimoto, N., Takahashi, H., Smith, F.W., Yamaya, T., Saito, K., 2002. Two distinct high-affinity sulfate transporters with different inducibilities mediate uptake of sulfate in *Arabidopsis* roots. Plant J. 29, 465–473.

Yoshimoto, N., Inoue, E., Saito, K., Yamaya, T., Takahashi, H., 2003. Phloem-localizing sulfate transporter, Sultr1;3, mediates re-distribution of sulfur from source to sink organs in *Arabidopsis*. Plant Physiol. 131, 1511–1517.

Yoshimoto, N., Inoue, E., Watanabe-Takahashi, A., Saito, K., Takahashi, H., 2007. Posttranscriptional regulation of high-affinity sulphate transporters in *Arabidopsis* by sulphur nutrition. Plant Physiol. 145, 378–388.

This page intentionally left blank

CHAPTER FIVE

Metabolic Pathways in the Apicoplast of Apicomplexa

Frank Seeber[*,†] *and* Dominique Soldati-Favre[‡]

Contents

1. Introduction 162
2. Morphology, Acquisition, and Evolutionary Origin of the Apicoplast 164
3. Genome, Proteome, and Protein Trafficking 165
4. Potential and Limitations of *In Silico* Predictions of Metabolic Pathways 168
5. Biosynthesis of Various Metabolites and Factors 170
   5.1. Isoprenoids 170
   5.2. Abscisic acid 188
   5.3. Fatty acids 190
   5.4. Lipoic acid 194
   5.5. Iron–sulfur clusters 197
   5.6. Heme 203
6. Apicoplast Metabolic Pathways as Drug Targets and the Phenomenon of Delayed Death 208
7. Conclusions 210
Acknowledgments 211
References 211

Abstract

Intracellular parasites of the phylum Apicomplexa harbor a plastid-like organelle called apicoplast that is the most reduced organelle of this type known. Due to the medical importance of some members of Apicomplexa, a number of fully sequenced genomes are available that have allowed to assemble metabolic pathways also from the apicoplast and have revealed initial clues to its essential nature for parasite survival in the host. We provide a compilation of Internet resources useful to access, reconstruct, verify, or annotate metabolic pathways. Then we show detailed and updated metabolic maps and discuss the three major biosynthetic pathways leading to the generation of isoprenoids, fatty acids, and

* Robert-Koch-Institut, Berlin, Germany
† FB Biologie/Parasitologie, Philipps-Universität Marburg, Marburg, Germany
‡ Department of Microbiology and Molecular Medicine, CMU, University of Geneva, Geneva, Switzerland

International Review of Cell and Molecular Biology, Volume 281
ISSN 1937-6448, DOI: 10.1016/S1937-6448(10)81005-6

heme, and compare these routes in the different species. Moreover, several auxiliary pathways, like iron–sulfur cluster assembly, are covered and put into context with the major metabolic routes. Finally, we highlight some aspects that emerged from recent publications and were not discussed previously with regard to Apicomplexa.

Key Words: Apicomplexa, Apicoplast, *Toxoplasma*, *Plasmodium*, Metabolism.

1. Introduction

The phylum Apicomplexa encompasses more than 5000 species (Levine, 1988), some of them being of considerable medical and economic importance, like *Plasmodium* sp., the causative agent of malaria; *Toxoplasma gondii*, causing toxoplasmosis of humans and animals; or *Eimeria tenella*, the causative agent of chicken coccidiosis. All these unicellular protists have an obligate intracellular parasitic lifestyle and rely to different degrees on their host cells for nutrients (Ginger, 2006; Saliba and Kirk, 2001; Seeber et al., 2008). In this review we will consider primarily the apicomplexan species that have their genomes fully sequenced. The preservation or loss of some metabolic pathways will be discussed in the context of the adaptation of parasites to their specific niches and lifestyles and will include the following species: *Plasmodium* sp., *T. gondii*, *Neospora caninum*, *Theileria parva*, *Theileria annulata*, and *Babesia bovis* (Table 5.1). Occasionally, we will make reference to *E. tenella* whose genome annotation is unfinished, and for comparative purposes, *Cryptosporidium parvum* and *Cryptosporidium hominis*, when suitable. For simplicity we will frequently use the term ''all Apicomplexa'' when we mean ''all sequenced apicoplast-containing parasites.''

The plastid-derived organelle of the Apicomplexa called ''apicoplast'' has been under intense experimental and bioinformatic investigation for more than a decade now. Consequently, various aspects of its cell biology, phylogeny, and biochemistry have been summarized in a number of excellent reviews (Feagin and Parsons, 2006; Fleige et al., 2010; Foth and McFadden, 2003; Marechal and Cesbron-Delauw, 2001; Obornik et al., 2009; Ralph et al., 2004; Roos et al., 1999; Seeber and Soldati, 2007; Vaishnava and Striepen, 2006; Waller and McFadden, 2005; Wilson, 2002, 2005; Wilson et al., 2003, and references in later chapters). Rather than repeating those facts we have attempted in this article to provide the currently known picture of the metabolic pathways in a comparative way and by detailed graphical representations of the biochemical steps that we hope can serve as a useful complement to those reviews. We have also

Table 5.1 Genome sizes, host cell types, and known metabolic pathways hosted by the apicoplast of the apicomplexan parasites discussed in this chapter

	Genome size (Mb) (no. of genes)	Host cell[a]	Fd/FNR[a]	[Fe–S][a]	DOXP[a]	LipA/B[a]	PDH[a]	FAS II[a]	Heme[a]
Babesia bovis	8.2 (3671)	Erythrocytes	+	+	+	−	−	−	−
Theileria parva	8.35 (4035)	Lymphocytes, erythrocytes	+	+	+	−	−	−	−
Plasmodium falciparum	23.27 (5595)	Erythrocytes, hepatocytes	+	+	+	+	+	+	+
Toxoplasma gondii	63.5 (9239)	All nucleated cells	+	+	+	+	+	+	+
Thalassiosira pseudonana[b]	32.4 (11776)	None (free-living diatom)	+	+	+	+	+	+	+

[a] Fd/FNR, ferredoxin redox system; [Fe–S], iron–sulfur cluster biosynthesis; DOXP, isoprenoid biosynthesis; LipA/B, lipoic acid metabolism; PDH; pyruvate dehydrogenase complex; FAS II, fatty acid biosynthesis type II; Heme, heme biosynthesis.

[b] The diatom *T. pseudonana*, member of the chromalevolates, is included as an example of a distantly related, free-living organism, possessing a secondary plastid of red algal origin and with an entirely sequenced genome.

highlighted some aspects that we cover in more detail and where we felt that recent publications warranted a closer look at these topics or were not discussed previously in the context of Apicomplexa.

2. Morphology, Acquisition, and Evolutionary Origin of the Apicoplast

More than 50 years ago, morphological studies on various apicomplexans performed by electron microscopy revealed the existence of a structure surrounded by multiple membranes (McFadden et al., 1997; Siddall, 1992). This organelle did not resemble either the typical mitochondrion, endoplasmatic reticulum, or Golgi apparatus, or any of the apical complex organelles name-giving to the phylum Apicomplexa, like micronemes, rhoptries, or dense granules. At that time, this organelle was given a refreshing number of different illuminating names, such as ''grosse Vakuole mit kräftiger Wandung (= big vacuole with a strong wall)'' in the case of *Eimeria*; ''Hohlzylinder'' (= hollow cylinder), ''Lamellärer Körper'' (= lamellar body), and Golgi adjunct and ''vésicule plurimembranaire'' (= multimembranous vesicle) in *T. gondii*, or spherical body in *Plasmodium* (Siddall, 1992). The discovery of a circular 35-kb extrachromosomal DNA element of *Plasmodium falciparum* encoding an RNA polymerase with striking similarity to respective chloroplast genes (Gardner et al., 1991) were the first evidence for a alga–Apicomplexa connection (Wilson et al., 1994) and raised the possibility for the presence of a remnant plastid in these organisms. In 1996/97, the 35-kb circular genome could be localized to the organelle by two studies (Köhler et al., 1997; McFadden et al., 1996). It was unambiguously assigned to the relic of a plastid and was named the apicoplast (*apico*mplexan *plast*id). We now know that the apicoplast resulted from a secondary endosymbiosis via the engulfment of a plastid-bearing alga. The organelle is a relic of the plastid composed of two membranes and surrounded by two more membranes originating from the plasma membrane of the alga and from the endocytotic membrane that served to engulf the alga, respectively. The presence of three versus four membranes has been the matter of debate (Foth and McFadden, 2003; Hopkins et al., 1999; Köhler, 2005; McFadden et al., 1997). Importantly, the recent description of *Chromera velia*, a close relative of the Apicomplexa and still photosynthetically active, possesses a four membrane-bound plastid (Moore et al., 2008). This indicates that the four membranes are ancestral and that those Apicomplexa with three membranes, if they exist, have subsequently lost one membrane.

An observation with presumably significant impact on metabolism as detailed below is the close physical association between the single apicoplast

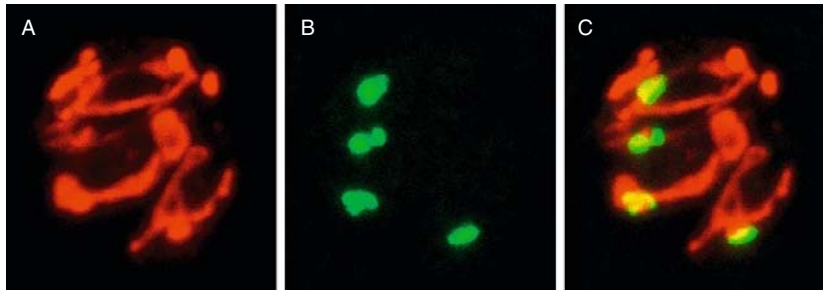

Figure 5.1 3D-reconstructions of four fluorescently tagged mitochondria (myc-tagged TgTPX1/2) (A) and apicoplasts (Ty-tagged TgICDH) (B) of *T. gondii* tachyzoites, respectively (Pino et al., 2007). The merged image in (C) documents the close association between both organelles.

and the single mitochondrion in Apicomplexa (see Fig. 5.1). Using fluorescently tagged organellar marker proteins in combination with significant improvements in bioimaging technologies, as well as EM studies on serial sections, a number of studies have provided a detailed picture of this phenomenon in *T. gondii* as well as *Plasmodium* sp. throughout intracellular development and also throughout the life cycle of these organisms (Dzierszinski et al., 2004; Hopkins et al., 1999; Köhler, 2006; Nishi et al., 2008; Okamoto et al., 2009; Stanway et al., 2009; van Dooren et al., 2005). These studies also impressively illustrate the complexity of tasks faced by the parasites to assure faithful inheritance of both organelles.

The nature of the algal prey (red or green) is not entirely clear but hotly debated (Obornik et al., 2009). Most data argue for a red algal endosymbiont that gave rise to the extant apicoplast, but it seems that genetic footprints of green algae evident in a number of chromalveolate genomes are an indication of a second endosymbiosis event by a green alga predating that of the apicoplast precursor (Moustafa et al., 2009). Chromalveolates (which include diatoms, dinoflagellates, and Apicomplexa; Keeling, 2009) thus appear to have gained genes from these two algal groups and the current repertoire of apicoplast genes could be a mixture of those genes.

3. Genome, Proteome, and Protein Trafficking

The pioneering work on the characterization of the 35-kb DNA element and its localization to the apicoplast paved the way to a series of seminal studies that revealed the unique features of the biology of this organelle but also led the foundation to unravel the biochemistry of

it (Foth and McFadden, 2003; McFadden et al., 1997; Roos et al., 1999; Waller and McFadden, 2005; Wilson, 2002, 2005). Therefore, in this section we will briefly summarize the essential features of the apicoplast genome and proteome as far as they are of interest in the context of this chapter.

The plastome (i.e., the genome of the apicoplast) is a circular 35-kb molecule that was first described in *P. falciparum*. This extrachromosomal DNA codes for an RNA polymerase more closely related to the polymerase of chloroplasts than to that of bacteria (Gardner et al., 1991). Furthermore, examination of the overall organization of the genes on the 35-kb molecule showed that it was very similar to the plastid genomes from algae, despite considerable deletions and reorganizations. These observations documented the first evolutionary connection between algae and parasites (Wilson et al., 1994, 1996). The definitive link was established by the localization of the 35-kb genome to the enigmatic multimembrane organelle (see above). Almost all known Apicomplexa have retained the plastid, with the notable exception of *Cryptosporidium* spp. (Abrahamsen et al., 2004) and possibly some gregarines (Toso and Omoto, 2007).

Depending on the Apicomplexa, the apicoplast hosts between 15 and 25 copies of the plastome (Matsuzaki et al., 2001), which can be replicated by two different modes also found in plants: the unidirectional single-stranded replication and the rolling circle mechanism (Williamson et al., 2001, 2002). To replicate the plastome, Apicomplexa rely on a most unusual multidomain polypeptide. This large nuclear gene codes for a contiguous DNA polymerase, DNA primase, and DNA helicase multi-domain polypeptide and was first characterized in *P. falciparum* (Seow et al., 2005). The sequence of the primase/helicase domain is phylogenetically related to the T7-bacteriophage gene 4 product and mammalian mitochondrial helicase. The DNA polymerase sequence is most closely related to those of the thermophilic *Aquifex* species and is inhibited by chloroquines and sumarin. This plastid replication and repair enzyme complex (PREX) is absent in *Cryptosporidium* spp. but found in other apicomplexans and was recently characterized in *T. gondii* (Mukhopadhyay et al., 2009). During the replication process the DNA molecules are subjected to torsional stress that is released by the action of topoisomerases. For this purpose, the apicomplexans possess a heterodimeric DNA gyrase belonging to the bacterial type II enzymes and which is composed of two nuclear-encoded subunits that are targeted to the apicoplast (Dar et al., 2007; Khor et al., 2005). Ciprofloxacin (a fluoroquinolone analog) is a powerful inhibitor of bacterial topoisomerases that efficiently also blocks apicoplast DNA replication of *P. falciparum* and *T. gondii* (Fichera and Roos, 1997; Williamson et al., 2002).

To date, all the sequenced plastomes of Apicomplexa are highly conserved with regard to size and composition (Cai et al., 2003; Wilson and Williamson, 1997). In contrast to the plastids of other organisms, the

apicoplast harbors the smallest plastome known, containing mainly genes involved in transcription and translation (Wilson and Williamson, 1997). The coding elements on the 35-kb molecule include a minimal but sufficient set of tRNAs for translation of the proteins, an rpoBC operon, and the ribosomal proteins necessary for the initial assembly of the small and large subunit, respectively. This arsenal is dedicated for transcription and translation of eight open reading frames, three of which code for genes with predicted known functions. The translation–elongation factor Tu (EF-Tu) is the product of the gene *tufA*. The gene *sufB* codes for a protein involved in the assembly of iron–sulfur clusters (see below), and *clpC* codes for a chaperone, which may function in the import of nuclear-encoded proteins (Howe and Purton, 2007). *Theileria* sp. and *B. bovis* plastomes exhibit the most prominent divergence from the other apicomplexans and a detailed comparison has been reviewed earlier (Fleige and Soldati-Favre, 2008).

Right from the beginning of apicoplast biology it was evident that the majority of proteins constituting the proteome of the apicoplast are nuclear-encoded and have to be transported to the organelle. This occurs via the secretory pathway (DeRocher et al., 2000; Waller et al., 2000), and import of soluble proteins into the organelle occurs via a two-step trafficking mechanism, which is probably shared by all plastid harboring apicomplexans (Parsons et al., 2007, 2009; Tonkin et al., 2008). An N-terminal extension composed of a bipartite motif was identified as the necessary and sufficient targeting signal for the apicoplast. This motif consists of a classical signal peptide, which mediates cotranslational insertion into the endoplasmic reticulum (ER), followed by a transit peptide, needed for routing to and import into the plastid (Foth et al., 2003; Harb et al., 2004; van Dooren et al., 2002). The unique features of the bipartite signal were exploited to perform bioinformatic predictions from the complete genome data of *P. falciparum*, leading to the identification of over 500 putatively apicoplast-localized proteins. More than 70% of the proteins that came out of this *in silico* screen were of unknown function (Ralph et al., 2004). Similar bioinformatic algorithms have not been developed so far for the other apicomplexans, and since not all proteins destined for the organelle show N-terminal extensions (see below), purification of the apicoplast combined with proteomic analyses will be ultimately required to define the individual proteomes.

The sequence determinants serving as trafficking signal, the route taken by proteins to reach the organelle, and the machinery implicated in the translocation have been intensely investigated and were recently reviewed (Parsons et al., 2007; Sheiner and Soldati-Favre, 2008; Tonkin et al., 2008). Some trafficking determinants have been shown to bring proteins to more than one destination, but in a rather unpredictable way. This is the case for some metabolic and antioxidant enzymes that are dually targeted to the mitochondrion and apicoplast (Pino et al., 2007; Saito et al., 2008). Another level of transport complexity was revealed while studying the trafficking

of membrane proteins. The nature of the trafficking determinant is often cryptic and import can be intimately linked to the parasite's cell cycle (Karnataki et al., 2007a,b, 2009). Interestingly, a protein of the thioredoxin family (ATrx1) has recently highlighted the existence of a population of vesicles in the vicinity of the apicoplast that may serve to transport some membrane proteins to the organelle (DeRocher et al., 2008; Lim et al., 2009).

The absence of classical and complete Tic/Toc complexes in apicomplexans that in plant plastids are instrumental for protein transport posed a dilemma as to how the proteins were eventually imported into the apicoplast (Gould et al., 2008). Two recent studies in *P. falciparum* and *T. gondii* have identified a second copy of proteins homologous to components of the endoplasmic reticulum-associated protein degradation (ERAD) system that target to the apicoplast (Agrawal et al., 2009; Spork et al., 2009). One of the components, Der1, is presumed to act as a pore of the apicoplast ERAD complex and has been demonstrated to be critical for protein import into the organelle and hence for survival of *T. gondii* (Agrawal et al., 2009).

4. Potential and Limitations of *In Silico* Predictions of Metabolic Pathways

A considerable amount of information presented and discussed in this chapter is based on apicomplexan genome sequence information, while biochemical and genetic studies performed on these parasites are still limited, compared to other organisms like bacteria, yeast, or mammalian cells. Luckily, a number of *in silico* methods developed during the course of apicomplexan genomes annotation efforts such as OrthoMCL (Chen et al., 2006) have been instrumental in putting gene annotations into the context of metabolism. However, open reading frames are not always correctly predicted despite the existence of good gene models (Dybas et al., 2008; Lu et al., 2007; Wakaguri et al., 2009). For instance, alternative splicing is known to contribute significantly to protein diversity in *Plasmodium* (Iriko et al., 2009, and references therein; van Dooren et al., 2002) as well as in *T. gondii* (Chaudhary et al., 2005; Delbac et al., 2001; Dybas et al., 2008; Ling et al., 2007). Moreover, large-scale proteomic analyses have also provided evidence that proteins exist whose corresponding genes show little or no detectable transcription in these organisms (Wastling et al., 2009; Xia et al., 2008). The N-termini of predicted proteins can considerably vary depending on the gene model and in consequence the deduced localization based on predictive algorithms need to be considered with great caution. Moreover, for some genes the sequence conservation between organisms might be too low to allow identification of homologs

by common sequence searches. This results in so-called pathway holes, that is, metabolic routes consisting of several successive enzymatic steps where one or more enzymes are missing in the constructed pathway (Green and Karp, 2004).

However, bioinformatics approaches relying on more sophisticated sequence search algorithms and structural comparisons can help spotting distantly related candidates (Green and Karp, 2004; Mohanty and Srinivasan, 2009), but in every case experimental biochemical confirmation is required. Moreover, even the number of pathways and pathway holes in a given organism is not something that different databases or researches can agree upon. Taking *P. falciparum* as an example, the manually created MPMP database (Ginsburg, 2006) reports 18 missing enzymes with EC numbers (from a total of 34 pathways), whereas another study lists 69 enzymes (Mohanty and Srinivasan, 2009). PlasmoCyc suggests that from 163 total pathways 115 are missing (totaling 320 proteins), whereby more than two-thirds of these pathways have three or more "holes." This most likely reflects the entire absence of such pathways in *Plasmodium*. The metaTIGER initially predicts 133 plasmodial metabolic pathways but after filtering for those that only contain a significant number of enzymes and not counting those enzymes that appear in many pathways, 52 remain (Whitaker et al., 2009).

However, pathway holes are not only due to annotation problems but sometimes can indicate real missing enzymes. One illustrating example is the missing enzyme in plasmodial folate synthesis, dihydroneopterin aldolase (DHNA), and the presence of an unusual ortholog of 6-pyruvoyltetrahydropterin synthase that provides a bypass for the missing DHNA enzyme (Dittrich et al., 2008). Another possibility is that a bifunctional enzyme carries out two successive steps in a chain, as it has been recently reported for the heme synthesis pathway in *P. falciparum* (see below) (Nagaraj et al., 2008).

Given the parasitic lifestyle of Apicomplexa, it is not surprising that host metabolites of various kinds are actively exploited as resource, and as a consequence that *in vitro* and *in vivo* growth conditions might differ substantially (Leroux et al., 2009). Although none of the Apicomplexa can be cultured under axenic conditions that would easily allow defining auxothrophies (and thus missing anabolic capabilities), some are known, like deficiencies in the synthesis of several amino acids (Chaudhary and Roos, 2005); pantothenate for *Plasmodium* (Saliba et al., 1998), and lipoic acid (LA) for both, *T. gondii* and *P. falciparum* (Allary et al., 2007; Crawford et al., 2006), to name some. Consequently, it is possible that a pathway hole could be compensated for by the "import" of a host metabolite. In this respect it is important to identify and characterize in detail the "transportome" of the parasites, that is, the set of transporters and solute carriers, especially at the parasite cell surface but in the case of *Plasmodium* also those

that are exported to the erythrocyte membrane (Martin et al., 2009). This allows a better picture of possible solute fluxes between parasite and host and thus contributes also to the understanding of metabolic dependencies of the parasite.

In principle, three methods exist for the prediction of metabolic pathways in any organism: fully automatic annotation either with or without subsequent manual curation, or the much more time-consuming fully manual compilation based on genome annotations, sequence homology searches, and profound biochemical knowledge. As pointed out by a recent discussion regarding *Plasmodium* databases, all methods have their advantages but also their limitations (Ginsburg, 2009; Whitaker et al., 2009), and as usual it is best to consult more than one source of information when available. As an aid Table 5.2 lists the most relevant general as well as parasite-specific databases with regard to metabolic pathway reconstructions, including some sources to allow verification of specific biochemical routes, reactions, and compounds. Also included are the genome portals for the Apicomplexa as far as implemented, which allows the verification of gene/protein predictions by a ''critical mind.'' Most of the pathways drawn in this chapter are based on MetaCyc, using the Pathway Tools software (Karp et al., 2002). Extensive crosschecks were performed with other databases and the literature.

5. Biosynthesis of Various Metabolites and Factors

5.1. Isoprenoids

This section stands somewhat in the center of this chapter since it not only covers the generation of an essential class of metabolites, the isoprenoids, and their distribution to other cellular compartments but also incorporates aspects of other required auxiliary pathways, like the source of carbon in the apicoplast as well as the provision of reducing power via the ferredoxin (Fd) redox system. Their discussion here rather than in separate sections illustrates best their connection to this essential metabolic pathway of all apicoplast-containing apicomplexans.

Isoprenoids are by far the largest and most diverse group of natural compounds, encompassing $>23{,}000$ known structures (Barton et al., 1999; Holstein and Hohl, 2004). Given this large number, they obviously fulfill a great diversity of cellular functions in all biological systems. Notably, isoprenoids are involved in cell signaling processes, protein modifications (prenylation), synthesis of the cofactor ubiquinone (coenzyme Q), and modifications of tRNAs. The basic precursors for all these structures are the isopentenyl diphosphate (IPP) and its isomeric form, dimethylallyl

Table 5.2 Compilation of useful Internet resources to access metabolic pathways and for their reconstruction, verification, and annotation

Database	Content and comments	URL	References
General Internet resources for enzymatic reactions and pathways			
KEGG (Kyoto Encyclopedia of Genes and Genomes)	Many search options and links; best known for its pathways that are directly linked to almost all sequenced organisms	http://www.genome.ad.jp/kegg/	Kanehisa et al. (2008)
	Among the many tools available for interacting with KEGG is the new web interface "Pathway Projector" that provides a simple way to query the database in different ways and to get and manipulate further information	http://www.g-language.org/PathwayProjector/index.html	Kono et al. (2009)
MetaCyc Biochemical Pathways	Multiorganism metabolic pathway and enzyme database. Contains >1400 metabolic pathways derived from >1800 organisms. Manually curated and commented	http://biocyc.org/metacyc/index.shtml	Caspi et al. (2009)
Biochemical Pathways (Roche/ExPASy)	The original "Boehringer Biochemical Pathways"; still a valuable resource with reaction schemes; with direct links to ENZYME	http://www.expasy.org/cgi-bin/search-biochem-index	Michal (1999)
	A different browser is "BioPath," which gives access to extended structural data, search options, etc.	http://www.molecular-networks.com/biopath/index.html	Reitz et al. (2004)
IUBMB-Nicholson Minimaps	Another site with a restricted collection of nice pathway maps	http://www.iubmb-nicholson.org/minimaps.html	

(*continued*)

Table 5.2 (*continued*)

Database	Content and comments	URL	References
Reactome	A curated knowledge base of biological human pathways, with cross-links to computationally inferred *P. falciparum* pathways	http://www.reactome.org/	Matthews et al. (2009)
The SEED	A database curated by expert annotators across many genomes. Contains also information on pathways, but from Apicomplexa it covers only *P. falciparum*. Not very intuitive to use; no graphical pathway maps	http://www.theseed.org/wiki/index.php/Main_Page	Overbeek et al. (2005)
BRENDA (Comprehensive Enzyme Information System)	Very comprehensive cross-kingdom information on enzymes, their substrates/inhibitors and biochemistry; with direct links to PubMed and other sources	http://www.brenda-enzymes.info/	Chang et al. (2009)
ENZYME (Enzyme nomenclature database at ExPASy)	Searches can be done by EC number or enzyme name; links to other databases	http://www.expasy.org/enzyme/	Gasteiger et al. (2003)
Internet resources for parasite-specific metabolism			
ApiCyc	Metabolic pathways from several *Plasmodium* species, *Cryptosporidium* and *T. gondii*. They are automatically generated based on MetaCyc and not manually curated. Not up-to-date with latest releases of the respective genome annotations. Gateway to the respective databases PlasmoCyc, ToxoCyc, CryptoCyc	http://apicyc.apidb.org/	Yeh et al. (2004)

MPMP (Metabolic Pathways of the Malaria Parasite)	This site contains manually generated pathways for *Plasmodium* only, using gene annotations (from GeneDB and PlasmoDB) and KEGG maps as template, and by additional annotations identified by the curator (Dr. Hagai Ginsburg, Jerusalem, Israel)	http://sites.huji.ac.il/malaria/	Ginsburg (2006)
metaTIGER	Database representing metabolic pathways automatically generated from genomic information from >120 eukaryotes and >400 prokaryotes. Also contains a comprehensive database of >2250 phylogenetic trees, allowing the judgment of the evolutionary origin of enzymes	http://www.bioinformatics.leeds.ac.uk/metatiger/index.html	Whitaker et al. (2009a)
EupathDB	Database integrating the individual databases from the eukaryotic pathogens *Cryptosporidium*, *Giardia*, *Leishmania*, *Neospora*, *Plasmodium*, *Toxoplasma*, *Trichomonas*, and *Trypanosoma* using the same web infrastructure. It offers an entry point to all these resources plus the opportunity to compare data across genera	http://eupathdb.org/eupathdb/	Aurrecoechea et al. (2010)
PlasmoDB	Comprehensive genome database for *Plasmodium* with many links	http://plasmodb.org/	Aurrecoechea et al. (2009)
ToxoDB	Comprehensive genome database for *T. gondii* with many links	http://toxodb.org/	Gajria et al. (2008)
CryptoDB	Comprehensive genome database for *Cryptosporidium* with many links	http://cryptodb.org/	Heiges et al. (2006)

(*continued*)

Table 5.2 (*continued*)

Database	Content and comments	URL	References
Eimeria tenella GeneDB	Access to *Eimeria tenella* genome data (still unfinished)	http://www.genedb.org/genedb/etenella/	Hertz-Fowler et al. (2004)
DFCI *E. tenella* Gene Index	Access to *Eimeria tenella* EST data. Contains rudimentary mapping of ESTs to pathway maps	http://compbio.dfci.harvard.edu/tgi/gi/etgi/GenInfo.html	
Theileria annulata GeneDB	Access to *Theileria annulata* genome data	http://www.genedb.org/genedb/annulata/	Hertz-Fowler et al. (2004)
Theileria parva genome	Currently no dedicated database like for the other Apicomplexa available. NCBI's Map Viewer gives a starting point for querying the genome	http://www.ncbi.nlm.nih.gov/mapview/map_search.cgi?taxid=5875	Gardner et al. (2005)
Babesia bovis genome	Currently no dedicated database like for the other Apicomplexa available. NCBI's Map Viewer gives a starting point for querying the genome	http://www.ncbi.nlm.nih.gov/mapview/map_search.cgi?taxid=5865	Brayton et al. (2007)

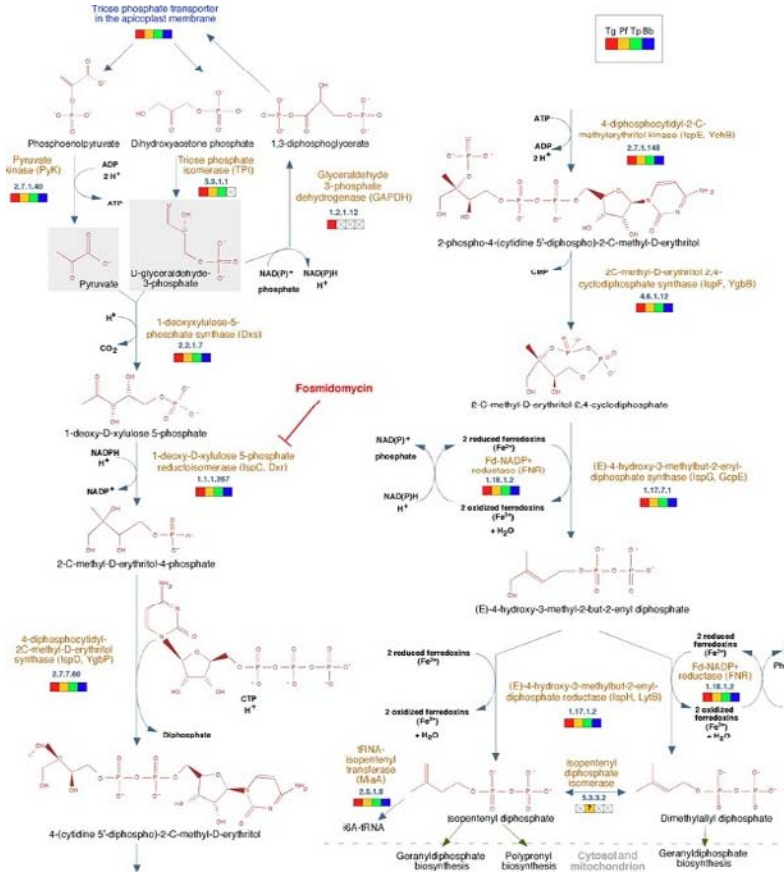

Figure 5.2 Synthesis of isoprenoid precursors IPP and DMAPP via the DOXP pathway. Starting point are the glycolysis-derived phosphoenol pyruvate (PEP) and dihydroxyacetone phosphate (DHAP), which both can be transported into the apicoplast via a membrane-resident triose phosphate translocator (Lim et al., 2010). In *T. gondii*, an apicoplast-resident glyceraldehyde-3-phosphate dehydrogenase (GAPDH) (Fleige et al., 2007) can potentially generate reducing power from glyceraldehyde-3-phosphate, but this enzyme has not been found in the other apicomplexan genomes. Otherwise, synthesis steps are similar to those defined in plants and bacteria. The step inhibited by Fos is indicated. The presence of an enzyme is color coded, as indicated by the legend (top right), whereas the presumed absence (= no homolog detected in the databases) is denoted by a white, crossed box. EC numbers (where assigned) are also shown below enzyme names.

diphosphate (DMAPP) (Fig. 5.2). Nature has invented two alternative routes for the synthesis for these two substances, whereby most eubacteria and plants follow the so-called 1-deoxy-D-xylulose-5-phosphate (DOXP) pathway (also called methylerythritol phosphate (MEP) pathway). In contrast,

eukaryotes and archaebacteria use the mevalonate (MEV) pathway (Eisenreich et al., 2004; Lichtenthaler, 1999; Rohmer, 1999; Rohmer et al., 1993). However, there are a number of exceptions to these rules. The majority of plants and a few bacteria (like *Listeria monocytogenes*) possess both pathways. In plants, the MEV pathway is cytosolic whereas the DOXP route is confined to the chloroplast (Rohmer, 1999). Some bacteria like *Streptococcus pyogenes* and *Staphylococcus aureus* use only the MEV pathway (Kirby and Keasling, 2009; Rohdich et al., 2005), while the green algae and the apicomplexans possess the entire set of genes coding for the bacterial DOXP pathway only (Clastre et al., 2007; Grauvogel and Petersen, 2007). Phylogenetic analyses of the DOXP pathway suggest that most of the genes were initially acquired by lateral transfer from eubacteria subsequently to the origin of plastids, and were later introduced into Apicomplexa and other Alveolata by acquisition of the apicoplast (Grauvogel et al., 2007; Lange et al., 2000; Matsuzaki et al., 2008).

The two pathways differ in the initial starting compounds (two molecules of acetyl-CoA for the MEV pathway; one molecule of D-glyceraldehyde-3-phosphate, and one molecule of pyruvate for the DOXP pathway). The intermediate products also differ, and only the formation of the two end products unifies both pathways. Given that the enzymes of the DOXP pathway are not found in humans, they constitute attractive candidate drug targets to combat the pathogens that rely on them (Moreno and Li, 2008; Rohdich et al., 2005; Singh et al., 2007; see below). Consequently, considerable efforts have dedicated to unravel the reaction mechanisms and the structures of the DOXP enzymes (deRuyck and Wouters, 2008; Hunter, 2007).

The first study on apicomplexan isoprenoid biosynthesis was published in 1999 and reported the potent *in vitro* and *in vivo* action of the antibiotic fosmidomycin (Fos) against *Plasmodium* sp. (Jomaa et al., 1999). This was the first evidence of the essential nature of the DOXP pathway for the malaria parasite, which was recently confirmed by the unsuccessful knockout attempts for DOXP reductoisomerase (Dxr) in *P. falciparum* (Odom and Van Voorhis, 2009). The DOXP pathway is functionally active in all intraerythrocytic stages of this organism, evidenced by the detection of most downstream intermediates (Cassera et al., 2004). In *T. gondii*, all the genes implicated in the DOXP pathway are present and possess a predicted bipartite targeting signal for the apicoplast, and antibodies raised against recombinant PfDxr decorate the plastid of both, *P. falciparum* and *T. gondii* (J. Wiesner, O. Harb, personal communication). Direct evidence for the importance of this pathway for the survival of apicomplexans has been recently obtained in *T. gondii* where essential genes can be conditionally disrupted. Turning off the expression of LytB, the last enzyme of the pathway, dramatically interferes with parasite replication (B. Striepen, personal communication).

This information is relevant in the context of the reported insensitivity of *T.gondii*, *E. tenella*, and *T. parva* to even high concentrations of Fos (Clastre et al., 2007; Jomaa et al., 1999; Ling et al., 2005; Lizundia

Table 5.3 Range of host cell types, IC_{50} values for Fos, and reported alteration of host cell plasma membrane permeability by different Apicomplexa

	Host cell type	IC_{50} Fos (μM) (References)	Alteration of membrane permeability (References)
Babesia sp.	Erythrocyte	<5 (Sivakumar et al., 2008)	Yes (Alkhalil et al., 2007)
Plasmodium falciparum	Erythrocyte	0.35 (Jomaa et al., 1999)	Yes (Staines et al., 2007)
Theileria parva, T. annulata	B and T lymphocytes, macrophages and erythocytes	>500 (Lizundia et al., 2009)	No
Eimeria tenella	Select enterocytes	>500 (Clastre et al., 2007)	No
Toxoplasma gondii	Virtually all nucleated cells	>500 (Ling et al., 2005)	No

et al., 2009) (Table 5.3). The unexpected failure to kill these apicomplexans despite the presence of the complete set of genes for this pathway could be explained in several ways: the pathway could be dispensable, the enzymes are resistant to Fos, or the drug is poorly bio-available in those parasites. However, homology modeling of Dxr from *T. gondii* with the known 3D structure from *Mycobacterium tuberculosum* Dxr shows the overall high structural similarity between both proteins and that the binding pocket with those amino acids interacting with Fos is expected to be highly similar in both proteins (Fig. 5.3). In the light of this information, TgDxr should be equally sensitive to the drug. Preliminary data indicate that the poor uptake of the drug by the host cell infected by *T. gondii*, *E. tenella*, or *T. parva*, respectively, is presumably responsible for resistance to Fos (Baumeister et al., unpublished). In contrast, *P. falciparum* and *Babesia* species are known to enhance the permeability of infected erythrocytes to diverse ions and metabolites (a phenomenon described as ''new permeability pathways'' or NPP, which is still poorly understood molecularly) (Kirk, 2001; Staines et al., 2007; see Table 5.3). The NPP increase the uptake of Fos and its related derivative FR900098 into the host cell (Baumeister et al., unpublished). Obviously, the host cell plasma membrane is not the only barrier that separates Fos from Dxr, and it is currently unknown how the other membranes are overcome in *P. falciparum* and *B. bovis*.

The DOXP pathway requires glyceraldehyde-3-phosphate (G3P) and pyruvate as precursors, both of which are generated in the apicoplast from either dihydroxyacetone phosphate (DHAP) or phosphoenol pyruvate (PEP), respectively (Fig. 5.2). G3P and pyruvate are the essential precursors

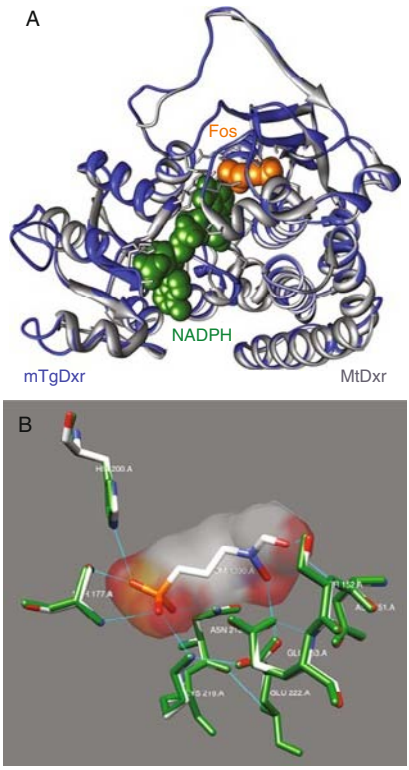

Figure 5.3 3D-modeling of *T. gondii* Dxr protein sequence onto *Mycobacterium tuberculosis* Dxr. (A) The model was built using the Swiss Model Server (Arnold et al., 2006) with the *M. tuberculosis* structure as template (PDB 2jcvA; Henriksson et al., 2007). The resulting structures were then compared using the TopMatch server (Sippl and Wiederstein, 2008). Visualization of the model was performed using Chimera (Pettersen et al., 2004). The bacterial structure is shown in gray (MtDxr) and the parasite chain in blue (mTgDxr). MtDxr-bound NADPH (green) and Fos (orange) are also shown. (B) Amino acids implicated in Fos interactions within the binding pocket of MtDxr (Henriksson et al., 2006) and their comparison with the corresponding aa from the modeled TgDxr (green). The numbers refer to the MtDxr sequence. The molecular surface of Fos is indicated.

of DOXP while acetyl-CoA and malonyl-CoA are required for fatty acid biosynthesis via FAS II (see below). PEP imported into the apicoplast is metabolized there into pyruvate due to the action of the pyruvate kinase type II (PyKII) recently characterized in both, *T. gondii* and *P. falciparum* (Maeda et al., 2009; Saito et al., 2008). Pyruvate is ultimately converted into acetyl-CoA by the action of the pyruvate dehydrogenase complex (PDH) exclusively found in the apicoplast (Crawford et al., 2006; Fleige et al., 2007; Foth et al., 2005). The plastidic translocators required to import PEP

from the cytosol (thereby connecting glycolysis to fatty acid (FA) and isoprenoid metabolism) have recently been identified and biochemically characterized. In plants sugar transport in plastids occurs through membrane transporters that function as antiport systems, exchanging phosphorylated C_3, C_5, and C_6 sugars. In *T. gondii*'s genome, a single apicoplast phosphate translocator (TgAPT1) localizes to multiple membranes of the apicoplast (Fleige et al., 2007; Karnataki et al., 2007a). Biochemical data indicated that TgAPT1 transports different substrates like triose phosphate and PEP (Brooks et al., 2010), and the conditional disruption of the TgATP1 gene established that transport of metabolites to the plastid is essential for parasite survival. This result is in agreement with the previously demonstrated importance of the FAS II pathway in *T. gondii* (Mazumdar et al., 2006). In *P. falciparum* two distinct genes coding for potential transporters have been reported to localize differentially to the inner (PfiTPT/PfAPT1) and the outer membrane (PfoTPT/PfAPT2) of the apicoplast, respectively (Mullin et al., 2006). The substrate preferences of these transporters were recently assessed using a novel cell-free assay system and indicated that they can account for the transport of phosphorylated metabolites (PEP, DHAP, 3PGA) from the parasite cytosol into the plastid (Lim et al., 2010).

While the sources and the route of uptake for carbon to the apicoplast have been fairly well characterized, the processes by which energy and reducing power are produced in the organelle are less obvious. In *T. gondii*, the 10 enzymes forming the glycolytic pathway are found in the cytosol. In addition, for some glycolytic enzymes the parasite also possesses a second isoform that each is localized to the apicoplast (Fleige et al., 2007). Together, they might contribute to the local production of ATP. For example, an apicoplast-resident second GAPDH isoenzyme (Fast et al., 2001; Pino et al., 2007) could be involved in the generation of NAD(P)H from D-glyceraldehyde-3-phosphate (Fig. 5.2; Ralph et al., 2004). Surprisingly, such a GAPDH gene is not apparent in the other genomes (Harper and Keeling, 2003), and if true, its functional consequences (if any) are currently not known. The further steps of IPP/DMAPP synthesis follow those initially defined in plant and bacterial cells, unless noted otherwise (see Fig. 5.2; for biochemical details see reviews by Eisenreich et al., 2004; Eoh et al., 2009; Hunter, 2007; Kirby and Keasling, 2009; Rohmer, 1999; Wiesner and Jomaa, 2007, and Table 5.4). Whether the end products IPP and DMAPP are produced simultaneously at a 5:1 ratio, as reported *in vitro* (Röhrich et al., 2005), or whether an IPP isomerase might be required *in vivo*, is not known. Recently, a gene showing distant similarity to a functional domain found in IPP isomerases has been identified in *P. falciparum* (PFE071w) (Mohanty and Srinivasan, 2009) and other apicomplexans. Whether this gene indeed codes for an IPP isomerase still awaits further characterization.

Table 5.4 Compilation of apicoplast-localized proteins involved in metabolic pathways

Pathway	Enzyme name/function[a]	Abbreviation	EC number	*T. gondii*[b]	*P. falciparum*[c]	*T. parva*[d]	*B. bovis*[e]	Key references from Apicomplexa[f]
Coenzyme A biosynthesis	Dephospho-CoA kinase	DPCK	2.7.1.24	TGME49_030990	PF14_0415	TP01_0811	BBOV_IV009580	Spry et al. (2008)
[Fe–S] synthesis	NifU-like scaffold protein	NFU		TGME49_021920	PFI1050c	TP01_0062	BBOV_III006970	–
	Plant-type ferredoxin	ptFd		TGME49_015070	MAL13P1.95	TP04_0049	BBOV_II005080	Balconi et al. (2009), Kimata-Ariga et al. (2007), Vollmer et al. (2001)
	Plant-type ferredoxin-$NADP^+$-reductase	ptFNR	1.18.1.2	TGME49_098990	PFF1115w	TP01_1180	BBOV_IV011290	Balconi et al. (2009), Milani et al. (2007), Vollmer et al. (2001)
	SufA [Fe–S] shuttle protein	SufA		TGME49_097930	PFE1135w	–	–	–
	SufB, ABC transporter	SufB		TogoCp26	PFC10_-API0012	–	–	–
	SufC, ABC transporter	SufC		TGME49_025800	PF14_0133	TP02_0460	BBOV_I000600	–
	SufD, complexed with SufB, C	SufD		TGME49_073450	PF11_0044	–	–	–
	SufE, desulfurase activator and sulfide "transferase"	SufE		TGME49_077010	PFB0270w	–	–	–
	Cysteine desulfurase	SufS	2.8.1.7	TGME49_016170	PF07_0068	TP01_1094	BBOV_IV003350	–
	High chlorophyll fluorescence phenotype protein (*)	HCF101		TGME49_118590	PF11_0296	TP03_0848	BBOV_I000220	–
	Glutaredoxin 14(16)-like (*)	Grx14 (16)		TGME49_047580	PF07_0036	TP01_0735	BBOV_IV010730 (?)	–
	Chaperonin 60	Cpn60		TGME49_040600	PFL1545c	TP03_0206	BBOV_IV007010	Sato and Wilson (2004)
	Chaperonin 20	Cpn20		TGME49_073960	PF13_0180	TP02_0311	BBOV_III006630	Sato and Wilson (2005)

Heme biosynthesis and metabolism	Porphobilinogen synthase	HemB (ALAD)	4.2.1.24	TGME49_053900	PF14_0381	–	BBOV_II001120	Dhanasekaran et al. (2004), Sato and Wilson (2002)
	Porphobilinogen deaminase	HemC (PBGD)	2.5.1.61	TGME49_071420	PFL0480w	–	–	Nagaraj et al. (2008)
	5-Aminolevulinate synthase	HemA (ALAS)	2.3.1.37	TGME49_058690	PFL2210w	–	–	Sato et al. (2004), Varadharajan et al. (2002)
	Uroporphyrinogen-III synthase	HemD (UROS)	4.2.1.75	TGME49_114040	(PFL2285c?)	–	–	Mohanty and Srinivasan (2009), Nagaraj et al. (2008)
	Uroporphyrinogen decarboxylase	HemE (UROD)	4.1.1.37	TGME49_089940	PFF0360w	–	–	Nagaraj et al. (2009a)
	Coproporphyrinogen oxidase	HemF (CPO)	1.3.3.3	TGME49_023020	PF11_0436	–	–	Nagaraj et al. (2009b)
	Protoporphyrinogen oxidase	HemG (PPO)	1.3.3.4	TGME49_072490	PF10_0275	–	–	–
	Ferrochelatase	HemH (FC)	4.99.1.1	TGME49_058650	MAL13P1.326	–	–	Nagaraj et al. (2009c), Sato and Wilson (2003), Varadharajan et al. (2004)
	Heme oxygenase (*)	HO	1.14.99.3	TGME49_059190	PF10_0116	TP01_0873 (C-term)	BBOV_IV009020 (N-term)	Okada (2009)
	Cytochrome *c* (c_1) heme lyase (*)	CCHL		TGME49_114040 TGME49_093390	PFL1185c PFL0180w	TP02_0784 TP01_0886	BBOV_IV008890 BBOV_III011500A	Bernard et al. (2003)
FAS II synthesis	Acetyl-CoA carboxylase 1	ACC1	6.4.1.2	TGME49_021320	PF14_0664	–	–	Zuther et al. (1999)
	Biotin-acetyl-CoA carboxylase ligase (*)	BirA	6.3.4.15	TGME49_089760	PF10_0409 PF14_0573	–	–	–
	Acyl carrier protein	ACP		TGME49_064080	PFB0385w	–	–	Gallagher and Prigge (2010), Waller et al. (1998), Waters et al. (2002)

(*continued*)

Table 5.4 (*continued*)

Pathway	Enzyme name/function[a]	Abbreviation	EC number	*T. gondii*[b]	*P. falciparum*[c]	*T. parva*[d]	*B. bovis*[e]	Key references from Apicomplexa[f]
	Holo-[acyl carrier protein] synthase	ACPS-PPT	2.7.8.7	TGME49_003420	PFD0980w	–	–	Cai et al. (2005)
	β-Hydroxyacyl-(acyl carrier protein) dehydratase	FabZ	4.2.1.–	TGME49_121570	PF13_0128	–	–	Dautu et al. (2008), Sharma et al. (2003)
	β-Ketoacyl synthase I/II	FabB/F (KAS I/II)	2.3.1.41	TGME49_093590	PFF1275c	–	–	Lack et al. (2006), Prigge et al. (2003)
	Malonyl-CoA-(acyl carrier protein) transacylase	FabD (MCAT)	2.3.1.39	TGME49_025990	PF13_0066	–	–	Prigge et al. (2003)
	β-Ketoacyl-(acyl carrier protein) synthase III	FabH (KAS III)	2.3.1.180	TGME49_031890	PFB0505c	–	–	Waters et al. (2002)
	3-Oxoacyl-(acyl carrier protein) reductase	FabG	1.1.1.100	TGME49_017740	PFI1125c	–	–	Pillai et al. (2003)
	Enoyl-(acyl carrier protein) reductase	FabI (ENR)	1.3.1.9	TGME49_051930	PFF0730c	–	–	McLeod et al. (2001), Muench et al. (2007), Surolia and Surolia, (2001), Wickramasinghe et al. (2006)
Lipoic acid synthesis	Lipoate synthase	LipA	2.8.1.8	TGME49_026400	MAL13P1.220	–	–	Thomsen-Zieger et al. (2003), Wrenger and Müller (2004)
	Octanoyl-(ACP): protein *N*-octanoyltransferase	LipB	2.3.1.181	TGME49_115640	MAL8P1.37	–	–	Günther et al. (2007), Wrenger and Müller (2004)

	Lipoic acid protein ligase A2	LiplA2	2.7.7.63	TGME49_094900	PFI1160w	–	–	Allary et al. (2007), Günther et al. (2009a,b), Wrenger and Müller (2004)
Pyruvate metabolism	PDH E1 alpha	PDH E1 alpha	1.2.4.1	TGME49_045670	PF11_0256	–	–	Fleige et al. (2007), Foth et al. (2005)
	PDH E1 beta	PDH E1 beta	1.2.4.1	TGME49_072290	PF14_0441	–	–	Fleige et al. (2007), Foth et al. (2005)
	PDH E2	PDH E2	2.3.1.12	TGME49_006610	PF10_0407	–	–	Crawford et al. (2006), Fleige et al. (2007), Foth et al. (2005)
	PDH E3	PDH E3	1.8.1.4	TGME49_105980	PF08_0066	–	–	Fleige et al. (2007), Foth et al. (2005)
	Pyruvate kinase II	PyKII	2.7.1.40	TGME49_099070	PF10_0363	TP02_0134	BBOV_III010130	Maeda et al. (2009), Saito et al. (2008)
Isoprenoid biosynthesis and metabolism	1-Deoxy-D-xylulose-5-phosphate synthase	Dxs	2.2.1.7	TGME49_008820	PF13_0207	TP01_0516	BBOV_III002600	–
	1-Deoxy-D-xylulose-5-phosphate reductoisomerase	Dxr	1.1.1.267	TGME49_014850	PF14_0641	TP02_0073	BBOV_III010740	Jomaa et al. (1999), Odom and Van Voorhis (2010)
	2-C-Methyl-D-erythritol-4-phosphate cytidylyltransferase	YgbP	2.7.7.60	TGME49_106260	PFA0340w	TP03_0057	BBOV_III003490	–
	4-Diphosphocytidyl-2-C-methyl-D-erythritol kinase	YchB	2.7.1.148	TGME49_106550	PFE0150c	TP02_0681	BBOV_II007070	–
	2-C-Methyl-D-erythritol-2,4-cyclodiphosphate synthase	YgbB	4.6.1.12	TGME49_055680	PFB0420w	TP03_0365	BBOV_IV002810	–

(*continued*)

Table 5.4 (*continued*)

Pathway	Enzyme name/function[a]	Abbreviation	EC number	*T. gondii*[b]	*P. falciparum*[c]	*T. parva*[d]	*B. bovis*[e]	Key references from Apicomplexa[f]
	(*E*)-4-Hydroxy-3-methyl-but-2-enyl-diphosphate synthase	GcpE	1.17.7.1	TGME49_062430	PF10_0221	TP02_0667	BBOV_II006930	–
	(*E*)-4-Hydroxy-3-methyl-but-2-enyl diphosphate reductase	LytB	1.17.1.2	TGME49_027420	PFA0225w	TP03_0674	BBOV_III001660	Röhrich et al. (2005)
	Isopentenyl diphosphate isomerase	IPPI	5.3.3.2	–	PFE0710w?	–	–	Mohanty and Srinivasan (2009)
	tRNA delta(2)-isopenteny-lpyrophosphate transferase	MiaA	2.5.1.8	TGME49_112520	PFL0380c	TP01_0445	fuse BBOV_IV006320 and BBOV_IV006330	–
	Dimethylallyl adenosine tRNA methylthio-transferase	MiaB		TGME49_073140	PFF1070c	TP04_0588	–	–
Carotenoid synthesis	Phytoene synthase (*)	PSY	2.5.1.32	TGME49_069430	PFB0130w	TP03_0238	BBOV_IV007310	Tonhosolo et al. (2005, 2009)
Transporter	Triose phosphate/phosphate translocator	TPT			PFE1510c	TP01_0715	BBOV_IV009970	Lim et al. (2009, 2010), Mullin et al. (2006)
	Apicoplast phosphate translocator	APT		TGME49_061070	PFE0410w	TP03_0536	BBOV_I004960	Fleige et al. (2007), Karnataki et al. (2007a,b), Mullin et al. (2006)

Energy and reducing power generating enzymes	Triosephosphate isomerase II	TPI II	5.3.1.1	TGME49_033500	PFC0831w	–	–	–
	Glyceraldehyde-3-phosphate dehydrogenase II	GAPDH II	1.2.1.12	TGME49_069190	–	–	–	Fast et al. (2001), Pino et al. (2007)
	Phosphoglycerate kinase II	PGK II	2.7.2.3	TGME49_022020	–	–	–	Fleige et al. (2007)

[a] All enzymes except those of the heme metabolism (see Table 5.6) are predicted or proved to be apicoplast-localized at least in one apicomplexan, unless no clear assignments are currently possible but reasonable analogy to plant plastids is visible (indicated by *).
[b] ToxoDB accession numbers for strain ME49.
[c] PlasmoDB accession numbers for *P. falciparum*.
[d] Initial TIGR annotation numbers for *T. parva*. Data can be accessed via Uniprot, KEGG, or NCBI queries.
[e] NCBI accession numbers for *B. bovis*.
[f] Key references are given to articles related to biochemical and/or localization studies of a respective apicomplexan gene product. If no reference is given then this protein has not been studied in more detail and reviews cited in the main text should be consulted.

The last two steps of the DOXP pathway require a source for reducing equivalents. Currently, the only known redox system in the apicoplast consists of the small acidic [2Fe–2S] plant-type ferredoxin (ptFd) protein and its associated reductase, ferredoxin $NADP^+$-reductase (ptFNR) (Vollmer et al., 2001). *In vitro* experiments strongly suggest that the electron donor in the apicoplast is NADPH and that reduced ptFd transfers it to LytB via direct protein–protein interaction (Röhrich et al., 2005). These results are corroborated by similar data for GcpE in plant and algal systems (Okada and Hase, 2005; Seemann et al., 2006) as well as in *Escherichia coli*, where this task is performed by flavodoxin 1 (Puan et al., 2005). Therefore, a strong link between the DOXP pathway and the ptFd redox system exists, and this dependency can be extended to the possible involvement of ptFd in [Fe–S] synthesis since LytB and GcpE are two [4Fe–4S]-containing proteins (see below). In addition, the ptFd/FNR system is presumably also involved in the redox balance in the organelle (Krapp et al., 2002), which seems to be a highly reducing environment (Gallagher and Prigge, 2010).

Two resistance mechanisms to Fos have been described to date. In plant plastids, the amount of DOXP enzymes increases by a mechanism coupled to Clp-dependent proteolysis (Flores-Perez et al., 2008). When this post-translational control mechanism is inactivated then Fos resistance can occur. Whether similar mechanisms are operative in Apicomplexa is unknown, but a Clp-like protease system is also present in the apicoplast (Wilson et al., 1996). Alternatively, an amplification of the Dxr locus has been reported to confer drug resistance both in plants and in *P. falciparum* (Carretero-Paulet et al., 2006; Dharia et al., 2009). In the malaria parasite, gene amplification was achieved by *in vitro* selection of cultures for their ability to grow in the presence of eightfold higher Fos concentrations (Dharia et al., 2009). Interestingly, no naturally occurring Fos-resistant Dxr enzyme has been reported so far.

In the apicoplast, tRNAs are presumably modified by isoprenylation, as it is the case in plant plastids (Miyawaki et al., 2006; Persson et al., 1994). The modified base (isopentenyladenosine in the anticodon loop) has been shown to be necessary for correct binding of the charged tRNA to the ribosome–mRNA complex, and also to suppress several stop codons and frameshift mutations that are frequently observed in apicoplast genomes (Cai et al., 2003; Lang-Unnasch and Aiello, 1999; Preiser et al., 1995; Wilson et al., 1996). All apicoplast-bearing parasite genomes contain a gene for a tRNA isopentenylpyrophosphate transferase (miaA) that is presumably plastid-targeted (Ralph et al., 2004). Moreover, another enzyme required for further tRNA base modifications, miaB (methylthiolase), can be identified in the apicomplexans. Whether the cytosolic tRNAs are also modified by isoprenylation is currently not known. Intriguingly, Cryptosporidia that lack the apicoplast and do not possess the genes coding for either the MEV or the alternative MEP pathway (Clastre et al., 2007), nevertheless contain miaA

and miaB homologs in their genomes. The presence of miaA and miaB suggests that Cryptosporidia manage to scavenge isoprenoid precursors from their host (Clastre et al., 2007; Ginger, 2006).

The synthesis of thiamine pyrophosphate (TPP), the active form of vitamin B1 (thiamin), was initially predicted to be dependent on DOXP and possibly localized to the apicoplast (Ralph et al., 2004). TPP is an essential cofactor of the E1-subunit of the PDH-complex and the DOXP-synthase in the apicoplast as well as for the E1-subunit of the mitochondrial α-ketoglutarate dehydrogenase complex. However, experimental evidence from *Plasmodium* indicates that TPP synthesis is cytosolic (Knöckel et al., 2008; Wrenger et al., 2006, 2008). Homologs for the bacterial enzymes that use DOXP as precursor for TPP synthesis (ThiG, ThiH) cannot be found in the plasmodial genomes (Müller and Kappes, 2007). Consequently, an alternative route independent of DOXP is probably used for the synthesis of vitamin B1 in *Plasmodium*. It is currently unclear to what extent vitamin B1 synthesis occurs in other Apicomplexa since the respective genes are missing in *T. gondii* and *Eimeria* (Wrenger et al., 2008). The synthesis of vitamin B6 also appears to take place via a DOXP-independent pathway in *Plasmodium* and *T. gondii*, respectively (Knöckel et al., 2007; Müller et al., 2010).

In summary, the DOXP pathway is present in the apicoplast of all apicomplexan species studied to date, but it is unclear whether this pathway is required for any other purpose than isoprenoid production. Moreover, how TPP reaches the apicoplast and mitochondrion is currently unknown but likely depends on the uptake by a specific transporter. Further bioinformatic examinations as carried out on the predicted transportome of *P. falciparum* should help to identify such proteins (Martin et al., 2009).

The current view is that isoprenoids synthesized in the apicoplast are also used in other subcellular compartments of the parasite (although it is possible that the host-derived isoprenoid pool might be ''parasitized''). A study in *P. falciparum* provided evidence that Fos treatment of blood stage parasites decreased the levels of intermediates of ubiquinone and dolichol biosynthesis (Cassera et al., 2007), thus affecting pathways outside the apicoplast. How IPP/DMAPP could leave the organelle is currently not known. Although plants possess an additional cytosolic MEV pathway, it is well established that exchange of different MEP intermediates is possible between cytosol and chloroplast (Bick and Lange, 2003; Flügge and Gao, 2005; Hemmerlin et al., 2003). However, the molecular nature of the implicated transporters is ill defined. Transport of DOXP into chloroplasts is driven by an exchange with inorganic phosphate, possibly with the help of members of the plastidic phosphate translocator family, which includes the triose phosphate/phosphate translocator TPT (Flügge and Gao, 2005). Whether the reported fairly broad substrate specificity of PfTPT (Lim et al., 2010) also allows IPP/DMAPP transport needs to be investigated.

The enzyme farnesyl-pyrophosphate synthase (FFPS) that condensates IPP and DMAPP in the next step toward the formation of more complex isoprenoids is located in the mitochondrion of *T. gondii* (Ling et al., 2007). There, it is likely involved in the generation of precursor molecules for the isoprenyl modification of, for example, ubiquinone (de Macedo et al., 2002). This leaves open the question whether the mitochondrion-derived isoprenoids are used for the reported prenylation and farnesylation of cytosolic proteins in *T. gondii* and *P. falciparum* (Chakrabarti et al., 1998, 2002; de Macedo et al., 2003; Ibrahim et al., 2001; Kimmel et al., 2003; Tonhosolo et al., 2005; Wiesner et al., 2004).

5.2. Abscisic acid

A recent study revealed the unanticipated presence of high nanomolar concentrations of the plant hormone (+) abscisic acid (ABA) in *T. gondii* (Nagamune et al., 2008a). Nagamune et al. showed that ABA controls Ca^{2+}-mediated parasite egress from the host cell by production of the second-messenger cyclic ADP-ribose (cADPR). Administration of the known ABA synthesis inhibitor fluoridone to *T. gondii* cultures accelerated the developmental switch to the bradyzoite stage *in vitro* and also led to growth arrest in mice. The sensitivity to this compound is so far the clearest evidence that ABA biosynthesis takes place in *T. gondii* (and possibly also in *Plasmodium* sp., Nagamune et al., 2008a). In plants, the so-called indirect pathway is plastid-localized and starts formally from β-carotene (see Fig. 5.4) and proceeds through a number of hydroxylation and oxidation steps to the final product ABA (Nambara and Marion-Poll, 2005). Fluoridone acts on phytoene synthase, a step upstream of β-carotene synthesis, from the isoprenoid precursors IPP and DMAPP. ABA synthesis can thus be regarded as a continuation of this pathway (Fig. 5.2). In plants the last three steps, starting from xanthoxin, mark the cytosolic localization of the synthesis route (Fig. 5.4), whereas all earlier steps are confined to the plastid (Seo and Koshiba, 2002). In contrast, some fungi use a more direct pathway starting from farnesyl-diphosphate based on a very different chemistry and fewer steps to produce ABA (Inomata et al., 2004). Since neither pathway is very well defined at the molecular level, homology-based gene hunts in *T. gondii* and *Plasmodium* genomes have been of limited value to unravel how ABA is produced in apicomplexans (Nagamune et al., 2008b). It seems obvious, however, to assume that both parasites use the plant-derived route, given the fact that fluoridone targets phytoene synthase, which is absent in the fungal pathway.

Most recently, a bifunctional enzyme possessing octaprenyl pyrophosphate synthase as well as phytoene synthase activity has been described in *P. falciparum* (Tonhosolo et al., 2009). Strikingly, neither this nor the homologous proteins from other Apicomplexa show a predicted signal sequence, usually indicative of a plastid-targeting domain. Localization studies in *P. falciparum*

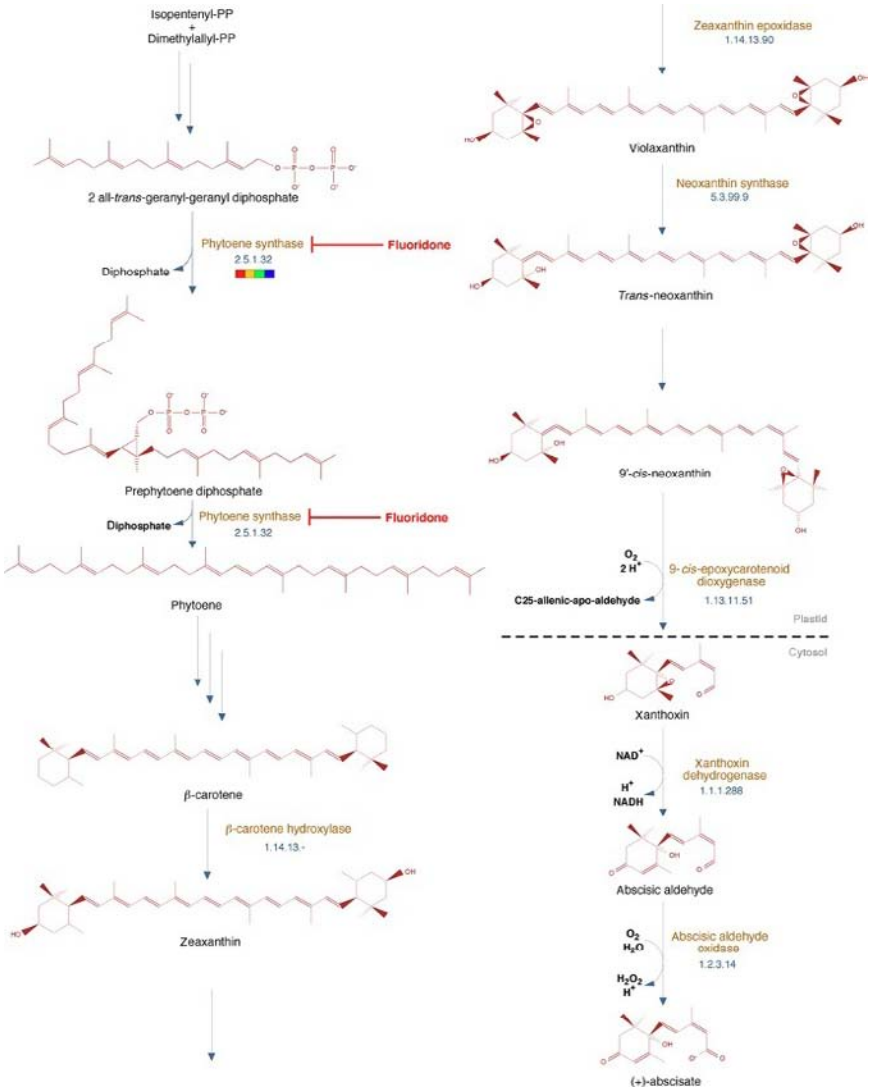

Figure 5.4 Abscisic acid synthesis in plant plastids. So far the only known enzymatic activity that can be assigned to known genes in Apicomplexa is the dual phytoene synthase/octaprenyl pyrophosphate synthase enzyme, which should also be the target of fluoridone.

were not very conclusive due to the low spatial resolution of the microscopic images provided, but a dual localization in both, mitochondrion and apicoplast, cannot be excluded at present (Tonhosolo et al., 2009). A more definitive assessment of the localization and the importance of ABA synthesis

in apicomplexans still await further investigations. Whether *P. falciparum* and other apicopmplexans also use carotenoid synthesis as a precursor for ABA production or if this pathway has been retained as a generator of antioxidant activity needs to be clarified. The recent *in vitro* reconstitution of the signaling pathway subsequent to ABA generation in plants should be instrumental to the elucidation of the signaling process occurring in apicomplexans (Fujii et al., 2009).

5.3. Fatty acids

Fatty acids (FA) play fundamental roles in any living cell, serving as building blocks of membrane lipids and also as energy storage molecules; for posttranslational modifications of proteins, precursors for second messengers and cofactors, etc. Apicomplexa have presumably a high demand for lipids and phospholipids since, in addition to the usual eukaryotic membrane-bound compartments like nucleus, ER, Golgi, and mitochondria, they possess a number of additional unique organelles such as micronemes, rhoptries, dense granules, the apicoplast, the pellicular complex, and the growing parasitophorous vacuole membrane (Bisanz et al., 2006; Charron and Sibley, 2002; Coppens and Vielemeyer, 2005; Krishnegowda and Gowda, 2003).

Most organisms are capable of synthesizing FA of different lengths but this can be achieved in two different ways. The eukaryotic fatty acid synthase type I (FAS I) combines all enzymatic steps for FA synthesis in one huge cytosolic multifunctional "nanomachine" (2.6 MDa in yeast and 540 kDa in animals; Leibundgut et al., 2008) which essentially produces palmitate (C_{16}). In contrast, the individual steps of the prototypic bacterial FA synthesis is carried out by distinct protein entities (dissociated or bacterial-type, FAS II; White et al., 2005) and the chain length produced is usually C_8 and longer. This dissociated FAS type is not confined to bacteria only but also found in mitochondria of many eukaryotes (Hiltunen et al., 2010) where it mainly provides the octanoic acid precursor for the biosynthesis of the essential cofactor lipoic acid (LA) (see below). Nevertheless, the underlying biochemistry for both FAS pathways is the same (Fig. 5.5), and the intermediates of each step are taken over by the next enzyme entity. In general, synthesis of palmitate (C_{16}) can be summarized by the following equation:

$$\begin{aligned}&\text{acetyl} - \text{CoA} + 7\,\text{malonyl} - \text{CoA} + 14\,\text{NADPH} + 14\,\text{H}^+ \Rightarrow\\ &\text{palmitoic acid}\,(\text{C}_{16}) + 7\,\text{CO}_2 + 8\,\text{CoA} + 14\,\text{NADP}^+ + 6\,\text{H}_2\text{O}\end{aligned}$$

In addition, the generation of seven molecules of malonyl-CoA, starting from acetyl-CoA, consumes seven ATP:

$$\begin{aligned}&7\,\text{acetyl} - \text{CoA} + 7\,\text{ATP} + 7\,\text{HCO}^{3-} + 7\,\text{H}^+ \Rightarrow\\ &7\,\text{malonyl} - \text{CoA} + 7\,\text{ADP} + 7\,\text{P}_\text{i}\end{aligned}$$

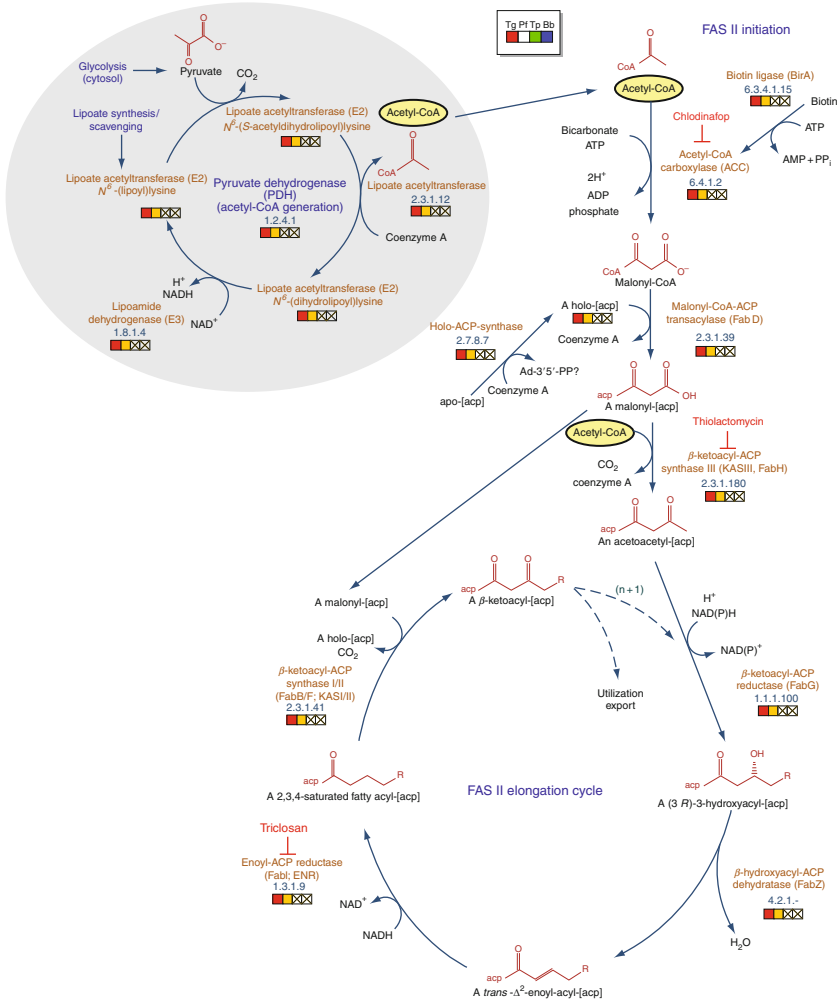

Figure 5.5 Generation of acetyl-CoA and its connection to fatty acid synthesis in the apicoplast. Depicted are the individual reactions of the PDH complex at the lipoylated E2-subunit that result in the decarboxylation of pyruvate, and the transfer of the activated acetyl group to coenzyme A (top left). The resulting acetyl-CoA serves for the generation of malonyl-ACP and also for the initiation of the first elongation cycle (top right). In subsequent cycles, only malonyl-ACP is fed in at the FabB/F step (elongation cycle). After several cycles the respective even-numbered FA-ACP is likely utilized in the apicoplast and possibly exported in undefined way(s). Known enzyme inhibitors are indicated.

Thus, FA synthesis is an energy-hungry process and it is therefore not surprising that apicomplexan parasites have found different ways to minimize this expenditure (see below).

The bacterial-type FAS II was the first metabolic pathway that could be assigned to the apicoplast, based on gene sequence comparisons and targeting experiments (Waller et al., 1998). Waller et al. showed that in *T. gondii* and *P. falciparum*, FAS II enzymes FabH, FabZ, and ACP are nuclear-encoded proteins that are targeted for transport to the apicoplast via N-terminal extensions (Waller et al., 1998). This feature and the high level of sequence homology to the respective bacterial enzymes has allowed the complete annotation of apicomplexan FAS II genes and predicted their targeting to the apicoplast. Like the isoprenoid pathway, the general biochemistry of the individual reactions is very similar to the bacterial steps (White et al., 2005). For in-depth reviews on the apicomplexan FAS II pathway, see Gornicki (2003), Surolia et al. (2004), Goodman and McFadden (2007), and Mazumdar and Striepen (2007).

The complete FAS II pathway is dependent on three vitamins/cofactors that have to reach the apicoplast: biotin, pantothenic acid (PA), and LA. The biotin carboxylase domain of the acetyl-CoA carboxylase (ACC) requires biotinylation for activity; a similar modification occurs by LA at the E2-domain of the PDH (see below), and the activated acyl groups are attached to the acyl carrier protein (ACP) via a coenzyme A (CoA)-derived pantothenate linker (Perham, 2000) (Fig. 5.5). While the synthesis of LA takes place in the apicoplast (see below), biotin and PA are scavenged from the host cell and their transport into the organelle has not been elucidated to date (Spry and Saliba, 2009).

Comparative analysis of the completed genomes of different apicomplexans revealed the absence of FAS II in the apicoplast of *Theileria* sp. and *B. bovis* (Table 5.4). These parasites not only lack the genes corresponding to FAS II but also those coding for proteins functionally connected to it, including the members of the PDH complex, the proteins required for LA synthesis and LA and biotin ligation (BirA, LipA, LipB, LplA2) (see below and Fig. 5.5). The implication of this loss for these organisms is the necessity to scavenge FA from their host cells. This is presumably facilitated by the rapid disappearance of a parasitophorous vacuole membrane (PVM) following invasion, which allows more direct access to host FA and at the same time a lower demand for FA and lipids for its maintenance and growth. *Plasmodium* sp., on the other hand, was long thought to be dependent on its FAS II during the erythrocytic cycle since a number of different compounds known to inhibit bacterial FAS II enzymes (like the FabI-inhibitor triclosan) were reported to have a strong parasiticidal activity *in vitro* and also against *P. berghei* in the mouse *in vivo* model (Surolia and Surolia, 2001; Waller et al., 2003). This view was recently challenged by two studies that generated FAS II gene knockouts in *P. falciparum* as well as *P. berghei* and *P. yoelii* (Tarun et al., 2009; Vaughan et al., 2008; Yu et al., 2008). Initially, an absence of correlation was observed with derivatives of triclosan showing improved and potent inhibitory activity against the recombinant FabI enzyme but poor

in vitro activity on infected erythrocytes. Subsequent genetic deletion studies of FabI (Vaughan et al., 2008; Yu et al., 2008) as well as FabB/F and FabZ (Vaughan et al., 2008) proved that each of the enzymes and thus the whole FAS II pathway was dispensable for growth of the erythrocytic stages. However, FA synthesis proved to be essential in the late hepatic stage that precedes merosome formation, indicating that these liver-stage parasites have a requirement for endogenous FA that cannot be supplied in enough quantity or quality by the host cell or by the parasite FA elongases (Tarun et al., 2009). Likewise, knockout of the *P. yoelii* E1α or E3 subunits of the PDH complex result in similar phenotypes (Pei et al., 2010). Glycosyl-phosphatidylinositol-anchors, neutral glycerolipids, and phospholipids seem to be among those FAS II-dependent molecules responsible for the observed phenotype in the knockout strains (Yu et al., 2008). In contrast to liver stages, FAS II-deficient blood-stage parasites seem to be able to fully compensate for the loss of FA synthesis by importing and salvaging host FA. These can obviously be elongated and desaturated by parasite-encoded elongases, desaturases, and acyl-CoA synthases to C_{16}–C_{18} and $C_{16:1}$, $C_{18:1}$ FA (Gratraud et al., 2008; Hashimoto et al., 2008; Mazumdar and Striepen, 2007; Yu et al., 2008). *T. gondii* is also known to import host-derived FA (Charron and Sibley, 2002) whereas *T. parva* and *B. bovis* should have direct access to host FA since no vacuolar membrane restricts their access to the parasite.

The above results raise the question how triclosan and other FAS II inhibitors affect the blood stages of *P. falciparum* at the molecular level if FAS II is not the target. Triclosan is known to kill *T. parva* and *Babesia*, although at fairly high concentrations (IC_{50} = 20–300 μM) (Bork et al., 2003; Lizundia et al., 2009). Given that both parasites lack the FAS II, off-targets must be considered as an explanation for the observed effect. Triclosan was reported to be very effective in killing tachyzoites *in vitro* and *in vivo* (McLeod et al., 2001). Notably, no triclosan-resistant parasites could be generated in a transgenic strain overexpressing a putative triclosan-insensitive FabI gene (Crawford et al., 2006). However, the conditional knockout of TgACP that codes for the essential acyl group carrier (Fig. 5.5) in *T. gondii* provided firm evidence that in this parasite, the FAS II pathway is essential for survival, both in tissue culture and in the mouse model (Mazumdar et al., 2006). It points again to significant off-target effects of triclosan in killing apicomplexan parasites.

To what extent and how FA are exported from the apicoplast is currently uncertain; however, the recently described membrane contact sites between apicoplast and ER could play an important role in this respect (Tomova et al., 2009), similar to the situation in plant plastids (Benning, 2009). In this regard, it is noteworthy that the gene previously suspected to be an apicoplast-resident stearoyl-CoA desaturase (PFE0555w) in *P. falciparum* (Ralph et al., 2004) has recently been localized to the ER

(Gratraud et al., 2008). Apicoplast-resident acyl-ACP thioesterase-like proteins have not been described in any apicomplexan genome but are expected to be required for release of FA from ACP to allow their subsequent traversal of the apicoplast membranes, as it is the case in plant plastids (Benning, 2009; Koo et al., 2004). There is clearly a gap of knowledge regarding the traffic of FA in apicomplexans.

5.4. Lipoic acid

As mentioned in the previous section, the PDH-complex converts glucose-derived PEP via pyruvate to acetyl-CoA in the apicoplast, and the enzymatic activity of the complex relies on an E2 subunit that is modified by LA at a specific lysine residue within a characteristic lipoylation domain (Perham, 2000). PDH and proteins involved in this lipoylation process are therefore usually in the same compartment, as it is the case in mitochondria of eukaryotes that possess an acetyl-CoA-fueled TCA cycle. In plants, which possess PDH complexes in both FA synthesizing organelles (mitochondria and plastids), a lipoylating activity is found in both compartments (Yasuno and Wada, 2002). Unexpectedly, all four components of the PDH complex have been shown to be exclusively located in the apicoplast and are absent from the mitochondrion of *P. falciparum* and *T. gondii* (Crawford et al., 2006; Fleige et al., 2007; Foth et al., 2005). This unique situation has important functional consequences for mitochondrial metabolism, especially the TCA cycle (Seeber et al., 2008; Vaidya and Mather, 2009; van Dooren et al., 2006).

The knowledge on LA metabolism (detailed in Fig. 5.6) is primarily derived from studies on *E. coli*, but it seems that the biochemical principles are fairly similar in all eukaryotes examined to date (Cronan et al., 2005; Nesbitt et al., 2008) although some deviations exist (Ewald et al., 2007; Schonauer et al., 2009). The synthesis of LA, a dithiol-containing C_8 FA, is dependent on FAS II, which generates octanoyl-ACP as precursor (Fig. 5.6). This FA is then transferred onto the lysine residue in the apodomain of an acceptor protein like PDH-E2 by an octanoyl-(ACP):protein *N*-octanoyltransferase (LipB). In the following, chemically unique reaction, the enzyme lipoic acid synthase (LipA) converts the octanoyl group on the protein into LA by inserting two sulfur atoms successively at the C_8 and C_6 positions. It requires the assistance of *S*-adenosyl-L-methionine (SAM) radicals, and consequently LipA belongs to the large group of iron–sulfur cluster ([Fe–S])-containing radical SAM enzymes (Frey et al., 2008). Given all the reagents needed for LA synthesis (octanoyl-ACP, [Fe–S], SAM), it is considered as a highly energy-demanding process, and in consequence scavenging or recycling LA is certainly advantageous. Many organisms including the apicomplexans are thus exploiting this economically attractive alternative (Fig. 5.6). The enzyme lipoyl protein ligase A (LplA) can activate

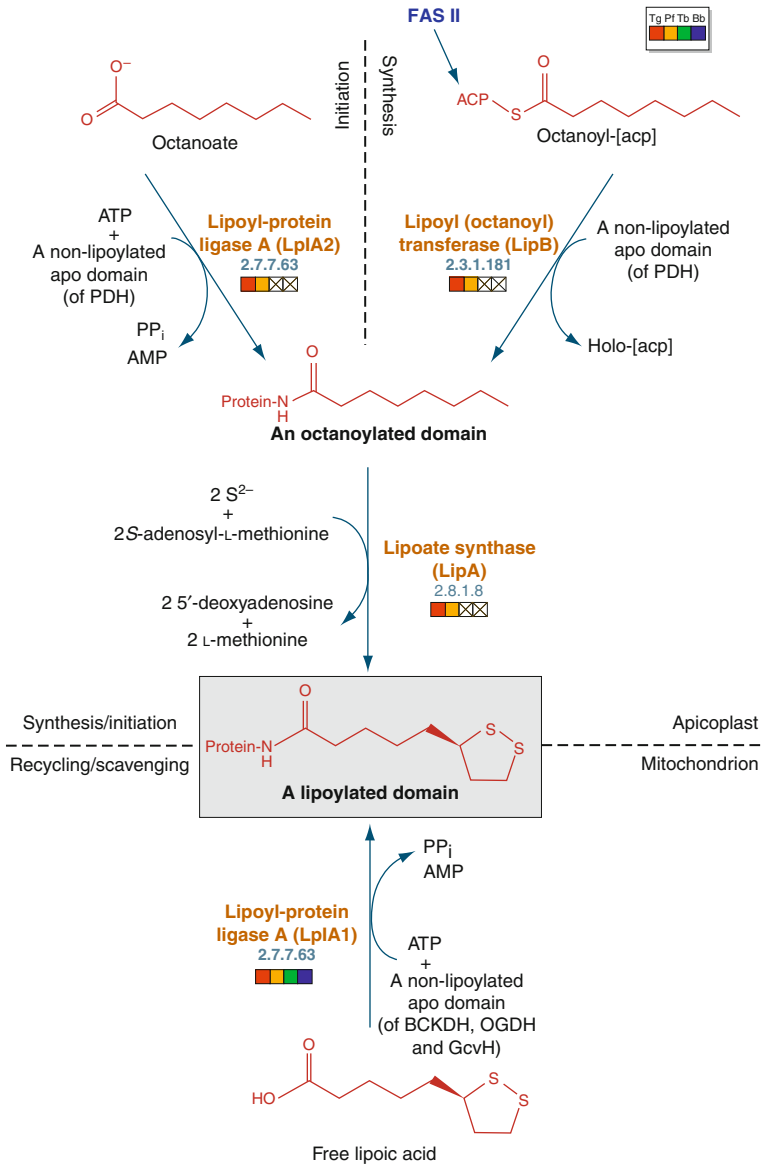

Figure 5.6 Lipoic acid metabolism in the apicoplast and mitochondrion of Apicomplexa. Top right depicts the synthesis of LA on PDH, with FAS II-derived octanoyl-ACP as precursor. On the left the hypothetical initiation of PDH lipoylation from free octanoate and the concerted action of LplA2 and LipA is shown. The sulfur for the LipA reaction is presumably donated by the iron–sulfur cluster of LipA (Cicchillo and Booker, 2005). At the bottom of the figure the insertion of free LA via LplA1 into the three known mitochondrial proteins requiring LA as cofactor is shown. See text for details.

free LA using ATP or GTP and then transfer the resulting compound onto the apo-domain (in mammals, activation and transfer is performed by two separate enzymes; Fujiwara et al., 2001). Thus, only one mole of ATP (GTP) is required per mole attached LA, which is definitely less than what is needed for LA synthesis.

Compartmentalization of LA metabolism in Apicomplexa has turned out to be more complex than initially anticipated when the first characterization of *T. gondii lipA* and *lipB* genes was published (Thomsen-Zieger et al., 2003) and the exclusive apicoplast localization of PDH in these organisms was not yet known. A new picture has emerged from several studies that investigated the localization of LipA, LipB, and two LplA isoforms (LplA1, LplA2) in *T. gondii* and *Plasmodium* (Allary et al., 2007; Günther et al., 2007, 2009a,b; Thomsen-Zieger et al., 2003; Wrenger and Müller, 2004).

As depicted in Figs. 5.5 and 5.6, nonlipoylated PDH is nonfunctional and thus no acetyl-CoA can be generated. Consequently, also LA cannot be synthesized and a potential "chicken-or-egg" problem arises. The described temporary localization of a LplA-like protein (PfLplA2) in the apicoplast of *P. falciparum* (Günther et al., 2007) could provide a reasonable solution to this dilemma since the starting LA molecules that could initially lipoylate and thus activate the PDH-complex do not have to be produced by FAS II. Instead, it could be derived from free octanoic acid (scavenged from the host or via recycling from internal sources, respectively) and possibly serving as a substrate for PfLplA2, similar to what has been described recently in *E. coli* (Hermes and Cronan, 2009) (Fig. 5.6). LipA could then insert the sulfur atoms, thereby generating LA bound to PDH-E2. In addition, LplA2 could recycle preformed LA. A long open reading frame coding for a protein related to PfLplA2 with a predicted mitochondrial targeting sequence is also present in *T. gondii*, and bimodal targeting of TgLplA2 to the mitochondrion and apicoplast might occur.

Once FAS II is operating it generates ACP-bound octanoate, attaches this with the help of LipB to the apo-domain of the E2-subunit of PDH, on which in the next step LipA performs the sulfur insertion. The currently available experimental data suggest that very little if any LA finds its way to the parasite's mitochondrion (Allary et al., 2007; Crawford et al., 2006) and since LipA and LipB are exclusively apicoplast-localized, the mitochondrion can be considered as auxotrophic for LA. As a consequence, the three enzymes that require lipoylation in the mitochondrion (the E2 subunits of the branched-chain ketoacid dehydrogenase, BCKDH, and of the α-ketoglutarate dehydrogenase, KGDH, as well as the H-protein of the glycine cleavage complex, GcvH) are dependent on LA transfer by LplA1, which is localized to the mitochondrion (Wrenger and Müller, 2004). The source of LA is most likely the host cell, and it is tempting to speculate that in the case of *T. gondii* the host mitochondria lining up at the vacuolar

membrane that surrounds the parasites can serve as immediate ''supplier'' of this cofactor and that the intimate contact between both compartments might be important for transfer of LA (Crawford et al., 2006). In the hepatic stage of *P. falciparum*, such a direct interaction is not readily apparent (Bano et al., 2007), but since hepatocytes are packed with mitochondria a more transient interaction might be sufficient for LA transfer. Since the level of LA in the blood is fairly high, the erythrocytic stages can readily obtain this metabolite from the host (Constantinescu et al., 1995; Teichert and Preiss, 1992). Taken together, LA metabolism is uniquely compartmentalized in *T. gondii* and *Plasmodium* sp. and it provides an example that not in every case the close physical contact of apicoplast and mitochondrion automatically translates into metabolite exchange. Phylogenetic analyses of LipA indicate that the selective loss of mitochondrial LipA and LipB occurred after the acquisition of the apicoplast (Crawford et al., 2006). Therefore, the dependence on host LA must have been compensated for by a gain of other, so far unknown advantages.

5.5. Iron–sulfur clusters

Iron–sulfur clusters ([Fe–S]) are $Fe^{2+/3+}$ and S^{2-} ions, usually coordinated in various numbers and complexities to mainly cysteine or histidine residues in diverse protein domains (Meyer, 2008). Due to this flexibility in structure, number, and overall tasks, it is difficult to predict by sequence analysis alone which proteins contain [Fe–S] (Johnson et al., 2005). In all organisms, from bacteria to man, [Fe–S]-containing proteins play key roles in electron-donating and -sensing processes, but also as structural components (Johnson et al., 2005; Lill, 2009; Xu and Møller, 2008). In contrast to earlier views derived from *in vitro* reconstitution experiments of [Fe–S], it is clear now that [Fe–S] proteins do not form spontaneously *in vivo*. They rather require a coordinated interplay between a complex cellular machinery, consisting of various proteins in different cellular compartments. Most of the knowledge on [Fe–S] biogenesis has been acquired from studies performed in yeast and bacteria, but it seems that the underlying principle of this process is rather conserved in all organisms (Johnson et al., 2005; Lill, 2009). It basically consists of the assembly of the [Fe–S] derived from iron ions and sulfide (cysteine-derived by the action of a desulfurase) on a protein scaffold. This labile cluster is subsequently transferred either directly onto the target apo-protein or, in the case of eukaryotes, it is transported out of the mitochondrion prior to its transfer onto cytosolic or nuclear apo-proteins (Fig. 5.7).

In bacteria up to three machineries for [Fe–S] synthesis coexist in the same cell (so-called ISC, SUF, and NIF systems, respectively) with partially overlapping tasks. In eukaryotes, cellular compartmentalization in organelles, each having its own requirement for [Fe–S] proteins, has resulted

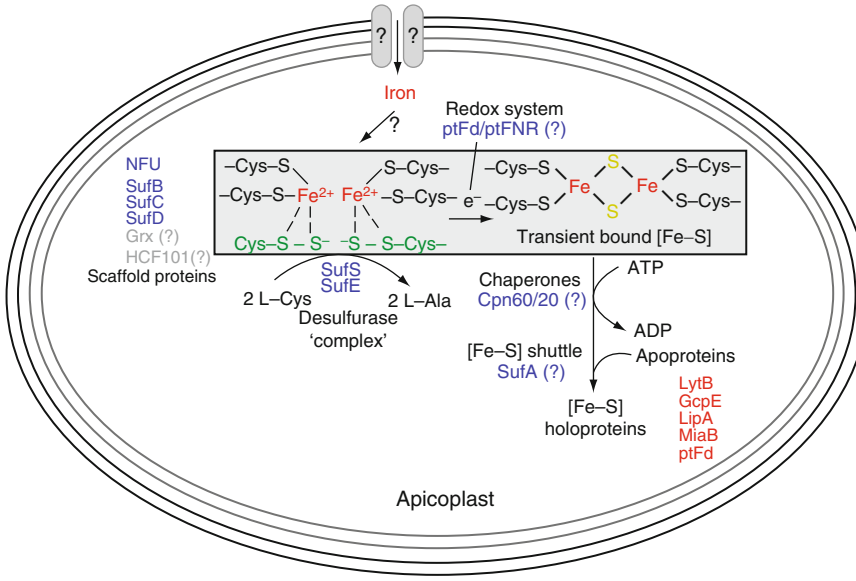

Figure 5.7 Hypothetical model for [Fe–S] biosynthesis in the apicoplast of *T. gondii* and *P. falciparum*, based on the current knowledge of the bacterial and plant SUF system. The basic concept of [Fe–S] formation on a scaffold protein/complex, with sulfide coming from desulfuration of cysteine, and the transfer of a labile, scaffold-bound [Fe–S] to the apoprotein with the aid of chaperones and a redox system is the same as in mitochondria, but the molecular players are different. Note that [Fe–S] synthesis in *Theileria* and *Babesia* involves apparently less proteins. See text for details.

in distinct but to some extent interdependent [Fe–S] generation and assembly systems (Lill and Mühlenhoff, 2008). The "raison d'etre" for separate organellar machineries is presumably that during protein transport through mitochondrial or plastid membranes, the polypeptide chains are unfolded and as a consequence [Fe–S] could either impair this process or the clusters could get lost during transport. Consequently, in plants four compartments (cytosol, nucleus, mitochondria, and plastids) are known to contain components required for distinct steps of the generation and/or final assembly of different types of [Fe–S]. Here we will focus entirely on the plastidial [Fe–S] biogenesis components, and the reader is referred to recent reviews that cover the bacterial, mitochondrial, cytosolic, and nuclear [Fe–S] synthesis pathways (Ayala-Castro et al., 2008; Johnson et al., 2005; Lill, 2009; Lill and Mühlenhoff, 2006, 2008; Meyer, 2008).

Compared to bacterial and mitochondrial [Fe–S] biogenesis, little is known on the plastidial process (Balk and Lobréaux, 2005; Kessler and Papenbrock, 2005; Pilon et al., 2006; Xu and Møller, 2008), and virtually nothing has been reported experimentally in the case of the apicoplast.

Obviously, a number of proteins are required to allow this process to proceed in a coordinated fashion, and apparently the bacterial SUF system (a stress-responsive [Fe–S] assembly system in bacteria; Johnson et al., 2005) and its accessory proteins are the major players in plastids (Balk and Lobréaux, 2005), and based on bioinformatic analyses also in the apicoplast (Ellis et al., 2001; Seeber, 2002) (Table 5.5). The least debated step in this pathway is the generation of sulfide from L-cysteine by the desulfurase SufS, in complex with its activator and final sulfide transferase SufE (Layer et al., 2007). The actual iron donor for the [Fe–S] as well as how Fe ions enter the organelle is unknown. SufSE passes on the sulfide to the scaffold protein(s) for assembly of the transient [Fe–S]. At this point, the nature and number of proteins being involved is unclear. One class of proteins able to coordinate

Table 5.5 Known and presumed proteins involved in plastid [Fe–S] biogenesis (top) and currently known [Fe–S]-containing proteins in the apicoplast with their presumed type of [Fe–S] (bottom)

[Fe–S] biogenesis[a]	Putative function
NFU	NifU-like scaffold protein
ptFd	Plant-type ferredoxin
ptFNR	Plant-type ferredoxin-NADP reductase
SufA	[Fe–S] transfer protein[b]
SufB	ABC transporter[b]
SufC	ABC transporter[b]
SufD	Unknown, complexed with SufB, C[b]
SufE	Desulfurase activator and sulfide "transferase"[b]
SufS	Cysteine desulfurase
Hcf101 (?)	Scaffold protein for [4Fe–4S]
Cpn60 (?)	Chaperone 60
Cpn20 (?)	Chaperone 20
GrxS 14, 16 (?)	Glutaredoxin-like scaffold protein
Apicoplast [Fe–S] proteins[a,c]	
LipA	Lipoic acid synthase[b] [4Fe–4S]
LytB	(*E*)-4-Hydroxy-3-methyl-but-2-enyl diphosphate reductase [4Fe–4S]
GcpE	1-Hydroxy-2-methyl-2-(*E*)-butenyl-4-diphosphate synthase [4Fe–4S]
MiaB	Dimethylallyl adenosine tRNA methylthiotransferase [4Fe–4S]
ptFd	Plant-type ferredoxin [2Fe–2S]

[a] For gene accession numbers see Table 5.4. (?) indicates uncertain roles in Apicomplexa.
[b] Absent in *T. parva* and *B. bovis*.
[c] Scaffold proteins could also be regarded as [Fe–S] proteins, but they only transiently bind [Fe–S], in contrast to ptFd, which also has functions outside [Fe–S] synthesis.

transient [Fe–S] are the so-called A-type carriers (Vinella et al., 2009), with SufA representing the SUF system. Initially considered a scaffold protein, the latest model supported by genetic and protein–protein interactions data suggests that SufA rather fulfills a shuttle function, transferring [Fe–S] from other scaffolds to apo-proteins (Chahal et al., 2009; Vinella et al., 2009). In the SUF system, this scaffold is a complex of the three proteins SufB, C, and D. Whether this model, as proposed for *E. coli*, is also valid as a main player for plastids remains to be determined.

In light of recent studies, it became clear that different scaffold proteins are involved in the generation of different forms of [Fe–S] (like [2Fe–2S], [4Fe–4S], etc.). At least one more potential scaffold protein, the U-type carrier NFU, could be involved in the assembly of a different set of [Fe–S] in the apicoplast. Furthermore, HCF101-like proteins are P-loop NTPases that have recently been implicated in the assembly of [4Fe–4S] proteins in plant plastids, thereby acting as a scaffold protein for the assembly of this type of cluster (Lezhneva et al., 2004; Schwenkert et al., 2009). In the apicoplast, at least four proteins contain [4Fe–4S], based on the known cluster types from other organisms (see Table 5.5), and therefore it would be important to know whether HCF101-like proteins could fulfill the function of a [4Fe–4S] scaffold protein in this organelle.

Four classes of HCF101-like proteins have been defined based on sequence features that are found in either bacterial, mitochondrial, cytosolic, or plastid proteins, respectively (Lezhneva et al., 2004; Schwenkert et al., 2009). Genes coding for HCF101-like proteins are present in the genomes of all Apicomplexa including *C. parvum* (Fig. 5.8). The subcellular distributions of these proteins have been tentatively predicted based on the classification of Schwenkert et al. The combined results of our analysis are shown in Fig. 5.8. A number of features would mark the HCF101-like sequences from *T. gondii*, *P. falciparum*, and *C. parvum* as class I (plastid-localized) isoforms (Fig. 5.8A and B): the exchange of a cysteine for a glycine in the P-loop sequence, the presence of two protein domains of unknown function (DUF59 at the N-terminus and DUF971 at the C-terminus), the absence of an otherwise conserved tryptophan in signature 2 as well as the phylogenetic clustering of the core sequence of HCF101 (without the DUF sequences). However, other sequence characteristics are not easily reconciled with this assignment: (i) absence of a predicted targeting signal that would indicate an apicoplast localization; (ii) the patterns of other cysteine residues differ from those conserved in plant HCF101; (iii) the proteins found in *B. bovis* and *T. parva* clustering with the plant sequences lack the DUF domains; and (iv) these proteins are also found in organisms that lack a plastid (like *C. parvum* and *Paramecium*; although both might have secondarily lost the organelle; Keeling, 2009). Moreover, a second HCF101-like isoform exists in all Apicomplexa, including *Cryptosporidium*, for which a signal peptide sequence is predicted for most of them

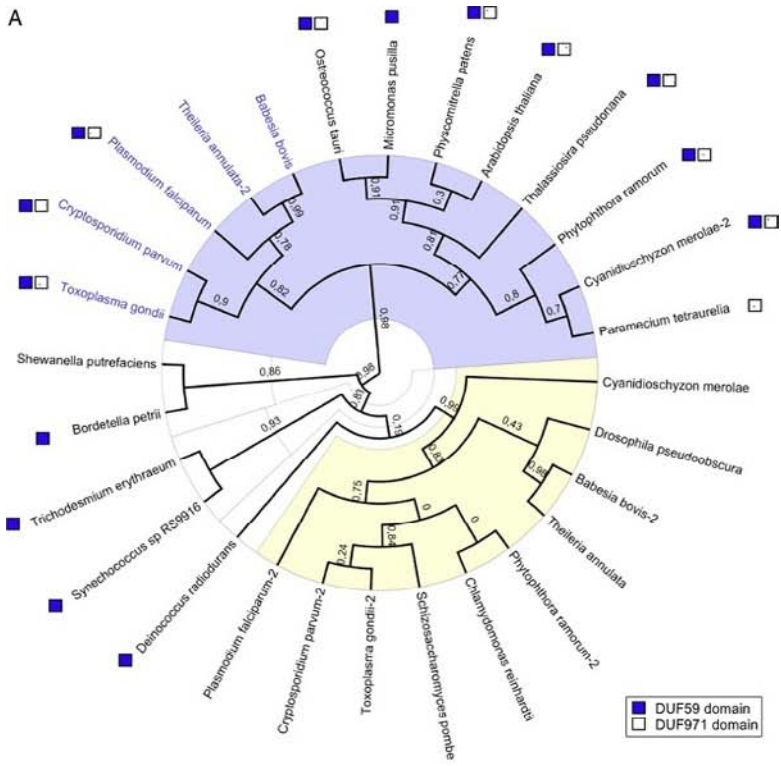

Organism	P-loop	Signature 2	TargetP	SignalP HMM	PProwler plant	PProwler non-plant	Predotar
P. falciparum-2	SGKGGVGKS	VIRGPKK	s	s	s	m	er
T. gondii-2	SGKGGVGKS	VVRGPKK	m	s	s		
T. annulata	SGKGGVGKS	ISRGAKK					
B. bovis-2	SGKGGVGKS	VVRGPKK	s		s		
C. parvum-2	SGKGGVGKS	VIRGPKK	s		s		er
P. ramorum-2	SGKGGVGKS	IIRGPKK					
C. merolae	ANKGGCGKS	VARGARK					
C. reinhardtii	SGKGGVGKS	VIRGPRK	c	s			
D. pseudoobscura	SGKGGVGKS	VIRGPKK					
S. pombe	SGKGGVGKS	VIRGPKK					
S. putrefaciens	SGKGGVGKS	AVRGPMA					
T. erythraeum	SGKGGVGKS	VIRGPML					
B. petrii	SGKGGVGKS	MIRGPMA					
D. radiodurans	SGKGGVGKS	LVRGPML					
Synechococcus sp	SGKGGVGKS	VIRGPML					
B. bovis	SGKGGVGKS	AAYRGPII					
T. annulata-2	SGKGGVGKS	SAYRGPIV					
P. falciparum	SGKGGVGKS	SSFRGPIL					
T. gondii	SGKGGVGKS	SALRGPFA					
C. parvum	SGKGGVGKS	SILRGPIA					
T. pseudonana	SGKGGVGKS	AIMRGPMV					
O. tauri	SGKGGVGKS	AIMRGPMV					
C. merolae-2	SAKGGVAKS	AMLRGPMV		s	m		c
P. tetraurelia	SGKGGVGKS	AIIRGPMV	s		m		m
P. ramorum	SGKGGVGKS	AVMRGAMV	m		m	m	m
A. thaliana	SGKGGVGKS	AIMRGPMV	c		c	m	
P. patens	SGKGGVGKS	AIMRGPMV	c		c		c
M. pusilla	SGKGGVGKS	AIMRGPMV	c	s	c	m	c

Figure 5.8 Phylogenetic clustering and sequence signatures of apicomplexan HCF101-like proteins. (A) Phylogenetic analysis of selected sequences was performed with the Phylogeny.fr server (Dereeper et al., 2008) using MUSCLE for alignment and PhyML for clustering. Numbers denote the statistical support for branch points (using aLRT as test). The HCF101 proteins from plastid-bearing organisms and one of the

by one or the other algorithm but otherwise lack features of the plastid-type HCF101 proteins (Fig. 5.8B). Taken together, it is currently unclear where in the apicomplexan cell the HCF101-like proteins reside in.

Glutaredoxins GrxS 14 and 16 belong to another class of [2Fe–2S] scaffold proteins located in plant plastids (Bandyopadhyay et al., 2008; Rouhier et al., 2010). Grx are thiol-disulfide oxidoreductases with a 3D-fold similar to thioredoxin and a Cxx[C/S] active site motif. The apicomplexans possess Grx-like sequences, but again sequence analysis alone is not sufficient to draw conclusions as to where in the cell the proteins are located and hence to infer their possible function (data not shown).

The two chaperones, Cpn60 and Cpn20, have been experimentally characterized in *P. falciparum* (Sato and Wilson, 2004, 2005); however, no data have been published from Apicomplexa or plants that would indicate an involvement of these proteins in the assembly of the labile [Fe–S] on the scaffold protein or in the subsequent transfer to apo-proteins (Weiss et al., 2009; see Fig. 5.7). In contrast, in the mitochondrial and bacterial systems, type I (DnaK-like) chaperones have been implicated in [Fe–S] assembly (Vickery and Cupp-Vickery, 2007), and an involvement of this class of proteins in the apicoplast would also be plausible. Although Cpn20 is annotated as mitochondrial in ToxoDB, an alternative gene model predicts the presence of a signal peptide, suggesting its localization in the apicoplast (Sato and Wilson, 2005). A similar predicted signal is found in the *B. bovis* and *T. parva* Cpn20 sequences.

The involvement of the plant-type ferredoxin redox system (ptFd/FNR) (Vollmer et al., 2001) in the biogenesis of [Fe–S] in plastids has been postulated (Seeber et al., 2005). ptFd/FNR can be considered a likely functional homolog of the mitochondrial ferredoxin (adrenodoxin) or the bacterial ferredoxin/flavodoxin redox systems, based on structural and biochemical features (Wan and Jarrett, 2002; Zanetti et al., 2001). The bacterial FNR shows significant structural similarity to ptFNRs that include the apicomplexan enzymes (Aliverti et al., 2008). Although Fd is not an essential protein in *E. coli*, it is located in the ISC operon in many bacteria. Moreover, reduced *E. coli* Fd can efficiently donate electrons to flavodoxins Fld1 and Fld2 (Wan and Jarrett, 2002), and since Fld1 is essential (Gaudu

apicomplexan isoform clearly cluster together with high statistical support (green/dark background) and most of them also contain the DUF59 and DUF971 domains. (B) The same sequences also group together when sequence conservation in the P-loop and signature 2, respectively, is compared (green/dark background). However, subcellular localization prediction based on N-terminal targeting sequences is at odds with those apicomplexan sequences being apicoplast-localized since they show no signal peptide prediction by any algorithm (TargetP and SignalP HMM at http://www.cbs.dtu.dk/services/; PProwler at http://pprowler.imb.uq.edu.au/; Predotar at http://urgi.versailles.inra.fr/predotar/predotar.html). For details see text.

and Weiss, 2000) this could explain the dispensability of EcFd. To date the precise role of Fd in [Fe–S] biogenesis has not been elucidated in any system, possibly due to experimental limitations owing to the vital role Fd is playing as electron donor also in other cellular processes. However, at various sites of [Fe–S] synthesis would electrons be required, like (i) reduction of iron ions, (ii) the generation of sulfide from cysteine-derived S_0 sulfur, (iii) possibly the release of the labile clusters from the scaffolds, or (iv) the proposed fusion of two [2Fe–2S] clusters to form a single [4Fe–4S] cluster (Lill, 2009). Moreover, even the most reduced organellar [Fe–S] systems, like those found in the protists *Giardia* sp., *Trichomonas vaginalis* or the microsporidian *Encephalitozoon cuniculi*, contain [2Fe–2S]-based Fd redox systems (Goldberg et al., 2008; Tachezy et al., 2001).

The genomes of *Theileria* and *Babesia* predict at least four apicoplast-targeted [Fe–S] proteins (LytB, GcpE, ptFd, and MiaB; see Table 5.5), suggesting that [Fe–S] synthesis must occur in their apicoplast (Gardner et al., 2005; Seeber, 2002). However, these apicomplexans only contain a SufS-like desulfurase gene and an NFU-like scaffold protein but lack all the other Suf components that are known in other systems to enhance SufS' activity (SufE and the SufBCD complex) (Ayala-Castro et al., 2008) and that are present in *T. gondii* and *Plasmodium* sp. A plastid-targeted tRNA thiolation enzyme (MnmA) showing considerable sequence homology with the sulfur-binding domain of SufE in its unique N-terminal domain was postulated to substitute for the function of SufE (Gardner et al., 2005). Alternatively, some organisms appear to get along with only a desulfurase and a scaffold protein for [Fe–S] synthesis, like *Helicobacter pylori* and *Entamoeba histolytica* (Ali et al., 2004; Olson et al., 2000). In addition, the 3D structure of the scaffold protein IscU of *Haemophilus influenzae* has strong structural homology to the known structure of SufE from *E. coli*, despite the absence of significant primary sequence identity between the two proteins (Ayala-Castro et al., 2008). It is therefore plausible that the *Theileira* NFU-type scaffold proteins could act like a SufE-type protein for SufS activation. Taken together, [Fe–S] biosynthesis in *Theileria* and *Babesia* seems to operate in the apicoplast, although presumably quite differently compared to *T. gondii* and *P. falciparum*. They represent attractive systems to investigate deviations from the general route of [Fe–S] synthesis.

5.6. Heme

Among the known biochemical pathways in the apicoplast, the biosynthesis of heme is unique in many respects. This pathway is split between the apicoplast and the mitochondrion and also the cytosol. This is strikingly contrasting with animals where heme biosynthesis is exclusively mitochondrial (Heinemann et al., 2008), and with plants where it resides in large part

in the plastid (Tanaka and Tanaka, 2007). In apicomplexans, the phylogenetic origins and localizations of the individual enzymes reflect a mosaic of plant and animal pathways. For instance, the HemC, HemE and ferrochelatase (FC) are of proteobacterial origin (Oborník and Green, 2005) and hence would be expected to be mitochondrial but they have instead been shown to be targeted to the apicoplast in *P. falciparum* (Table 5.6).

Heme is a cyclic tetrapyrrole complexed with iron and found as a prosthetic group in several essential proteins, including catalase and cytochromes. Since cytochromes and cytochrome *c* oxidase are present in the genomes of all Apicomplexa, heme biosynthesis is anticipated to be important, although a complete set of enzymes is only found in *Plasmodium* sp. and, in contrast to a statement in a recent publication (Wasmuth et al.,

Table 5.6 Experimentally confirmed localization of the enzymes involved in heme metabolism in *P. falciparum* and *T. gondii*

	P. falciparum		*T. gondii*	
Enzyme	Experimental localization[a]	References	Experimental localization[a]	References
HemA (ALAS)	m	Varadharajan et al. (2002), Sato et al. (2004)	m	Wu (2006)
HemB (ALAD)	a	Sato et al. (2004)	a	Wu (2006)
HemC (PBGD)	a	Sato et al. (2004)	a	Wu (2006)
HemD (UROS)	?[b]		a	Wu (2006)
HemE (UROD)	a	Nagaraj et al. (2009a)	c	Wu (2006)
HemF (CPO)	c	Nagaraj et al. (2009b)	c	Wu (2006)
HemY (PPO)	?	–	m	Wu (2006)
HemH (FC)	m	Nagaraj et al. (2009c), van Dooren et al. (2006)	m	Wu (2006)
HO	a (?)	Okada (2009)	?	–
CCHL/ CC_1HL	?	–	?	–

[a] a, apicoplast; m, mitochondrion; c, cytosol; ?, unknown.
[b] Function presumably taken over by HemC (see also text for details).

2009), also in *T. gondii* (Wu, 2006; see also Table 5.4). However, *B. bovis* and *T. parva* appear to lack heme biosynthesis entirely and it remains to be determined whether the host cells they reside in serve as a plausible source for heme. Unexpectedly, *B. bovis* possesses a single enzyme of the pathway, HemB (ALAD), but its functional significance in heme metabolism is unknown. A considerable number of prokaryotes are unable to synthesize heme and do not appear to possess a known system for its uptake (Cavallaro et al., 2008). Interestingly, archaebacteria that lack HemE, F, G, and H can synthesize protoheme IX via a shortcut, the so-called precorrin-2 pathway (Buchenau et al., 2006). *Babesia* would still require the presence of HemC and D proteins to adopt such a strategy. Alternatively, membrane-localized heme uptake systems (mostly for the acquisition of iron) have been described in bacterial and eukaryotic species (Krishnamurthy et al., 2007; Shayeghi et al., 2005), and since both *Theileria* and *Babesia* replicate freely in the cytosol, the presence of such an uptake mechanism at the parasite plasma membrane could be a plausible scenario.

The overall biochemistry of apicomplexan heme biosynthesis at each individual enzymatic steps apparently does not deviate much from other organisms (Heinemann et al., 2008; Ralph et al., 2004; Tanaka and Tanaka, 2007; Wilson, 2005), unless otherwise noted below. In *P. falciparum* and *T. gondii*, heme synthesis starts in the mitochondrion with an enzymatic reaction also occurring in animals, fungi, or α-proteobacteria (for details see Fig. 5.9 and Table 5.6). The enzyme δ-aminolevulinate synthase (ALAS) utilizes glycine and succinyl-CoA to generate 5-aminolevulinate (ALA). The overall importance of the TCA cycle for energy generation in Apicomplexa is still unclear (Seeber et al., 2008; Vaidya and Mather, 2009; van Dooren et al., 2006); however, the need for succinyl-CoA for this first step in heme synthesis might justify its maintenance. The next three steps are catalyzed by HemB, HemC, and HemD and presumably take place in the apicoplast of both *T. gondii* and *P. falciparum*. The localization as well as the phylogenetic clustering of these enzymes (Wu, 2006) mark these steps as plastidial in origin. HemD (uroporphyrinogen-III synthase) was originally thought to be absent in *Plasmodium* sp.; however, a recent study has provided experimental evidence that the recombinant PfHemC also possesses HemD activity, thus filling this apparent "pathway hole" (Nagaraj et al., 2008). Notably, a recent bioinformatic approach set out to close such gaps identified a plasmodial sequence (PFL2285c) with a C-terminal part resembling a HemD domain (Mohanty and Srinivasan, 2009). Further experimental investigations will be required to determine if this protein has the predicted activity. The subcellular compartments where the next three steps take place are either uncertain or appear to differ between *P. falciparum* and *T. gondii* (Table 5.6). HemE is found in the apicoplast of *P. falciparum* and in the cytosol of *T. gondii*, whereas HemF is cytosolic in both parasites. Localization of HemY is unknown in *Plasmodium* and targets to the mitochondrion in

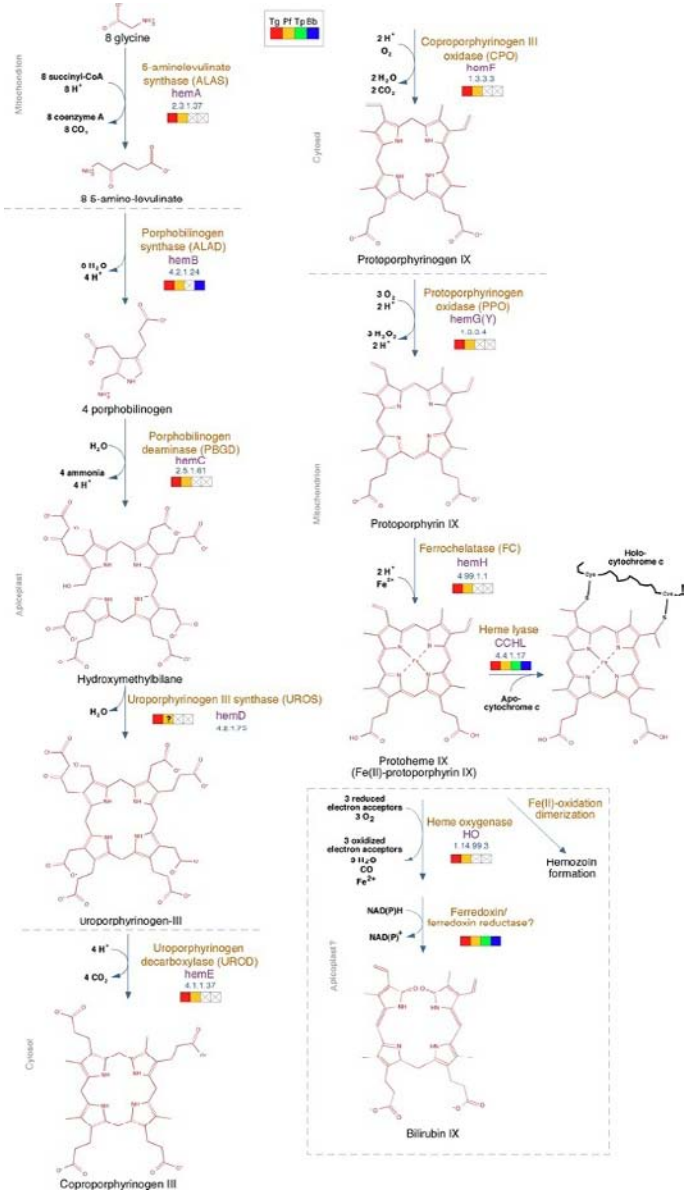

Figure 5.9 Heme synthesis and metabolism in Apicomplexa. The indicated intracellular compartments where the individual steps occur are those for *T. gondii* (see also Table 5.6). The boxed part indicates degradation of protoheme IX via heme oxygenase. For completeness, heme detoxification via hemozoin formation of heme in erythrocytic stages of *Plasmodium* (derived from engulfed host hemoglobin degradation) is also indicated (Egan, 2008).

T. gondii. The localization of the last enzyme FC has been a matter of debate for some time but is now assumed to be mitochondrial in both parasites (Nagaraj et al., 2009c; van Dooren et al., 2006; Wilson, 2005). The apicomplexan FC lack sequence motifs known in other organisms to coordinate a [2Fe–2S] but which is not strictly required for activity (Dailey and Dailey, 2002; Sato and Wilson, 2003; Shepherd et al., 2006).

Two genes annotated as cytochrome *c* (c_1) heme lyase (CCHL; also called cytochrome *c* synthetase) are found in all apicomplexans. These proteins covalently attach heme to cytochrome *c* and c_1 and are found in the intermembrane space of mitochondria (Hamel et al., 2009; Kranz et al., 2009). Their substrate specificity for the parasite cytochromes has not been determined. While the sequence motif implicated in heme binding (CPx) was reported to be absent in the *P. falciparum* CC_1HL protein (Bernard et al., 2003), this is not consistently observed with the other parasite sequences.

As a consequence of the extensive compartmentalization of the heme biosynthesis pathway, several intermediates have to cross multiple membranes. Due to the charged propionyl side chains, the tetrapyrroles are considered unable to diffuse through lipid bilayers (Krishnamurthy et al., 2007). Consequently, how the heme intermediates are transported between the organelles of Apicomplexa is currently a mystery. There is no molecular evidence in the parasites for a so-called type II, CcsA/B-based cytochrome *c* synthesis and transport system typically found in plastids and some bacteria (Allen et al., 2008; Hamel et al., 2009; Hamza, 2006; Kranz et al., 2009). These two proteins act in concert, forming a channel for heme in the bacterial or plastid membrane and at the same time participate in the covalent attachment of heme to a conserved CXXCH sequence motif in cytochrome *c* (Frawley and Kranz, 2009). ABC-type transporters as well as other solute transporters have been implicated in heme export/import processes in mammals (Hamza, 2006; Krishnamurthy et al., 2007). The close physical association between the apicoplast and the mitochondrion might underscore the existence of general metabolite channeling between the two organelles. In *P. falciparum* the interaction is evident throughout the asexual cycle (Hopkins et al., 1999; van Dooren et al., 2005), whereas in *T. gondii* a shorter time window for this association has been described, encompassing the G1 and apicoplast elongation stages before daughter cell formation (Nishi et al., 2008). Whether membrane contact sites exist between both organelles similar to what has been recently described for *T. gondii* between ER and apicoplast (Tomova et al., 2009) needs further assessment. Intriguingly, the dissociation of the two organelles has been resistant to various experimental attempts (He et al., 2001a; Kobayashi et al., 2007). This could be an indication for physical membrane continuities between apicoplast and mitochondrion, thus greatly facilitating metabolite exchange.

Recently, a hypothesis has been put forward for *P. falciparum* infected erythrocytes, suggesting that several host enzymes accumulate in the cytosol of the parasite, where they carry out all the synthesis steps subsequent to the

initial mitochondrial generation of ALA by the plasmodial HemA enzyme (Padmanaban et al., 2007). The hypothesis is based on the previously reported detection of erythrocytic HemB and FC in the parasite and on biochemical evidence, suggesting that the host enzymes are functional (Bonday et al., 1997, 2000; Dhanasekaran et al., 2004; Varadharajan et al., 2004). However, before such a model can be generally accepted, a number of issues need to be experimentally addressed. For instance, although plasmodial proteins are efficiently exported to the erythrocyte cytosol and plasma membrane (Maier et al., 2009), it is unclear how the reverse process could operate, that is, how host proteins could be transported across the PVM and the parasite plasma membrane.

A recent report adds some more questions to the already perplexing picture of the dispersed nature of heme metabolism in Apicomplexa. A *P. falciparum* protein with *in vitro* heme oxygenase (HO) activity has been described, which could be involved in the degradation of heme (Okada, 2009). In general, HO is important for the recycling of iron from heme, and simultaneously for generating carbon monoxide, a gas implicated in signaling events, and biliverdin, a potent antioxidant (Kikuchi et al., 2005). The *P. falciparum* HO sequence is distantly related to plant HOs but has related sequences in other Apicomplexa (Table 5.4). The localization of this protein is presently unclear, although it contains a predicted targeting signal for the apicoplast. It was suggested that the plastidial Fd/FNR redox system together with NADPH could be the natural electron donor to HO for the generation of bilirubin IX in this organelle, thus obviating the need for a dedicated biliverdin reductase (Okada, 2009). Further experiments are required to substantiate these observations, like the further route of bilirubin disposal and the role of the related proteins in *Theileria* and *Babesia*. In these organisms the complete heme synthesis pathway is missing; however, the HO enzyme is present. The implications of this need to be determined.

6. Apicoplast Metabolic Pathways as Drug Targets and the Phenomenon of Delayed Death

In the above description of the individual pathways, the steps and enzymes that are considered as attractive drug targets to inhibit parasite growth have already been highlighted. It is out of the scope of this chapter to provide more detail on this topic, and a number of recent reviews give a comprehensive overview of these and further experimental compounds found to inhibit apicoplast functions in the medically and economically important Apicomplexa (Fleige et al., 2010; Goodman and McFadden, 2007; Lizundia et al., 2009; Moreno and Li, 2008; Seeber, 2009;

Schlitzer, 2008; Wiesner and Jomaa, 2007; Wiesner and Seeber, 2005; Wiesner et al., 2008). Here we only want to emphasize the importance this aspect had and still has for the interest on research on apicoplast biology and biochemistry. This is in particular the case for *P. falciparum* where the ongoing race between emergence of drug resistance in the parasite and development of new, safe, and affordable medication by scientists and pharmaceutical companies around the world still sees no winner (Dondorp et al., 2009; Noedl et al., 2008; Olliaro and Wells, 2009).

Right from the beginning of its characterization in the mid-1990s, the apicoplast has attracted the attention of many scientists interested in drug development for quite obvious reasons: the plant-like nature of the known metabolic pathways as detailed above provides a rich source of potential targets with no direct mammalian counterparts (Wilson et al., 1994). Therefore, the hope has been to be able to develop small inhibitory compounds tailored to inhibit apicoplast-resident enzymes with little side effects on the host. In principle, this approach is not restricted to metabolic pathways since other proteins required for the inheritance and maintenance of the apicoplast are putative targets based on the same reasoning. For example, in *P. falciparum*, the immunosuppressant 15-deoxyspergualin has been shown to inhibit the trafficking of nuclear-encoded, apicoplast-localized proteins, resulting in apicoplast miss-segregation during subsequent cell divisions and ultimately death of the parasites (Ramya et al., 2007a). Although an immunosuppressant is certainly not a good drug candidate for malaria patients, it serves as proof of principle to demonstrate that small molecules can target this pathway that is crucial for the maintenance of the organelle (Agrawal et al., 2009).

The first definitive evidence of the essential nature of the apicoplast came from studies in *T. gondii* showing that parasites treated with the antibiotic ciprofloxacin failed to replicate the organelle by blocking the apicoplast-encoded DNA gyrase, finally killing the parasites (Fichera and Roos, 1997). Since then, many more antibiotics known to inhibit prokaryotic-type transcription, translation, and replication processes (so-called housekeeping functions) have been shown to target the apicoplast (Beckers et al., 1995; Dahl and Rosenthal, 2008; Fleige and Soldati-Favre, 2008). Some of these antibiotics have actually been used against malaria or toxoplasmosis for years before their molecular targets became apparent (e.g., clindamycin; Camps et al., 2002).

One intriguing phenomenon that is still not understood at the molecular level but has significant consequences when considering the apicoplast as a drug target is the so-called ''delayed death phenotype'' (Burkhardt et al., 2007; Dahl and Rosenthal, 2007, 2008; Goodman et al., 2007; Ramya et al., 2007b). Initially described in *T. gondii* (Fichera et al., 1995), the delayed death phenotype refers to the fact that treatment of intracellular parasites with inhibitors of housekeeping functions has no immediate effect

on replication and egress of these parasites. However, after entering a new host cell during a second replicative cycle, the parasites stop growing and die, even in the absence of drug. One hypothesis to explain this delay could be the delivery of formylated Met-tRNA from the apicoplast to the nearby mitochondrion (Howe and Purton, 2007). *T. gondii* imports tRNAs from the cytosol to the mitochondrion, and formylated Met-tRNA is presumably required to start the prokaryotic-type mitochondrial translation. However, there is only one gene coding for Met-tRNA formyltransferase (FMT) and the enzyme is exclusively found in the apicoplast and absent from the mitochondrion (Pino et al., submitted). While the provision of formylated Met-tRNA from the apicoplast to the mitochondrion is an interesting possibility, the absence of protein deformylase (PDF) in the mitochondrion argue for a translation in the absence of Met-tRNA formylation. Consistent with this hypothesis is that the *Babesia* and *Theileria* genomes lack both FMT and PDF genes. In these parasites, translation in the absence of Met-tRNA formylation not only occurs in the mitochondrion but also in the apicoplast.

In contrast to the inhibition of housekeeping functions of the apicoplast, the action of Fos that inhibits the MEP pathway is fast even at low drug concentrations (Jomaa et al., 1999; Surolia et al., 2004). This needs to be reconciled with the observation that an apicoplast segregation mutant of *T. gondii*, where all tachyzoites within a vacuole except one have no plastid, are still able to establish a new host cell infection before finally collapsing in a delayed fashion (He et al., 2001b). Taken at face value it means that the single remaining apicoplast supplies some product to all the tachyzoites within the vacuole and that transfer to plastid-less parasites can occur. This yet-unidentified compound of the apicoplast is either generated in large quantities or required only in minute amounts so that one plastid per vacuole is sufficient, and clearly more work is required to solve this puzzle. The three main anabolic pathways are attractive drug targets due to their fast killing, which is a favorable effect in the case of severe acute malaria. But also the ''slow killers'' like clindamycin, when for example combined with Fos, can be of great value in combination therapy against this disease (Borrmann et al., 2004).

7. Conclusions

The proteome of the extant apicoplast has been shaped over time through a process of ''reductive evolution'' to reach its current state. Comparative genomics of free living and intracellular chromalveolates can give illuminating insights into these processes and help to understand the overall metabolism of these intracellular parasites and how it adapted to the different environmental niches (Gould et al., 2008; Parker et al., 2008). As

one example, while the common ancestor of the Apicomplexa almost certainly had a cytosolic MEP pathway (as the phylogenetically related free-living diatoms still do) to synthesize isoprenoids for the generation of cholesterol, Apicomplexa could lose this pathway upon arrival of the plastid. This was possible after they had "learned" how to scavenge this compound either from the host cell (as in *T. gondii*) or live without it (Coppens and Vielemeyer, 2005), and at the same time how to provide IPP/DMAPP to the other cellular compartments of the cell where they are required. It is not too surprising that during this evolutionary process, complex mosaics of genes and pathways occurred.

ACKNOWLEDGMENTS

Own work cited by the authors was supported by funds from the Deutsche Forschungsgemeinschaft (Se 642/3) to F. S., and the Swiss SystemsX.ch initiative, grant LipidX-2008/011, to D. S.

REFERENCES

Abrahamsen, M.S., Templeton, T.J., Enomoto, S., Abrahante, J.E., Zhu, G., Lancto, C.A., et al., 2004. Complete genome sequence of the apicomplexan, *Cryptosporidium parvum*. Science 304, 441–445.

Agrawal, S., Van Dooren, G.G., Beatty, W.L., Striepen, B., 2009. Genetic evidence that an endosymbiont-derived ERAD system functions in import of apicoplast proteins. J. Biol. Chem. 284, 33683–33691.

Ali, V., Shigeta, Y., Tokumoto, U., Takahashi, Y., Nozaki, T., 2004. An intestinal parasitic protist, *Entamoeba histolytica*, possesses a non-redundant nitrogen fixation-like system for iron–sulfur cluster assembly under anaerobic conditions. J. Biol. Chem. 279, 16863–16874.

Aliverti, A., Pandini, V., Pennati, A., Derosa, M., Zanetti, G., 2008. Structural and functional diversity of ferredoxin-$NADP^+$ reductases. Arch. Biochem. Biophys. 474, 283–291.

Alkhalil, A., Hill, D.A., Desai, S.A., 2007. Babesia and plasmodia increase host erythrocyte permeability through distinct mechanisms. Cell. Microbiol. 9, 851–860.

Allary, M., Lu, J.Z., Zhu, L., Prigge, S.T., 2007. Scavenging of the cofactor lipoate is essential for the survival of the malaria parasite *Plasmodium falciparum*. Mol. Microbiol. 63, 1331–1344.

Allen, J.W., Jackson, A.P., Rigden, D.J., Willis, A.C., Ferguson, S.J., Ginger, M.L., 2008. Order within a mosaic distribution of mitochondrial c-type cytochrome biogenesis systems? FEBS J. 275, 2385–2402.

Arnold, K., Bordoli, L., Kopp, J., Schwede, T., 2006. The SWISS-MODEL workspace: a web-based environment for protein structure homology modelling. Bioinformatics 22, 195–201.

Aurrecoechea, C., Brestelli, J., Brunk, B.P., Dommer, J., Fischer, S., Gajria, B., et al., 2009. PlasmoDB: a functional genomic database for malaria parasites. Nucleic Acids Res. 37, D539–D543.

Aurrecoechea, C., Brestelli, J., Brunk, B.P., Fischer, S., Gajria, B., Gao, X., et al., 2010. EuPathDB: a portal to eukaryotic pathogen databases. Nucleic Acids Res. 38, D415–D419.

Ayala-Castro, C., Saini, A., Outten, F.W., 2008. Fe–S cluster assembly pathways in bacteria. Microbiol. Mol. Biol. Rev. 72, 110–125.

Balconi, E., Pennati, A., Crobu, D., Pandini, V., Cerutti, R., Zanetti, G., et al., 2009. The ferredoxin-NADP(+) reductase/ferredoxin electron transfer system of *Plasmodium falciparum*. FEBS J. 76, 3825–3836.

Balk, J., Lobréaux, S., 2005. Biogenesis of iron–sulfur proteins in plants. Trends Plant Sci. 10, 324–331.

Bandyopadhyay, S., Gama, F., Molina-Navarro, M.M., Gualberto, J.M., Claxton, R., Naik, S.G., et al., 2008. Chloroplast monothiol glutaredoxins as scaffold proteins for the assembly and delivery of [2Fe–2S] clusters. EMBO J. 27, 1122–1133.

Bano, N., Romano, J.D., Jayabalasingham, B., Coppens, I., 2007. Cellular interactions of *Plasmodium* liver stage with its host mammalian cell. Int. J. Parasitol. 37, 1329–1341.

Barton, D., Nakanishi, K., Meth-Cohn, O., 1999. Comprehensive Natural Products Chemistry: Isoprenoids Including Carotenoids and Steroids. Elsevier, Amsterdam.

Beckers, C.J., Roos, D.S., Donald, R.G., Luft, B.J., Schwab, J.C., Cao, Y., et al., 1995. Inhibition of cytoplasmic and organellar protein synthesis in *Toxoplasma gondii*. Implications for the target of macrolide antibiotics. J. Clin. Invest. 95, 367–376.

Benning, C., 2009. Mechanisms of lipid transport involved in organelle biogenesis in plant cells. Annu. Rev. Cell. Dev. Biol. 25, 71–91.

Bernard, D.G., Gabilly, S.T., Dujardin, G., Merchant, S., Hamel, P.P., 2003. Overlapping specificities of the mitochondrial cytochrome *c* and c_1 heme lyases. J. Biol. Chem. 278, 49732–49742.

Bick, J.A., Lange, B.M., 2003. Metabolic cross talk between cytosolic and plastidial pathways of isoprenoid biosynthesis: unidirectional transport of intermediates across the chloroplast envelope membrane. Arch. Biochem. Biophys. 415, 146–154.

Bisanz, C., Bastien, O., Grando, D., Jouhet, J., Marechal, E., Cesbron-Delauw, M.F., 2006. *Toxoplasma gondii* acyl-lipid metabolism: de novo synthesis from apicoplast-generated fatty acids versus scavenging of host cell precursors. Biochem. J. 394, 197–205.

Bonday, Z.Q., Taketani, S., Gupta, P.D., Padmanaban, G., 1997. Heme biosynthesis by the malarial parasite. Import of delta-aminolevulinate dehydrase from the host red cell. J. Biol. Chem. 272, 21839–21846.

Bonday, Z.Q., Dhanasekaran, S., Rangarajan, P.N., Padmanaban, G., 2000. Import of host [delta]-aminolevulinate dehydratase into the malarial parasite: identification of a new drug target. Nat. Med. 6, 898–903.

Bork, S., Yokoyama, N., Matsuo, T., Claveria, F.G., Fujisaki, K., Igarashi, I., 2003. Growth inhibitory effect of triclosan on equine and bovine Babesia parasites. Am. J. Trop. Med. Hyg. 68, 334–340.

Borrmann, S., Issifou, S., Esser, G., Adegnika, A.A., Ramharter, M., Matsiegui, P.B., et al., 2004. Fosmidomycin-clindamycin for the treatment of *Plasmodium falciparum* malaria. J. Infect. Dis. 190, 1534–1540.

Brayton, K.A., Lau, A.O., Herndon, D.R., Hannick, L., Kappmeyer, L.S., Berens, S.J., et al., 2007. Genome sequence of *Babesia bovis* and comparative analysis of apicomplexan hemoprotozoa. PLoS Pathog. 3, 1401–1413.

Brooks, C.F., Johnsen, H., van Dooren, G.G., Muthalagi, M., Lin, S.S., Bohne, W., et al., 2010. The *Toxoplasma* apicoplast phosphate translocator links cytosolic and apicoplast metabolism and is essential for parasite survival. Cell Host Microbe 7, 62–73.

Buchenau, B., Kahnt, J., Heinemann, I.U., Jahn, D., Thauer, R.K., 2006. Heme biosynthesis in *Methanosarcina barkeri* via a pathway involving two methylation reactions. J. Bacteriol. 188, 8666–8668.

Burkhardt, D., Wiesner, J., Stoesser, N., Ramharter, M., Uhlemann, A.C., Issifou, S., et al., 2007. Delayed parasite elimination in human infections treated with clindamycin parallels 'delayed death' of *Plasmodium falciparum* in vitro. Int. J. Parasitol. 37, 777–785.

Cai, X., Fuller, A.L., McDougald, L.R., Zhu, G., 2003. Apicoplast genome of the coccidian *Eimeria tenella*. Gene 321, 39–46.

Cai, X., Herschap, D., Zhu, G., 2005. Functional characterization of an evolutionarily distinct phosphopantetheinyl transferase in the apicomplexan *Cryptosporidium parvum*. Eukaryot. Cell 4, 1211–1220.

Camps, M., Arrizabalaga, G., Boothroyd, J., 2002. An rRNA mutation identifies the apicoplast as the target for clindamycin in *Toxoplasma gondii*. Mol. Microbiol. 43, 1309–1318.

Carretero-Paulet, L., Cairó, A., Botella-Pavía, P., Besumbes, O., Campos, N., Boronat, A., et al., 2006. Enhanced flux through the methylerythritol 4-phosphate pathway in *Arabidopsis* plants overexpressing deoxyxylulose 5-phosphate reductoisomerase. Plant Mol. Biol. 62, 683–695.

Caspi, R., Altman, T., Dale, J.M., Dreher, K., Fulcher, C.A., Gilham, F., et al., 2010. The MetaCyc database of metabolic pathways and enzymes and the BioCyc collection of pathway/genome databases. Nucleic Acids Res. 38, D473–D479.

Cassera, M.B., Gozzo, F.C., D'Alexandri, F.L., Merino, E.F., del Portillo, H.A., Peres, V.J., et al., 2004. The methylerythritol phosphate pathway is functionally active in all intraerythrocytic stages of *Plasmodium falciparum*. J. Biol. Chem. 279, 51749–51759.

Cassera, M.B., Merino, E.F., Peres, V.J., Kimura, E.A., Wunderlich, G., Katzin, A.M., 2007. Effect of fosmidomycin on metabolic and transcript profiles of the methylerythritol phosphate pathway in *Plasmodium falciparum*. Mem. Inst. Oswaldo Cruz 102, 377–383.

Cavallaro, G., Decaria, L., Rosato, A., 2008. Genome-based analysis of heme biosynthesis and uptake in prokaryotic systems. J. Proteome Res. 7, 4946–4954.

Chahal, H.K., Dai, Y., Saini, A., Ayala-Castro, C., Outten, F.W., 2009. The SufBCD Fe–S scaffold complex interacts with SufA for Fe–S cluster transfer. Biochemistry 48, 10644–10653.

Chakrabarti, D., Azam, T., DelVecchio, C., Qiu, L., Park, Y.I., Allen, C.M., 1998. Protein prenyl transferase activities of *Plasmodium falciparum*. Mol. Biochem. Parasitol. 94, 175–184.

Chakrabarti, D., Da Silva, T., Barger, J., Paquette, S., Patel, H., Patterson, S., et al., 2002. Protein farnesyltransferase and protein prenylation in *Plasmodium falciparum*. J. Biol. Chem. 277, 42066–42073.

Chang, A., Scheer, M., Grote, A., Schomburg, I., Schomburg, D., 2009. BRENDA, AMENDA and FRENDA the enzyme information system: new content and tools in 2009. Nucleic Acids Res. 37, D588–D592.

Charron, A.J., Sibley, L.D., 2002. Host cells mobilizable lipid resources for the intracellular parasite *Toxoplasma gondii*. J. Cell Sci. 115, 3049–3059.

Chaudhary, K., Roos, D.S., 2005. Protozoan genomics for drug discovery. Nat. Biotechnol. 23, 1089–1091.

Chaudhary, K., Donald, R.G., Nishi, M., Carter, D., Ullman, B., Roos, D.S., 2005. Differential localization of alternatively spliced hypoxanthine-xanthine-guanine phosphoribosyltransferase isoforms in *Toxoplasma gondii*. J. Biol. Chem. 280, 22053–22059.

Chen, F., Mackey, A.J., Stoeckert Jr., C.J., Roos, D.S., 2006. OrthoMCL-DB: querying a comprehensive multi-species collection of ortholog groups. Nucleic Acids Res. 34, D363–D368.

Cicchillo, R.M., Booker, S.J., 2005. Mechanistic investigations of lipoic acid biosynthesis in *Escherichia coli*: both sulfur atoms in lipoic acid are contributed by the same lipoyl synthase polypeptide. J. Am. Chem. Soc. 127, 2860–2861.

Clastre, M., Goubard, A., Prel, A., Mincheva, Z., Viaudmassuart, M., Bout, D., et al., 2007. The methylerythritol phosphate pathway for isoprenoid biosynthesis in coccidia: presence and sensitivity to fosmidomycin. Exp. Parasitol. 116, 375–384.

Constantinescu, A., Pick, U., Handelman, G.J., Haramaki, N., Han, D., Podda, M., et al., 1995. Reduction and transport of lipoic acid by human erythrocytes. Biochem. Pharmacol. 50, 253–261.

Coppens, I., Vielemeyer, O., 2005. Insights into unique physiological features of neutral lipids in Apicomplexa: from storage to potential mediation in parasite metabolic activities. Int. J. Parasitol. 35, 597–615.

Crawford, M.J., Thomsen-Zieger, N., Ray, M., Schachtner, J., Roos, D.S., Seeber, F., 2006. *Toxoplasma gondii* scavenges host-derived lipoic acid despite its de novo synthesis in the apicoplast. EMBO J. 25, 3214–3222.

Cronan, J.E., Zhao, X., Jiang, Y., 2005. Function, attachment and synthesis of lipoic acid in *Escherichia coli*. Adv. Microb. Physiol. 50, 103–146.

Dahl, E.L., Rosenthal, P.J., 2007. Multiple antibiotics exert delayed effects against the *Plasmodium falciparum* apicoplast. Antimicrob. Agents Chemother. 51, 3485–3490.

Dahl, E.L., Rosenthal, P.J., 2008. Apicoplast translation, transcription and genome replication: targets for antimalarial antibiotics. Trends Parasitol. 24, 279–284.

Dailey, T.A., Dailey, H.A., 2002. Identification of [2Fe–2S] clusters in microbial ferrochelatases. J. Bacteriol. 184, 2460–2464.

Dar, M.A., Sharma, A., Mondal, N., Dhar, S.K., 2007. Molecular cloning of apicoplast-targeted *Plasmodium falciparum* DNA gyrase genes: unique intrinsic ATPase activity and ATP-independent dimerization of PfGyrB subunit. Eukaryot. Cell 6, 398–412.

Dautu, G., Ueno, A., Munyaka, B., Carmen, G., Makino, S., Kobayashi, Y., et al., 2008. Molecular and biochemical characterization of *Toxoplasma gondii* beta-hydroxyacyl-acyl carrier protein dehydratase (FABZ). Parasitol. Res. 102, 1301–1309.

de Macedo, C.S., Uhrig, M.L., Kimura, E.A., Katzin, A.M., 2002. Characterization of the isoprenoid chain of coenzyme Q in *Plasmodium falciparum*. FEMS Microbiol. Lett. 207, 13–20.

de Macedo, C.S., Shams-Eldin, H., Smith, T.K., Schwarz, R.T., Azzouz, N., 2003. Inhibitors of glycosyl-phosphatidylinositol anchor biosynthesis. Biochimie 85, 465–472.

Delbac, F., Sanger, A., Neuhaus, E.M., Stratmann, R., Ajioka, J.W., Toursel, C., et al., 2001. *Toxoplasma gondii* myosins B/C: one gene, two tails, two localizations, and a role in parasite division. J. Cell Biol. 155, 613–623.

Dereeper, A., Guignon, V., Blanc, G., Audic, S., Buffet, S., Chevenet, F., et al., 2008. Phylogeny.fr: robust phylogenetic analysis for the non-specialist. Nucleic Acids Res. 36, W465–W469.

DeRocher, A., Hagen, C.B., Froehlich, J.E., Feagin, J.E., Parsons, M., 2000. Analysis of targeting sequences demonstrates that trafficking to the *Toxoplasma gondii* plastid branches off the secretory system. J. Cell Sci. 113, 3969–3977.

DeRocher, A.E., Coppens, I., Karnataki, A., Gilbert, L.A., Rome, M.E., Feagin, J.E., et al., 2008. A thioredoxin family protein of the apicoplast periphery identifies abundant candidate transport vesicles in *Toxoplasma gondii*. Eukaryot. Cell 7, 1518–1529.

deRuyck, J., Wouters, J., 2008. Structure-based drug design targeting biosynthesis of isoprenoids: a crystallographic state of the art of the involved enzymes. Curr. Prot. Pept. Sci. 9, 117–137.

Dhanasekaran, S., Chandra, N.R., Chandrasekhar Sagar, B.K., Rangarajan, P.N., Padmanaban, G., 2004. Delta-aminolevulinic acid dehydratase from *Plasmodium falciparum:* indigenous versus imported. J. Biol. Chem. 279, 6934–6942.

Dharia, N.V., Sidhu, A.B., Cassera, M.B., Westenberger, S.J., Bopp, S.E., Eastman, R.T., et al., 2009. Use of high-density tiling microarrays to identify mutations globally and elucidate mechanisms of drug resistance in *Plasmodium falciparum*. Genome Biol. 10, R21.

Dittrich, S., Mitchell, S.L., Blagborough, A.M., Wang, Q., Wang, P., Sims, P.F., et al., 2008. An atypical orthologue of 6-pyruvoyltetrahydropterin synthase can provide the missing link in the folate biosynthesis pathway of malaria parasites. Mol. Microbiol. 67, 609–618.

Dondorp, A.M., Nosten, F., Yi, P., Das, D., Phyo, A.P., Tarning, J., et al., 2009. Artemisinin resistance in *Plasmodium falciparum* malaria. N. Engl. J. Med. 361, 455–467.

Dybas, J.M., Madrid-Aliste, C.J., Che, F.Y., Nieves, E., Rykunov, D., Angeletti, R.H., et al., 2008. Computational analysis and experimental validation of gene predictions in *Toxoplasma gondii*. PLoS ONE 3, e3899.

Dzierszinski, F., Nishi, M., Ouko, L., Roos, D.S., 2004. Dynamics of *Toxoplasma gondii* differentiation. Eukaryot. Cell 3, 992–1003.

Egan, T.J., 2008. Recent advances in understanding the mechanism of hemozoin (malaria pigment) formation. J. Inorg. Biochem. 102, 1288–1299.

Eisenreich, W., Bacher, A., Arigoni, D., Rohdich, F., 2004. Biosynthesis of isoprenoids via the non-mevalonate pathway. Cell. Mol. Life Sci. 61, 1401–1426.

Ellis, K.E.S., Clough, B., Saldanah, J.W., Wilson, R.J.M., 2001. Nifs and Sufs in malaria. Mol. Microbiol. 41, 973–981.

Eoh, H., Brennan, P., Crick, D., 2009. The *Mycobacterium tuberculosis* MEP (2C-methyl-D-erythritol 4-phosphate) pathway as a new drug target. Tuberculosis 89, 1–11.

Ewald, R., Kolukisaoglu, U., Bauwe, U., Mikkat, S., Bauwe, H., 2007. Mitochondrial protein lipoylation does not exclusively depend on the mtKAS pathway of de novo fatty acid synthesis in *Arabidopsis*. Plant Physiol. 145, 41–48.

Fast, N.M., Kissinger, J.C., Roos, D.S., Keeling, P.J., 2001. Nuclear-encoded, plastid-targeted genes suggest a single common origin for apicomplexan and dinoflagellate plastids. Mol. Biol. Evol. 18, 418–426.

Feagin, J.E., Parsons, M., 2006. The apicoplast and mitochondrion of *Toxoplasma gondii*. In: Weiss, L.M., Kim, K. (Eds.), *Toxoplasma gondii*: The Model Apicomplexan. Academic Press, Amsterdam, pp. 207–244.

Fichera, M.E., Roos, D.S., 1997. A plastid organelle as a drug target in apicomplexan parasites. Nature 390, 407–409.

Fichera, M.E., Bhopale, M.K., Roos, D.S., 1995. In vitro assays elucidate peculiar kinetics of clindamycin action against *Toxoplasma gondii*. Antimicrob. Agents Chemother. 39, 1530–1537.

Fleige, T., Soldati-Favre, D., 2008. Targeting the transcriptional and translational machinery of the endosymbiotic organelle in apicomplexans. Curr. Drug Targets 9, 948–956.

Fleige, T., Fischer, K., Ferguson, D.J., Gross, U., Bohne, W., 2007. Carbohydrate metabolism in the *Toxoplasma gondii* apicoplast: localization of three glycolytic isoenzymes, the single pyruvate dehydrogenase complex, and a plastid phosphate translocator. Eukaryot. Cell 6, 984–996.

Fleige, T., Limenitakis, J., Soldati-Favre, D., 2010. Apicoplast: keep it or leave it. Microbes Infect. 12, 253–262.

Flores-Perez, U., Sauret-Gueto, S., Gas, E., Jarvis, P., Rodriguez-Concepcion, M., 2008. A mutant impaired in the production of plastome-encoded proteins uncovers a mechanism for the homeostasis of isoprenoid biosynthetic enzymes in *Arabidopsis plastids*. Plant Cell 20, 1303–1315.

Flügge, U.-I., Gao, W., 2005. Transport of isoprenoid intermediates across chloroplast envelope membranes. Plant Biol. 7, 91–97.

Foth, B.J., McFadden, G.I., 2003. The apicoplast: a plastid in *Plasmodium falciparum* and other apicomplexan parasites. Int. Rev. Cytol. 224, 57–110.

Foth, B.J., Ralph, S.A., Tonkin, C.J., Struck, N.S., Fraunholz, M., Roos, D.S., et al., 2003. Dissecting apicoplast targeting in the malaria parasite *Plasmodium falciparum*. Science 299, 705–708.

Foth, B.J., Stimmler, L.M., Handman, E., Crabb, B.S., Hodder, A.N., McFadden, G.I., 2005. The malaria parasite *Plasmodium falciparum* has only one pyruvate dehydrogenase complex, which is located in the apicoplast. Mol. Microbiol. 55, 39–53.

Frawley, E.R., Kranz, R.G., 2009. CcsBA is a cytochrome c synthetase that also functions in heme transport. Proc. Natl. Acad. Sci. USA 106, 10201–10206.

Frey, P.A., Hegeman, A.D., Ruzicka, F.J., 2008. The radical SAM superfamily. Crit. Rev. Biochem. Mol. Biol. 43, 63–88.

Fujii, H., Chinnusamy, V., Rodrigues, A., Rubio, S., Antoni, R., Park, S.-Y., et al., 2009. In vitro reconstitution of an abscisic acid signalling pathway. Nature 462, 660–664.

Fujiwara, K., Takeuchi, S., Okamura-Ikeda, K., Motokawa, Y., 2001. Purification, characterization, and cDNA cloning of lipoate-activating enzyme from bovine liver. J. Biol. Chem. 276, 28819–28823.

Gajria, B., Bahl, A., Brestelli, J., Dommer, J., Fischer, S., Gao, X., et al., 2008. ToxoDB: an integrated *Toxoplasma gondii* database resource. Nucleic Acids Res. 36, D553–D556.

Gallagher, J., Prigge, S., 2010. *Plasmodium falciparum* acyl carrier protein crystal structures in disulfide-linked and reduced states and their prevalence during blood stage growth. Proteins 78, 575–588.

Gardner, M.J., Williamson, D.H., Wilson, R.J., 1991. A circular DNA in malaria parasites encodes an RNA polymerase like that of prokaryotes and chloroplasts. Mol. Biochem. Parasitol. 44, 115–123.

Gardner, M.J., Bishop, R., Shah, T., de Villiers, E.P., Carlton, J.M., Hall, N., et al., 2005. Genome sequence of *Theileria parva*, a bovine pathogen that transforms lymphocytes. Science 309, 134–137.

Gasteiger, E., Gattiker, A., Hoogland, C., Ivanyi, I., Appel, R.D., Bairoch, A., 2003. ExPASy: The proteomics server for in-depth protein knowledge and analysis. Nucleic Acids Res. 31, 3784–3788.

Gaudu, P., Weiss, B., 2000. Flavodoxin mutants of *Escherichia coli* K-12. J. Bacteriol. 182, 1788–1793.

Ginger, M.L., 2006. Niche metabolism in parasitic protozoa. Phil. Trans. R. Soc. B 361, 101–118.

Ginsburg, H., 2006. Progress in in silico functional genomics: the malaria Metabolic Pathways database. Trends Parasitol. 22, 238–240.

Ginsburg, H., 2009. Caveat emptor: limitations of the automated reconstruction of metabolic pathways in *Plasmodium*. Trends Parasitol. 25, 37–43.

Goldberg, A.V., Molik, S., Tsaousis, A.D., Neumann, K., Kuhnke, G., Delbac, F., et al., 2008. Localization and functionality of microsporidian iron–sulphur cluster assembly proteins. Nature 452, 624–628.

Goodman, C.D., McFadden, G.I., 2007. Fatty acid biosynthesis as a drug target in apicomplexan parasites. Curr. Drug Targets 8, 15–30.

Goodman, C.D., Su, V., McFadden, G.I., 2007. The effects of anti-bacterials on the malaria parasite *Plasmodium falciparum*. Mol. Biochem. Parasitol. 152, 181–191.

Gornicki, P., 2003. Apicoplast fatty acid biosynthesis as a target for medical intervention in apicomplexan parasites. Int. J. Parasitol. 33, 885–896.

Gould, S.B., Waller, R.F., Mcfadden, G.I., 2008. Plastid evolution. Annu. Rev. Plant. Biol. 59, 491–517.

Gratraud, P., Huws, E., Falkard, B., Adjalley, S., Fidock, D.A., Berry, L., et al., 2008. Oleic acid biosynthesis in *Plasmodium falciparum*: characterization of the stearoyl-CoA desaturase and investigation as a potential therapeutic target. PLoS ONE 4, e6889.

Grauvogel, C., Petersen, J., 2007. Isoprenoid biosynthesis authenticates the classification of the green alga *Mesostigma viride* as an ancient streptophyte. Gene 396, 125–133.

Grauvogel, C., Reece, K.S., Brinkmann, H., Petersen, J., 2007. Plastid isoprenoid metabolism in the oyster parasite *Perkinsus marinus* connects dinoflagellates and malaria pathogens—new impetus for studying alveolates. J. Mol. Evol. 65, 725–729.

Green, M.L., Karp, P.D., 2004. A Bayesian method for identifying missing enzymes in predicted metabolic pathway databases. BMC Bioinf. 5, 76.

Günther, S., Wallace, L., Patzewitz, E.M., McMillan, P.J., Storm, J., Wrenger, C., et al., 2007. Apicoplast lipoic acid protein ligase B is not essential for *Plasmodium falciparum*. PLoS Pathog. 3, e189.

Günther, S., Matuschewski, K., Müller, S., 2009a. Knockout studies reveal an important role of *Plasmodium* lipoic acid protein ligase A1 for asexual blood stage parasite survival. PLoS ONE 4, e5510.

Günther, S., Storm, J., Müller, S., 2009b. *Plasmodium falciparum*: organelle-specific acquisition of lipoic acid. Int. J. Biochem. Cell Biol. 41, 748–752.

Hamel, P., Corvest, V., Giege, P., Bonnard, G., 2009. Biochemical requirements for the maturation of mitochondrial c-type cytochromes. Biochim. Biophys. Acta 1793, 125–138.

Hamza, I., 2006. Intracellular trafficking of porphyrins. ACS Chem. Biol. 1, 627–629.

Harb, O.S., Chatterjee, B., Fraunholz, M.J., Crawford, M.J., Nishi, M., Roos, D.S., 2004. Multiple functionally redundant signals mediate targeting to the apicoplast in the apicomplexan parasite *Toxoplasma gondii*. Eukaryot. Cell 3, 663–674.

Harper, J.T., Keeling, P.J., 2003. Nucleus-encoded, plastid-targeted glyceraldehyde-3-phosphate dehydrogenase (GAPDH) indicates a single origin for chromalveolate plastids. Mol. Biol. Evol. 20, 1730–1735.

Hashimoto, K., Yoshizawa, A.C., Okuda, S., Kuma, K., Goto, S., Kanehisa, M., 2008. The repertoire of desaturases and elongases reveals fatty acid variations in 56 eukaryotic genomes. J. Lipid Res. 49, 183–191.

He, C.Y., Striepen, B., Pletcher, C.H., Murray, J.M., Roos, D.S., 2001a. Targeting and processing of nuclear-encoded apicoplast proteins in plastid segregation mutants of *Toxoplasma gondii*. J. Biol. Chem. 276, 28436–28442.

He, C.Y., Shaw, M.K., Pletcher, C.H., Striepen, B., Tilney, L.G., Roos, D.S., 2001b. A plastid segregation defect in the protozoan parasite *Toxoplasma gondii*. EMBO J. 20, 330–339.

Heiges, M., Wang, H., Robinson, E., Aurrecoechea, C., Gao, X., Kaluskar, N., et al., 2006. CryptoDB: a *Cryptosporidium* bioinformatics resource update. Nucleic Acids Res. 34, D419–D422.

Heinemann, I.U., Jahn, M., Jahn, D., 2008. The biochemistry of heme biosynthesis. Arch. Biochem. Biophys. 474, 238–251.

Hemmerlin, A., Hoeffler, J.F., Meyer, O., Tritsch, D., Kagan, I.A., Grosdemange-Billiard, C., et al., 2003. Cross-talk between the cytosolic mevalonate and the plastidial methylerythritol phosphate pathways in tobacco bright yellow-2 cells. J. Biol. Chem. 278, 26666–26676.

Henriksson, L., Bjorkelid, C., Mowbray, S., Unge, T., 2006. The 1.9 A resolution structure of *Mycobacterium tuberculosis* 1-deoxy-d-xylulose 5-phosphate reductoisomerase, a potential drug target. Acta Cryst. D62, 807–813.

Henriksson, L.M., Unge, T., Carlsson, J., Aqvist, J., Mowbray, S.L., Jones, T.A., 2007. Structures of *Mycobacterium tuberculosis* 1-deoxy-D-xylulose-5-phosphate reductoisomerase provide new insights into catalysis. J. Biol. Chem. 282, 19905–19916.

Hermes, F.A., Cronan, J.E., 2009. Scavenging of cytosolic octanoic acid by mutant LplA lipoate ligases allows growth of *Escherichia coli* strains lacking the LipB octanoyltransferase of lipoic acid synthesis. J. Bacteriol. 191, 6796–6803.

Hertz-Fowler, C., Peacock, C.S., Wood, V., Aslett, M., Kerhornou, A., Mooney, P., et al., 2004. GeneDB: a resource for prokaryotic and eukaryotic organisms. Nucleic Acids Res. 32, D339–D343.

Hiltunen, J., Chen, Z., Haapalainen, A., Wierenga, R., Kastaniotis, A., 2010. Mitochondrial fatty acid synthesis - an adopted set of enzymes making a pathway of major importance for the cellular metabolism. Prog. Lipid Res. 29, 27–45.

Holstein, S.A., Hohl, R.J., 2004. Isoprenoids: remarkable diversity of form and function. Lipids 39, 293–309.

Hopkins, J., Fowler, R., Krishna, S., Wilson, I., Mitchell, G., Bannister, L., 1999. The plastid in *Plasmodium falciparum* asexual blood stages: a three-dimensional ultrastructural analysis. Protist 150, 283–295.

Howe, C.J., Purton, S., 2007. The little genome of apicomplexan plastids: its raison d'etre and a possible explanation for the 'delayed death' phenomenon. Protist 158, 121–133.

Hunter, W.N., 2007. The non-mevalonate pathway of isoprenoid precursor biosynthesis. J. Biol. Chem. 282, 21573–21577.

Ibrahim, M., Azzouz, N., Gerold, P., Schwarz, R.T., 2001. Identification and characterisation of *Toxoplasma gondii* protein farnesyltransferase. Int. J. Parasitol. 31, 1489–1497.

Inomata, M., Hirai, N., Yoshida, R., Ohigashi, H., 2004. The biosynthetic pathway to abscisic acid via ionylideneethane in the fungus *Botrytis cinerea*. Phytochemistry 65, 2667–2678.

Iriko, H., Jin, L., Kaneko, O., Takeo, S., Han, E.-T., Tachibana, M., et al., 2009. A small-scale systematic analysis of alternative splicing in *Plasmodium falciparum*. Parasitol. Int. 58, 196–199.

Johnson, D.C., Dean, D.R., Smith, A.D., Johnson, M.K., 2005. Structure, function, and formation of biological iron–sulfur clusters. Annu. Rev. Biochem. 74, 247–281.

Jomaa, H., Wiesner, J., Sanderbrand, S., Altincicek, B., Weidemeyer, C., Hintz, M., et al., 1999. Inhibitors of the nonmevalonate pathway of isoprenoid biosynthesis as antimalarial drugs. Science 285, 1573.

Kanehisa, M., Araki, M., Goto, S., Hattori, M., Hirakawa, M., Itoh, M., et al., 2008. KEGG for linking genomes to life and the environment. Nucleic Acids Res. 36, D480–D484.

Karnataki, A., Derocher, A., Coppens, I., Nash, C., Feagin, J.E., Parsons, M., 2007a. Cell cycle-regulated vesicular trafficking of *Toxoplasma* APT1, a protein localized to multiple apicoplast membranes. Mol. Microbiol. 63, 1653–1668.

Karnataki, A., Derocher, A.E., Coppens, I., Feagin, J.E., Parsons, M., 2007b. A membrane protease is targeted to the relict plastid of toxoplasma via an internal signal sequence. Traffic 8, 1543–1553.

Karnataki, A., DeRocher, A.E., Feagin, J.E., Parsons, M., 2009. Sequential processing of the *Toxoplasma* apicoplast membrane protein FtsH1 in topologically distinct domains during intracellular trafficking. Mol. Biochem. Parasitol. 166, 126–133.

Karp, P.D., Paley, S., Romero, P., 2002. The pathway tools software. Bioinformatics 18 (Suppl. 1), S225–S232.

Keeling, P.J., 2009. Chromalveolates and the evolution of plastids by secondary endosymbiosis. J. Eukaryot. Microbiol. 56, 1–8.

Kessler, D., Papenbrock, J., 2005. Iron–sulfur cluster biosynthesis in photosynthetic organisms. Photosynth. Res. 86, 391–407.

Khor, V., Yowell, C., Dame, J.B., Rowe, T.C., 2005. Expression and characterization of the ATP-binding domain of a malarial *Plasmodium vivax* gene homologous to the B-subunit of the bacterial topoisomerase DNA gyrase. Mol. Biochem. Parasitol. 140, 107–117.

Kikuchi, G., Yoshida, T., Noguchi, M., 2005. Heme oxygenase and heme degradation. Biochem. Biophys. Res. Commun. 338, 558–567.

Kimata-Ariga, Y., Kurisu, G., Kusunoki, M., Aoki, S., Sato, D., Kobayashi, T., et al., 2007. Cloning and characterization of ferredoxin and ferredoxin-NADP+ reductase from human malaria parasite. J. Biochem. 141, 421–428.

Kimmel, J., Ogun, S.A., de Macedo, C.S., Gerold, P., Vivas, L., Holder, A.A., et al., 2003. Glycosylphosphatidyl-inositols in murine malaria: *Plasmodium yoelii yoelii*. Biochimie 85, 473–481.

Kirby, J., Keasling, J.D., 2009. Biosynthesis of plant isoprenoids: perspectives for microbial engineering. Annu. Rev. Plant. Biol. 60, 335–355.
Kirk, K., 2001. Membrane transport in the malaria-infected erythrocyte. Physiol. Rev. 81, 495–537.
Knöckel, J., Müller, I.B., Bergmann, B., Walter, R.D., Wrenger, C., 2007. The apicomplexan parasite *Toxoplasma gondii* generates pyridoxal phosphate de novo. Mol. Biochem. Parasitol. 152, 108–111.
Knöckel, J., Bergmann, B., Müller, I.B., Rathaur, S., Walter, R.D., Wrenger, C., 2008. Filling the gap of intracellular dephosphorylation in the *Plasmodium falciparum* vitamin B1 biosynthesis. Mol. Biochem. Parasitol. 157, 241–243.
Kobayashi, T., Sato, S., Takamiya, S., Komaki-Yasuda, K., Yano, K., Hirata, A., et al., 2007. Mitochondria and apicoplast of *Plasmodium falciparum:* behaviour on subcellular fractionation and the implication. Mitochondrion 7, 125–132.
Köhler, S., 2005. Multi-membrane-bound structures of Apicomplexa: I. The architecture of the *Toxoplasma gondii* apicoplast. Parasitol. Res. 96, 258–272.
Köhler, S., 2006. Multi-membrane-bound structures of Apicomplexa: II. The ovoid mitochondrial cytoplasmic (OMC) complex of *Toxoplasma gondii* tachyzoites. Parasitol. Res. 98, 355–369.
Köhler, S., Delwiche, C.F., Denny, P.W., Tilney, L.G., Webster, P., Wilson, R.J., et al., 1997. A plastid of probable green algal origin in Apicomplexan parasites. Science 275, 1485–1489.
Kono, N., Arakawa, K., Ogawa, R., Kido, N., Oshita, K., Ikegami, K., et al., 2009. Pathway projector: web-based zoomable pathway browser using KEGG atlas and Google Maps API. PLoS One 4, e7710.
Koo, A.J., Ohlrogge, J.B., Pollard, M., 2004. On the export of fatty acids from the chloroplast. J. Biol. Chem. 279, 16101–16110.
Kranz, R.G., Richard-Fogal, C., Taylor, J.S., Frawley, E.R., 2009. Cytochrome c biogenesis: mechanisms for covalent modifications and trafficking of heme and for heme-iron redox control. Microbiol. Mol. Biol. Rev. 73, 510–528.
Krapp, A.R., Rodriguez, R.E., Poli, H.O., Paladini, D.H., Palatnik, J.F., Carrillo, N., 2002. The flavoenzyme ferredoxin (flavodoxin)-NADP(H) reductase modulates NADP(H) homeostasis during the soxRS response of *Escherichia coli*. J. Bacteriol. 184, 1474–1480.
Krishnamurthy, P., Xie, T., Schuetz, J.D., 2007. The role of transporters in cellular heme and porphyrin homeostasis. Pharmacol. Ther. 114, 345–358.
Krishnegowda, G., 2003. Intraerythrocytic *Plasmodium falciparum* incorporates extraneous fatty acids to its lipids without any structural modification. Mol. Biochem. Parasitol. 132, 55–58.
Lack, G., Homberger-Zizzari, E., Folkers, G., Scapozza, L., Perozzo, R., 2006. Recombinant expression and biochemical characterization of the unique elongating beta-ketoacyl-acyl carrier protein synthase involved in fatty acid biosynthesis of *Plasmodium falciparum* using natural and artificial substrates. J. Biol. Chem. 281, 9538–9546.
Lange, B.M., Rujan, T., Martin, W., Croteau, R., 2000. Isoprenoid biosynthesis: the evolution of two ancient and distinct pathways across genomes. Proc. Natl. Acad. Sci. USA 97, 13172–13177.
Lang-Unnasch, N., Aiello, D.P., 1999. Sequence evidence for an altered genetic code in the *Neospora caninum* plastid. Int. J. Parasitol. 29, 1557–1562.
Layer, G., Gaddam, S.A., Ayala-Castro, C.N., Ollagnier-de Choudens, S., Lascoux, D., Fontecave, M., et al., 2007. SufE transfers sulfur from SufS to SufB for iron–sulfur cluster assembly. J. Biol. Chem. 282, 13342–13350.
Leibundgut, M., Maier, T., Jenni, S., Ban, N., 2008. The multienzyme architecture of eukaryotic fatty acid synthases. Curr. Opin. Struct. Biol. 18, 714–725.

Leroux, M., Lakshmanan, V., Daily, J., 2009. *Plasmodium falciparum* biology: analysis of in vitro versus in vivo growth conditions. Trends Parasitol. 25, 474–478.
Levine, N., 1988. The Protozoan Phylum Apicomplexa. CRC Press, Boca Raton, Fla.
Lezhneva, L., Amann, K., Meurer, J., 2004. The universally conserved HCF101 protein is involved in assembly of [4Fe–4S]-cluster-containing complexes in *Arabidopsis thaliana* chloroplasts. Plant J. 37, 174–185.
Lichtenthaler, H.K., 1999. The 1-deoxy-D-xylulose-5-phosphate pathway of isoprenoid biosynthesis in plants. Annu. Rev. Plant Physiol. Plant Mol. Biol. 50, 47–65.
Lill, R., 2009. Function and biogenesis of iron–sulphur proteins. Nature 460, 831–838.
Lill, R., Mühlenhoff, U., 2006. Iron–sulfur protein biogenesis in eukaryotes: components and mechanisms. Annu. Rev. Cell. Dev. Biol. 22, 457–486.
Lill, R., Mühlenhoff, U., 2008. Maturation of iron–sulfur proteins in eukaryotes: mechanisms, connected processes, and diseases. Annu. Rev. Biochem. 77, 669–700.
Lim, L., Kalanon, M., McFadden, G.I., 2009. New proteins in the apicoplast membranes: time to rethink apicoplast protein targeting. Trends Parasitol. 25, 197–200.
Lim, L., Linka, M., Mullin, K.A., Weber, A.P., Mcfadden, G.I., 2010. The carbon and energy sources of the non-photosynthetic plastid in the malaria parasite. FEBS Lett. 584, 549–554.
Ling, Y., Sahota, G., Odeh, S., Chan, J.M.W., Araujo, F.G., Moreno, S.N.J., et al., 2005. Bisphosphonate inhibitors of *Toxoplasma gondii* growth: in vitro, QSAR, and in vivo investigations. J. Med. Chem. 48, 3130–3140.
Ling, Y., Li, Z.-H., Miranda, K., Oldfield, E., Moreno, S.N.J., 2007. The farnesyl-diphosphate/geranylgeranyl-diphosphate synthase of *Toxoplasma gondii* is a bifunctional enzyme and a molecular target of bisphosphonates. J. Biol. Chem. 282, 30804–30816.
Lizundia, R., Werling, D., Langsley, G., Ralph, S.A., 2009. The *Theileria* apicoplast as a target for chemotherapy. Antimicrob. Agents Chemother. 53, 1213–1217.
Lu, F., Jiang, H., Ding, J., Mu, J., Valenzuela, J.G., Ribeiro, J.M., et al., 2007. cDNA sequences reveal considerable gene prediction inaccuracy in the *Plasmodium falciparum* genome. BMC Genomics 8, 255.
Maeda, T., Saito, T., Harb, O.S., Roos, D.S., Takeo, S., Suzuki, H., et al., 2009. Pyruvate kinase type-II isozyme in *Plasmodium falciparum* localizes to the apicoplast. Parasitol. Int. 58, 101–105.
Maier, A.G., Cooke, B.M., Cowman, A.F., Tilley, L., 2009. Malaria parasite proteins that remodel the host erythrocyte. Nat. Rev. Microbiol. 7, 341–354.
Marechal, E., Cesbron-Delauw, M.F., 2001. The apicoplast: a new member of the plastid family. Trends Plant Sci. 6, 200–205.
Martin, R., Ginsburg, H., Kirk, K., 2009. Membrane transport proteins of the malaria parasite. Mol. Microbiol. 74, 519–528.
Matthews, L., Gopinath, G., Gillespie, M., Caudy, M., Croft, D., de Bono, B., et al. (2009). Reactome knowledgebase of human biological pathways and processes. Nucleic Acids Res. 37, D619–D622.
Matsuzaki, M., Kikuchi, T., Kita, K., Kojima, S., Kuroiwa, T., 2001. Large amounts of apicoplast nucleoid DNA and its segregation in *Toxoplasma gondii*. Protoplasma 218, 180–191.
Matsuzaki, M., Kuroiwa, H., Kuroiwa, T., Kita, K., Nozaki, H., 2008. A cryptic algal group unveiled: a plastid biosynthesis pathway in the oyster parasite *Perkinsus marinus*. Mol. Biol. Evol. 25, 1167–1179.
Mazumdar, J., Striepen, B., 2007. Make it or take it: fatty acid metabolism of apicomplexan parasites. Eukaryot. Cell 6, 1727–1735.
Mazumdar, J., Wilson, E.H., Masek, K., Hunter, C.A., Striepen, B., 2006. Apicoplast fatty acid synthesis is essential for organelle biogenesis and parasite survival in *Toxoplasma gondii*. Proc. Natl. Acad. Sci. USA 103, 13192–13197.

McFadden, G.I., Reith, M.E., Munholland, J., Lang-Unnasch, N., 1996. Plastid in human parasites. Nature 381, 482.
McFadden, G.I., Waller, R.F., Reith, M.E., Lang-Unnasch, N., 1997. Plastids in apicomplexan parasites. Plant Syst. Evol. 11 (Suppl.), 261–287.
McLeod, R., Muench, S.P., Rafferty, J.B., Kyle, D.E., Mui, E.J., Kirisits, M.J., et al., 2001. Triclosan inhibits the growth of *Plasmodium falciparum* and *Toxoplasma gondii* by inhibition of apicomplexan Fab I. Int. J. Parasitol. 31, 109–113.
Meyer, J., 2008. Iron–sulfur protein folds, iron–sulfur chemistry, and evolution. J. Biol. Inorg. Chem. 13, 157–170.
Michal, G. (1999). ''Biochemical Pathways.'' Spektrum Akademischer Verlag, Heidelberg.
Milani, M., Balconi, E., Aliverti, A., Mastrangelo, E., Seeber, F., Bolognesi, M., et al., 2007. Ferredoxin-NADP(+) reductase from *Plasmodium falciparum* undergoes NADP(+)-dependent dimerization and inactivation: functional and crystallographic analysis. J. Mol. Biol. 367, 501–513.
Miyawaki, K., Tarkowski, P., Matsumoto-Kitano, M., Kato, T., Sato, S., Tarkowska, D., et al., 2006. Roles of *Arabidopsis* ATP/ADP isopentenyltransferases and tRNA isopentenyltransferases in cytokinin biosynthesis. Proc. Natl. Acad. Sci. USA 103, 16598–16603.
Mohanty, S., Srinivasan, N., 2009. Identification of missing metabolic proteins of *Plasmodium falciparum*: a bioinformatics approach. Prot. Pept. Lett. 16, 961–968.
Moore, R.B., Oborník, M., Janouškovec, J., Chrudimský, T., Vancová, M., Green, D.H., et al., 2008. A photosynthetic alveolate closely related to apicomplexan parasites. Nature 451, 959–963.
Moreno, S.N.J., Li, Z.-H., 2008. Anti-infectives targeting the isoprenoid pathway of *Toxoplasma gondii*. Expert Opin. Ther. Targets 12, 253–263.
Moustafa, A., Beszteri, B., Maier, U.G., Bowler, C., Valentin, K., Bhattacharya, D., 2009. Genomic footprints of a cryptic plastid endosymbiosis in diatoms. Science 324, 1724–1726.
Muench, S.P., Prigge, S.T., McLeod, R., Rafferty, J.B., Kirisits, M.J., Roberts, C.W., et al., 2007. Studies of *Toxoplasma gondii* and *Plasmodium falciparum* enoyl acyl carrier protein reductase and implications for the development of antiparasitic agents. Acta Crystallogr. D Biol. Crystallogr. 63, 328–338.
Mukhopadhyay, A., Chen, C.Y., Doerig, C., Henriquez, F.L., Roberts, C.W., Barrett, M.P., 2009. The *Toxoplasma gondii* plastid replication and repair enzyme complex, PREX. Parasitology 136, 747–755.
Müller, S., Kappes, B., 2007. Vitamin and cofactor biosynthesis pathways in *Plasmodium* and other apicomplexan parasites. Trends Parasitol. 23, 112–121.
Müller, I., Hyde, J., Wrenger, C., 2010. Vitamin B metabolism in *Plasmodium falciparum* as a source of drug targets. Trends Parasitol. 26, 35–43.
Mullin, K.A., Lim, L., Ralph, S.A., Spurck, T.P., Handman, E., McFadden, G.I., 2006. Membrane transporters in the relict plastid of malaria parasites. Proc. Natl. Acad. Sci. USA 103, 9572–9577.
Nagamune, K., Hicks, L.M., Fux, B., Brossier, F., Chini, E.N., Sibley, L.D., 2008a. Abscisic acid controls calcium-dependent egress and development in *Toxoplasma gondii*. Nature 451, 207–210.
Nagamune, K., Xiong, L., Chini, E., Sibley, L., 2008b. Plants, endosymbionts and parasites: abscisic acid and calcium signaling. Commun. Integr. Biol. 1, 62–65.
Nagaraj, V.A., Arumugam, R., Gopalakrishnan, B., Jyothsna, Y.S., Rangarajan, P.N., Padmanaban, G., 2008. Unique properties of *Plasmodium falciparum* porphobilinogen deaminase. J. Biol. Chem. 283, 437–444.
Nagaraj, V.A., Prasad, D., Rangarajan, P.N., Padmanaban, G., 2009a. Mitochondrial localization of functional ferrochelatase from *Plasmodium falciparum*. Mol. Biochem. Parasitol. 168, 109–112.

Nagaraj, V.A., Arumugam, R., Chandra, N.R., Prasad, D., Rangarajan, P.N., Padmanaban, G., 2009b. Localisation of *Plasmodium falciparum* uroporphyrinogen III decarboxylase of the heme-biosynthetic pathway in the apicoplast and characterisation of its catalytic properties. Int. J. Parasitol. 39, 559–568.

Nagaraj, V.A., Prasad, D., Arumugam, R., Rangarajan, P.N., Padmanaban, G., 2009c. Characterization of coproporphyrinogen III oxidase in *Plasmodium falciparum* cytosol. Parasitol. Int. doi:10.1016/j.parint.2009.1012.1001.

Nambara, E., Marion-Poll, A., 2005. Abscisic acid biosynthesis and catabolism. Annu. Rev. Plant. Biol. 56, 165–185.

Nesbitt, N.M., Cicchillo, R.M., Lee, K., Grove, T.L., Booker, S.J., 2008. Lipoic acid biosynthesis. In: Patel, S.P., Packer, L. (Eds.), Lipoic Acid: Energy Production, Antioxidant Activity and Health Effects. CRC Press, Boca Raton, FL, pp. 11–56.

Nishi, M., Hu, K., Murray, J.M., Roos, D.S., 2008. Organellar dynamics during the cell cycle of *Toxoplasma gondii*. J. Cell Sci. 121, 1559–1568.

Noedl, H., Se, Y., Schaecher, K., Smith, B.L., Socheat, D., Fukuda, M.M., Artemisinin Resistance in Cambodia 1 Study, C, 2008. Evidence of artemisinin-resistant malaria in western Cambodia. N. Engl. J. Med. 359, 2619–2620.

Oborník, M., Green, B.R., 2005. Mosaic origin of the heme biosynthesis pathway in photosynthetic eukaryotes. Mol. Biol. Evol. 22, 2343–2353.

Obornik, M., Janouskovec, J., Chrudimsky, T., Lukes, J., 2009. Evolution of the apicoplast and its hosts: from heterotrophy to autotrophy and back again. Int. J. Parasitol. 39, 1–12.

Odom, A.R., Van Voorhis, W.C., 2010. Functional genetic analysis of the *Plasmodium falciparum* deoxyxylulose 5-phosphate reductoisomerase gene. Mol. Biochem. Parasitol. 170, 108–111.

Okada, K., 2009. The novel heme oxygenase-like protein from *Plasmodium falciparum* converts heme to bilirubin IXα in the apicoplast. FEBS Lett. 583, 313–319.

Okada, K., Hase, T., 2005. Cyanobacterial non-mevalonate pathway: (*E*)-4-hydroxy-3-methylbut-2-enyl diphosphate synthase interacts with ferredoxin in *Thermosynechococcus elongatus* BP-1. J. Biol. Chem. 280, 20672–20679.

Okamoto, N., Spurck, T.P., Goodman, C.D., McFadden, G.I., 2009. Apicoplast and mitochondrion in gametocytogenesis of *Plasmodium falciparum*. Eukaryot. Cell 8, 128–132.

Olliaro, P., Wells, T.N., 2009. The global portfolio of new antimalarial medicines under development. Clin. Pharmacol. Ther. 85, 584–595.

Olson, J.W., Agar, J.N., Johnson, M.K., Maier, R.J., 2000. Characterization of the NifU and NifS Fe–S cluster formation proteins essential for viability in *Helicobacter pylori*. Biochemistry 39, 16213–16219.

Overbeek, R., Begley, T., Butler, R. M., Choudhuri, J. V., Chuang, H. Y., Cohoon, M., et al. (2005). The subsystems approach to genome annotation and its use in the project to annotate 1000 genomes. Nucleic Acids Res. 33, 5691-5702.

Padmanaban, G., Nagaraj, V.A., Rangarajan, P.N., 2007. An alternative model for heme biosynthesis in the malarial parasite. Trends Biochem. Sci. 32, 443–449.

Parker, M.S., Mock, T., Armbrust, E.V., 2008. Genomic insights into marine microalgae. Annu. Rev. Genet. 42, 619–645.

Parsons, M., Karnataki, A., Feagin, J.E., DeRocher, A., 2007. Protein trafficking to the apicoplast: deciphering the apicomplexan solution to secondary endosymbiosis. Eukaryot. Cell 6, 1081–1088.

Parsons, M., Karnataki, A., Derocher, A.E., 2009. Evolving insights into protein trafficking to the multiple compartments of the apicomplexan plastid. J. Eukaryot. Microbiol. 56, 214–220.

Pei, Y., Tarun, A.S., Vaughan, A.M., Herman, R.W., Soliman, J.M.B., Erickson-Wayman, A., et al., 2010. *Plasmodium* pyruvate dehydrogenase activity is only essential

for the parasite's progression from liver infection to blood infection. Mol. Microbiol. 75, 957–971.
Perham, R.N., 2000. Swinging arms and swinging domains in multifunctional enzymes: catalytic machines for multistep reactions. Annu. Rev. Biochem. 69, 961–1004.
Persson, B.C., Esberg, B., Olafsson, O., Bjork, G.R., 1994. Synthesis and function of isopentenyl adenosine derivatives in tRNA. Biochimie 76, 1152–1160.
Pettersen, E.F., Goddard, T.D., Huang, C.C., Couch, G.S., Greenblatt, D.M., Meng, E.C., et al., 2004. UCSF Chimera–a visualization system for exploratory research and analysis. J. Comput. Chem. 25, 1605–1612.
Pillai, S., Rajagopal, C., Kapoor, M., Kumar, G., Gupta, A., Surolia, N., 2003. Functional characterization of beta-ketoacyl-ACP reductase (FabG) from *Plasmodium falciparum*. Biochem. Biophys. Res. Commun. 303, 387–392.
Pilon, M., Abdel-Ghany, S.E., Van Hoewyk, D., Ye, H., Pilon-Smits, E.A., 2006. Biogenesis of iron–sulfur cluster proteins in plastids. Genet. Eng. (N Y) 27, 101–117.
Pino, P., Foth, B.J., Kwok, L.-Y., Sheiner, L., Schepers, R., Soldati, T., et al., 2007. Dual targeting of antioxidant and metabolic enzymes to the mitochondrion and the apicoplast of *Toxoplasma gondii*. PLoS Pathog. 3, e115.
Preiser, P., Williamson, D.H., Wilson, R.J., 1995. tRNA genes transcribed from the plastid-like DNA of *Plasmodium falciparum*. Nucleic Acids Res. 23, 4329–4336.
Prigge, S.T., He, X., Gerena, L., Waters, N.C., Reynolds, K.A., 2003. The initiating steps of a type II fatty acid synthase in *Plasmodium falciparum* are catalyzed by pfacp, pfmcat, and pfKASIII. Biochemistry 42, 1160–1169.
Puan, K.J., Wang, H., Dairi, T., Kuzuyama, T., Morita, C.T., 2005. fldA is an essential gene required in the 2-C-methyl-D-erythritol 4-phosphate pathway for isoprenoid biosynthesis. FEBS Lett. 579, 3802–3806.
Ralph, S.A., Van Dooren, G.G., Waller, R.F., Crawford, M.J., Fraunholz, M.J., Foth, B.J., et al., 2004. Metabolic maps and functions of the *Plasmodium falciparum* apicoplast. Nat. Rev. Micro. 2, 203–216.
Ramya, T.N., Karmodiya, K., Surolia, A., Surolia, N., 2007a. 15-deoxyspergualin primarily targets the trafficking of apicoplast proteins in *Plasmodium falciparum*. J. Biol. Chem. 282, 6388–6397.
Ramya, T.N., Mishra, S., Karmodiya, K., Surolia, N., Surolia, A., 2007b. Inhibitors of nonhousekeeping functions of the apicoplast defy delayed death in *Plasmodium falciparum*. Antimicrob. Agents Chemother. 51, 307–316.
Reitz, M., Sacher, O., Tarkhov, A., Trumbach, D., Gasteiger, J., 2004. Enabling the exploration of biochemical pathways. Org. Biomol. Chem. 2, 3226–3237.
Rohdich, F., Bacher, A., Eisenreich, W., 2005. Isoprenoid biosynthetic pathways as anti-infective drug targets. Biochem. Soc. Trans. 33, 785–791.
Rohmer, M., 1999. The discovery of a mevalonate-independent pathway for isoprenoid biosynthesis in bacteria, algae and higher plants. Nat. Prod. Rep. 16, 565–574.
Rohmer, M., Knani, M., Simonin, P., Sutter, B., Sahm, H., 1993. Isoprenoid biosynthesis in bacteria: a novel pathway for the early steps leading to isopentenyl diphosphate. Biochem. J. 295, 517–524.
Röhrich, R., Englert, N., Troschke, K., Reichenberg, A., Hintz, M., Seeber, F., et al., 2005. Reconstitution of an apicoplast-localised electron transfer pathway involved in the isoprenoid biosynthesis of *Plasmodium falciparum*. FEBS Lett. 579, 6433–6438.
Roos, D.S., Crawford, M.J., Donald, R.G., Kissinger, J.C., Klimczak, L.J., Striepen, B., 1999. Origin, targeting, and function of the apicomplexan plastid. Curr. Opin. Microbiol. 2, 426–432.
Rouhier, N., Couturier, J., Johnson, M., Jacquot, J., 2010. Glutaredoxins: roles in iron homeostasis. Trends Biochem. Sci. 35, 43–52.

Saito, T., Nishi, M., Lim, M.I., Wu, B., Maeda, T., Hashimoto, H., et al., 2008. A novel GDP-dependent pyruvate kinase isozyme from *Toxoplasma gondii* localizes to both the apicoplast and the mitochondrion. J. Biol. Chem. 283, 14041–14052.

Saliba, K.J., Kirk, K., 2001. Nutrient acquisition by intracellular apicomplexan parasites: staying in for dinner. Int. J. Parasitol. 31, 1321–1330.

Saliba, K.J., Horner, H.A., Kirk, K., 1998. Transport and metabolism of the essential vitamin pantothenic acid in human erythrocytes infected with the malaria parasite *Plasmodium falciparum*. J. Biol. Chem. 273, 10190–10195.

Sato, S., Wilson, R.J., 2002. The genome of *Plasmodium falciparum* encodes an active delta-aminolevulinic acid dehydratase. Curr. Genet. 40, 391–398.

Sato, S., Wilson, R.J., 2003. Proteobacteria-like ferrochelatase in the malaria parasite. Curr. Genet. 42, 292–300.

Sato, S., Wilson, R., 2004. The use of DsRED in single-and dual-color fluorescence labeling of mitochondrial and plastid organelles in *Plasmodium falciparum*. Mol. Biochem. Parasitol. 134, 175–179.

Sato, S., Wilson, R., 2005. Organelle-specific cochaperonins in apicomplexan parasites. Mol. Biochem. Parasitol. 141, 133–143.

Sato, S., Clough, B., Coates, L., Wilson, R.J., 2004. Enzymes for heme biosynthesis are found in both the mitochondrion and plastid of the malaria parasite *Plasmodium falciparum*. Protist 155, 117–125.

Schlitzer, M., 2008. Antimalarial drugs—what is in use and what is in the pipeline. Arch. Pharm. 341, 149–163.

Schonauer, M., Kastaniotis, A., Kursu, V., Hiltunen, J., Dieckmann, C., 2009. Lipoic acid synthesis and attachment in yeast mitochondria. J. Biol. Chem. 284, 23234–23242.

Schwenkert, S., Netz, D., Frazzon, J., Pierik, A., Bill, E., Gross, J., Lill, R., Meurer, J., 2009. Chloroplast HCF101 is a scaffold protein for [4Fe-4S] cluster assembly. Biochem J. 425, 207–214.

Seeber, F., 2002. Biogenesis of iron–sulfur clusters in amitochondriate and apicomplexan protists. Int. J. Parasitol. 32, 1207–1217.

Seeber, F., 2009. Malaria and anti-malarials—a focused view. In: Selzer, P.M. (Ed.), Anti-parasitic and Antibacterial Drug Discovery: From Molecular Targets to Drug Candidates. Wiley-VCH, Weinheim, pp. 277–298.

Seeber, F., Soldati, D., 2007. The metabolic functions of the mitochondrion and the apicoplast. In: Ajioka, J., Soldati, D. (Eds.), Toxoplasma: Molecular and Cellular Biology. Horizon Bioscience, Norfolk, pp. 409–435.

Seeber, F., Aliverti, A., Zanetti, G., 2005. The plant-type ferredoxin-$NADP^+$-reductase/ferredoxin redox system as a possible drug target against apicomplexan human parasites. Curr. Pharm. Design 11, 3159–3172.

Seeber, F., Limenitakis, J., Soldati-Favre, D., 2008. Apicomplexan mitochondrial metabolism: a story of gains, losses and retentions. Trends Parasitol. 24, 468–478.

Seemann, M., Tsesumbui, B., Wolff, M., Miginiacmaslow, M., Rohmer, M., 2006. Isoprenoid biosynthesis in plant chloroplasts via the MEP pathway: direct thylakoid/ferredoxin-dependent photoreduction of GcpE/IspG. FEBS Lett. 580, 1547–1552.

Seo, M., Koshiba, T., 2002. Complex regulation of ABA biosynthesis in plants. Trends Plant Sci. 7, 41–48.

Seow, F., Sato, S., Janssen, C.S., Riehle, M.O., Mukhopadhyay, A., Phillips, R.S., et al., 2005. The plastidic DNA replication enzyme complex of *Plasmodium falciparum*. Mol. Biochem. Parasitol. 141, 145–153.

Sharma, S.K., Kapoor, M., Ramya, T.N., Kumar, S., Kumar, G., Modak, R., et al., 2003. Identification, characterization, and inhibition of *Plasmodium falciparum* beta-hydroxyacyl-acyl carrier protein dehydratase (FabZ). J. Biol. Chem. 278, 45661–45671.

Shayeghi, M., Latunde-Dada, G.O., Oakhill, J.S., Laftah, A.H., Takeuchi, K., Halliday, N., et al., 2005. Identification of an intestinal heme transporter. Cell 122, 789–801.
Sheiner, L., Soldati-Favre, D., 2008. Protein trafficking inside *Toxoplasma gondii*. Traffic 9, 636–646.
Shepherd, M., Dailey, T.A., Dailey, H.A., 2006. A new class of [2Fe–2S]-cluster-containing protoporphyrin (IX) ferrochelatases. Biochem. J. 397, 47–52.
Siddall, M.E., 1992. Hohlzylinders. Parasitol. Today 8, 90–91.
Singh, N., Cheve, G., Avery, M.A., McCurdy, C.R., 2007. Targeting the methyl erythritol phosphate (MEP) pathway for novel antimalarial, antibacterial and herbicidal drug discovery: inhibition of 1-deoxy-D-xylulose-5-phosphate reductoisomerase (DXR) enzyme. Curr. Pharm. Des. 13, 1161–1177.
Sippl, M.J., Wiederstein, M., 2008. A note on difficult structure alignment problems. Bioinformatics 24, 426–427.
Sivakumar, T., Aboulaila, M., Khukhuu, A., Iseki, H., Alhassan, A., Yokoyama, N., et al., 2008. In vitro inhibitory effect of fosmidomycin on the asexual growth of *Babesia bovis* and *Babesia bigemina*. J. Protozool. Res. 18, 71–78.
Spork, S., Hiss, J.A., Mandel, K., Sommer, M., Kooij, T.W., Chu, T., et al., 2009. An unusual ERAD-like complex is targeted to the apicoplast of *Plasmodium falciparum*. Eukaryot. Cell 8, 1134–1145.
Spry, C., Saliba, K.J., 2009. The human malaria parasite *Plasmodium falciparum* is not dependent on host coenzyme A biosynthesis. J. Biol. Chem. 284, 24904–24913.
Spry, C., Kirk, K., Saliba, K.J., 2008. Coenzyme A biosynthesis: an antimicrobial drug target. FEMS Microbiol. Rev. 32, 56–106.
Staines, H., Alkhalil, A., Allen, R., Dejonge, H., Derbyshire, E., Egee, S., et al., 2007. Electrophysiological studies of malaria parasite-infected erythrocytes: current status. Int. J. Parasitol. 37, 475–482.
Stanway, R.R., Witt, T., Zobiak, B., Aepfelbacher, M., Heussler, V.T., 2009. GFP-targeting allows visualization of the apicoplast throughout the life cycle of live malaria parasites. Biol. Cell 101, 415–430.
Surolia, N., Surolia, A., 2001. Triclosan offers protection against blood stages of malaria by inhibiting enoyl-ACP reductase of *Plasmodium falciparum*. Nat. Med. 7, 167–173.
Surolia, A., Ramya, T.N., Ramya, V., Surolia, N., 2004. 'FAS't inhibition of malaria. Biochem. J. 383, 401–412.
Tachezy, J., Sanchez, L.B., Muller, M., 2001. Mitochondrial type iron–sulfur cluster assembly in the amitochondriate eukaryotes *Trichomonas vaginalis* and *Giardia intestinalis*, as indicated by the phylogeny of IscS. Mol. Biol. Evol. 18, 1919–1928.
Tanaka, R., Tanaka, A., 2007. Tetrapyrrole biosynthesis in higher plants. Annu. Rev. Plant Biol. 58, 321–346.
Tarun, A., Vaughan, A., Kappe, S., 2009. Redefining the role of de novo fatty acid synthesis in *Plasmodium* parasites. Trends Parasitol. 25, 545–550.
Teichert, J., Preiss, R., 1992. HPLC-methods for determination of lipoic acid and its reduced form in human plasma. Int. J. Clin. Pharmacol. Ther. Toxicol. 30, 511–512.
Thomsen-Zieger, N., Schachtner, J., Seeber, F., 2003. Apicomplexan parasites contain a single lipoic acid synthase located in the plastid. FEBS Lett. 547, 80–86.
Tomova, C., Humbel, B.M., Geerts, W.J.C., Entzeroth, R., Holthuis, J.C.M., Verkleij, A.J., 2009. Membrane contact sites between apicoplast and ER in *Toxoplasma gondii* revealed by electron tomography. Traffic 10, 1471–1480.
Tonhosolo, R., D'Alexandri, F.L., Genta, F.A., Wunderlich, G., Gozzo, F.C., Eberlin, M.N., et al., 2005. Identification, molecular cloning and functional characterization of an octaprenyl pyrophosphate synthase in intra-erythrocytic stages of *Plasmodium falciparum*. Biochem. J. 392, 117–126.

Tonhosolo, R., D'Alexandri, F.L., De Rosso, V.V., Gazarini, M.L., Matsumura, M.Y., Peres, V.J., et al., 2009. Carotenoid biosynthesis in intraerythrocytic stages of *Plasmodium falciparum*. J. Biol. Chem. 284, 9974–9985.

Tonkin, C.J., Kalanon, M., McFadden, G.I., 2008. Protein targeting to the malaria parasite plastid. Traffic 9, 166–175.

Toso, M.A., Omoto, C.K., 2007. *Gregarina niphandrodes* may lack both a plastid genome and organelle. J. Eukaryot. Microbiol. 54, 66–72.

Vaidya, A., Mather, M., 2009. Mitochondrial evolution and functions in malaria parasites. Annu. Rev. Microbiol. 63, 249–267.

Vaishnava, S., Striepen, B., 2006. The cell biology of secondary endosymbiosis—how parasites build, divide and segregate the apicoplast. Mol. Microbiol. 61, 1380–1387.

van Dooren, G.G., Su, V., D'Ombrain, M.C., McFadden, G.I., 2002. Processing of an apicoplast leader sequence in *Plasmodium falciparum* and the identification of a putative leader cleavage enzyme. J. Biol. Chem. 277, 23612–23619.

van Dooren, G.G., Marti, M., Tonkin, C.J., Stimmler, L.M., Cowman, A.F., McFadden, G.I., 2005. Development of the endoplasmic reticulum, mitochondrion and apicoplast during the asexual life cycle of *Plasmodium falciparum*. Mol. Microbiol. 57, 405–419.

van Dooren, G.G., Stimmler, L.M., McFadden, G.I., 2006. Metabolic maps and functions of the *Plasmodium* mitochondrion. FEMS Microbiol. Rev. 30, 596–630.

Varadharajan, S., Dhanasekaran, S., Bonday, Z.Q., Rangarajan, P.N., Padmanaban, G., 2002. Involvement of delta-aminolaevulinate synthase encoded by the parasite gene in de novo haem synthesis by *Plasmodium falciparum*. Biochem. J. 367, 321–327.

Varadharajan, S., Sagar, B.K., Rangarajan, P.N., Padmanaban, G., 2004. Localization of ferrochelatase in *Plasmodium falciparum*. Biochem. J. 384, 429–436.

Vaughan, A.M., O'neill, M.T., Tarun, A.S., Camargo, N., Phuong, T., Aly, A.S.I., et al., 2008. Type II fatty acid synthesis is essential only for malaria parasite late liver stage development. Cell. Microbiol. 11, 506–520.

Vickery, L.E., Cupp-Vickery, J.R., 2007. Molecular chaperones HscA/Ssq1 and HscB/Jac1 and their roles in iron–sulfur protein maturation. Crit. Rev. Biochem. Mol. Biol. 42, 95–111.

Vinella, D., Brochier-Armanet, C., Loiseau, L., Talla, E., Barras, F., 2009. Iron–sulfur (Fe/S) protein biogenesis: phylogenomic and genetic studies of A-type carriers. PLoS Genet. 5, e1000497.

Vollmer, M., Thomsen, N., Wiek, S., Seeber, F., 2001. Apicomplexan parasites possess distinct nuclear encoded but apicoplast-localized plant-type ferredoxin-$NADP^+$-reductase and ferredoxin. J. Biol. Chem. 276, 5483–5490.

Wakaguri, H., Suzuki, Y., Sasaki, M., Sugano, S., Watanabe, J., 2009. Inconsistencies of genome annotations in apicomplexan parasites revealed by 5′-end-one-pass and full-length sequences of oligo-capped cDNAs. BMC Genomics 10, 312.

Waller, R.F., McFadden, G.I., 2005. The apicoplast: a review of the derived plastid of apicomplexan parasites. Curr. Issues Mol. Biol. 7, 57–79.

Waller, R.F., Keeling, P.J., Donald, R.G., Striepen, B., Handman, E., Lang-Unnasch, N., et al., 1998. Nuclear-encoded proteins target to the plastid in *Toxoplasma gondii* and *Plasmodium falciparum*. Proc. Natl. Acad. Sci. USA 95, 12352–12357.

Waller, R.F., Reed, M.B., Cowman, A.F., McFadden, G.I., 2000. Protein trafficking to the plastid of *Plasmodium falciparum* is via the secretory pathway. EMBO J. 19, 1794–1802.

Waller, R.F., Ralph, S.A., Reed, M.B., Su, V., Douglas, J.D., Minnikin, D.E., et al., 2003. A type II pathway for fatty acid biosynthesis presents drug targets in *Plasmodium falciparum*. Antimicrob. Agents Chemother. 47, 297–301.

Wan, J.T., Jarrett, J.T., 2002. Electron acceptor specificity of ferredoxin (flavodoxin): NADP+ oxidoreductase from *Escherichia coli*. Arch. Biochem. Biophys. 406, 116–126.

Wasmuth, J., Daub, J., Peregrín-Alvarez, J., Finney, C., Parkinson, J., 2009. The origins of apicomplexan sequence innovation. Genome Res. 19, 1202–1213.

Wastling, J.M., Xia, D., Sohal, A., Chaussepied, M., Pain, A., Langsley, G., 2009. Proteomes and transcriptomes of the Apicomplexa–where's the message? Int. J. Parasitol. 39, 135–143.

Waters, N., Kopydlowski, K., Guszczynski, T., Wei, L., Sellers, P., Ferlan, J., et al., 2002. Functional characterization of the acyl carrier protein (PfACP) and beta-ketoacyl ACP synthase III (PfKASIII) from *Plasmodium falciparum*. Mol. Biochem. Parasitol. 123, 85–94.

Weiss, C., Bonshtien, A., Farchi-Pisanty, O., Vitlin, A., Azem, A., 2009. Cpn20: siamese twins of the chaperonin world. Plant Mol. Biol. 69, 227–238.

Whitaker, J.W., Westhead, D.R., Mcconkey, G.A., 2009. Alio intuitu: the automated reconstruction of the metabolic networks of parasites. Trends Parasitol. 25, 396–397.

White, S.W., Zheng, J., Zhang, Y.-M., Rock, C.O., 2005. The structural biology of type ii fatty acid biosynthesis. Annu. Rev. Biochem. 74, 791–831.

Wickramasinghe, S.R., Inglis, K.A., Urch, J.E., Muller, S., van Aalten, D.M., Fairlamb, A.H., 2006. Kinetic, inhibition and structural studies on 3-oxoacyl-ACP reductase from *Plasmodium falciparum*, a key enzyme in fatty acid biosynthesis. Biochem. J. 393, 447–457.

Wiesner, J., Jomaa, H., 2007. Isoprenoid biosynthesis of the apicoplast as drug target. Curr. Drug Targets 8, 3–13.

Wiesner, J., Seeber, F., 2005. The plastid-derived organelle of protozoan human parasites as a target of established and emerging drugs. Expert Opin. Ther. Targets 9, 23–44.

Wiesner, J., Kettler, K., Sakowski, J., Ortmann, R., Katzin, A.M., Kimura, E.A., et al., 2004. Farnesyltransferase inhibitors inhibit the growth of malaria parasites in vitro and in vivo. Angew. Chem. Int. Ed. Engl. 43, 251–254.

Wiesner, J., Reichenberg, A., Heinrich, S., Schlitzer, M., Jomaa, H., 2008. The plastid-like organelle of apicomplexan parasites as drug target. Curr. Pharm. Des. 14, 855–871.

Williamson, D.H., Denny, P.W., Moore, P.W., Sato, S., McCready, S., Wilson, R.J., 2001. The in vivo conformation of the plastid DNA of *Toxoplasma gondii*: implications for replication. J. Mol. Biol. 306, 159–168.

Williamson, D.H., Preiser, P.R., Moore, P.W., McCready, S., Strath, M., Wilson, R.J., 2002. The plastid DNA of the malaria parasite *Plasmodium falciparum* is replicated by two mechanisms. Mol. Microbiol. 45, 533–542.

Wilson, R.J., 2002. Progress with parasite plastids. J. Mol. Biol. 319, 257–274.

Wilson, R.J., 2005. Parasite plastids: approaching the endgame. Biol. Rev. Camb. Philos. Soc. 80, 129–153.

Wilson, R.J., Williamson, D.H., 1997. Extrachromosomal DNA in the Apicomplexa. Microbiol. Mol. Biol. Rev. 61, 1–16.

Wilson, R.J., Williamson, D.H., Preiser, P., 1994. Malaria and other Apicomplexans: the "plant" connection. Infect. Agents Dis. 3, 29–37.

Wilson, R.J., Denny, P.W., Preiser, P.R., Rangachari, K., Roberts, K., Roy, A., et al., 1996. Complete gene map of the plastid-like DNA of the malaria parasite *Plasmodium falciparum*. J. Mol. Biol. 261, 155–172.

Wilson, R.J., Rangachari, K., Saldanha, J.W., Rickman, L., Buxton, R.S., Eccleston, J.F., 2003. Parasite plastids: maintenance and functions. Philos. Trans. R Soc. Lond. B Biol. Sci. 358, 155–162.

Wrenger, C., Müller, S., 2004. The human malaria parasite *Plasmodium falciparum* has distinct organelle-specific lipoylation pathways. Mol. Microbiol. 53, 103–113.

Wrenger, C., Eschbach, M.-L., Müller, I.B., Laun, N.P., Begley, T.P., Walter, R.D., 2006. Vitamin B1 de novo synthesis in the human malaria parasite *Plasmodium falciparum*

depends on external provision of 4-amino-5-hydroxymethyl-2-methylpyrimidine. Biol. Chem. 387, 41–51.
Wrenger, C., Knöckel, J., Walter, R.D., Müller, I.B., 2008. Vitamin B1 and B6 in the malaria parasite: requisite or dispensable? Braz. J. Med. Biol. Res. 41, 82–88.
Wu, B., 2006. Heme Biosynthetic Pathway in Apicomplexan Parasites. Department of Biology, University of Pennsylvania, Philadelphia. http://repository.upenn.edu/dissertations/AAI3246256/.
Xia, D., Sanderson, S.J., Jones, A.R., Prieto, J.H., Yates, J.R., Bromley, E., et al., 2008. The proteome of *Toxoplasma gondii*: integration with the genome provides novel insights into gene expression and annotation. Genome Biol. 9, R116.
Xu, X.M., Møller, S.G., 2008. Iron–sulfur cluster biogenesis systems and their crosstalk. ChemBioChem 9, 2355–2362.
Yasuno, R., Wada, H., 2002. The biosynthetic pathway for lipoic acid is present in plastids and mitochondria in *Arabidopsis thaliana*. FEBS Lett. 517, 110–114.
Yeh, I., Hanekamp, T., Tsoka, S., Karp, P.D., Altman, R.B., 2004. Computational analysis of *Plasmodium falciparum* metabolism: organizing genomic information to facilitate drug discovery. Genome Res. 14, 917–924.
Yu, M., Kumar, T.R.S., Nkrumah, L.J., Coppi, A., Retzlaff, S., Li, C.D., et al., 2008. The fatty acid biosynthesis enzyme FabI plays a key role in the development of liver-stage malarial parasites. Cell Host Microbe 4, 567–578.
Zanetti, G., Binda, C., Aliverti, A., 2001. The [2Fe–2S] ferredoxins. In: Messerschmidt, A., Huber, T., Poulos, T., Wieghardt, K. (Eds.), Handbook of Metalloproteins. Wiley & Sons, Chichester, pp. 532–542.
Zuther, E., Johnson, J.J., Haselkorn, R., McLeod, R., Gornicki, P., 1999. Growth of *Toxoplasma gondii* is inhibited by aryloxyphenoxypropionate herbicides targeting acetyl-CoA carboxylase. Proc. Natl. Acad. Sci. USA 96, 13387–13392.

CHAPTER SIX

Molecular Mechanisms of Pathogenesis of Parkinson's Disease

M.I. Shadrina, P.A. Slominsky, *and* S.A. Limborska

Contents

1. Introduction 230
2. Clinical Features of Parkinson's Disease 231
3. Neuropathology of Parkinson's Disease 233
4. Genetic Causes of Parkinson's Disease 234
   4.1. Monogenic forms of Parkinson's disease 235
   4.2. Genes and biological processes involved in the pathogenesis of sporadic Parkinson's disease 246
5. Conclusion 256
References 257

Abstract

Parkinson's disease is a complex disease characterized by a progressive degeneration of nigrostriatal dopaminergic neurons. The development of this condition is defined by the interaction between the genetic constitution of an organism and environmental factors. Analysis of the genes associated with development of monogenic forms of disease has allowed pointing out several mechanisms involved in Parkinson's disease pathogenesis such as the ubiqutin–proteasome degradation, differentiation of dopaminergic neurons, mitochondrial dysfunction, oxidative damage, and others. In this review, a variety of data which throw light on molecular mechanisms underlying pathogenesis of Parkinson's disease will be considered.

Key Words: Parkinson's disease, Pathogenesis, Genetic factors, Ubiquitin–proteasome system, Mitochondrial dysfunction.

Institute of Molecular Genetics, Russian Academy of Sciences, Moscow, Russia

International Review of Cell and Molecular Biology, Volume 281
ISSN 1937-6448, DOI: 10.1016/S1937-6448(10)81006-8

1. Introduction

Parkinson's disease (idiopathic or primary parkinsonism; PD) refers to a group of chronically progressing neurodegenerative disorders linked to disturbances in the brain basal ganglia activity. Descriptions of PD-like symptoms have existed for thousands of years and they have been found in the texts of Ayurveda (a system of ancient Indian medicine) and in ancient Chinese manuscripts. Even so, it is universally accepted that PD was described for the first time by the English physician James Parkinson in his illustrious ''Essay on the Shaking Palsy,'' in which he brought together observations of six patients, with their emaciation and quivering considered to be the main manifestation of the disease. Seventy years later, the prominent French neurologist Jean-Martin Charcot gave his first clinical description of the disease and named it Parkinson's disease eponymously in honor of James Parkinson.

As regards the frequency of neurodegenerative disorders, PD occupies the second position after Alzheimer's disease. All in all, the number of PD patients in the world approaches four million people, and no less than 1% of the world population aged above 50 years (Golubev et al., 2000), or greater than 2–4% of the population aged over 65 years (Polymeropoulos et al., 1996), on average, suffer from idiopathic parkinsonism. The number of idiopathic parkinsonism patients is growing and the starting age of the disease is decreasing (Forno, 1996).

The occurrence of the disease strongly differs among various ethnic groups and depends on their geographical location. For instance, the lowest incidence of PD, 10–15 patients per 100,000 population, has been stated for Chinese residents of continental China, the second-highest incidence of PD has been observed in Australia, at 414 patients, and the highest in Argentina, at 650 patients per 100,000 of the entire population. The average spread in PD incidence in European countries is from 100 to 200 patients per 100,000 persons (BenMoyal-Segal and Soreq, 2006). In Russia, the incidence of the disease does not differ from the average in Europe and constitutes 180 patients per 100,000 persons of the population (Golubev et al., 2000).

The average starting age for the disease is about 57 years, with the first symptoms of the disease showing earlier, before 40 years of age, in about 5–10% of patients, and sometimes the disease may start in children or in teenagers (juvenile parkinsonism). However, independent of the etiology and age of the start of disease development, the duration of life in the patients considerably shortens. The mortality among PD patients is about three times as great as in a general population, allowance being made for the patients' age, sex, and ethnic group. Ten years after the start of the disease, 60% of patients become severe invalids or die; 15 years after, this rate

reaches 80%. The average duration of life of patients with PD is 9 years, counting from the start of the disease, although individual variations lie within the range of 1–33 years (Kontakos and Stokes, 1999).

The forms of PD are familial and sporadic. The familial form of PD can be inherited according to both autosomal-dominant and autosomal-recessive types and develop at an early (up to 45 years of age), middle (45–60 years of age), and late (after 65 years) age. Juvenile autosomal-recessive parkinsonism begins at up to 20 years of age, and forms a separate group of the familial forms of parkinsonism. Two forms represent the sporadic PD, one with an early start of the disease (before 45 years of age) and the other with a later start of PD (after 45 years of age).

The familial form of PD was described for the first time at the beginning of the twentieth century, and it is now well acknowledged that 10–12% of PD patients are characterized by positive familial anamneses. However, the majority of PD patients suffer from a sporadic form determined by the complicated interrelationship between the organism's genetic constitution and environmental factors. In the idiopathic parkinsonism patients' relatives, the combination of a similar genetic background and the mode of life raises two- to sevenfold the risk of acquiring the same disease.

To date, 17 loci in the human genome have been revealed as being involved, in one way or another, in PD pathogenesis. Analysis of all hitherto-revealed loci allows several mechanisms that cause the disease to be suggested. They are primarily processes associated with the ubiquitin-dependent proteosome degradation of proteins, mitochondrial dysfunction, dopaminergic neuron differentiation, the functioning of synapses and lysosomes, dopamine exchange, and other processes.

In this review, we shall focus both on individual genes whose mutations lead to monogenic PDs and on various biological processes and genetic systems whose disturbances might cause the development of a sporadic form of the disease.

2. Clinical Features of Parkinson's Disease

PD is a permanently progressing condition characterized by a classical tetrad of clinical traits, namely, resting tremor, facial and manual skeletal muscle rigidity, bradykinesia (slowness of movement), and postural instability (disturbed coordination of movements after sleeping). These motional symptoms generally arise as asymmetrical and gradually affect the opposite part of the body. However, that half of the body that was involved initially remains most strongly afflicted during the entire course of the disease (Weintraub et al., 2008).

Usually, most PD patients (70–90%) are inflicted with resting tremor at the start of the disease, which emerges independent of a motor action, an essential difference from the intentional tremor found in cerebellar insufficiency that is only shown during active motion. At the start of PD, tremor involves the distal portions of the upper extremities and takes the form of a typical ''pill-rolling'' movement. In the subsequent course of the disease, the tremor spreads over the proximal portions of the upper and lower extremities, the lower jaw, the articulation organs, and the body. It should be noted that tremor is the most distinctly marked symptom in young patients, whereas the elderly show a more pronounced manifestation of bradykinesia that is found in 80–90% of the patients and is expressed not only by lowered spontaneous motional activity but also by the disturbed qualitative structure of their movement. In this case, the coordinate movement of the extremities (synkinesia) is observed and the accuracy of movements suffers considerably. Akinesia, the difficulty in the initiation of a movement, constitutes the final stage of bradykinesia and considerably reduces the patient's working ability and his ability to live without help. Rigidity is displayed clinically by enhanced muscular tonus of the patient's extremities, the body, the facial muscles, and is observed in virtually all PD patients. Enhanced muscular tone is accompanied by uniform resistance at all stages of passive movement, and the so-called ''cogwheel'' phenomenon, that is, rhythmical variations of the degree of rigidity. Owing to the muscle strain prevalence in the flexor muscles, the patient's posture grows stooped, conditioning the typical round-backed posture of PD patients. Postural instability, or disturbed balance, is displayed at later stages of the disease. There exist several body balance-supporting processes; they are the orientation via somatic and sensor, vestibular and visual stimuli, the maintenance of the basic muscle tone, and the regulation of coordinate movement. With PD, all of these processes are impaired to some degree, although disturbances of motor functions play the first-order role in the development of postural instability (Bronte-Stewart et al., 2002; Golubev et al., 2000; Weintraub et al., 2008). All the above-mentioned clinical signs are the most typical for PD, that is, in most PD cases, the initial manifestations of the disease are motional symptoms.

Apart from the basic symptoms, the patients suffer from vegetative disorders, such as a change of dietary preferences and of the functioning of the intestines (constipation), excessive salivation, and frequency of urination. Pathologies of speech and memory are observed, as well as cognitive dysfunction that progresses to dementia in 20–80% of patients. Depression also develops. At later stages of PD, organic psychosis with hallucination and paranoid manifestations or chronic delirium (temporal and spatial disorientation, confusion of conscience, verbal impairment, hallucination, and deliration) emerge (Golubev et al., 2000; Weintraub et al., 2008).

3. Neuropathology of Parkinson's Disease

The neurodegenerative changes associated with PD are linked with the selective death of different types of neurons. In the first place, reduction of dopaminergic neurons in the compact portion of the *substantia nigra*, in basal nuclei, and in the *tectum mesencephalicum* is observed. The death of *substantia nigra* nerve cells leads to a decrease of the dopamine level in the *putamen* and in the *corpus striatum*, which leads to the emergence of motor symptoms, namely, tremor, rigidity, and, most importantly, bradykinesia. It is now believed that the typical clinical signs of PD are displayed after the death of 60–80% of dopaminergic neurons of the compact part of the *substantia nigra* and an 80% decrease of the dopamine level in the *putamen* (Bernheimer et al., 1973; Cookson et al., 2008).

One of the most indicative features of PD is the presence of eosinophilic fibrillary intracellular inclusions in neuronal bodies and appendages. Those are the so-called Lewy bodies and Lewy neurites, both discovered in the *substantia innominata* by the German neurologist Frederic Lewy in 1912. They constitute spherical aggregates of various 15 μm-sized proteins, fats, and polysaccharides, with α-synuclein, neurofilaments, ubiquitin, parkin, and synphilin being the main protein components of Lewy bodies and neurites. However, at present, both the formation initiation mechanisms of Lewy bodies and the chronological order of their formation remain unknown (Beyer et al., 2009).

The role of Lewy bodies in the death of neuronal cells remains unelucidated and open to debate. On the one hand, these inclusions can exert a toxic effect on neurons by isolation of the normal proteins needed for cell functioning. On the other hand, Lewy bodies can protect nerve cells by aggregating the damaged cellular proteins (Beyer et al., 2009). Lewy bodies can be revealed in other neurodegenerative diseases, such as multiple systemic atrophy and the condition of diffusely distributed Lewy bodies, Alzheimer's disease, and in healthy elderly persons (Gibb and Lees, 1988). However, it is believed that the presence of Lewy bodies together with the death of *substantia nigra* neurons is a neuropathological feature that distinguishes idiopathic parkinsonism from other similar diseases (Golubev et al., 2000). At the same time, such inclusions are not revealed in all the PD cases and cannot be regarded as obligatory histological markers of the disease. Lewy bodies are usually missing in patients with juvenile autosomal and recessive parkinsonism with mutations in the *PARK2* gene. In PD coupled with mutations in the PARK8 gene, Lewy bodies can be both absent and present (Mori et al., 1998; Takahashi et al., 1994).

One more characteristic feature of the neurodegenerative changes in PD is the development of gliosis (Orr et al., 2002), where anomalous

enhancement of the proliferation of different glial cell types is observed in the *corpus striatum* and in the *substantia nigra*. The leading role in the development of gliosis most likely belongs to the activation of microglia, which is important in the inflammatory processes, the expression of the major histocompatibility complex class II genes being increased (Croisier and Graeber, 2006).

The reduction of the amount of neurons and the formation of Lewy bodies takes place not only in the *substantia nigra*, basal nuclei, and the *tectum mesencephalicum*, but degenerative processes are also observed in the *locus coeruleus*, the *pedunculopontine* nucleus, the *raphe nucleus*, the dorsal motor nucleus of the vagal nerve, in olfactory bulbs, parasympathetic and sympathetic postganglionic neurons, in the Meynert nucleus, the amygdaloid nucleus, and the cerebral cortices. Damage in the structures mentioned leads to the development of nonmotor clinical symptoms. Recently, the German neuropathologists, Braak et al. (2004), proposed a six-stage development scheme of degeneration processes during PD, which was based on studying postmortem nerve tissue samples and took into consideration the preclinical stages of the disease. According to this scheme, the first stage of the disease starts with pathological changes in the vagal nerve's dorsal motor neurons. In the second stage, the pathogenic processes spread over the *medulla oblongata*, the *tectum mesencephalicum*, and the olfactory apparatus, which leads to olfactory disturbances, constipation, and sleep disorders. The marked clinical pattern of PD only develops in the third stage when the *substantia nigra* and the limbic system are involved. Death of *substantia nigra* neurons produces a decrease of the dopamine level in the *putamen* and the *corpus striatum* and subsequent symptoms typical for PD, namely, tremor in rest, rigidity, and most importantly, bradykinesia. In the final, sixth stage, the pathology affects the neocortex, which causes loss of memory and cognitive disorders.

4. Genetic Causes of Parkinson's Disease

The putative role of genetic factors in the pathogenesis of PD has long been discussed, and the data collected during analyses of family and twin studies confirm the significance of the genetic constituent in the progress of the disease. For instance, studying twins has demonstrated that, even in PD discordant twins, concordance was observed with regard to nigrostriatal function disturbance (45% in monozygotic twins and 29% in dizygotic twins) (Burn et al., 1992). Studies using positron emission tomography have stated a high concordance (75% in monozygotic twins and 22% in dizygotic twins) for the subclinical dopaminergic dysfunction level (Piccini et al., 1999). Analysis of families with PD has shown that the risk of the

disease in the relatives of idiopathic (sporadic) parkinsonism patients is three- to 14-fold, provided the genetic backgrounds and the mode of life are similar (Pankratz and Foroud, 2004). Families have also been revealed showing Mendelian inheritance of PD, autosomal recessively and autosomal dominantly. The first direct proof in favor of a significant role of genetic factors in PD pathogenesis was obtained at the end of the twentieth century when the *SNCA* gene, whose mutations lead to the development of PD, was first identified in studies of the autosomal-dominant form of the disease in an Italian–American family. This gene encodes the protein α-synuclein, a basic protein component of Lewy bodies. Presently, 17 different loci have been discovered, which are, in one way or another, involved in the pathogenesis of PD (Tables 6.1 and 6.2), with only seven loci so far revealed for which the disease-implicated genes have been identified (Table 6.1). At present, evidence concerning 10 more loci is available (Table 6.2), allowing only assumptions to be made with regard to their association with PD.

However, the incidence of familial PD forms is only 10–15%, and in most cases the disease is sporadic and idiopathic. Many problems, which are called forth by the complicated pattern of the disease, come out in determination of the role of genetic factors in the development of the sporadic PD form. Factors that considerably complicate the investigation of the genetic causes of PD include: the delayed start of the disease; in a majority of cases, incomplete penetrance of the genetic factors involved; the genetic heterogeneity of the disease; and the ponderous contribution of environmental factors to PD pathogenesis. In both forms of PD (monogenic and sporadic), however, the common pattern of neuropathology is observed, linked with the degeneration of dopaminergic neurons of the *substantia nigra*. The familial and the sporadic forms of PD are indistinguishable at the clinical level, a possible indication of the existence of common pathogenetic mechanisms.

Analysis of all hitherto-revealed loci allows several mechanisms to be suggested, which account for the causes of the selective and the progressive death of dopaminergic neurons. Those are, in the first instance, processes connected with the ubiquitin-dependent proteasomal protein degradation, mitochondrial dysfunction, the differentiation of dopaminergic neurons, the functioning of synapses and lysosomes, the exchange of dopamine, and other processes.

4.1. Monogenic forms of Parkinson's disease

4.1.1. PARK1 (PARK4) locus

As mentioned above, the *SNCA* gene mapped on chromosome 4q21 (locus PARK1), and coding for the protein α-synuclein was historically the first identified gene associated with the familial form of PD. At present, three missense mutations (A53T, A30P, and E46K) have been described in the

Table 6.1 Loci and genes with conclusive evidence for Parkinson's disease pathogenesis

Locus	Map position	Gene/protein	Putative function	Inheritance pattern/ phenotype PD	Mutation in familial PD	Variants and risk of sporadic PD
PARK1/ PARK4	4q21	SNCA/α-synuclein	Presynaptic protein, component of Lewy bodies, dopamine transmission	AD/EOPD with rapid progression and dementia, sporadic	PM and genomic duplication and triplication	Promoter polymorphism, 5′ and 3′ variants ↑ risk for PD
PARK2	6q25–q27	PARK2/E3 ubiquitin-protein ligase parkin	Ubiquitin E3 ligase, has neuroprotective function	AR/juvenile and EOPD with slow progression, dystonia; sporadic	Various mutations, exonic deletions, duplication, triplication	Promoter polymorphism and HM ↑ risk for PD
PARK5	4p14	UCH-L1/ubiquitin carboxyl-terminal hydrolase isozyme L1	Ubiquitin hydrolase	AD/LOPD	I93M	S18R variant may ↓ risk for PD
PARK6	1p35–p36	PINK1/serine, threonine-protein kinase PINK1	Mitochondrial protein kinase, has neuroprotective function	AR/EOPD with slow progression, tremor	PM and large deletions	HM may ↑ risk for PD
PARK7	1p36	PARK7/protein DJ-1	Chaperone, antioxidant	AR/EOPD, dystonia, psychiatric symptoms	PM and large deletions	HM may ↑ risk for PD
PARK8	12q12	LRRK2/leucine-rich repeat serine/ threonine-protein kinase 2	Protein kinase, protect cells from stress-induced mitochondrial dysfunction	AD/LOPD, tremor	Different mutations and missense variants	HM may ↑ risk for PD
PARK9	1p36	ATP13A2/probable cation-transporting ATPase 13A2	Lysosomal ATPase	AR/juvenile Kufor-Rakeb syndrome, EOPD	PM	unknown

AD, autosomal-dominant; AR, autosomal-recessive; EO, early onset; LO, late onset; PM, point mutations; HM, heterozygous mutations.

Table 6.2 Loci and genes with suggestive role in Parkinson's disease pathogenesis

Locus	Map position	Gene/protein	Putative function	Inheritance pattern/ phenotype PD	Mutation in familial PD	Variants and risk of sporadic PD
PARK3?	2p13	SPR/sepiapterin reductase	Catalyzes the NADPH-dependent reduction and is important in the biosynthesis of tetrahydrobiopterin (BH4)	AD/LOPD, dementia	Not identified	SPR variants may ↑ risk for PD
PARK10?	1p32	UPS24/ubiquitin carboxyl-terminal hydrolase 24	Involved in the ubiquitin-dependent proteolytic pathway	Unclear/LOPD	Not identified	UPS24 variants may ↑ risk PD
PARK11?	2q36–q37	GIGYF2/PERQ amino acid-rich with GYF domain-containing protein 2	Involved in regulation of tyrosine kinase receptor signaling	AD/LOPD	PM	Not identified
PARK12	Xq12–q25	Unknown	Unknown	Unclear	Not identified	Unknown
PARK13	2p13	HTRA2/serine protease HTRA2, mitochondrial	Serine protease, may be involved in mitochondrial dysfunction	Unclear	Not identified	HTRA2 variants may contribute to risk PD

(*continued*)

Table 6.2 (*continued*)

Locus	Map position	Gene/protein	Putative function	Inheritance pattern/ phenotype PD	Mutation in familial PD	Variants and risk of sporadic PD
PARK14?	22q13.1	PLA2G6/85 kDa calcium-independent phospholipase A2	Catalyzes the release of fatty acids from phospholipids	AR/juvenile, levodopa-responsive dystonia parkinsonism	PM	Not investigated
PARK15?	22q12–q13	FBXO7/F-box only protein 7	Involved in the ubiquitin-dependent proteolytic pathway	AR/EO, parkinsonian-pyramidal syndrome	PM	Not investigated
Not assigned	2q22–q23	NR4A2/nuclear receptor subfamily 4 group A member 2	Probable nuclear receptor. May function as a general coactivator of gene transcription	AD?	PM	NR4A2 variants may ↑ risk
Not assigned	5q23.1–q23.3	SNCAIP/ synphilin-1	Interact with α-synuclein, is substrate of parkin and is a part of Lewy body	Unknown	Unknown	PM of SNCAIP may contribute to risk PD
Not assigned	15q25	POLG/DNA polymerase subunit gamma-1	Mitochondrial DNA polymerase catalytic subunit	AD, AR/ EOPD	PM	POLG polyglutamine tract variants may contribute to risk PD

AD, autosomal-dominant; AR, autosomal-recessive; EO, early onset; LO, late onset; PM, point mutations; HM, heterozygous mutations.

α-synuclein gene; they are encountered very rarely and lead to the development of PD with the autosomal and dominant character of inheritance (Krüger et al., 1998; Polymeropoulos et al., 1997; Zarranz et al., 2004). The A53T mutation discovered in at least 13 families is the most frequent one. Interestingly, 12 such families originated from Greece and Italy, and, in all probability, had a common ancestor (Lesage and Brice, 2009). No point mutations in gene *SNCA* have ever been found in families from the Russian population (Illarioshkin et al., 2000).

Recently, data were reported showing that mutations linked with changed α-synuclein doses are likely to play an important role in the development of Parkinson's disease. Duplication and triplication (earlier named the PARK4 locus) of the 0.4–6.37 Mb region occur with the α-synuclein gene. Multiplications of gene *SNCA* are found more frequently than point mutations and they were revealed in families with the autosomal and dominant form of the disease from France (Chartier-Harlin et al., 2004), America (Singleton et al., 2003), Japan (Nishioka et al., 2006), and Korea (Ahn et al., 2008). The presence of both the duplication (the Swedish branch) and the triplication (the American branch) has been shown in a Swedish–American family. Clinical and genetic studies of families with *SNCA* gene duplications showed that, with an increase of the number of gene copies from duplications to triplications, the disease starts progressing at an earlier age and adopts a more severe form (with dementia arising in the patients) (Fuchs et al., 2007).

The *SNCA* gene encodes the 140 amino acid residue-sized protein α-synuclein that contains no folded structures in its native state and includes three functional portions, an N-end region with an amphipathic α-helical domain, a hydrophobic central area bearing a nonamyloid-b component domain (the NAC domain), and an acidic C-end region. The exact function of the protein remains unknown. Data are available that it is likely to be a molecular chaperone, to regulate protein–protein and protein–lipid interactions and to play an important role in the exchange of synaptic vesicles, in the storage and compartmentalization of neurotransmitters, primarily, dopamine (Yavich et al., 2004). It is well known that α-synuclein protofibrils constitute the main component of Lewy bodies in PD, an indication of the important role of the α-synuclein aggregation processes in PD pathogenesis (Fortin et al., 2004). Similar accumulation of α-synuclein might be because of a change of the amount of α-synuclein and an elevation of its expression level (occurring in the duplications and triplications of the *SNCA* gene area) or because of changes in the proteolytic degradation processes of α-synuclein mutant forms.

4.1.2. PARK2 locus

The *PARK2* gene was mapped on chromosome 6q25.2–q27 in 1997, and its mutations were described for the first time for a family from Japan with the juvenile autosomal-recessive parkinsonism (Kitada et al., 1998).

Later these mutations were found in members of different ethnic groups. At the present time, it is well accepted that *PARK2* gene mutations are most often the cause of the development of PD, and that homozygosity or compound heterozygosity at *PARK2* gene mutations cause the disease in about 50% of patients with juvenile autosomal-recessive parkinsonism (Oliveira et al., 2003). Over 120 different mutations in the *PARK2* gene have so far been revealed in families with the autosomal-recessive juvenile form of the disease, the main portion of them being missense mutations (over 50 amino acid substitutions identified) and mutations with a change in the abundance of individual exons or groups of exons (deletions, duplications, and triplications) (Hedrich et al., 2002; Illarioshkin et al., 2003; Kann et al., 2002; Rashmi et al., 2005). The high mutation frequency with abundant changes provides a characteristic trait of the mutation range in the juvenile form of PD. These mutations are revealed in 33–67% of patients with the juvenile form of PD (Bertoli-Avella et al., 2005; Hedrich et al., 2002; Periquet et al., 2003). In the Russian population, 35% of patients suffering from the juvenile autosomal-recessive form of PD showed mutations with changed abundance (Slominsky et al., 2003). Thus, most patients with mutations in the *PARK2* gene have no Lewy bodies and neurites typical for other PD forms deserves to be mentioned. In these patients, development of typical clinical PD symptoms is observed. However, in patients with mutations in the *PARK2* gene, an early and more symmetrical beginning of the development of PD symptoms is apparent; a slow progression of the disease, with dystonia as the first clinical sign, hyperreflexia and weakly expressed postural disorders are typical (Lohmann et al., 2003).

Locus PARK2 consists of 12 exons and codes for the protein parkin bearing 465 amino acid residues and showing ubiquitin ligase activity. The structural and functional analysis of the *PARK2* gene and the protein parkin has shown this protein to be an E3 ubiquitin ligase and a member of the RBR family of ubiquitin ligases. The direct function of parkin is the transfer of ubiquitin from ubiquitin-conjugating enzymes to specific substrates, namely, α-synuclein, synphilin-1, parkin, Sept-4 (CDCrel-2), PAEL-R, cyclin E, JTV1 (p38), synaptotagmin XI, tubulin, the p38 subunit of amino acyl t-RNA synthetase and proteins with polyglutamine repeats (Shimura et al., 2000). Insufficiency of parkin can lead to disturbance of ubiquitination processes and to the accumulation of proteins in the cell that are parkin substrates, in turn leading to neuronal death. Currently, data have been collected suggesting that parkin acts as a complex neuroprotector protein in a number of toxic inflictions critical for the survival of dopaminergic neurons (Cookson, 2005). Data are available indicating that parkin can participate in the functioning of mitochondria and may therefore be involved in mitochondrial dysfunction. For instance, it was stated that parkin is able to affect mitochondrial functions such as mitochondrial morphogenesis in spermatogenesis and to enhance mitochondrial biogenesis

in cell proliferation via mitochondrial DNA transcription and replication (Kuroda et al., 2006).

4.1.3. PARK6 locus

Locus PARK6 was mapped for the first time in a large family of Italian origin with the autosomal-recessive form of PD on chromosome 1p35–p36 (Valente et al., 2001). *PINK1* gene coding for serine/threonine-protein kinase PINK1 was identified in 2004 in three families of European origin with autosomal-recessive parkinsonism (Valente et al., 2004a). Over 50 missense substitutions were revealed in the *PINK1* gene as well as point mutations causing transcription frame shifting and reduced protein variants. Recently, a 50 kb deletion covering gene *PINK1*'s exons 6, 7, and 8 was discovered (Li et al., 2005), and it is believed at present that mutations in this gene are the most frequent cause of the PD form characterized by an early start of its development. They have a relatively uniform distribution over the whole gene, and their frequency varies from 1% to 9% in different ethnic populations (Tan and Skipper, 2007).

It was established that homozygosity and the compound heterozygosity at these mutations led to the development of different PD forms of a broad phenotypic range, from the early-onset (from 32 to 48 years of age) and atypically progressing (levodopa-sensitive dyskinesia with a slow progression of the disease) conditions to diseases with a late onset and with typical PD symptoms (Schiesling et al., 2008; Valente et al., 2001, 2004a).

Protein PINK1 contains 581 amino acid residues and has an N-end motif responsible for linking with mitochondria and a highly conserved protein kinase domain similar to serine/threonine kinases of the Ca^{2+} calmodulin family. The protein is widely spread in different types of tissues and cells, and a detailed analysis of its expression allows the assumption that it is preferentially localized to mitochondria. One of its features is its weak dissolution ability and hence the inclination to aggregate that is likely to account for the presence of this protein in 10% of Lewy bodies in the sporadic PD form (Gandhi et al., 2006).

At present, little is known about the actual properties of PINK1. Data are available that indicate that PINK1 can function as a mitochondrial kinase and protect neurons from oxidant stress (Schiesling et al., 2008; Valente et al., 2004a).

4.1.4. PARK7 locus

In 2001, the seventh PD locus, PARK7, was identified during analysis of a family from Denmark with early-onset autosomal-recessive PD, and it was mapped on chromosome 1p36 (van Duijn et al., 2001). Two years later, a large chromosomal deletion and the missense substitution L166P at a gene coding for the protein DJ-1 and located at the area of the *PARK7* gene locus were discovered in the above-mentioned family and in a family from Italy.

In the homozygotic state, they lead to the development of a slowly progressing juvenile PD accompanied by the complete absence of DJ-1 protein synthesis, resulting from the blocking of protein synthesis or from its very rapid posttranslational degradation (Bonifati et al., 2003). In the *PARK7* gene, both point mutations in homozygotic and heterozygotic states and exon deletions and triplications have been found. All the described mutations lead to the progression of rare forms of autosomal-recessive PD with an early starting period (usually at the age of 20–40). Overall, mutations in the *PARK7* gene are encountered in no more than 1–2% of patients with the early PD form (Bonifati et al., 2003). In patients with mutations in this gene, the typical clinical symptoms are accompanied by the symptoms of dystonia and psychiatric signs including psychotic episodes (van Duijn et al., 2001).

DJ-1 is a highly conserved protein made up of 189 amino acid residues, and it belongs to the DJ-1/Thi/PfpI protein superfamily. The protein is widely distributed in different mammalian tissues, including the brain. It is well established that DJ-1 is preferentially localized in the cytoplasm, albeit in small amounts, being linked with mitochondria (Zhang et al., 2005).

The DJ-1 protein gene was described for the first time, prior to the elucidation of its role in the development of PD, as a proto-oncogene implicated in the sperm maturation processes and in fertilization. It was later shown to possess antioxidant properties and to be able to protect cells against oxidant stress by removing the peroxide compounds through self-oxidation. Moreover, data have been reported that DJ-1 can be involved in the regulation of apoptosis processes and that it can behave as a reduction–oxidation chaperone inhibiting α-synuclein aggregation. Evidence is available that DJ-1 is able to bind with parkin at a time of oxidant stress, suggesting the existence of a common role in neuroprotection mechanisms of the two proteins (Mandemakers et al., 2007).

4.1.5. PARK8 locus

Locus PARK8 was mapped in 2002 in a family with autosomal-dominant PD (Funayama et al., 2002). In 2004, two independent research teams identified the *LRRK2* gene, coding for serine/threonine-protein kinase 2 with leucine-rich repeats or dardarin, in families with an autosomal-dominant early-onset form of PD (Paisan-Ruiz et al., 2004; Zimprich et al., 2004). At present, over 50 different variants, among them mostly missense mutations and some point substitutions leading to splicing disturbances, have been revealed in the *LRRK2* gene. All mutations are rather uniformly distributed over the gene and have been shown to make an essential contribution to the etiology of both familial and sporadic PD. The total frequency of the mutations in the *LRRK2* gene in different world populations can reach 15% of the familial PD cases and 3.6% of sporadic PD. It should be noted, however, that the pathogenic role of mutations in PD development has been completely proven for only seven mutations. This is associated, first, with the low

penetrance of the mutations in the *LRRK2* gene, the presence of phenocopies, and a late onset of the disease, all of which impedes segregation analysis (Krüger, 2008; Lesage and Brice, 2009).

The G2019S mutation, the most frequent in the *LRRK2* gene, located at exon 41, belongs to the mutations with demonstrated proof of their pathogenic significance. It has been stated that, in addition, this mutation is the most frequent of all the point mutations ever described for PD. The G2019S mutation has been found in patients with both familial and sporadic PD and belonging to different populations. Its frequency in European populations reaches 4.6% of sporadic Parkinson's disease cases and 11.5% of the familial parkinsonism cases; its frequency in the Ashkenazi Jews is as high as 13.3% in the sporadic patients and 29.7% in familial PD cases; in Arabs from South Africa, it has been found in 40.8% of the sporadic cases and in 37.0% of the familial PD cases (Lesage et al., 2006; Ozelius et al., 2006). At the same time, this mutation is extremely rare in Mongoloids (Tan, 2006). In the Russian population, this mutation has been found in both patients from the families with autosomal-dominant PD (at a frequency of 13%) and in patients with sporadic PD forms (5%) (Illarioshkin et al., 2007; Shadrina et al., 2007a).

Analysis of the G2019S mutation-linked haplotypes testifies that, most probably, this mutation emerged more than once in the evolution of man. At present, three different haplotypes have been discovered. The most frequent one, referred to as haplotype 1, is found in 95% of the mutation G2019S carriers from Europe, South America, North America, and in Ashkenazi Jews. It has been proposed that this mutation emerged for the first time in the Near East several thousand years ago. The second haplotype was revealed in five families of European origin, and the third one was found in carriers of the mutation from Japan and in a family from Turkey (Lesage and Brice, 2009).

The range of clinical manifestations of the G2019S mutation varies strongly, and this mutation is not completely penetrative. The penetrance of this mutation can vary from 28% in PD patients aged 59 years to 74% in PD patients aged 79 years (Healy et al., 2008). Overall, patients with mutations in the *LRRK2* gene show a late onset of the development of the disease and a broad range of clinical symptoms, which even vary within the same family.

The *LRRK2* gene consists of 51 exons and codes for dardarin, a 275 kDa protein bearing 2527 amino acid residues, belonging to the ROCO subfamily of the Ras HTPs family and characterized by the presence of several functional domains, namely, two Roc domains, the COR domain, the WD40 domain, a leucine-rich repeats area, and a tyrosine kinase catalytic domain (Zimprich et al., 2004). It is actively expressed in the liver, lungs, kidneys, heart, and different parts of the brain, including the dopaminergic neurons of the *substantia nigra*. Dardarin is preferentially localized in the

cytoplasm, mainly in the Golgi apparatus, synaptic vesicles of the cytoplasm membrane, and it is probably connected with the outer mitochondrial membrane (Hatano et al., 2007). Presently, little is known about the principal biological characteristics of dardarin, although it has been established that the protein shows kinase activity, which was proven in experiments in cell culture (West et al., 2007). It is assumed that dardarin can also exert the HTPase activity typical of the ROCO family proteins. Data are available that LRRK2 can take part in the control of the exchange of synaptic vesicles, in axon growth and branching, and in the functioning of the Golgi apparatus, lysosomes, and mitochondria (MacLeod et al., 2006; Zhu et al., 2006).

4.1.6. Locus PARK5

Locus PARK5 and its corresponding gene *UCH-L1* were identified when studying a family from Germany with an autosomal-dominant form of PD with an early onset of the disease at about 50 years of age. The 193M mutation in the *UCH-L1* gene was revealed in four out of the seven members of the family (Leroy et al., 1998). In spite of intense research, no other mutations in the *UCH-L1* gene and no other families with the development of PD linked with locus PARK5 have been found. Patients with the 193M mutation display clinical symptoms typical for PD, including olfactory disorders and progressive cognitive dysfunction at later stages of the disease.

The *UCH-L1* gene, consisting of nine exons was mapped on chromosome 4p14. It encodes the 223 amino acid residues at the C-end of ubiquitin hydrolase 1 (UCH-L1), which is a component of Lewy bodies and neurites, and is one of the most represented proteins in the brain. Its concentration is 1–2% of the total protein content of the brain (Wilkinson et al., 1989). Biochemical studies have shown UCH-L1 to be implicated in the ubiquitin-dependent proteasomal degradation of proteins and to play a double role in this process. As a monomer, it hydrolyzes the polyubiquitin chains, and as a dimer, it plays the role of an E3 ligase. The presence of the 193M mutation contributes to the dimerization of the protein by enhancing its ligase function and abating ubiquitin realization, which in turn results in accumulation of ubiquitin residues and in their aggregation (Liu et al., 2002).

4.1.7. PARK9 locus

The ninth locus of PD is mapped on chromosome 1p36; the *ATP13A2* gene whose mutations were revealed in two independent families with the Kufor-Rakeb syndrome has been identified (Hamprhire et al., 2001; Ramirez et al., 2006). This syndrome constitutes the atypical form of the recessively inherited levodopa-responsive parkinsonism with a very early onset (11–16 years), the patients displaying a rapid progression of the

disease, pyramidal degeneration, dementia, supranuclear gaze palsy, along with globus pallidus atrophy, and later, generalized brain atrophy (Najim al-Din et al., 1994; Williams et al., 2005). Recently, new mutations in the *ATP13A2* gene were brought to light in patients from Brazil and Italy with a more typical parkinsonism and an early start of the disease (Di Fonzo et al., 2007).

The *ATP13A2* gene contains 29 exons and encodes a P-type lysosomal ATPase forming a part of the ATPase P_5 superfamily and bearing 1180 amino acid residues and 10 transmembrane domains. The precise physiological role of the protein remains obscure, although other proteins of this family are well known to be transporters of various substrates, and in the first place, of inorganic cations. The *ATP13A2* gene is preferentially expressed in brain tissues, especially in the dopaminergic neurons of the *substantia nigra*. Studies of cell cultures have shown the wild-type *ATP13A2* protein to be preferentially localized in the lysosomal membrane, whereas the protein's mutant shortened variants return to the endoplasmic reticulum to be subjected to proteasomal degradation (Ramirez et al., 2006).

4.1.8. Other loci

Locus PARK3 has been mapped on chromosome 2p13, and is linked with the progression of the autosomal-dominant PD form with a delayed onset at about 61 years, the patients showing the same clinical signs as those with the sporadic PD form, with dementia revealed in some of the patients (Gasser et al., 1998). At present, some researchers maintain the assumption that the *SPR* gene is involved in the synthesis of dopamine, and might be coupled with this locus (Karamohamed et al., 2003; Takazawa et al., 2003).

The 10th locus (PARK10) was identified in a population from Iceland, using broad-scale genomic scanning. It has been stated that the clinical symptoms observed in PD patients are similar to those typical of the sporadic form of the disease, with the age of the disease onset averaging 65.8 years (Hicks et al., 2002). In 2009, over 1000 SNPs in the area of locus PARK10 were analyzed in a population from the Norway (PD patients and controls), the results allowing the assumption that the *UPS24* gene is associated with PD development and localized in the area of locus PARK10 (Haugarvoll et al., 2009). However, in order to confirm the data obtained, it is necessary to conduct screening of mutations in these genes in families linked with locus PARK10.

Recently, evidence was obtained suggesting that the *GIGYF2* gene is coupled with locus PARK10, which was earlier mapped on the long shoulder of chromosome 2. Ten substitutions in 16 PD patients from France and Italy, with the frequency of mutations in the *GIGYF2* gene being 6.4%, were revealed in two independent samples of PD patients with the familial form of PD (Lautier et al., 2008; Pankratz et al., 2003). The *GIGYF2* gene encodes PERQ amino acid-rich with GYF domain-containing protein 2.

This can participate in the regulation of the tyrosine kinase receptor signal path including IGF1 and the insulin receptor. Locus PARK12 was mapped on the long shoulder of the X-chromosome in a wide-scale screening of patients with no family history of the disease (Pankratz et al., 2002). However, no gene corresponding to this locus, whose mutations could have led to the development of PD, has been discovered so far.

The *HTRA2* gene localized on chromosome 2 near locus PARK3 is the candidate gene for locus PARK3. Two mutations (G399S and R404W) and one polymorph variant (A141S) were found in this gene in an analysis of sporadic PD patients from Belgium and Germany (Bogaerts et al., 2008; Strauss et al., 2005), although screening of families with PD showed no mutations to exist in this gene. The *HTRA2* gene is universally expressed and encodes the serine protease HTRA2, which shows proteolytic activity, is localized in the intermembrane area, and is liberated into the cytosol during apoptosis. It has been established that *HTRA2* gene knockout mice possess the neurodegenerative Parkinson phenotype (Martins et al., 2004). It was shown in *in vitro* experiments that the mutant variant 399S and the allelic variant 141S can cause mitochondrial dysfunction linked with a change of mitochondrial morphology. It was shown, besides, that cells with superexpression of the mutant variant 399S are more sensitive to stress-induced death than wild-type cells (Strauss et al., 2005).

Loci PARK14 and PARK15 were identified when families with rare atypical forms of parkinsonism were studied. For instance, homozygous missense mutations in the *PLA2G6* gene (locus PARK14) localized on chromosome 22 and encoding calcium-dependent phospholipase 2 were found in studying two unrelated Pakistani families with autosomal-recessive adult-onset levodopa-responsive dystonia parkinsonism. Moreover, when studying families from Iran, Italy, and Denmark with the autosomal-recessive parkinsonian-pyramidal syndrome, homozygotic and compound-heterozygotic mutations in the *FBXO7* gene (locus PARK15) were revealed. The *FBXO7* gene is also localized on chromosome 22; it codes for the F-box family protein involved in the ubiquitin-dependent proteasomal degradation of proteins (Di Fonzo et al., 2009; Shojaee et al., 2008). We note that as far as genes *PLA2G6* and *FBXO7* are concerned, no data have been found regarding whether their mutations are likely to lead to the development of typical PD forms.

4.2. Genes and biological processes involved in the pathogenesis of sporadic Parkinson's disease

4.2.1. Dysfunction of the ubiquitin–proteasome system

Ubiquitin-dependent proteolysis of proteins via the 26S proteasome system plays an important role in the regulation of such processes as DNA replication and transcription, and cell differentiation in response to exogenous and

endogenous stimuli (Ciechanover and Brundin, 2003). The disturbing role in processes of proteins' normal proteasomal degradation by way of ubiquitin-dependent proteolysis in 26S proteasomes in the pathogenesis of PD is unquestioned, because the three monogenic forms of the disease are conditioned by gene mutations directly involved in proteasome degradation processes (*SNCA*, *PARK2*, and *UCHL1*). Decrease in the activity of the 26S proteasome complex is observed in the substantia nigra in Parkinson patients' brains, in turn causing the accumulation of oxygenated protein forms in cells (Fig. 6.1) (Jenner and Olanow, 1998).

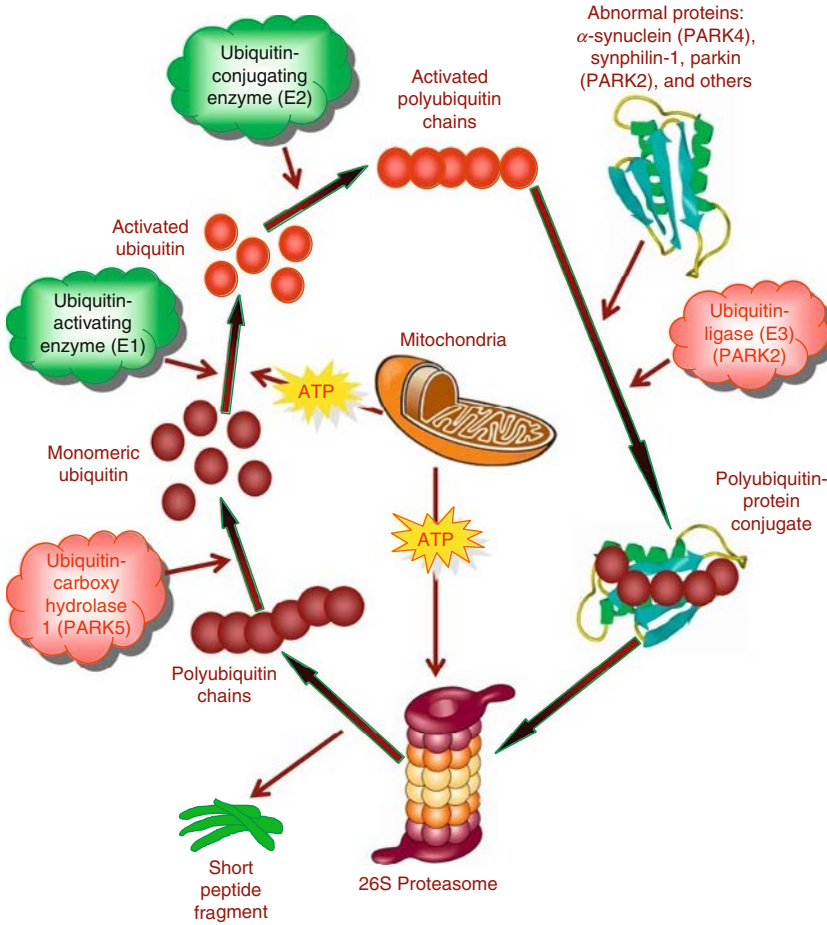

Figure 6.1 The ubiquitin–proteasome system: genes involved in Parkinson's disease pathogenesis.

Data are available indicating that genes encoding proteins for ubiquitin-dependent proteasomal degradation (*SNCA*, *PARK2*, *UCHLI*, and *SNCAIP*) may be involved in the pathogenesis of the sporadic form of PD. For instance, several intron SNPs and dinucleotide polymorphism in the promoter region of *SNCA* have been revealed and their association with PD in different populations is established. It is presumed that these polymorphisms can influence the stability of mRNA and the transcriptional activity of *SNCA* (Brighina et al., 2008; Cronin et al., 2009; Mellick et al., 2005).

Homozygosity or compound heterozygosity at mutations in *PARK2* lead to the development of the disease in 10–20% of sporadic from PD patients with an early (before 50 years of age) onset of the condition (Hedrich et al., 2004; Shadrina et al., 2007b; Sironi et al., 2008). Data are available suggesting that, even in the heterozygotic state, the mutation can cause development of the disease or elevate the organism's sensitivity to environmental factors. Moreover, several point polymorphous variants (both synonymous and nonsynonymous) that influence the risk of PD development have been discovered (Lücking et al., 2003; Tan and Skipper, 2007; West et al., 2002).

Ubiquitin carboxyl hydrolase (UCH-L1), which releases ubiquitin from its complex with protein, plays an important role at the final stage of protein degradation processes. Association between the risk of development of PD and the frequent S18Y polymorphism in the gene's coding region has been revealed for *UCH-L1*, and it has been established that the 18Y variant reduces the risk of development of the disease (Belin and Westerlund, 2008; Maraganore et al., 1999).

Besides ubiquitin, proteins NEDDS and SUMO-1, the functional analogs of ubiquitin, can take part in the processes of ubiquitin-dependent proteolysis, the former being revealed in Lewy bodies, and SUMO-1 playing a role in DJ-1 protein modification (Dil Kuazi et al., 2003). These data allow the genes of these proteins to be regarded as possible candidate genes for PD. Moreover, parkin target proteins, including sinfilin-1, may be involved in PD pathogenesis. Like α-synuclein, sinfilin-1 forms part of Lewy bodies. Polymorphism R621C, with its established either presence or absence of association with PD in different populations, has been revealed in the sinfilin-1 gene (*SNCAIP*) (Myhre et al., 2008).

4.2.2. Mitochondrial dysfunction and oxidative stress

Data concerning a possible role of mitochondrial dysfunction in PD pathogenesis were acquired as long ago as the 1980s. It was demonstrated that young people who abused crudely manufactured MPPP (1-methyl-4-phenyl-4-propionoxypiperidine) showed symptoms of parkinsonism because of the neurotoxic action of the MPTP (1-methyl-4-phenyl-1,2,3,6-tetrahydropyridine) by-product from MPPP ''heroin'' synthesis, which inhibits the mitochondrial complex I (Betarbet et al., 2000; Mandemakers et al., 2007). Insufficient activity of the mitochondrial

complex I and a decrease in the amount of this complex's particular subunits in the neurons in the central nervous system in PD patients and their blood thrombocytes have been observed (Swerdlow et al., 1996). Genes connected with the development of familial PD forms *SNCA*, *PARK2*, *DJ-1*, *PINK1*, and *LRRK2* in turn encode proteins playing a significant role in the functioning of mitochondria (Fig. 6.2).

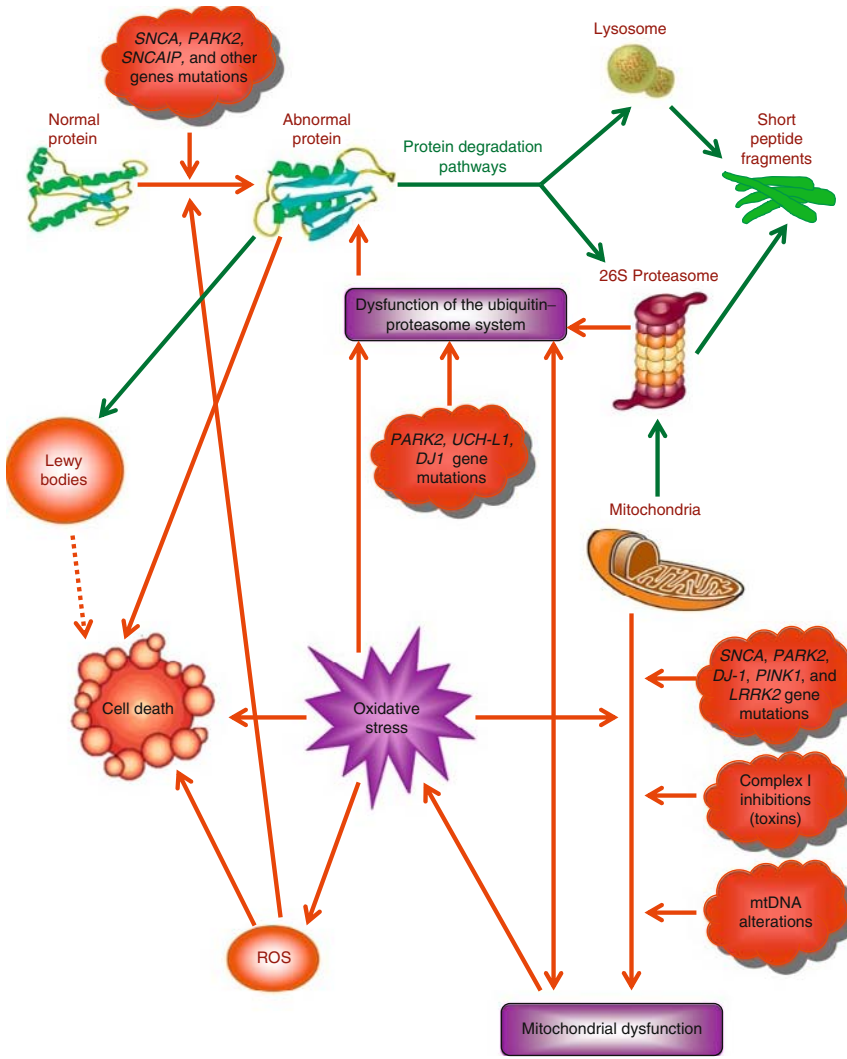

Figure 6.2 The interaction between oxidative stress, mitochondrial dysfunction, and abnormal protein degradation in Parkinson's disease pathogenesis (simplified view).

Data are available suggesting that the modulation of mitochondrial function by α-synuclein is responsible for resistance to mitochondrial toxins (Biskup et al., 2005; Klivenyi et al., 2006), possibly because α-synuclein can become localized on the mitochondria's inner membrane at the expense of the cryptic mitochondrial targeting signal discovered at the protein's N-terminal end. The authors also showed that aggregated α-synuclein can obstruct the normal functioning of the mitochondrial complex I (Devi et al., 2008).

A large amount of data has been hitherto accumulated, concerning the direct localization and involvement of genes *PARK2*, *PINK1*, *DJ-1*, and *LRRK2* in mitochondria functioning (for details see Section 4.1). As in the case of *PARK2*, it was established that individual pathologically significant mutations in heterozygotic states of genes *PINK1*, *DJ-1*, and *LRRK2* can influence the risk of the development of a sporadic form of PD (Abou-Sleiman et al., 2006; Lesage and Brice, 2009; Valente et al., 2004b).

HTRA2 and *POLG1* must also be referred to as genes whose mutations may lead to mitochondrial dysfunction. *HTRA2* codes for the mitochondrial serine protease HTRA2, which shows proteolytic activity, is localized in the intermembrane area of mitochondria, and is released into the cytosol during apoptosis. A polymorphous variant (A141S) of this gene that is associated with an increased risk of PD development has been discovered (for details see Section 4.1.8).

POLG1 is a mitochondrial DNA polymerase localized on the inner membrane of mitochondria. A cluster of rare CAG repeat variants in *POLGI1*, whose occurrence could be regarded as a PD-predisposing factor, has been revealed (Luoma et al., 2007). Moreover, association between mitochondrial monotypes and the risk of development of sporadic parkinsonism has been discovered, and it has been shown that the risk of the disease is considerably lower in Europeans with monotypes J and K as compared with the carriers of monotype H, the most frequently found monotype in Europeans (Van der Walt et al., 2003).

4.2.3. Genes associated with the synapse

Synaptic exchange plays an important role in the vital activity of neurons, including dopaminergic neurons. At least four proteins (α-synuclein, parkin, dardarin, and ubiquitin carboxy hydrolase) encoded by the genes for PD monogenic forms are involved in synapse functioning. For instance, α-synuclein is important in the maintenance of synaptic vesicles and also in the storage and compartmentalization of neurotransmitters, including dopamine (Yavich et al., 2004). These data allow one to presume that mutations in *SNCA* can lead to presynaptic changes in dopaminergic neurons.

As was mentioned earlier, parkin (E3 ubiquitin ligase) participates in the proteasomal degradation of such presynaptic proteins as α-synuclein and synfilin-1, this process taking place not only in the perikaryon, but also in

dendrites. Furthermore, not long ago parkin was shown to influence the functioning of the G-protein coupled receptor (GPR31), which interacts with the dopamine DAT1 transporter (Marazziti et al., 2007). In addition to parkin, UCLH1 participates in the proteasomal degradation of presynaptic proteins, an indirect indication of its role in the functioning of synapses. It was also discovered that transduction of *UCLH1* to mice with a murine model of Alzheimer's disease led to recovery of normal enzymatic activity in synapses and to normalization of their functioning. Moreover, the mice showed improvement of their damaged cognitive functions (Gong et al., 2006).

Biological characteristics of *LRRK2*-encoded dardarin are not yet fully elucidated. However, evidence exists that this protein can be involved in synaptic exchange. Dardarin, for instance, was found in presynaptic terminals, and it was established that dardarin had some involvement with vesicles and endosomes (Zhu et al., 2006). Shin et al. (2008) showed dardarin could regulate synaptic vesicular endocytosis by way of direct interaction with the early endosome marker protein Rab5.

4.2.4. Genes associated with the lysosome

It was recently discovered that besides ubiquitin-dependent proteasomal protein utilization, processes of lysosomal autophagia, especially those with a long (over 10 h) half-life, play an important role in protein utilization processes (Pan et al., 2008). Data regarding an increase in the level of α-synuclein after lysosome inhibition suggest the hypothesis that degradation of α-synuclein may not be entirely proteasomal. During lysosome inhibition, α-synuclein becomes bound to lysosome receptors instead of selective migration within the organelle. It was also shown that a mutant α-synuclein was mainly bound to lysosomal membrane receptors, thereby blocking both its own lysosome autophagia-induced degradation and the degradation of other protein substrates (Cuervo et al., 2004). Lysosomal P-type ATPase encoded by *ATP13A2* is another protein connected with lysosome functioning. Mutations in this gene were revealed in two unrelated families with the Kufor-Rakeb parkinsonism syndrome (Hamprhire et al., 2001; Ramirez et al., 2006) as well as in patients with more typical parkinsonism and its early onset (Di Fonzo et al., 2007).

Glucocerebrosidase (GBA), catalyzing the formation of ceramide and glucose from glycolipid glucosylceramide, is another lysosomal protein likely to be involved in PD pathogenesis. Mutations in *GBA* lead to the development of Gaucher's disease with its typical symptoms of parkinsonism. Analysis of patients with sporadic PD revealed a large number of heterozygotic carriers of pathogenically important *GBA* variants, including L445P, D409H, E326K, and H255Q. The large frequency of such mutations in PD patients speaks in favor of *GBA* being involved in PD pathogenesis.

The occurrence of mutations at this gene can considerably boost the risk of PD development (DePaolo et al., 2009; Nichols et al., 2009).

4.2.5. Genes involved in the differentiation, survival, and maintenance of dopaminergic neurons

The role of disturbance of dopaminergic neuron differentiation processes in PD pathogenesis has been confirmed by the discovery of two mutations in the transcription factor Nurr1 (*NR4A2*) exon 1 in familial PD patients (Le et al., 2003). A number of polymorphous variants of this gene, which influence the risk of the disease, have been revealed (Chen et al., 2007; Sleiman et al., 2009). Gene *NR4A2* encodes the transcriptional factor required for differentiation of postmitotic dopaminergic neurons and controlling the expression of the genes whose protein products are associated with the synthesis and retention of dopamine, those are especially tyrosine hydro carboxylase (TH), dopamine transporter (DAT1), monoamine vesicular transporter (VMAT2), and aromatic amino acid decarboxylase (AADC) (Chinta and Andrersen, 2005).

Other transcription factors, such as Titx3 and Lmx1b, needed for the differentiation of dopaminergic neurons, can also contribute to the pathogenesis of the sporadic form of PD. At present, two polymorphisms located in intron 1 in the immediate proximity of the 5′-end of *PITX3* and associated with the sporadic form of PD have been found in the gene of one of these factors, namely the Pitx3 factor specific for the dopaminergic neurons of the ventral and ventromedial portions of the substantia nigra (Bergman et al., 2010).

In addition, the brain growth factor, BDNF, the glial growth factor, GDNF, and the transforming growth factor α (TGFα) all play an important role in the differentiation and maintenance of the normal functioning of dopaminergic neurons. BDNF and GDNF are well known to influence dopamine exchange in the substantia nigra. However, only one of the proteins, namely BDNF, which regulates the expression of the dopamine receptor D3 on striatum neurons, has polymorphism V66M revealed and associated with sporadic PD in a Japanese population (Toda et al., 2003). Analysis of this polymorphous variant and other polymorphisms in the gene of BDNF in European populations showed no association with PD (Hakansson et al., 2003; Xiromerisiou et al., 2007).

4.2.6. Genes involved in dopamine synthesis, metabolism, and functioning

PD symptoms result from a decrease in dopamine synthesis in the substantia nigra and its decline in concentration in the striatum. One of the reasons for the decreases might be a disturbance of dopamine exchange system functioning—that is, its synthesis, transport, synaptic release, and reception.

The rate of the dopamine synthesis is limited by the dopamine conversion to DOPA reaction, catalyzed by tryptophan hydrolyze (TPH). Therefore, *TPH* can be regarded as one of the most likely candidate genes for PD. However, no associations of any kind between *TPH* polymorphous variants and the development of the disease have been hitherto discovered. On the other hand, proteins regulating the activity of tyrosine hydroxylase (α-synuclein) and the transcription of the gene for this enzyme (Nurr1) play a large role in PD pathogenesis. Alongside this, disturbance of the synthesis of tetrahydrobiopterin (BH4), the cofactor for tyrosine hydroxylase, can play a role in PD onset. In some cases, mutations in the gene for GTP cyclohydrolase (*GCH1*), the first enzyme in the BH4 biosynthesis cycle, lead to the development of a PD-like phenotype, nonclassical DOPA-dependent torsion distension (Bressman, 2003). The gene for the SRR enzyme, catalyzing the final stage of BH4 biosynthesis, is mapped in the PARK3 locus area, and it cannot be ruled out that it is the mutations in this gene that are responsible for the PARK3-form of PD (Karamohamed et al., 2003; Sharma et al., 2006).

The level of dopamine in the cell is also dependent on the rate of its degradation under the action of dopamine-β-hydrolase and monoamine oxidases A and B (MAO-A and MAO-B). Associations of different polymorphous variants with the evolution of PD have been disclosed for all the genes of these enzymes (Healy et al., 2004a,b; Kang et al., 2006; Mellick et al., 1999; Yoritaka et al., 1997).

Nor can we rule out the role—in PD development—of the reverse transport system of dopamine and dopamine receptors. Changing of the expression of receptors of dopamine D3, whose level declines 40–45% in the area of the nucleus accumbens and in the tegmentum, and of dopamine D4, whose level in the tegmentum rises as much as 15% (Ryoo et al., 1998). However, at present no data are available regarding any association between the genes for dopamine receptors and PD. At the same time, Ritz et al. (2009) recently showed not long ago that definite polymorphous variants of the dopamine transporter gene, *DAT1*, especially if in combination with the long influence of pesticides, can enhance the risk of PD development.

4.2.7. Genes involved in inflammation

Microglia activation in the substantia nigra area takes place during PD, with this process being prior to the death of neurons and likely to initiate apoptosis (On et al., 2002). Activated microglia can produce different anti-inflammatory cytokines (such as TNF-α, γ-interferon, and various interleukins). At the same time, activation of the expression of neuronal nitric oxide synthase (nNOS) takes place and in its turn leads to increased levels of nitric oxide and oxidative stress. Moreover, activation of cytokines causes activation of the transcription factor, NF-κB (Hunot et al., 1997;

Zhang et al., 2000), with gene *NR4A2* being one of its targets, which enhances the sensitivity of dopaminergic neurons to oxidative stress and the probability of their death.

Analysis of polymorphous variants of the genes for anti-inflammatory cytokines and their target genes revealed a number of SNPs associated with PD development. For instance, association between the 308G/A polymorphism of the promoter region affecting the gene for TNF-α and PD development has been found. The rarer allelic variant 308A exerts higher transcriptional activity and raises the risk of PD (Krüger et al., 2000). In the interleukin-1β gene, polymorphism 551C/T confers the risk of PD development (Manila et al., 2002; Wahner et al., 2007). Parkinsonism-associated polymorphisms have been described in genes of neuronal (Lo et al., 2002) and inducible (Levecque et al., 2003) nitric oxide synthases.

4.2.8. Other genes associated with Parkinson's disease

The whole range of possible paths to the etiopathogenesis of the sporadic form of PD cannot be simply reduced to only the above-mentioned mechanisms and genes.

Development of PD may also be linked with the toxic action of various xenobiotics. In this connection, the enzymes in their detoxication systems can play an important role in the pathogenesis of the disease. Analysis of the polymorphous variants of genes of the enzymes involved in their detoxication processes brought to light a number of SNPs associated with PD development. Currently, under active investigation, are both enzymes for the first stage in the processes, the proteins of the cytochrome P450 superfamily (CYP2E1, CYP2D6) that are activated by xenobiotics, and enzymes of the second stage that are involved in the detoxication of endogenous and exogenous toxins, for example, glutathione-*S*-transferases (GSTT1, GSTM1, GSTP1) and *N*-acetyl transferase (NAT2). A number of SNPs located in the genes of the above-mentioned enzymes are associated with PD development (Jenner, 1999; Kelada et al., 2003; Shahabi et al., 2009; Singh et al., 2008; Tan et al., 2000).

Disturbance of the normal iron homeostasis may also exert toxic action that could lead to PD development. PD risk-affecting polymorphous variants have been found in the transferrin gene involved in the blood plasma iron transport, in the protein HFE gene regulating iron absorption and in the hemoxy kinase 1 gene linked with the reverse iron transport system in cells (Borie et al., 2002; Buchanan et al., 2002; Kimpara et al., 1997).

A chromosome 8p region strictly connected with PD was found in a search for new loci involved in PD pathogenesis (Scott et al., 2001), with genes *NEFH* and *NEFL* both coding for the heavy and light chains of neurofilaments, which are one of the main components of Lewy bodies. Three different missense mutations in gene *NEFH* were found in three patients, one with juvenile autosomal-recessive parkinsonism and two with the sporadic form

of PD (Krüger et al., 2003; Lavedan et al., 2002). These data suggest the hypothesis that gene *NEFH* might be associated with PD development.

Microtubule-associated protein tau (MAPT) is also a component of Lewy bodies. Mutations leading to the development of an atypical PD form (frontotemporal dementia with parkinsonism) were found in gene *MAPT* (Dumanchin et al., 1998) alongside with several haplotypes in the promoter region of this gene, which influence its transcriptional activity. Clear-cut association with the risk of PD development was has been established for one of them, the common haplotype H1 (Healy et al., 2004a,b; Kalinderi et al., 2009; Tobin et al., 2008).

At the present time, a number of data have been generated pointing to the microRNA contribution to neuron development and differentiation. Quite a number of different microRNAs have been revealed, with a majority of them being unique and only found in neurons (Kosik, 2006; Vreugdenhil and Berezikov, 2009). One of them, miR-133b, has been shown to participate in the maturation and functional regulation of dopaminergic neurons of the mesencephalon (Kim et al., 2007). The binding site of another microRNA, miR-433, has been shown to be located in the mRNA of the fibroblast growth factor 20 gene (*FGF20*), where a PD-associated SNP has been identified and a binding site for miR-433 has been found disturbed in gene *FGF20* in one allelic variant for this polymorphism. The disturbance of this binding site leads to enhanced *FGF20* RNA translation, which correlates with an increase in the levels of α-synuclein. It has also been shown that it is this allelic variant of gene *FGF20* that is associated with an increased risk of PD development (Wang et al., 2008).

4.2.9. Genome-wide association studies in Parkinson's disease

The genome-wide association study (GWAS) has recently been widely employed for the discovery of genes involved in the pathogenesis of diseases. Some studies of this kind were performed for PD. No positive associations at genome-wide significance levels were found in two of them (Fung et al., 2006; Maraganore et al., 2005). In a third study, the combined analysis strategy using genome-wide data bases and meta-analytic techniques was used, and, as a result, a new polymorphous variant was identified in the GAK/DGKQ region on chromosome 4 influencing the risk of PD; thereby confirming the involvement of genes *SNCA* and *MAPT* in PD pathogenesis (Pankratz et al., 2009). However, the involvement of the locus on chromosome 4 in PD pathogenesis has not been confirmed during the most extended GWAS analysis of PD, in which over 20,000 PD patients and healthy controls, either Europeans or Asians, were examined. A highly reliable association of PD with the DNA marker rs 11931074 from the *SNCA* region was shown for the two ethnic groups, whereas the association of PD with the MAPT locus appeared specific only for the Europeans (Simón-Sánchez et al., 2009).

Genome-wide studies have confirmed the previously described associations of *SNCA* with PD onset, but they have not yet helped to reveal any principally new candidate genes for the disease. To find them, a combination of the GWAS technology with genome-wide expression analysis methods might be appropriate. Similar combined analysis of the substantia nigra neuron transcriptome from PD patients and healthy controls and polymorphous DNA markers in differentially transcribing genes was undertaken by Prokisch et al. (Elstner et al., 2009) and resulted in the discovery of four candidate genes for PD (*MTND2*, *PDXK*, *SGAP3*, and *TRPPC4*); subsequent analysis, however, confirmed PD association with only one of them, the pyridoxal kinase-coding gene *PDXK*.

5. Conclusion

In conclusion, considerable progress in PD genetic basis studies has marked the last number of years, and the number of genes revealed to involve in the pathogenesis of familial PD has been greatly increased. Thus, knowledge regarding the etiopathogenesis of the disease has been extended and more studies aimed at the investigation of the genetic factors of the more frequent, sporadic PD forms have been initiated. Analysis of the contribution of the development of mutations to sporadic PD and polymorphisms of genes involved in the pathogenesis of monogenic forms of PD is actively underway. Indeed, a number of candidate genes directly accounting for sporadic PD have been revealed. In this connection, the possibility of preclinical DNA diagnostics of the disease becomes an urgent question because it will allow the elaboration of principles of and approaches to preventive treatments at the moment when the degeneration of dopaminergic neurons is at its early stage and has only inflicted damage upon a limited number of these neurons. Accomplishment of these studies will make it possible to generate new methods of therapy, which could decelerate (if not stop) the development of pathologic processes in the nervous tissue, thereby shifting the clinical onset age of the disease toward a later period and reducing its clinical gravity.

Difficulties can be expected on this path, for our concepts regarding the genetic basis of the disease are not yet thorough and allow no unambiguous interconnection to be established between particular features of an individual genome and the risk of PD. Moreover, even where monogenic forms of a pathogenetically significant mutation are revealed, nowadays we cannot, in a majority of the cases, be completely confident that PD will develop in the carrier of the mutation, because of the incomplete penetrative ability of mutations and variability, if any, of their clinical expression. We will have to elucidate those environmental and genetic factors that determine the

manifestation and the degree of the disease when a particular concrete mutation has evolved. Nonetheless, further analysis of the genetically determined group of PD development risk and employment of modern clinical and biochemical methods will contribute to the accumulation of more detailed knowledge of PD pathogenesis, and this contribution will be significant for the elaboration of new approaches to the early diagnostics and treatment of PD.

REFERENCES

Abou-Sleiman, P.M., Muqit, M.M., McDonald, N.Q., Yang, Y.X., Gandhi, S., Healy, D.G., et al., 2006. A heterozygous effect for PINK1 mutations in Parkinson's disease? Ann. Neurol. 60, 414–419.

Ahn, T.B., Kim, S.Y., Kim, J.Y., Park, S.S., Lee, D.S., Min, H.J., et al., 2008. Alpha-synuclein gene duplication is present in sporadic Parkinson disease. Neurology 70, 43–49.

Belin, A.C., Westerlund, M., 2008. Parkinson's disease: a genetic perspective. FEBS J. 275, 1377–1383.

BenMoyal-Segal, L., Soreq, H., 2006. Gene–environment interactions in sporadic Parkinson's disease. J. Neurochem. 97, 1740–1755.

Bergman, O., Håkansson, A., Westberg, L., Nordenström, K., Carmine Belin, A., Sydow, O., et al., 2010. PITX3 polymorphism is associated with early onset Parkinson's disease. Neurobiol. Aging 31, 114–117.

Bernheimer, H., Birkmayer, W., Hornykiewicz, O., Jellinger, K., Seitelberger, F., 1973. Brain dopamine and the syndromes of Parkinson and Huntington. Clinical, morphological and neurochemical correlations. J. Neurol. Sci. 20, 415–455.

Bertoli-Avella, A.M., Giroud-Benitez, J.L., Akyol, A., Barbosa, E., Schaap, O., van der Linde, H. C., et al., 2005. Novel parkin mutations detected in patients with early-onset Parkinson's disease. Mov. Disord. 20, 424–431.

Betarbet, R., Sherer, T.B., MacKenzie, G., Garcia-Osuna, M., Panov, A.V., Greenamyre, J.T., 2000. Chronic systemic pesticide exposure reproduces features of Parkinson's disease. Nat. Neurosci. 3, 1301–1306.

Beyer, K., Domingo-Sàbat, M., Ariza, A., 2009. Molecular pathology of Lewd body diseases. Int. J. Mol. Sci. 10, 724–745.

Biskup, S., Gerlach, M., Kupsch, A., Reichmann, H., Riederer, P., Vieregge, P., et al., 2005. Genes associated with Parkinson syndrome. J. Neurol. 255, 8–17.

Bogaerts, V., Nuytemans, K., Reumers, J., Pals, P., Engelborghs, S., Pickut, B., et al., 2008. Genetic variability in the mitochondrial serine protease HTRA2 contributes to risk for Parkinson disease. Hum. Mutat. 29, 832–840.

Bonifati, V., Rizzu, P., van Baren, M.J., Schaap, O., Breedveld, G.J., Krieger, E., et al., 2003. Mutations in the DJ-1 gene associated with autosomal recessive early-onset parkinsonism. Science 299, 256–259.

Borie, C., Gasparini, F., Verpillat, P., Bonnet, A.M., Agid, Y., Hetet, G., et al., 2002. French Parkinson's disease genetic study group. Association study between iron-related genes polymorphisms and Parkinson's disease. J. Neurol. 249, 801–804.

Braak, H., Ghebremedhin, E., Rüb, U., Bratzke, H., Del Tredici, K., 2004. Stages in the development of Parkinson's disease-related pathology. Cell Tissue Res. 318, 121–134.

Bressman, S.B., 2003. Dystonia: phenotypes and genotypes. Rev. Neurol. (Paris) 159, 849–856.

Brighina, L., Frigerio, R., Schneider, N.K., Lesnick, T.G., de Andrade, M., Cunningham, J.M., et al., 2008. Alpha-synuclein, pesticides, and Parkinson disease: a case-control study. Neurology 70, 1461–1469.

Bronte-Stewart, H.M., Minn, Y., Rodrigues, R., Buckley, E.L., Nashner, L.M., 2002. Postural instability in idiopathic Parkinson's disease: the role of medication and unilateral pallidotomy. Brain 125, 2100–2114.

Buchanan, D.D., Silburn, P.A., Chalk, J.B., Le Couteur, D.G., Mellick, G.D., 2002. The Cys282Tyr polymorphism in the HFE gene in Australian Parkinson's disease patients. Neurosci. Lett. 327, 91–94.

Burn, D.J., Mark, M.H., Playford, E.D., Maraganore, D.M., Zimmerman, T.R., Duvoisin, R.C., et al., 1992. Parkinson's disease in twins studied with 18F-dopa and positron emission tomography. Neurology 42, 1894–1900.

Chartier-Harlin, M.C., Kachergus, J., Roumier, C., Mouroux, V., Douay, X., Lincoln, S., et al., 2004. Alpha-synuclein locus duplication as a cause of familial Parkinson's disease. Lancet 364, 1167–1169.

Chen, C.M., Chen, I.C., Chang, K.H., Chen, Y.C., Lyu, R.K., Liu, Y.T., et al., 2007. Nuclear receptor NR4A2 IVS6 + 18insG and brain derived neurotrophic factor (BDNF) V66M polymorphisms and risk of Taiwanese Parkinson's disease. Am. J. Med. Genet. B Neuropsychiatr. Genet. 144B, 458–462.

Chinta, S.I., Andrersen, J.K., 2005. Dopaminergic neurons. Int. J. Biochem. Cell Biol. 37, 942–946.

Ciechanover, A., Brundin, P., 2003. The ubiquitin proteasome system in neurodegenerative diseases: sometimes the chicken, sometimes the egg. Neuron 40, 427–446.

Cookson, M.R., 2005. The biochemistry of Parkinson's disease. Annu. Rev. Biochem. 74, 29–52.

Cookson, M.R., Hardy, J., Lewis, P.A., 2008. Genetic neuropathology of Parkinson's disease. Int. J. Clin. Exp. Pathol. 1, 217–231.

Croisier, E., Graeber, M.B., 2006. Glial degeneration and reactive gliosis in alpha-synucleinopathies: the emerging concept of primary gliodegeneration. Acta Neuropathol. 112, 517–530.

Cronin, K.D., Ge, D., Manninger, P., Linnertz, C., Rossoshek, A., Orrison, B.M., et al., 2009. Expansion of the Parkinson disease-associated SNCA-Rep1 allele upregulates human α-synuclein in transgenic mouse brain. Hum. Mol. Genet. 18, 3274–3285.

Cuervo, A.M., Stefanis, L., Fredenburg, R., Lansbury, P.T., Sulzer, D., 2004. Impaired degradation of mutant alpha-synuclein by chaperone-mediated autophagy. Science 305 (5688), 1292–1295.

DePaolo, J., Goker-Alpan, O., Samaddar, T., Lopez, G., Sidransky, E., 2009. The association between mutations in the lysosomal protein glucocerebrosidase and parkinsonism. Mov. Disord. 24, 1571–1578.

Devi, L., Raghavendran, V., Prabhu, B.M., Avadhani, N.G., Anandatheerthavarada, H.K., 2008. Mitochondrial import and accumulation of alpha-synuclein impair complex I in human dopaminergic neuronal cultures and Parkinson disease brain. J. Biol. Chem. 283, 9089–9100.

Di Fonzo, A., Chien, H.F., Socal, M., Giraudo, S., Tassorelli, C., Iliceto, G., et al., 2007. ATP13A2 missense mutations in juvenile parkinsonism and young onset Parkinson disease. Neurology 68, 1557–1562.

Di Fonzo, A., Dekker, M.C., Montagna, P., Baruzzi, A., Yonova, E.H., Correia Guedes, L., et al., 2009. FBXO7 mutations cause autosomal recessive, early-onset parkinsonian-pyramidal syndrome. Neurology 72, 240–245.

Dil Kuazi, A., Kito, K., Abe, Y., Shin, R.W., Kamitani, T., Ueda, N., 2003. NEDD8 protein is involved in ubiquitinated inclusion bodies. J. Pathol. 199, 259–266.

Dumanchin, C., Camuzat, A., Campion, D., Verpillat, P., Hannequin, D., Dubois, B., et al., 1998. Segregation of a missense mutation in the microtubule-associated protein tau gene with familial frontotemporal dementia and parkinsonism. Hum. Mol. Genet. 7, 1825–1829.

Elstner, M., Morris, C.M., Heim, K., Lichtner, P., Bender, A., Mehta, D., et al., 2009. Single-cell expression profiling of dopaminergic neurons combined with association analysis identifies pyridoxal kinase as Parkinson's disease gene. Ann. Neurol. 66, 792–798.

Forno, L.S., 1996. Neuropathology of Parkinson's disease. J. Neuropathol. Exp. Neurol. 55, 259–272.

Fortin, D.L., Troyer, M.D., Nakamura, K., Kubo, S., Anthony, M.D., Edwards, R.H., 2004. Lipid rafts mediate the synaptic localization of alpha-synuclein. J. Neurosci. 24, 6715–6723.

Fuchs, J., Nilsson, C., Kachergus, J., Munz, M., Larsson, E.M., Schüle, B., et al., 2007. Phenotypic variation in a large Swedish pedigree due to SNCA duplication and triplication. Neurology 68, 1–7.

Funayama, M., Hasegawa, K., Kowa, H., Saito, M., Tsuji, S., Obata, F., 2002. A new locus for Parkinson's disease (PARK8) maps to chromosome 12p11.2–q13.1. Ann. Neurol. 51, 296–301.

Fung, H.C., Scholz, S., Matarin, M., Simón-Sánchez, J., Hernandez, D., Britton, A., et al., 2006. Genome-wide genotyping in Parkinson's disease and neurologically normal controls: first stage analysis and public release of data. Lancet Neurol. 5, 911–916.

Gandhi, S., Muqit, M.M., Stanyer, L., Healy, D.G., Abou-Sleiman, P.M., Hargreaves, I., et al. 2006. PINK1 protein in normal human brain and Parkinson's disease. Brain. 129, 1720–1731.

Gasser, T., Muller-Myhsok, B., Wszolek, Z.K., Oehlmann, R., Calne, D.B., Bonifati, V., et al., 1998. A susceptibility locus for Parkinson's disease maps to chromosome 2p13. Nat. Genet. 18, 262–265.

Gibb, W.R., Lees, A.J., 1988. The relevance of the Lewy body to the pathogenesis of idiopathic Parkinson's disease. J. Neurol. Neurosurg. Psychiatry 51, 745–752.

Golubev, V.L., Levin, Ya.I., Wein, A.M., 2000. Parkinson's Disease and Parkinsonism Syndrome. MEDpress, Moscow.

Gong, B., Cao, Z., Zheng, P., Vitolo, O.V., Liu, S., Staniszewski, A., et al., 2006. Ubiquitin hydrolase Uch-L1 rescues beta-amyloid-induced decreases in synaptic function and contextual memory. Cell 126, 775–788.

Hakansson, A., Melke, J., Westberg, L., Shahabi, H.N., Buervenich, S., Carmine, A., et al., 2003. Lack of association between the BDNF Val166 Met polymorphism and Parkinson's disease in Swedish population. Ann. Neurol. 53, 823.

Hamprhire, D.J., Roberts, E., Crow, Y., Hoad, J., Mubaidin, A., Wriekat, A.L., et al., 2001. Kufor–Rakeb syndrome, pallido-pyramidal degeneration with supranuclear upgaze paresis and dementia, maps to 1p 36. J. Med. Genet. 38, 680–682.

Hatano, T., Kubo, S., Imai, S., Maeda, M., Ishikawa, K., Mizuno, Y., et al., 2007. Leucine-rich repeat kinase 2 associates with lipid rafts. Hum. Mol. Genet. 16, 678–690.

Haugarvoll, K., Toft, M., Skipper, L., Heckman, M.G., Crook, J.E., Soto, A., et al., 2009. Fine-mapping and candidate gene investigation within the PARK10 locus. Eur. J. Hum. Genet. 17, 336–343.

Healy, D.G., Abou-Sleiman, P.M., Lees, A.J., Casas, J.P., Quinn, N., Bhatia, K., et al., 2004a. Tau gene and Parkinson's disease: a case-control study and meta-analysis. J. Neurol. Neurosurg. Psychiatry 75 (7), 962–965.

Healy, D.G., Abou-Sleiman, P.M., Ozawa, T., Lees, A.J., Bhatia, K., Ahmadi, K.R., et al., 2004b. A functional polymorphism regulating dopamine beta-hydroxylase influences against Parkinson's disease. Ann. Neurol. 55, 443–446.

Healy, D.G., Falchi, M., O'sullivan, S.S., Bonifati, V., Durr, A., Bressman, S., et al., 2008. Phenotype, genotype, and worldwide genetic penetrance of LRRK2-associated Parkinson's disease: a case–control study. Lancet Neurol. 7, 583–590.

Hedrich, K., Marder, K., Harris, J., Kann, M., Lynch, T., Meija-Santana, H., et al., 2002. Evaluation of 50 probands with early-onset Parkinson's disease for parkin mutations. Neurology 58, 1239–1246.

Hedrich, K., Eskelson, C., Wilmot, B., Marder, K., Harris, J., Garrels, J., et al., 2004. Distribution, type, and origin of Parkin mutations: review and case studies. Mov. Disord. 19, 1146–1157.

Hicks, A.A., Pétursson, H., Jónsson, T., Stefánsson, H., Jóhannsdóttir, H.S., Sainz, J., et al., 2002. A susceptibility gene for late-onset idiopathic Parkinson's disease. Ann. Neurol. 52, 549–555.

Hunot, S., Brugg, B., Ricard, D., Michel, P.P., Muriel, M.P., Ruberg, M., et al., 1997. Nuclear translocation of NF-κ is increased in dopaminergic neurons of patients with Parkinson's disease. Proc. Natl. Acad. Sci. USA 94, 7531–7536.

Illarioshkin, S.N., Ivanova-Smolenskaya, I.A., Markova, E.D., Zagorovskaya, T.B., Brice, A., 2000. Lack of alpha-synuclein gene mutations in families with autosomal dominant Parkinson's disease in Russia. J. Neurol. 247, 968–969.

Illarioshkin, S.N., Periquet, M., Rawal, N., Lücking, C.B., Zagorovskaya, T.B., Slominsky, P.A., et al., 2003. Mutation analysis of the parkin gene in Russian families with autosomal recessive juvenile parkinsonism. Mov. Disord. 18, 914–919.

Illarioshkin, S.N., Shadrina, M.I., Slominsky, P.A., Bespalova, E.V., Zagorovskaya, T.B., Bagyeva, G.Kh., et al., 2007. A common leucine-rich repeat kinase 2 gene mutation in familial and sporadic Parkinson's disease in Russia. Eur. J. Neurol. 14, 413–417.

Jenner, P., 1999. Genetic susceptibility and the occurrence of Parkinson's disease. Parkinsonism Relat. Disord. 5, 173–177.

Jenner, P., Olanow, C.W., 1998. Understanding cell death in Parkinson's disease. Ann. Neurol. 44, 72–84.

Kalinderi, K., Fidani, L., Katsarou, Z., Clarimón, J., Bostantjopoulou, S., Kotsis, A., 2009. GSK3beta polymorphisms, MAPT H1 haplotype and Parkinson's disease in a Greek cohort. Neurobiol. Aging [Epub ahead of print].

Kang, S.J., Scott, W.K., Li, Y.J., Hauser, M.A., van der Walt, J.M., Fujiwara, K., et al., 2006. Family-based case-control study of MAOA and MAOB polymorphisms in Parkinson disease. Mov. Disord. 21, 2175–2180.

Kann, M., Jacobs, H., Mohrmann, K., Schumacher, K., Hedrich, K., Garrels, J., et al., 2002. Role of parkin mutations in 111 community-based patients with early-onset parkinsonism. Ann. Neurol. 51, 621–625.

Karamohamed, S., DeStefano, A.L., Wilk, J.B., Shoemaker, C.M., Golbe, L.I., Mark, M.H., et al., 2003. A haplotype at the PARK3 locus influences onset age for Parkinson's disease: the Gene PD study. Neurology 61, 1557–1561.

Kelada, S.N., Stapleton, P.L., Farin, F.M., Bammler, T.K., Eaton, D.L., Smith-Weller, T., et al., 2003. Glutathione S-transferase M1, T1, and P1 polymorphisms and Parkinson's disease. Neurosci. Lett. 30, 5–8.

Kim, J., Inoue, K., Ishii, J., Vanti, W.B., Voronov, S.V., Murchison, E., et al., 2007. A microRNA feedback circuit in midbrain dopamine neurons. Science 317, 1220–1224.

Kimpara, T., Takeda, A., Watanabe, K., Itoyama, Y., Ikawa, S., Watanabe, M., et al., 1997. Microsatellite polymorphism in the human heme oxygenase-1 gene promoter and its application in association studies with Alzheimer and Parkinson disease. Hum. Genet. 100, 145–147.

Kitada, T., Asakawa, S., Hattori, N., Hattori, N., Matsumine, H., Yamamura, Y., et al., 1998. Mutations in the parkin gene cause autosomal recessive juvenile parkinsonism. Nature 392, 605–608.

Klivenyi, P., Siwek, D., Gardian, G., Yang, L., Starkov, A., Cleren, C., et al., 2006. Mice lacking alpha-synuclein are resistant to mitochondrial toxins. Neurobiol. Dis. 21, 541–548.

Kontakos, N., Stokes, J., 1999. Monograph series on aging-related diseases: XII. Parkinson's disease-recent developments and new directions. Chronic Dis. Can. 20, 58–76.

Kosik, K.S., 2006. The neuronal microRNA system. Nat. Rev. Neurosci. 7, 911–920.

Krüger, R., 2008. *LRRK2* in Parkinson's disease—drawing the curtain of penetrance: a commentary. BMC Med. 6, 33.

Krüger, R., Kuhn, W., Muller, T., Woitalla, D., Graeber, M., Kösel, S., et al., 1998. Ala30Pro mutation in the gene encoding alpha-synuclein in Parkinson's disease. Nat. Genet. 18, 106–108.

Krüger, R., Hardt, C., Tschentscher, F., Jäckel, S., Kuhn, W., Müller, T., et al., 2000. Genetic analysis of immunomodulating factors in sporadic Parkinson's disease. J. Neural Transm. 107, 553–562.

Krüger, R., Fischer, C., Schulte, T., Strauss, K.M., Müller, T., Woitalla, D., et al., 2003. Mutation analysis of the neurofilament M gene in Parkinson's disease. Neurosci. Lett. 351, 125–129.

Kuroda, Y., Mitsui, T., Kunishige, M., Shono, M., Akaike, M., Azuma, H., et al., 2006. Parkin enhances mitochondrial biogenesis in proliferating cells. Hum. Mol. Genet. 15, 883–895.

Lautier, C., Goldwurm, S., Durr, A., Giovannone, B., Tsiaras, W.G., Pezzoli, G., et al., 2008. Mutations in the GIGYF2 (TNRC15) gene at the PARK11 locus in familial Parkinson disease. Am. J. Hum. Genet. 82, 822–833.

Lavedan, C., Buchholtz, S., Nussbaum, R.L., Albin, R.L., Polymeropoulos, M.H., 2002. A mutation in the human neurofilament M gene in Parkinson's disease that suggests a role for the cytoskeleton in neuronal degeneration. Neurosci. Lett. 322, 57–61.

Le, W.D., Xu, P., Jankovic, J., Jiang, H., Appel, S.H., Smith, R.G., et al., 2003. Mutations in NR4A2 associated with familial Parkinson disease. Nat. Genet. 33, 85–89.

Leroy, E., Boyer, R., Auburger, G., Leube, B., Ulm, G., Mezey, E., et al., 1998. The ubiquitin pathway in Parkinson's disease. Nature 395, 451–452.

Lesage, S., Brice, A., 2009. Parkinson's disease: from monogenic forms to genetic susceptibility factors. Hum. Mol. Genet. 18, 48–59.

Lesage, S. ., Durr, A., Tazir, M., Lohmann, E., Leutenegger, A.L., Janin, S., et al., 2006. LRRK2 G2019S as a cause of Parkinson's disease in North African Arabs. N. Engl. J. Med. 354, 422–423.

Levecque, C., Elbaz, A., Clavel, J., Richard, F., Vidal, J.S., Amouyel, P., et al., 2003. Association between Parkinson's disease and polymorphisms in the nNOS and iNOS series in a community-based case-control study. Hum. Mol. Genet. 12, 79–86.

Li, Y., Tomiyama, H., Sato, K., Hatano, Y., Yoshino, H., Atsumi, M., et al., 2005. Clinicogenetic study of PINK1 mutations in autosomal recessive early-onset Parkinsonism. Neurology 64, 1955–1957.

Liu, Y., Fallon, L., Lashuel, H.A., Liu, Z., Lansbury, P.T., 2002. The UCH-L1 gene encodes two opposing enzymatic activities that affect alpha-synuclein degradation and Parkinson's disease susceptibility. Cell 111, 209–218.

Lo, H.S., Hogan, E.L., Soong, B.W., 2002. 5V-flanking region polymorphism of the neuronal nitric oxide synthase gene with Parkinson's disease in Taiwan. J. Neurol. Sci. 194, 11–13.

Lohmann, E., Periquet, M., Bonifati, V., Wood, N.W., De Michele, G., Bonnet, A.M., et al., 2003. How much phenotypic variation can be attributed to parkin genotype. Ann. Neurol. 54, 176–185.

Lücking, C., Chesneau, V., Lohmann, E., Verpillat, P., Dulac, C., Bonnet, A., et al., 2003. Coding polymorphisms in the parkin gene and susceptibility to Parkinson disease. Arch. Neurol. 60, 1253–1256.

Luoma, P.T., Eerola, J., Ahola, S., Hakonen, A.H., Hellström, O., Kivistö, K.T., et al., 2007. Mitochondrial DNA polymerase gamma variants in idiopathic sporadic Parkinson disease. Neurology 69, 1152–1159.

MacLeod, D., Dowman, J., Hammond, R., Leete, T., Inoue, K., Abeliovich, A., 2006. The familial Parkinsonism gene LRRK2 regulates neurite process morphology. Neuron 52, 587–593.

Mandemakers, W., Morais, V.A., De Strooper, B., 2007. A cell biological perspective on mitochondrial dysfunction in Parkinson disease and other neurodegenerative diseases. J. Cell Sci. 120, 1707–1716.

Manila, K.M., Rinne, J.O., Lehtimaki, T., Röyttä, M., Ahonen, J.P., Hurme, M., 2002. Association of an interleukin IB gene polymorphism (-511) with Parkinson's disease in Finnish patients. J. Med. Genet. 39, 400–402.

Maraganore, D.M., Farrer, M.J., Hardy, J.A., Lincoln, S.J., McDonnell, S.K., Rocca, W.A., 1999. Case-control study of the ubiquitin carboxy-terminal hydrolase L1 gene in Parkinson's disease. Neurology 53, 1858–1860.

Maraganore, D.M., de Andrade, M., Lesnick, T.G., Strain, K.J., Farrer, M.J., Rocca, W.A., et al., 2005. High-resolution whole-genome association study of Parkinson disease. Am. J. Hum. Genet. 77, 685–693.

Marazziti, D., Mandillo, S., Di Pietro, C., Golini, E., Matteoni, R., Tocchini-Valentini, G.P., 2007. GPR37 associates with the dopamine transporter to modulate dopamine uptake and behavioral responses to dopaminergic drugs. Proc. Natl. Acad. Sci. USA 104, 9846–9851.

Martins, L.M., Morrison, A., Klupsch, K., Fedele, V., Moisoi, N., Teismann, P., et al., 2004. Neuroprotective role of the reaper-related serine protease HtrA2/Omi revealed by targeted deletion in mice. Mol. Cell. Biol. 24, 9848–9862.

Mellick, G.D., Buchanan, D.D., McCann, S.J., James, K.M., Johnson, A.G., Davis, D.R., et al., 1999. Variations in the monoamine oxidase B (MAOB) gene are associated with Parkinson's disease. Mov. Disord. 14, 219–224.

Mellick, G.D., Maraganore, D.M., Silburn, P.A., 2005. Australian data and meta-analysis lend support for alpha-synuclein (NACPRep1) as a risk factor for Parkinson's disease. Neurosci. Lett. 375, 112–116.

Mori, H., Kondo, T., Yokochi, M., Matusmine, H., Nakagawa-Hattori, Y., Miyake, T., et al., 1998. Pathologic and biochemical studies of juvenile Parkinsonism linked to chromosome 6q. Neurology 51, 890–892.

Myhre, R., Klungland, H., Farrer, M.J., Aasly, J.O., 2008. Genetic association study of synphilin-1 in idiopathic Parkinson's disease. BMC Med. Genet. 9, 19.

Najim al-Din, A.S., Wriekat, A., Mubaidin, A., Dasouki, M., Hiari, M., 1994. Pallidopyramidal degeneration, supranuclear upgaze paresis and dementia: Kufor-Rakeb syndrome. Acta Neurol. Scand. 89, 347–352.

Nichols, W.C., Pankratz, N., Marek, D.K., Pauciulo, M.W., Elsaesser, V.E., Halter, C.A., et al., 2009. Parkinson Study Group-PROGENI Investigators. Mutations in GBA are associated with familial Parkinson disease susceptibility and age at onset. Neurology 72, 310–316.

Nishioka, K., Hayashi, S., Farrer, M.J., Singleton, A.B., Yoshino, H., Imai, H., et al., 2006. Clinical heterogeneity of alpha-synuclein gene duplication in Parkinson's disease. Ann. Neurol. 59, 298–309.

Oliveira, S.A., Scott, W.K., Martin, E.R., Nance, M.A., Watts, R.L., Hubble, J.P., et al., 2003. Parkin mutations and susceptibility alleles in late-onset Parkinson's disease. Ann. Neurol. 53, 624–629.

On, C.F., Rowe, D.B., Halliday, G.V., 2002. An inflammatory review of Parkinson's disease. Prog. Neurobiol. 68, 325–340.
Orr, C.F., Rowe, D.B., Halliday, G.M., 2002. An inflammatory review of Parkinson's disease. Prog. Neurobiol. 68, 325–340.
Ozelius, L.J., Senthil, G., Saunders-Pullman, R., Ohmann, E., Deligtisch, A., Tagliati, M., et al., 2006. LRRK2 G2019S as a cause of Parkinson's disease in Ashkenazi Jews. N. Engl. J. Med. 354, 424–425.
Paisan-Ruiz, C., Jain, S., Evans, E.W., Gilks, W.P., Simón, J., van der Brug, M., et al., 2004. Cloning of the gene containing mutations that cause PARK8-linked Parkinson's disease. Neuron 44, 595–600.
Pan, T., Kondo, S., Le, W., Jankovic, J., 2008. The role of autophagy-lysosome pathway in neurodegeneration associated with Parkinson's disease. Brain 131, 1969–1978.
Pankratz, H., Foroud, T., 2004. Genetics of Parkinson disease. NeuroRx 1, 235–242.
Pankratz, N., Nichols, W.C., Uniacke, S.K., Halter, C., Rudolph, A., Shults, C., et al., 2002. Genome screen to identify susceptibility genes for Parkinson disease in a sample without parkin mutations. Am. J. Hum. Genet. 71, 124–135.
Pankratz, N., Nichols, W.C., Uniacke, S.K., Halter, C., Rudolph, A., Shults, C., et al., 2003. Significant linkage of Parkinson disease to chromosome 2q36–37. Am. J. Hum. Genet. 72, 1053–1057.
Pankratz, N., Wilk, J.B., Latourelle, J.C., Destefano, A.L., Halter, C., Pugh, E.W., PSG-PROGENI and GenePD Investigators, Coordinators and Molecular Genetic Laboratories, 2009. Genomewide association study for susceptibility genes contributing to familial Parkinson disease. Hum. Genet. 124, 593–605.
Periquet, M., Latouche, M., Lohmann, E., Rawal, N., De Michele, G., Ricard, S., et al., 2003. Parkin mutations are frequent in patients with isolated early-onset parkinsonism. Brain 126, 1271–1278.
Piccini, P., Burn, D., Ceravolo, R., Maraganore, D., Brooks, D., 1999. The role of inheritance in sporadic Parkinson's disease: evidence from a longitudinal study of dopaminergic function in twins. Ann. Neurol. 45, 577–582.
Polymeropoulos, M.H., Higgins, J.J., Golbe, L.I., Johnson, W.G., Ide, S.E., Di Iorio, G., et al., 1996. Mapping of a gene for Parkinson's disease to chromosome 4q21–q23. Science 274, 1197–1199.
Polymeropoulos, M.H., Lavedan, C., Leroy, E., Ide, S.E., Dehejia, A., Dutra, A., et al., 1997. Mutation in the alpha-synuclein gene identified in families with Parkinson's disease. Science 276, 2045–2047.
Ramirez, A., Heimbach, A., Gründemann, J., Stiller, B., Hampshire, D., Cid, L.P., et al., 2006. Hereditary Parkinsonism with dementia is caused by mutations in ATP13A2, encoding a lysosomal type 5 P-type ATPase. Nat. Genet. 38, 1184–1191.
Rashmi, S., Racette, B., Perlmutter, J.S., Parsian, A., 2005. Prevalence of parkin gene mutations and variations in idiopathic Parkinson's disease. Parkinsonism Relat. Disord. 11, 341–347.
Ritz, B.R., Manthripragada, A.D., Costello, S., Lincoln, S.J., Farrer, M.J., Cockburn, M., et al., 2009. Dopamine transporter genetic variants and pesticides in Parkinson's disease. Environ. Health Perspect. 117, 964–969.
Ryoo, H.L., Pierrotti, D., Joyce, J.N., 1998. Dopamine D3 receptor is decreased and D2 receptor is elevated in the striatum of Parkinson's disease. Mov. Disord. 13, 788–797.
Schiesling, C., Kieper, N., Seidel, K., Kruger, R., 2008. Review: familial Parkinson's disease—genetics, clinical phenotype and neuropathology in relation to the common sporadic form of the disease. Neuropathol. Appl. Neurobiol. 34, 255–271.
Scott, W.K., Nance, M.A., Watts, R.L., Hubble, J.P., Koller, W.C., Lyons, K., et al., 2001. Complete genomic screen in Parkinson disease: evidence for multiple genes. JAMA 286, 2239–2244.

Shadrina, M.I., Illarioshkin, S.N., Bagyeva, G.Kh., Bespalova, E.V., Zagorodskaia, T.B., Slominskiĭ, P.A., et al., 2007a. A PARK8 form of Parkinson's disease: a mutational analysis of the LRRK2 gene in Russian population. Zh. Nevrol. Psikhiatr. Im. S. S. Korsakova 107, 46–50.

Shadrina, M.I., Semenova, E.V., Slominsky, P.A., Bagyeva, G.H., Illarioshkin, S.N., Ivanova-Smolenskaia, I.I., et al., 2007. Effective quantitative real-time polymerase chain reaction analysis of the parkin gene (PARK2) exon 1-12 dosage. BMC Med. Genet. 8, 6.

Shahabi, H.N., Westberg, L., Melke, J., Håkansson, A., Belin, A.C., Sydow, O., et al., 2009. Cytochrome P450 2E1 gene polymorphisms/haplotypes and Parkinson's disease in a Swedish population. J. Neural Transm. 116, 67–73.

Sharma, M., Mueller, J.C., Zimprich, A., Lichtner, P., Hofer, A., Leitner, P., et al., 2006. The sepiapterin reductase gene region reveals association in the PARK3 locus: analysis of familial and sporadic Parkinson's disease in European populations. J. Med. Genet. 43, 557–562.

Shimura, H., Hattori, N., Kubo, S., Mizuno, Y., Asakawa, S., Minoshima, S., et al., 2000. Familial Parkinson disease gene product, parkin, is a ubiquitin-protein ligase. Nat. Genet. 25, 302–305.

Shin, N., Jeong, H., Kwon, J., Heo, H.Y., Kwon, J.J., Yun, H.J., et al., 2008. LRRK2 regulates synaptic vesicle endocytosis. Exp. Cell Res. 314, 2055–2065.

Shojaee, S., Sina, F., Banihosseini, S.S., Kazemi, M.H., Kalhor, R., Shahidi, G.A., et al., 2008. Genome-wide linkage analysis of a Parkinsonian-pyramidal syndrome pedigree by 500 K SNP arrays. Am. J. Hum. Genet. 82, 1375–1384.

Simón-Sánchez, J., Schulte, C., Bras, J.M., Sharma, M., Gibbs, J.R., Berg, D., et al., 2009. Genome-wide association study reveals genetic risk underlying Parkinson's disease. Nat. Genet. 41, 1308–1312.

Singh, M., Khan, A.J., Shah, P.P., Shukla, R., Khanna, V.K., Parmar, D., 2008. Polymorphism in environment responsive genes and association with Parkinson disease. Mol. Cell. Biochem. 312, 131–138.

Singleton, A.B., Farrer, M., Johnson, J., Singleton, A., Hague, S., Kachergus, J., et al., 2003. a-Synuclein locus triplication causes Parkinson's disease. Science 302, 841.

Sironi, F., Primignani, P., Zini, M., Tunesi, S., Ruffmann, C., Ricca, S., et al., 2008. Parkin analysis in early onset Parkinson's disease. Parkinsonism Relat. Disord. 14, 326–333.

Sleiman, P.M., Healy, D.G., Muqit, M.M., Yang, Y.X., Van Der Brug, M., Holton, J.L., et al., 2009. Characterisation of a novel NR4A2 mutation in Parkinson's disease brain. Neurosci. Lett. 457, 75–79.

Slominsky, P.A., Miloserdova, O.V., Popova, S.N., Giliazova, I.R., Khidiiatova, I.V., Magzhanov, R.V., et al., 2003. Analysis of deletion mutations in the *PARK2* gene in idiopathic Parkinson's disease. Genetika 39, 23–28.

Strauss, K.M., Martins, L.M., Plun-Favreau, H., Marx, F.P., Kautzmann, S., Berg, D., et al., 2005. Loss of function mutations in the gene encoding Omi/HtrA2 in Parkinson's disease. Hum. Mol. Genet. 14, 2099–2111.

Swerdlow, R.H., Parks, J.K., Miller, S.W., Tuttle, J.B., Trimmer, P.A., Sheehan, J.P., et al., 1996. Origin and functional consequences of the complex I defect in Parkinson's disease. Ann. Neurol. 40, 663–671.

Takahashi, H., Ohama, E., Suzuki, S., Horikawa, Y., Ishikawa, A., Morita, T., et al., 1994. Familial juvenile Parkinsonism, clinical and pathologic study in a family. Neurology 44, 437–441.

Takazawa, C., Karamohamed, S., DeStefano, A.L., Wilk, J.B., Shoemaker, C.M., Golbe, L.I., et al., 2003. A haplotype at the PARK3 locus influences onset age for Parkinson's disease: the GenePD study. Neurology 61, 1557–1561.

Tan, E.K., 2006. Identification of a common genetic risk variant(G2385A) in Parkinson's disease. Ann. Acad. Med. 35, 840–842.
Tan, E., Skipper, L.M., 2007. Pathogenic mutations in Parkinson disease. Hum. Mutat. 28, 641–653.
Tan, E.K., Khajavi, M., Thornby, J.I., Nagamitsu, S., Jankovic, J., Ashizawa, T., 2000. Variability and validity of polymorphism association studies in Parkinson's disease. Neurology 55, 533–538.
Tobin, J.E., Latourelle, J.C., Lew, M.F., Klein, C., Suchowersky, O., Shill, H.A., et al., 2008. Haplotypes and gene expression implicate the MAPT region for Parkinson disease: the GenePD Study. Neurology 71, 28–34.
Toda, T., Momose, Y., Murata, M., Tamiya, G., Yamamoto, M., Hattori, N., et al., 2003. Toward identification of susceptibility genes for sporadic Parkinson's disease. J. Neurol. 250, 40–44.
Valente, E.M., Bentivoglio, A.R., Dixon, P.H., Ferraris, A., Ialongo, T., Frontali, M., et al., 2001. Localization of a novel locus for autosomal recessive early-onset parkinsonism, PARK6, on human chromosome 1p35–p36. Am. J. Hum. Genet. 68, 895–900.
Valente, E.M., Abou-Sleiman, P.M., Caputo, V., Muqit, M.M., Harvey, K., Gispert, S., et al., 2004a. Hereditary earlyonset Parkinson's disease caused by mutations in PINK1. Science 304, 1158–1160.
Valente, E.M., Salvi, S., Ialongo, T., Marongiu, R., Elia, A.E., Caputo, V., 2004b. PINK1 mutations are associated with sporadic early-onset parkinsonism. Ann. Neurol. 56, 336–341.
Van der Walt, J.M., Nicodemus, K.K., Martin, E.R., Scott, W.K., Zhang, F., Nance, M.A., et al., 2003. Mitochondrial polymorphisms significantly reduce the risk of Parkinson disease. Am. J. Hum. Genet. 72, 804–811.
van Duijn, C.M., Dekker, M.C., Bonifati, V., Galjaard, R.J., Houwing-Duistermaat, J.J., Snijders, P.J., et al., 2001. Park7, a novel locus for autosomal recessive early-onset parkinsonism, on chromosome 1p36. Am. J. Hum. Genet. 69, 629–634.
Vreugdenhil, E., Berezikov, E., 2009. Fine-tuning the brain: microRNAs. Front. Neuroendocrinol. [Epub ahead of print].
Wahner, A.D., Sinsheimer, J.S., Bronstein, J.M., Ritz, B., 2007. Inflammatory cytokine gene polymorphisms and increased risk of Parkinson disease. Arch. Neurol. 64, 836–840.
Wang, G., van der Walt, J.M., Mayhew, G., Li, Y.J., Züchner, S., Scott, W.K., et al., 2008. Variation in the miRNA-433 binding site of FGF20 confers Risk for Parkinson disease by overexpression of α-synuclein. Am. J. Hum. Genet. 82, 283–289.
Weintraub, D., Comella, C.L., Horn, S., 2008. Parkinson's disease—Part 1: Pathophysiology, symptoms, burden, diagnosis, and assessment. Am. J. Manag. Care 14, 40–48.
West, A.B., Maraganore, D., Crook, J., Lesnick, T., Lockhart, P.J., Wilkes, K.M., et al., 2002. Functional association of the parkin gene promoter with idiopathic Parkinson's disease. Hum. Mol. Genet. 11, 2787–2792.
West, A.B., Moore, D.J., Choi, C., Andrabi, S.A., Li, X., Dikeman, D., et al., 2007. Parkinson's disease-associated mutations in LRRK2 link enhanced GTP-binding and kinase activities to neuronal toxicity. Hum. Mol. Genet. 16, 223–232.
Wilkinson, K.D., Lee, K.M., Deshpande, S., Duerksen-Hughes, P., Boss, J.M., Pohl, J., 1989. The neuron-specific protein PGP 9.5 is a ubiquitin carboxyl-terminal hydrolase. Science 246, 670–673.
Williams, D.R., Hadeed, A., AlDin, A.S., Wreikat, A.L., Lees, A.J., 2005. Kufor Rakeb disease: autosomal recessive, levodopa-responsive parkinsonism with pyramidal degeneration, supranuclear gaze palsy, and dementia. Mov. Disord. 20, 1264–1271.
Xiromerisiou, G., Hadjigeorgiou, G.M., Eerola, J., Fernandez, H.H., Tsimourtou, V., Mandel, R., et al., 2007. BDNF tagging polymorphisms and haplotype analysis in sporadic Parkinson's disease in diverse ethnic groups. Neurosci. Lett. 415, 59–63.

Yavich, L., Tanila, H., Vepsalainen, S., Jakala, P., 2004. Role of alpha-synuclein in presynaptic dopamine recruitment. J. Neurosci. 24, 11165–11170.

Yoritaka, A., Hattori, N., Yoshino, H., Mizuno, Y., 1997. Catechol-*O*-methyltransferase genotype and susceptibility to Parkinson's disease in Japan. Short communication. J. Neural Transm. 104, 1313–1317.

Zarranz, J.J., Alegre, J., Gomez-Esteban, J.C., Lezcano, E., Ros, R., Ampuero, I., et al., 2004. The new mutation, E46K, of alpha-synuclein causes Parkinson and Lewy body dementia. Ann. Neurol. 55, 164–173.

Zhang, Y., Dawson, V.L., Dawson, T.M., 2000. Oxidative stress and genetics in the pathogenesis of Parkinson's disease. Neurobiol. Dis. 7, 240–250.

Zhang, L., Shimoji, M., Thomas, B., Moore, D.J., Yu, S.W., Marupudi, N.I., et al., 2005. Mitochondrial localization of the Parkinson's disease related protein DJ-1: implications for pathogenesis. Hum. Mol. Genet. 14, 2063–2073.

Zhu, X., Siedlak, S.L., Smith, M.A., Perry, G., Chen, S.G., 2006. LRRK2 protein is a component of Lewy bodies. Ann. Neurol. 60, 617–618.

Zimprich, A., Biskup, S., Leitner, P., Lichtner, P., Farrer, M., Lincoln, S., et al., 2004. Mutations in LRRK2 cause autosomal-dominant parkinsonism with pleomorphic pathology. Neuron 44, 601–607.

Index

A

Abscisic acid (ABA)
  apicomplexa
    metabolites, biosynthesis, 188–190
    P. falciparum, 188–190
    Toxoplasma gondii, 188
  barley grain development
    embryo desiccation, 74
    endopolyploidization, 73–74
    endosperm cellularization, 73–74
    endosperm storage activities, 74
    programmed cell death, 65–66
Apicomplexa
  abscisic acid
    P. falciparum, 188–190
    Toxoplasma gondii, 188
  apicoplast
    acquisition, 164–165
    evolutionary origin, 165
    genome, 166
    morphology, 164
    proteome, 167
    trafficking mechanism, 167–168
  delayed death phenotype, 209–210
  drug targets
    antibiotics, 209
    immunosuppressant 15-deoxyspergualin, 209
  fatty acid synthesis
    acetyl-CoA generation, 191
    apicoplast-resident acyl-ACP thioesterase-like proteins, 194
    apicoplast-resident stearoyl-CoA desaturase (PFE0555w), 193
    FAS II pathway, 192–193
    palmitate (C_{16}), 190
  heme biosynthesis
    cytochrome c (c1) heme lyase, 207
    energy generation, TCA cycle, 205
    enzyme localization, 204
    erythrocyte infection, *P. falciparum*, 207–208
    heme oxygenase (HO) activity, 208
    membrane-localized heme uptake system, 205
    metabolism, 206
    metabolite exchange, 207
  iron–sulfur cluster biosynthesis
    bacterial SUF system, 199–200
    chaperones (Cpn60 and Cpn20), 202
    components, 197–198
    glutaredoxins, 202
    HCF101-like proteins, 200–202
    hypothetical model, 197–198
    plant-type ferredoxin redox system, 202–203
    scaffold proteins, 200
  isoprenoids (*see also* 1-Deoxy-D-xylulose-5-phosphate (DOXP) pathway)
    apicoplast-localized protein compilation, 180–185
    carbon source and uptake route, 179
    mevalonate (MEV) pathway, 176
    new permeability pathway, 177
    T. gondii's apicoplast phosphate translocator (TgAPT1), 179
  lipoic acid metabolism
    lipoyl protein ligase A (LplA), 194, 196
    LplA-like protein (PfLplA2), 196
    mitochondrion lipoylation, 196–197
    PDH complex, 194
  metabolites, biosynthesis
    abscisic acid, 188–190
    fatty acids (FA), 190–194
    heme, 203–208
    iron–sulfur clusters, 197–203
    isoprenoids (*see* Isoprenoids, apicomplexa)
    lipoic acid, 194–197
  in silico prediction, gene annotation
    alternative splicing, 168
    internet resources, 171–174
    metabolic dependencies, parasite, 169–170
    methods, 170
    missing enzymes, 169
    pathway holes, 168–169
Arabidopsis thaliana
  molecular mechanism
    CLE peptide-related nodulation, 17–18
    miR169, nitrogen starvation, 17
    miR399, phosphate starvation, 16–17
  phylogenetic tree, 134
  sulfate transport
    cis-acting element, 148
    cytokinin, 147
    feedback regulation, 145
    high-affinity transporters, 135–136
    molybdate transporter, 144
    O-acetylserine, 146

Arabidopsis thaliana (*cont.*)
oxyanions transport, 143–144
phloem companion cells, 141
root-to-shoot transport, 137–138
sulfur transport to seed, 141–142
symbiotic sulfate transporter, 142
vacuolar transport, 139–140
Arbuscular mycorrhiza (AM)
Arabidopsis molecular mechanism, AM symbiosis
CLE peptide-related nodulation, 17–18
miR169, nitrogen starvation, 17
miR399, phosphate starvation, 16–17
colonization
barley, 25–26
genome sequencing, 16
liverworts, 14–15
nitrogen uptake reduction, 28
plant growth response, 25
responsive and nonresponsive plants, 24–25
maize, 23
model legumes
common symbiosis pathway, 5–8
nutrient trading, 9–10
nutrient transporters, 10–14
prepenetration apparatus, 4–5
signal molecules, 3–4
transcriptome profiling, 8–9
pea and alfalfa, 24
plant interaction, 2
potato and tomato, 23–24
rice *(Oryza sativa)*
AM colonization, 21–22
dynamics aspects, 20–21
OsPT11-GFP fluorescence, 19–20
in planta imaging, 19
presymbiotic and endosymbiotic phase, 18
soybeans, 22–23
sustainable agriculture
abiotic and biotic stress tolerance, 27–28
agricultural resource crisis, 26–27
crop yield, normal conditions, 28–30
fertilizer phosphate reuse, 30–32

B

Barley grain development
abscisic acid (ABA)-influences
endosperm cellularization and endopolyploidization, 73–74
endosperm storage activities and embryo desiccation, 74
barley seed, 50
data integration, 51
developmental stages, 51–52
endosperm
cellularization, 52
storage capacity, 54–55
endosperm transfer cells (ETC), 52, 54, 66–67
high-resolution caryopsis 3-D model
biological variability, 55–56
MALDI imaging, 56–57
magnetic resonance-based 4-D modeling, 57–58
morphology and histology, 52–53
nucellar projection (NP), 52, 54
omics technologies and molecular physiology
expressed sequence tags (EST), 59
nucellar projection role, 63–64
nucellus role, 62–63
pericarp role, 60, 62
transcriptome data, 59–60
programmed cell death (PCD)
ABA biosynthesis, 65–66
α-amylase, 64–65
ethylene biosynthesis, 65–66
jasmonic acid (JA) biosynthesis, 65
seed maturation regulatory genes, 74–76
storage metabolism
ATP/ADP ratio, 72
fermentative enzymes, 70–71
oxygen distribution, 71–72
respiration, 69–70
systems biology
data generation, storage, integration, and visualization, 77–78
modeling, 78–79
transcriptional reprograming
seed filling, 67–68
sink strength, 68
storage protein synthesis, 68–69
transcriptome analysis, 51

C

Caldesmon (CAD) and tropomyosin (Tm)
actin cytoskeleton regulation, 108
actin dynamics
actin polymerization, 113–114
pyrene fluorescence, 112–113
cancer, 114–116
cell phosphorylation
CAD regulation, 110–111
CaD–tropomyosin interaction, 112
Tm phosphorylation, 111–112
expression, 108–109
podosomes, 109–110
smooth muscle, 101–102
Cancer metastasis, 114–116
Chaperones (Cpn60 and Cpn20), 202
Chlamydomonas, 144
Chromosome 8p, 254–255
Common symbiosis pathway (CSP), 5–7
Cytokinin, 147–148
Cytoskeletal tropomyosin, 94, 99, 101, 105

D

Delayed death phenotype, 209–210
1-Deoxy-D-xylulose-5-phosphate (DOXP) pathway
  Clp-dependent proteolysis, 186
  DOXP reductoisomerase (Dxr), *P. falciparum*, 176
  glyceraldehyde-3-phosphate (G3P), 177–178
  pyruvate, 178
  redox system, 186
  thiamine pyrophosphate (TPP), 187
Detoxication system, 254
Dihydroneopterin aldolase (DHNA), 169
Dopamine, Parkinson disease, 252–253

E

Embryo desiccation, 74
Endoplasmic reticulum-associated protein degredation (ERAD), 168
Endopolyploidization, 73–74
Endosperm cellularization, 52, 73–74
Endosperm storage capacity, 54–55, 74
Endosperm transfer cells (ETC), 51
  cellulose synthase, 66
  endosperm cellularization, 52
  function, 66
  gene expression, 66–67
  PCD, 64, 67
  scheme, 54
  transcriptome analysis, 59
  trehalose, 67

F

Familial Parkinson's disease
  characterization, 231
  dopaminergic neuron, 252
  GIGYF2 gene, 245
  G2019S mutation, 243
  incidence, 235
  LRRK2 gene, 242
  mitochondria function, 249
  SNCA gene, 242
Fatty acid synthesis, apicomplexa
  acetyl-CoA generation, 191
  apicoplast-resident acyl-ACP thioesterase-like proteins, 194
  apicoplast-resident stearoyl-CoA desaturase (PFE0555w), 193
  FAS II pathway, 192–193
  palmitate (C_{16}), 190
Flux balance analysis (FBA), 78–79

G

Gibberellic acid (GA), 54, 63, 73
Glomus intraradices, 14–15
Glutaredoxins, 202

H

HCF101-like proteins, 200–202
Heme biosynthesis, apicomplexa
  cytochrome c (c1) heme lyase, 207
  energy generation, TCA cycle, 205
  enzyme localization, 204
  erythrocyte infection, *P. falciparum*, 207–208
  heme oxygenase (HO) activity, 208
  membrane-localized heme uptake system, 205
  metabolism, 206
  metabolite exchange, 207
Heme oxygenase (HO) activity, 208

I

Inflammation, 253–254
Iron homeostasis, 254
Iron–sulfur cluster biosynthesis, apicomplexa
  bacterial SUF system, 199–200
  chaperones (Cpn60 and Cpn20), 202
  components, 197–198
  glutaredoxins, 202
  HCF101-like proteins, 200–202
  hypothetical model, 197, 198
  plant-type ferredoxin redox system, 202–203
  scaffold proteins, 200
Isoprenoids, apicomplexa
  apicoplast-localized protein compilation, 180–185
  carbon source and uptake route, 179
  1-deoxy-D-xylulose-5-phosphate (DOXP) pathway
    Clp-dependent proteolysis, 186
    DOXP reductoisomerase (Dxr), *P. falciparum*, 176
    glyceraldehyde-3-phosphate (G3P), 177–178
    pyruvate, 178
    redox system, 186
    thiamine pyrophosphate (TPP), 187
  mevalonate (MEV) pathway, 176
  new permeability pathway, 177
  T. gondii's apicoplast phosphate translocator (TgAPT1), 179

L

Legume–arbuscular mycorrhiza fungi interaction
  common symbiosis pathway (CSP)
    genes, 6–7
    root nodule formation and AM symbosis, 5–6
  nutrient exchange
    AMT2-type ammonium transporter, 13
    carbon import, 10
    hexoses, 10
    L. japonicus, 11–13
    M. truncatula, 10–11
    phosphate and ammonium, 9–10

Legume–arbuscular mycorrhiza fungi interaction (*cont.*)
prepenetration apparatus (PPA)
formation, 4–5
hyphopodia, 4
symbiosomes, 5
signal molecules
Myc factor, 4
Nod factor, 3–4
transcriptome profiling, 8–9
Lotus japonicus, 3, 5, 142. *See also* Legume–arbuscular mycorrhiza fungi interaction
LjAMT2;2 gene, 13
LjPT3/LjPT4 gene, 11–13
Lysosome, 251–252

M

Maize (Zea mays), 23
Marchantia foliacea, 14
Medicago truncatula, 3, 5. *See also* Legume–arbuscular mycorrhiza fungi interaction
Membrane-localized heme uptake system, 205
Methylerythritol phosphate (MEP) pathway, 175–176
MicroRNA, 255
MicroRNA-395, 151–152
Microtubule-associated protein tau (MAPT), 255
Mitochondrial dysfunction and oxidative stress, 248–250
Molybdate transporter, 144–145

N

New permeability pathway (NPP), 177

O

O-acetylserine (OAS), 146–147
Omics technologies and molecular physiology, barley
expressed sequence tags (EST), 59
molecular-physiological events, caryopsis development, 61
nucellar projection role, 63–64
nucellus role, 62–63
pericarp role, 60, 62
transcriptome data, 59–60
Oxyanion transport, 143–144

P

Parkinson's disease (PD)
clinical features, 231–232
evidence, 236
familial form, 231
genes and biological process
chromosome 8p, 254–255
detoxication system, 254
dopamine, 252–253
dopaminergic neurons, 252
genome-wide association study (GWAS), 255–256
inflammation, 253–254
iron homeostasis, 254
lysosome, 251–252
microRNA, 255
microtubule-associated protein tau (MAPT), 255
mitochondrial dysfunction and oxidative stress, 248–250
synapse, 250–251
ubiquitin–proteasome system, 246–248
loci and genes role, 237–238
monogenic forms
PARK1 (PARK4) locus, 235, 239
PARK2 locus, 239–241
PARK3 locus, 245, 246
PARK5 locus, 244
PARK6 locus, 241
PARK7 locus, 241–242
PARK8 locus, 242–244
PARK9 locus, 244–245
PARK10 locus, 245–246
PARK12 locus, 246
PARK14 locus, 246
PARK15 locus, 246
neuropathology, 233–234
occurrence, 230
symptoms, 230–231
PCD. *See* Programmed cell death (PCD)
Plant-type ferredoxin redox system, 202–203
Plastid replication and repair enzyme complex (PREX), 166
Plastome
replication, 166
transcription and translation, 166–167
Potato *(Solanum tuberosum)*, 23–24
Prepenetration apparatus (PPA), 4–5
Programmed cell death (PCD)
ABA and ethylene ratio, 74
ABA biosynthesis, 65–66
α-amylase, 64–65
early-and mid-storage phase, 55
ETC, 67
ethylene biosynthesis, 65–66
indicators, 63
jasmonic acid (JA) biosynthesis, 65
pericarp, 62
vacuolar-processing enzyme, 62
Protein deformylase (PDF), 210

R

Rice *(Oryza sativa)*–arbuscular mycorrhiza interaction
AM colonization, 21–22, 24

localization and dynamics, 20–21
OsPT11-GFP fluorescence, 19–20
in planta imaging, 19
presymbiotic and endosymbiotic phase, 18
Root-to-shoot sulfate transport
horizontal transport, 137
low-affinity transport functional interplay, 138
SULTR2;1 function, 137–138

S

Source-to-sink transport
sulfate transport
phloem companion cells, 141
phloem parenchyma cells, 140–141
sulfur transport to seeds, 141–142
Soybean *(Glycine max)*, 22–23
Sporadic Parkinson's disease
development, 231
genes and biological process
chromosome 8p, 254–255
detoxication system, 254
dopamine, 252–253
dopaminergic neurons, 252
genome-wide association study (GWAS), 255–256
inflammation, 253–254
iron homeostasis, 254
lysosome, 251–252
microRNA, 255
microtubule-associated protein tau (MAPT), 255
mitochondrial dysfunction and oxidative stress, 248–250
synapse, 250–251
ubiquitin–proteasome system, 246–248
genetic factors, 235
G2019S mutation, 243
HTRA2 gene, 246
Storage metabolism, barley
ATP/ADP ratio, 72
fermentative enzymes, 70–71
oxygen distribution, 71–72
respiration, 69–70
Strigolactones, 3–4
Stylosanthes hamata, 133
Sulfate transport and assimilation
function, 131–132
illustration, 130–131
leaf tissues, 143
microorganisms, 130
molybdate transporter, 144–145
oxyanion transport, 143–144
regulation effectors
cytokinin, 147–148
feedback regulation, 145
O-acetylserine (OAS), 146–147
regulatory elements
microRNA-395, 151–152
SLIM1, 149–151
sulfur-responsive *cis*-acting element, 148
root-to-shoot transport
horizontal transport, 137
low-affinity transport functional interplay, 138
SULTR2;1 function, 137–138
source-to-sink transport
phloem companion cells, 141
phloem parenchyma cells, 140–141
seeds, 141–142
sulfate uptake
Arabidopsis, 135–136
mechanism, 132–133
SULTR1;1 and SULTR1;2 characteristics, 136–137
transporter, 133–134
symbiotic sulfate transporter, 142–143
vacuolar transport
control sulfate transport, 140
mechanism, 139
vacuolar sulfate remobilization, 139–140
Sulfur limitation1 (SLIM1) mutant, 149–151
Sustainable agriculture, arbuscular mycorrhiza
abiotic and biotic stress tolerance
arsenate and arsenite, 27–28
bacterial pathogen, 28
Cu-binding capacity, 28
nitrate poisoning, 28
agricultural resource crisis
AM inoculation, positive plant growth, 27
phosphate resources, 26
crop yield
nonresponsive crops, 29–30
plant transplantation, AM colonization, 28–29
fertilizer phosphate reuse, 30–32
Symbiotic sulfate transporter, 142–143
Systems biology, barley grain development
data generation, storage, integration, and visualization, 77–78
modeling, 78–79

T

Thiamine pyrophosphate (TPP) synthesis, 187
Tomato *(Solanum lycopersicum)*, 23–24
Transcriptome analysis, barley, 51
molecular-physiological events, 61
omics technologies, 59–60
transcriptional reprograming
seed filling, 67–68
sink strength, 68
storage protein synthesis, 68–69
Tropomyosin (Tm)
actin–tropomyosin interaction, myosin II, 107–108

Tropomyosin (Tm) (*cont.*)
biochemical properties, 98–99
caldesmon (CAD) and Tm
actin cytoskeleton regulation, 108
actin dynamics, 112–114
CAD regulation, phosphorylation, 110–111
CaD–tropomyosin interaction, 112
expression, 108–109
podosomes, 109–110
Tm phosphorylation, 111–112
cancer metastasis
cell migration, 114
l-CaD and Tm interaction, 115–116
metastatic and nonmetastatic cell line, 114–115
class I myosins, cell membrane, 108
gene structure
alternative splicing, 92, 94
schematics, 92–93
α-, β-, γ-Tm, 94–95
isoform distribution
brain, 105–106
local signaling, 106
muscle-specific isoforms, 105
nonmuscle, 105–106
nonmuscle cells
actin filament dynamics, 104
cell division and actomyosin-II ATPase, 103
lamellipodium and lamellum, 103–104
organelle transport, 103
Tm–actin interaction, 104
protein structure
actin binding, 96–97
Ca^{2+}-sensitive movement, 98
coiled-coil structure, 95
crystal structure, 97
dimers, 95–96
three-dimensional reconstruction, 97–98
smooth muscle
actomyosin activation, 101–102
caldesmon (h-CaD) concentration, 102
inhibitory action, 102
striated muscle contraction
cytoskeletal Tm, 101
myosin-binding site, 100
α-Tm, 100
β-and γ-Tm, 100–101
troponin, 99–100
Troponin, 92, 96–102

U

Ubiquitin–proteasome system, 246–248

V

Vacuolar sulfate transport
control sulphate transport, 140
mechanism, 139
vacuolar sulfate remobilization, 139–140

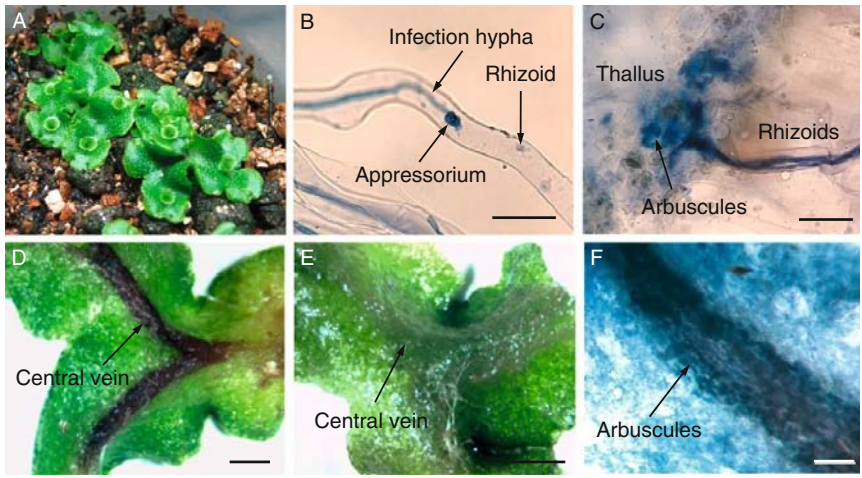

Shingo Hata et al., Figure 1.3 Colonization of a liverwort with an AM fungus. (A) Photograph of *Marchantia paleacea* var. *diptera* (a gift from Prof. H. Takano, Kumamoto University), which had been inoculated with spores of *Glomus intraradices*. (B) Trypan blue-staining shows that fungal hyphae formed an appressorium on the surface of the rhizoids, penetrated into the cells, and extended to the thallus. (C) Arbuscules developed in the thallus (40 dpi). (D) AM fungi mainly colonized the central vein of the thallus of *M. paleacea* and brown to red pigments were accumulated around the colonized area. (E) In contrast to in panel (D), coloration was not observed in a noninoculated control. (F) Trypan blue-staining indicates that arbuscules were densely formed in the central vein (60 dpi). Bar = 50 μm (B and C), 2 mm (D and E), and 0.5 mm (F).

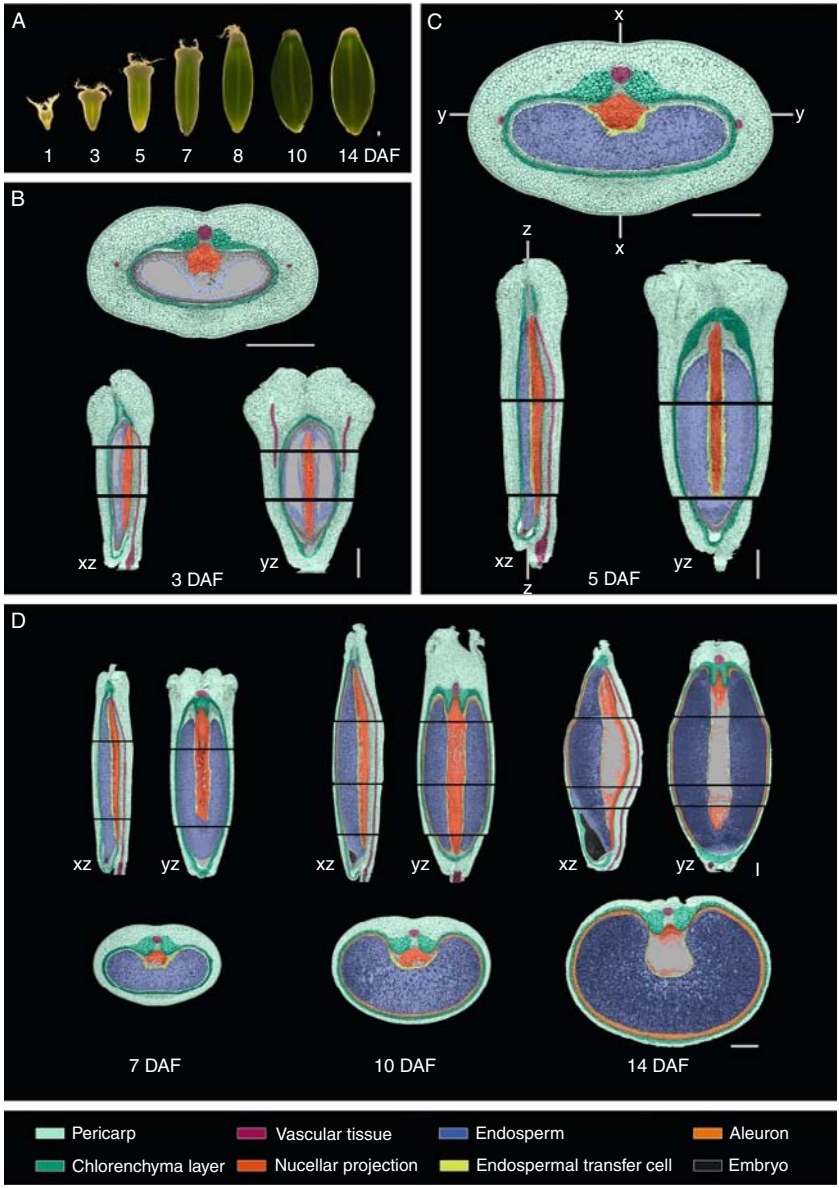

Nese Sreenivasulu et al., Figure 2.1 The developing barley grain. (A) Barley grains at different developmental stages. Glumes and awn were removed before taking photographs. (B)–(D) Median transverse, longitudinal (xz), and saggital (yz) sections of barley grains at different developmental stages. The x, y, and z position of the sections is given in (C). Longitudinal and saggital sections are created from simulated artificial grains generated by a combination of thin transverse sections from plastic-embedded material. Black bars dividing the longitudinal and saggital sections into pieces result from cutting of the native caryopses necessary for optimal fixation and embedding. Colors representing individual tissues are shown at the bottom panel of the figure. The white patches within the nucellar projection in (D) indicate degeneration of tissue resulting into the endosperm cavity. Bars, 500 μm. DAF, days after flowering.

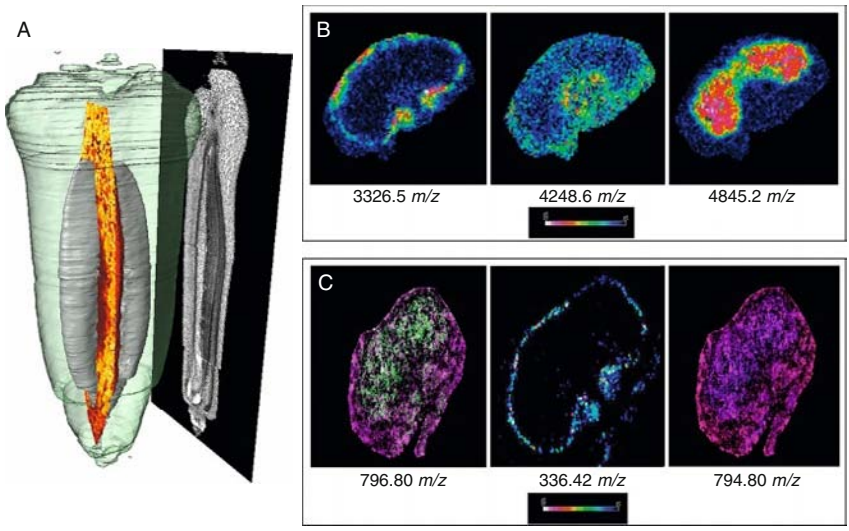

Nese Sreenivasulu et al., Figure 2.3 Model of an individual barley grain at 7 DAF with an integrated matrix-assisted laser desorption/ionization imaging mass spectrometry (MALDI-IMS) median section visualizing the distribution of an unidentified substance of a mass of $m/z = 9.595$ and a simulated median section (A) and MALDI-IMS cross sections depicting yet unidentified peptides (B) or low-molecular-weight compounds (C). Images were taken with spatial resolutions of 50 μm (B) or 15 μm (C).

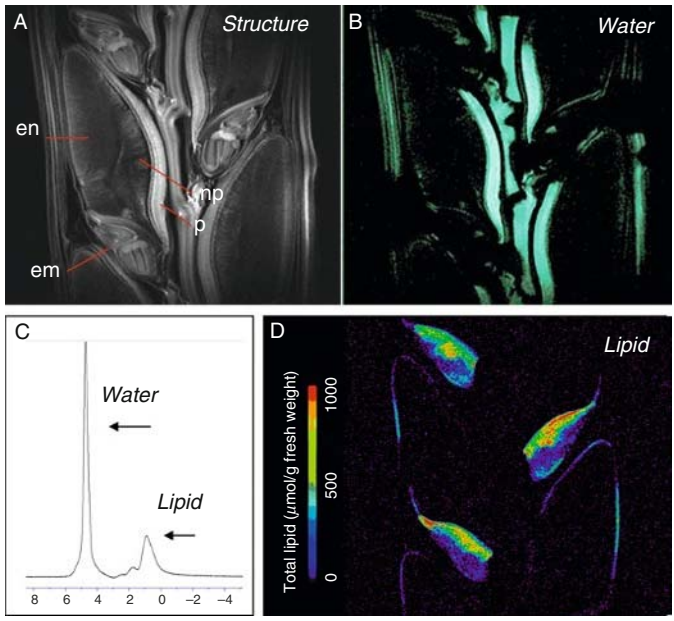

Nese Sreenivasulu et al., Figure 2.4 Noninvasive visualization of a barley spike section using nuclear magnetic resonance (NMR). (A) Internal grain structure *in vivo* at 35 μm resolution; (B) visualization of the *in vivo* water distribution; (C) water and lipid peaks in the NMR spectrum; (D) quantitative map representing the *in vivo* lipid deposition within grains (mainly within the embryo and the aleuron layer). Lipid content is color-coded. Abbreviations: em, embryo; en, endosperm; np, nucellar projection; p, pericarp.

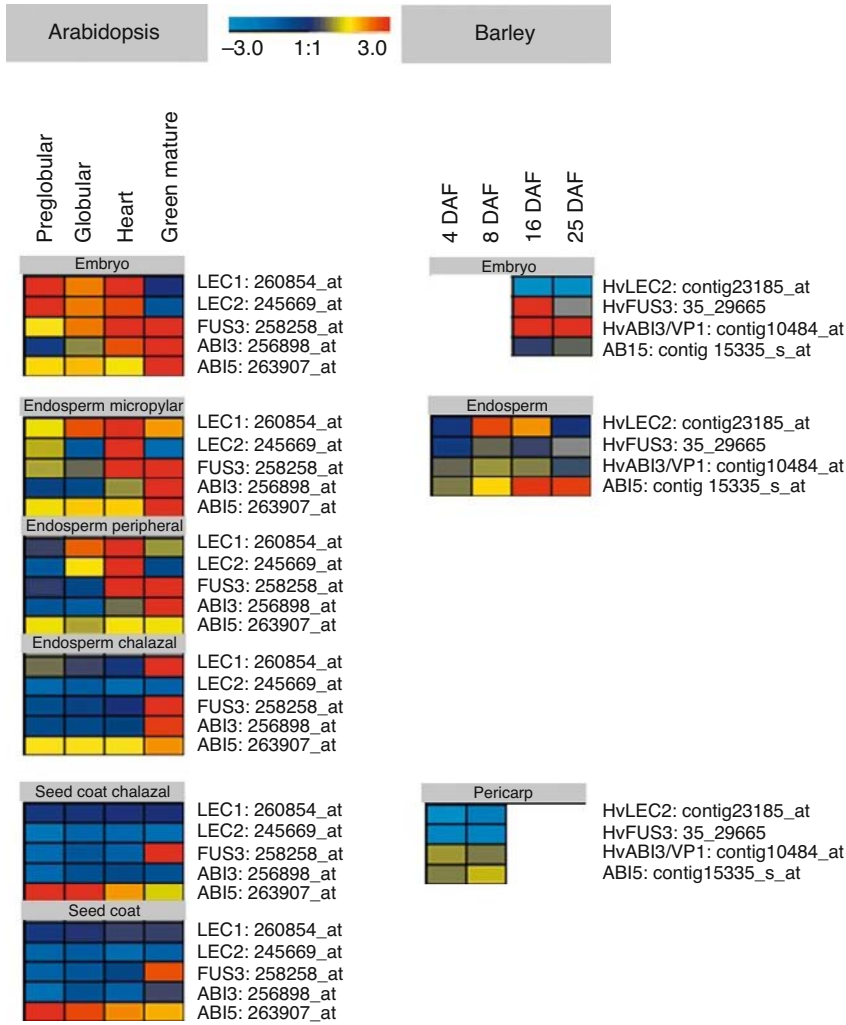

Nese Sreenivasulu et al., Figure 2.6 Tissue-specific expression patterns of key seed maturation regulatory genes in *Arabidopsis* and barley. First, the barley sequences homologs to the *Arabidopsis* genes *LEC1*, *LEC2*, *FUS3*, *ABI3*, and *ABI5* were defined. Second, publicly available Affymetrix expression data of microdissected *Arabidopsis* seed tissues (Series GSE12402, GSE11262, GSE15160, GSE15165) and our own data obtained from manually dissected tissues of three major barley grain tissues (Series GSE9365) were subjected to Robust Multiarray normalization, and the expression patterns of the key regulators are shown as heat maps. Signal intensities are color coded: red, high expression; yellow, moderate expression; dark blue, low expression; light blue, very low expression. LEC, leafy cotyledon; FUS3, FUSCA3; ABI, abscisic acid insensitive.

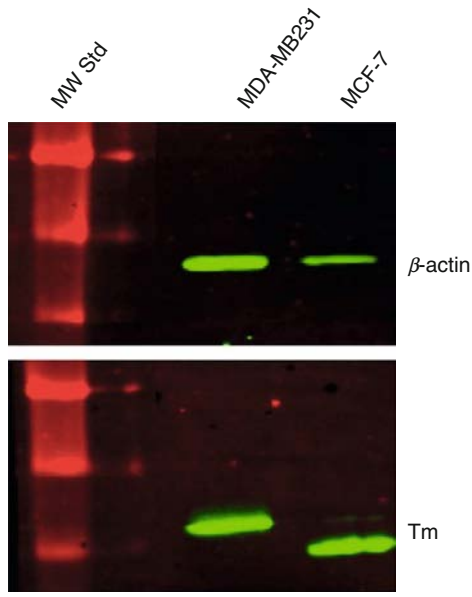

C.-L. Albert Wang and Lynne M. Coluccio, Figure 3.4 Metastatic and nonmetastatic human breast tumor cells contain different Tms. Western blot analysis with Odyssey software showing that the Tm in the two types of tumor cells, MDA-MB231 (metastatic) and MCF-7 (nonmetastatic), exhibit different mobilities on SDS–polyacrylamide gels (lower panel). β-Actin was used as a reference for loading (upper panel).

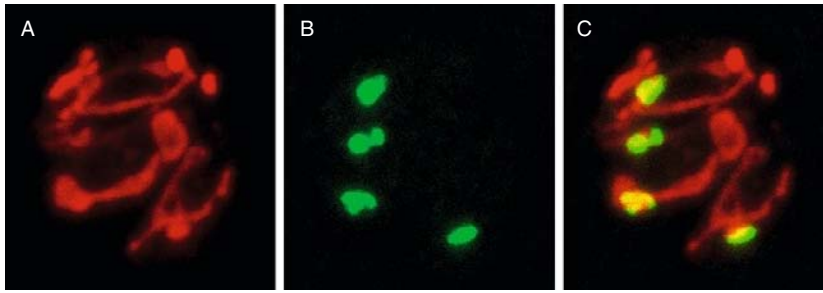

Frank Seeber and Dominique Soldati-Favre, Figure 5.1 3D-reconstructions of four fluorescently tagged mitochondria (myc-tagged TgTPX1/2) (A) and apicoplasts (Ty-tagged TgICDH) (B) of *T. gondii* tachyzoites, respectively (Pino et al., 2007). The merged image in (C) documents the close association between both organelles.

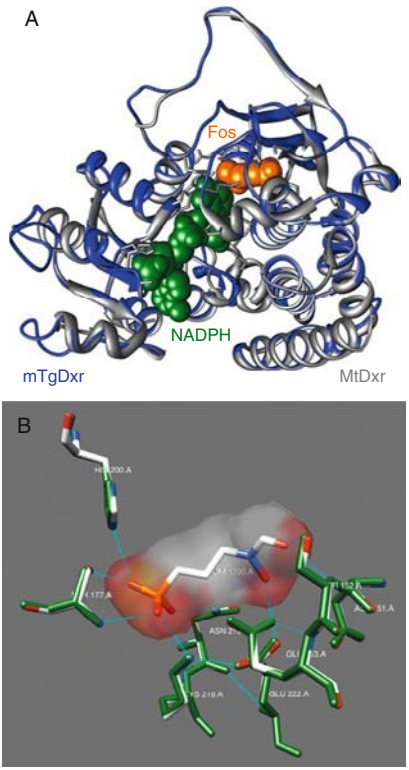

Frank Seeber and Dominique Soldati-Favre, Figure 5.3 3D-modeling of *T. gondii* Dxr protein sequence onto *Mycobacterium tuberculosis* Dxr. (A) The model was built using the Swiss Model Server (Arnold et al., 2006) with the *M. tuberculosis* structure as template (PDB 2jcvA; Henriksson et al., 2007). The resulting structures were then compared using the TopMatch server (Sippl and Wiederstein, 2008). Visualization of the model was performed using Chimera (Pettersen et al., 2004). The bacterial structure is shown in gray (MtDxr) and the parasite chain in blue (mTgDxr). MtDxr-bound NADPH (green) and Fos (orange) are also shown. (B) Amino acids implicated in Fos interactions within the binding pocket of MtDxr (Henriksson et al., 2006) and their comparison with the corresponding aa from the modeled TgDxr (green). The numbers refer to the MtDxr sequence. The molecular surface of Fos is indicated.